



HAL
open science

Inverse problems for stochastic neutronics

Corentin Houpert

► **To cite this version:**

Corentin Houpert. Inverse problems for stochastic neutronics. Statistics [math.ST]. Institut Polytechnique de Paris, 2022. English. NNT : 2022IPPAX124 . tel-04106674

HAL Id: tel-04106674

<https://theses.hal.science/tel-04106674v1>

Submitted on 25 May 2023

HAL is a multi-disciplinary open access archive for the deposit and dissemination of scientific research documents, whether they are published or not. The documents may come from teaching and research institutions in France or abroad, or from public or private research centers.

L'archive ouverte pluridisciplinaire **HAL**, est destinée au dépôt et à la diffusion de documents scientifiques de niveau recherche, publiés ou non, émanant des établissements d'enseignement et de recherche français ou étrangers, des laboratoires publics ou privés.



INSTITUT
POLYTECHNIQUE
DE PARIS

NNT : 2022IPPAX124

Thèse de doctorat



Inverse problem for stochastic neutronics

Thèse de doctorat de l'Institut Polytechnique de Paris
préparée à École polytechnique

École doctorale n°574 Ecole Doctorale de Mathématiques Hadamard (EDMH)
Spécialité de doctorat : Mathématiques appliquées

Thèse présentée et soutenue à Palaiseau, le 8 décembre 2022, par

CORENTIN HOUPERT

Composition du Jury :

| | |
|---|-----------------------|
| Sébastien Da Veiga Professeur, ENSAI - CREST (UMR 9194) | Président, Rapporteur |
| Anil Prinja Professeur émérite, University of New Mexico | Rapporteur |
| Emmanuel Gobet Professeur, École polytechnique (UMR 7641) | Examineur |
| Céline Helbert Maîtresse de conférences, ICJ École Centrale de Lyon (UMR 5208) | Examinatrice |
| Josselin Garnier Professeur, École polytechnique (UMR 7641) | Directeur de thèse |
| Philippe Humbert Ingénieur de recherche, CEA DAM DIF | Co-encadrant de thèse |
| Marie Ducauze-Philippe Ingénieure de recherche, CEA DAM DIF | Invitée |

Inverse problem for Stochastic Neutronics
CEA et École polytechnique

Corentin Houpert

December 8, 2022

Nomenclature

Nuclear constants

| | |
|---------------|---|
| $\bar{\nu}$ | Mean number of neutrons emitted by a fission event |
| $\bar{\nu}_S$ | Mean number of neutrons emitted by a source event |
| λ_C | Capture rate by time unit |
| λ_F | Fission rate by time unit |
| λ_T | Total reaction rate by time unit |
| ν_i | Moment of order i of the number of neutrons emitted by the induced fission |
| θ | Mean lifetime of neutrons |
| D_2 | Diven factor of the fission of order 2 |
| D_3 | Diven factor of the fission of order 3 |
| D_{2S} | second order Diven factor of the source |
| D_{3S} | third order Diven factor of the source |
| f_ν | Probability the fission emits ν neutrons |
| $f_{\nu,S}$ | Probability that the spontaneous fission emits ν neutrons during a source event |

Nuclear parameters

| | |
|-----------------|---|
| α | Decreasing coefficient of the neutronic system |
| \bar{S} | Mean number of neutrons generated by the sources by unit of time (neutrons/units of time) |
| \mathbf{p} | Vector of the parameters of the system |
| x | spontaneous fission rate |
| ε_C | Capture efficiency |
| ε_F | Fission efficiency |

| | |
|------------|---|
| k_{eff} | Multiplication factor |
| M_L | the leakage multiplication |
| S | Intensity of the sources |
| S_α | Intensity of the Poisson type source |
| S_F | Intensity of the compound Poisson type source |

Observations and model outputs

| | |
|-------------------------|---|
| $\bar{\nu}_{II}$ | Mean number of the neutrons present in the system at T knowing there was 0 in the system at t in presence of a source |
| $\bar{\nu}_\pi$ | Mean number of the neutron present in the system at T knowing there was 1 in the system at t in the absence of a source |
| $\bar{\nu}_{II,\infty}$ | Mean of the number of neutrons present in the system in presence of a source during the stationary regime |
| \mathbf{M} | Vector of the first three simple statistical moments, the model |
| $\hat{\mathbf{M}}$ | Estimation of the first three simple moments of $N_{[0,t]}$ |
| $\hat{\mathbf{M}}$ | Vector of the first three simple empirical moments, the measures |
| $\mathcal{G}(x, t)$ | Generating function associated to the probability distribution $(Q_n(t))_{n \in \mathbb{N}}$ |
| \mathcal{M}_p | Mean number of q -combination of q detections between t and T when there is a number of neutrons at t with a stationary distribution and when there is a source |
| $\nu_{k,II,\infty}$ | Factorial moment of order k of the number of neutrons present in the system in presence of a source during the stationary regime |
| $\nu_{k,II}$ | Factorial moment of order k of the neutrons present in the system at T knowing there was 0 in the system at t in presence of a source |
| $\nu_{k,\pi}$ | Moment of order k of the neutrons present in the system at T knowing there was 1 in the system at t in the absence of a source |
| $\Pi_n(t)$ | Probability that n neutrons be present at final time T knowing there was 0 at t in presence of a source |
| $\Pi_{\nu,\infty}$ | Probability that ν neutrons are present in the system in presence of a source and during the stationary regime |
| $\pi_{n,1}(t)$ | Probability of presence of n neutrons at final time T knowing the fact there was 1 neutron at t in the absence of a source |
| $\pi_{n,\nu}(t)$ | Probability of presence of n neutrons at final time T knowing the fact there was ν neutrons at t in the absence of a source |

- $g(x, t)$ Generating function associated to the probability distribution $(p_n(t))_{n \in \mathbb{N}}$
- $g^{\Pi}(x, t)$ Generating function associated to the probability distribution $(p_j^{\Pi}(t))_{j \in \mathbb{N}}$
- $g_{\nu}(x, t)$ Generating function associated to the probability distribution $(p_{n,\nu}(t))_{n \in \mathbb{N}}$
- G_{Π} Generating function associated to the distribution of the number of neutrons present in presence of a source Π
- g_{π} Generating function associated to the distribution of the number of neutrons present in the absence of a source π
- $G_{\Pi, \infty}(z)$ Generating function of the probability distribution $(\Pi_{n, \infty})_{n \in \mathbb{N}}$ when the stationary regime is established
- $g_{\pi, \infty}(z)$ Generating function associated to the probability distribution $(\pi_{n, \infty})_{n \in \mathbb{N}}$ when the stationary regime is settled
- m_n Mean number of n -combination of n detections between t and T when there is a neutron at t in the absence of a source
- M_q Mean number of q -combination of q detections between t and T when there is a neutron at t in presence of source
- $N_{[t, T]}$ Random variable representing the number of neutrons detected during the interval $[t, T]$
- $P_n(t)$ Probability of counting n neutrons between t and T knowing the fact there is 0 neutron at time t (with external source)
- $p_{n,1}(t)$ Probability of detecting n neutrons at final time T knowing the fact there was 1 neutron at t in the absence of a source
- $P_{n,\nu}(t)$ Probability of counting n neutrons between t and T knowing the fact there is ν neutrons at time t (with external source)
- $p_{n,\nu}(t)$ Probability of detecting n neutrons at final time T knowing the fact there was ν neutrons at t in the absence of a source
- $Q_n(t)$ Probability of counting n neutrons on the interval $[t, T]$ knowing the number of neutrons has stationary distributions $(\Pi_{\nu, \infty})_{\nu \in \mathbb{N}}$ (with external source)
- X_T Random variable representing the number of neutrons present in the system at T

Remerciements

Je tiens en premier lieu à remercier Josselin. Lorsque j'ai appris que j'allais pouvoir faire cette thèse, j'ai été très agréablement surpris. J'avais lu une partie du livre "Mathématiques tout-en-un pour la Licence L3" de Buff et al., et je venais d'apprendre que je pouvais faire ma thèse avec un des auteurs d'un des livres de référence pour l'agrégation. J'ai beaucoup appris grâce en travaillant avec toi, ma vision des maths et leurs applications s'est nettement améliorée depuis mes années d'études. Merci de m'avoir accordé ton temps. J'ai pu apprendre en faisant des erreurs, et en m'améliorant, même si ça a été laborieux. J'ai pu donner beaucoup plus de profondeur à ma perception, et j'espère pouvoir encore l'améliorer pour apporter quelque chose de plus. Merci également de m'avoir permis de terminer mes travaux dans de bonnes conditions.

Je remercie ensuite Philippe pour avoir proposé ce sujet, la simplicité du modèle ponctuel permet d'avoir une bonne ouverture sur la neutronique, et d'aller plus loin. Merci pour d'avoir proposé des solutions qui ont un sens physique, c'est ce que je cherchais dans ma formation. L'aspect pratique a son importance, et tu l'as bien montré.

Je tiens à remercier Anil K. Prinja et Sébastien Da Veiga pour leur travail de relecture.

Ces travaux vont se poursuivre grâce à Paul Lartaud, je lui souhaite de mener à bien toutes les idées qu'il aura, et qu'elles seront fructueuses.

Merci à tous les membres de la team Emmanuel pour les bons moments qu'on a pu avoir. Merci donc à Florian Bourgey, Manon Rivoire, Emmanuel Gobet, Marine Saux, Clara Lage, Maxime Grangereau, Wanqing Wang, Dorinel, David Métivier.

Je tiens à remercier Pierre et Sylvain pour toutes les fois où je leur ai demandé de l'aide concernant l'informatique. Je remercie spécialement François Alouges pour ses encouragements et son soutien. Je remercie aussi Matthieu Aussal pour les conversations autour de la thèse que nous avons eu. Je souhaite pleins de succès sportifs aux randoms runners, en particulier à Laurent et Hélène.

Ce doctorat s'est très bien déroulé grâce à de nombreux stagiaires, doctorants ou post-doctorants au CEA ou au CMAP. Je tiens à remercier Solange, Mickael, Louis R., Arthur, Aurélien, Thomas B., Dominik, Vianney, Julie, Imke, Vincent, Rémy, Frédéric, Guillaume B., Guillaume C., Célia, Yoann, Kévin, Eugénie, Pierre Lavigne, Matthias, Charles, Ward, Emmanuel, Antoine V., Jules, Raphaël, Shanqing, Kang, Baptiste, Clément, Naoufal, Amin, Victor, Olivier, Pablo, Louise, Mathilde, Ronan, Bastien, Mathieu, Marie, Antoine C., Jean-Cédric, Albertine, Eric, Adrien, Cécile, Sébastien, Christina, Grégoire, Pauline, Étienne, Joël, Haythem, Kevish, Tuan Anh,

Alexis Cousin, Thomas V., Alexandre B., Achille, Leïla, Olga, Fedor, Ludovic, Ignacio, Quentin Canu, Benjamin, Gabriel, Tom, Armand, Baptiste G., Paul T., Louis G., Mario, Florian F., Geneviève, Aude, Claire, Corentin C., Mathilde, Ruben, Benoît Dagallier, Maëlle, Pierre W., Maksim, Nikita, Thomas Langlade, Richard, Anna, Omar, Josué, Angèle, Josselin M. et Constantin.

Je vous souhaite à tous pleins de réussite !

Au sein des labos de l'École polytechnique, j'ai pu trouver de précieux conseils grâce à Antigoni, Lucia, Charles Bertucci, Aymeric Dieuleveut, Marylou Gabrié, Vincent Bansaye, Thierry Bodineau, Cyril Marzouk, Giovanni, Igor, Yang Qi, Aldjia Mazari, Nizar Touzi et Carl Graham. Je les remercie pour le temps qu'ils m'ont accordé.

Remerciements particuliers à Sébastien Notre-Dame.

Je remercie le personnel soignant qui m'a aidé au cours de cette thèse, à savoir Murielle, Valérie, Denis Michard. Plus particulièrement, je tiens à remercier et féliciter Florence Robin, Anne Delaigue ainsi Pascale Tessier pour le soutien qu'elles m'ont apporté.

J'ai pris du temps pour élargir ma vision de la Science durant cette thèse. C'est en particulier grâce à Emmanuel Ferrand, Matthieu Piquerez, Thibaut Damour, Laurent Lafforgue, Étienne Ghys, Jean-François Colonna, Nicolas Brosse, Denis Gratias, Éric Moulines et Emmanuel Gobet, je les en remercie.

Je tiens à remercier les équipes du Palais de la découverte et leur souhaiter bonne suite, en particulier à Laure Cornu, Robin Jamet et Guillaume Reuillier.

Mon travail est passé par le CEA, où je tiens à remercier Julien Cartier, David Denis-Petit, François-Xavier Hugot, Davide Mancusi, Marie Philippe, Marianne Sécheresse, Matthieu De Sequeira, Patrick Rémy et Andrea Zoia pour leur aide, et leur ouverture au monde du nucléaire.

Mes études universitaires sont passées par Nantes et j'ai pu faire des mathématiques fondamentales et appliquées. Merci à Eddy, Hélène, Jérémy, Pierre, Solène et Germain d'avoir été là à ce moment. Germain, tu m'accompagnes depuis cette période, tes conseils me sont très utiles, et ce, depuis longtemps. J'ai pu passer par les mathématiques fondamentales grâce aux conseils de Barbara Héreau-Dostal, et j'ai eu la chance d'avoir comme professeurs Christophe Berthon, Sylvain Gervais, Frédéric Héreau, Hélène Mathis, François Nicoleau et Laurent Thomann; je salue leur pédagogie et leur sympathie.

Ces études se sont poursuivies à l'ONERA grâce à Florent Renac, Éric Savin, Marc Errera et Odile. Je les remercie de m'avoir fait part de leur passion pour la recherche et l'aéronautique.

Le skateboard a occupé une grande partie de mon temps pendant mes études, et j'ai rencontré Jean Tain au skatepark de l'Hôtel-Dieu de Nantes. Merci Jean pour ces petits moments, tes conseils, qui font que je conçois cette pratique autrement. Je garderai longtemps souvenir du lieu où sont stockés les livres chez toi.

Je remercie mes parents, mon frère Adrien, mes sœurs Élisa et Hortense, pour leur soutien et leur présence.

Je fais un petit coucou à mes amis de lycée Thomas Authier, Raphaël Calixte,

Ilyès Charrick, Dimitri Grivollat et Thomas Januel.

Enfin, j'espère n'avoir oublié personne, si c'est le cas, je te souhaite le meilleur.

Contents

| | | |
|----------|---|-----------|
| 1 | Introduction | 11 |
| 1.0.1 | Contexte | 12 |
| 1.0.2 | Motivations | 12 |
| 1.0.3 | Context | 15 |
| 1.0.4 | Motivations | 15 |
| 1.1 | Discrete probabilistic tools | 16 |
| 1.1.1 | Basic probability distributions | 16 |
| 1.1.2 | Generating functions | 18 |
| 1.2 | Discrete-time sto. pro. | 20 |
| 1.3 | Discrete-time Markov chains | 20 |
| 1.3.1 | Some general properties of the Markov motion | 22 |
| 1.3.2 | Stability of a Markov system | 24 |
| 1.3.3 | Recurrence times | 27 |
| 1.3.4 | Ergodicity | 30 |
| 1.4 | Continuous-time sto. pro. | 31 |
| 1.5 | Continuous-time Markov pro. | 32 |
| 1.5.1 | The infinitesimal transition scheme | 34 |
| 1.5.2 | Forward and backward Chapman-Kolmogorov equations | 34 |
| 1.5.3 | Continuous time Markov chain behaviour | 36 |
| 1.5.4 | Ergodicity | 38 |
| 1.6 | Stochastic neutronics | 39 |
| 1.6.1 | Basic of neutron physics | 39 |
| 1.6.2 | Stochastic neutronic equations | 48 |
| 1.6.3 | Feynman moments | 69 |
| 1.6.4 | Panjer formula | 71 |
| 1.7 | U.Q. and Inverse problems | 72 |
| 1.7.1 | Tikhonov's regularisation from linear to non-linear | 73 |
| 1.7.2 | Bayesian inverse problems | 78 |

| | | |
|----------|--|------------|
| 1.7.3 | MCMC Sampling methods, Bayesian sampling | 86 |
| 2 | Direct problem | 88 |
| 2.1 | The process of the number of neutrons present in the system | 89 |
| 2.1.1 | Factorial Cumulants | 92 |
| 2.2 | Pop. and detec. | 95 |
| 2.3 | The "Counting" code, a MC code in the point model approximation . | 101 |
| 2.4 | Num. exp. | 103 |
| 2.4.1 | A first case | 103 |
| 2.4.2 | A second case | 120 |
| 2.4.3 | A third case | 123 |
| 2.5 | Two Cases | 125 |
| 2.5.1 | Modelisation of the data of a first case | 126 |
| 2.5.2 | Modelling of the data of the second case | 138 |
| 3 | Inverse problem | 146 |
| 3.1 | Inv. prob. | 146 |
| 3.1.1 | Analytical inversion method | 148 |
| 3.1.2 | The observations | 157 |
| 3.1.3 | The mean square error, a first consideration for the inverse problem | 158 |
| 3.1.4 | Simulated annealing | 163 |
| 3.1.5 | Use of Bayesian methods | 177 |
| 3.2 | Posterior distributions | 183 |
| 3.2.1 | A posteriori distribution of $(k_{eff}, \varepsilon_C, S)$ given the three first moments of $N_{[0,T]}$ for $k_{eff} = 0.95$ | 183 |
| 3.2.2 | A posteriori distribution of $(k_{eff}, \varepsilon_C, S)$ given the three first moments of $N_{[0,T_1]}, N_{[0,T_2]}$ for $T_1 = \frac{1}{\alpha}$ and $T_2 = \frac{10}{\alpha}$ for $k_{eff} = 0.95191$ | |
| 3.2.3 | A posteriori distribution of $(k_{eff}, \varepsilon_C, S)$ given the three first moments of $N_{[0,T]}$ where $T = \frac{1}{\alpha}$ or $T = \frac{10}{\alpha}$ and $k_{eff} = 0.5$. . . | 192 |
| 3.2.4 | A posteriori distribution of $(k_{eff}, \varepsilon_C, S)$ given the three first moments of $N_{[0,T_1]}, N_{[0,T_2]}$ where $T_1 = \frac{1}{\alpha}, T_2 = \frac{10}{\alpha}$ and $k_{eff} = 0.5199$ | |
| 3.2.5 | Influence of the prior distribution | 203 |
| 4 | Conclusion | 207 |
| 4.1 | Conclusions | 207 |
| 4.2 | Perspectives | 208 |
| A | Appendix | 210 |

| | | |
|--------|--|-----|
| A.1 | Note on the state-of-the-art | 210 |
| A.1.1 | Markov chains on finite set of space | 211 |
| A.1.2 | Linear algebra | 211 |
| A.1.3 | Classical methods of estimation in statistics | 211 |
| A.2 | Direct prob. | 212 |
| A.2.1 | Some key integrals | 212 |
| A.2.2 | Cumulants of the distribution of presence | 213 |
| A.2.3 | Moments of the distribution of presence $\pi_n(t)$ and $\Pi_n(t)$. . . | 214 |
| A.2.4 | Moments of the distribution of detection $p_n(t)$, $P_n(t)$, $Q_n(t)$. | 222 |
| A.2.5 | Generating functions | 244 |
| A.2.6 | Feynman moments tools | 248 |
| A.2.7 | Feynman and simple moments: passage formula | 250 |
| A.2.8 | Euler's method for the moments of the neutrons detected . . . | 251 |
| A.2.9 | Panjer formula | 253 |
| A.2.10 | Link between $Q_n(t)$ and $P_n(t)$ | 253 |
| A.2.11 | About ε_F , ε_C | 254 |
| A.2.12 | MCNP-6 and Tripoli-4 parameters | 255 |
| A.3 | Inv. prob. | 257 |
| A.3.1 | The program ntc0b_cov2 | 257 |
| A.3.2 | Vectorial version of CLT | 257 |
| A.3.3 | Confidence interval | 259 |
| A.3.4 | Approximation of the likelihood | 260 |
| A.3.5 | Delta method | 262 |
| A.3.6 | Numerical results | 262 |
| A.4 | Tools | 263 |
| A.4.1 | Computation of confidence interval | 263 |
| A.4.2 | Differentiate for the computation of the empirical likelihood $\tilde{\mathbb{P}}(\mathbf{p} \mathbf{y}_{obs})$ | 265 |
| A.4.3 | Distributions for induced fission | 266 |

Chapter 1

Introduction

Le scientifique a une grande expérience en matière d'ignorance, de doute et d'incertitude, et cette expérience est d'une très grande importance, je pense. Quand le scientifique ne connaît pas la réponse, il est ignorant. Quand il a une intuition de ce que le résultat est, il est incertain. Et quand il est sacrément sûr de ce que le résultat sera, il est encore dans le doute. La connaissance scientifique est un ensemble d'affirmations à différents degrés de certitude – certains plus incertains, d'autres à peu près sûrs, mais pas absolument certains.

Richard Feynman "The Value of Science," discours à l'Académie nationale des sciences (Automne 1955)

1.0.1 Contexte

Le contexte de la thèse est principalement la détection passive de neutrons corrélés pour la sûreté et les garanties nucléaires.

La sûreté est le moyen pour empêcher les incidents nucléaires et protéger l'environnement, le public et les travailleurs des risques d'exposition aux rayonnements. Les garanties nucléaires sont une façon de vérifier que chaque état remplisse les accords internationaux sur le nucléaire en ce qui concerne la production d'explosifs nucléaires. Les méthodes de détection passives permettent d'obtenir la connaissance de l'état du système neutronique sans manipulation supplémentaire [Ens+98]. Cela arrive pendant le contrôle d'une installation nucléaire ou lorsque l'on assure sa sûreté. Du fait des interactions aléatoires (en particulier lors des collisions), le fait de détecter des neutrons sera considéré comme un processus aléatoire. Ici, nous sommes spécifiquement concernés par les mesures de corrélations temporelles des neutrons. D'autres sujets d'intérêt sont la comptabilité matière, la physique des réacteurs, les mesures de réactivité, l'interprétation des benchmarks sous-critiques, la réactivité des réacteurs sous-critiques (réacteur hybride piloté par accélérateur - ADS) [PP08]. La comptabilité matière se réfère à l'évaluation et l'enregistrement de la quantité et du type de matériaux nucléaires présents dans les installations. Les benchmarks sous-critiques aident les spécialistes en sûreté à vérifier les données nucléaires. En ce qui concerne la physique des réacteurs, il y a deux types de fluctuations du flux des neutrons : le bruit à puissance nulle et le bruit à puissance non-nulle. Le bruit à puissance non-nulle résulte des fluctuations macroscopiques comme les vibrations mécaniques des barres de contrôle. Dans les réacteurs à puissance nulle, la source d'aléa est due à des phénomènes microscopiques, e.g. réactions nucléaires, fission. La détermination de la réactivité d'un assemblage nucléaire sous-critique peut être établie par l'utilisation de deux méthodes standard, Feynman-alpha et Rossi-alpha. Ces méthodes sont basées sur l'analyse statistique de la liste des instants de détection, qui permet de déterminer les paramètres neutroniques d'un système fissile.

1.0.2 Motivations

Le but de ce travail est l'estimation de paramètres nucléaires à partir des mesures de corrélations neutroniques. Il s'agit d'un problème inverse avec des observations bruitées, ce n'est pas une exception à la citation de Feynman. La physique des systèmes neutroniques fournit quelques intuitions du comportement des observations, alors nous serons incertains comme suggéré par la remarque de Feynman. Comme l'indique ce point de vue, il est nécessaire de quantifier le niveau d'incertitude : la quantification d'incertitude apparaît comme un moyen adéquat.

Les données expérimentales sont une liste du nombre de détections durant des intervalles de temps de même durée. Une analyse statistique basée sur les moments du nombre de détections est effectuée pour l'inférence sur les paramètres.

Les neutrons de fission sont produits par paquets (entre 2 et 3 en moyenne). Les neutrons provenant d'une même fission sont corrélés en temps. L'émission des neutrons sources est un processus de Poisson composé. Lors de la détection, il va y avoir un excès de variance à la loi de Poisson. Ce fait est exploité par la méthode

de Feynman. En général, du fait des corrélations neutroniques, les moments d'ordre supérieur à la moyenne contiennent de l'information à propos du système.

Comme nous ne cherchons pas qu'une estimation ponctuelle, mais plutôt la distribution complète des paramètres, nous considérerons l'inférence bayésienne et les méthodes de Monte-Carlo par chaînes de Markov (MCMC) d'échantillonnage de la distribution a posteriori des paramètres.

En ce qui concerne les calculs directs des paramètres, un modèle simple où l'espace des phases est réduit à un point unique est mis en œuvre. Avec ce modèle ponctuel, les moments ont des expressions analytiques et peuvent être calculés de manière efficace et rapide. Cette thèse est structurée comme suit.

Dans un premier temps, nous rappelons l'état de l'art des bases de probabilités, du modèle ponctuel du neutron et ses équations, de la quantification d'incertitudes et des problèmes inverses.

Puis, dans une seconde partie, nous établirons les expressions des observations que l'on obtient à partir des instants de détections : les moments empiriques de la distribution du nombre de neutrons détectés. Après, dans une troisième partie, nous étudierons le problème inverse associé, i.e. connaissant les observations quels sont les paramètres et leurs incertitudes. Cela sera fait par l'utilisation de méthodes MCMC telles que l'algorithme de Metropolis-Hastings avec adaptation de matrices de covariance.

Finalement, nous pourrions conclure quant aux apports amenés par la thèse et ce qui peut être poursuivi après ce travail.

The scientist has a lot of experience with ignorance and doubt and uncertainty, and this experience is of very great importance, I think. When a scientist doesn't know the answer to a problem, he is ignorant. When he has a hunch as to what the result is, he is uncertain. And when he is pretty damn sure of what the result is going to be, he is still in some doubt. Scientific knowledge is a body of statements of varying degrees of certainty – some most unsure, some nearly sure, but none absolutely certain.

Richard Feynman "The Value of Science," address to the National Academy of Sciences (Autumn 1955)

1.0.3 Context

The context of the thesis is mainly the passive detection of correlated neutrons for nuclear safety and safeguards.

Nuclear safety is the means to prevent nuclear accidents and protect the environment, the public and the workers from excessive radiation risks. Safeguards are a way of verifying that each country complies with the international agreement on nuclear materials concerning the production of nuclear explosives. Passive detection methods allow to know the state of a neutron system without additional handling [Ens+98]. This happens in particular during the control of a nuclear installation or when ensuring its safety. Due to random interactions (especially when colliding), the action of detecting neutrons will be considered as a random process. Here, we are specifically concerned with neutron time correlation measurements. Other area of concern are material accounting, reactor physics, reactivity measurements, interpretation of subcritical benchmarks, monitoring the reactivity of subcritical reactors (Accelerator Driven Systems - ADS) [PP08]. Material accountancies refers to the evaluation and recording of the quantity and type of nuclear material present in an installation. The subcritical benchmark helps the safety specialist to verify the nuclear data. In reactor physics, there are two types of neutron flux fluctuations : zero power and power noise. Power noise results from macroscopic fluctuations such as mechanical vibrations of the control bars. In zero power noise reactors, the source of randomness is due to microscopic phenomena, e.g. nuclear reactions, fission. The determination of the subcritical reactivity of a nuclear assembly can be established by using two standard methods, Feynman-alpha and Rossi-alpha. These methods are based on statistical analysis of the time detection list, which makes it possible to determine the neutron parameters of the measured fissile system.

1.0.4 Motivations

The aim of this work is the estimation of nuclear parameters from neutron correlation measurements. It is an inverse problem with noisy observations, this is not an exception to Feynman's quote. The physics of the neutron provides some clues about the behaviour of the observations, then we will be uncertain as the Feynman's remark suggests. As this viewpoint indicates, it is necessary to quantify the level of certainty: uncertainty quantification appears as a good choice.

The experimental data is the list of the number of neutrons detected during time intervals of the same duration. A statistical analysis based on the moments of the number of detections is performed for parameter inference. Fission neutrons are produced by bunches (between 2 and 3 on average). Neutrons from the same fission are correlated in time. The emission of source neutrons is a compound Poisson process. In the detections, there will be an excess of variance compared to a Poisson process. This fact is exploited in the Feynman method. In general, due to the correlations, the moments of higher order than the mean contain information about the system. Since we are not only looking for point estimates but also the probability distribution of the parameters, we will consider Bayesian inference and Markov chain Monte Carlo sampling (MCMC) of the a posteriori distribution. With regard to the direct calculation of the parameters, a simple model where the phase space is reduced

to a single point is implemented. With this point model, moments have analytical expressions and can be calculated efficiently and quickly. The thesis is structured as follows.

First, we recall the state of the art on the basic probability, neutron point model and neutron equations, uncertainty quantification and inverse problem.

Then, in a second part, we will establish the expressions of the observations that we obtain from the detection times: the empirical moments of the distribution of the number of detected neutrons. Then in a third part we will study the associated inverse problem i.e. knowing the observations, what are the parameters and their uncertainties. This will be done using MCMC methods with the Metropolis algorithm and covariance matrix adaptation.

Finally, we will conclude on the improvements made by the thesis and what could be continued after this work.

This chapter presents the tools needed to define the direct problem of neutron counting, and also consider the neutrons present in the system. Then, in the next chapter, we will study the direct problem of neutron counting i.e. knowing the inputs of the model considered, what are the observations. Then, in the last chapter we will consider the corresponding inverse problem, i.e. knowing the observations of our model what the inputs are. This chapter also provides the tools to study the inverse problem.

First, we recall some elementary probabilistic tools such as generating functions, Markov chains on integer states, continuous time Markov chains and their ergodicities. Then, we recall the basics of neutron physics and state the neutron equations to obtain the expression of the simple moments of the joint process of the number of neutrons present in the system at time t and the neutrons detected during $[0, t]$. Thus, the tools needed to correctly define the direct problem are presented. Then, we will present the tools for obtaining an answer to an ill-posed inverse problem in the Hadamard sense. In a first part, we will present methods for solving the mean-squares problem, such as the Tikhonov regularisation. In a second part, we will present Bayesian methods for sampling the a posteriori distribution of inputs knowing the observations. The sampling methods are Markov Chain Monte Carlo (MCMC) methods.

1.1 Discrete probabilistic tools

First, we present the basic discrete-time tools needed for the direct neutron counting problem.

In our context, the neutron point model, we will consider probability distributions with finite moments.

1.1.1 Basic probability distributions

From a probabilistic point of view, the branching process of fission can be modeled by elementary distributions [PS12; Hag10]. Here are some examples.

We now define the Bernoulli distribution, the binomial distribution and other elementary discrete distributions.

Definition 1.1.1. *Bernoulli distribution*

A random variable X has a Bernoulli distribution of probability $\varepsilon \in [0, 1]$ when

$$\begin{cases} \mathbb{P}(X = 1) = \varepsilon \\ \mathbb{P}(X = 0) = 1 - \varepsilon \end{cases} \quad (1.1)$$

$\mathbb{P}(X = 1)$ refers to the probability of success of the probabilistic experiment, and $\mathbb{P}(X = 0)$ of failure.

Example 1.1.2. Here ε could be the probability that a captured neutron is detected (i.e. the detector efficiency); or the probability that a neutron left alone in the system induces a fission, in the absence of a source (cf. 1.136).

In [Hag10], we use the Binomial distribution in order to compute the probability for detecting n neutrons in the interval $[0, t]$

Definition 1.1.3. *Binomial distribution*

A random variable X has a binomial distribution of parameters n, ε when its distribution is given by

$$\mathbb{P}(X = k) = \binom{n}{k} \varepsilon^k (1 - \varepsilon)^{n-k}, \quad 0 \leq k \leq n. \quad (1.2)$$

It can be seen as a Bernoulli experiment of parameter ε repeated n times. $\mathbb{P}(X = k)$ is the probability of k successes during n independent Bernoulli experiments.

Then we define the Poisson distribution

Definition 1.1.4. *Poisson distribution*

The distribution of a Poisson law of parameter $\lambda, \mathcal{P}(\lambda)$, is given by

$$\mathbb{P}(X = k) := \frac{\lambda^k}{k!} e^{-\lambda}, \quad \forall k \in \mathbb{N} \quad (1.3)$$

Remark 1.1.5. The Binomial distribution can be approximated by a Poisson distribution of parameter $\lambda = \varepsilon n$ using the Stirling formula when $\varepsilon \rightarrow 0, n \rightarrow +\infty$ and $\varepsilon n = O(1)$.

Finally, we introduce a continuous random variable.

Definition 1.1.6. *Exponential distribution*

A random variable X is said to have an exponential probability distribution of parameter $\Lambda > 0$ when its probability density function is

$$f(x) = \Lambda e^{-\Lambda x} \mathbf{1}_{x \geq 0}, \quad \forall x \in \mathbb{R} \quad (1.4)$$

The basics of probability for stochastic neutronics can be found in [PE08], more details on probability can be found in [Bre69; Fel71; GMT19]. Simple definitions can be found in [Bas19].

1.1.2 Generating functions

In this study, we will consider probability distributions on the integers that is why we choose to use generating functions. The generating function of probability distributions will enable better computation of the characteristics of the current processes.

In this context the usual random variables will be integer valued; the generating function is a tool dedicated to the study of this kind of random variables.

Definition 1.1.7. *Generating function*

Let X be a random variable with nonnegative integer values, with probability distribution $\mathbb{P}(X = k)_{k \in \mathbb{N}}$, the associated generating function is

$$G_{\mathbb{P}_X}(z) := \sum_{k=0}^{+\infty} z^k \mathbb{P}(X = k), \forall z \in [0, 1] \quad (1.5)$$

and so, for all $z \in [0, 1]$, $G_{\mathbb{P}_X}(z) = \mathbb{E}[z^X]$.

We can also consider the link between generating function and the probability distribution.

Proposition 1.1.8. *Probability and generating function*

Let X be a random variable with nonnegative integer values, with probability distribution $\mathbb{P}(X = k)_{k \in \mathbb{N}}$ and generating function $G_{\mathbb{P}_X}(z)$. The probability distribution can be expressed in function of the generating function through

$$\mathbb{P}(X = k) = \frac{1}{k!} \left[\frac{\partial^k G_{\mathbb{P}_X}}{\partial z^k} \right]_{z=0}, \forall k \in \mathbb{N} \quad (1.6)$$

Then we can define the moments of a random variable, more precisely those that will be used in this work.

Definition 1.1.9. *Moments of a distribution*

Let X be a random variable on \mathbb{N} with probability distribution $\mathbb{P}(X = k)_{k \in \mathbb{N}}$. The simple moments of X of order l is

$$\mathbb{E}[X^l] := \sum_{k=0}^{+\infty} k^l \mathbb{P}(X = k), \forall l \in \mathbb{N}^*. \quad (1.7)$$

The l -th factorial moments of X is

$$\mathbb{M}_l := \mathbb{E}[X(X-1) \cdots (X-l+1)], \forall l \in \mathbb{N}^*. \quad (1.8)$$

Let $G_{\mathbb{P}_X}$ be the generating function associated to the probability distribution of X . Then, we can define

$$K_{\mathbb{P}_X} := \log G_{\mathbb{P}_X} \quad (1.9)$$

Then we can also define the binomial cumulants of X of order l

$$\Gamma_{\mathbb{P}_X, l} := \frac{1}{l!} \left[\frac{\partial^l}{\partial z^l} K_{\mathbb{P}_X} \right]_{z=1}, \forall l \in \mathbb{N}^* \quad (1.10)$$

These three versions of moments are equivalent and can be deduced one from another.

Proposition 1.1.10. *For a random variable X on \mathbb{N} with probability distribution $\mathbb{P}(X = k)_{k \in \mathbb{N}}$, and $G_{\mathbb{P}_X}$ associated generating function.*

X is integrable if and only if $G_{\mathbb{P}_X}$ is differentiable in $z = 1$ at left. Then we can compute the mean of X

$$\mathbb{E}[X] = \left[\frac{\partial}{\partial z} G_{\mathbb{P}_X} \right]_{z=1}. \quad (1.11)$$

More generally, for $l \in \mathbb{N}^$, the random variable $X(X-1)\cdots(X-l+1)$ is integrable (i.e. X admits a factorial moment of order l), if and only if $G_{\mathbb{P}_X}$ is l differentiable in $z = 1$ at left, and we then have*

$$\mathbb{E}[X(X-1)\cdots(X-l+1)] = \left[\frac{\partial^l}{\partial z^l} G_{\mathbb{P}_X} \right]_{z=1}. \quad (1.12)$$

In particular, for the simple moments

$$\mathbb{E}[X^2] = \left[\frac{\partial^2}{\partial z^2} G_{\mathbb{P}_X} + \frac{\partial}{\partial z} G_{\mathbb{P}_X} \right]_{z=1}, \quad (1.13)$$

$$\text{Var}[X] = \left[\frac{\partial^2}{\partial z^2} G_{\mathbb{P}_X} \right]_{z=1} + \left[\frac{\partial}{\partial z} G_{\mathbb{P}_X} \right]_{z=1} - \left[\frac{\partial}{\partial z} G_{\mathbb{P}_X} \right]_{z=1}^2 \quad (1.14)$$

and

$$\mathbb{E}[X^3] = \left[\frac{\partial^3}{\partial z^3} G_{\mathbb{P}_X} \right]_{z=1} + 3 \left[\frac{\partial^2}{\partial z^2} G_{\mathbb{P}_X} + \frac{\partial}{\partial z} G_{\mathbb{P}_X} \right]_{z=1} - 2 \left[\frac{\partial}{\partial z} G_{\mathbb{P}_X} \right]_{z=1}^2 \quad (1.15)$$

The proof of this proposition is in the annexes.

The following provides a characterisation of the generating function.

Proposition 1.1.11. *The generating function characterizes the law*

Let X and Y be two random variables with probability distribution \mathbb{P}_X and \mathbb{P}_Y . Then

$$G_{\mathbb{P}_X} = G_{\mathbb{P}_Y} \quad (1.16)$$

if and only if X and Y have the same distribution.

Proof. Two power series are equal if and only if their have the same coefficients. \square

We will consider several distributions and their generating functions.

Proposition 1.1.12. *For two independent random variables X and Y on \mathbb{N} with probability distribution $\mathbb{P}(X = k)_{k \in \mathbb{N}}$ and $\mathbb{P}(Y = l)_{l \in \mathbb{N}}$, and $G_{\mathbb{P}_X}$ and $G_{\mathbb{P}_Y}$ associated generating functions. Then*

$$G_{\mathbb{P}_{X+Y}} = G_{\mathbb{P}_X} G_{\mathbb{P}_Y} \quad (1.17)$$

Proof. Using the Cauchy product is the key of the computations. \square

Example 1.1.13. When $X \sim \mathcal{P}(\lambda)$ and $Y \sim \mathcal{P}(\mu)$, then

$$\begin{aligned} G_{\mathbb{P}_{X+Y}} &= \mathbb{E}[z^{X+Y}] \\ &= \mathbb{E}[z^X]\mathbb{E}[z^Y] \text{ by independence} \\ &= e^{\lambda(z-1)}e^{\mu(z-1)} \\ &= e^{(\lambda+\mu)(z-1)} \end{aligned} \tag{1.18}$$

That is the generating function of $\mathcal{P}(\lambda + \mu)$, then by uniqueness of the generating function and the property 1.1.8 $X + Y \sim \mathcal{P}(\lambda + \mu)$.

The proposition 1.1.12 will be useful for the analysis of the generating function of $N_{[0,t]}$ the distribution of the number of neutrons detected during a time gate t . In this context, we will start from the distribution of the number of neutrons present in the system (in the absence of a source, in presence of a source and during the transitional phase; or in presence of a source when the stationary regime is established).

1.2 Discrete-time stochastic processes

Now we introduce some discrete time stochastic processes such as the branching process and then the discrete Markov chains for the description of the neutronic system.

In order to have a more specific approach of the system we consider, we need to have a clear definition of the Markov processes. On the one hand with discrete time Markov chains, then on the other hand with continuous time Markov chains.

We define the symmetric random walk (cf. [M 03])

Definition 1.2.1. *Symmetric random walk on \mathbb{Z}^d*

The sequence of random variables $(X_n)_{n \in \mathbb{N}^}$ is called a random walk on \mathbb{Z}^d when*

$$X_k = X_0 + \sum_{j=1}^k Z_j \tag{1.19}$$

where $Z_j \in \mathbb{Z}^d$ refers to the successive moves that are independent and identically distributed. If the walk is only possible to its neighbors, the walk is said simple. Moreover, if the movement to each of its nearest neighbors occurs with probability $\frac{1}{2d}$ the random walk is said symmetric.

This example will be taken as a counter example when talking about the ergodicity of discrete-time Markov chains.

1.3 Discrete-time Markov chains

In a first time, we define the Markov chains on integer states, give some properties and define time-continuous Markov chains that will be the basis of our neutronic

model. Here all the set of states will be named FCS and for the whole chapter $FCS = \mathbb{N}$ which is the context of our application. The notation FCS could refer to a more general view with a finite or countable set, and all the following results related to Markov chains will be true, the interested reader can consult [Bre69].

Definition 1.3.1. *The sequence of random variables X_0, X_1, \dots will be named Markov chain if for all state sequence $\{x_0, x_1, \dots, x_{k+1}\} \in FCS$,*

$$\mathbb{P}(X_{k+1} = x_{k+1} | X_k = x_k, \dots, X_0 = x_0) = \mathbb{P}(X_{k+1} = x_{k+1} | X_k = x_k) \quad (1.20)$$

that we will call the Markov property. We define the conditional probability

$$p_k(x'|x) := \mathbb{P}(X_{k+1} = x' | X_k = x) \quad (1.21)$$

the probability of jumping from state x to state x' at step $k + 1$.

A noteworthy property of the Markov chains is the following:

Property 1.3.2. *Let X_0, X_1, \dots be a Markov chain and let $\{x_0, x_1, \dots, x_{k+1}, x_{k+2}\} \in FCS$ be a state sequence then*

$$\mathbb{P}(X_{k+2} = x_{k+2}, X_{k+1} = x_{k+1} | X_k = x_k, \dots, X_0 = x_0) = \mathbb{P}(X_{k+2} = x_{k+2}, X_{k+1} = x_{k+1} | X_k = x_k) \quad (1.22)$$

Proof. We use the Bayes formula

$$\mathbb{P}(A \cap B | C) = \mathbb{P}(A | B \cap C) \mathbb{P}(B | C), \quad (1.23)$$

with the Markov property.

Thus we have

$$\begin{aligned} & \mathbb{P}(X_{k+2} = x_{k+2}, X_{k+1} = x_{k+1} | X_k = x_k, \dots, X_0 = x_0) \\ &= \mathbb{P}(X_{k+2} = x_{k+2} | X_{k+1} = x_{k+1}, X_k = x_k, \dots, X_0 = x_0) \mathbb{P}(X_{k+1} = x_{k+1} | X_k = x_k, \dots, X_0 = x_0) \\ &= \mathbb{P}(X_{k+2} = x_{k+2} | X_{k+1} = x_{k+1}, X_k = x_k) \mathbb{P}(X_{k+1} = x_{k+1} | X_k = x_k) \\ &= \mathbb{P}(X_{k+2} = x_{k+2}, X_{k+1} = x_{k+1} | X_k = x_k) \end{aligned} \quad (1.24)$$

□

Definition 1.3.3. *Homogeneous chain*

A Markov chain is homogeneous when $\forall k \in \mathbb{N}, \forall (x', x) \in FCS$,

$$p_k(x'|x) = p(x'|x) \quad (1.25)$$

Moreover, the initial distribution is the quantity

$$p_0(x) := \mathbb{P}(X_0 = x) \quad (1.26)$$

If a Markov chain is homogeneous, then the distributions of its transitions can be represented by its transition matrix $(\mathbf{P}_{x',x})_{x',x \in FCS^2}$. The transition matrix describes the probability of transition from x to x'

$$\mathbf{P}_{x',x} = p(x'|x), \quad (1.27)$$

and satisfies to

$$\forall (x', x) \in FCS^2, \mathbf{P}_{x',x} \geq 0, \text{ and } \forall x \in FCS, \sum_{x' \in FCS} \mathbf{P}_{x',x} = 1 \quad (1.28)$$

Then we can introduce the example of the branching process (see [Mé03])

Definition 1.3.4. *Branching process*

Let X_n the random variable representing the population size at time n , then X_0 is the number of individuals at the beginning. Let $Y_{n,i}$ the random variable representing the number of direct successors of individual $i \leq X_n$ at time n . The dynamics of the population size is

$$X_{n+1} = \sum_{i=1}^{X_n} Y_{n,i} \tag{1.29}$$

where the sum is null when $X_n = 0$ and the $Y_{n,i}$ which are i.i.d random variables on \mathbb{N} . Then the chain X_n forms a homogeneous Markov chain on \mathbb{N} , with transition matrix $\mathbf{P}_{j,i}$ where

$$\mathbf{P}_{0,0} = 1, \quad \mathbf{P}_{j,i} = \mathbb{P}\left(\sum_{k=1}^i Y_{0,k} = j\right), \forall (i, j) \in \mathbb{N}^* \times \mathbb{N} \tag{1.30}$$

The fission will be modeled as a branching process.

In the following, we consider that the Markov chain is homogeneous. The two elements we have introduced enable us to deduce the evolution of the model.

Proposition 1.3.5. *A model consisting of a Markov chain with stationary transition probabilities is completely defined when the transition probabilities and the initial distribution are given.*

Proof. By using the conditional probability formula by recurrence

$$\begin{aligned} & \mathbb{P}(X_{k+1} = x_{k+1}, X_k = x_k, \dots, X_0 = x_0) \\ &= \mathbb{P}(X_{k+1} = x_{k+1} | X_k = x_k, \dots, X_0 = x_0) \mathbb{P}(X_k = x_k | X_{k-1} = x_{k-1}, \dots, X_0 = x_0) \dots \mathbb{P}(X_0 = x_0) \end{aligned} \tag{1.31}$$

$$\forall \{x_0, x_1, \dots, x_{k+1}\} \in FCS \tag{1.31} \quad \square$$

1.3.1 Some general properties of the Markov motion

We recall here the set of states x will be $FCS = \mathbb{N}$.

Definition 1.3.6. *For a subset A of FCS , we define*

$$p(A|x) := \sum_{y \in A} p(y|x) \tag{1.32}$$

The non-empty set A will be said closed when

$$p(A|x) = 1 \tag{1.33}$$

for all $x \in A$.

Definition 1.3.7. *Irreducible motion or states*

The motion or states will be said irreducible when the set of states does not contain 2 or more disjoint closed sets of states.

Definition 1.3.8. We define the k -th transition probability as,

$$\mathbb{P}(X_k \in A | X_0 = x) := p^{(k)}(A|x) \quad (1.34)$$

which is exactly the probability of going in k steps from x to $A \subset FCS$. Then the k -th transition probability is defined by:

$$p^{(k)}(x'|x) := \mathbb{P}(X_k = x' | X_0 = x) \quad (1.35)$$

These k -th transition probability can be obtained from the first transition probability by an important identity: the Chapman-Kolmogorov equation.

As example, we show how to obtain $p^{(2)}(x'|x), x, x' \in \mathbb{N}$ (the same goes for FCS).

Proof. As the system of events $\{X_1 = y\}, y \in \mathbb{N}$ is complete, we can apply the formula

$$\begin{aligned} \mathbb{P}(X_2 = x' | X_0 = x) &= \sum_y \mathbb{P}(X_2 = x', X_1 = y | X_0 = x) \\ &= \sum_y \mathbb{P}(X_2 = x' | X_1 = y) \mathbb{P}(X_1 = y | X_0 = x) \end{aligned} \quad (1.36)$$

This enables us to deduce

$$p^{(2)}(x'|x) = \sum_y p(x'|y)p(y|x) \quad (1.37)$$

In the same manner, we can deduce by recurrence:

$$p^{(k+l)}(x'|x) = \sum_y p^{(k)}(x'|y)p^{(l)}(y|x) \quad (1.38)$$

which is a particular case of the Chapman-Kolmogorov equation for the discrete states. \square

We will call in the following

Definition 1.3.9. The transition from state $x \in FCS$ to state $x' \in FCS$, labeled $x \rightarrow x'$ exists when $\exists k \in \mathbb{N}^*$ such as

$$p^{(k)}(x'|x) > 0 \quad (1.39)$$

Then we will say the transition $x \rightarrow x'$ is possible. If each transition from x to x' and x' to x is possible then we will claim the state x and x' communicate and we will note $x \leftrightarrow x'$.

Property 1.3.10. If for each state couple $x \in FCS$ and $x' \in FCS$, at least one of the transitions x to x' or x' to x is possible, then the motion is irreducible.

Proof. Suppose we have two closed disjoint state sets $A_1 \subset FCS$ and $A_2 \subset FCS$. Then starting from any state x in A_1 , we stay in A_1 (the same goes for x' in A_2) because A_1 is closed. This means $x \rightarrow x'$ and $x' \rightarrow x$ are not possible, because if we start in x we will stay in A_1 and we can not go to x' . This concludes the proof. \square

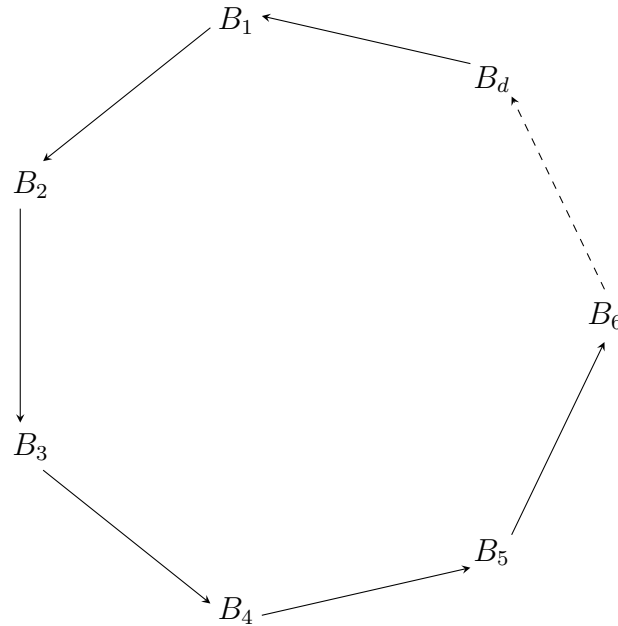


Figure 1.1: Periodic motion of a Markov chain on B_1, \dots, B_d

1.3.2 Stability of a Markov system

Let us start from the integer state $x \in FCS$ at time zero and observe the motion of the resulting system. We wonder if that process will converge to a stationary limiting process in the following sense. More precisely, the question we are asking is the stability one: Will the system, independently of its initial state, converge to a limit distribution?

In a more precise way, we wonder: Does it exist a limiting probability $\bar{p}(A)$ such that

$$p^{(k)}(A|x) \rightarrow \bar{p}(A) \tag{1.40}$$

when $k \rightarrow \infty$ for all starting states $x \in FCS$?

When the answer is yes, we will call the system stable.

We remark the stability aspect is a property depending only on the transition probability and not on the initial condition because the definition is accurate for all the starting states $x \in FCS$. In order to analyse the stability, we will focus on the transition probability.

Definition 1.3.11. *Periodic motion*

Let $d \in \mathbb{N}$ be the largest integer such that $A \subset FCS$ can be decomposed into d disjoint parts, B_1, \dots, B_d each of which is closed under the d -step transition probability. Let $d' \in \llbracket 1, d \rrbracket$. Consider $x \in B_{d'}$ such that there exists an integer k where $p^{(k)}(x|x) > 0$; then we define k as a period of x . We consider $d_x = \gcd\{k \text{ period on } x\}$. The chain is periodic on the integers D which are multiples of d_x . Moreover, when $x \leftrightarrow y$, $d_x = d_y$. Consider the system cycles among the B_1, \dots, B_d . If the starting state is in B_1 , then the next state will always be in the same one of the other sets, say B_2 , then from B_2 in one step it can only go to B_3 , and so on. Finally, from B_d it has to go back to B_1 . Thus, we have the motion we see in the figure 1.1.

We can see there is no chance to get stability when the motion is reducible or periodic.

When the motion is reducible, let A_1, A_2 be two disjoint closed sets of states. Then $\forall x \in FCS$,

$$p^{(k)}(A_1|x) = \begin{cases} 0, & x \in A_2 \\ 1, & x \in A_1 \end{cases} \quad (1.41)$$

Now, we suppose the motion to be periodic where $d = 2$ is the period, and claim that the motion is alternate between two sets B_1 and B_2 .

Remark 1.3.12. *A motion is said periodic of period $d = 2$ if FCS is reducible in 2 disjoint closed parts B_1 and B_2 such that*

$$\begin{aligned} p^{(2)}(B_1|x) &= 1, \quad \forall x \in B_1, \\ p^{(2)}(B_2|x) &= 1, \quad \forall x \in B_2 \end{aligned} \quad (1.42)$$

Then, for k even,

$$p^{(k)}(B_1|x) = \begin{cases} 0, & x \in B_2, \\ 1, & x \in B_1, \end{cases} \quad (1.43)$$

and 0 and 1 are reversed for the k odd.

These probabilities can clearly not converge when k tends to $+\infty$.

That is why we will suppose in the following the motion is irreducible and non-periodic.

When the system is stable, then the motion settles and has long term properties. This can be interpreted by the fact that for any set of states A the proportion of time spent in A tends to a limiting value given by $\bar{p}(A)$ for any starting state.

Theorem 1.3.13. *Let $\Pi(A)$ be a probability distribution such that*

$$\Pi(A) = \sum_x p(A|x)\Pi(x) \quad (1.44)$$

for all $A \subset FCS$ where $p(A|x)$ is the transition probability of the chain.

Then if $\Pi(A)$ is used as an initial probability distribution for the chain, i.e.

$$\mathbb{P}(X_0 \in A) = \Pi(A), \quad (1.45)$$

then the sequence of integer states has the same distribution. In other words,

$$\mathbb{P}(X_k \in A) = \Pi(A), \quad (1.46)$$

for all $k \in \mathbb{N}$.

Proof. In order to prove this, we proceed by recurrence. We give here the idea enabling us to get the recurrence relation: we compute the distribution of X_1 using the conditional probability rule,

$$\mathbb{P}(X_1 \in A) = \sum_x \mathbb{P}(X_1 \in A|X_0 = x)\mathbb{P}(X_0 = x) \quad (1.47)$$

the right part of the equation is exactly $\Pi(A) = \sum_x p(A|x)\Pi(x)$.
 In the same manner, we know that

$$\mathbb{P}(X_2 \in A) = \sum_x \mathbb{P}(X_2 \in A|X_1 = x)\mathbb{P}(X_1 = x) \quad (1.48)$$

but as we have already established $\mathbb{P}(X_1 = x) = \Pi(x)$, by the use of the same argument, we can deduce that

$$\mathbb{P}(X_2 \in A) = \Pi(A) \quad (1.49)$$

Thus, by recurrence, we can deduce the announced result. \square

Definition 1.3.14. *Any measure Π satisfying to 1.44 is called an invariant measure. Furthermore, when the measure Π is a probability, it is called a stationary distribution.*

For the proof of the two following results, we will refer to [Bre69]

Theorem 1.3.15. *When the chain is irreducible, there is at most one stationary distribution.*

We can find the following theorem in [Bre69] p. 172.

Theorem 1.3.16. *Let $A \subset FCS$ a set of states. For an irreducible chain, non-periodic with transition probability $p(A|x)$ such as for two states $x \in FCS$ and $y \in FCS$ that communicate, $x \leftrightarrow y$, one of the two alternatives holds:*

- *Either 1.44 has no solution, and for each finite set K and state $y \in FCS$*

$$p^{(k)}(K|y) \rightarrow 0 \quad (1.50)$$

- *1.44 has a solution $\Pi(A)$, and for each starting state y*

$$p^{(k)}(A|y) \rightarrow \Pi(A) \quad (1.51)$$

We precise what it means. How a system can be instable? Only if it tends to $+\infty$, because the first point of the previous theorem states that for all finite sets of points B and initial distribution

$$\mathbb{P}(X_k \in B) \rightarrow 0 \quad (1.52)$$

This implies that the probability of finding a particle outside any finite set of points tends to 1 if the system continues for quite a long time.

1.3.3 Recurrence times

As the states of the Markov chains are assumed to be counted on the integers, there is a beautiful theory highlighting the ins and outs of the asymptotic behaviour of the chain.

The theory is based on the simple observation that if the system begins at a state $x \in FCS$, then at each return of the system to this state the whole system can be considered as starting again at the start independently of what happened previously. We illustrate the usefulness of this idea as follows: Let r_x be the probability that the system, beginning from x , returns to state $x \in FCS$. Of course $0 \leq r_x \leq 1$.

Property 1.3.17. *If $r_x < 1$, then the system returns to the state $x \in FCS$ at maximum a finite number of times a.s.*

The reader is referred to [Bre69] for a proof.

Definition 1.3.18. *If for a state $x \in FCS$,*

- $r_x < 1$, we will say the state is transient;
- $r_x = 1$, we will say the state is recurrent;

Property 1.3.19. *If $r_x = 1$ for a state $x \in FCS$, the system starting from $x \in FCS$ returns to $x \in FCS$, infinitely often a.s.*

The following introduces filtration and stopping time, what can be found in [Bod20].

Definition 1.3.20. *Filtration*

Let $(\Omega, \mathcal{A}, \mathbb{P})$ a probability space. A filtration of \mathcal{A} is an increasing sequence $\mathbb{F} = \{\mathcal{F}_n\}_{n \geq 0}$ of sub- σ -algebras of \mathcal{A} such that,

$$\mathcal{F}_0 \subset \mathcal{F}_1 \subset \dots \subset \mathcal{A}. \quad (1.53)$$

Thus, we claim $(\Omega, \mathcal{A}, \mathbb{F}, \mathbb{P})$ is a filtrated probability space.

In particular, if $(X_n)_{n \geq 0}$ is a random process. Then the sequence

$$\mathcal{F}_n = \sigma(X_i, i \leq n), \quad n \geq 0, \quad (1.54)$$

is called the natural filtration of the process $(X_n)_{n \geq 0}$.

Definition 1.3.21. *Let $\mathbb{F} = \{\mathcal{F}_n\}_{n \geq 0}$ a filtration of \mathcal{A} . The process $\{X_n\}_{n \geq 0}$ is said adapted to the filtration \mathbb{F} if X_n is \mathcal{F}_n -measurable for all $n \geq 0$.*

Definition 1.3.22. *Stopping time*

A stopping time T (for the filtration $\mathbb{F} = \{\mathcal{F}_n\}_{n \geq 0}$) is a random variable with values in $\mathbb{N} \cup \infty$ such that

$$\{T = n\} \in \mathcal{F}_n, \forall n \geq 0 \quad (1.55)$$

Let $\mathcal{F}_n = \sigma(X_i, i \leq n)$ the natural filtration of X . Let $n \in \mathbb{N}$. The variable $\mathbf{1}_{\{T=n\}}$ can be expressed as a function of the $n + 1$ first observations

$$\mathbf{1}_{\{T=n\}} = \phi_n(X_0, \dots, X_n) \quad (1.56)$$

where ϕ_n is a measurable function. We recall an important class of stopping time, corresponding to the first time of reaching the state A

$$T_A = \inf_{n \geq 0} \{X_n \in A\} \quad (1.57)$$

by convention $\inf \emptyset = \infty$.

Definition 1.3.23. For a Markov chain $\{X_k\}_{k \in \mathbb{N}}$, when the distribution of the initial value X_0 is μ_0 , we denote

$$\mathbb{P}_{\mu_0}(X_1 = x_1, \dots, X_k = x_k) := \sum_{x \in FCS} \mu_0(x) \mathbb{P}(X_1 = x_1, \dots, X_k = x_k | X_0 = x) \quad (1.58)$$

We can also define

Definition 1.3.24. Previous σ -algebra to T

Let T a stopping time and $A \in \mathcal{A}$. A is called previous event to T if:

$$\forall n \in \mathbb{N}, A \cap \{T = n\} \in \mathcal{F}_n. \quad (1.59)$$

The set of the previous events to T is a sub- σ -algebra of \mathcal{A} . This is called previous σ -algebra to T and this is denoted \mathcal{F}_T .

Now, we can state the strong Markov property

Theorem 1. Strong Markov property

For a stopping time T of the Markov chain X , and an element B of \mathcal{F}_T

$$\begin{aligned} & \mathbb{P}_{\mu_0}(\{X_{T+1} = x_1, \dots, X_{T+k} = x_k\} \cap B | \{X_T = x\} \cap \{T < +\infty\}) \\ &= \mathbb{P}(X_1 = x_1, \dots, X_k = x_k | X_0 = x) \mathbb{P}_{\mu_0}(B | \{X_T = x\} \cap \{T < +\infty\}) \end{aligned} \quad (1.60)$$

Proof. Let B an event in \mathcal{F}_T . Then for all integer n , the event $B \cap \{T = n\}$ is determined by $\{X_0, \dots, X_n\}$. Then we can establish for all $k \in \mathbb{N}^*$

$$\begin{aligned} & \mathbb{P}_{\mu_0}(\{X_{T+1} = x_1, \dots, X_{T+k} = x_k\} \cap B \cap \{T = n\} \cap \{X_T = x\}) \\ &= \mathbb{P}_{\mu_0}(\{X_{n+1} = x_1, \dots, X_{n+k} = x_k\} \cap B \cap \{T = n\} \cap \{X_n = x\}) \\ &= \mathbb{P}(X_1 = x_1, \dots, X_k = x_k | X_0 = x) \mathbb{P}_{\mu_0}(\{X_{n+1} = x_1, \dots, X_{n+k} = x_k\} \cap B \cap \{T = n\} \cap \{X = x\}) \end{aligned} \quad (1.61)$$

thanks to the conditional probabilities' equation, and the Markov property applied at time n . Then we sum all of these equations on $n \in \mathbb{N}^*$ and we obtain

$$\begin{aligned} & \mathbb{P}_{\mu_0}(\{X_{T+1} = x_1, \dots, X_{T+k} = x_k\} \cap B \cap \{X_T = x\} \cap \{T < +\infty\}) \\ &= \mathbb{P}(X_1 = x_1, \dots, X_k = x_k | X_0 = x) \mathbb{P}_{\mu_0}(B \cap \{X_T = x\} \cap \{T < +\infty\}) \end{aligned} \quad (1.62)$$

In order to conclude this theorem, we rebuild the conditional probabilities by dividing the two members of the equation by $\mathbb{P}_{\mu_0}(\{X_T = x\} \cap \{T < +\infty\})$

$$\begin{aligned} & \mathbb{P}_{\mu_0}(\{X_{T+1} = x_1, \dots, X_{T+k} = x_k\} \cap B | \{X_T = x\} \cap \{T < +\infty\}) \\ &= \mathbb{P}(X_1 = x_1, \dots, X_k = x_k | X_0 = x) \mathbb{P}_{\mu_0}(B | \{X_T = x\} \cap \{T < +\infty\}) \end{aligned} \quad (1.63)$$

□

Definition 1.3.25. *Return time*

Let $x \in FCS$ be a recurrent state. Starting from x , we define $T_1^{(x)}$ the first recurrence time (or return time) as the first time that the system returns to the state x .

In the same way, we define the second time of recurrence; which is $T_2^{(x)}$ the time of the second return.

This enables us to define the sequence of return times $T_1^{(x)}, T_2^{(x)}, T_3^{(x)}, \dots$

We can express

$$T_k^{(x)} := \inf_{j \geq 1} \{X_{T_{k-1}^{(x)}+j} = x\} \text{ and } T_0 = 0 \quad (1.64)$$

Theorem 1.3.26. *The sequence $T_1^{(x)}, T_2^{(x)}, T_3^{(x)}, \dots$ is constituted of i.i.d. random variables.*

Proof. The sketch of proof is based on the following ideas:

- Each time the system returns in $x \in FCS$, it restarts as if it started from the beginning. Thus, the probability distribution of $T_2^{(x)}$, the time needed to get back to x from its first restart, should be as the distribution of $T_1^{(x)}$.
- These times are independent, because as they return to the state x the time to get back does not depend on the time to return the first time.

□

Definition 1.3.27. *We denote $t(x) = \mathbb{E}[T_1^{(x)}]$.*

We will say the state x is

- *positive-recurrent if $t(x) < +\infty$, and*
- *null-recurrent if $t(x) = \infty$.*

By the law of large numbers, we find the mean

$$\frac{T_1^{(x)} + \dots + T_j^{(x)}}{j} \xrightarrow{j \rightarrow +\infty} t(x) \text{ a.s.} \quad (1.65)$$

We can find different applications of this result. Especially to the unbounded symmetrical random walk where all the states are non-recurrent.

Definition 1.3.28. *Certain transition*

A transition of a state $x' \rightarrow x$ is said certain if, starting from a state $x' \in FCS$, there is a probability 1 that the system goes through the state $x \in FCS$.

Theorem 1.3.29. *Let $x \in FCS$ and $x' \in FCS$ two states.*

- *If the transition $x \rightarrow x'$ is possible, and if x is recurrent, then x' is recurrent and each $x \rightarrow x', x' \rightarrow x$ is certain.*
- *And x and x' communicate, then they are either both transient either both positive-recurrent, or either all null-recurrent.*

This theorem is important, its proof (cf [Bre69]) enables us to establish the following scheme:

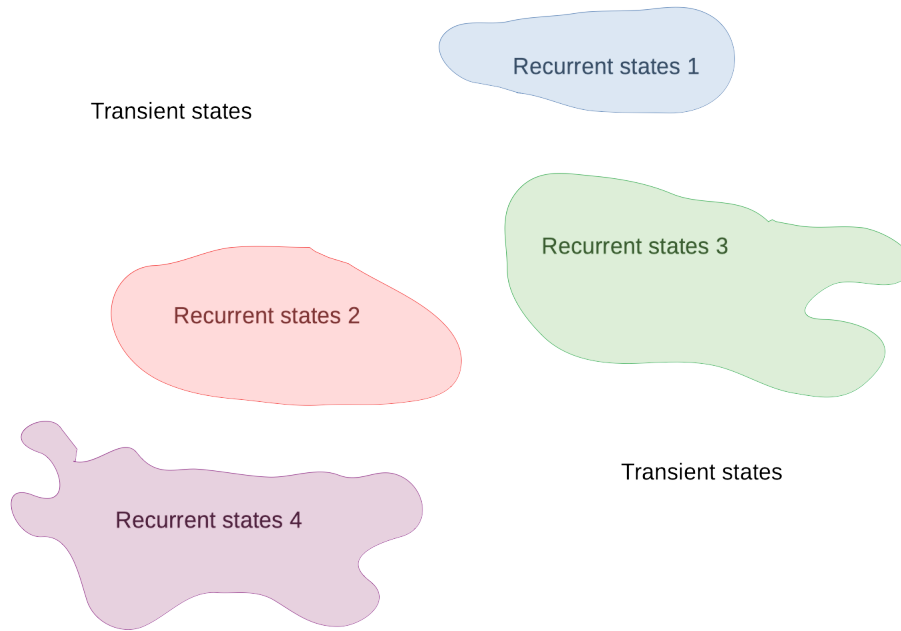


Figure 1.2: Disposition of the recurrent and the transient states with respect to the theorem 1.3.29

We summarize what indicates the scheme [Bre69].

- If the motion is irreducible, then either all the states are transient or there is only one closed irreducible set of recurrent states surrounded by any number of transient states.
If there is only a finite number of transient states, then the system starting from any transient state must eventually enter into the set of recurrent states. But, if there is an infinite number of transient states the system may never enter into the recurrent states.

1.3.4 Ergodicity

We are still in the case of $FCS = \mathbb{N}$.

We recall that a distribution satisfying 1.44 is called an invariant measure and that a stationary distribution is a probability distribution satisfying 1.44.

We introduce now the theorem of existence of an invariant measure

Theorem 2. *Existence and uniqueness of an invariant probability distribution*
For an irreducible Markov chain on FCS the two following sentences are equivalent

- *the chain is positive-recurrent*
- *there exists an invariant probability distribution Π*

Moreover, the invariant probability distribution is unique and given by

$$\Pi(x) = \frac{1}{\mathbb{E}_x[T_1^{(x)}]}, \quad \forall x \in FCS \quad (1.66)$$

Proof. Proof can be found in [Bod20]. \square

Remark 1.3.30. When the Markov chain is irreducible and null-recurrent we can show that there exists an invariant measure, but it can not be normalized. As example, the measure $\Pi(x) = 1$ is an invariant measure for the symmetric random walk on \mathbb{Z} (see 1.2.1). Some irreducible and transient Markov chains can admit no invariant measure.

Theorem 3. Ergodicity for a positive recurrent Markov chain

Let X a positive-recurrent and irreducible Markov chain on FCS. Let Π be its unique invariant probability distribution.

Let f a function of FCS in \mathbb{R} which is integrable with respect to Π , i.e. $\mathbb{E}_\Pi[|f|] = \sum_{x \in FCS} |f(x)|\Pi(x) < \infty$.

We assume the initial data X_0 is distributed by μ on FCS.

The means along the trajectories converge almost surely

$$\frac{1}{l} \sum_{k=0}^{l-1} f(X_k) \xrightarrow{l \rightarrow +\infty} \mathbb{E}_\Pi[f] \quad (1.67)$$

Proof. Proof can be found in [Bod20]. \square

1.4 Continuous-time stochastic process

Secondly, we recall the basic continuous-time tools needed in order to define the observations of the direct problem of the neutron count.

Definition 1.4.1. Counting process

A counting process is an increasing process $(N_t)_{t \geq 0}$, càdlàg (right continuous with left limits) with values in \mathbb{N} such that $N_0 = 0$ and satisfying

- N_t is integer valued ($N_t < +\infty$), a.s.

Example 1.4.2. The fact of counting neutrons using a detector is a counting process.

Definition 1.4.3. Poisson process

Let $(\tau_i)_{i \in \mathbb{N}^*}$ be a set of i.i.d random variables following a law $\mathcal{E}(\lambda)$.

Let $T_0 = 0$, $T_i = \sum_{j=1}^i \tau_j$, $i \geq 1$, the Poisson process associated to the jump times $(T_j)_{j=0}^\infty$ is

$$N_t := \text{card}\{i \geq 1 \text{ s.t. } T_i \leq t\}, \quad \forall t \geq 0. \quad (1.68)$$

Property 1.4.4. Property of the Poisson process

Let $(N_t)_{t \geq 0}$ be a Poisson process.

For all $t_1 < \dots < t_n$, $(N_{t_j} - N_{t_{j-1}})_{j=2}^n$ are independent of law $\mathcal{P}(\lambda(t_j - t_{j-1}))$.

Example 1.4.5. *The jump times of a Poisson process consist of a point process. This process will be important in the neutronic system considered because the source emission is modeled as a Poisson process in some cases, or a compound Poisson process.*

Example 1.4.6. *Poisson process and generating function*

We can consider a Poisson process of intensity λ denoted $(N_t)_{t \geq 0}$, then

$$\mathbb{P}(N_t = k) = \frac{(\lambda t)^k}{k!} e^{-\lambda t} \quad (1.69)$$

Then applying the expression of a Poisson distribution, the generating function associated to this distribution is

$$\boxed{G_{N_t} = G_{\mathcal{P}(\lambda t)} = e^{\lambda t(z-1)}} \quad (1.70)$$

Now we introduce the compound Poisson process, and so the Poisson process that is a particular case of the compound Poisson process.

Definition 1.4.7. *Compound Poisson process*

A compound Poisson process is a random process indexed by time, which can be written

$$Z_t = \sum_{i=1}^{N_t} Y_i$$

where $(N_t)_{t \in [0, +\infty[}$ is a Poisson process and $(Y_i)_{i \in \mathbb{N}}$ is a sequence of random variables independent and identically distributed and independent of N_t .

Example 1.4.8. *It is interesting to notice that when we take $Y_i = 1, \forall i \in \mathbb{N}$, we recover a Poisson process*

$$Z_t = \sum_{i=1}^{N_t} 1 = N_t \quad (1.71)$$

1.5 Continuous-time Markov process

We recall the reader that the exposed results in this part comes from the reading of [Bre69]. We consider here $FCS = \mathbb{N}$, more precisely we will consider time-continuous integer-valued Markov processes.

We define the continuous time Markov process as follows.

Definition 1.5.1. *Given a stochastic process $X = \{X_t\}_{t \geq 0}$, the finite-dimensional distributions of X are the distributions of all the vectors $(X_{t_1}, \dots, X_{t_k})$ for all $0 \leq t_1 < \dots < t_k$ and $k \in \mathbb{N}$.*

Now, we make explicit the definition of a continuous time Markov chain.

Definition 1.5.2. *Considering a device moving from state to state in continuous time, where $FCS = \mathbb{N}$. For $\{X_t\}_{0 \leq t}$, the state at time t , we can model the considered system by a Markov process if for all times $0 \leq t_1 < t_2 < \dots < t_k < t$ and $0 \leq \tau$,*

$$\mathbb{P}(X_{t+\tau} = x' | X_t = x, X_{t_k} = x_k, \dots, X_{t_1} = x_1) = \mathbb{P}(X_{t+\tau} = x' | X_t = x), \forall t, \tau \geq 0, \\ \text{and state } x_1, x_2, \dots, x_k, x, x' \in FCS. \quad (1.72)$$

This statement is the generalization of the Markov property to the continuous time case.

Then a system that satisfies this property is called a continuous time Markov chain.

We can also consider the stationary transition probability,

Definition 1.5.3. *A Markov process will be said having homogeneous probability transition $p_\tau(x'|x)$ when*

$$p_\tau(x'|x) := \mathbb{P}(X_{t+\tau} = x' | X_t = x), \forall t, \tau \geq 0, \text{ and states } x, x' \in FCS. \quad (1.73)$$

Property 1.5.4. *Specifying this transition probabilities $p_t(x'|x)$ for all $t \geq 0, \forall x, x' \in FCS$ and the initial probability completely determines the distribution for a Markov process.*

Now we ask: What condition must a set of functions defined for all $t \geq 0, x, x' \in FCS$ satisfy to be transition probabilities of a Markov process?

There are two evident conditions:

$$p_t(x'|x) \geq 0 \quad (1.74)$$

$$\sum_{x'} p_t(x'|x) = 1 \quad (1.75)$$

The third condition is less evident.

How to pass from a state x to a state x' in a time t ? We use the argument of the intermediate states, so we take into account all the states by which the system can go.

That is why, we consider

$$\mathbb{P}(X_{t+\tau} = x', X_\tau = y | X_0 = x) = \mathbb{P}(X_{t+\tau} = x' | X_\tau = y) \mathbb{P}(X_\tau = y | X_0 = x) \\ = p_t(x'|y) p_\tau(y|x) \quad (1.76)$$

In this case, the transition probabilities must satisfy the continuous time Chapman-Kolmogorov

$$p_{t+\tau}(x'|x) = \sum_y p_t(x'|y) p_\tau(y|x) \quad (1.77)$$

Finally, we want to control the possibility that the system leaves the state x . What can be translated in the following manner:

$$\lim_{\tau \downarrow 0} p_\tau(x|x) = 1, \text{ for all } x \in FCS \quad (1.78)$$

Theorem 1.5.5. *A set of functions $p_t(x'|x)$ is said to be transition probabilities for a Markov process without instant jumps if, and only if, the conditions 1.74, 1.75, 1.77 and 1.78 are satisfied.*

1.5.1 The infinitesimal transition scheme

To be more precise on the Chapman-Kolmogorov equations:

$$p_{t+\tau}(x'|x) = \sum_y p_t(x'|y)p_\tau(y|x) \quad (1.79)$$

It is notable that if we have the knowledge of the transition probabilities $p_t(x'|x)$ for all $x', x \in FCS$ and $t \in [0, \delta]$ then we can obtain the transition probabilities for all times.

Taking $t, \tau \in [0, \delta]$, $t + \tau \in [0, 2\delta]$ and so we obtain the transition probabilities for double size interval.

We repeat the procedure in order to know all the transition probabilities. As knowing the transition probabilities for small times enables us to determine it for all times, we will focus on the infinitesimal transition scheme. We make the assumption that for dt small transition probabilities can be given by

$$p_{dt}(y|x) = q(y|x)dt + o(dt), y \neq x \quad (1.80)$$

Of course, as

$$\sum_y p_{dt}(y|x) = 1, \quad (1.81)$$

then by summing on $y \neq x$,

$$\begin{aligned} p_{dt}(x|x) &= 1 - dt \sum_{y \neq x} q(y|x) + o(dt) \\ &= 1 - dtQ(x) + o(dt) \end{aligned} \quad (1.82)$$

where $Q(x) = \sum_{y \neq x} q(y|x)$. The constants $q(y|x), y \neq x$ governs the infinitesimal transition scheme.

1.5.2 Forward and backward Chapman-Kolmogorov equations

Let $[t_0, t]$ be a fixed time interval and $x', x \in FCS$.

As a particular case of the Chapman-Kolmogorov equations, we dispose of

$$\mathbb{P}(X_{t+dt} = x'|X_{t_0} = x) = \sum_y \mathbb{P}(X_{t+dt} = x'|X_t = y)\mathbb{P}(X_t = y|X_{t_0} = x) \quad (1.83)$$

Using the infinitesimal transitions given by the previous diagram, we have

$$\begin{aligned} \mathbb{P}(X_{t+dt} = x'|X_{t_0} = x) &= \mathbb{P}(X_{t+dt} = x'|X_t = x')\mathbb{P}(X_t = x'|X_{t_0} = x) \\ &+ \sum_{y \neq x'} \mathbb{P}(X_{t+dt} = x'|X_t = y)\mathbb{P}(X_t = y|X_{t_0} = x) \\ &= (1 - Q(x)dt)\mathbb{P}(X_t = x'|X_{t_0} = x) \\ &+ dt \sum_{y \neq x} q(x'|y)\mathbb{P}(X_t = y|X_{t_0} = x) + o(dt) \end{aligned} \quad (1.84)$$

Moving the $\mathbb{P}(X_t = x'|X_{t_0} = x)$ to the left, dividing by dt then letting tend $dt \rightarrow 0$, we obtain the *forward* Chapman-Kolmogorov equation:

$$\frac{d}{dt}\mathbb{P}(X_t = x'|X_{t_0} = x) = -Q(x)\mathbb{P}(X_t = x'|X_{t_0} = x) + \sum_{y \neq x} q(x'|y)\mathbb{P}(X_t = y|X_{t_0} = x) \quad (1.85)$$

For the *backward* equations, we start again from the Chapman-Kolmogorov equations

$$\begin{aligned} \mathbb{P}(X_t = x'|X_{t_0} = x) &= \sum_y \mathbb{P}(X_t = x', X_{t_0+dt_0} = y|X_{t_0} = x) \\ &= \sum_y \mathbb{P}(X_t = x'|X_{t_0+dt_0} = y)\mathbb{P}(X_{t_0+dt_0} = y|X_{t_0} = x) \end{aligned} \quad (1.86)$$

Moreover, the infinitesimal transition scheme are given by

$$\mathbb{P}(X_{t_0+dt_0} = y|X_{t_0} = x) = \begin{cases} q(y|x)dt_0 + o(dt_0), & \text{if } y \neq x \\ 1 - Q(x)dt_0 + o(dt_0), & \text{if } y = x \end{cases} \quad (1.87)$$

Then we understand that

$$\begin{aligned} \mathbb{P}(X_t = x'|X_{t_0} = x) &= \mathbb{P}(X_t = x'|X_{t_0+dt_0} = x) + dt_0 \sum_{y \neq x} q(y|x)\mathbb{P}(X_t = x'|X_{t_0+dt_0} = y) \\ &\quad - dt_0 \sum_{y \neq x} q(y|x)\mathbb{P}(X_t = x'|X_{t_0+dt_0} = x) + o(dt_0) \end{aligned} \quad (1.88)$$

By a limited expansion of $\mathbb{P}(X_t = x'|X_{t_0+dt_0} = y)$ and $\mathbb{P}(X_t = x'|X_{t_0+dt_0} = x)$, we obtain

$$\begin{aligned} \mathbb{P}(X_t = x'|X_{t_0} = x) &= \mathbb{P}(X_t = x'|X_{t_0+dt_0} = x) + dt_0 \sum_{y \neq x} q(y|x)\mathbb{P}(X_t = x'|X_{t_0} = y) \\ &\quad - dt_0 \sum_{y \neq x} q(y|x)\mathbb{P}(X_t = x'|X_{t_0} = x) + o(dt_0) \end{aligned} \quad (1.89)$$

This enables us to deduce

$$\begin{aligned} &\frac{\mathbb{P}(X_t = x'|X_{t_0+dt_0} = x) - \mathbb{P}(X_t = x'|X_{t_0} = x)}{dt_0} \\ &= \sum_{y \neq x} q(y|x)\mathbb{P}(X_t = x'|X_{t_0} = y) - \mathbb{P}(X_t = x'|X_{t_0} = x) \sum_{y \neq x} q(y|x) + o(1) \end{aligned} \quad (1.90)$$

But, we made the assumption the motion is homogeneous in time (cf. [PE08]), we have

$$-\frac{d}{dt_0}\mathbb{P}(X_t = x'|X_{t_0} = x) = \frac{d}{dt}\mathbb{P}(X_t = x'|X_{t_0} = x) \quad (1.91)$$

Finally, we obtain the Chapman-Kolmogorov equations by letting dt_0 go to 0,

$$\frac{d}{dt}\mathbb{P}(X_t = x'|X_{t_0} = x) = \sum_{y \neq x} q(y|x)\mathbb{P}(X_t = x'|X_{t_0} = y) - \mathbb{P}(X_t = x'|X_{t_0} = x) \sum_{y \neq x} q(y|x) \quad (1.92)$$

1.5.3 Continuous time Markov chain behaviour

The following results and evidence are from [Bre69].

First, we give the waiting time definition for a given state in the set of states

Definition 1.5.6. *Waiting time*

Let x be a state in the set of states FCS. Given $X_0 = x$, the waiting time of the continuous time Markov chain $(X_t)_{t \geq 0}$ is

$$T_x = \inf\{t \geq 0, X_t \neq x\} \quad (1.93)$$

For a given x in the set of states, we can obtain the distribution of T_x as follows. The probability that there is no transition during the time interval of duration dt is approximately

$$\mathbb{P}(\text{no transition during } dt|X_0 = x) = 1 - Q(x)dt \quad (1.94)$$

Then the probability that the particle leaves the state x during this time interval is

$$\mathbb{P}(\text{the particle leaves state } x \text{ during } dt|X_0 = x) = Q(x)dt \quad (1.95)$$

Thanks to the Markov property and the stationarity of the transition probabilities, we know that the situation is the same for a particle in a state x at time t as it is for a particle starting from the state x at time zero.

Proposition 1.5.7. *Let x in the set of states, T_x the waiting time in state x has an exponential distribution with parameter $Q(x)$.*

Then we can consider a particle moving on time-continuous Markov chain. The time of motion can be considered of several sub-intervals of length dt , dt' , etc... Then after dt we consider independent trial of transition with probability $Q(x)dt$ and no transition $1 - Q(x)dt$. And so the particle remains at state x until the trial occurs as a transition.

Now we can question ourselves about the possibilities for the particle motion after transition x . The skeleton of the chain is

$$p(y|x) = \begin{cases} 0, & y = x \\ \frac{q(y|x)}{Q(x)}, & y \neq x \end{cases} \quad (1.96)$$

We recall that

$$Q(x) = \sum_{y \neq x} q(y|x), \quad (1.97)$$

thus the quantity $\frac{q(y|x)}{Q(x)}$ is, for the terms of order $o(dt)$, the probability of transition to state y at time dt given that a transition has occurred in this time. Thanks to

$$\sum_{y \neq x} p(y|x) = 1 \quad (1.98)$$

the $p(y|x)$ are one-step transition probabilities of discrete time Markov process. These are called *first – jump probabilities*. Let Y be the position of the particle after its first transition out of its initial state x . We now show the independence of the position Y and the waiting time T_x

Proposition 1.5.8. *Let $x \in FCS$. Y and T_x are independent and*

$$\mathbb{P}(Y = y|X_0 = x) = p(y|x), \quad y \in FCS \quad (1.99)$$

Proof. Consider $y \neq x$. We have

$$\mathbb{P}(X_{t+dt} = y|t + dt > T_x \geq t) = \frac{\mathbb{P}(X_{t+dt} = y, t + dt > T_x \geq t)}{\mathbb{P}(t + dt > T_x \geq t)} \quad (1.100)$$

But $X_{t+dt} = y$ implies $t + dt > T_x$. This simplifies the numerator of the previous expression

$$\mathbb{P}(X_{t+dt} = y, t+dt > T_x \geq t) = \mathbb{P}(X_{t+dt} = y, T_x \geq t) = \mathbb{P}(X_{t+dt} = y|T_x \geq t)\mathbb{P}(T_x \geq t) \quad (1.101)$$

Using the Markov property provides

$$\mathbb{P}(X_{t+dt} = y|T_x \geq t) = \mathbb{P}(X_{t+dt} = y|X_t = x) = q(y|x)dt + o(dt) \quad (1.102)$$

Reinjecting this result into 1.101 and using

$$\mathbb{P}(t + dt > T_x \geq t) = Q(x)e^{-Q(x)t}dt + o(dt) \quad (1.103)$$

provides

$$\mathbb{P}(X_{t+dt} = y|t+dt > T_x \geq t) = \frac{q(y|x)dt e^{-Q(x)t} + o(dt)}{Q(x)e^{-Q(x)t}dt + o(dt)} = \frac{q(y|x) + o(1)}{Q(x) + o(1)} = p(y|x) + o(1) \quad (1.104)$$

Letting $dt \rightarrow 0$, we conclude

$$\mathbb{P}(Y = y|T_x = t) = p(y|x), \forall t \geq 0.$$

This enables us to conclude also that Y and T_x are independent and the distribution of Y is $p(y|x)$. \square

In summary, a continuous-time Markov chain moves from state x to state y with probability $p(y|x)$ and each transition time T_x is distributed with an exponential distribution of parameter $Q(x)$. These two processes are independent of each other.

Proposition 1.5.9. *Let $(Y_j)_{j \geq 0}$ be a Markov chain with the infinitesimal generator $p(y|x)$ (with $p(x|x) = 0 \forall x$). Conditionally to $(Y_j)_{j \geq 0}$, let $T_0 = 0$ and $(T_j)_{j \geq 1}$ be a sequence of independent random variables with exponential distribution with parameter $Q(Y_{j-1})$. Let $X_t = Y_j$ if $\sum_{i=0}^j T_i \leq t < \sum_{i=0}^{j+1} T_i$. Then $(X_t)_{t \geq 0}$ is a continuous time Markov process with the infinitesimal scheme $q(y|x) = Q(x)p(y|x)$.*

1.5.4 Ergodicity

We consider time-continuous integer-valued Markov processes, so we are in the case of $FCS = \mathbb{N}$, the skeleton of the chain is $p(y|x)$ and the waiting time distribution T_x is given by the exponential distribution of parameter $Q(x)$. The notion of invariant distribution for the continuous time Markov process can be defined as follows.

Definition 1.5.10. *Invariant measure for a continuous time Markov process*
A probability distribution Π_{CT} such that

$$\sum_{y \neq x} q(x|y) \Pi_{CT}(y) = Q(x) \Pi_{CT}(x) \quad (1.105)$$

for all $x \in FCS$ is called an invariant distribution.

Indeed, if Π_{CT} satisfies (1.105), then

$$\sum_{y \in FCS} \mathbb{P}(X_{dt} = x | X_0 = y) \Pi_{CT}(y) = [1 - Q(x)dt] \Pi_{CT}(x) + \sum_{y \neq x} q(x|y) dt \Pi_{CT}(y) = \Pi_{CT}(x)$$

We make the assumption that the skeleton $p(y|x)$ is irreducible and positive recurrent, and that $Q(x)$ is bounded from above by a positive constant. Let $\Pi_S(x)$ be the invariant distribution for the transition probabilities $p(x|y)$ [it satisfies $\Pi_S(x) = \sum_{y \in FCS} p(x|y) \Pi_S(y)$]. Then

$$\Pi_{CT}(x) = \frac{\Pi_S(x) Q(x)^{-1}}{\sum_{y \in FCS} \Pi_S(y) Q(y)^{-1}} \quad (1.106)$$

is clearly an invariant distribution for the time-continuous process.

As in the discrete case, we can define the first recurrence time $T_1^{(x)}$.

Definition 1.5.11. *Return time*

Starting from x , we define $T_x^{(1)}$ the first recurrence time (or return time) as the first time that the system returns to the state x :

$$T_x^{(1)} := \inf\{t > T_x, X_t = x\} \quad (1.107)$$

The stationary distribution of a continuous time Markov process is related to the mean waiting time and mean return time as follows [Bre92, p. 345]

Theorem 4. $\mathbb{E}_x[T_x^{(1)}] < +\infty$ for all x if and only if the Markov process has a unique invariant distribution, which is then given by

$$\Pi_{CT}(x) = \frac{\mathbb{E}_x[T_x]}{\mathbb{E}_x[T_x^{(1)}]}, \quad \forall x \in FCS \quad (1.108)$$

Then we get the ergodicity of the continuous time Markov chain

Theorem 5. *Ergodicity of a continuous time Markov chain*

$$\lim_{t \rightarrow +\infty} \frac{1}{t} \int_0^t f(X_s) ds = \mathbb{E}_{\Pi_{CT}}[f], \quad a.s. \quad (1.109)$$

We now expose the stochastic neutronics aspects of the problem. We will apply the Markov chain theory to our problem.

1.6 Stochastic neutronics

In this section, we present the neutron phenomena in order to establish our direct problem, in the context of neutron counting.

In most applications, only the average neutron population is taken into account. However, for the study of neutron time correlations, it is necessary to take into account the phenomenon of neutron fluctuations (cf. [PE08]).

Historically, the Feynman moments have been considered [FHS56; FI67]. In our context, we will consider the first three simple moments of the neutron population and the number of detections during a time interval.

In a first part, we will establish the elementary neutron processes. Then, in a second part, we will explain how to obtain the stochastic equations for the number of neutrons present in the system (in the absence of a source or in the presence of a source), and for the joint process of the number of neutrons present in the system in the presence of a source and the number of neutrons detected during $[0, T]$.

1.6.1 Basic of neutron physics

Point model approximation

The point model is a simple model in neutronics, which is useful in this work to quickly calculate the simple moments and obtain the a posteriori distribution of the system parameters knowing the measurements of a nuclear system (thanks to the Bayes theorem).

Definition 1.6.1. *The point model approximation*

The medium is infinite, homogeneous and isotropic. The detector is also infinite and homogeneous. The neutrons are point particles moving at the same speed. In addition, the life of the neutron is considered to end with capture (with or without detection) or fission. Neutrons are produced by fission and by Poisson or compound Poisson sources. This involves a branching process. It is important to consider the correlation over time [HC85]. In neutronics, two detected neutrons are called correlated if they belong to the same fission chain, produced by induced or spontaneous fission.

Remark 1.6.2. *Delayed neutrons are a subject of interest [Bre16]. They are neglected here because we focus on correlated neutrons detected during a time interval much shorter than the average lifetime of delayed neutron precursors.*

As the medium is infinite, there is no neutron leakage. However, leakage can be taken into account as a capture or when a neutron does not induce fission.

Reaction rates

Now, we define the microscopic and macroscopic cross-section to define the reaction rates.

The intuition of neutron microscopic cross-section is

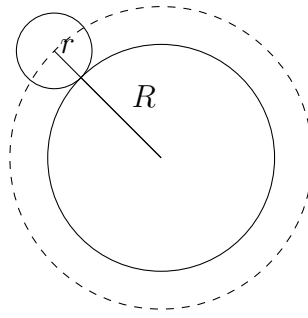


Figure 1.3: Microscopic cross-section intuition [Reu03]

This is the area of the circle with radius $r + R$ where r is the radius of the incident particle and R of the target. This defines the probability of interaction of the neutron with the atomic nucleus under consideration.

Definition 1.6.3. *Cross-section and reaction rates*

Let N be the atomic density of the medium (that can be expressed in nb/cm^3) and σ (that can be expressed in cm^2) the effective microscopic cross-section of the considered reaction. The macroscopic cross-section

$$\Sigma = N\sigma \quad (1.110)$$

is equal to the probability of reaction per unit length traveled by the neutron at the speed v and

$$\lambda = v\Sigma \quad (1.111)$$

is the number of reactions per unit time (s^{-1}), i.e. the reaction rate.

The occurrence of nuclear reactions and source events are Poisson processes. The reaction rate λ is the intensity of the considered Poisson process; it is also the average number of events per time unit.

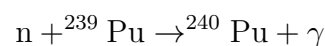
We will specify the rate of capture and fission reactions later.

We can now consider all elementary neutron processes such as fission, capture, source, detection and introduce the concept of criticality.

Capture

In our system, a neutron ends its life by fission or capture. When a neutron is captured, it may involve detection.

Neutron capture is when a neutron is killed in an absorption reaction. An example is the radiative capture of a thermal neutron by a plutonium isotope.



We will see that capture reactions are also used for neutron detection.

The capture reaction is sterile; it has no descendant.

Definition 1.6.4. *The capture rate by unit of time is*

$$\lambda_C := \text{capture rate per unit of time} \quad (1.112)$$

We can then define fission and its parameters.

Fission

Fission occurs when a neutron collides with a fissile isotope such as ^{235}U or ^{239}Pu . This fissile isotope is split into two fragments, with the production of new neutrons. The reaction can be written as



where ${}_Z^{A^*} X$ refers to the element X with A^* the nucleons number Z its proton number; the fission reaction provides two fission products where ${}_{Z1}^{A1} \text{FP1}$ refers to the element $FP1$ with $A1$ nucleons and $Z1$ protons, and ${}_{Z2}^{A2} \text{FP2}$ refers to the element $FP2$ with $A2$ nucleons and $Z2$ protons.

In the case of ^{235}U the energy released by a fission is 207 MeV. For fast neutrons, the most likely emission energy is 0.75 MeV, their average energy is about 2 MeV.

We define the reaction rates as

Definition 1.6.5. *Fission and total reaction rate, neutron decay constant α*
The fission rate per unit time is

$$\lambda_F := \text{fission rate per unit of time} \quad (1.113)$$

The rate of reactions by unit of time is

$$\lambda_T := \lambda_F + \lambda_C \quad (1.114)$$

Definition 1.6.6. *The probability distribution of the number of neutrons produced by a fission is as follows,*

$$f_\nu := \text{Probability that the induced fission emits } \nu \text{ neutrons} \quad (1.115)$$

where ν goes from 0 to the maximum number of neutrons emitted by the fission ν_{max} , and

$$\bar{\nu} := \sum_{\nu=0}^{\nu_{max}} \nu f_\nu \quad (1.116)$$

is the mean number of neutrons emitted by one fission event. When a fission occurs, $\bar{\nu}$ neutrons are emitted on average. Moreover, we can consider the moments of fission process

$$\begin{aligned} \nu_2 &:= \sum_{\nu} \frac{\nu(\nu-1)}{2} f_\nu \\ \nu_3 &:= \sum_{\nu} \frac{\nu(\nu-1)(\nu-2)}{6} f_\nu \end{aligned} \quad (1.117)$$

For the fission distribution, we can use the Terrel distribution [Ter57], a truncated and discretized Gaussian distribution.

Definition 1.6.7. *Diven factor*

The second and third order Diven factors of the fission probability distribution [Div+56], [OYS00] are

$$D_2 := \frac{2\nu_2}{\bar{\nu}^2}, \quad D_3 := \frac{6\nu_3}{\bar{\nu}^3} \quad (1.118)$$

Finally, we can define

Definition 1.6.8. *Neutron decay constant*

The neutron decay constant is

$$\alpha := \lambda_T - \bar{\nu}\lambda_F \quad (1.119)$$

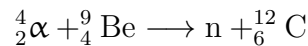
α is the number of neutrons destructed per unit of time minus the number of neutrons created per unit of time.

Source

The considered neutron sources are (α, n) and spontaneous fission.

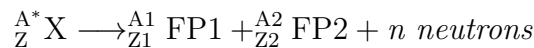
An (α, n) source is a Poisson source, i.e. the times of the source events form a Poisson process, and each source event produces one neutron. An example of (α, n) source is the (Am,Be) Source. It is made by mixing radioisotopes of americium with beryllium. Alpha particles emitted by americium interact with beryllium to produce neutrons.

(α, n) reactions are as follows. An alpha reaction occurs with Am. And then the beryllium stabilises by producing a neutron



These reactions enabled Chadwick to demonstrate the existence of the neutron in 1933.

The other example is spontaneous fission sources: [BFG11] provides the following observations. When we consider the really heavy nuclei, most of them are artificial, it may happen the electrostatic forces between protons can be stronger than the nuclear forces. In this case, the nucleus splits into two parts, called fission fragments, and emits a certain amount of neutrons.



This phenomenon, called spontaneous fission, is another way of building neutron sources. A spontaneous fission source event produces a random number of neutrons, generally ranging from zero to eight neutrons. As an example, ${}^{252}\text{Cf}$ emits an average of 3.73 neutrons per source event. Neutron production by spontaneous fission is a compound Poisson process.

The source processes are Poissonian. The system under consideration can be in the presence of different types of sources: Poisson and compound Poisson sources. Thus, the first emits one neutron per source event, the other several.

Definition 1.6.9. *The source can be composed of two types: a Poisson type source of intensity S_α and a source of compound Poisson type of intensity S_F . Then S can be defined as the total intensity of the sources, taking into account the Poisson and the compound Poisson type sources. More precisely,*

$$\begin{aligned} S_\alpha &:= \text{intensity of the Poisson type source} \\ S_F &:= \text{intensity of the compound Poisson type source} \\ S &:= \text{total intensity of the sources} \end{aligned} \quad (1.120)$$

Therefore, we can conclude

$$S = S_\alpha + S_F \quad (1.121)$$

The time of emission of the sources is distributed by a Poisson process of intensity S . We also have

$$\bar{S} := \text{mean number of neutrons generated by the sources by unit of time} \quad (1.122)$$

The unit of this quantity is in the number of neutrons emitted per unit time ($n.ms^{-1}$). The probability distribution of the number of neutrons emitted by a spontaneous source event is given by

$$f_{\nu,S} := \text{Probability that one spontaneous fission emits } \nu \text{ neutrons} \quad (1.123)$$

where ν goes from 0 to the maximum number of neutrons emitted by the source $\nu_{max,S}$. The mean number of neutrons emitted by a spontaneous source event of the compound Poisson type source is

$$\bar{\nu}_S := \sum_{\nu=0}^{\nu_{max,S}} \nu f_{\nu,S}. \quad (1.124)$$

Then, we have,

$$\bar{S} = S_\alpha + \bar{\nu}_S S_F \quad (1.125)$$

As previously, we can define

$$\begin{aligned} \nu_{2S} &:= \sum_{\nu=0}^{\nu_{max,S}} \frac{\nu(\nu-1)}{2} f_{\nu,S} \\ \nu_{3S} &:= \sum_{\nu=0}^{\nu_{max,S}} \frac{\nu(\nu-1)(\nu-2)}{6} f_{\nu,S} \end{aligned} \quad (1.126)$$

Therefore, the probability of occurrence of a source event during the interval $[t, t+dt]$ is given by Sdt . As before, we obtain the formulas for the second and third order Diven factors of the source: D_{2S} , D_{3S} .

More precisely, a source event occurs with probability Sdt during the time interval dt . Given there is a source event, the probability that one neutron is emitted by the (α, n) source is $\frac{S_\alpha}{S}$; and the probability that the spontaneous fission emits neutrons is $\frac{S_F}{S}$ (which emits a random number of neutrons, with mean $\bar{\nu}_S$).

Example 1.6.10. *An example of spontaneous fission source is ^{252}Cf of intensity $2.34 \cdot 10^{12} n.g^{-1}.s^{-1}$ [al.98]. Other examples are ^{240}Pu of intensity $1.02 \cdot 10^3 n.g^{-1}.s^{-1}$ and ^{238}U $0.0136 n.g^{-1}.s^{-1}$.*

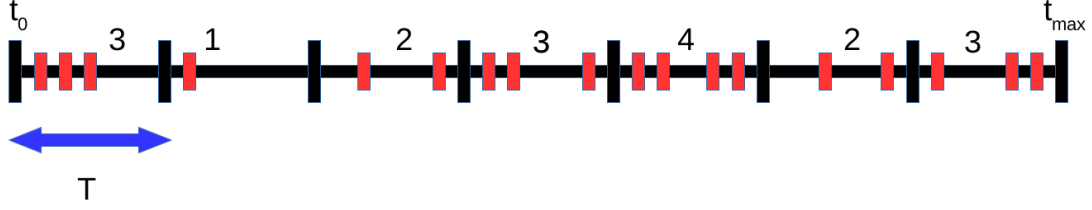


Figure 1.4: Measurements of the number of neutrons detected during a time gate T between t_0 and t_{max} : $N_{1,[0,T]} = 3$, $N_{2,[0,T]} = 1$, $N_{3,[0,T]} = 2, \dots$

The fissile mass is proportional to the intensity of the spontaneous fission source.

In the system, the proportion of spontaneous fission will be qualified by

Definition 1.6.11. *The spontaneous fission proportion is given by*

$$\boxed{x = \frac{\bar{\nu}_S S_F}{S_\alpha + \bar{\nu}_S S_F}} \quad (1.127)$$

Therefore, $x \in [0, 1]$.

Remark 1.6.12. *Note that this parameter only exists when the system is in the presence of the source. It makes sense when there is at least one source of type (α, n) or spontaneous fission.*

Detection

There are different types of neutron detectors. In this work, we consider capture detectors. They are used to count the number of neutrons captured in a sensitive material. In general, the material chosen is helium-3 [TL15]. The proton that emerges from the reaction causes an electric current. These detectors can be used in list mode (e.g. [Hum18]). During a time interval of duration T_{meas} , each detection time is stored as a list in a file (see Fig. 1.4).

By processing this time list file, we can extract the number of counts during time intervals of different durations (time gates T) and calculate the empirical moments of the corresponding distributions. Detection efficiency can be defined as the average number of detections per capture in the system (capture efficiency ε_C).

Definition 1.6.13. *We define the capture efficiency as*

$$\boxed{\varepsilon_C := \text{Probability that a captured neutron is detected}} \quad (1.128)$$

An estimator of this quantity is

$$\hat{\varepsilon}_C := \frac{\text{number of detections during } [0, T]}{\text{number of captures during } [0, T]} \quad (1.129)$$

We define the fission efficiency ε_F as

$$\boxed{\varepsilon_F := \text{number of detections per induced fission in the system}} \quad (1.130)$$

An estimator of this quantity is

$$\hat{\varepsilon}_F := \frac{\text{number of detections during } [0, T]}{\text{number of fissions during } [0, T]} \quad (1.131)$$

Therefore, we can define

Proposition 1.6.14. *The capture and fission efficiencies are linked by:*

$$\lambda_C \varepsilon_C = \lambda_F \varepsilon_F \quad (1.132)$$

where λ_C (resp. λ_F) is the capture rate (resp. fission rate) per unit of time, and ε_F the fission efficiency.

Proof. The result can be deduced from the previous definitions. \square

We will consider the observations during a time gate T :

$$\varepsilon_C(t') = \begin{cases} \varepsilon_C, & \text{if } t' \in [0, T] \\ 0, & \text{else.} \end{cases} \quad (1.133)$$

Remark 1.6.15. *When $\varepsilon_C = 0$ this means that the detector is closed.*

Moreover, $\varepsilon_C(t') = \varepsilon_C H_1(t - t') H_1(T - t')$ where H_1 is the Heaviside step function.

Criticality

To illustrate the qualitative behaviour of the neutron population in a fissile system, we obtain, in the point model approximation, the average neutron number equation. Let $n_t := \mathbb{E}[X_t]$ the average number of neutrons present in the fissile system at time t . The equilibrium equation taking into account the creation and disappearance of neutrons during a time interval $[t, t + dt]$ is

$$\begin{cases} n_{t+dt} = n_t + \bar{S}dt + \bar{\nu}\lambda_F dt n_t - \lambda_T dt n_t, \\ n_{t=0} = n_0 \end{cases} \quad (1.134)$$

Then the average number of neutrons is the solution of the differential equation

$$\frac{d}{dt} n_t + \alpha n_t = \bar{S} \quad (1.135)$$

We can define

Definition 1.6.16. *Multiplication factor*

$$k_{eff} = \frac{\bar{\nu}\lambda_F}{\lambda_T} \quad (1.136)$$

is the mean number of children of a neutron.

The mean lifetime of neutrons is

$$\theta := \frac{1}{\lambda_T} \quad (1.137)$$

Using these notations, the decay constant can also be written as

$$\alpha = \frac{1 - k_{eff}}{\theta} \quad (1.138)$$

Definition 1.6.17. For a neutron population, reactivity can be defined from the multiplication k_{eff}

$$\rho := \frac{k_{eff} - 1}{k_{eff}} \quad (1.139)$$

Remark 1.6.18. In nuclear physics one typically expresses reactivity with per cent mille (p.c.m.) which means the actual value has to be multiplied by 10^{-5} .

The behaviour of the fissile system is characterised by the coefficient k_{eff} , α , or ρ .

For an initial population of a system without external sources, Figure 1.5

$$n_t = n_0 e^{-\alpha t} = n_0 e^{\frac{k_{eff}-1}{\theta} t} \quad (1.140)$$

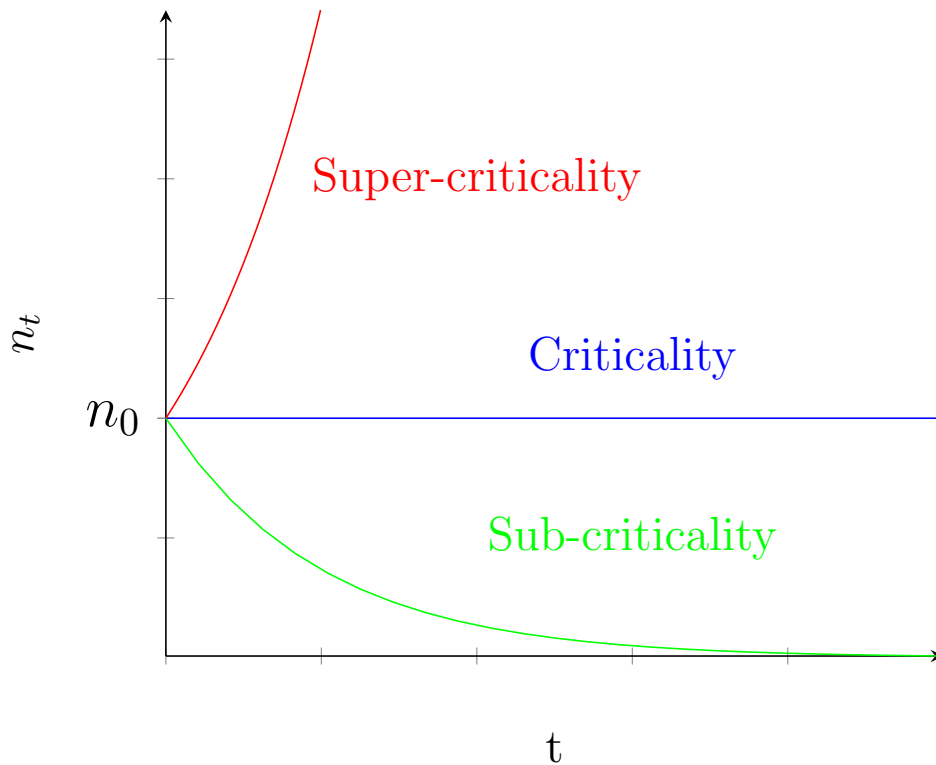


Figure 1.5: Evolution of the average population of neutrons present in the system in the absence of source $n_t = \mathbb{E}[X_t]$ in function of the regime

Then, $k_{eff} < 1$, ($\alpha > 0$, $\rho < 0$) the mean population is decreasing, the system is sub-critical.

$k_{eff} = 1$, ($\alpha = 0$, $\rho = 0$) the mean population is constant, the system is critical (note that the Galton-Watson theory (see [Har02]) ensures that the population almost surely goes to zero except in the trivial case $\lambda_C = \lambda_F = 0$).

$k_{eff} > 1$, ($\alpha < 0$, $\rho > 0$) the mean population is increasing, the system is super-critical.

For an initial population of a system with an external source, Figure 1.6

We note the different regimes.

$$\text{If } \alpha \neq 0, n_t = (n_0 - \frac{\bar{S}}{\alpha})e^{-\alpha t} + \frac{\bar{S}}{\alpha}$$

$$\text{If } \alpha = 0, n_t = n_0 + \bar{S}t$$

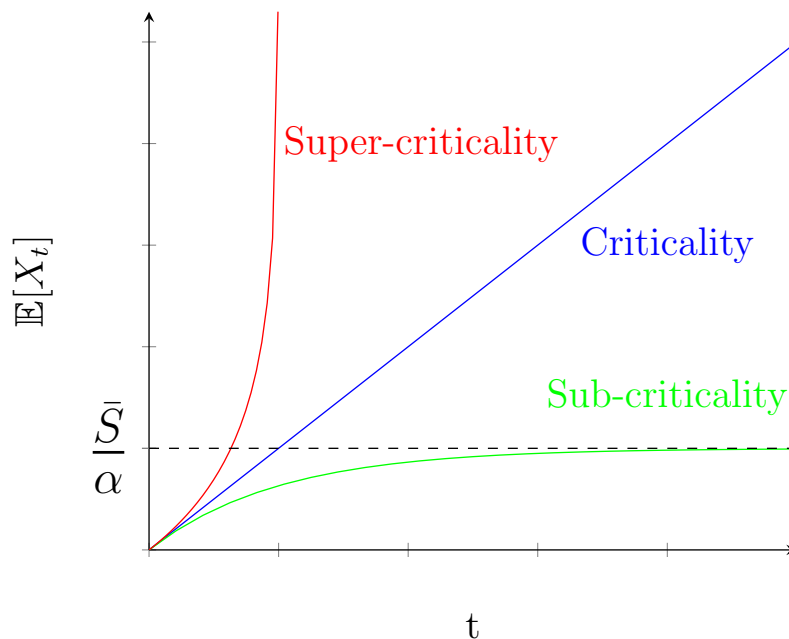


Figure 1.6: Evolution of the mean number of neutrons present in the system when an external source is present $n_t = \mathbb{E}[X_t]$ in function of the regime

The Figure 1.6 shows the evolution of the average population of neutrons present in the system at t in the presence of a source

- in sub-critical regime, the mean population stabilizes to $\frac{\bar{S}}{\alpha}$,
- in critical regime, the mean population grows linearly,
- in super-critical regime, the mean population grows exponentially.

We will consider the joint process of the number of neutrons present in the system at time t and the number of neutrons detected during a time gate of duration t , for a sub-critical system. We will study two phases: the transitory regime and the stationary regime.

The measurements are performed, during the stationary regime. This gives us the number of neutrons detected during a time gate t

$$N_{[0,t]} := \text{the number of neutrons detected during the time interval } [0, t] \quad (1.141)$$

We will use the results of [PE08] 3.2 in order to establish the expression of the generating function of the distribution of the number of neutrons in the presence of a source.

In the context of the point model approximation, we consider the process of the number of neutrons present in the system and the joint process of the number of neutrons present in the system and the number of neutrons detected during a time gate t : $(X_t, N_{[0,t]})$.

The number of neutrons present in the system at time t X_t is a Markov process. We can establish the Chapman-Kolmogorov equation for the number of neutrons present in the system.

The number of neutrons detected in the system during a time gate t $N_{[0,t]}$ is not a Markov process. Indeed, this quantity needs to be associated to the number of neutrons present in the system $(X_t, N_{[0,t]})$ to be Markov.

1.6.2 Stochastic neutronic equations

We want to establish the Chapman-Kolmogorov equations for the number of neutrons present in the system (in the absence of a source or in the presence of a source), or for the joint process of the number of neutrons present in the system and the number of neutrons detected during a time gate t in the presence of a source. The aim of the computations is to obtain the expression of the three first moments of the joint process (number of neutrons present in the system at time t , number of neutrons detected during the time interval $[0, t]$) in the case of sub-critical reactor with a stationary distribution with a source.

To obtain the expressions for the moments of the various quantities of interest, we will consider the transition scheme of the considered Markov process. Then the backward Chapman-Kolmogorov equations (ODE) give the expression for the generating function [Bel65; Pà58; Pà62; Reu03] for the considered cases, and then we deduce the equations of the moments. The use of the forward Chapman-Kolmogorov equations could also be considered, but it provides a PDE which is more difficult to solve, so the use of the backward Chapman-Kolmogorov equations is recommended.

Another approach to the calculations considers the moment of the distribution of the number of neutrons detected between 0 and T knowing the fact there was 0 neutrons at $t \in [-\infty, 0]$. This approach is not developed here, but is close to the experimental process.

The full calculation of the analytical formula can be found in the appendix and is presented in the next chapter.

Remark 1.6.19. *When we consider the forward equation, the associated generating function must take into account the number of neutrons present in the system at t and the number of neutrons detected during $[0, t]$. Then the associated generating function has two spatial variables.*

We define

Definition 1.6.20. *The stochastic process representing the number of neutrons in the system is as follows*

$$X_t := \text{number of neutrons present in the system at } t \quad (1.142)$$

We sum up the dynamic of the system in the absence of an external source by the infinitesimal transition scheme for fission or capture

| <u>Transitions</u> | <u>Probabilities</u> | | |
|--------------------|------------------------|---|-----------------------|
| n | $\nearrow n + \nu - 1$ | $n\lambda_F f_\nu dt$ | fission, $\nu \neq 1$ |
| | $\longrightarrow n$ | $1 - n\lambda_F(\sum_{\nu \neq 1} f_\nu)dt - n\lambda_C dt$ | nothing or fission |
| | $\searrow n - 1$ | $n\lambda_F f_0 dt + n\lambda_C dt$ | fission or capture |

Figure 1.7: Table of infinitesimal transitions for the problem with fission or capture

The infinitesimal transition scheme for a compound Poisson source is

| <u>Transitions</u> | <u>Probabilities</u> | | |
|--------------------|----------------------|-----------------|---|
| n | $\nearrow n + \nu$ | $Sf_{\nu,S} dt$ | source emits ν neutrons, $\nu \neq 0$ |
| | $\searrow n$ | $1 - Sdt$ | nothing |

Figure 1.8: Table of infinitesimal transitions for the problem with a source (Poisson or compound Poisson), remember that we assume $f_{0,S} = 0$

X_t **the number of neutrons present in the system at t is time-continuous Markov process** In this paragraph, we will show X_t is a time-continuous Markov process using the characterisation 1.5.7.

Proposition 1.6.21. *X_t is a time-continuous Markov process. The skeleton of X_t is, for $x \in \mathbb{N}$*

$$q(y|x) = \begin{cases} \frac{x\lambda_F f_{y-x+1} + S f_{y-x,S}}{Q(x)}, & \text{if } y > x \\ \frac{x\lambda_F f_0 + x\lambda_C}{Q(x)}, & \text{if } y = x - 1 \end{cases} \quad (1.143)$$

and, conditionally to $X_0 = x$, T_x the waiting time between two transitions of the skeleton has the distribution

$$T_x \sim \text{Exp}(Q(x)), \text{ where } Q(x) = S + x\lambda_F(\sum_{\nu \neq 1} f_\nu) + x\lambda_C \quad (1.144)$$

Proof. Thanks to the characterisation 1.5.7, we know a time-continuous Markov chain is characterised by its skeleton and the parameter of the exponential distribution of the jump process. The set of states of X_t is defined by the values taken by X_t .

Thanks to the infinitesimal transition schemes for the problem with fission and capture (see Figure 1.7), and the problem with source (see Figure 1.8) the infinitesimal transition scheme of the process X_t is given by

$$p_{dt}(y|x) = \begin{cases} x\lambda_F f_{y-x+1}dt + S f_{y-x,S}dt, & \text{if } y > x \\ 1 - x\lambda_F(\sum_{\nu \neq 1} f_\nu)dt - Sdt - x\lambda_C dt, & \text{if } y = x \\ x\lambda_F f_0 dt + x\lambda_C dt, & \text{if } y = x - 1 \end{cases} \quad (1.145)$$

Then, thanks to the characterisation of the skeleton of a time continuous Markov process (see eq. 1.96), we have

$$q(y|x) = \begin{cases} \frac{x\lambda_F f_{y-x+1} + S f_{y-x,S}}{Q(x)}, & \text{if } y > x \\ \frac{x\lambda_F f_0 + x\lambda_C}{Q(x)}, & \text{if } y = x - 1 \end{cases} \quad (1.146)$$

Conditionally to $X_0 = x$, the waiting time between two transitions of the skeleton is distributed by the exponential law of parameter $Q(x) = S + x\lambda_F(\sum_{\nu \neq 1} f_\nu) + x\lambda_C$

$$T_x \sim \text{Exp}(Q(x)) \quad (1.147)$$

□

And so X_t is a Markov chain time-continuous. We will show the same kind of result for $(X_t, N_{[0,t]})$.

The processes X_t and $(X_t, N_{[0,t]})$ are used in order to prove their continuous-time behavior. For the analytical computations, we will consider X_T and $(X_T, N_{[t,T]})$.

Definition 1.6.22. Let $N_{[0,t]}$ be the number of neutrons detected during the time interval $[0, t]$.

Let $(X_t, N_{[0,t]})$ be the stochastic process representing the number of neutrons present in the system at t and the number of neutrons detected during the interval $[0, t]$.

$(X_t, N_{[0,t]})$, the joint number of neutrons present in the system at t and detected during a time gate t is time-continuous Markov process In this paragraph we will show $(X_t, N_{[0,t]})$ is a time-continuous Markov process using the characterisation 1.5.7.

Proposition 1.6.23. $(X_t, N_{[0,t]})$ is a time-continuous Markov process of skeleton, for $(x, n) \in \mathbb{N}^2$

$$q(y, m|x, n) = \begin{cases} \frac{x\lambda_F f_{y-x+1} + S f_{y-x,S}}{Q(x)}, & \text{if } y > x \text{ and } m = n \\ \frac{x\lambda_C \varepsilon_C}{Q(x)}, & \text{if } y = x - 1 \text{ and } m = n + 1 \\ \frac{x\lambda_C(1-\varepsilon_C)}{Q(x)}, & \text{if } y = x - 1 \text{ and } m = n \\ 0, & \text{else} \end{cases} \quad (1.148)$$

and $T_{(x,n)}$ the waiting time between two transition of the skeleton has the exponential law

$$T_{(x,n)} \sim \text{Exp}(Q(x)), \text{ where } Q(x) = S + x\lambda_F(\sum_{\nu \neq 1} f_\nu) + x\lambda_C \quad (1.149)$$

Proof. Thanks to the characterization 1.5.7, we know that a continuous Markov chain in time is characterized by its skeleton and the parameter of the exponential distribution of the jump process. The infinitesimal transition scheme of $(X_t, N_{[0,t]})$ is deduced from

$$p_{dt}(y, m|x, n) = \begin{cases} x\lambda_F f_{y-x+1} + S f_{y-x,S}, & \text{if } y > x \text{ and } m = n \\ x\lambda_C \varepsilon_C, & \text{if } y = x - 1 \text{ and } m = n + 1 \\ x\lambda_C(1 - \varepsilon_C), & \text{if } y = x - 1 \text{ and } m = n \\ 0, & \text{else} \end{cases} \quad (1.150)$$

Then the skeleton of the process is

$$q(y, m|x, n) = \begin{cases} \frac{x\lambda_F f_{y-x+1} + S f_{y-x,S}}{Q(x)}, & \text{if } y > x \text{ and } m = n \\ \frac{x\lambda_C \varepsilon_C}{Q(x)}, & \text{if } y = x - 1 \text{ and } m = n + 1 \\ \frac{x\lambda_F f_0 + x\lambda_C(1 - \varepsilon_C)}{Q(x)}, & \text{if } y = x - 1 \text{ and } m = n \\ 0, & \text{else} \end{cases} \quad (1.151)$$

The waiting time between two transitions of the skeleton is distributed by the exponential law of parameter $Q(x) = S + x\lambda_F(\sum_{\nu \neq 1} f_\nu) + x\lambda_C$

$$T_{(x,n)} \sim \text{Exp}(Q(x)) \quad (1.152)$$

□

As we consider continuous-time Markov processes, we can settle the Kolmogorov equations that govern the evolution in time of the distributions we will consider, they also characterize these equations. More explicitly, we consider

- $\pi_n(t)$: The distribution of the number of neutrons present in the system at time T given the fact there was 1 neutron at time t in the absence of a source
- $\Pi_n(t)$: The distribution of the number of neutrons present in the system at T given the fact there was 0 neutrons at time t in the presence of a source in the transitional regime
- $\Pi_{n,\infty}$: The distribution of the number of neutrons present in the system at T given the presence of a source at t during the stationary regime
- $p_n(t)$: The distribution of the number of neutrons detected during $[t, T]$ given the fact there was 1 neutron at time t in the absence of a source
- $P_n(t)$: The distribution of the number of neutrons detected during $[t, T]$ given the fact there was 0 neutrons at time t in the presence of a source in the transitional regime
- $Q_n(t)$: The distribution of the number of neutrons detected during $[t, T]$ in the presence of a source in the stationary regime

Number of neutrons present in the system

Population induced by one initial neutron We are now dealing with the distribution of the number of neutrons present in the system at T given the fact there was 1 neutron at time t in the absence of a source $\pi_n(t)$.

By taking a backward point of view (considering scheme 1.7), we take into account the neutrons that provide the output of the system in the absence of an external source. First we focus on the number of neutrons present in the system, then we will focus on the number of neutrons detected in the system.

Definition 1.6.24. *Probabilities of presence in the absence of a source*
The probability of detecting n neutrons at time T knowing the fact there were ν neutrons at time t in the absence of a source is

$$\pi_{n,\nu}(t) := \mathbb{P}(n \text{ neutrons present at } T | \nu \text{ neutrons present in the system at } t) \quad (1.153)$$

We will focus here more on

$$\pi_n(t) = \pi_{n,1}(t) = \mathbb{P}(n \text{ neutrons present at } T | 1 \text{ neutron present in the system at } t) \quad (1.154)$$

Remark 1.6.25. *During sub-critical regime, in the absence of a source, the system turns off. It means the number of neutrons present in the system decreases.*

So during a time dt , we observe what happens to neutrons between $t - dt$ and t

- nothing may happen
- there may be a capture (event with probability $\lambda_C dt$ which decreases the number of neutrons present by 1)
- there may be a fission (event with probability $\lambda_F dt$ which changes the number of neutrons according to the fission distribution)

then we can deduce

$$\begin{aligned} \pi_n(t - dt) &= (1 - \lambda_F \left(\sum_{i \neq 1} f_i \right) dt - \lambda_C dt) \pi_n(t) + (\lambda_F f_0 dt + \lambda_C dt) \pi_{n,0}(t) \\ &\quad + \lambda_F f_2 dt \pi_{n,2}(t) \\ &\quad + \lambda_F f_3 dt \pi_{n,3}(t) \\ &\quad + \dots \\ &\quad + \lambda_F f_m dt \pi_{n,m}(t) + o(dt) \end{aligned} \quad (1.155)$$

It is difficult to obtain the solutions of these equations directly. A simple way to overcome this difficulty is to use the generating function method. We define the generating function associated to $\pi_n(t)$, $n \in \mathbb{N}$.

Definition 1.6.26. We will also obtain the generating function of the number of neutrons present in the system in the absence of source

$$g_\pi(x, t) := \sum_{n=0}^{\infty} \pi_n(t) x^n \quad (1.156)$$

Moreover, we define

$$g_{\pi, \nu}(x, t) := \sum_{n=0}^{\infty} \pi_{n, \nu}(t) x^n \quad (1.157)$$

Now, we can establish the property

Proposition 1.6.27. The generating function $g_{\pi, i}$ can be expressed as

$$g_{\pi, i} = g_\pi^i \quad (1.158)$$

Proof. We show $g_{\pi, i}(t) = g_\pi^i(t)$. By definition,

$$\pi_{j, i}(t) = \sum_{j_1, \dots, j_i \text{ such that } j_1 + \dots + j_i = j} \pi_{j_1}(t) \pi_{j_2}(t) \cdots \pi_{j_i}(t) \quad (1.159)$$

Thus, multiplying by x^n and adding over $n \in \mathbb{N}^*$ gives

$$g_{\pi, i}(t) = g_\pi^i(t) \quad (1.160)$$

□

We multiply by x^n , sum on n , and use the equation for the generating property

$$g_{\pi, i} = g_\pi^i \quad (1.161)$$

Then the generating function equation is

$$\boxed{-\frac{\partial g_\pi}{\partial t}(x, t) = -(\lambda_F \sum_{i \neq 1} f_i + \lambda_C) g_\pi(x, t) + (\lambda_F f_0 + \lambda_C) g_\pi^0(x, t) + \lambda_F \sum_i f_i g_\pi^i(x, t), \quad g_\pi(x, T) = 1} \quad (1.162)$$

Definition 1.6.28. We introduce the mean of the distribution $\pi_n(t)$, the distribution of the number of neutrons present in the system in the absence of a source.

$$\bar{\nu}_\pi(t) := \left[\frac{\partial g_\pi}{\partial x} \right]_{x=1} = \sum_{n=0}^{\infty} n \pi_n(t) \quad (1.163)$$

the mean number of the neutrons present in the system at time T knowing there was 1 in the system at t in the absence of a source. In the same manner, we can introduce the factorial moments of order 2 and 3 of this distribution

$$\begin{aligned} \nu_{2, \pi}(t) &:= \frac{1}{2} \left[\frac{\partial^2 g_\pi}{\partial x^2} \right]_{x=1} = \sum_{n=2}^{\infty} \frac{n(n-1)}{2} \pi_n(t) \\ \nu_{3, \pi}(t) &:= \frac{1}{6} \left[\frac{\partial^3 g_\pi}{\partial x^3} \right]_{x=1} = \sum_{n=3}^{\infty} \frac{n(n-1)(n-2)}{6} \pi_n(t) \end{aligned} \quad (1.164)$$

More generally, we can consider

$$\nu_{k,\pi}(t) := \frac{1}{k!} \left[\frac{\partial^k g_\pi}{\partial x^k} \right]_{x=1} = \sum_{n=k}^{\infty} \frac{n(n-1)\cdots(n-k+1)}{k!} \pi_n(t), \forall k \in \mathbb{N}^* \quad (1.165)$$

We obtained the Chapman-Kolmogorov equation for the distribution of the number of neutrons present in the system at T knowing the fact there was 1 neutron in the system at time t in the absence of a source. Now we can compute the equations for the moments $\nu_{i,\pi}(t), i \in \llbracket 1, 3 \rrbracket$.

$$-\frac{\partial}{\partial t} \frac{\partial g_\pi}{\partial x} = -(\lambda_F \sum_{i \neq 1} f_i + \lambda_C) \frac{\partial g_\pi}{\partial x} + \lambda_F \sum_i i f_i \frac{\partial g_\pi}{\partial x} g_\pi^{i-1}(t) \quad (1.166)$$

Then evaluating in $x = 1$, we obtain

$$\begin{aligned} -\frac{d\bar{\nu}_\pi}{dt} &= -(\lambda_F \sum_{i \neq 1} f_i + \lambda_C) \bar{\nu}_\pi + \lambda_F \sum_{i=2}^m i f_i \bar{\nu}_\pi \\ &= -\lambda_C \bar{\nu}_\pi + \lambda_F \sum_i (i-1) f_i \bar{\nu}_\pi \end{aligned} \quad (1.167)$$

That becomes

$$\boxed{\frac{d\bar{\nu}_\pi}{dt} = \bar{\nu}_\pi \alpha, \quad \bar{\nu}_\pi(T) = 1} \quad (1.168)$$

Differentiating a second time the differential equation verified by g_π , we obtain

$$\begin{aligned} -\frac{\partial}{\partial t} \frac{\partial^2 g_\pi}{\partial x^2}(x, t) &= -(\lambda_F \sum_{i \neq 1} f_i + \lambda_C) \frac{\partial^2 g_\pi}{\partial x^2}(x, t) + \lambda_F \sum_{i=2} i f_i \left(\frac{\partial^2 g_\pi}{\partial x^2}(x, t) g_\pi(x, t) \right. \\ &\quad \left. + (i-1) \left(\frac{\partial g_\pi}{\partial x}(x, t) \right)^2 g_\pi^{i-2}(x, t) \right) \end{aligned} \quad (1.169)$$

However by definition

$$\nu_{2,\pi} = \frac{1}{2} \left[\frac{\partial^2 g_\pi}{\partial x^2} \right]_{x=1} \quad (1.170)$$

And so we can deduce

$$\begin{aligned} -\frac{d}{dt} \nu_{2,\pi} &= -(\lambda_F \sum_{i \neq 1} f_i + \lambda_C) \nu_{2,\pi} + \lambda_F (\bar{\nu} \nu_{2,\pi} + \nu_{2,\pi} \bar{\nu}_\pi^2) \\ &= (\lambda_F \sum_{i \neq 1} (i-1) f_i - \lambda_C) \nu_{2,\pi} + \nu_{2,\pi} \lambda_F \bar{\nu}_\pi^2 \end{aligned} \quad (1.171)$$

Which becomes

$$\boxed{\frac{d}{dt} \nu_{2,\pi} = \alpha \nu_{2,\pi} - \nu_{2,\pi} \lambda_F \bar{\nu}_\pi^2, \quad \nu_{2,\pi}(T) = 0} \quad (1.172)$$

Starting again from the differentiate equation on g_π differentiated 3 times with respect to x

$$-\frac{\partial}{\partial t} \frac{\partial^3 g_\pi}{\partial x^3} = -(\lambda_F \sum_{i \neq 1} f_i - \lambda_C) \frac{\partial^3 g_\pi}{\partial x^3} + \lambda_F \sum_i i f_i \left(\frac{\partial^3 g_\pi}{\partial x^3} g_\pi^{i-1} + 3(i-1) \frac{\partial^2 g_\pi}{\partial x^2} \frac{\partial g_\pi}{\partial x} g_\pi^{i-2} + (i-1)(i-2) \left(\frac{\partial g_\pi}{\partial x} \right)^3 g_\pi^{i-3} \right) \quad (1.173)$$

Evaluating in $x = 1$, we obtain

$$-\frac{d}{dt} \nu_{3,\pi} = (\lambda_F \sum_{i \neq 1} (i-1) f_i - \lambda_C) \nu_{3,\pi} + \lambda_F (2\nu_2 \nu_{2,\pi} \bar{\nu}_\pi + \nu_3 \bar{\nu}_\pi^3) \quad (1.174)$$

What becomes

$$\boxed{\frac{d}{dt} \nu_{3,\pi} = \alpha \nu_{3,\pi} - \lambda_F (2\nu_2 \nu_{2,\pi} \bar{\nu}_\pi + \nu_3 \bar{\nu}_\pi^3), \quad \nu_{3,\pi}(T) = 0} \quad (1.175)$$

These equations will be solved in the next chapter, the whole computations are in the appendix.

Population induced by an external source Then we can consider the distribution of the number of neutrons present in the system at T given the fact there was 0 neutron at time t in the presence of a source in the transitional regime $\Pi_n(t)$.

The probability that n neutrons are in the system at final time T with ν neutrons at time t , in the presence of a source is noted $\Pi_{n,\nu}(t)$. We consider the events

- $\mathcal{A}_{\nu,j} = \{\text{there is a source, there is } \nu \text{ neutrons in the system at } t, \text{ we detect } j \text{ neutrons between } t \text{ and } T\}$,
- $\mathcal{B}_{\nu,j} = \{\text{there is no source, there is } \nu \text{ neutrons in the system at } t, \text{ we detect } j \text{ neutrons between } t \text{ and } T\}$.

We have

$$\mathcal{A}_{0,n-j} \cap \mathcal{B}_{\nu,j}, \quad j = 0, \dots, n \text{ is a partition of } \mathcal{A}_{\nu,n} \quad (1.176)$$

and $\mathcal{A}_{0,n-j}$ and $\mathcal{B}_{\nu,j}$ are independent.

Then, $\Pi_{n,\nu}(t)$ can be decomposed as

$$\Pi_{n,\nu}(t) = \sum_{j=0}^n \pi_{j,\nu}(t) \Pi_{n-j}(t) \quad (1.177)$$

We consider a compound Poisson neutron source of intensity $S = S_F$ ($S_\alpha = 0$). The probability of one source event during dt is Sdt . Each source event produces ν neutrons with the probability $f_{\nu,S}$.

Thanks to the scheme 1.8, we know the possible source events during the time interval $[t - dt, t]$ are : no emission with probability $1 - Sdt$, or one source emission producing $\nu = 1, 2, 3, \dots$ neutrons with probability $Sdt f_{\nu,S}$.

$$II_n(t - dt) = (1 - Sdt)II_n(t) + Sdt \sum_{\nu=0}^{\nu_{max,S}} f_{\nu,S} II_{n,\nu}(t) + o(dt) \quad (1.178)$$

Considering a (α, n) source and a compound Poisson source would have meant adding a $S_\alpha dt II_{n,1}(t)$ term in our calculations.

Then dividing by dt and making it tend to 0, we obtain the Kolmogorov backward equation for the source problem.

$$-\frac{d}{dt} II_n(t) = S \left(\sum_{\nu=0}^{\nu_{max,S}} f_{\nu,S} II_{n,\nu}(t) - II_n(t) \right), \quad II_n(T) = \delta_{n,0} \quad (1.179)$$

Definition 1.6.29. *The generating function of the number of neutrons present in the system with source is*

$$G_{II}(z, t) := \sum_{n=0}^{\infty} II_n(t) z^n \quad (1.180)$$

By 1.177 and 1.179 we obtain

$$\frac{\partial G_{II}}{\partial t}(z, t) = S \left\{ 1 - \sum_{\nu=0}^{\nu_{max,S}} f_{\nu,S} g_\pi^\nu(z, t) \right\} G_{II}(z, t) \quad (1.181)$$

where $g_\pi(z, t) := \sum_{n=0}^{\infty} \pi_n(t) z^n$. Knowing the initial condition $\lim_{t \rightarrow T} G_{II}(z, t) = 1$, we can integrate the previous backward equation in order to find the Sevast'yanov formula for the number of neutrons present in the system in presence of a source

$$\boxed{G_{II}(z, t) = \exp\left(S \int_t^T \left(\sum_{\nu=0}^{\nu_{max,S}} f_{\nu,S} g_\pi^\nu(z, t') - 1 \right) dt'\right)} \quad (1.182)$$

By doing a change of variable $s = T - t'$, we obtain

$$G_{II}(z, t) = \exp\left(S \int_0^{T-t} \left(\sum_{\nu=0}^{\nu_{max,S}} f_{\nu,S} g_\pi^\nu(z, T - s) - 1 \right) ds\right). \quad (1.183)$$

Then when $t \rightarrow -\infty$

$$G_{II,\infty}(z) = \exp\left(S \int_0^{\infty} \left(\sum_{\nu=0}^{\nu_{max,S}} f_{\nu,S} g_\pi^\nu(z, T - t') - 1 \right) dt'\right) \quad (1.184)$$

In the following, $S = S_F$ will refer to the intensity of the source and $S_\alpha = 0$.

Definition 1.6.30. *When the stationary regime is established, we note*

$II_{\nu,\infty} :=$ the probability that ν neutrons are present in the system in the presence of a source. (1.185)

Definition 1.6.31. We introduce the mean of the distribution $(\Pi_n(t))_n$.

$$\bar{\nu}_{\Pi}(t) := \sum_{n=0}^{\infty} n \Pi_n(t) \quad (1.186)$$

the mean number of neutrons present in the system at T knowing there was 0 in the system at t in presence of a source. When it comes to the use of the mean number of neutrons present in the system in presence of a source during the stationary regime we will use

$$\bar{\nu}_{\Pi,\infty} := \sum_{n=0}^{\infty} n \Pi_{n,\infty}. \quad (1.187)$$

In the same manner, we can introduce the factorial moments of order 2 and 3 of this distribution

$$\begin{aligned} \nu_{2,\Pi}(t) &:= \frac{1}{2} \left[\frac{\partial^2 G_{\Pi}}{\partial x^2} \right]_{x=1} = \sum_{n=2}^{\infty} \frac{n(n-1)}{2} \Pi_n(t) \\ \nu_{3,\Pi}(t) &:= \frac{1}{6} \left[\frac{\partial^3 G_{\Pi}}{\partial x^3} \right]_{x=1} = \sum_{n=3}^{\infty} \frac{n(n-1)(n-2)}{6} \Pi_n(t) \end{aligned} \quad (1.188)$$

The same definitions works for $(\Pi_{\nu,\infty})_{\nu \in \mathbb{N}}$.

We take back the Chapman-Kolmogorov equation

$$-\frac{\partial G_{\Pi}}{\partial t} = -S G_{\Pi} + S \sum_{\nu} f_{\nu,S} G_{\Pi} g_{\pi}^{\nu} \quad (1.189)$$

By differentiating with respect to x we obtain

$$-\frac{\partial^2 G_{\Pi}}{\partial t \partial x} = -S \frac{\partial G_{\Pi}}{\partial x} + S \sum_{\nu} f_{\nu,S} \left(\frac{\partial G_{\Pi}}{\partial x} g_{\pi}^{\nu} + G_{\Pi} \nu \frac{\partial g_{\pi}}{\partial x} g_{\pi}^{\nu-1} \right) \quad (1.190)$$

Finally, by evaluating in $x = 1$, we have

$$\boxed{-\frac{d\bar{\nu}_{\Pi}}{dt} = \bar{\nu}_S S \bar{\nu}_{\pi}(t), \quad \bar{\nu}_{\Pi}(T) = 0} \quad (1.191)$$

The equation 1.190 differentiated with respect to x is

$$-\frac{\partial}{\partial t} \frac{\partial^2 G_{\Pi}}{\partial x^2} = -S \frac{\partial^2 G_{\Pi}}{\partial x^2} + S \sum_{\nu} f_{\nu,S} \left(\frac{\partial^2 G_{\Pi}}{\partial x^2} g_{\pi}^{\nu} + 2 \frac{\partial G_{\Pi}}{\partial x} \nu \frac{\partial g_{\pi}}{\partial x} g_{\pi}^{\nu-1} + G_{\Pi} \nu \left(\frac{\partial^2 g_{\pi}}{\partial x^2} g_{\pi}^{\nu-1} + (\nu-1) \left(\frac{\partial g_{\pi}}{\partial x} \right)^2 g_{\pi}^{\nu-2} \right) \right) \quad (1.192)$$

Because

$$\frac{\partial}{\partial x} \left(\frac{\partial G_{\Pi}}{\partial x} g_{\pi}^{\nu} + G_{\Pi} \nu \frac{\partial g_{\pi}}{\partial x} \right) = \frac{\partial^2 G_{\Pi}}{\partial x^2} g_{\pi}^{\nu} + 2 \frac{\partial G_{\Pi}}{\partial x} \nu \frac{\partial g_{\pi}}{\partial x} g_{\pi}^{\nu-1} + G_{\Pi} \nu \left(\frac{\partial^2 g_{\pi}}{\partial x^2} + (\nu-1) \left(\frac{\partial g_{\pi}}{\partial x} \right)^2 g_{\pi}^{\nu-2} \right) \quad (1.193)$$

Where

$$\boxed{-\frac{d\nu_{2,\Pi}}{dt} = \bar{\nu}_S S(\bar{\nu}_\Pi \bar{\nu}_\pi + \nu_{2,\pi}) + \nu_{2S} S \bar{\nu}_\pi^2, \nu_{2,\Pi}(T) = 0} \quad (1.194)$$

Differentiating the equation 1.190 three times with respect to x , we obtain

$$\begin{aligned} -\frac{\partial}{\partial t} \frac{\partial^3 G_\Pi}{\partial x^3} &= -S \frac{\partial^3 G_\Pi}{\partial x^3} + S \sum_\nu f_{\nu,S} \left(\frac{\partial^3 G_\Pi}{\partial x^3} g_\pi^\nu + 3\nu \frac{\partial^2 G_\Pi}{\partial x^2} \frac{\partial g_\pi}{\partial x} g_\pi^{\nu-1} \right. \\ &\quad \left. + 3 \frac{\partial G_\Pi}{\partial x} \nu \left(\frac{\partial^2 g_\pi}{\partial x^2} g_\pi^{\nu-1} + (\nu-1) \left(\frac{\partial g_\pi}{\partial x} \right)^2 g_\pi^{\nu-2} \right) \right. \\ &\quad \left. + G_\Pi \nu \left(\frac{\partial^3 g_\pi}{\partial x^3} g_\pi^{\nu-1} + 3(\nu-1) \frac{\partial g_\pi}{\partial x} \frac{\partial^2 g_\pi}{\partial x^2} g_\pi^{\nu-2} + (\nu-1)(\nu-2) \left(\frac{\partial g_\pi}{\partial x} \right)^3 g_\pi^{\nu-3} \right) \right) \\ &= -S \frac{\partial^3 G_\Pi}{\partial x^3} + S \sum_\nu f_{\nu,S} \left[\frac{\partial^3 G_\Pi}{\partial x^3} g_\pi^\nu \right. \\ &\quad \left. + 3\nu \frac{\partial^2 G_\Pi}{\partial x^2} \frac{\partial g_\pi}{\partial x} g_\pi^{\nu-1} + 3 \frac{\partial G_\Pi}{\partial x} \left(\nu \frac{\partial^2 g_\pi}{\partial x^2} g_\pi^{\nu-1} + \nu(\nu-1) \left(\frac{\partial g_\pi}{\partial x} \right)^2 g_\pi^{\nu-2} \right) \right. \\ &\quad \left. + G_\Pi \left(\nu \frac{\partial^3 g_\pi}{\partial x^3} g_\pi^{\nu-1} + 3\nu(\nu-1) \frac{\partial^2 g_\pi}{\partial x^2} \frac{\partial g_\pi}{\partial x} g_\pi^{\nu-2} + \nu(\nu-1)(\nu-2) \left(\frac{\partial g_\pi}{\partial x} \right)^3 g_\pi^{\nu-3} \right) \right] \end{aligned} \quad (1.195)$$

Dividing by 6 and evaluating in $x = 1$, we obtain

$$\boxed{-\frac{d}{dt} \nu_{3,\Pi} = S(\nu_{2,\Pi} \bar{\nu}_\pi \bar{\nu}_S + \nu_\Pi (\nu_{2\pi} \bar{\nu}_S + \bar{\nu}_\pi^2 \nu_{2S}) + \nu_{3,\pi} \bar{\nu}_S + 2\bar{\nu}_\pi \nu_{2,\pi} \nu_{2S} + \bar{\nu}_\pi^3 \nu_{3S}), \nu_{3,\Pi}(T) = 0} \quad (1.196)$$

The moments in the stationary regime are the limits of the one of $P_n(t)$ by taking $t \rightarrow -\infty$

Ergodicity of X_t , and some properties of the chain The expression

$$G_\Pi(x, t) = \exp \left(S \int_t^T \left(\sum_{\nu=0}^{\nu_{max,S}} f_{\nu,S} g_\pi^\nu(x, t') - 1 \right) dt' \right)$$

will enable us to conclude the ergodicity of the chain X_t .

First, we recall that

$$\sum_{\nu=0}^{\nu_{max,S}} f_{\nu,S} g_\pi^\nu(x, t') - 1 = \sum_{\nu=0}^{\nu_{max,S}} f_{\nu,S} (g_\pi^\nu(x, t') - 1) \quad (1.197)$$

since $(f_{\nu,S})_\nu$ is a probability distribution.

By definition, we know

$$\sum_{n \neq 0} \pi_n(t) \leq \sum_{n \neq 0} n \pi_n(t) = e^{-\alpha(T-t)} \quad (1.198)$$

So the quantity $\pi_0(t)$ satisfies the inequalities

$$\begin{aligned} 1 \geq \pi_0(t) &= 1 - \sum_{n \neq 0} \pi_n(t) \geq 1 - \sum_{n \neq 0} n \pi_n(t) \\ &\geq 1 - \bar{\nu}_\pi(t) \\ &\geq 1 - e^{-\alpha(T-t)} \end{aligned} \quad (1.199)$$

and then converges to 1 when $T - t \rightarrow +\infty$.

Moreover, we can add

$$\begin{aligned} 1 - e^{-\alpha(T-t)} &\leq \pi_0(t) \\ (1 - e^{-\alpha(T-t)})^\nu &\leq \pi_0^\nu(t) \\ \sum_{k=0}^{\nu} \binom{\nu}{k} (-1)^k e^{-\alpha k(T-t)} &\leq \pi_0^\nu(t) \text{ using binomial theorem} \\ 0 \leq 1 - \pi_0^\nu(t) &\leq 1 + \sum_{k=0}^{\nu} \binom{\nu}{k} (-1)^{k+1} e^{-\alpha k(T-t)} = \sum_{k=1}^{\nu} \binom{\nu}{k} (-1)^{k+1} e^{-\alpha k(T-t)} \end{aligned} \quad (1.200)$$

the last right member of the equation is the sum of integrable functions when $T - t \rightarrow +\infty$.

Definition 1.6.32. *Two functions f , g are said equivalent in the neighbourhood of A when $x \rightarrow A$, when*

$$\lim_{x \rightarrow A} \frac{f(x)}{g(x)} = 1 \quad (1.201)$$

it will be denoted $f(x) \underset{x \rightarrow A}{\sim} g(x)$.

Then, in first approximation

$$g_\pi(t) = \sum_n x^n \pi_n(t) \underset{t \rightarrow -\infty}{\sim} \pi_0(t) \quad (1.202)$$

Then, when $T - t \rightarrow +\infty$

$$0 \leq 1 - g_\pi^\nu(t) \leq \sum_{k=1}^{\nu} \binom{\nu}{k} (-1)^{k+1} e^{-\alpha k(T-t)} \quad (1.203)$$

Then $G_{II}(x, t)$ has a non-trivial limit when $T - t \rightarrow +\infty$. This proves that the process X_t is ergodic.

Stationary regime

Then we can define the stationary regime of the neutronic system

Definition 1.6.33. *For $k_{eff} < 1$, the stationary regime is when the ergodicity for X_t is achieved, which is the case thanks to the previous subsection.*

Number of neutrons detected

Detections induced by one initial neutron We are now working on the distribution of the number of neutrons detected between t and T given the fact there was 1 neutron at time t in the absence of a source $p_n(t)$.

Definition 1.6.34. *Probabilities of detection in the absence of a source*

The probability of detecting n neutrons between t and T knowing the fact there were ν neutrons at time t in the absence of a source is

$$p_{n,\nu}(t) := \mathbb{P}(n \text{ neutrons detected between } t \text{ and } T | \nu \text{ neutrons present in the system at } t) \quad (1.204)$$

We will focus here more on

$$p_{n,1}(t) = \mathbb{P}(n \text{ neutrons detected between } t \text{ and } T | 1 \text{ neutron present in the system at } t) \quad (1.205)$$

The neutrons present in the system are counted when the detector is open, i.e. during $[t, T]$.

During $[t - dt, t]$

- nothing may happen
- there may be a capture with detection (event with probability $\lambda_C \varepsilon_C dt$ which decreases the number of neutrons present by 1 and increases the number of neutrons detected by 1)
- there may be a capture without detection (event with probability $\lambda_C(1 - \varepsilon_C)dt$ which decreases the number of neutrons present by 1)
- there may be a fission (event with probability $\lambda_F dt$ which changes the number of neutrons according to the fission distribution)

We establish the backward Chapman-Kolmogorov equation for the counting probability $p_n(t)$, by taking into account the probabilities $p_{n,\nu}(t)$.

$$\begin{aligned} p_n(t - dt) &= \left(1 - (\lambda_F \sum_i f_i - \lambda_C) dt \right) p_n(t) + \lambda_F dt \sum_{\nu} f_{\nu} p_{n,\nu}(t) \\ &\quad + \lambda_C dt (\varepsilon_C \delta_{n,1} + (1 - \varepsilon_C) \delta_{n,0}) + o(dt), \\ p_n(T) &= \delta_{n,0} \end{aligned} \quad (1.206)$$

which becomes

$$\boxed{-\frac{dp_n}{dt}(t) + \lambda_T p_n(t) = \lambda_F \sum_{\nu=0}^{\nu_{max}} f_{\nu} p_{n,\nu}(t) + \lambda_C (\varepsilon_C \delta_{n,1} + (1 - \varepsilon_C) \delta_{n,0}), \quad p_n(T) = \delta_{n,0}} \quad (1.207)$$

As previously, we use the generating function

Definition 1.6.35. *The generating function associated to the distribution $(p_n(t))_{n \in \mathbb{N}}$ is given by:*

$$g(x, t) := \sum_{n=0}^{+\infty} x^n p_n(t) \quad (1.208)$$

In the same manner, we define the associated generating function to the probability distribution $(p_{n,\nu}(t))_{(n,\nu) \in \mathbb{N}^2}$

$$g_\nu(x, t) := \sum_{n=0}^{+\infty} x^n p_{n,\nu}(t) \quad (1.209)$$

Property 1.6.36. *In order to find 1.207 from the generating equation function, we will use*

$$p_{n,\nu}(t) = \frac{1}{n!} \left[\frac{\partial^n g^\nu}{\partial x^n} \right]_{x=0}, \forall (n, \nu) \in \mathbb{N} \times \mathbb{N}^* \quad (1.210)$$

and

$$p_{n,1}(t) = \frac{1}{n!} \left[\frac{\partial^n g}{\partial x^n} \right]_{x=0}, \forall n \in \mathbb{N} \quad (1.211)$$

The equation in $x = 0$, enables us to obtain the probabilities from the generating function.

We remark

$$p_{n,\nu}(t) = \sum_{k_1, \dots, k_\nu \text{ such that } k_1 + \dots + k_\nu = n} p_{k_1}(t) \cdots p_{k_\nu}(t) \quad (1.212)$$

then

$$g_\nu = g^\nu \quad (1.213)$$

Then, from the generating function expression as well as the equation 1.207, we can deduce the following result

$$\boxed{-\frac{\partial g}{\partial t}(x, t) + \lambda_T g(x, t) = \lambda_F \sum_{\nu=0}^{\nu_{max}} f_\nu g^\nu(x, t) + \lambda_C(\varepsilon_C x + (1 - \varepsilon_C)), g(x, T) = 1} \quad (1.214)$$

Remark 1.6.37. *One of the first interests of using the generating function is to transform the term $p_{n,\nu}(t)$ of 1.207 by g^ν in 1.214. This last equation is simplified from this fact.*

By a power series expansion of g in 1, we find the formula

$$g(x) = \sum_{p=0}^{\infty} (x-1)^p \frac{1}{p!} \left[\frac{\partial^p g}{\partial x^p} \right]_{x=1} \quad (1.215)$$

By identifying the general terms of the power series, we derive the following definition.

Definition 1.6.38. *The combinatorial moment m_n is the mean number of n -combination of n detections between t and T when there is a neutron at t in the absence of a source.*

On the other hand, the evaluation in $x = 1$ enables us to obtain the moments of the distribution concerned.

$$m_n(t) := \frac{1}{n!} \left[\frac{\partial^n g}{\partial x^n} \right]_{x=1}, \forall n \in \mathbb{N} \quad (1.216)$$

We will also compute the combinatorial moments of n detections for ν neutrons present at initial time.

$$m_{n,\nu}(t) := \frac{1}{n!} \left[\frac{\partial^n g^\nu}{\partial x^n} \right]_{x=1}, \forall (n, \nu) \in \mathbb{N} \times \mathbb{N}^* \quad (1.217)$$

Then we can compute the equations for the moments $m_n(t), n \in \llbracket 1, 3 \rrbracket$.

For the moment of order 1, by differentiating the equation 1.214 with respect to x then evaluating in $x = 1$, we obtain

$$-\frac{dm_1}{dt}(t) + \lambda_T m_1(t) = \lambda_F \sum_{\nu=0}^{\infty} \nu f_\nu m_1(t) + \lambda_C \varepsilon_C, \quad m_1(T) = 0 \quad (1.218)$$

which becomes

$$-\frac{dm_1}{dt}(t) + (\lambda_T - \lambda_F \bar{\nu}) m_1(t) = \lambda_C \varepsilon_C \quad (1.219)$$

but, as $\alpha = \lambda_T - \lambda_F \bar{\nu}$, we can deduce that

$$-\frac{1}{\alpha} \frac{dm_1}{dt}(t) + m_1(t) = \frac{\lambda_F \varepsilon_F}{\alpha} \quad (1.220)$$

Moreover, we know the fact that

$$\begin{aligned} \frac{\lambda_F}{\alpha} &= \frac{\lambda_F}{\lambda_T - \bar{\nu} \lambda_F} \\ &= \frac{1}{\bar{\nu}} \frac{1}{\frac{\lambda_T}{\bar{\nu} \lambda_F} - 1} \\ &= \frac{1}{-\rho \bar{\nu}} \end{aligned} \quad (1.221)$$

because $\rho = 1 - \frac{\lambda_T}{\bar{\nu} \lambda_F}$.

The knowledge of the differential equations enables to obtain the simple moments in the absence of a source, we need to compute them.

Computing the simple moment of order 1 in the absence of a source, we will solve the differential equation in the next chapter.

$$\boxed{-\frac{1}{\alpha} \frac{dm_1}{dt} + m_1 = \frac{1}{-\rho \bar{\nu}} \varepsilon_F, \quad m_1(T) = 0} \quad (1.222)$$

Differentiating two times the equation 1.214 with respect to x then evaluating in $x = 1$, we obtain

$$\boxed{-\frac{1}{\alpha} \frac{dm_2}{dt} + m_2 = \frac{\nu_2}{-\rho\bar{\nu}} m_1^2, \quad m_2(T) = 0} \quad (1.223)$$

Deriving three times the equation 1.214 with respect to x then evaluating in $x = 1$, we are in presence of

$$\boxed{-\frac{1}{\alpha} \frac{dm_3}{dt} + m_3 = \frac{1}{-\rho\bar{\nu}} (\nu_3 m_1^3 + 2\nu_2 m_1 m_2), \quad m_3(T) = 0} \quad (1.224)$$

Remark 1.6.39. *Similar notations for different types of moments will be used later. Their expressions will follow the same type of reasoning.*

Detections induced by an external source Now we can consider the distribution of the number of neutrons detected between t and T given the fact there was 0 neutrons at time t in the presence of a source in the transitional regime $P_n(t)$. We still consider $S = S_F$ the intensity of the source and $S_\alpha = 0$.

Definition 1.6.40. $P_n(t)$ is the probability of detecting n neutrons between t and T knowing the fact there were 0 neutrons at time t in presence of a source. Similarly, $P_{n,\nu}(t)$ is the probability of detection of n neutrons between t and T knowing the fact there were ν neutrons at time t in presence of a source.

During the infinitesimal time interval $[t - dt, t]$ there can be no source event with probability $(1 - Sdt)$ or one source event with probability Sdt . A source event gives birth to ν neutrons with probability $f_{\nu,S}$.

Using the backward formalism of the Chapman-Kolmogorov equations applied to $P_n(t)$ we can deduce

$$P_n(t - dt) = P_n(t)(1 - Sdt) + Sdt \sum_{\nu=0}^{\nu_{max,S}} f_{\nu,S} P_{n,\nu}(t) + o(dt) \quad (1.225)$$

Dividing by dt and making it tend towards 0, we obtain

$$-\frac{dP_n}{dt}(t) = -SP_n(t) + S \sum_{\nu=0}^{\nu_{max,S}} f_{\nu,S} P_{n,\nu}(t), \quad P_n(T) = \delta_{n,0} \quad (1.226)$$

We consider the events

- $A_{\nu,j} = \{\text{there is a source, there are } \nu \text{ neutrons in the system at } t, \text{ we detect } j \text{ neutrons between } t \text{ and } T\}$,
- $B_{\nu,j} = \{\text{there is no source, there are } \nu \text{ neutrons in the system at } t, \text{ we detect } j \text{ neutrons between } t \text{ and } T\}$.

We have

$$A_{0,n-j} \cap B_{\nu,j}, \quad j = 0, \dots, n \text{ is a partition of } A_{\nu,n} \quad (1.227)$$

and $A_{0,n-j}$ and $B_{\nu,j}$ are independent.

Then, we obtain

$$P_{n,\nu}(t) = \sum_{j=0}^n p_{j,\nu}(t) P_{n-j}(t) \quad (1.228)$$

$$-\frac{dP_n}{dt}(t) = S \left(\sum_{j=0}^n P_{n-j}(t) \sum_{\nu=0}^M f_{\nu,S} p_{j,\nu}(t) - P_n(t) \right) \quad (1.229)$$

Using equation 1.229, we obtain the equation of associated generating function $G(x, t)$:

$$\begin{cases} -\frac{dG}{dt}(x, t) = SG(x, t) (\sum_{\nu=0}^{\nu_{max,S}} f_{\nu,S} g^{\nu}(x, t) - 1) \\ G(x, T) = 1 \end{cases} \quad (1.230)$$

We deduce the Sevast'yanov formula, i.e. the generating function expression:

$$\boxed{G(x, t) = \exp\left(\int_t^T S \left(\sum_{\nu=0}^{\nu_{max,S}} f_{\nu,S} g^{\nu}(x, s) - 1\right) ds\right)} \quad (1.231)$$

Definition 1.6.41. *The combinatorial moments of the counting distribution are given by:*

$$M_q := \frac{1}{q!} \left[\frac{\partial^q G}{\partial x^q} \right]_{x=1} \quad (1.232)$$

The generating function associated to the distribution induced by one initial source event is:

$$g_F = \sum_{\nu=0}^{\infty} f_{\nu,S} g^{\nu} \quad (1.233)$$

We already have an expression of the evaluation in $x = 1$ of the following expression

$$\frac{\partial G}{\partial x} = \int_0^{T-t} S \frac{\partial g_F}{\partial x}(x, T-s) ds G \quad (1.234)$$

Then evaluating in $x = 1$

$$\boxed{M_1(t) = \bar{\nu}_S S \int_0^{T-t} m_1(T-s) ds} \quad (1.235)$$

Then, we can look forward to

$$\frac{\partial^2 G}{\partial x^2} = \int_0^{T-t} S \frac{\partial^2 g_F}{\partial x^2}(x, T-s) ds G + \int_0^{T-t} S \frac{\partial g_F}{\partial x}(x, T-s) ds \frac{\partial G}{\partial x} \quad (1.236)$$

by definition of G .

But

$$\begin{aligned}
\frac{\partial^2 g_F(x, t)}{\partial x^2} &= \frac{\partial}{\partial x} \sum_{\nu=0}^{\nu_{max,S}} \nu f_{\nu,S} \frac{\partial g}{\partial x} g^{\nu-1}(x, t) \\
&= \sum_{\nu=0}^{\nu_{max,S}} \nu f_{\nu,S} \left(\frac{\partial^2 g}{\partial x^2} g^{\nu-1}(x, t) + (\nu - 1) \left(\frac{\partial g}{\partial x} \right)^2 g^{\nu-2}(x, t) \right) \\
&= \frac{\partial^2 g}{\partial x^2} \left(\sum_{\nu=0}^{\nu_{max,S}} \nu f_{\nu,S} g^{\nu-1}(x, t) \right) + \left(\frac{\partial g}{\partial x} \right)^2 \left(\sum_{\nu=0}^{\nu_{max,S}} \nu(\nu - 1) f_{\nu,S} g^{\nu-2}(x, t) \right)
\end{aligned} \tag{1.237}$$

This enables us to obtain

$$\begin{aligned}
\frac{\partial^2 G}{\partial x^2} &= \int_0^{T-t} S \left\{ \frac{\partial^2 g}{\partial x^2} \left(\sum_{\nu=0}^{\nu_{max,S}} \nu f_{\nu,S} g^{\nu-1}(x, T-s) \right) + \left(\frac{\partial g}{\partial x} \right)^2 \sum_{\nu=0}^{\nu_{max,S}} \nu(\nu - 1) f_{\nu,S} g^{\nu-2}(x, T-s) \right\} ds G \\
&\quad + \left(\int_0^{T-t} S \frac{\partial g}{\partial x} \left(\sum_{\nu=0}^{\nu_{max,S}} \nu f_{\nu,S} g^{\nu-1}(x, T-s) \right) ds \right)^2 G
\end{aligned} \tag{1.238}$$

evaluating in $x = 1$, we obtain

$$\boxed{
\begin{aligned}
M_2(t) &= \int_0^{T-t} S(m_2(T-s)\bar{\nu}_S + m_1^2(T-s)\nu_2S) ds \\
&\quad + \frac{\left(\int_0^{T-t} S\bar{\nu}_S m_1(T-s) ds \right)^2}{2}
\end{aligned}
} \tag{1.239}$$

$$\begin{aligned}
\frac{\partial^3 G}{\partial x^3} &= \frac{\partial}{\partial x} \left\{ \int_0^{T-t} S \frac{\partial^2 g_F}{\partial x^2}(x, T-s) ds G + \int_0^{T-t} S \frac{\partial g_F}{\partial x}(x, T-s) ds \frac{\partial G}{\partial x} \right\} \\
&= \int_0^{T-t} S \frac{\partial^3 g_F}{\partial x^3}(x, T-s) ds G + 3 \int_0^{T-t} S \frac{\partial^2 g_F}{\partial x^2}(x, T-s) ds \frac{\partial G}{\partial x} \\
&\quad + \left(\int_0^{T-t} S \frac{\partial g_F}{\partial x}(x, T-s) ds \right)^2 \frac{\partial G}{\partial x}
\end{aligned} \tag{1.240}$$

because $\frac{\partial G}{\partial x} = \int_0^{T-t} S \frac{\partial g_F}{\partial x}(x, T-s) ds G$.

To conclude, we obtain

$$\begin{aligned}
\frac{\partial^3 G}{\partial x^3} &= \int_0^{T-t} S \frac{\partial^3 g_F}{\partial x^3}(x, T-s) ds G \\
&\quad + \left(3 \int_0^{T-t} S \frac{\partial^2 g_F}{\partial x^2}(x, T-s) ds + \left[\int_0^{T-t} S \frac{\partial g_F}{\partial x}(x, T-s) ds \right]^2 \right) \frac{\partial G}{\partial x}
\end{aligned} \tag{1.241}$$

Evaluating the previous expression in $x = 1$ and using the results of the annexes A.2.5, we obtain

$$M_3(t) = \int_0^{T-t} S(\bar{\nu}_S m_3(T-s) + 2\nu_{2S} m_1(T-s)m_2(T-s) + \nu_{3S} m_1^3(T-s)) ds + \left(\int_0^{T-t} S(\bar{\nu}_S m_2(T-s) + \nu_{2S} m_1^2(T-s)) ds + \frac{1}{6} \left(\int_0^{T-t} S \bar{\nu}_S m_1(T-s) ds \right)^2 \right) M_1(t) \quad (1.242)$$

Neutron detection given the presence of a source in the stationary regime

Finally, we take into account the distribution of the neutron detected during $[t, T]$ given the fact of the presence of a source in the stationary regime $Q_n(t)$.

By doing a power series expansion in 1, we get the formula

$$\mathcal{G}(x) = \sum_{p=0}^{\infty} (x-1)^p \frac{1}{p!} \left[\frac{\partial^p \mathcal{G}}{\partial x^p} \right]_{x=1} \quad (1.243)$$

Which gives

$$\mathcal{G}(x) = \sum_{p=0}^{\infty} (x-1)^p \mathcal{M}_p \quad (1.244)$$

where \mathcal{M}_p refers to the mean number of combinations of p detected neutrons (correlated and uncorrelated).

Definition 1.6.42. *By identification of the general terms of the power series, we can deduce that*

$$\mathcal{M}_p := \frac{1}{p!} \left[\frac{\partial^p \mathcal{G}}{\partial x^p} \right]_{x=1} \quad (1.245)$$

Definition 1.6.43. *We define*

$$Q_n(t) := \mathbb{P}(n \text{ neutrons detected on } [t, T] | (\Pi_{\nu, \infty})_{\nu \in \mathbb{N}})$$

the probability of counting n neutrons during the interval $[t, T]$ knowing the number of neutrons has stationary distribution $(\Pi_{\nu, \infty})_{\nu \in \mathbb{N}}$.

By definition, we know that

$$Q_n(t) = \sum_{j=0}^n \sum_{\nu=0}^{\infty} \Pi_{\nu, \infty} P_{n-j}(t) p_{j, \nu}(t) \quad (1.246)$$

This enables us to get

$$Q_n(t) = \sum_{j=0}^n P_{n-j}(t) \sum_{\nu=0}^{\infty} \Pi_{\nu, \infty} p_{j, \nu}(t) \quad (1.247)$$

As previously, it is appropriate for us to introduce a new object

Definition 1.6.44. We define

$$p_j^{\Pi}(t) := \sum_{\nu=0}^{\infty} \Pi_{\nu,\infty} p_{j,\nu}(t)$$

We note \mathcal{G} the generating function associated to $Q_n(t)$. Henceforth, we can write

$$\begin{aligned} \mathcal{G}(x, t) &= \sum_{n=0}^{\infty} x^n \sum_{j=0}^n P_{n-j}(t) p_j^{\Pi}(t) \\ &= \sum_{n=0}^{\infty} \sum_{j=0}^n x^{n-j} P_{n-j}(t) x^j p_j^{\Pi}(t) \\ &= \left(\sum_{n=0}^{\infty} x^n P_n(t) \right) \left(\sum_{n=0}^{\infty} x^n p_n^{\Pi}(t) \right) \end{aligned} \quad (1.248)$$

as we are in the presence of a Cauchy product.

As a result, we dispose of an equation on the generating function \mathcal{G} of the distribution of the count number on the interval $[t, T]$ knowing the number of neutrons has a stationary distribution $(\Pi_{\nu,\infty})_{\nu}$

$$\boxed{\mathcal{G}(x, t) = G(x, t) G_{\Pi,\infty}(g(x, t))} \quad (1.249)$$

Remark 1.6.45. The generating function associated to $p_j^{\Pi}(t)$ is computed by the following way

$$g^{\Pi}(x, t) = \sum_{\nu=0}^{\infty} \Pi_{\nu,\infty} g(x, t)^{\nu} = G_{\Pi,\infty}(g(x, t)) \quad (1.250)$$

Thus, the generating function associated to $(Q_n(t))_{n \in \mathbb{N}}$ enables us to obtain the associated distribution and its moments.

Derivating one time

$$\begin{aligned} \frac{\partial \mathcal{G}}{\partial x}(x, t) &= \frac{\partial G}{\partial x}(x, t) \sum_{\nu=0}^{+\infty} \Pi_{\nu,\infty} g(x, t)^{\nu} + G(x, t) \sum_{\nu=0}^{+\infty} \nu \Pi_{\nu,\infty} \frac{\partial g}{\partial x}(x, t) g(x, t)^{\nu-1} \\ \left[\frac{\partial \mathcal{G}}{\partial x} \right]_{x=1}(t) &= \left[\frac{\partial G}{\partial x} \right]_{x=1}(t) + \left[\frac{\partial g}{\partial x} \right]_{x=1}(t) \sum_{\nu=0}^{\infty} \nu \Pi_{\nu,\infty} \end{aligned} \quad (1.251)$$

And so,

$$\boxed{\mathbb{E}[N_{[t,T]}] = \mathcal{M}_1(t) = M_1(t) + \bar{\nu}_{\Pi,\infty} m_1(t)} \quad (1.252)$$

Then we compute

$$\begin{aligned} \frac{\partial^2 \mathcal{G}}{\partial x^2} &= \frac{\partial^2 G}{\partial x^2} G_{\Pi,\infty}(g, t) + 2 \frac{\partial G}{\partial x} \frac{\partial g}{\partial x} \frac{\partial G_{\Pi,\infty}}{\partial x} + G \left(\frac{\partial^2 g}{\partial x^2} \frac{\partial G_{\Pi,\infty}}{\partial x} + \left(\frac{\partial g}{\partial x} \right)^2 \frac{\partial^2 G_{\Pi,\infty}}{\partial x^2}(g, t) \right) \\ &= \frac{\partial^2 G}{\partial x^2} G_{\Pi,\infty}(g, t) + 2 \frac{\partial G}{\partial x} \frac{\partial g}{\partial x} \frac{\partial G_{\Pi,\infty}}{\partial x} + G \frac{\partial^2 g}{\partial x^2} \frac{\partial G_{\Pi,\infty}}{\partial x} + G \left(\frac{\partial g}{\partial x} \right)^2 \frac{\partial^2 G_{\Pi,\infty}}{\partial x^2}(g, t) \end{aligned} \quad (1.253)$$

This enables us to deduce

$$\boxed{\mathcal{M}_2(t) = M_2(t) + \bar{\nu}_{II,\infty} M_1(t) m_1(t) + \bar{\nu}_{II,\infty} m_2(t) + \nu_{2,II,\infty} m_1^2(t)} \quad (1.254)$$

The expression of the simple moments as a function of the $(\mathcal{M}_i)_{i=1,2}$ is

$$\boxed{\mathbb{E}[N_{[t,T]}^2] = 2\mathcal{M}_2(t) + \mathcal{M}_1(t)} \quad (1.255)$$

The equation 1.249 enables us to make this computation from this knowledge on $(\Pi_{\nu,\infty})_{\nu \in \mathbb{N}}$, g and G .

$$\begin{aligned} \frac{\partial^3 \mathcal{G}}{\partial x^3} &= \frac{\partial^3 G}{\partial x^3} G_{II,\infty}(g, t) + \frac{\partial^2 G}{\partial x^2} \frac{\partial g}{\partial x} \frac{\partial G_{II,\infty}}{\partial x} \\ &+ 2 \left(\frac{\partial^2 G}{\partial x^2} \frac{\partial g}{\partial x} \frac{\partial G_{II,\infty}}{\partial x} + \frac{\partial G}{\partial x} \left(\frac{\partial^2 g}{\partial x^2} \frac{\partial G_{II,\infty}}{\partial x} + \left(\frac{\partial g}{\partial x} \right)^2 \frac{\partial^2 G_{II,\infty}}{\partial x^2} \right) \right) \\ &+ \frac{\partial G}{\partial x} \frac{\partial^2 g}{\partial x^2} \frac{\partial G_{II,\infty}}{\partial x} + G \left(\frac{\partial^3 g}{\partial x^3} \frac{\partial G_{II,\infty}}{\partial x} + \frac{\partial g}{\partial x} \frac{\partial^2 g}{\partial x^2} \frac{\partial^2 G_{II,\infty}}{\partial x^2} \right) \\ &+ \frac{\partial G}{\partial x} \left(\frac{\partial g}{\partial x} \right)^2 \frac{\partial^2 G_{II,\infty}}{\partial x^2} + G \left(2 \frac{\partial g}{\partial x} \frac{\partial^2 g}{\partial x^2} \frac{\partial^2 G_{II,\infty}}{\partial x^2} + \left(\frac{\partial g}{\partial x} \right)^3 \frac{\partial^3 G_{II,\infty}}{\partial x^3} \right) \end{aligned} \quad (1.256)$$

Which we can simplify by

$$\begin{aligned} \frac{\partial^3 \mathcal{G}}{\partial x^3} &= \frac{\partial^3 G}{\partial x^3} G_{II,\infty}(g, t) \\ &+ 3 \left(\frac{\partial^2 G}{\partial x^2} \frac{\partial g}{\partial x} \frac{\partial G_{II,\infty}}{\partial x} + \frac{\partial G}{\partial x} \left(\frac{\partial^2 g}{\partial x^2} \frac{\partial G_{II,\infty}}{\partial x} + \left(\frac{\partial g}{\partial x} \right)^2 \frac{\partial^2 G_{II,\infty}}{\partial x^2} \right) \right) \\ &+ G \left(\frac{\partial^3 g}{\partial x^3} \frac{\partial G_{II,\infty}}{\partial x} \right) + G \left(3 \frac{\partial g}{\partial x} \frac{\partial^2 g}{\partial x^2} \frac{\partial^2 G_{II,\infty}}{\partial x^2} + \left(\frac{\partial g}{\partial x} \right)^3 \frac{\partial^3 G_{II,\infty}}{\partial x^3} \right) \end{aligned} \quad (1.257)$$

Evaluating the previous expression in $x = 1$, we obtain

$$\mathcal{M}_3 = M_3 + \bar{\nu}_{II,\infty} (M_2 m_1 + M_1 m_2) + \nu_{2,II,\infty} M_1 m_1^2 + \bar{\nu}_{II,\infty} m_3 + 2\nu_{2,II,\infty} m_1 m_2 + \nu_{3,II,\infty} m_1^3 \quad (1.258)$$

That is better to write

$$\boxed{\mathcal{M}_3 = M_3 + \bar{\nu}_{II,\infty} (M_2 m_1 + M_1 m_2 + m_3) + \nu_{2,II,\infty} (M_1 m_1^2 + 2m_1 m_2) + \nu_{3,II,\infty} m_1^3} \quad (1.259)$$

The expression of the simple moments as a function of the $(\mathcal{M}_i)_{i=1,2,3}$ is

$$\boxed{\mathbb{E}[N_{[t,T]}^3] = 6(\mathcal{M}_3(t) + \mathcal{M}_2(t)) + \mathcal{M}_1(t)} \quad (1.260)$$

The basics of these computations can be used in order to measure the margin to criticality in reactor cores, in accelerator driven system, in nuclear safeguards [PE08; Nag21].

In a more elaborated model [Sax17; SWE16; JEMSE18] et al. considered the time and space evolution of neutron using the backward master equations in order to compute the distributions of the number of neutrons detected in the presence of a source. In [MP22], the authors use a combination of low-order count probabilities and low-order statistical moments. This combination is optimal. They are useful in order to reconstruct distributions valid for all count number.

A classic approach is to consider the binomial cumulants and the Feynman moments.

1.6.3 Feynman moments

We will consider here the number of detections during $[0, t]$.

During the Manhattan Project Feynman et al. [FHS44; FHS56] suggest the use of what becomes the second order Feynman moments $Y_2(t)$ in order to determine the Diven factor of order 2. The key idea of this process is to consider the excess of relative variance to the mean of $N_{[0,t]}$.

$$Y_2(t) = \frac{\mathbb{E}[(N_{[0,t]} - \mathbb{E}[N_{[0,t]}])^2]}{\mathbb{E}[N_{[0,t]}]} - 1 \quad (1.261)$$

This quantity enables to characterize the system when there are fissile materials.

Neutrons are correlated when they belong to the same fission chain.

Since we want to identify the different parameters of the system, we can consider the variance excess compared to a Poisson law.

Then this quantity is null when the neutrons are not correlated.

The Feynman function can be generalized by considering the number $\Gamma_p(t)$ of combinations of p correlated neutrons.

Definition 1.6.46. *We introduce the following function*

$$\mathcal{K}_{Q_n(t)}(x) := \log \mathcal{G}(x, t) \quad (1.262)$$

We define the binomial cumulants as

$$\Gamma_p(t) := \frac{1}{p!} \left[\frac{\partial^p}{\partial x^p} \mathcal{K}_{Q_n(t)} \right]_{x=1}, \forall p \in \mathbb{N}^* \quad (1.263)$$

Then $\mathcal{K}_{Q_n(t)}(x)$ is the generating function of the factorial cumulants of the number of neutrons detected during a time gate t .

In our context, we will consider $\Gamma_1(t)$, $\Gamma_2(t)$ and $\Gamma_3(t)$.

Remark 1.6.47. *The $\Gamma_p(t)$ are the binomial cumulants of the number of detections.*

Since $\mathcal{G}(x, t) = G(x, t)G_{\Pi, \infty}(g(x, t))$, we can deduce

$$\mathcal{K} = \log \mathcal{G} = \log G + \log G_{\Pi, \infty}(g(x, t)) \quad (1.264)$$

Then we consider

$$\begin{aligned} K &= \log G \\ K_{\Pi, \infty} &= \log G_{\Pi, \infty} \end{aligned} \quad (1.265)$$

Then,

Definition 1.6.48. *We define*

$$Y_p(t) = \frac{p! \Gamma_p(t)}{\Gamma_1(t)} \quad (1.266)$$

Remark 1.6.49. *In practice, the Feynman factors of order greater than three are not commonly used because their measurements are too noisy. When the efficiency of the detector is high, the moment of order four can be considered.*

The analysis of the triples was introduced by [FI67].

The average detection number of correlated p -uples is calculated by integrating the one-initial source event moment with the source strength.

The Feynman moments can also be written using the centered moments

$$\begin{aligned} Y_2(t) &= \frac{\mu_2(t)}{\mu(t)} - 1 \\ Y_3(t) &= \frac{\mu_3(t)}{\mu(t)} - 1 - 3\left(\frac{\mu_2(t)}{\mu(t)} - 1\right) \end{aligned} \quad (1.267)$$

where

$$\begin{aligned} \mu(t) &:= \mathbb{E}[N_{[0,t]}] \\ \mu_2(t) &:= \mathbb{E}[(N_{[0,t]} - \mathbb{E}[N_{[0,t]}])^2] \\ \mu_3(t) &:= \mathbb{E}[(N_{[0,t]} - \mathbb{E}[N_{[0,t]}])^3] \end{aligned} \quad (1.268)$$

are the centered moments of order 1, 2 and 3 of $N_{[0,t]}$. We will use $Y_2(t)$ in order to refer to the Feynman moment of order 2, the Feynman moment of order 3 $Y_3(t)$ is also called X of Furuhashi.

Within the point model approximation, the Feynman moments can be written in closed form. In the point model approximation, in the case of a spontaneous fission source, during the stationary regime and for a time gate of duration t we have the following analytical expressions for Y_2 and Y_3 (from [FHS44] and [FI67])

$$\begin{aligned} Y_2(t) &= \frac{\varepsilon_F D_2}{\rho^2} \left(1 - x\rho \frac{\bar{\nu}_S D_{2S}}{\bar{\nu} D_2}\right) \left(1 - \frac{1 - e^{-\alpha t}}{\alpha t}\right) \\ Y_3(t) &= 3 \left(\frac{\varepsilon_F D_2}{-\rho^2}\right)^2 \left(1 - x\rho \frac{\bar{\nu}_S D_{2S}}{\bar{\nu} D_2}\right) \left(1 + e^{-\alpha t} - 2 \frac{1 - e^{-\alpha t}}{\alpha t}\right) \\ &\quad - \frac{\varepsilon_F^2 D_3}{\rho^3} \left(1 - x\rho \frac{\bar{\nu}_S D_{3S}}{\bar{\nu} D_3}\right) \left(1 - \frac{3 - 4e^{-\alpha t} + 2e^{-2\alpha t}}{2\alpha t}\right) \end{aligned} \quad (1.269)$$

Furuashi and Izumi extended the notion to the order 3 using the factorial cumulants of the neutron counts distribution. We can define

$$\begin{aligned} Y_{2,\infty} &:= \frac{\varepsilon_F D_2}{\rho^2} \left(1 - x\rho \frac{\bar{\nu}_S D_{2S}}{\bar{\nu} D_2} \right) \\ Y_{3,\infty} &:= 3 \left(\frac{\varepsilon_F D_2}{-\rho^2} \right)^2 \left(1 - x\rho \frac{\bar{\nu}_S D_{2S}}{\bar{\nu} D_2} \right) - \frac{\varepsilon_F^2 D_3}{\rho^3} \left(1 - x\rho \frac{\bar{\nu}_S D_{3S}}{\bar{\nu} D_3} \right) \end{aligned} \quad (1.270)$$

Remark 1.6.50. *Furuashi et al. [FI67] developed Y_3 taking into account the delayed neutrons.*

The Binomial moments M_p can be calculated from the binomial cumulants Γ_n by using the Panjer recurrence formula [Pan81; SJ81] applied to compound Poisson distributions. Factorial moments can also be used as in [Bö85], that was corrected by [PEP09].

1.6.4 Panjer formula

For $\Gamma_p(t)$

Starting from the equation

$$\frac{\partial G}{\partial x}(x, t) = \left\{ \int_t^T S \frac{\partial g_F}{\partial x} ds \right\} G(x, t) \quad (1.271)$$

Using a Taylor formula in $x = 1$ of the generating function G in order to obtain the moments, we dispose of

$$\begin{aligned} \frac{\partial}{\partial x} \left(\sum_{n=0}^{\infty} (x-1)^n M_n \right) &= \int_t^T S \left(\frac{\partial}{\partial x} \sum_{p=1}^{\infty} (x-1)^p m_p^F \right) dt \sum_{q=0}^{\infty} (x-1)^q M_q \\ \sum_{n=1}^{\infty} n(x-1)^{n-1} M_n &= \left(\sum_{p=1}^{\infty} p(x-1)^{p-1} \Gamma_p \right) \sum_{q=0}^{\infty} (x-1)^q M_q = \sum_{p=1}^{\infty} p(x-1)^{p-1} \Gamma_p \sum_{q=0}^{\infty} (x-1)^q M_q \\ \sum_{n=1}^{\infty} \binom{n}{n} M_n (x-1)^{n-1} &= \sum_{n=1}^{\infty} \left(\sum_{p=1}^n p \Gamma_p M_{n-p} \right) (x-1)^{n-1} \end{aligned} \quad (1.272)$$

By identification the general term of the power series, we conclude that

$$\boxed{nM_n = \sum_{p=1}^n \Gamma_p M_{n-p}} \quad (1.273)$$

Using this formula we can express the Feynman moments in function of the M_j .

$$\begin{aligned} M_0 &= 1 \\ M_1 &= \Gamma_1 \\ 2M_2 &= \Gamma_1 M_1 + 2\Gamma_2 \\ 3M_3 &= \Gamma_2 M_1 + 2\Gamma_2 M_1 + 3\Gamma_3 \end{aligned} \quad (1.274)$$

Then we conclude

$$\begin{aligned} Y_2 &= 2 \frac{\Gamma_2}{\Gamma_1} = 2 \frac{M_2}{M_1} - M_1 \\ Y_3 &= 6 \frac{\Gamma_3}{\Gamma_1} = 6 \frac{M_3}{M_1} - 6M_2 + 2M_1^2 \end{aligned} \tag{1.275}$$

We can get use of more detailed models by using 3D Monte Carlo transport codes like MCNP-6 or Tripoli-4.

1.7 Uncertainty quantification and inverse problems

Uncertainty quantification will be used in order to tackle the inverse problem. These techniques are at the interface of probability, statistics and numerical analysis. [Gar17; Sul15] are good sources of these developments.

Here, two sources of error can be considered: the noise measurements and the model imperfection. These errors cause variations in the outputs, and in general they are of the same order of magnitude. This can be explained by improvements in measurement techniques and theoretical knowledge of physical phenomena; measurement techniques are used to improve knowledge about the model and conversely knowledge of the model enables for more accurate measurement tools. All of this is explained in 1.3 part of [Tar05].

A direct problem is defined as follows

Definition 1.7.1. *Given an input $\mathbf{p} \in \mathcal{P}$ of a model $\mathbf{M} : \mathcal{P} \mapsto \mathcal{Y}$, we obtain \mathbf{y} the observations such that*

$$\mathbf{y} = \mathbf{M}(\mathbf{p}) \tag{1.276}$$

In the context of this work the direct problem we consider is 3.6.

An inverse problem is the reciprocal of the direct problem [Sul15]

Definition 1.7.2. *Given the observations \mathbf{y} , we want to determine the input \mathbf{p}^* of the model \mathbf{M} such that*

$$\mathbf{y} = \mathbf{M}(\mathbf{p}^*) \tag{1.277}$$

According to Hadamard, a problem is said ill-posed when one of the following statements occurs

- The solution does not exist
- The solution is not unique
- The solution depends discontinuously on the observations (An arbitrary small perturbation of the observations can cause an arbitrary large perturbation of the solution)

In many physical applications, the inverse problem is ill-posed, especially in our case.

We now assume the detector provided $\mathbf{y}_{obs} \in \mathcal{Y}$. Then the problem can be reformulated as minimizing of the square norm

$$\underset{\mathbf{p} \in \mathcal{P}}{\operatorname{argmin}} \|\mathbf{y}_{obs} - \mathbf{M}(\mathbf{p})\|^2 \quad (1.278)$$

In neutron noise measurements, the detector provides noisy observations $\mathbf{y}_{obs} \in \mathcal{Y}$. The number of neutrons detected during a time gate t is $N_{[0,t]}$, the associated vector of the model is

$$\mathbf{M}(\mathbf{p}) = \begin{pmatrix} \mathbb{E}[N_{[0,t]}] \\ \mathbb{E}[N_{[0,t]}^2] \\ \mathbb{E}[N_{[0,t]}^3] \end{pmatrix}$$

we define the covariance matrix of the observations

Definition 1.7.3. *The covariance matrix of $(N_{[0,t]}^k)_{k=1,3}$ is*

$$\mathbf{Cov}(\mathbf{p}) := \begin{pmatrix} \mathbb{E}[N^2] - \mathbb{E}[N]^2 & \mathbb{E}[N^3] - \mathbb{E}[N]\mathbb{E}[N^2] & \mathbb{E}[N^4] - \mathbb{E}[N]\mathbb{E}[N^3] \\ \mathbb{E}[N^3] - \mathbb{E}[N]\mathbb{E}[N^2] & \mathbb{E}[N^4] - \mathbb{E}[N^2]^2 & \mathbb{E}[N^5] - \mathbb{E}[N^2]\mathbb{E}[N^3] \\ \mathbb{E}[N^4] - \mathbb{E}[N]\mathbb{E}[N^3] & \mathbb{E}[N^5] - \mathbb{E}[N^2]\mathbb{E}[N^3] & \mathbb{E}[N^6] - \mathbb{E}[N^3]^2 \end{pmatrix} \quad (1.279)$$

We made several measurements of $N_{[0,t]}$, then the observations are the vector of the empirical means

$$\mathbf{y}_{obs} = \begin{pmatrix} \widehat{\mathbb{E}[N_{[0,t]}]} \\ \widehat{\mathbb{E}[N_{[0,t]}^2]} \\ \widehat{\mathbb{E}[N_{[0,t]}^3]} \end{pmatrix} \quad (1.280)$$

where, for $n \in \mathbb{N}^*$,

$$\widehat{\mathbb{E}[N_{[0,t]}^j]} = \frac{1}{n} \sum_{l=1}^n N_{l,[0,t]}^j \quad (1.281)$$

The Central Limit theorem claims that, for n realisations of $N_{[0,t]}$

$$\mathbf{y}_{obs} \sim \mathcal{N}(\mathbf{M}(\mathbf{p}), \frac{1}{n} \mathbf{Cov}(\mathbf{p})) \quad (1.282)$$

So, we can deduce

$$\mathbf{y}_{obs} = \mathbf{M}(\mathbf{p}) + \eta \quad (1.283)$$

where $\eta \sim \mathcal{N}(\mathbf{0}, \frac{1}{n} \mathbf{Cov}(\mathbf{p}))$.

1.7.1 Tikhonov's regularisation from linear to non-linear

When the problem is linear ($\mathbf{p} \in \mathbb{R}^r$ and $\mathbf{y} \in \mathbb{R}^s$) it can be expressed as

$$\mathbf{M}\mathbf{p} = \mathbf{y} \quad (1.284)$$

where \mathbf{p} is the unknown, the classical method in order to solve this kind of problem is the least square [Tar05]

$$\underset{\mathbf{p}}{\operatorname{argmin}} \|\mathbf{y} - \mathbf{M}\mathbf{p}\|^2 \quad (1.285)$$

where $\|\cdot\|$ refers to the Euclidian norm. [Tar05] highlights the fact that the calculations of this method are simple despite a lack of robustness (the strong sensitivity to a few large errors in the set of data). Some pathological cases occur when the linear operator \mathbf{M} is not invertible or even ill-conditioned. Then there are plenty of solutions.

As explained in [Gar17; Sul15], we have

Theorem 1.7.4. *Set of solutions*

We define the set of solution \mathcal{S} of the problem 1.285, then

$$\mathbf{p} \in \mathcal{S} \text{ if, and only if, } \mathbf{M}^T(\mathbf{y} - \mathbf{M}\mathbf{p}) = \mathbf{0}$$

We need to define the pseudoinverse of a matrix.

Definition 1.7.5. *Let \mathbf{M} be a matrix of dimension $s \times r$ of rank r_k . The pseudoinverse can be defined by different manners*

$$\begin{aligned} \mathbf{M}^+ &= \lim_{\delta \rightarrow 0} (\mathbf{M}^T \mathbf{M} + \delta \mathbf{I})^{-1} \mathbf{M}^T, \\ \mathbf{M}^+ &= \mathbf{V} \Sigma^+ \mathbf{U}^T, \end{aligned} \quad (1.286)$$

where $\mathbf{U} \Sigma \mathbf{V}^T$ is the singular value decomposition of \mathbf{M} , so \mathbf{V} and \mathbf{U} are unitary matrices, and Σ is a rectangular diagonal matrix containing the singular values of \mathbf{M} in the diagonal $(\sigma_i)_{i=1, r_k}$; Σ^+ is the rectangular diagonal matrix with the values $(\frac{1}{\sigma_i})_{i=1}^{r_k}$ on the diagonal.

Then \mathcal{S} can be characterized by

Proposition 1.7.6. *Let \mathbf{M} be a matrix of dimension $s \times r$ of rank r_k . The set of solution of 1.285 is of the form*

$$\mathcal{S} = \left\{ \mathbf{M}^+ \mathbf{y} + \sum_{i=r_k+1}^r a_i \mathbf{v}_i, a_i \in \mathbb{R}, i = r_k + 1, \dots, r \right\} \quad (1.287)$$

where \mathbf{M}^+ is the pseudoinverse of \mathbf{M} and \mathbf{v}_i is the i -th column of \mathbf{V} , with $\mathbf{U} \Sigma \mathbf{V}^T$ the SVD decomposition of \mathbf{M} . This means that the set of solutions to the least-square problem is of the form $\mathbf{M}^+ \mathbf{y}$ plus an arbitrary vector that is in the kernel of \mathbf{M} .

The vector $\mathbf{M}^+ \mathbf{y}$ can be written in explicit form as a function of the SVD of \mathbf{M} by

$$\mathbf{M}^+ \mathbf{y} = \sum_{i=1}^{r_k} \frac{y_i}{\sigma_i} \mathbf{v}_i \quad (1.288)$$

where y_i are the coefficients of the decomposition of \mathbf{y} in the orthonormal basis \mathbf{u}_i (the columns of \mathbf{U})

$$\mathbf{y} = \sum_{i=1}^s y_i \mathbf{u}_i, y_i = \mathbf{y} \cdot \mathbf{u}_i \quad (1.289)$$

and then the residual error is

$$\|\mathbf{y} - \mathbf{M}\mathbf{p}\|^2 = \sum_{i=r_k+1}^s y_i^2 \quad (1.290)$$

Among all the solution to 1.285, we can choose one particular solution which is the one with minimal norm

Definition 1.7.7.

$$\mathbf{p}_{LS} := \underset{\mathbf{p} \in \mathcal{S}}{\operatorname{argmin}} \|\mathbf{p}\| \quad (1.291)$$

This solution is given by

$$\mathbf{p}_{LS} = \mathbf{M}^+ \mathbf{y} \quad (1.292)$$

When the vector \mathbf{y} comes from \mathbf{p}^* , $\mathbf{y} = \mathbf{M}\mathbf{p}^*$, then

$$\mathbf{p}_{LS} = \mathbf{M}^+ \mathbf{M}\mathbf{p}^* \quad (1.293)$$

Using the SVD of $\mathbf{M} = \mathbf{U}\Sigma\mathbf{V}^T$, by decomposing the \mathbf{p}^* in the basis of the columns of \mathbf{V}

$$\mathbf{p}^* = \sum_{i=1}^r p_i^* \mathbf{v}_i, \quad p_i^* = \mathbf{v}_i \cdot \mathbf{p}^* \quad (1.294)$$

then we have

$$\mathbf{p}_{LS} = \sum_{i=1}^{r_k} p_i^* \mathbf{v}_i \quad (1.295)$$

then the estimation error is

$$\|\mathbf{p}_{LS} - \mathbf{p}^*\|^2 = \sum_{i=r_k+1}^r (p_i^*)^2. \quad (1.296)$$

Hence, we cannot rebuild the components that are in the kernel of \mathbf{M} (which is coherent with the fact that they disappear in the observations). But we can build all the other components.

Now, we search a solution of the problem 1.285, but we observe

$$\mathbf{y}_{obs}^\eta = \mathbf{y} + \boldsymbol{\eta} \quad (1.297)$$

where $\boldsymbol{\eta}$ is a vector of noise. As an example, we will consider $\boldsymbol{\eta}$ as a vector of i.i.d. components, Gaussian centred and of variance σ_{mes} .

If we apply the formula 1.292, we find

$$\mathbf{p}_{LS}^\eta = \mathbf{M}^+ \mathbf{y}_{obs}^\eta \quad (1.298)$$

we would like to find $\mathbf{p}_{LS} = \mathbf{M}^+ \mathbf{y}$. We would like the error $\|\mathbf{p}_{LS}^\eta - \mathbf{p}_{LS}\|^2$ to be small when σ_{mes}^2 is small. This is not always true. The error is centred and of variance

$$\mathbb{E}[\|\mathbf{p}_{LS}^\eta - \mathbf{p}_{LS}\|^2] = \sum_{i=1}^{r_k} \frac{\sigma_{mes}^2}{\sigma_i^2} \quad (1.299)$$

This shows that when \mathbf{M} has small singular values then the quadratic error of estimation can be colossal.

To show this, we compute

$$\mathbb{E}[\|\mathbf{p}_{LS}^\eta - \mathbf{p}_{LS}\|^2] = \mathbb{E}[\|\mathbf{M}^+ \mathbf{y}\|^2] = \mathbb{E}\left[\sum_{i=1}^{r_k} \frac{(\mathbf{u}_i \cdot \boldsymbol{\eta})^2}{\sigma_i}\right] \quad (1.300)$$

But $\mathbf{U}\boldsymbol{\eta}$ is a centered Gaussian vector with covariance matrix $\sigma_{mes}^2 \mathbf{U}\mathbf{U}^T = \sigma_{mes}^2 \mathbf{I}$. The random variables $(\mathbf{u}_i \cdot \boldsymbol{\eta})_i$ are centered Gaussian with variance σ_{mes}^2 , which gives the result.

When the data comes from \mathbf{p}^* , $\mathbf{y} = \mathbf{M}\mathbf{p}^*$, then the error term contains a bias term and a variance term

$$\mathbb{E}[\|\mathbf{p}_{LS}^\eta - \mathbf{p}^*\|^2] = \|\mathbf{p}_{LS} - \mathbf{p}^*\|^2 + \mathbb{E}[\|\mathbf{p}_{LS}^\eta - \mathbf{p}_{LS}\|^2] \quad (1.301)$$

with

$$\|\mathbf{p}_{LS} - \mathbf{p}^*\|^2 = \sum_{i=r_k+1}^r (p_i^*)^2 \quad (1.302)$$

and

$$\mathbb{E}[\|\mathbf{p}_{LS}^\eta - \mathbf{p}_{LS}\|^2] = \sum_{i=1}^{r_k} \frac{\sigma_{mes}^2}{\sigma_i^2}. \quad (1.303)$$

This is not satisfactory.

In order to give priority to coherent solutions of the problem 1.285, we introduce a regularisation term in the minimisation of the norm: this is the regularisation of Tikhonov

$$\underset{\mathbf{p}}{\operatorname{argmin}} \|\mathbf{y} - \mathbf{M}\mathbf{p}\|^2 + \|\mathbf{R}\mathbf{p}\|^2 \quad (1.304)$$

the operator \mathbf{R} is often chosen as $\alpha \mathbf{Id}$. This improves the conditioning of the system and focuses on the solution with low norms. This operator represents the prior knowledge on what the solution should look like, e.g. the expert instructions.

Then the solution minimizing the norm is

$$\tilde{\mathbf{p}} = (\mathbf{M}^T \mathbf{M} + \mathbf{R}^T \mathbf{R})^{-1} \mathbf{M}^T \mathbf{y} \quad (1.305)$$

Remark 1.7.8. When the regularization matrix is vanishing (i.e. $\mathbf{R} \rightarrow 0$) we find the Moore-Penrose pseudoinverse [Sul15] bottom of page 95.

Now we provide some examples with linear problem.

Example: L^2 regularisation, the ridge regression. We set $\mathcal{P} = \mathbb{R}^r$ and $\mathcal{Y} = \mathbb{R}^s$, $\mathbf{M}(\mathbf{p}) = \mathbf{M}\mathbf{p}$ where \mathbf{M} is a $s \times r$ the matrix of rank r_k . Let $\alpha > 0$. We are looking for

$$\underset{\mathbf{p}}{\operatorname{argmin}} (\|\mathbf{y} - \mathbf{M}\mathbf{p}\|^2 + \alpha \|\mathbf{p}\|^2) \quad (1.306)$$

Since $\mathbf{M}^T \mathbf{M} + \alpha \mathbf{I}$ is positive definite, there is a unique solution to the minimization problem 1.306 denoted by

$$\hat{\mathbf{p}}_\alpha = (\mathbf{M}^T \mathbf{M} + \alpha \mathbf{I})^{-1} \mathbf{M}^T \mathbf{y} \quad (1.307)$$

Using the singular value decomposition of $\mathbf{M} = \mathbf{U}\Sigma\mathbf{V}^T$, where \mathbf{u}_i is the i -th column of \mathbf{U} , \mathbf{v}_i is the i -th column of \mathbf{V} and σ_i , called singular values, the eigenvalues of $\mathbf{M}\mathbf{M}^T$, then we obtain

$$\hat{\mathbf{p}}_\alpha = \sum_{i=1}^{r_k} \frac{\sigma_i}{\sigma_i^2 + \alpha} y_i \mathbf{v}_i, y_i = \mathbf{v}_i^T \mathbf{y} \quad (1.308)$$

When $\mathbf{y} = \mathbf{M}\mathbf{p}^*$ with $\mathbf{p}^* = \sum_i \mathbf{p}_i^* \mathbf{v}_i$, $\mathbf{p}_i^* = \mathbf{v}_i^T \mathbf{p}^*$, then $y_i = \sigma_i \mathbf{p}_i^*$. Then

$$\hat{\mathbf{p}}_\alpha - \mathbf{p}^* = \sum_{i=1}^{r_k} \frac{\alpha}{\sigma_i^2 + \alpha} \mathbf{p}_i^* \mathbf{v}_i \quad (1.309)$$

the correct solution is obtained when $\alpha = 0$.

When $\mathbf{y} = \mathbf{M}\mathbf{p}^* + \boldsymbol{\eta}$, with $\boldsymbol{\eta} \sim \mathcal{N}(0, \sigma_{mes}^2 \mathbf{I})$, then, we find

$$\hat{\mathbf{p}}_\alpha = \sum_{i=1}^{r_k} \frac{\alpha}{\sigma_i^2 + \alpha} \mathbf{p}_i^* \mathbf{v}_i + \sum_{i=1}^{r_k} \frac{\sigma_i}{\sigma_i^2 + \alpha} \boldsymbol{\eta}_i \mathbf{v}_i, \boldsymbol{\eta}_i = \mathbf{v}_i^T \boldsymbol{\eta} \quad (1.310)$$

As the $\boldsymbol{\eta}_i$ are i.i.d with law $\mathcal{N}(0, \sigma_{mes}^2)$

$$\begin{aligned} \mathbb{E}[\|\hat{\mathbf{p}}_\alpha - \mathbf{p}^*\|^2] &= \mathbb{E}[\|\hat{\mathbf{p}}_\alpha - \mathbb{E}[\hat{\mathbf{p}}_\alpha]\|^2] + \|\mathbb{E}[\hat{\mathbf{p}}_\alpha] - \mathbf{p}^*\|^2 \\ &= \sum_{i=1}^{r_k} \frac{\sigma_i^2}{(\sigma_i^2 + \alpha)^2} \sigma_{mes}^2 + \sum_{i=1}^{r_k} \frac{\sigma_i^2}{(\sigma_i^2 + \alpha)^2} (\mathbf{p}_i^*)^2 \end{aligned} \quad (1.311)$$

The variance term does not explode when the singular values are small, it is majored by $\frac{\rho \sigma_{mes}^2}{4\alpha}$ uniformly in $(\sigma_i)_{i=1}^{r_k}$.

Letting a little bias, we reduce drastically the variance.

We are looking for the α in order to minimize $\mathbb{E}[\|\hat{\mathbf{p}}_\alpha - \mathbf{p}^*\|^2]$

The optimal α depends on \mathbf{p}^* and \mathbf{M} , it exists and is strictly positive. This shows that regularization is profitable.

For the L^0 regularization, we dispose of

$$\|\mathbf{M}\mathbf{p} - \mathbf{y}\|^2 + \alpha \|\mathbf{p}\|_0 \quad (1.312)$$

where $\|\mathbf{p}\|_0 = \sum_{i=1}^{r_k} \mathbf{1}_{\mathbf{p}_i \neq 0}$. A solution is said sparse when $\|\mathbf{p}\|_0$ is small (cf. [Sul15] p. 97). We look for an optimal solution, which is also sparse. This kind of problems are numerically hard.

L^1 regularization, LASSO (Least Absolute Shrinkage and Selection Operator) regression [Tib96]

$$\|\mathbf{M}\mathbf{p} - \mathbf{y}\|^2 + \alpha \|\mathbf{p}\|_1 \quad (1.313)$$

with $\|\mathbf{p}\|_1 = \sum_{i=1}^{r_k} |\mathbf{p}_i|$ For some good matrices (with the restricted isometric property, RIP, see annexes A.1.2) the solution of the regularized L^1 problem is the same as for the L^0 one. This kind of problem is numerically hard but not impossible (in particular when the solution is sparse).

In practice, we choose α such that $\|\mathbf{y} - \mathbf{M}\hat{\mathbf{p}}_\alpha\|^2 \approx \mathbb{E}[\|\boldsymbol{\eta}\|^2] = s\sigma_{mes}^2$ we do not look for the adjustment of the model with a precision superior to the level of noise. This is called the Morozov's discrepancy principle (cf. [Sch93]).

The Bayesian viewpoint enables to get the distribution of the parameters \mathbf{p} given the observations \mathbf{y} , which is more interesting than the Tikhonov regularization, which only provide a point estimation. The research of the mode of this a posteriori distribution can be reformulated by a minimization problem of a regularized square norm minimization. The Bayesian approach enables how to consider the penalization term, and to refine the results by giving more information on the structure of the solution.

1.7.2 Bayesian inverse problems

We consider two finite dimension spaces ¹ $\mathcal{P} = \mathbb{R}^r$ and $\mathcal{Y} = \mathbb{R}^s$ and we have some a priori information about the parameters whose a priori distribution is μ_0 .

We are still in the context of noisy observations

$$\mathbf{y}_{obs} = \mathbf{M}(\mathbf{p}) + \eta \quad (1.314)$$

The modelling of the problem may lead to different points of view.

Gaussian case

We dispose here of $\mathcal{P} = \mathbb{R}^r$ and $\mathcal{Y} = \mathbb{R}^s$. Moreover, we suppose that the a priori distribution μ_0 of the parameters \mathbf{p} is Gaussian $\mathcal{N}(\mathbf{m}_0, \Sigma_0)$ and that the random variable η which represents the observation noise

$$\mathbf{y}_{obs} = \mathbf{M}(\mathbf{p}) + \eta \quad (1.315)$$

also has a Gaussian law $\mathcal{N}(\mathbf{0}, \Gamma)$, where Γ is an invertible matrix. The Bayes' theorem states that the a posteriori distribution of the parameters \mathbf{p} knowing the observations \mathbf{y}_{obs} has the form

$$\mu_{\mathbf{y}}(\mathbf{p}|\mathbf{y}_{obs}) \approx \exp\left(-\frac{1}{2}\|\mathbf{y}_{obs} - \mathbf{M}(\mathbf{p})\|_{\Gamma}^2 - \frac{1}{2}\|\mathbf{p} - \mathbf{m}_0\|_{\Sigma_0}^2\right) \quad (1.316)$$

where $\|\mathbf{y}\|_{\Gamma}^2 := \mathbf{y}^T \Gamma^{-1} \mathbf{y}$. We remark in the general case the a posteriori distribution is not Gaussian, except when the model \mathbf{M} is linear.

If we focus on the mode of the a posteriori distribution, which is the most likely value of \mathbf{p} , then we find the maximum a posteriori.

$$\underset{\mathbf{p}}{\operatorname{argmin}} \|\mathbf{y}_{obs} - \mathbf{M}(\mathbf{p})\|_{\Gamma}^2 + \|\mathbf{p} - \mathbf{m}_0\|_{\Sigma_0}^2 \quad (1.317)$$

We get back the minimization problem of regularized mean square. Moreover, the Bayesian formulation provides more than the MAP. The a posteriori distribution can

¹The infinite dimensional case can be found in [Tar05]

sometimes be computed and explicitly characterized (as example when \mathbf{M} is linear as we will see below), but it is also possible to sample μ_y by a MCMC technique (as example Metropolis-Hastings) easily, because we dispose of an expression of its distribution up to a multiplicative constant.

Under determined problem

We take into account $\mathcal{P} = \mathbb{R}^r$ and $\mathcal{Y} = \mathbb{R}$ with $r > 1$, and the observations are in the form

$$y_{obs} = \mathbf{M}^T \mathbf{p} + \eta \quad (1.318)$$

for some $\mathbf{M} \in \mathbb{R}^r$. We suppose the noise Gaussian $\eta \sim \mathcal{N}(\mathbf{0}, \gamma^2)$ and $\mu_0 \sim \mathcal{N}(\mathbf{0}, \boldsymbol{\Sigma}_0)$. Then $\mu_y \sim \mathcal{N}(\mathbf{m}_y, \boldsymbol{\Sigma})$ and

$$\mathbf{m}_y = \frac{y_{obs}}{\gamma^2 + \mathbf{M}^T \boldsymbol{\Sigma}_0 \mathbf{M}} \boldsymbol{\Sigma}_0 \mathbf{M}, \quad \boldsymbol{\Sigma} = \boldsymbol{\Sigma}_0 - \frac{1}{\gamma^2 + \mathbf{M}^T \boldsymbol{\Sigma}_0 \mathbf{M}} \boldsymbol{\Sigma}_0 \mathbf{M} (\boldsymbol{\Sigma}_0 \mathbf{M})^T \quad (1.319)$$

When the observation noise gets small

$$\begin{aligned} \mathbf{m}_y^+ &= \lim_{\gamma \rightarrow 0} \mathbf{m}_y = \frac{y_{obs}}{\mathbf{M}^T \boldsymbol{\Sigma}_0 \mathbf{M}} \boldsymbol{\Sigma}_0 \mathbf{M}, \\ \boldsymbol{\Sigma}^+ &= \lim_{\gamma \rightarrow 0} \boldsymbol{\Sigma} = \boldsymbol{\Sigma}_0 - \frac{1}{\mathbf{M}^T \boldsymbol{\Sigma}_0 \mathbf{M}} \boldsymbol{\Sigma}_0 \mathbf{M} (\boldsymbol{\Sigma}_0 \mathbf{M})^T \end{aligned} \quad (1.320)$$

We obtain $\boldsymbol{\Sigma}^+ \mathbf{M} = \mathbf{0}$ and $\mathbf{m}_y^+ \mathbf{M} = y_{obs}$. The fact that $\boldsymbol{\Sigma}^+ \mathbf{M} = \mathbf{0}$ shows that the knowledge on \mathbf{p} in the direction of \mathbf{M} becomes certain. In the direction non-collinear to \mathbf{M} , the uncertainty remains, with a degree that is determined by an interaction between the properties of the prior and the observation operator.

Over determined problem

We take into account $\mathcal{P} = \mathbb{R}$ and $\mathcal{Y} = \mathbb{R}^s$ with $s > 1$, and the observations are in the form

$$\mathbf{y}_{obs} = \mathbf{M} \mathbf{p} + \eta \quad (1.321)$$

for some $\mathbf{M} \in \mathbb{R}^s$. We suppose the noise Gaussian $\eta \sim \mathcal{N}(\mathbf{0}, \gamma^2 \mathbf{I})$ and $\mu_0 \sim \mathcal{N}(0, \sigma_0^2)$. Then $\mu_y \sim \mathcal{N}(m_y, \sigma)$ and

$$m_y = \frac{\mathbf{M}^T \mathbf{y}}{\gamma^2 \sigma_0^{-2} + \|\mathbf{M}\|^2}, \quad \sigma^2 = \frac{\gamma^2}{\gamma^2 \sigma_0^{-2} + \|\mathbf{M}\|^2} \quad (1.322)$$

When the observation noise gets small

$$m_y^+ = \lim_{\gamma \rightarrow 0} m_y = \frac{\mathbf{M}^T \mathbf{y}}{\|\mathbf{M}\|^2}, \quad (\sigma^+)^2 = \lim_{\gamma \rightarrow 0} \sigma^2 = 0 \quad (1.323)$$

The point m_y^+ is the solution of the mean square error of the linear overdetermined problem $\mathbf{y} = \mathbf{M} \mathbf{p}$

$$m_y^+ = \underset{p \in \mathbb{R}}{\operatorname{argmin}} \|\mathbf{y} - \mathbf{M} \mathbf{p}\|^2 \quad (1.324)$$

Equilibrated problem

We suppose that $\mathcal{P} = \mathbb{R}^r = \mathcal{Y}$. Moreover, we consider $\mathbf{M} \in \mathcal{C}^2(\mathbb{R}^r, \mathbb{R}^r)$ and the equation $\mathbf{y} = \mathbf{M}(\mathbf{p})$ has a unique solution $\mathbf{p} = \mathbf{N}(\mathbf{y})$. Moreover, there exists $C > 0$ such that $\forall \mathbf{y}, \delta \in \mathbb{R}^r$

$$\|\mathbf{y} - \mathbf{M}(\mathbf{N}(\mathbf{y}) + \delta)\|^2 \geq C \min(1, \|\delta\|^2) \quad (1.325)$$

We suppose the a priori to be Gaussian $\mu_0 \sim \mathcal{N}(\mathbf{m}_0, \sigma_0)$ and the noise of observation to be $\eta \sim \mathcal{N}(\mathbf{0}, \gamma^2 \mathbf{I})$

When noise of observation tends to zero, the a posteriori distribution converges weakly to $\delta_{\mathbf{N}(\mathbf{y})}$ when $\gamma \rightarrow 0$. The uncertainty disappears, and the prior as no influence. More information at page 202 of [Tar05].

Linear case

We assume $\mathcal{P} = \mathbb{R}^r$ and $\mathcal{Y} = \mathbb{R}^s$. Moreover, we consider the model to be linear $\mathbf{M} \in \mathcal{M}_{r,s}$ and the observations are

$$\mathbf{y} = \mathbf{M}\mathbf{p} + \eta \quad (1.326)$$

We assume the observation noise is centered and of covariance Γ (we do not suppose the noise to be Gaussian). We want to establish a link between the mean square problem and the estimation of \mathbf{p} knowing \mathbf{y} . We begin by characterizing the best estimator of \mathbf{p} knowing the observations \mathbf{y} . The following definition defines what the best linear unbiased estimator (BLUE) is

Definition 1.7.9. *Best Linear Unbiased Estimator* The BLUE (Best Linear Unbiased Estimator) is, among the linear unbiased estimators of \mathbf{p} knowing \mathbf{y} , the one that minimizes the mean square error $\mathbb{E}[\|\hat{\mathbf{p}} - \mathbf{p}\|^2]$.

Then we have the following property

Proposition 1.7.10. *Best Linear Unbiased Estimator*

When $\mathbf{M}^T \Gamma^{-1} \mathbf{M}$ is invertible, the best linear unbiased estimator of \mathbf{p} given \mathbf{y} is given by

$$\hat{\mathbf{p}} = (\mathbf{M}^T \Gamma^{-1} \mathbf{M})^{-1} \mathbf{M}^T \mathbf{y} \quad (1.327)$$

This estimator has for covariance matrix

$$\mathbb{E}[(\mathbf{p} - \hat{\mathbf{p}})^T (\mathbf{p} - \hat{\mathbf{p}})] = (\mathbf{M}^T \Gamma^{-1} \mathbf{M})^{-1} \quad (1.328)$$

Proof. First, we check the estimator 1.327 is unbiased

$$\mathbb{E}[\hat{\mathbf{p}}] = (\mathbf{M}^T \Gamma^{-1} \mathbf{M})^{-1} \mathbf{M}^T \Gamma^{-1} \mathbf{M} \mathbf{p} = \mathbf{p} \quad (1.329)$$

and its covariance matrix is 1.328

$$\mathbb{E}[(\hat{\mathbf{p}} - \mathbf{p})(\hat{\mathbf{p}} - \mathbf{p})^T] = ((\mathbf{M}^T \Gamma^{-1} \mathbf{M})^{-1} \mathbf{M}^T \Gamma^{-1}) \Gamma ((\mathbf{M}^T \Gamma^{-1} \mathbf{M})^{-1} \mathbf{M}^T \Gamma^{-1})^T \quad (1.330)$$

Then, we take into account an arbitrary linear estimator $\check{\mathbf{p}} = \mathbf{L}\mathbf{y}$, and we write $\mathbf{L} = (\mathbf{M}^T \Gamma^{-1} \mathbf{M})^{-1} \mathbf{M}^T \Gamma^{-1} + \mathbf{R}$. If we suppose that this estimator is unbiased, then we would have $\mathbf{R}\mathbf{M} = 0$. The covariance matrix of $\check{\mathbf{p}}$ is:

$$\begin{aligned} \mathbb{E}[(\hat{\mathbf{p}} - \mathbf{p})(\hat{\mathbf{p}} - \mathbf{p})^T] &= \mathbf{L}\Gamma\mathbf{L}^T \\ &= (\mathbf{M}^T \Gamma^{-1} \mathbf{M})^{-1} + (\mathbf{M}^T \Gamma^{-1} \mathbf{M})^{-1} \mathbf{M}^T \Gamma^{-1}) \Gamma \mathbf{R}^T \\ &\quad + \mathbf{R} \Gamma ((\mathbf{M}^T \Gamma^{-1} \mathbf{M})^{-1} \mathbf{M}^T \Gamma^{-1})^T + \mathbf{R} \Gamma \mathbf{R}^T \end{aligned} \quad (1.331)$$

As $\mathbf{R}\mathbf{M} = 0$,

$$(\mathbf{M}^T \Gamma^{-1} \mathbf{M})^{-1} \mathbf{M}^T \Gamma^{-1}) \Gamma \mathbf{R}^T = \mathbf{M}^T \Gamma^{-1} \mathbf{M})^{-1} \mathbf{M}^T \mathbf{R}^T = \mathbf{M}^T \Gamma^{-1} \mathbf{M})^{-1} (\mathbf{R}\mathbf{M})^T = 0, \quad (1.332)$$

and then

$$\mathbb{E}[(\hat{\mathbf{p}} - \mathbf{p})(\hat{\mathbf{p}} - \mathbf{p})^T] = (\mathbf{M}^T \Gamma^{-1} \mathbf{M})^{-1} + \mathbf{R} \Gamma \mathbf{R}^T. \quad (1.333)$$

As $\mathbf{R} \Gamma \mathbf{R}^T$ is a positive semi-definite matrix, we have $\mathbb{E}[(\hat{\mathbf{p}} - \mathbf{p})(\hat{\mathbf{p}} - \mathbf{p})^T] \geq (\mathbf{M}^T \Gamma^{-1} \mathbf{M})^{-1}$. Then using the trace we obtain

$$\mathbb{E}[|\hat{\mathbf{p}} - \mathbf{p}|^2] = \text{Tr}(\mathbb{E}[(\hat{\mathbf{p}} - \mathbf{p})(\hat{\mathbf{p}} - \mathbf{p})^T]) = \text{Tr}((\mathbf{M}^T \Gamma^{-1} \mathbf{M})^{-1}) + \text{Tr}(\mathbf{R} \Gamma \mathbf{R}^T) \quad (1.334)$$

the last term is positive since it is the sum of the eigenvalues of a positive definite matrix and a positive semi-definite matrix. \square

This implies that the BLUE exists and is unique, minimizes also $\mathbb{E}_{\mathbf{p}}[|\hat{\mathbf{p}} - \mathbf{p}|^2]$.

The following proposition makes the link between the linear inverse problem and the minimisation of the normal equations of a weighted mean square problem.

Proposition 1.7.11. *Let $\mathbf{M} \in \mathcal{M}_{r,s}$ and $\Gamma \in \mathcal{M}_{r,r}$ be the invertible covariance matrix. We define*

$$J(\mathbf{p}) = \frac{1}{2} \|\mathbf{M}\mathbf{p} - \mathbf{y}\|_{\Gamma}^2 \quad (1.335)$$

$$\hat{\mathbf{p}} \in \underset{\mathbf{p} \in \mathbb{R}^r}{\text{argmin}} J(\mathbf{p}) \text{ iff } (\mathbf{M}^T \Gamma^{-1} \mathbf{M}) \hat{\mathbf{p}} = \mathbf{M}^T \mathbf{y} \quad (1.336)$$

Proof. If $\hat{\mathbf{p}}$ is a minimiser of the quadratic form $J(\mathbf{p})$ then it is a critical point. However,

$$J(\mathbf{p}) = \frac{1}{2} (\mathbf{p}^T \mathbf{M}^T \Gamma^{-1} \mathbf{M} \mathbf{p} - 2 \mathbf{p}^T \mathbf{M}^T \Gamma^{-1} \mathbf{y} + \mathbf{y}^T \Gamma^{-1} \mathbf{y}), \quad (1.337)$$

then

$$\nabla J(\mathbf{p}) = \mathbf{M}^T \Gamma^{-1} \mathbf{M} \mathbf{p} - \mathbf{M}^T \Gamma^{-1} \mathbf{y}, \quad (1.338)$$

what concludes the direct reasoning. Conversely, when $\hat{\mathbf{p}}$ satisfies the normal equations, then

$$\begin{aligned} \forall \mathbf{q}, J(\hat{\mathbf{p}} + \mathbf{q}) &= \frac{1}{2} ((\hat{\mathbf{p}} + \mathbf{q})^T \mathbf{M}^T \Gamma^{-1} \mathbf{M} (\hat{\mathbf{p}} + \mathbf{q}) - 2(\hat{\mathbf{p}} + \mathbf{q})^T \mathbf{M}^T \Gamma^{-1} \mathbf{y} + \mathbf{y}^T \Gamma^{-1} \mathbf{y}) \\ &= \hat{\mathbf{p}}^T \mathbf{M}^T \Gamma^{-1} \mathbf{M} \hat{\mathbf{p}} + \mathbf{q}^T \mathbf{M}^T \Gamma^{-1} \mathbf{M} \mathbf{q} + \mathbf{y}^T \Gamma^{-1} \mathbf{y} \\ &= \frac{1}{2} \|\mathbf{M}\mathbf{p}\|^2 + J(\hat{\mathbf{p}}) \end{aligned} \quad (1.339)$$

which is always greater than $J(\hat{\mathbf{p}})$, what proves the reciprocal. \square

Combining the two previous results, we obtain the Gauss-Markov theorem:

Theorem 1.7.12. *Under the condition of the Proposition 1.7.10 the BLUE $\hat{\mathbf{p}}$ given by 1.327 is the estimator of the mean square*

$$\hat{\mathbf{p}} = \underset{\mathbf{p} \in \mathbb{R}^r}{\operatorname{argmin}} J(\mathbf{p}), \quad J(\mathbf{p}) = \frac{1}{2} \|\mathbf{y} - \mathbf{M}\mathbf{p}\|_{\Gamma}^2 \quad (1.340)$$

Finally, we underline the gradient and the Hessian of $J(\mathbf{p})$ are

$$\begin{aligned} \nabla J(\mathbf{p}) &= \mathbf{M}^T \Gamma^{-1} \mathbf{M} \hat{\mathbf{p}} - \mathbf{M}^T \mathbf{y}, \\ \nabla \otimes \nabla J(\mathbf{p}) &= \mathbf{M}^T \Gamma^{-1} \mathbf{M}, \end{aligned} \quad (1.341)$$

We can notice the second identity claims that the inverse of the Hessian matrix of J is the inverse of the covariance matrix of the BLUE 1.328.

In the case where $\mathbf{M}^T \Gamma^{-1} \mathbf{M}$ is not invertible, then we use the estimator

$$\hat{\mathbf{p}} = (\mathbf{M}^T \Gamma^{-1} \mathbf{M})^+ \mathbf{M}^T \Gamma^{-1} \mathbf{y}, \quad (1.342)$$

where \mathbf{N}^+ is the pseudoinverse of \mathbf{N} . However this solution has some disadvantages such as instability.

Linear and Gaussian case

We assume the observation noise to be Gaussian $\eta \sim \mathcal{N}(\mathbf{0}, \Gamma)$ with an invertible covariance matrix Γ . When $\mathbf{M}^T \Gamma^{-1} \mathbf{M}$ is not invertible or is invertible but ill-conditioned, we need an a priori law μ_0 on \mathbf{p} in order to regularize the problem.

Proposition 1.7.13. *We suppose the observation noise to be Gaussian and the prior Gaussian, with invertible covariance matrix. Then the a posteriori law $\mu_{\mathbf{y}}$ on \mathbf{p} knowing \mathbf{y} is $\mathcal{N}(\mathbf{m}_{\mathbf{y}}, \Sigma)$ with*

$$\begin{aligned} \mathbf{m}_{\mathbf{y}} &= (\mathbf{M}^T \Gamma^{-1} \mathbf{M} + \Sigma_0)^{-1} (\mathbf{M}^T \Gamma^{-1} \mathbf{y} + \Sigma_0^{-1} \mathbf{m}_0^{-1}) \\ \Sigma &= (\mathbf{M}^T \Gamma^{-1} \mathbf{M} + \Sigma_0^{-1})^{-1} \end{aligned} \quad (1.343)$$

In an equivalent manner, we can reformulate the result with the Woodbury formula (see linear algebra dedicated annexes A.8).

Proof. $\mu_{\mathbf{y}}$ has for density

$$\pi_{\mathbf{y}}(\mathbf{p}) \approx \exp\left(-\frac{1}{2} \|\mathbf{y} - \mathbf{M}\mathbf{p}\|_{\Gamma}^2 - \frac{1}{2} \|\mathbf{p} - \mathbf{m}_0\|_{\Sigma_0}^2\right) \quad (1.344)$$

Developing the square we find the argument of the exponential is a quadratic form in \mathbf{p} we can put in the form (up to a multiplicative constant):

$$\pi_{\mathbf{y}}(\mathbf{p}) \approx \exp\left(-\frac{1}{2} \|\mathbf{p} - \mathbf{m}_{\mathbf{y}}\|_{\Sigma}^2\right) \quad (1.345)$$

□

The best estimator of \mathbf{p} (in the sense it is unbiased, and it minimizes the mean square error among all of the estimators of \mathbf{p}) is the BLUE

$$\hat{\mathbf{p}} = \mathbf{m}_y. \quad (1.346)$$

It is a consequence of the Gaussian nature of the joint law of (\mathbf{p}, \mathbf{y}) (which comes from the Gaussian nature of the a priori distributions and the observations) that the conditional expectation of \mathbf{p} knowing \mathbf{y} (which provides the best estimator) is linear in \mathbf{y} , see A.1.4, and that is also the mode of the a posteriori distribution, i.e. the MAP:

$$\hat{\mathbf{p}} = \underset{\mathbf{p} \in \mathbb{R}^r}{\operatorname{argmin}} \frac{1}{2} \|\mathbf{y} - \mathbf{M}\mathbf{p}\|_{\Gamma}^2 + \frac{1}{2} \|\mathbf{p} - \mathbf{m}_0\|_{\Sigma_0}^2 \quad (1.347)$$

We examine what the a posteriori distribution μ_y becomes when the observation noise becomes tiny. We recall \mathbf{p} refers to the parameters.

If $r \geq s$ and $\operatorname{Ker}(\mathbf{M}) = \{0\}$ (over-determined problem case), and if $\Gamma = \gamma^2 \Gamma_0$, then μ_y converges weakly to $\delta_{\mathbf{m}_y^+}$ when $\gamma \rightarrow 0$ with

$$\mathbf{m}_y^+ = \underset{\mathbf{p} \in \mathbb{R}^r}{\operatorname{argmin}} \|\mathbf{y} - \mathbf{M}\mathbf{p}\|_{\Gamma_0}^2 \quad (1.348)$$

The uncertainty disappears and the prior do not play any role.

If $s \leq r$ (under-determined problem), $\mathbf{M} \in \mathcal{M}_{r,s}$ of rank r , and $\Gamma = \gamma^2 \Gamma_0$, then it exists an invertible matrix $\mathbf{M}_0 \in \mathcal{M}_{r,r}$ and an orthogonal matrix $\mathbf{Q} \in \mathcal{M}_{s,s}$ such that

$$\mathbf{M} = (\mathbf{M}_0 \ \mathbf{0})\mathbf{Q}^T \quad (1.349)$$

The matrix \mathbf{Q} is in the form $\mathbf{Q} = (\mathbf{Q}_1 \ \mathbf{Q}_2)$ with \mathbf{Q}_2^T projection on $\mathcal{O} = \operatorname{Ker}(\mathbf{M})$ and projection on \mathcal{O}^\perp . We write

$$\mathbf{Q}^T \Sigma_0^{-1} \mathbf{Q} = \begin{pmatrix} \mathbf{L}_{1,1} & \mathbf{L}_{1,2} \\ \mathbf{L}_{1,2}^T & \mathbf{L}_{2,2} \end{pmatrix} \quad (1.350)$$

Then μ_y converges weakly to $\mathcal{N}(\mathbf{m}_y^+, \Sigma^+)$ when $\gamma \rightarrow 0$, when

$$\mathbf{m}_y^+ = \mathbf{Q} \begin{pmatrix} \mathbf{z} \\ \mathbf{z}' \end{pmatrix}, \quad \Sigma^+ = \mathbf{Q}_2 \mathbf{L}_{2,2}^{-1} \mathbf{Q}_2^T, \quad (1.351)$$

$\mathbf{z} = \mathbf{Q}_1^T \mathbf{M}_0^{-1} \mathbf{y}$, and $\mathbf{z}' = -\mathbf{L}_{2,2}^{-1} \mathbf{L}_{1,2}^T \mathbf{z} + \mathbf{L}_{2,2}^{-1} \mathbf{Q}_2^T \Sigma_0^{-1} \mathbf{m}_0$. In a more equivalent manner, one can claim μ_y converges weakly to $\delta_{\mathbf{z}} \otimes \mathcal{N}(\mathbf{z}', \mathbf{L}_{2,2}^{-1})$ which is a probability distribution on $\mathcal{O} \oplus \mathcal{O}^\perp$. This shows that, in the limit of a small observation noise, we can determine with certainty the solution in \mathcal{O}^\perp , but uncertainty remains in \mathcal{O} .

Moreover, the prior plays a role in the a posteriori distribution in this limit.

In the context of neutron noise measurements, we dispose of the observations $\hat{\mathbf{M}}$ which are the estimated moments of $N_{[0,t]}$. Moreover, the Bayes theorem [Tar05] states

$$\underset{\text{a posteriori distribution}}{\mathbb{P}(\mathbf{p}|\hat{\mathbf{M}})} \propto \underset{\text{likelihood}}{\mathbb{P}(\hat{\mathbf{M}}|\mathbf{p})} \underset{\text{a priori distribution}}{\mathbb{P}(\mathbf{p})} \quad (1.352)$$

where the likelihood and the a priori distribution are as follows

1. Thanks to the CLT, given the parameter \mathbf{p} the measures are Gaussian with mean $\mathbf{M}(\mathbf{p})$ and covariance $\frac{1}{n}\mathbf{Cov}(\mathbf{p})$ where \mathbf{M} refers to the expression of the exact simple moments of the distribution of $N_{[0,t]}$, $\mathbf{Cov}(\mathbf{p})$ the covariance matrix of the three first simple moments, n the number of realizations.

This gives explicitly

$$\mathbb{P}(\hat{\mathbf{M}}|\mathbf{p}) \propto \frac{1}{\sqrt{\det(\frac{1}{n}\mathbf{Cov}(\mathbf{p}))}} e^{-\frac{1}{2} {}^t(\hat{\mathbf{M}}-\mathbf{M}(\mathbf{p}))\mathbf{Cov}(\mathbf{p})^{-1}(\hat{\mathbf{M}}-\mathbf{M}(\mathbf{p}))n} \quad (1.353)$$

which is the expression of the likelihood up to a multiplicative constant. The computation of $\mathbf{Cov}(\mathbf{p})$ needs the expression of the simple moments up to the order 6, and this is too complex to be computed analytically. So we will use the empirical covariance matrix $\widehat{\mathbf{Cov}}$.

$$\tilde{\mathbb{P}}(\hat{\mathbf{M}}|\mathbf{p}) \propto \frac{1}{\sqrt{\det(\frac{1}{n}\widehat{\mathbf{Cov}})}} e^{-\frac{1}{2} {}^t(\hat{\mathbf{M}}-\mathbf{M}(\mathbf{p}))\widehat{\mathbf{Cov}}^{-1}(\hat{\mathbf{M}}-\mathbf{M}(\mathbf{p}))n} \quad (1.354)$$

2. The a priori distribution is assumed to be uniform on $[\varepsilon_{C,min}, \varepsilon_{C,max}] \times [k_{min}, k_{max}] \times [S_{min}, S_{max}]$.

Our goal is to sample the a posteriori distribution 1.352. We will use two different methods: a discrete sampling with a regular mesh and Adaptive Metropolis with Covariance matrix adaptation.

Consistency of Bayesian methods from a frequentist perspective

The following considerations come from [Sul15].

In this sub-sub-section we will search to show, with large amount of data, the Bayesian method finds the right answer for any a priori distribution (under some technical restrictions), in the sense of the a posteriori distribution is concentrated around the real value of the parameter.

We consider the following situation:

- we dispose of the a priori distribution μ_0 on \mathcal{P}
- the output is in the form $\mathbf{y} = \mathbf{M}(\mathbf{p}^*) + \eta$ where η has a known probability distribution and \mathbf{p}^* is unknown
- we observe N outputs $\mathbf{y}_1, \dots, \mathbf{y}_n$, corresponding to n independent realisations of η

We want to that the a posteriori distribution of \mathbf{p} knowing the n observations converges to a Dirac measure in \mathbf{p}^* when $n \rightarrow +\infty$.

In order to simplify, we suppose μ_0 and the law of η are absolute continuous with respect to the Lebesgue measure on \mathcal{P} and \mathcal{Y} , respectively and have for probability

distribution π_0 and μ respectively. Then the likelihood of the outputs given the parameter \mathbf{p} then is

$$\mathcal{L}(\mathbf{y}_1, \dots, \mathbf{y}_n | \mathbf{p}) = \prod_{i=1}^n \mu(\mathbf{y}_i - \mathbf{M}(\mathbf{p})) \quad (1.355)$$

First, we can study the convergence of the likelihood maximum. Then, we have the following property

Proposition 1.7.14. *Consistency of the Maximum Likelihood Estimator*

We suppose

- \mathcal{P} is compact, \mathbf{M} is continuous and injective, μ is continuous and strictly positive.
- $\mathbf{Y}_1, \dots, \mathbf{Y}_n$ are i.i.d. and have the law $\mathbf{Y} = \mathbf{M}(\mathbf{p}^*) + \eta$. Then the maximum likelihood estimator

$$\hat{\mathbf{p}} \in \underset{\mathbf{p} \in \mathcal{P}}{\operatorname{argmax}} \mathcal{L}(\mathbf{Y}_1, \dots, \mathbf{Y}_N | \mathbf{p}) \quad (1.356)$$

converges in probability to \mathbf{p}^* when $n \rightarrow +\infty$.

The maximum likelihood estimator could not exist for a certain N or not be unique. But, from a certain rank, it exists and for all chosen versions, it verifies the consistency theorem.

In order to have a refined result, we will suppose the following regularity conditions

- \mathcal{P} is compact and \mathbf{p}^* is in the interior of \mathcal{P}
- \mathbf{M} is injective and \mathcal{C}^2 class (at least around \mathbf{p}^*)
- μ is strictly positive and \mathcal{C}^2 class, and verifies $\partial_{y_k} \log \mu \in L^1(\mathcal{Y})$ and $\partial_{y_k y_l} \log \mu \in L^1(\mathcal{Y})$
- The Fisher matrix defined by 1.358 is invertible

We then study the normality and efficiency of the maximum of likelihood

Proposition 1.7.15. *Under the stated regularity conditions, the estimator of the likelihood maximum is asymptotically normal and satisfies*

$$\sqrt{N}(\hat{\mathbf{p}}_N - \mathbf{p}^*) \rightarrow \mathcal{N}(\mathbf{0}, \mathbf{I}_F(\mathbf{p}^*)) \quad (1.357)$$

in law, where the Fisher matrix of information of size (r, r) is defined by (for $i, j \in \llbracket 1, r \rrbracket^2$):

$$\mathbf{I}_F(\mathbf{p})_{i,j} = \int_{\mathbb{R}^n} \frac{\partial \log(\mu(\mathbf{y} - \mathbf{M}(\mathbf{p})))}{\partial p_i} \frac{\partial \log(\mu(\mathbf{y} - \mathbf{M}(\mathbf{p})))}{\partial p_j} \mu(\mathbf{y} - \mathbf{M}(\mathbf{p})) d\mathbf{y}. \quad (1.358)$$

Finally, the following theorem (Bernstein-von Mises theorem) shows that the a posteriori distribution of \mathbf{p} knowing the data becomes normal and efficient asymptotically (i.e. its asymptotic covariance matrix is the Fisher information matrix) when $N \rightarrow +\infty$.

An intuition of the theorem of Bernstein-von Mises can be found in [Nic13].

We study here the normality and efficiency of the maximum a posteriori (MAP)

Theorem 6. *Bernstein-von Mises*

Conditions of regularity of \mathbf{M} and μ , when π_0 is continuous and strictly positive in the neighborhood of \mathbf{p}^ , and when we note μ_N the a posteriori law of \mathbf{p} knowing $\mathbf{Y}_1, \dots, \mathbf{Y}_N$, then*

$$\mathcal{P}(\|\mu_N - \mathcal{N}(\hat{\mathbf{p}}_N, \frac{1}{N}\mathbf{I}_F(\mathbf{p}^*))\|_{TV} > \varepsilon) \quad (1.359)$$

We recall here what is the total variation

$$\|\mu - \nu\|_{TV} := \sup_{B \in \mathcal{B}(\mathbb{R})^r} |\mu(B) - \nu(B)| \quad (1.360)$$

where $\mathcal{B}(\mathbb{R})^r$ refers to the Borel algebra on \mathbb{R}^r and when μ, ν have density p_μ and p_ν , then $\|\mu - \nu\|_{TV} = \frac{1}{2}\|p_\mu - p_\nu\|_{L^1}$.

The Bernstein-von Mises theorem shows that, when the a priori distribution has a strictly positive density, the a posteriori distribution concentrates around the real parameter \mathbf{p}^* with whom were drawn the data.

1.7.3 MCMC Sampling methods, Bayesian sampling

In practice, we have measurements lasting 1 hour, which is large in front of the time gate duration (in ms) which is proportional to $\frac{1}{\alpha}$. Then the statistics on the empirical moments is computed with a high number of realisations. And so the support of the a posteriori distribution on the inputs knowing the data is really thin. Since we want to sample this a posteriori distribution, we can use two strategies : an explicit sampling on a regular tensorised grid and normalised sampling or a MCMC sampling.

First, we can consider the regular tensorised and normalised grid sampling. It can be used in dimension 1 to 3. But, in dimension 4 and more this computation is too complex and cost effective when it comes to compute an a posteriori distribution with a really thin support, the grid must be dense. It is equivalent to compute a 4 or 5D integral.

To overcome these defects we use MCMC methods. Classic MCMC methods such as the Metropolis-Hastings will fail to correctly sample the distribution because of the thinness of the support. Then we suggest tackling this issue with Metropolis algorithm with an adaptation matrix covariance using the last accepted points (see chapter 3).

While the resolution of the problem requires computing a 5D integral, what can be really cost-effective, the use of Markov Chain Monte-Carlo is more subtle method in order to get the a posteriori distribution of the parameters \mathbf{p} knowing

the observations \mathbf{y}_{obs} . This a posteriori distribution will be the target distribution of the Monte-Carlo by Markov Chains algorithm. And so we get a sample of the target distribution π . Moreover, the Markov chain Monte-Carlo algorithm has only one unique stationary distribution (up to a multiplicative constant) and this is the target distribution.

Algorithm 1: Pseudocode of the independent sampler algorithm

Initial proposition $\mathbf{p}_0 \sim \mu^0$

for $i = 1, N_{maxiter}$ **do**

- $\mathbf{q}_{i+1} \sim \mu^0$
- Computation of the local acceptance rate using the likelihood of the proposal and the previous accepted point

$$\alpha(\mathbf{q}_{i+1}, \mathbf{p}_i) = \min\left(1, \frac{\pi(\mathbf{q}_{i+1})}{\pi(\mathbf{p}_i)}\right)$$

Then $\mathbf{p}_{i+1} = \mathbf{q}_{i+1}$ with probability α ; $\mathbf{p}_{i+1} = \mathbf{p}_i$ with probability $1 - \alpha$.

The independent sampler has a low acceptance rate when the support of the target distribution is small. A classic MCMC method is the Metropolis-Hastings algorithm, which is the following algorithm

Algorithm 2: Pseudocode of the Metropolis-Hastings algorithm [RS94]

Initial parameter \mathbf{p}_0 , chosen uniformly on $\bigotimes_{k=1}^r [\mathbf{p}_{k,min}, \mathbf{p}_{k,max}]$

for $i = 1, N_{maxiter}$ **do**

- Proposition $\mathbf{q}_{i+1} \sim \mathcal{N}(\mathbf{p}_i, \mathbf{C}_i)$ as instrumental law, with \mathbf{C}_i a covariance matrix.
- Computation of the local acceptance rate using the likelihood of the proposal and the previous accepted point

$$\alpha(\mathbf{q}_{i+1}, \mathbf{p}_i) = \min\left(1, \frac{\pi(\mathbf{q}_{i+1})}{\pi(\mathbf{p}_i)}\right)$$

Then $\mathbf{p}_{i+1} = \mathbf{q}_{i+1}$ with probability α ; $\mathbf{p}_{i+1} = \mathbf{p}_i$ with probability $1 - \alpha$.

This algorithm will be enhanced by a matrix covariance adaptation in the Chapter 3 because the support of the likelihood we want to sample is really thin.

The advantage of the MCMC methods is to provide the uncertainty about the input parameters, which is faster than computing a r D integral. [For09]

Chapter 2

The neutron noise direct problem

We recall the general form of the direct problem

$$\begin{aligned} \mathbf{M} : \mathbb{R}^5 &\rightarrow \mathbb{R}^3 \\ \mathbf{p} &\mapsto \mathbf{M}(\mathbf{p}) \end{aligned} \tag{2.1}$$

where $\mathbf{p} = (\varepsilon_C, k_{eff}, S, \mathbf{x}, \alpha)$ with $S = S_F$ refers to the intensity of the source, $S_\alpha = 0$ and $\mathbf{M}_j(\mathbf{p}) = \mathbb{E}[N_{[t,T]}^j]$ where $N_{[t,T]}^j$, $j \in \llbracket 1; 3 \rrbracket$ refers to the j -th power of the distribution of the neutrons counted during $[t, T]$ in the stationary regime (see Def 1.6.33 of the state-of-the-art). This allows us to study the outputs of our model as a function of the inputs. We will distinguish three different types of regimes:

- in the absence of a source,
- in transitional regime with an external source,
- in stationary regime with an external source.

And we will also consider two groups of neutrons: the number of neutrons present in the system X_T at time T and the number of neutrons detected $N_{[t,T]}$ during a time gate $T - t$.

We will check the theoretical formulas for the first three moments of the distribution considered

- $\pi_n(t)$: The distribution of the number of neutrons present in the system at time T given that there was 1 neutron at time t in the absence of a source
- $\Pi_n(t)$: The distribution of the number of neutrons present in the system at T given that there were 0 neutrons at time t in the presence of a source in the transitional regime
- $\Pi_{n,\infty}$: The distribution of the number of neutrons present in the system at T given the presence of a source in the stationary regime.
- $p_n(t)$: The distribution of the number of neutrons detected during $[t, T]$ given that there was 1 neutron at time t in the absence of a source

- $P_n(t)$: Distribution of the number of neutrons detected during $[t, T]$ given that there were 0 neutrons at time t in the presence of a source in transitional regime
- $Q_n(t)$: The distribution of the number of neutrons detected during $[t, T]$ given the fact the presence of a source in stationary regime (i.e. when $\Pi_{n,\infty}$ is the number of neutrons present in the system)

We will also consider factorial cumulants which allow us to calculate the first three moments of the number of neutrons present in the system at time T knowing that there are 0 neutrons present in the system at time t in the presence of an external source and in stationary state. Thus, the outputs of the point model will be verified numerically. A sensitivity analysis can be found in [PM07].

There are at least two functions of the moments of the distribution of the number of neutrons detected during a time gate $N_{[t,T]}$ that can be taken into account for the a posteriori calculation of the parameters: the simple moments $(\mathbb{E}[N_{[t,T]}^i])_{i \in \llbracket 1;3 \rrbracket}$ calculated from the number of neutrons present in the system X_T and the number of neutrons detected during a time gate $[t, T]$, and the Feynman moments from the equations on the moments of $N_{[t,T]}$.

We recall that the full calculation of the analytical formulas can be found in the annex.

2.1 The process of the number of neutrons present in the system

Calculation of the distribution of neutrons present in the system at time T knowing that there was 1 at time t and in the absence of an external source

We recall here the equations on the transition probability from the state-of-the-art (deduced from equation 1.155), the reader is also referred to the annexes A.2.3

$$\begin{aligned}
 -\frac{\partial \pi_n}{\partial t} &= -(\lambda_F \sum_{i \neq 1} f_i + \lambda_C) \pi_n(t) + (\lambda_F f_0 + \lambda_C) \pi_{n,0}(t) \\
 &\quad + \lambda_F f_2 \pi_{n,2}(t) \\
 &\quad + \lambda_F f_3 \pi_{n,3}(t) \\
 &\quad + \dots \\
 &\quad + \lambda_F f_m \pi_{n,\nu_{max}}(t)
 \end{aligned}$$

From which we can obtain the equation on the generating function from the state-of-the-art (deduced from equation 1.162)

$$-\frac{\partial g_\pi}{\partial t}(x, t) = -(\lambda_F \sum_{i \neq 1} f_i + \lambda_C) g_\pi(x, t) + (\lambda_F f_0 + \lambda_C) g_\pi^0(x, t) + \lambda_F \sum_i f_i g_\pi^i(x, t) \quad (2.2)$$

Deriving with respect to x , we obtain

$$-\frac{\partial}{\partial t} \frac{\partial g_\pi}{\partial x} = -(\lambda_F \sum_{i \neq 1} f_i + \lambda_C) \frac{\partial g_\pi}{\partial x} + \lambda_F \sum_i i f_i \frac{\partial g_\pi}{\partial x} g_\pi^{i-1}(t)$$

Since we are in sub-critical regime $\alpha > 0$, in the absence of a source, the number of neutrons decreases to 0, as there is only induced fission and detection.

We begin our calculations with the first three moments of the neutrons present in the system at T knowing that there was 1 at time t and in the absence of an external source. By deriving 1.162 with respect to x and evaluating in $x = 1$ we are able to access the average number of neutrons present in the system at time T knowing that there was 1 neutron at time t .

Proposition 2.1.1. *The average number of neutrons present in the system at T given that there was 1 neutron at time t in the absence of a source is*

$$\boxed{\bar{\nu}_\pi(t) = e^{-\alpha(T-t)}} \quad (2.3)$$

and thus

$$\boxed{\bar{\nu}_{\pi,\infty} = 0} \quad (2.4)$$

In the same way, we can calculate the moments of order 2.

Proposition 2.1.2. *The second order factorial moment of the number of neutrons present in the system at time T knowing that there was 1 neutron in the system at time t in the absence of a source is*

$$\boxed{\nu_{2,\pi}(t) = \frac{\nu_2}{-\rho\bar{\nu}} e^{-\alpha(T-t)} (1 - e^{-\alpha(T-t)})} \quad (2.5)$$

This enables us to deduce

$$\boxed{\nu_{2,\pi,\infty} = 0} \quad (2.6)$$

Moreover, we calculate the differential equation of $\nu_{3,\pi}$ to deduce its analytical expression.

Proposition 2.1.3. *The third order factorial moment of the number of neutrons present in the system at T given that there were 1 neutron at t in the system in the absence of a source is*

$$\boxed{\nu_{3,\pi}(t) = \frac{e^{-\alpha(T-t)}}{-\rho\bar{\nu}} \left(\frac{\nu_2^2}{-\rho\bar{\nu}} (1 - e^{-\alpha(T-t)})^2 + \nu_3 \frac{1 - e^{-2\alpha(T-t)}}{2} \right)} \quad (2.7)$$

Moreover, its asymptotic value when $T - t \rightarrow +\infty$ is

$$\boxed{\nu_{3,\pi,\infty} = 0} \quad (2.8)$$

These expressions conclude the calculation of the moments of the neutron distribution present in the system in the absence of an external source. Now we calculate the moments of the neutron distribution present in the system in the presence of an external source.

Calculation of the neutron distribution in the system at T knowing that there was 0 at t and in the presence of an external source

We propose to calculate the first three moments of the distribution $(\Pi_{n,\infty})_{n \in \mathbb{N}}$. We recall $S = S_F$ refers to the intensity of the source and $S_\alpha = 0$.

Proposition 2.1.4. *The first moment of the distribution of the number of neutrons present with the source is*

$$\bar{\nu}_{\Pi}(t) = \bar{\nu}_S S \frac{1 - e^{-\alpha(T-t)}}{\alpha} \quad (2.9)$$

In addition, when the stationary state is established, we have

$$\bar{\nu}_{\Pi,\infty} = \frac{\bar{\nu}_S S}{\alpha} \quad (2.10)$$

Proposition 2.1.5. *The second moment of the distribution of the number of neutrons present with the source is*

$$\nu_{2,\Pi}(t) = \bar{\nu}_S S \left(\frac{\bar{\nu}_S S}{\alpha} + \frac{\nu_2}{-\rho\bar{\nu}} \right) \frac{1 - e^{-\alpha(T-t)}}{\alpha} + \left(-\bar{\nu}_S S \left(\frac{\bar{\nu}_S S}{\alpha} + \frac{\nu_2}{-\rho\bar{\nu}} \right) + \nu_{2S} S \right) \frac{1 - e^{-2\alpha(T-t)}}{2\alpha} \quad (2.11)$$

In addition, it can be noted that

$$\nu_{2,\Pi,\infty} = \frac{S}{2\alpha} \left(\bar{\nu}_S \frac{\nu_2}{-\rho\bar{\nu}} + \nu_{2S} \right) + \frac{\bar{\nu}_S^2 S^2}{2\alpha^2} \quad (2.12)$$

Proposition 2.1.6. *The third moment of the distribution of the number of neutrons present with the source is*

$$\begin{aligned} \nu_{3,\Pi}(t) = & \left[\left(\frac{(\bar{\nu}_S S)^2}{2\alpha} \left(\frac{\bar{\nu}_S S}{\alpha} + 3 \frac{\nu_2}{-\rho\bar{\nu}} \right) + \frac{\bar{\nu}_S \nu_{2S} S^2}{2\alpha} \right) + \frac{\bar{\nu}_S S}{-\rho\bar{\nu}} \left(\frac{\nu_2^2}{-\rho\bar{\nu}} + \frac{\nu_3}{2} \right) \right] \frac{1 - e^{-\alpha(T-t)}}{\alpha} \\ & + \left[- \left(\frac{(\bar{\nu}_S S)^2}{\alpha} \left(\frac{\bar{\nu}_S S}{\alpha} + 3 \frac{\nu_2}{-\rho\bar{\nu}} \right) \right) + \frac{\bar{\nu}_S \nu_{2S} S^2}{\alpha} - 2\bar{\nu}_S S \frac{\nu_2^2}{(-\rho\bar{\nu})^2} + 2\nu_{2S} S \frac{\nu_2}{-\rho\bar{\nu}} \right] \frac{1 - e^{-2\alpha(T-t)}}{2\alpha} \\ & + \left[\left(\frac{(\bar{\nu}_S S)^2}{2\alpha} \left(\frac{\bar{\nu}_S S}{\alpha} + 3 \frac{\nu_2}{-\rho\bar{\nu}} \right) - \frac{3\bar{\nu}_S \nu_{2S} S^2}{2\alpha} \right) \right. \\ & \left. + \frac{\bar{\nu}_S S}{-\rho\bar{\nu}} \left(\frac{\nu_2^2}{-\rho\bar{\nu}} - \frac{\nu_3}{2} \right) - 2\nu_{2S} S \frac{\nu_2}{-\rho\bar{\nu}} + \nu_{3S} S \right] \frac{1 - e^{-3\alpha(T-t)}}{3\alpha} \end{aligned} \quad (2.13)$$

The third asymptotic moment of the distribution of the number of neutrons present with the source is

$$\nu_{3,\Pi,\infty} = \frac{S}{3\alpha} \left(\frac{\bar{\nu}_S}{-\rho\bar{\nu}} \left(\frac{\nu_2^2}{-\rho\bar{\nu}} + \nu_3 \right) + \frac{\nu_2 \nu_{2S}}{-\rho\bar{\nu}} + \nu_{3S} \right) + \frac{\bar{\nu}_S S}{\alpha} \frac{S}{2\alpha} \left(\bar{\nu}_S \frac{\nu_2}{-\rho\bar{\nu}} + \nu_{2S} \right) + \frac{\bar{\nu}_S^3 S^3}{6\alpha^3} \quad (2.14)$$

2.1.1 Factorial Cumulants

Here we define the multiplicity rates from V. Multiplicity Mathematics, section H. [al.98].

Definition 2.1.7. *Multiplicities rates*

We define the rate of singles, doubles and triples as the average number of detections of i among n for $i = 1, 2, 3$ respectively, more precisely

$$\begin{aligned} \text{Singles} &:= \sum_{n \in \mathbb{N}^*} n Q_n(t) \\ \text{Doubles} &:= \sum_{n \in \mathbb{N}^*} \frac{n(n-1)}{2} Q_n(t) \\ \text{Triples} &:= \sum_{n \in \mathbb{N}^*} \frac{n(n-1)(n-2)}{6} Q_n(t) \end{aligned} \quad (2.15)$$

The use of factorial cumulants is the simplest way to calculate observations. It is used in [PP08], generally converted into singles, doubles and triples [al.98]. These will be used to calculate the first three moments of X_t .

We define the generating function of the factorial cumulants as follows

Definition 2.1.8. *Let the following quantity be*

$$K_{\Pi}(x, t) := \log(G_{\Pi}(x, t)) \quad (2.16)$$

This leads us to

Proposition 2.1.9. *The generating function of the factorial cumulants is*

$$K_{\Pi}(x, t) = S \int_0^{T-t} \left(\sum_{\nu=0}^{\infty} f_{\nu, S} g_{\pi}^{\nu}(x, T-s) - 1 \right) ds \quad (2.17)$$

Proof. Using 1.182

$$G_{\Pi}(x, t) = \exp\left(S \int_0^{T-t} \left(\sum_{\nu=0}^{\infty} f_{\nu, S} g_{\pi}^{\nu}(x, T-s) - 1 \right) ds\right) \quad (2.18)$$

Since $K_{\Pi}(x, t) = \log(G_{\Pi}(x, t))$ then

$$K_{\Pi}(x, t) = S \int_0^{T-t} \left(\sum_{\nu=0}^{\infty} f_{\nu, S} g_{\pi}^{\nu}(x, T-s) - 1 \right) ds \quad (2.19)$$

□

Moreover,

Definition 2.1.10. *The binomial cumulants are given by*

$$\Gamma_{\Pi}(x, t) := \frac{1}{n!} \left(\frac{\partial^n K_{\Pi}}{\partial x^n}(t) \right)_{x=1} = S \int_0^{T-t} \sum_{\nu=0}^{\infty} \frac{f_{\nu, S}}{n!} \left(\frac{\partial^n g_{\pi}^{\nu}}{\partial x^n} \right)_{x=1} (T-s) ds \quad (2.20)$$

But also,

Definition 2.1.11. *The moment of order n of the distribution of neutrons present in the absence of a source in the system at T knowing that there were i neutrons at t is*

$$\nu_{\pi,n,i}(t) := \frac{1}{n!} \sum_{j=1}^{\infty} j(j-1) \cdots (j-n+1) \pi_{j,i}(t) \quad (2.21)$$

A direct calculation shows

Proposition 2.1.12.

$$\nu_{\pi,n,i}(t) = \frac{1}{n!} \left(\frac{\partial^n g_{\pi}^i}{\partial x^n} \right)_{x=1} (t) \quad (2.22)$$

Proof. We use again the proof of the proposition. By differentiating n times the previous equation with respect to x and dividing by $n!$ we obtain the expected result. \square

Then, we define

Definition 2.1.13. *For $i \in \mathbb{N}^*$, we define*

$$\nu_{S\pi,i} := \sum_{\nu=0}^{\nu_{max,S}} f_{\nu,S} \nu_{\pi,i,\nu} \quad (2.23)$$

where $\bar{\nu}_S, \nu_{2S}, \nu_{3S}$ are defined in the equations 1.124 and 1.126 of the state-of-the-art in the source subsection.

Proposition 2.1.14. *The first three moments $\nu_{\pi,n,i}(t), n \in \llbracket 1; 3 \rrbracket$ have the property*

$$\begin{aligned} \nu_{S\pi,1} &= \bar{\nu}_S \bar{\nu}_{\pi} \\ \nu_{S\pi,2} &= \bar{\nu}_S \nu_{2,\pi} + \nu_{2S} \bar{\nu}_{\pi}^2 \\ \nu_{S\pi,3} &= \bar{\nu}_S \bar{\nu}_{\pi} + \nu_{3S} \bar{\nu}_{\pi}^3 + 2\nu_{2S} \bar{\nu}_{\pi} \nu_{2,\pi} \end{aligned} \quad (2.24)$$

Proof. By definition, we can deduce

$$\begin{aligned} \frac{\partial g_{\pi}^i}{\partial x} &= i \frac{\partial g_{\pi}}{\partial x} g_{\pi}^{i-1} \\ \frac{1}{2} \frac{\partial^2 g_{\pi}^i}{\partial x^2} &= \frac{i}{2} \left(\frac{\partial^2 g_{\pi}}{\partial x^2} g_{\pi}^{i-2} + (i-1) \left(\frac{\partial g_{\pi}}{\partial x} \right)^2 g_{\pi}^{i-2} \right) \\ \frac{1}{6} \frac{\partial^3 g_{\pi}^i}{\partial x^3} &= \frac{i}{6} \left(\frac{\partial^3 g_{\pi}}{\partial x^3} g_{\pi}^{i-3} + 3(i-1) \frac{\partial g_{\pi}}{\partial x} \frac{\partial^2 g_{\pi}}{\partial x^2} g_{\pi}^{i-3} + (i-1)(i-2) \left(\frac{\partial g_{\pi}}{\partial x} \right)^3 g_{\pi}^{i-3} \right) \end{aligned} \quad (2.25)$$

By evaluating in $x = 1$, we find

$$\begin{aligned} \nu_{\pi,1,\nu} &= \nu \bar{\nu}_{\pi} \\ \nu_{\pi,2,\nu} &= \nu \nu_{2,\pi} + \frac{\nu(\nu-1)}{2} \bar{\nu}_{\pi}^2 \\ \nu_{\pi,3,\nu} &= \nu \bar{\nu}_{\pi} + \frac{\nu(\nu-1)(\nu-2)}{6} \bar{\nu}_{\pi}^3 + \nu(\nu-1) \bar{\nu}_{\pi} \nu_{2,\pi} \end{aligned} \quad (2.26)$$

This allows us to conclude the result. \square

We can therefore deduce

Proposition 2.1.15. *The first three asymptotic binomial cumulants are given by*

$$\begin{aligned} \Gamma_{II,1,\infty} &= \frac{\bar{\nu}_S S}{\alpha} \\ \Gamma_{II,2,\infty} &= \frac{S}{2\alpha} \left(\bar{\nu}_S \frac{\nu_2}{-\rho\bar{\nu}} + \nu_2 S \right) \\ \Gamma_{II,3,\infty} &= \frac{S}{3\alpha} \left(\frac{\bar{\nu}_S}{-\rho\bar{\nu}} \left(\frac{\nu_2^2}{-\rho\bar{\nu}} + \nu_3 \right) + \frac{\nu_2 \nu_2 S}{-\rho\bar{\nu}} + \nu_3 S \right) \end{aligned} \quad (2.27)$$

Proof. We refer the reader to the appendix A.2.2 to understand the calculation of integrals. \square

By differentiating the generating function three times, we obtain

$$\begin{aligned} G'_{II} &= K'_{II} G_{II} \\ G''_{II} &= (K''_{II} + K'^2_{II}) G_{II} \\ G'''_{II} &= (K'''_{II} + 3K'_{II} K''_{II} + K'^3_{II}) G_{II} \end{aligned} \quad (2.28)$$

Where

$$\begin{aligned} \bar{\nu}_{II,\infty} &= \Gamma_{II,\infty} \\ \nu_{2,II,\infty} &= \Gamma_{II,2,\infty} + \frac{\Gamma^2_{II,\infty}}{2} \\ \nu_{3,II,\infty} &= \Gamma_{II,3,\infty} + \Gamma_{II,\infty} \Gamma_{II,2,\infty} + \frac{\Gamma^3_{II,\infty}}{6} \end{aligned} \quad (2.29)$$

So, we have

$$\begin{aligned} \bar{\nu}_{II,\infty} &= \frac{\bar{\nu}_S S}{\alpha} \\ \nu_{2,II,\infty} &= \frac{S}{2\alpha} \left(\bar{\nu}_S \frac{\nu_2}{-\rho\bar{\nu}} + \nu_2 S \right) + \frac{\bar{\nu}_S^2 S^2}{2\alpha^2} \\ \nu_{3,II,\infty} &= \frac{S}{3\alpha} \left(\frac{\bar{\nu}_S}{-\rho\bar{\nu}} \left(\frac{\nu_2^2}{-\rho\bar{\nu}} + \nu_3 \right) + \frac{\nu_2 \nu_2 S}{-\rho\bar{\nu}} + \nu_3 S \right) + \frac{\bar{\nu}_S S}{\alpha} \frac{S}{2\alpha} \left(\bar{\nu}_S \frac{\nu_2}{-\rho\bar{\nu}} + \nu_2 S \right) + \frac{\bar{\nu}_S^3 S^3}{6\alpha^3} \end{aligned} \quad (2.30)$$

From now on, we propose to obtain the first moments of the distribution $(Q_n(t))_n$, the distribution of the number of neutrons detected in the time interval $[t, T]$ given the presence of a source and during the stationary regime.

2.2 The joint process of the number of neutrons present in the system and the number of neutrons detected in $[t, T]$

In order to study the inverse problem, we need to have a forward problem as well-defined as possible. Here we compute some functions of the distribution of the detection number $N_{[t,T]}$: the measures. We then consider the joint process $(X_T, N_{[t,T]})$ which is a time-continuous Markov process.

In order to obtain the measurements, here the moments of the number of detections in the presence of a source, we start with the following explicit formula

$$\mathcal{G}(x, t) = G(x, t)G_{II,\infty}(g(x, t)) \quad (2.31)$$

from the state-of-the-art equation 1.249. It goes without saying that we proceed in a progressive way; the expression of the moments of \mathcal{G} are heavy.

Each of the moments considered will be calculated from the corresponding generating function. To this end, we recall how to calculate (for example, from the master equation it verifies).

Simple moments in the absence of a source

We start by calculating the first moment of g .

Proposition 2.2.1. *The moment of order 1 of the detection number on the interval $[t, T]$ in the absence of a source, defined in equation 1.216, is*

$$\mathbb{E}[N_{[t,T]}]_{(p_n(t))_n} = m_1(t) = \frac{\varepsilon_F}{-\rho\bar{\nu}}(1 - e^{-\alpha(T-t)}) \quad (2.32)$$

As a result, we know that

$$m_{2,\nu} = \frac{1}{2} \left[\frac{\partial^2 g^\nu}{\partial x^2} \right]_{x=1} = \frac{\nu(\nu-1)}{2} m_1^2 + \nu m_2 \quad (2.33)$$

This allows us to conclude

Proposition 2.2.2. *The moment of order 2 of the detection number on the interval $[t, T]$ in the absence of a source, defined in equation 1.216, is*

$$\mathbb{E}[N_{[t,T]}^2]_{(p_n(t))_n} = 2 \frac{\nu_2 \varepsilon_F^2}{(-\rho\bar{\nu})^3} (1 - 2\alpha(T-t)e^{-\alpha(T-t)} - e^{-2\alpha(T-t)}) + \frac{\varepsilon_F}{-\rho\bar{\nu}} (1 - e^{-\alpha(T-t)}) \quad (2.34)$$

We can notice

$$m_2(t) = \frac{\nu_2 \varepsilon_F^2}{(-\rho\bar{\nu})^3} (1 - 2\alpha(T-t)e^{-\alpha(T-t)} - e^{-2\alpha(T-t)}) \quad (2.35)$$

For the following calculations, we define

Definition 2.2.3. *The constants*

$$\begin{cases} A := \nu_3 \frac{\varepsilon_F^3}{(-\rho\bar{\nu})^4} \\ B := \nu_2^2 \frac{\varepsilon_F^3}{(-\rho\bar{\nu})^5} \end{cases} \quad (2.36)$$

are functions of the nuclear parameters ρ , ε_F and the moments of the fission process $(\bar{\nu}, \nu_2, \nu_3)$.

The only thing left to do is to calculate m_3 .

Proposition 2.2.4. *The moment of order 3 of the detection number on the interval $[t, T]$ in the absence of a source is*

$$\begin{aligned} \mathbb{E}[N_{[t,T]}^3]_{(p_n(t))_n} = & 6 \left(-\frac{1}{2}(-2(A+B) + (-(3A+B) + 2\alpha(T-t)(3A+B) + 2\alpha^2 B(T-t)^2)e^{-\alpha(T-t)} \right. \\ & + (2(3A+B) + 4\alpha B(T-t))e^{-2\alpha(T-t)} + (-A+B)e^{-3\alpha(T-t)}) \\ & \left. + \frac{\nu_2 \varepsilon_F^2}{(-\rho\bar{\nu})^3} (1 - 2\alpha(T-t)e^{-\alpha(T-t)} - e^{-2\alpha(T-t)}) \right) \\ & + \frac{\varepsilon_F}{-\rho\bar{\nu}} (1 - e^{-\alpha(T-t)}) \end{aligned} \quad (2.37)$$

We recall that m_3 , defined in equation 1.216, is

$$\begin{aligned} m_3(t) = & -\frac{1}{2}(-2(A+B) + (-(3A+B) + 2\alpha(T-t)(3A+B) + 2\alpha^2 B(T-t)^2)e^{-\alpha(T-t)} \\ & + (2(3A+B) + 4\alpha B(T-t))e^{-2\alpha(T-t)} \\ & + (-A+B)e^{-3\alpha(T-t)}) \end{aligned} \quad (2.38)$$

with the quantities A and B introduced earlier.

Remembering that these moments are involved in the calculation of the moments of \mathcal{G} (we can find an expression for 1.249) and allow us to solve our problem.

Considering the equation 1.249, we see that the calculation of the moments of \mathcal{G} requires that of G .

Simple moments in the presence of a source

We consider the number of neutrons detected during $[t, T]$ in the presence of a source knowing there was 0 neutrons at time t . In the equation 1.249, we obtained the formula of Sevast'yanov

$$G(x, t) = \exp\left(\int_t^T S\left(\sum_{\nu=0}^{+\infty} f_{\nu, S} g^\nu(x, s) - 1\right) ds\right). \quad (2.39)$$

with $S = S_F$ refers to the intensity of the source and $S_\alpha = 0$. We calculate the partial derivative of order 3 with respect to x of \mathcal{G} , so we will calculate that of G up to order 3 also.

As previously

Proposition 2.2.5. *The moment of order 1 of the detection number on the interval $[t, T]$ in the presence of a source, defined in equation 1.232, is*

$$\mathbb{E}[N_{[t,T]}]_{(P_n(t))_n} = M_1(t) = \bar{\nu}_S S \frac{\varepsilon_F}{-\rho\bar{\nu}} \left[(T-t) - \frac{1 - e^{-\alpha(T-t)}}{\alpha} \right] \quad (2.40)$$

Proof. To do this, we need the differentiation of 2.39 and evaluate it in $x = 1$. More details in the appendix A.2.8. \square

Proposition 2.2.6. *The moment of order 2 of the detection number on the interval $[t, T]$ in the presence of a source is*

$$\begin{aligned} \mathbb{E}[N_{[t,T]}^2]_{(P_n(t))_n} = & 2\bar{\nu}_S S \frac{\nu_2 \varepsilon_F^2}{(-\rho\bar{\nu})^3} \left[T-t + 2(T-t)e^{-\alpha(T-t)} - \frac{1 - e^{-\alpha(T-t)}}{\alpha} + \frac{1 - e^{-2\alpha(T-t)}}{2\alpha} \right] \\ & + 2\nu_2 S \frac{\varepsilon_F^2}{(-\rho\bar{\nu})^2} \left[T-t - 2\frac{1 - e^{-\alpha(T-t)}}{\alpha} + \frac{1 - e^{-2\alpha(T-t)}}{2\alpha} \right] \\ & + \left[\bar{\nu}_S S \frac{\varepsilon_F}{-\rho\bar{\nu}} \left\{ T-t - \frac{1 - e^{-\alpha(T-t)}}{\alpha} \right\} \right]^2 + \bar{\nu}_S S \frac{\varepsilon_F}{-\rho\bar{\nu}} \left\{ T-t - \frac{1 - e^{-\alpha(T-t)}}{\alpha} \right\} \end{aligned} \quad (2.41)$$

Moreover, we know that M_2 , defined in equation 1.232, is

$$\begin{aligned} M_2(t) = & \bar{\nu}_S S \frac{\nu_2 \varepsilon_F^2}{(-\rho\bar{\nu})^3} \left[T-t + 2(T-t)e^{-\alpha(T-t)} - \frac{1 - e^{-\alpha(T-t)}}{\alpha} + \frac{1 - e^{-2\alpha(T-t)}}{2\alpha} \right] \\ & + \nu_2 S \frac{\varepsilon_F^2}{(-\rho\bar{\nu})^2} \left[T-t - 2\frac{1 - e^{-\alpha(T-t)}}{\alpha} + \frac{1 - e^{-2\alpha(T-t)}}{2\alpha} \right] \\ & + \frac{1}{2} \left[\bar{\nu}_S S \frac{\varepsilon_F}{-\rho\bar{\nu}} \left\{ T-t - \frac{1 - e^{-\alpha(T-t)}}{\alpha} \right\} \right]^2 \end{aligned} \quad (2.42)$$

Proof. Let us continue our successive differentiations and evaluations in $x = 1$ in the annexes A.2.4. \square

Proposition 2.2.7. *The 3 order moment of the number of neutrons detected over the interval $[t, T]$ in the presence of a source $\mathbb{E}[N_{[t,T]}^3]_{P_n(t)}$ and $M_3(t)$ are given by*

the equations

$$\begin{aligned}
\mathbb{E}[N_{[t,T]}^3]_{(P_n(t))_n} = & 6 \left(-\frac{S\bar{\nu}_S}{2} \left(-2(A+B)(T-t) - (3A+B) \frac{1-e^{-\alpha(T-t)}}{\alpha} \right. \right. \\
& - 2(3A+B) \left((T-t)e^{-\alpha(T-t)} - \frac{1-e^{-\alpha(T-t)}}{\alpha} \right) \\
& + 2B(-\alpha(T-t)^2 e^{-\alpha(T-t)} - 2(T-t)e^{-\alpha(T-t)} + 2 \frac{1-e^{-\alpha(T-t)}}{\alpha}) \\
& + 2(3A+B) \frac{1-e^{-2\alpha(T-t)}}{2\alpha} - 2B \left((T-t)e^{-2\alpha(T-t)} - \frac{1-e^{-2\alpha(T-t)}}{2\alpha} \right) \\
& \left. \left. + (-A+B) \frac{1-e^{-3\alpha(T-t)}}{3\alpha} \right) \right) \\
& + 2\nu_2 S \frac{\nu_2 \varepsilon_F^3}{(-\rho\bar{\nu})^4} \left((T-t) + 2(T-t)e^{-\alpha(T-t)} - 3 \frac{1-e^{-\alpha(T-t)}}{\alpha} \right. \\
& \left. - (T-t)e^{-2\alpha(T-t)} + \frac{1-e^{-3\alpha(T-t)}}{3\alpha} \right) \\
& + \nu_3 S \frac{\varepsilon_F^3}{(-\rho\bar{\nu})^3} \left(T-t - 3 \frac{1-e^{-\alpha(T-t)}}{\alpha} + 3 \frac{1-e^{-2\alpha(T-t)}}{2\alpha} - \frac{1-e^{-3\alpha(T-t)}}{3\alpha} \right) \\
& + \left(\bar{\nu}_S S \frac{\nu_2 \varepsilon_F^2}{(-\rho\bar{\nu})^3} \left(T-t + 2 \left((T-t)e^{-\alpha(T-t)} - \frac{1-e^{-\alpha(T-t)}}{\alpha} \right) - \frac{1-e^{-2\alpha(T-t)}}{2\alpha} \right) \right. \\
& + \nu_2 S \frac{\varepsilon_F^2}{(-\rho\bar{\nu})^2} \left(T-t - 2 \frac{1-e^{-\alpha(T-t)}}{\alpha} + \frac{1-e^{-2\alpha(T-t)}}{2\alpha} \right) \\
& \left. + \frac{\bar{\nu}_S^2 S^2}{6} \frac{\varepsilon_F^2}{(-\rho\bar{\nu})^2} \left(T-t - \frac{1-e^{-\alpha(T-t)}}{\alpha} \right)^2 \right) \bar{\nu}_S S \frac{\varepsilon_F}{(-\rho\bar{\nu})} \left[\left(T-t - \frac{1-e^{-\alpha(T-t)}}{\alpha} \right) \right] \\
& + 6 \left(\bar{\nu}_S S \frac{\nu_2 \varepsilon_F^2}{(-\rho\bar{\nu})^3} \left[T-t + 2(T-t)e^{-\alpha(T-t)} - 2 \frac{1-e^{-\alpha(T-t)}}{\alpha} - \frac{1-e^{-2\alpha(T-t)}}{2\alpha} \right] \right. \\
& + \nu_2 S \frac{\varepsilon_F^2}{(-\rho\bar{\nu})^2} \left[T-t - 2 \frac{1-e^{-\alpha(T-t)}}{\alpha} + \frac{1-e^{-2\alpha(T-t)}}{2\alpha} \right] \\
& \left. + \frac{1}{2} \left[\bar{\nu}_S S \frac{\varepsilon_F}{-\rho\bar{\nu}} \left\{ T-t - \frac{1-e^{-\alpha(T-t)}}{\alpha} \right\} \right]^2 \right) \\
& + \bar{\nu}_S S \frac{\varepsilon_F}{-\rho\bar{\nu}} \left\{ T-t - \frac{1-e^{-\alpha(T-t)}}{\alpha} \right\}
\end{aligned}$$

(2.43)

and also, the expression of M_3 , defined in equation 1.232,

$$\begin{aligned}
M_3(t) = & -\frac{\bar{\nu}_S S}{2} \left(-2(A+B)(T-t) - (3A+B) \frac{1-e^{-\alpha(T-t)}}{\alpha} \right. \\
& - 2(3A+B) \left((T-t)e^{-\alpha(T-t)} - \frac{1-e^{-\alpha(T-t)}}{\alpha} \right) \\
& + 2B(-\alpha(T-t)^2 e^{-\alpha(T-t)} - 2(T-t)e^{-\alpha(T-t)} + 2 \frac{1-e^{-\alpha(T-t)}}{\alpha}) \\
& + 2(3A+B) \frac{1-e^{-2\alpha(T-t)}}{2\alpha} - 2B \left((T-t)e^{-2\alpha(T-t)} - \frac{1-e^{-2\alpha(T-t)}}{2\alpha} \right) \\
& \left. + (-A+B) \frac{1-e^{-3\alpha(T-t)}}{3\alpha} \right) \\
& + 2\nu_{2S} S \frac{\nu_2 \varepsilon_F^3}{(-\rho\bar{\nu})^4} \left((T-t) + 2(T-t)e^{-\alpha(T-t)} - 3 \frac{1-e^{-\alpha(T-t)}}{\alpha} \right. \\
& \left. - (T-t)e^{-2\alpha(T-t)} + \frac{1-e^{-3\alpha(T-t)}}{3\alpha} \right) \\
& + \nu_{3S} S \frac{\varepsilon_F^3}{(-\rho\bar{\nu})^3} \left(T-t - 3 \frac{1-e^{-\alpha(T-t)}}{\alpha} + 3 \frac{1-e^{-2\alpha(T-t)}}{2\alpha} - \frac{1-e^{-3\alpha(T-t)}}{3\alpha} \right) \\
& + \left(\bar{\nu}_S S \frac{\nu_2 \varepsilon_F^2}{(-\rho\bar{\nu})^3} \left(T-t + 2 \left((T-t)e^{-\alpha(T-t)} - \frac{1-e^{-\alpha(T-t)}}{\alpha} \right) - \frac{1-e^{-2\alpha(T-t)}}{2\alpha} \right) \right. \\
& + \nu_{2S} S \frac{\varepsilon_F^2}{(-\rho\bar{\nu})^2} \left(T-t - 2 \frac{1-e^{-\alpha(T-t)}}{\alpha} + \frac{1-e^{-2\alpha(T-t)}}{2\alpha} \right) \\
& \left. + \frac{\bar{\nu}_S^2 S^2}{6} \frac{\varepsilon_F^2}{(-\rho\bar{\nu})^2} \left(T-t - \frac{1-e^{-\alpha(T-t)}}{\alpha} \right)^2 \right) \bar{\nu}_S S \frac{\varepsilon_F}{(-\rho\bar{\nu})} \left[\left(T-t - \frac{1-e^{-\alpha(T-t)}}{\alpha} \right) \right]
\end{aligned} \tag{2.44}$$

Proof. It only remains for us to differentiate 1.236 in order to obtain our results, for explicit computation see annexes A.2.4. \square

To conclude, we have computed the first three moments of the generating function G required for the computation of the three first moments of the generating function \mathcal{G} . All that remains is to get on with the real purpose of this part: the first three simple moments of the number of detections on an interval $[t, T]$ in the presence of an external source and when the number of neutrons present in the system has a stationary distribution.

Simple moments in the presence of a source when the neutron number has a stationary distribution

We recall $S = S_F$ refers to the intensity of the source and $S_\alpha = 0$.

Proposition 2.2.8. *The simple moment of order 1 of the detection number in the presence of a source and when the neutron number has a stationary distribution*

$(\Pi_{\nu,\infty})_\nu$, defined in equation 1.245, is

$$\mathbb{E}[N_{[t,T]}]_{(Q_n(t))_n} = \mathcal{M}_1(t) = \bar{\nu}_S S \frac{\varepsilon_F}{-\rho \bar{\nu}} (T - t) \quad (2.45)$$

when $T - t$ is the length of the time gate considered.

Proof. We differentiate the composition of generating functions, the details are in the appendix A.2.4. \square

Proposition 2.2.9. *The simple moment of order 2 of the number of detections in the presence of a source and when the number of neutrons has a stationary distribution $(\Pi_{\nu,\infty})_\nu$ is*

$$\mathbb{E}[N_{[t,T]}^2]_{(Q_n(t))_n} = \nu_S^2 S^2 \frac{\varepsilon_F^2}{(-\rho \nu_2)^2} (T - t)^2 + \bar{\nu}_S S \frac{\varepsilon_F}{-\rho \bar{\nu}} (T - t) + 2 \frac{\varepsilon_F^2}{(-\rho \nu_2)^2} \left(\nu_S S \frac{\nu_2}{(-\rho \nu)} + \nu_{2S} S \right) \left(T - t - \frac{1 - e^{-\alpha(T-t)}}{\alpha} \right) \quad (2.46)$$

and also, \mathcal{M}_2 , defined in equation 1.245, is

$$\mathcal{M}_2(t) = \frac{1}{2} \nu_S^2 S^2 \frac{\varepsilon_F^2}{(-\rho \nu_2)^2} (T - t)^2 + \frac{\varepsilon_F^2}{(-\rho \nu_2)^2} \left(\nu_S S \frac{\nu_2}{(-\rho \nu)} + \nu_{2S} S \right) \left(T - t - \frac{1 - e^{-\alpha(T-t)}}{\alpha} \right) \quad (2.47)$$

Proof. The same techniques as previously are used, see annexes A.2.4. \square

Proposition 2.2.10. *The third simple moment of the number of neutrons detected in the presence of a source and when the number of neutrons has a stationary distribution $(\Pi_{\nu,\infty})_\nu$ is*

$$\mathbb{E}[N_{[t,T]}^3]_{(Q_n(t))_n} = \bar{\nu}_S S \frac{\varepsilon_F}{(-\rho \bar{\nu})} (T - t) 3 \left(\frac{\varepsilon_F D_2}{-\rho^2} \right)^2 \left(1 - \rho \frac{\bar{\nu}_S D_{2S}}{\bar{\nu} D_2} \right) \left(1 + e^{-\alpha(T-t)} - 2 \frac{1 - e^{-\alpha(T-t)}}{\alpha(T-t)} \right) - \frac{\varepsilon_F D_3}{\rho^3} \left(1 - \rho \frac{\bar{\nu}_S^2 D_{3S}}{\bar{\nu}^2 D_3} \right) \left(1 - \frac{3 - 4e^{-\alpha(T-t)} + 2e^{-2\alpha(T-t)}}{2\alpha(T-t)} \right) + 6 \frac{\varepsilon_F^2}{(-\rho \bar{\nu})^2} \left(\nu_S S \frac{\nu_2}{(-\rho \nu)} + \nu_{2S} S \right) \left(T - t - \frac{1 - e^{-\alpha(T-t)}}{\alpha} \right) \left(\bar{\nu}_S S \frac{\varepsilon_F}{(-\rho \bar{\nu})} (T - t) + 1 \right) + \bar{\nu}_S^3 S^3 \frac{\varepsilon_F^3}{(-\rho \bar{\nu})^3} (T - t)^3 + 6 \bar{\nu}_S^2 S^2 \frac{\varepsilon_F^2}{(-\rho \bar{\nu})^2} (T - t)^2 + 2 \bar{\nu}_S S \frac{\varepsilon_F}{(-\rho \bar{\nu})} (T - t) \quad (2.48)$$

where the above variables are expressed at the end of the computation. Due to too large size, the expression of \mathcal{M}_3 , defined in equation 1.245, can be found in the annexes A.2.4.

Proof. The reader is referred to the annexes A.2.4. □

These expressions can be checked by Monte-Carlo simulations of X_t or $(X_t, N_{[0,t]})$ using the next algorithm 3, or by using the explicit Euler method on each of the corresponding differential equations stated in the state-of-the-art or the annexes. In the following, we will be dealing with different test-cases in order to check the analytical formulas of the considered moments, then the forward problem of neutron counting will be settled.

2.3 The "Counting" code, a MC code in the point model approximation

In the point model approximation, we established the Monte-Carlo code 3, which is a kinetic Monte-Carlo code (a good introduction can be found in [Vot07]).

Algorithm 3: Counting code, the Monte-Carlo code in the point model approximation, generating a TimeList file

```

 $\lambda_{C,loc};$ 
 $\lambda_{F,loc};$ 
 $S;$ 
for  $i = 1$ , Number of realizations do
     $t = 0;$ 
     $X_t = 1;$ 
     $\lambda_C = X_t \lambda_{C,loc};$ 
     $\lambda_F = X_t \lambda_{F,loc};$ 
     $L = S + \lambda_C + \lambda_F;$ 
    while  $t < t_{max}$  do
         $u \sim \mathcal{U}[0, 1];$ 
         $dt = -\frac{\log(u)}{L};$ 
        CALL Simulations of either the source, the fission, the capture (with
            or without a detection) (algo 4);
         $\lambda_C = X_t \lambda_{C,loc};$ 
         $\lambda_F = X_t \lambda_{F,loc};$ 
         $L = S + \lambda_C + \lambda_F;$ 
        Storage of the values of  $X_t$  and  $t$  for post-treatment;
         $t = t + dt;$ 
    end
end

```

The algorithm 3 allows verifying the analytical formulas of the different moments by the Monte-Carlo method. More precisely, this code provides the detection times of the counts and the number of neutrons present in the system by the Monte-Carlo method, and thus a Time List file that can be analysed (in the presence or absence of a source). After processing the Time List file, we implemented the explicit Euler method for each of the quantities of interest (see next checks) and verified the analytical expressions with it.

Algorithm 4: Simulation of the events: source, fission or capture (with or without a detection)

```

 $invl = \frac{1}{L};$ 
 $p_S = S * invl;$ 
 $p_C = \lambda_C * invl;$ 
 $p_F = \lambda_F * invl;$ 
 $u \sim \mathcal{U}[0, 1];$ 
 $indiceprocessus = \mathbf{1}_{[0, p_S]}(u) + 2\mathbf{1}_{[p_S, p_S + p_C]}(u) + 3\mathbf{1}_{[p_S + p_C, 1]}(u);$ 
if  $indiceprocessus == 1$  (Source) then
    | % Computation of the random number of neutrons emitted by the
    | source;
    | Call number_of_emitted_neutrons_by_the_sources(nu);
    |  $X_t = X_t + nu;$ 
else if  $indiceprocessus == 2$  (Capture) then
    |  $X_t = X_t - 1;$ 
    |  $u \sim \mathcal{U}[0, 1];$ 
    |  $x_{compt} = \mathbf{1}_{[0, \varepsilon_C]}(u) + 2\mathbf{1}_{[\varepsilon_C, 1]}(u);$ 
    | if  $x_{compt} == 1$  then
    | | Storage of the time of detection;
    | | Number of detections = number of detections+1;
else if  $indiceprocessus == 3$  (Induced fission) then
    | % Computation of the random number of neutrons emitted by the
    | fission;
    | Call number_of_emitted_neutronsby_the_fission(ne);
    |  $X_t = X_t + ne - 1;$ 

```

Another part of the code provides the processing of the Time List file and the analytical and explicit Euler checks. It also provides detailed statistical analysis output, particularly for the direct problem.

The following section provides numerical checks and more details on the explicit Euler method used (see also A.2.8).

2.4 Numerical experiment from the direct problem

2.4.1 A first case

The parameters of the point model for the first case are

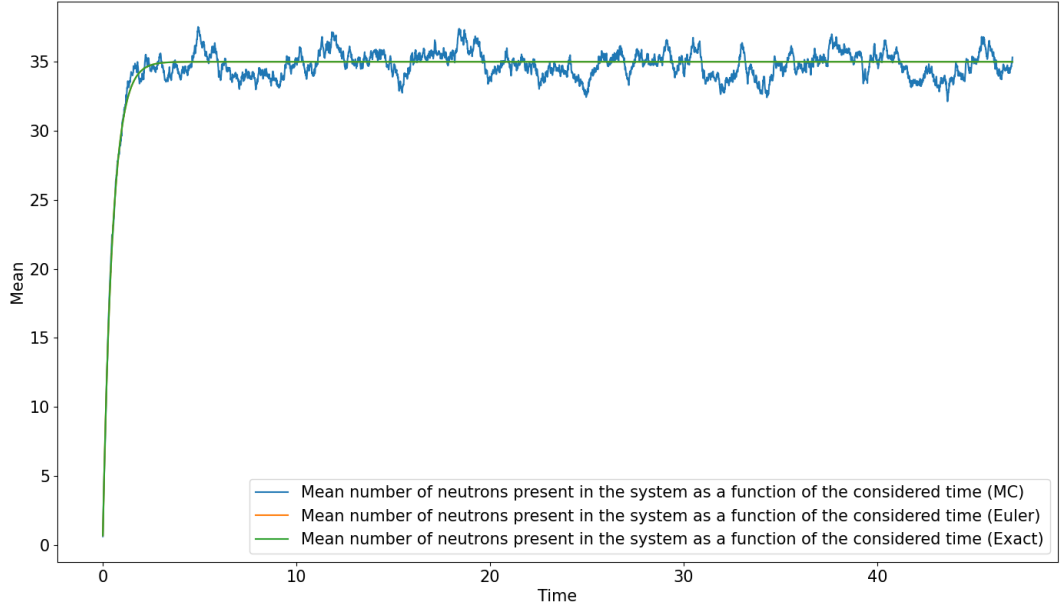
$$\mathbf{p}^* = \begin{pmatrix} S^* = 70 \text{ n.ms}^{-1} \\ \rho^* = -1 \\ \varepsilon_C^* = 0, 25 \cdot 10^{-2} \\ \mathbf{x}^* = 0 \\ \alpha^* = 2 \text{ ms}^{-1} \end{pmatrix} \quad (2.49)$$

where $\rho^* = -1$ corresponds to $k_{eff}^* = 0.5$. All calculations will be performed in ms^{-1} . The measurements are made for a duration of 3600 s. Spontaneous fission emits a maximum of 1 neutron, induced fission emits a maximum of 7 neutrons (with the Terrel distribution [Ter57] cf. appendix equation A.297) and the nuclear constants are

$$\begin{pmatrix} \bar{\nu} \\ D_2 \\ D_3 \end{pmatrix} = \begin{pmatrix} 2, 53108 \\ 0, 81168 \\ 0, 51843 \end{pmatrix} \quad \begin{pmatrix} \bar{\nu}_S \\ D_{2S} \\ D_{3S} \end{pmatrix} = \begin{pmatrix} 1 \\ 0 \\ 0 \end{pmatrix} \quad (2.50)$$

The "Counting" code 3 provides the Monte Carlo realisations obtained by the algorithm 3, the analytical formula and the explicit Euler resolution of the ODE for the previously introduced quantities such as

- $\bar{\nu}_{II}(t)$, $\sigma_{II}(t)$, $\nu_{3,II}(t)$, (see state-of-the-art eq. 1.191, 1.194 and 1.196 respectively for the ODE and eq. 2.9, 2.11 and 2.13 for the exact formula)
- $\nu_{3,\pi}(t)$, (see state-of-the-art eq. 1.175 and eq. 2.7 for the exact formula)
- $m_1(t)$, $\mathbb{E}[N^2]_{p_n(t)}$, $\mathbb{E}[N^3]_{p_n(t)}$, and induced quantities e.g. $\mathbb{E}[N^2]_{p_n(t)} - \mathbb{E}[N]_{p_n(t)}^2$ (see state-of-the-art eq. 1.222, 1.223 and 1.224 respectively for the ODE, and eq. 2.32, 2.34 and 2.37 for the exact formula)
- $M_1(t)$, $\mathbb{E}[N^2]_{P_n(t)}$, $\mathbb{E}[N^3]_{P_n(t)}$, and induced quantities (see appendix eq. A.207, A.209 and A.211 respectively for the ODE, and eq. 2.40, 2.41 and 2.43 for the exact formula)
- $\mathcal{M}_1(t)$, $\mathbb{E}[N^2]_{Q_n(t)}$, $\mathbb{E}[N^3]_{Q_n(t)}$ and induced quantities (see appendix eq. A.212, A.213 and A.214 respectively, and eq. 2.45, 2.46 and 2.48 for the exact formula)

Figure 2.1: $\bar{\nu}_{II}(t)$, t is in ms

All these calculations allow the results of the direct problem to be verified for the case under consideration. These checks can easily be done on another case. As some of these checks are really strong, we are sure that there is no problem.

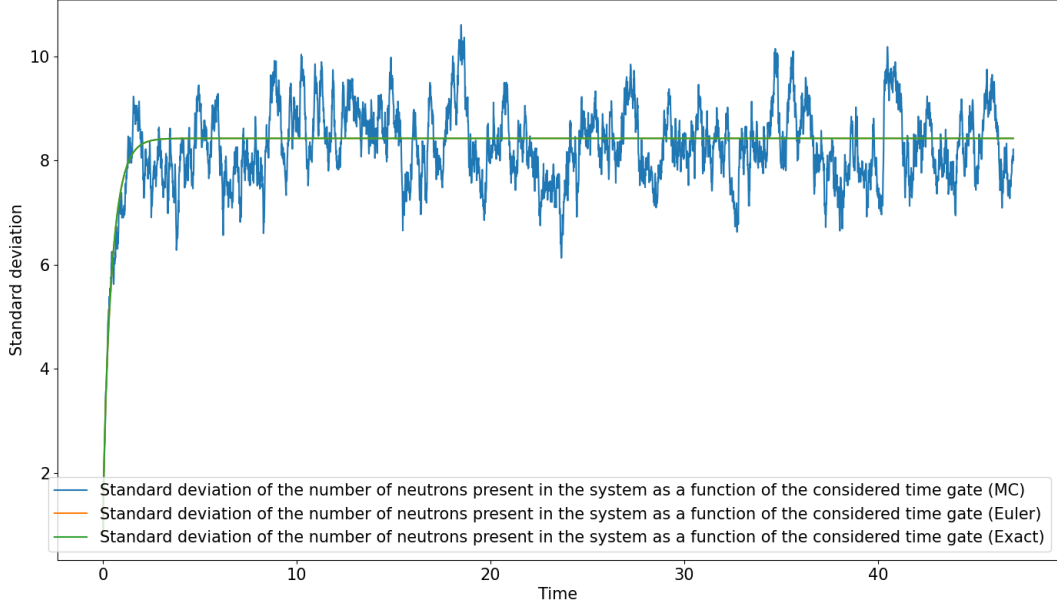
Moments of the number of neutrons present in the system We recall that we were talking about equations about the number of neutrons present in the system at time T knowing there was 0 neutrons at time t in the presence of a source. Here, we are talking about the number of neutrons present in the system at time t knowing there was 0 neutrons at time 0 in the presence of a source. The aim of this consideration is to have only a time length t in the computations.

We first calculate the average number of neutrons present in the system (cf. figure 2.1). As shown in equation 2.9, the average of the number of neutrons present in the system at time t converges to a stationary average value (cf. Prop 2.1.4) where $\bar{\nu}_S = 1$, $S = 70n.ms^{-1}$, $\alpha = 2ms^{-1}$. In the figure 2.1, we observe that the asymptotic value is 35, which is in agreement with our calculations. The Euler scheme (for the equation 1.191) and the exact formula are in agreement. On the other hand, we consider 1 MC realisation of duration 36s. Convergence can be achieved for a higher number of MC realisations.

We then calculate the standard deviation of the number of neutrons present in the system (cf. figure 2.2). We recall the expression of the standard deviation as a function of $\nu_{2,II}(t)$ and $\bar{\nu}_{II}(t)$.

$$\sigma_{II}(t) = \sqrt{2\nu_{2,II}(t) + \bar{\nu}_{II}(t) - \bar{\nu}_{II}^2(t)} \quad (2.51)$$

We recall the asymptotic value $2\nu_{2,II,\infty} = \frac{S}{\alpha}(\bar{\nu}_S \frac{\nu_2}{-\rho\bar{\nu}} + \nu_{2S}) + \frac{\bar{\nu}_S^2 S^2}{\alpha^2}$ and $\frac{\nu_2}{\bar{\nu}} = \frac{\bar{\nu} D_2}{2}$. Then,

Figure 2.2: $\sigma_{\Pi}(t)$, t is in ms

using the numerical values for this case, we conclude that $\sigma_{\Pi,\infty} \approx 8,42$ which is the approximate value of $\sigma_{\Pi,\infty}$ when we plot the figure. We consider 1 MC realisation of duration 36s.

The third order moment of the number of neutrons present in the system in the presence of a source has a complex expression. We will check this expression at different levels.

In Figure 2.3, the exact curve and the Euler explicit curves coincide. Then we have checks, with $\nu_{3,\Pi} - \frac{\nu_{\Pi}^3}{6}$ and $\nu_{3,\Pi} - \frac{\bar{\nu}\Pi\nu_{2,\Pi}}{3}$. Because there are components $\frac{\nu_{\Pi}^3}{6}$ and $\frac{\bar{\nu}\Pi\nu_{2,\Pi}}{3}$ in $\nu_{3,\Pi}$.

First, we plot the curve of $\nu_{3,\Pi}(t)$ with the exact, explicit Euler formula (for the equation 1.196) and with an MC estimate. The figure shows that the exact and explicit Euler curves are in agreement, the MC estimate fluctuates around the exact asymptote $\nu_{3,\Pi,\infty}$. As a first approach, the exact asymptotic value in this case is $\nu_{3,\Pi,\infty} \approx 7786,19$ which is approximately the asymptotic value we observe on figure 2.3 (we still used $\frac{\nu_2}{\bar{\nu}} = \frac{\bar{\nu}D_2}{2}$ and $\frac{\bar{\nu}^3D_3}{6}$).

Then we calculated the figure 2.4 because $\nu_{3,\Pi}(t)$ has a component $\frac{\nu_{\Pi}^3(t)}{6}$. Since we want to check the asymptotic value of $\nu_{3,\Pi}(t) - \frac{\nu_{\Pi}^3(t)}{6}$ we are interested in the long-term behaviour of this expression. We have $\nu_{3,\Pi,\infty} - \frac{\nu_{\Pi,\infty}^3}{6} \approx 640,36$ which is the approximate asymptotic value that we can see in the figure 2.4. This figure shows that the exact and explicit Euler expression (adding the results of the different schemes) converges to the same value, and that the MC estimate fluctuates around this expression. This could be a correct verification, but we will go further.

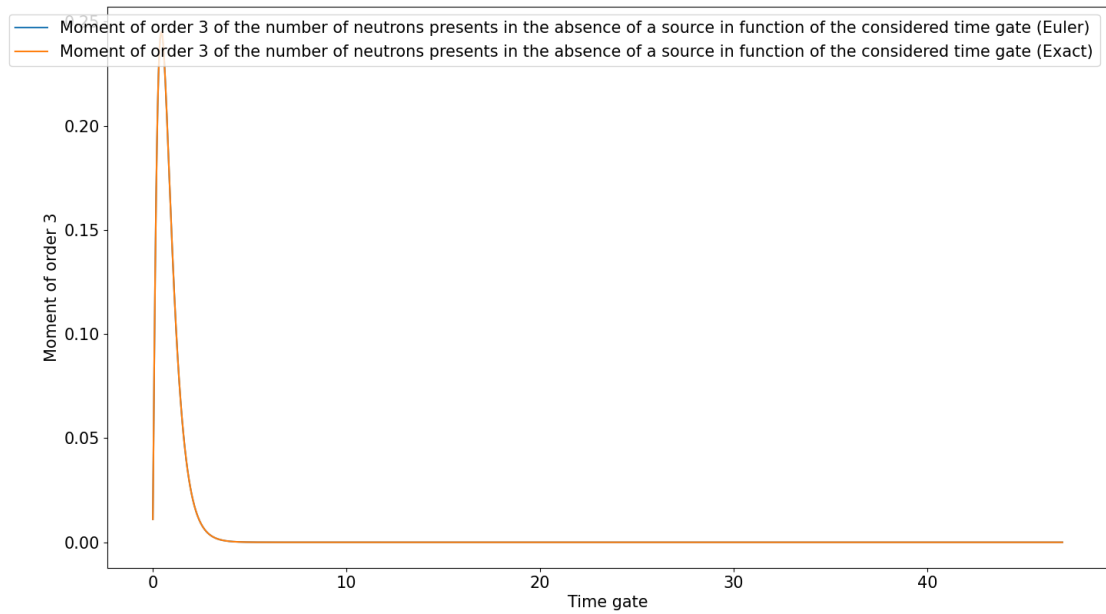


Figure 2.3: $\nu_{3,\Pi}(t)$, t is in ms

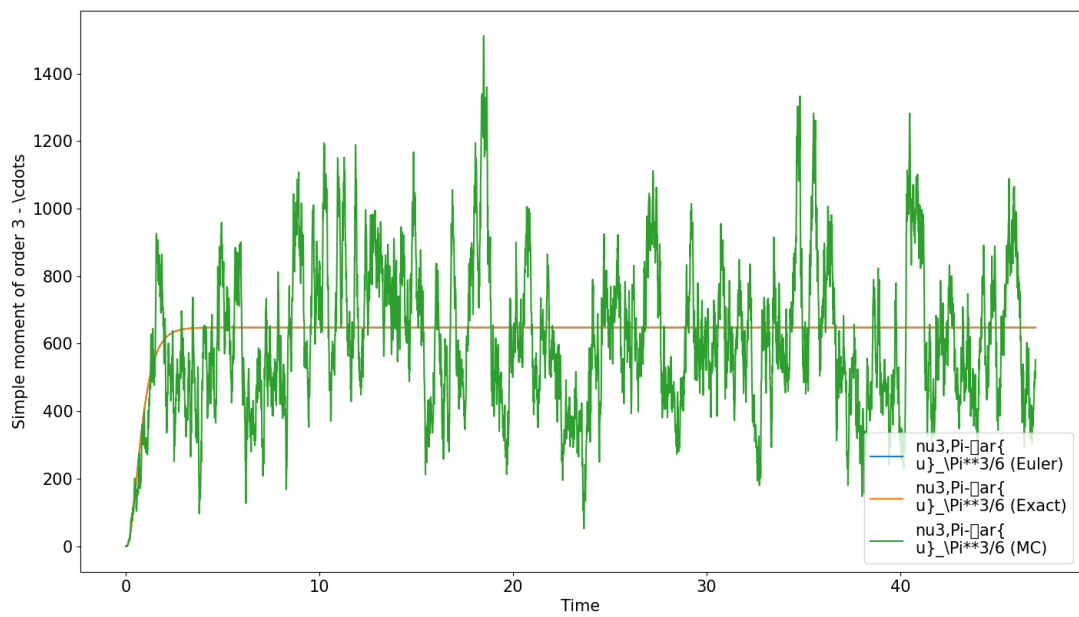


Figure 2.4: $\nu_{3,\Pi}(t) - \frac{\bar{\nu}^3}{6}$, t is in ms

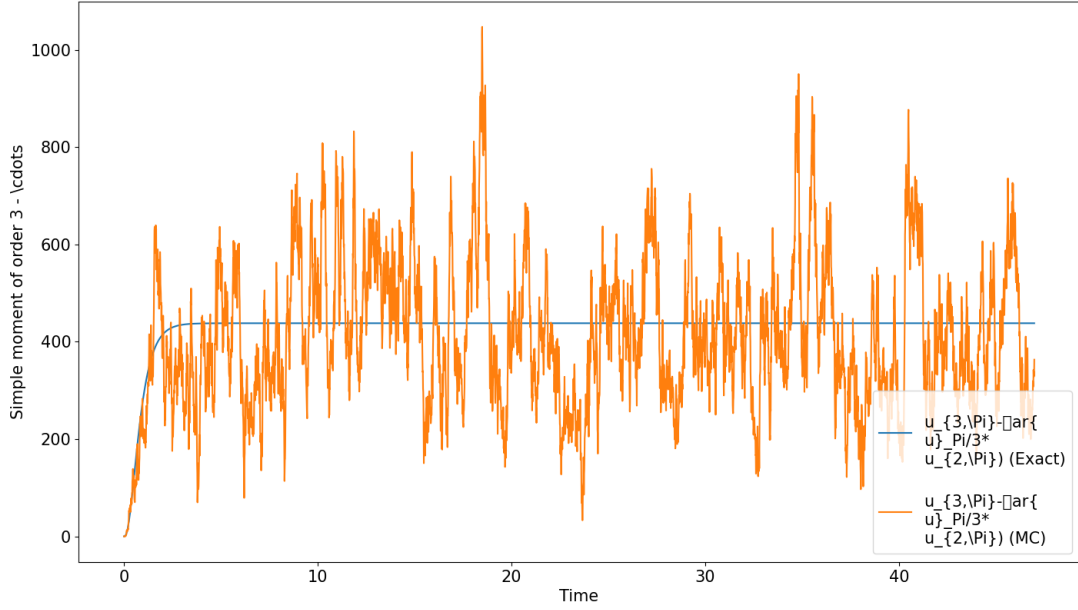


Figure 2.5: $\nu_{3, \Pi}(t) - \frac{\bar{\nu} \Pi^{\nu_{2, \Pi}}}{3}$, t is in ms

We also observe the asymptotic value of $\nu_{3, \Pi}(t)$ more precisely, thanks to the formula of cumulants, there is a component $\frac{\bar{\nu} \Pi^{(t) \nu_{2, \Pi}(t)}}{3}$. Then we will consider the expression $\nu_{3, \Pi}(t) - \frac{\bar{\nu} \Pi^{(t) \nu_{2, \Pi}(t)}}{3}$. At first sight, the expression should be calculated using the log, then we obtain the figure 2.5, and we observe that the MC estimate fluctuates around the asymptotic value of the exact curve. We compute the asymptotic values $\nu_{3, \Pi, \infty} - \frac{\bar{\nu} \Pi_{\infty}^{\nu_{2, \Pi, \infty}}}{3} \approx 438, 21$ which is approximately the value seen when zooming in on the figure 2.5.

This allows us to verify numerically the first 3 moments of the distribution of the number of neutrons present in the system in the presence of a source at time T knowing that there were 0 neutrons at t in the presence of a source $\Pi_n(t)$. We now propose to present the results of numerical experiments on the distribution of the number of neutrons detected in the absence or presence of a source.

Neutron number moments detected in the absence of a source

We recall the empirical moments of $N^j, \forall j \in \mathbb{N}^*$ are computed thanks to

$$\widehat{\mathbb{E}[N^j]} = \frac{1}{Nb} \sum_{k=1}^{Nb} N_k^j \quad (2.52)$$

where Nb is the number of realisations and N_k is the k -th realisation of N as in figure 1.4. When we are in the absence of source the system turns off, then we compute Nb times this extinction and take into account the empirical number of detections.

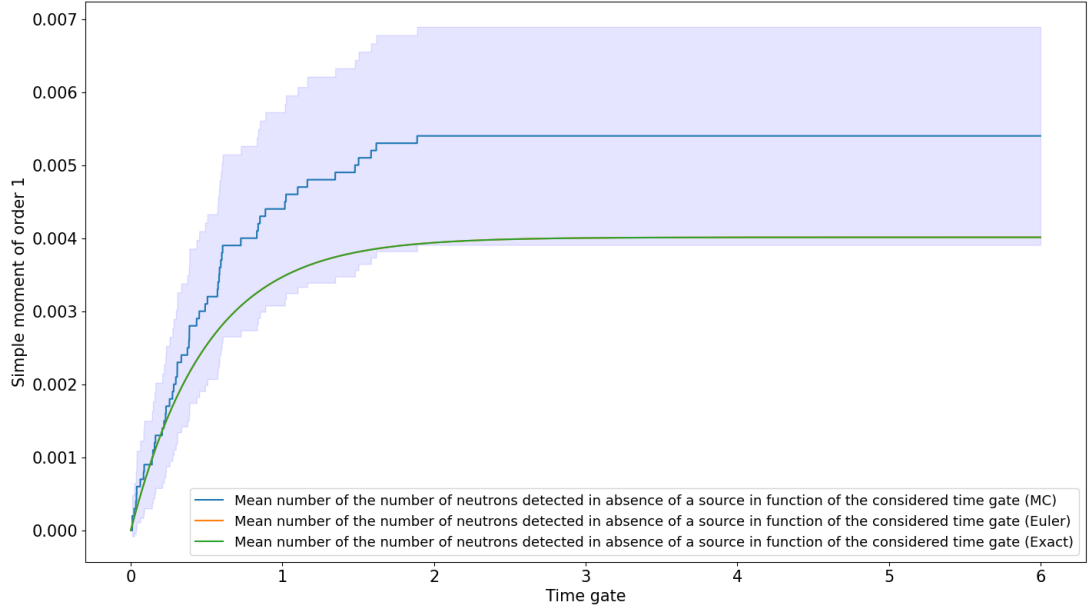


Figure 2.6: Moment of order 1 of the number of detected neutrons in absence of a source as a function of the length of the considered time gate $m_1(t)$, t is in ms

We will also compute the confidence interval for the quantities $\widehat{\mathbb{E}[N^j]} - \widehat{\mathbb{E}[N]^j}$ as shown in the annexes A.4.1.

The first moment in the absence of a source is shown in figure 2.6. The Monte Carlo (MC) curve is made with 10^4 realisations and there is a large $\sigma_{p_n(t)} = \sqrt{\widehat{\mathbb{E}[N^2]_{p_n(t)}} - \widehat{\mathbb{E}[N]^2_{p_n(t)}}$ corresponding, then the confidence interval at 95% is of order $\approx 15\%$. The MC average does not have much fluctuation for large values of the time gate because the number of neutrons detected is quite the same due to the characteristics of the case. The 95% empirical confidence intervals are calculated by computing the empirical moments $\widehat{\mathbb{E}[N^j]_{p_n(t)}}$ and the corresponding standard deviation $\widehat{\sigma_{j,p_n(t)}} = \sqrt{\widehat{\mathbb{E}[N^j]_{p_n(t)}} - \widehat{\mathbb{E}[N]^j_{p_n(t)}}$ and we plot the bar $\widehat{\mathbb{E}[N^j]_{p_n(t)}} \pm 2 \frac{\widehat{\sigma_{j,p_n(t)}}}{\sqrt{Nb}}$ where Nb is the number of MC realisations. Moreover, when the order of the moment is equal to 2 or 3, we want to check at a higher order. In particular, there is a $\mathbb{E}[N]^j$ in $\mathbb{E}[N^j]$ for the distribution under consideration, we make sure that $\widehat{\mathbb{E}[N^j]} - \widehat{\mathbb{E}[N]^j}$ converges to a unique solution for the three plotted curves.

In the following figures, the exact and explicit Euler curves are superimposed. The checks $\mathbb{E}[N^i] - \mathbb{E}[N]^i$ (for all the considered distributions $p_n(t)$, $P_n(t)$, $Q_n(t)$) the MC curve is taken by subtracting the MC estimation of $\mathbb{E}[N]^i$ to the MC estimation of $\mathbb{E}[N^i]$. We underline the fact that, in these cases, the confidence interval computation is non-trivial, the details of the computations are made in annexes A.4.1.

First, the equation 2.32 claims $m_1(t)$ has the asymptotical value $\frac{\varepsilon_F}{-\rho \bar{\nu}} \approx 4,01.10^{-3}$ what we observe on the figure 2.6. The second simple moment of the number of neutrons detected is in figure 2.7. The equation 2.34 shows the asymptotic value of $\mathbb{E}[N^2]_{p_n(t)}$ is $2 \frac{\nu_2 \varepsilon_F^2}{(-\rho \bar{\nu})^3} + \frac{\varepsilon_F}{-\rho \bar{\nu}} \approx 4.05.10^{-3}$ which is consistent with the asymptotic value in figure 2.7. Moreover, in the equation 2.37 we can see there is a component

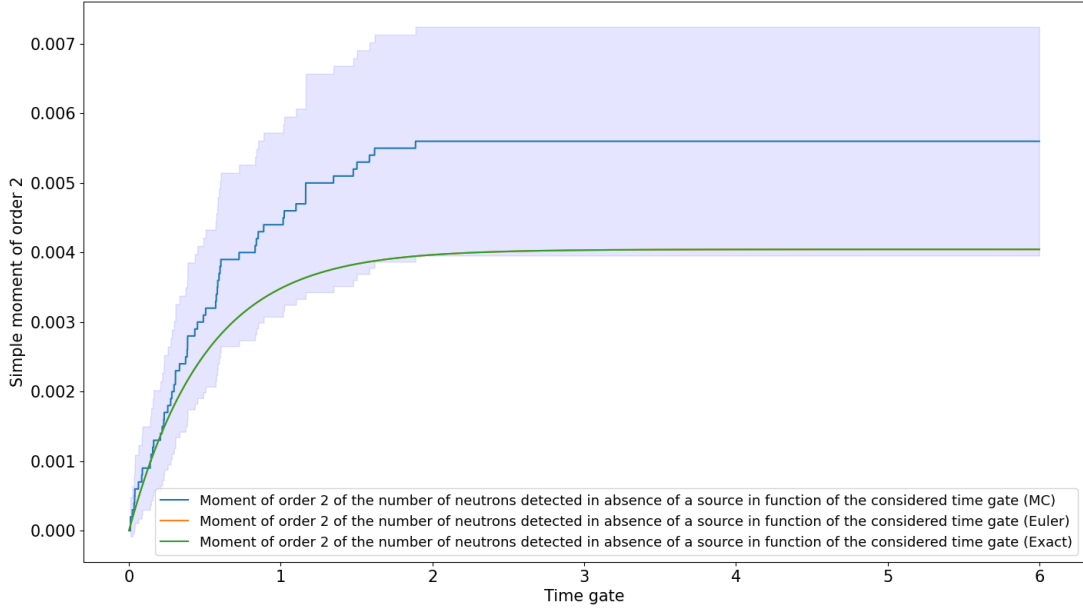


Figure 2.7: Simple moment of order 2 of the number of detected neutrons in absence of a source in function of the length of the considered time gate $\mathbb{E}[N^2]_{p_n(t)}$, t is in ms

$\mathbb{E}[N^2]_{p_n(t)}$ in $\mathbb{E}[N^2]_{p_n(t)}$ when $T - t$ is large, so we observe the asymptotical value on figure 2.8. The equation $2\frac{\nu_2\varepsilon_F^2}{(-\rho\nu)^3} + \frac{\varepsilon_F}{-\rho\nu} - (\frac{\varepsilon_F}{-\rho\nu})^2 \approx 4,03.10^{-3}$ which confirms the asymptotical value of $\mathbb{E}[N^2]_{p_n(t)} - \mathbb{E}[N^2]_{p_n(t)}$. Finally, we present the third simple moment of the neutron distribution detected in the absence of a source with an initial neutron (cf. 2.9). The figure 2.9 shows the asymptotical value of $\mathbb{E}[N^3]_{p_n(t)}$, which can be computed as $6(A + B + \frac{\nu_2\varepsilon_F^2}{(-\rho\nu)^3}) + \frac{\varepsilon_F}{-\rho\nu} \approx 4,11.10^{-3}$ which confirms the asymptotical values of $\mathbb{E}[N^3]_{p_n(t)}$ in figure 2.9. Since there is a component $\mathbb{E}[N^3]_{p_n(t)}$ in $\mathbb{E}[N^3]_{p_n(t)}$. We compute the difference $\mathbb{E}[N^3]_{p_n(t)} - \mathbb{E}[N^3]_{p_n(t)}$ and observe the behaviour of figure 2.10. We recall $6(A + B + \frac{\nu_2\varepsilon_F^2}{(-\rho\nu)^3}) + \frac{\varepsilon_F}{-\rho\nu} - (\frac{\varepsilon_F}{-\rho\nu})^3 \approx 4.11.10^{-3}$ which confirms the asymptotical values of $\mathbb{E}[N^3]_{p_n(t)} - \mathbb{E}[N^3]_{p_n(t)}$ in figure 2.10.

We can then conclude that the simple moments of order 1 to 3 of the detected neutron number distribution are valid thanks to the explicit Euler, the analytical formula and the Monte-Carlo comparison.

We now consider the numerical checks of the simple moments of the number of neutrons detected in the presence of a source of the distribution $(X_t, N_{[0,t]})$.

Moments of the number of neutrons detected in presence of a source

We remain in the configurations of the case presented at the beginning of the section.

Using the Monte Carlo code "Counting" 3, we present the following results of moment calculations in the transitional regime. We plot the analytical formula, the

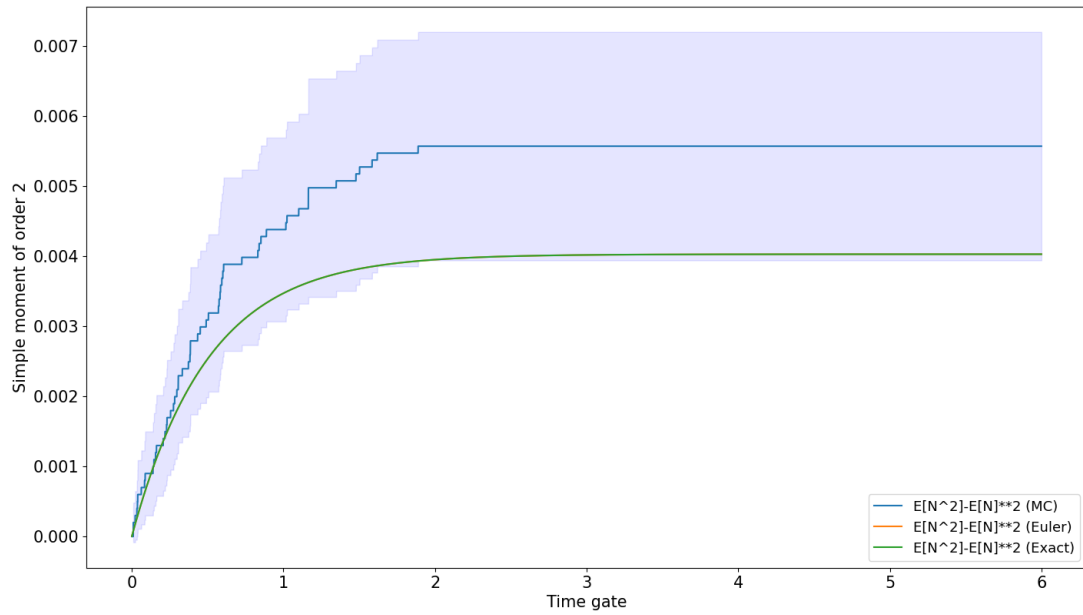


Figure 2.8: $\mathbb{E}[N^2]_{p_n(t)} - \mathbb{E}[N]_{p_n(t)}^2$, t is in ms

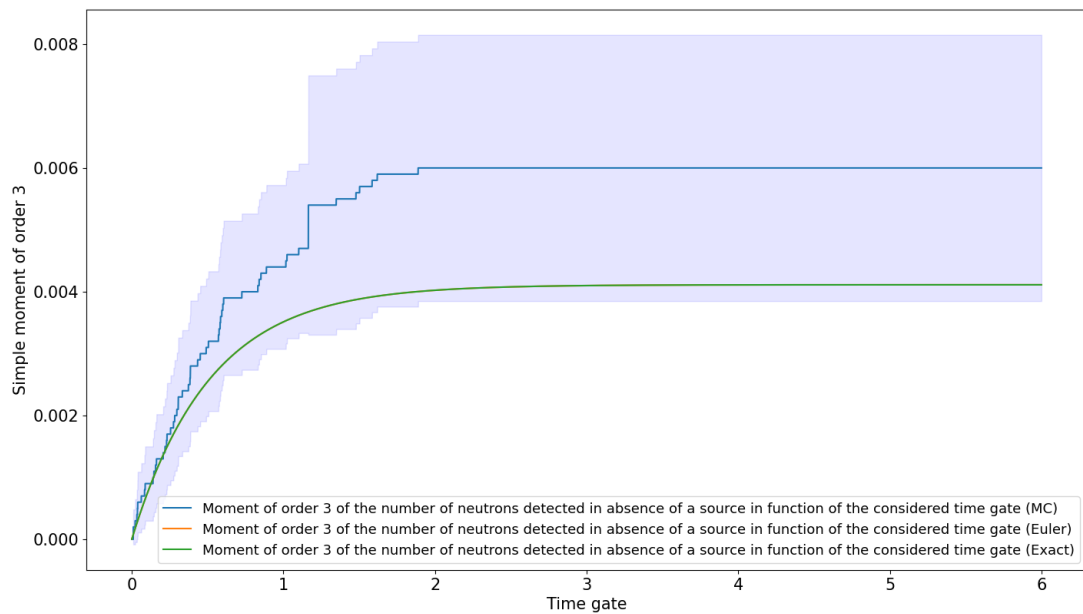


Figure 2.9: Simple moment of order 3 of the number of detected neutrons in absence of a source in function of the length of the considered time gate $\mathbb{E}[N^3]_{p_n(t)}$, t is in ms

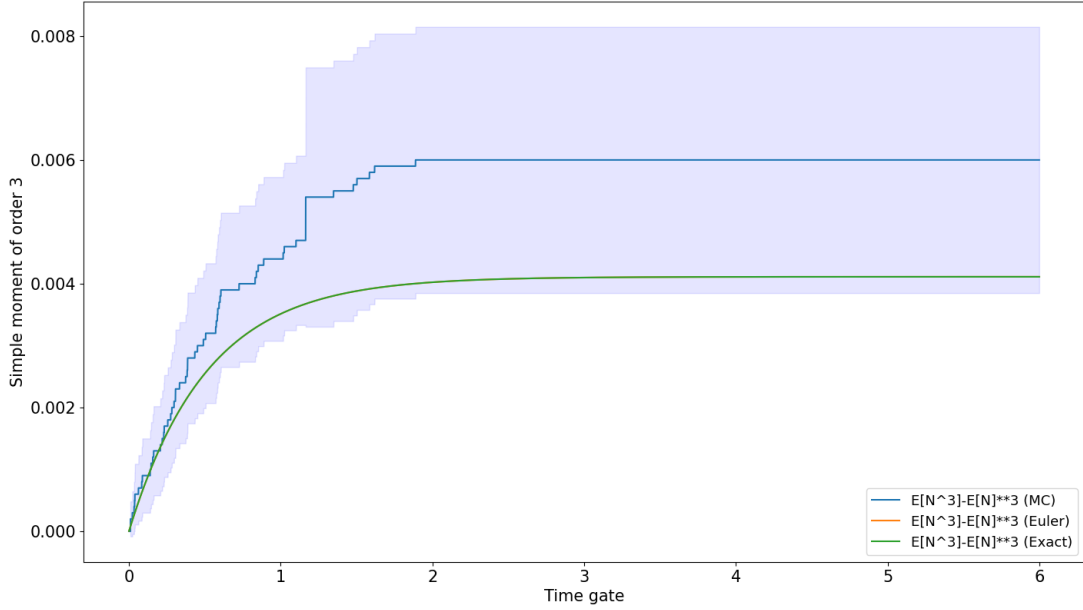


Figure 2.10: $\mathbb{E}[N^3]_{P_n(t)} - \mathbb{E}[N]_{P_n(t)}^3$, t is in ms

MC representation (with confidence interval 95%) and the explicit Euler. We have considered 100 MC realisations of 36s duration. We can observe satisfactory results for these simple moments.

We recall here that the curves of the exact formula and the explicit Euler scheme are superimposed. Moreover, on each curve representation, the $[0; 0, 01]$ part is not well-fitted to the other curves, this is due to the fact that the smallest time gate considered is $T - t = 0, 01\text{ms}$. Taking into account smaller time gates will allow obtaining a more accurate curve around $T - t = 0\text{ms}$. This detail has no impact on the overall verification performed here.

Regarding the stationary regime, the "Counting" code proceeds as follows: we let the MC code computes the number of neutrons present in the system until $t \gg \frac{1}{\alpha}$ and the detector is open.

The first moment of the number of neutrons detected is given in figure 2.11. We recall that the equation 2.40 has a linear part and an exponential part, i.e. when $T - t$ is low both quantities count, when $T - t \gg \frac{1}{\alpha}$ the linear part is dominant.

The second order simple moment of the number of neutrons detected is shown in figure 2.12. We recall the equation 2.41 has three different behaviours: a linear part, a quadratic part and an exponential part. When $T - t \gg \frac{1}{\alpha}$, the quadratic behaviour is dominant. The figure 2.12 confirms the quadratic formula is dominant when $T - t$ is large. Moreover, the equation 2.12 shows there is a component $\mathbb{E}[N^2]_{P_n(t)}$ in $\mathbb{E}[N^2]_{P_n(t)}$. Then, we use the following figure to confirm this. We plot $\mathbb{E}[N^2]_{P_n(t)} - \mathbb{E}[N]_{P_n(t)}^2$ in figure 2.13, and we observe only the linear behaviour as expected when $T - t \gg \frac{1}{\alpha}$ (we removed the quadratic part). The exponential behaviour is still present when $T - t \ll \frac{1}{\alpha}$.

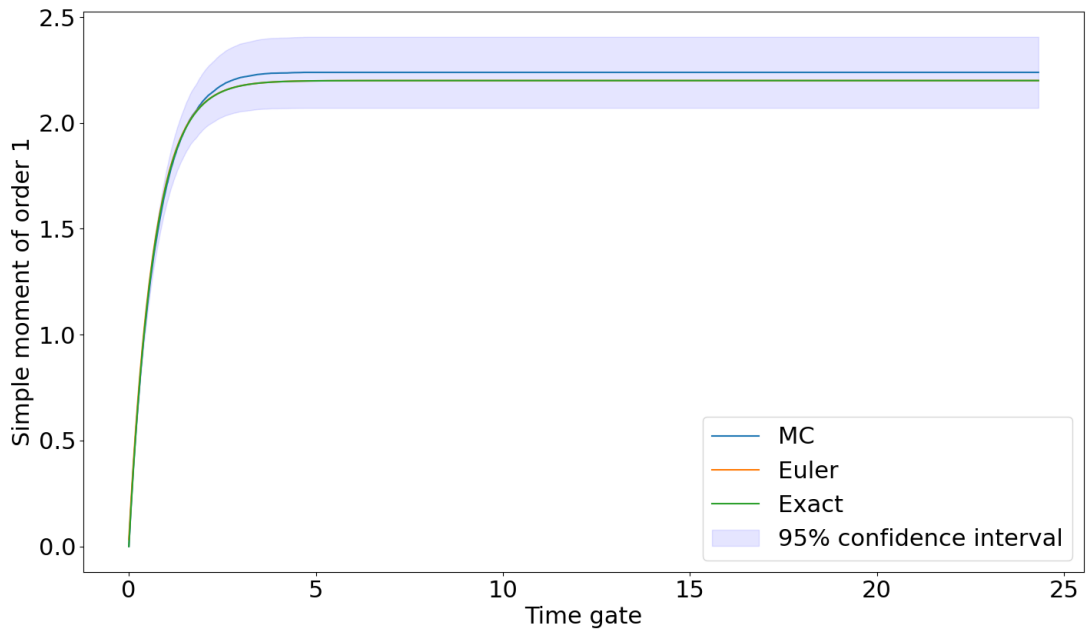


Figure 2.11: $M_1(t)$, t is in ms

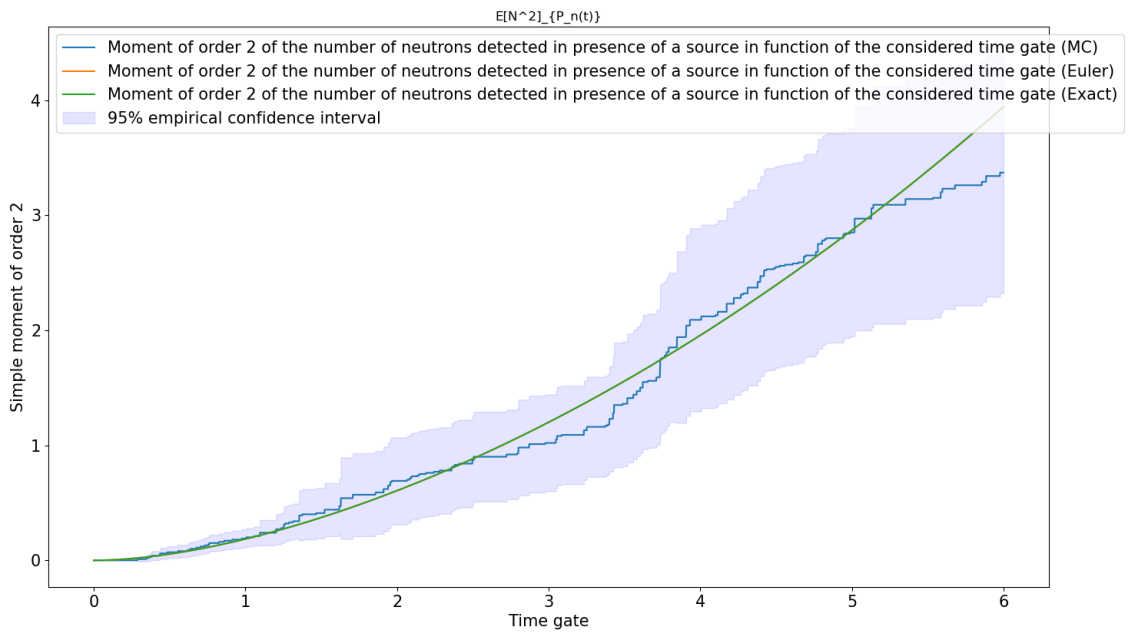


Figure 2.12: $\mathbb{E}[N^2]_{P_n(t)}$, t is in ms

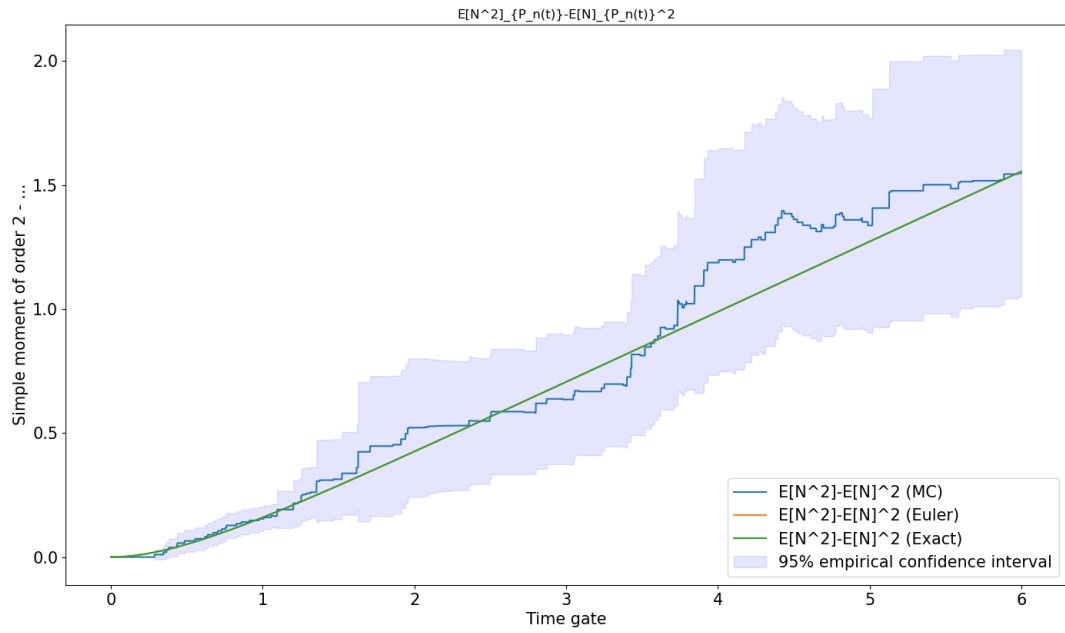


Figure 2.13: $\mathbb{E}[N^2]_{P_n(t)} - \mathbb{E}[N]_{P_n(t)}^2$, t is in ms

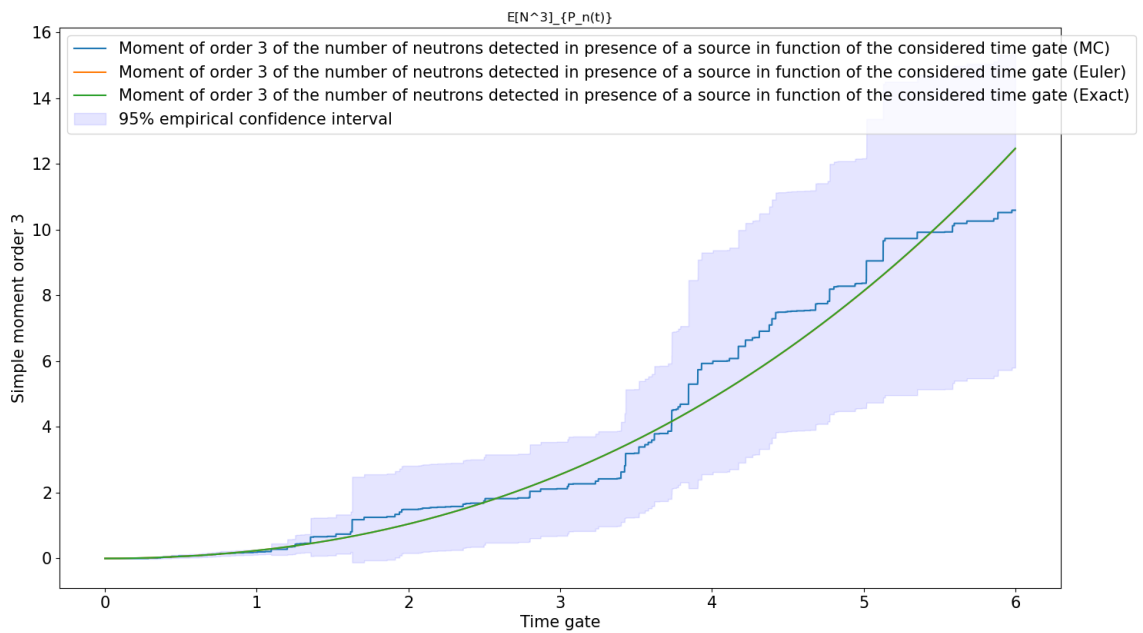


Figure 2.14: $\mathbb{E}[N^3]_{P_n(t)}$, t is in ms

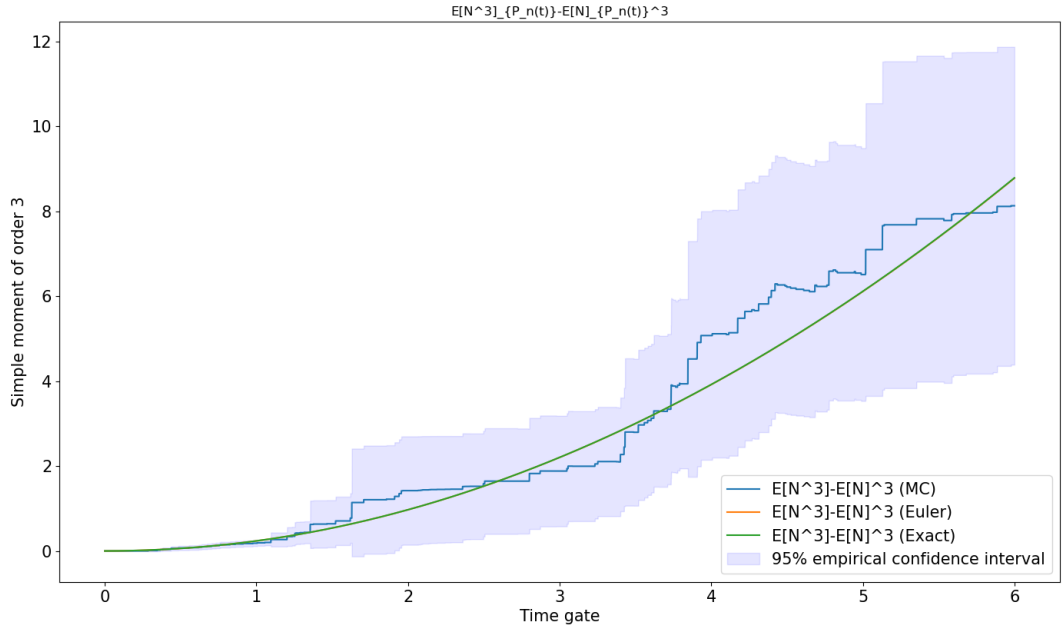


Figure 2.15: $\mathbb{E}[N^3]_{P_n(t)} - \mathbb{E}[N]_{P_n(t)}^3$, t is in ms

Finally, we can obtain the third-order simple momentum of the number of neutrons detected in figure 2.14. We recall the equation 2.43 shows four different behaviours: a linear, a quadratic, a cubic and an exponential behaviour. When $T - t \gg \frac{1}{\alpha}$, we see clearly the cubic behaviour of $\mathbb{E}[N^3]_{P_n(t)}$.

Then, we want to confirm the exact expression, to do so we plot $\mathbb{E}[N^3]_{P_n(t)} - \mathbb{E}[N]_{P_n(t)}^3$ in figure 2.15. When $T - t \gg \frac{1}{\alpha}$ we expect a quadratic behaviour, the figure 2.15 confirms.

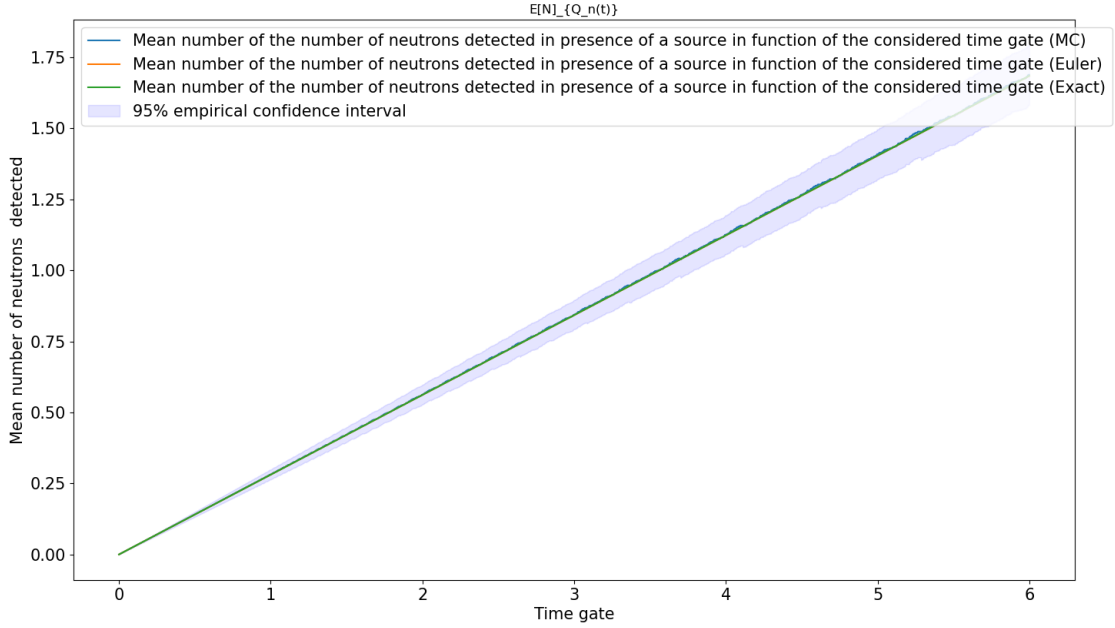
In conclusion, we have shown that the exact expressions of the simple moments of order 1 to 3 of the distribution of the number of neutrons detected during a time interval t are true and that they have a specific behaviour depending on the regime we consider.

Simple moments of the number of neutrons detected when the number of neutrons present in the system follows its stationary distribution

In the following we present our verification of the first three simple moments of the number of neutrons detected knowing that the number of neutrons present in the system has a stationary distribution.

The results for the simple moment of order one are given in the figure 2.16. The equation 2.45 shows a linear behaviour with a slope of $\bar{\nu}_S S \frac{\epsilon_F}{-\rho \bar{\nu}} \approx 0.28$ which is confirmed by the figure 2.16.

In figure 2.17 we show the simple second-order momentum of the neutron distribution detected in the presence of a source and with a stationary distribution. The equation 2.46 shows $\mathbb{E}[N^2]_{Q_n(t)}$ has three different behaviours: a linear term, a quadratic term and an exponential term. As before, the quadratic term is dominant

Figure 2.16: $\mathbb{E}[N]_{Q_n(t)}$, t is in ms

when $T - t \gg \frac{1}{\alpha}$. This is confirmed by the shape of the curve in figure 2.17.

The quadratic behaviour is dominant when $T - t \gg \frac{1}{\alpha}$, to confirm the linear term, we plot $\mathbb{E}[N^2]_{Q_n(t)} - \mathbb{E}[N]_{Q_n(t)}^2$ in figure 2.18. And so the figure shows a linear term of order $\bar{\nu}_S S \frac{\epsilon_F}{-\rho \bar{\nu}}$ as previously.

Finally, we present in figure 2.19 the results for the simple third-order moment of the distribution studied. The equation 2.48 shows four behaviour: a linear term, a quadratic term, a cubic term and an exponential term. When $T - t \gg \frac{1}{\alpha}$, we observe this cubic behaviour in figure 2.19.

To confirm the quadratic term in $\mathbb{E}[N^3]_{Q_n(t)}$ we plot $\mathbb{E}[N^3]_{Q_n(t)} - \mathbb{E}[N]_{Q_n(t)}^3$ in figure 2.20. We observe a quadratic behaviour and this confirm the expression of $\mathbb{E}[N^3]_{Q_n(t)} - \mathbb{E}[N]_{Q_n(t)}^3$ thanks to the figure 2.20.

In order to check more precisely $\mathcal{M}_1(t)$, we plot the theoretical 80% prediction interval (cf. figure 2.21 which computed by $\mathcal{M}_{1,exact}(t) \pm 1.3\sigma_{Q_n}(t)$).

In the figure 2.21, we dispose of the theoretical 80% prediction interval for $\mathcal{M}_1(t)$. This means that for every 10 MC realisations of $\hat{\mathcal{M}}_1(t)$ 8 realisations should be in the prediction interval (the orange interval). In this case, 2 of the 10 MC realisations are outside the prediction interval.

To conclude, the analytical expressions for the first three moments of $(X_t, N_{[0,t]})$ have been verified numerically.

Feynman moments

The correlated Feynman moments are calculated from the simple moments. The results for the second and third order Feynman moments are shown in the following

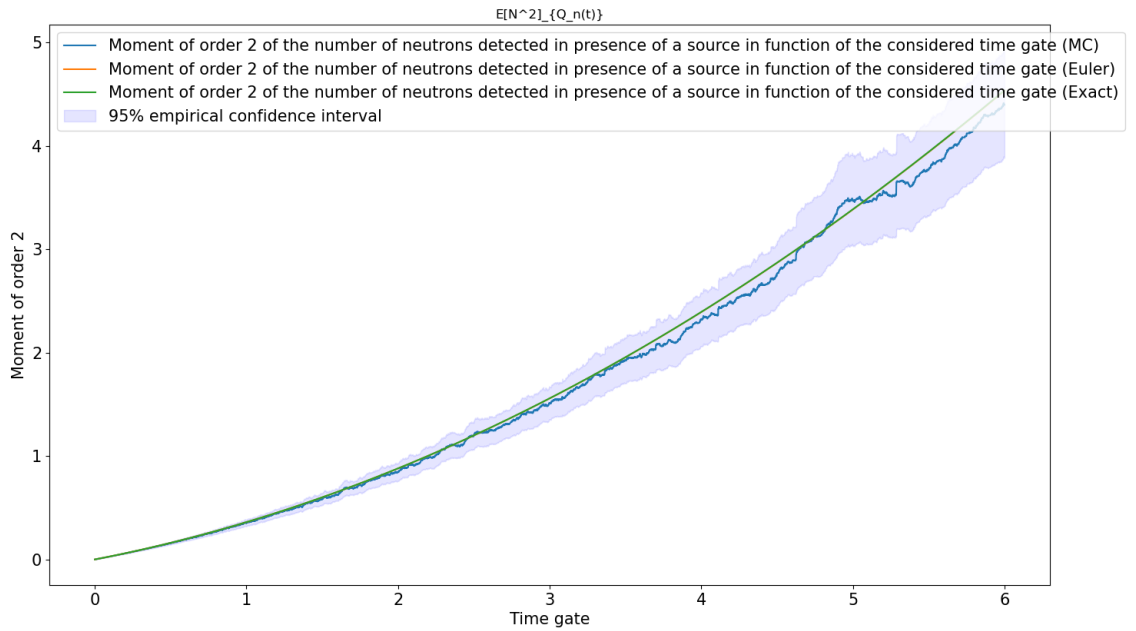


Figure 2.17: $\mathbb{E}[N^2]_{Q_n(t)}$, t is in ms

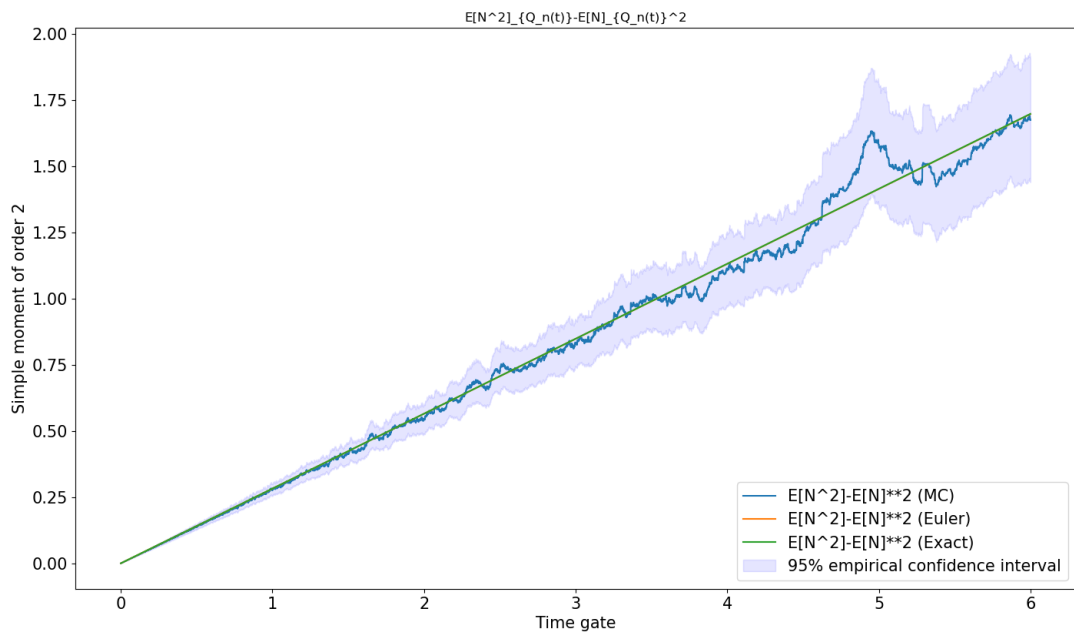


Figure 2.18: $\mathbb{E}[N^2]_{Q_n(t)} - \mathbb{E}[N]_{Q_n(t)}^2$, t is in ms

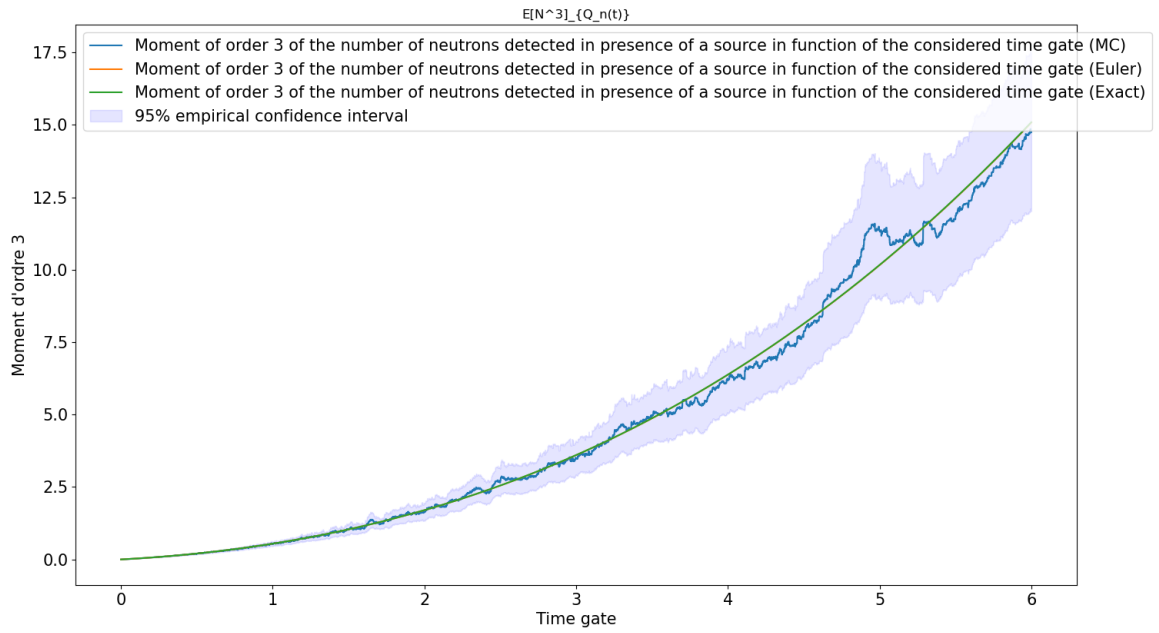


Figure 2.19: $\mathbb{E}[N^3]_{Q_n(t)}$, t is in ms

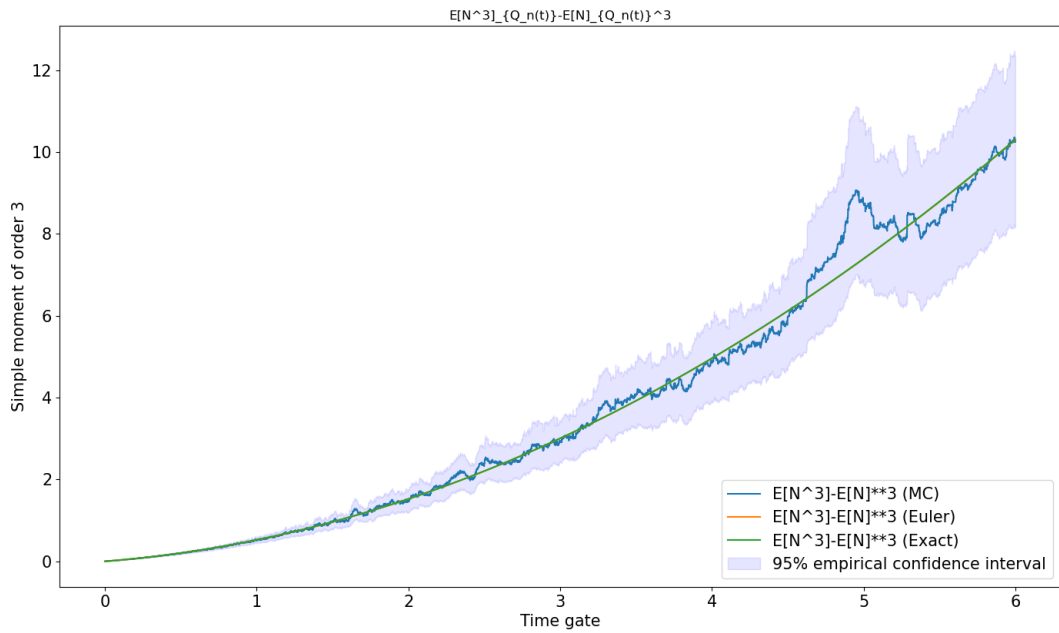


Figure 2.20: $\mathbb{E}[N^3]_{Q_n(t)} - \mathbb{E}[N]_{Q_n(t)}^3$, t is in ms

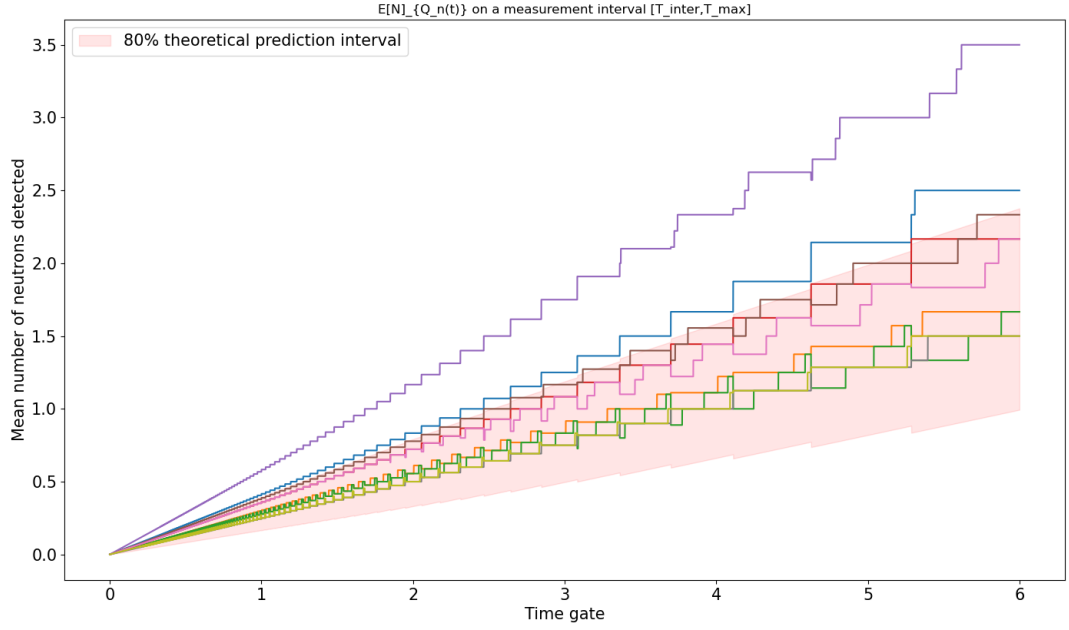


Figure 2.21: Theoretical 80% prediction interval for \mathcal{M}_1 and 10 realisations, t is in ms

figure 2.23 and 2.24 respectively. The empirical Feynman moments are estimated by Monte-Carlo simulations: we first calculate

$$\begin{pmatrix} \widehat{\mathbb{E}[N_{[0,t]}]} \\ \widehat{\mathbb{E}[N_{[0,t]}^2]} \\ \widehat{\mathbb{E}[N_{[0,t]}^3]} \end{pmatrix} \quad (2.53)$$

where, for $N_{realisations} \in \mathbb{N}^*$,

$$\widehat{\mathbb{E}[N_{[0,t]}^j]} = \frac{1}{N_{realisations}} \sum_{l=1}^{N_{realisations}} N_{l,[0,t]}^j \quad (2.54)$$

As shown in the figure 1.4, the realizations are calculated by storing the detection time (the red bars) over a measurement time between T_0 and T_{max} by subdividing them into time gates of length t providing the number of neutrons detected during the l -th time gate of length t : $N_{l,[0,t]}$.

Then the empirical Feynman moments are calculated using the transition formula (annexes A.2.7)

$$\begin{aligned} \widehat{Y}_2(t) &= \frac{\widehat{\mathbb{E}[N_{[0,t]}^2]}}{\widehat{\mathbb{E}[N_{[0,t]}]}^2} - \widehat{\mathbb{E}[N_{[0,t]}]} - 1 \\ \widehat{Y}_3(t) &= \frac{\widehat{\mathbb{E}[N_{[0,t]}^3]} - 3\widehat{\mathbb{E}[N_{[0,t]}^2]\widehat{\mathbb{E}[N_{[0,t]}]} + 2\widehat{\mathbb{E}[N_{[0,t]}]^3}}{\widehat{\mathbb{E}[N_{[0,t]}]}^3} - 3\left(\frac{\widehat{\mathbb{E}[N_{[0,t]}^2]}}{\widehat{\mathbb{E}[N_{[0,t]}]}^2} - \widehat{\mathbb{E}[N_{[0,t]}]} - 1\right) \end{aligned} \quad (2.55)$$

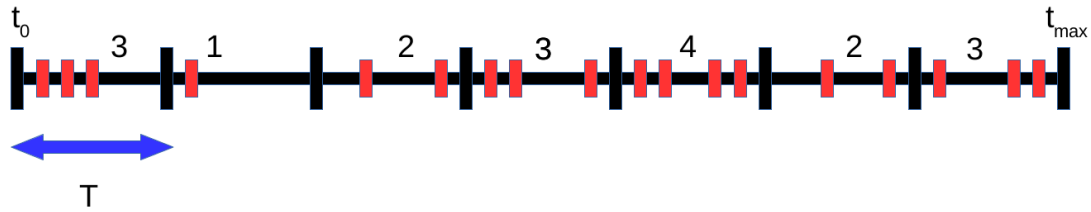


Figure 2.22: Measurements of the number of neutrons detected during a time gate T between t_0 and t_{max} : $N_{1,[0,T]} = 3$, $N_{2,[0,T]} = 1$, $N_{3,[0,T]} = 2, \dots$

The Feynman moment of order two, on figure 2.23, measures the difference in moments with respect to a Poisson process. In this case $x = 0$, the source is a Poisson process and there is induced fission, then $Y_{2,\infty} = \frac{\varepsilon_F D_2}{\rho^2} \approx 8,24 \cdot 10^{-3}$ which is small and this is what we observe: the exact curve increases to a constant value, the Monte Carlo estimate shows large fluctuations from the orange curve.

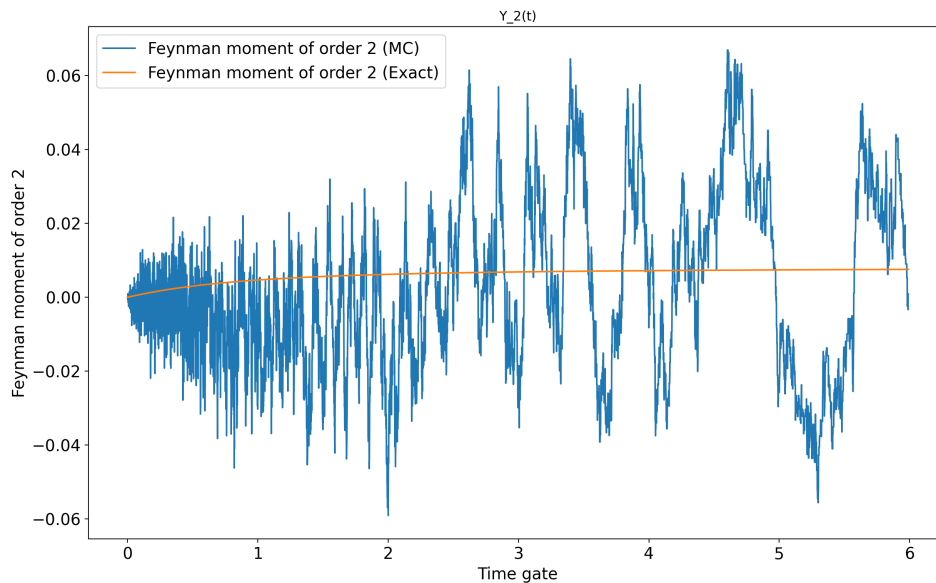


Figure 2.23: $Y_2(t) = \frac{\mathbb{E}[(N - \mathbb{E}[N])^2]_{Q_n(t)}}{\mathbb{E}[N]_{Q_n(t)}} - 1$, t is in ms

The Feynman moment of order three, on figure 2.24, measures also the difference to a Poisson process. The source is still a pure Poisson process, $x = 0$, then $Y_{3,\infty} = 3 \left(\frac{\varepsilon_F D_2}{-\rho^2} \right)^2 - \frac{\varepsilon_F^2 D_3}{\rho^3} \approx 2,04 \cdot 10^{-4}$ which is small and the observations show that the exact curve is constant, the Monte Carlo estimate shows large fluctuations from the orange curve.

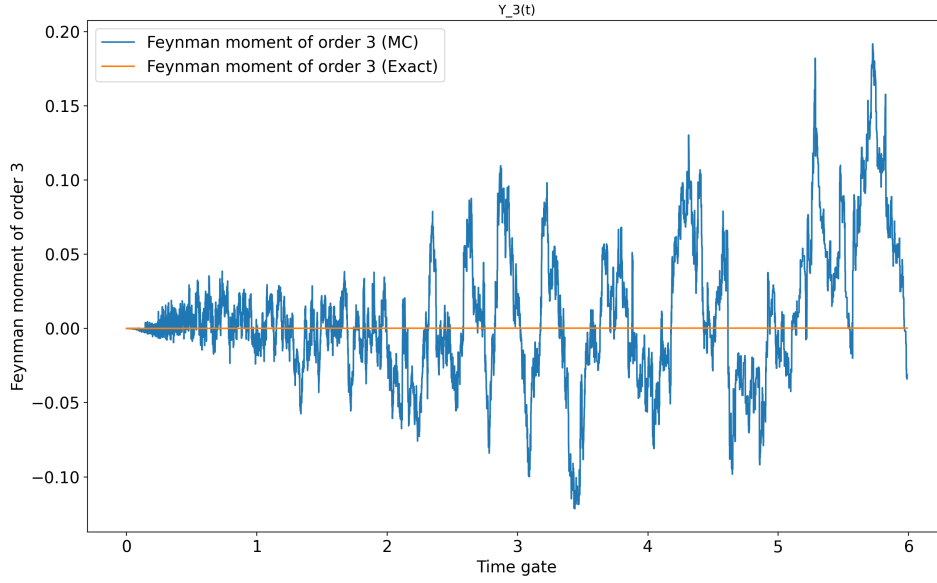


Figure 2.24: $Y_3(t) = \frac{\mathbb{E}[(N - \mathbb{E}[N])^3]_{Q_n(t)}}{\mathbb{E}[N]_{Q_n(t)}} - 1 - 3 \frac{\mathbb{E}[(N - \mathbb{E}[N])^2]_{Q_n(t)}}{\mathbb{E}[N]_{Q_n(t)}} - 1$, t is in ms

The fluctuations of the two Feynman moments show that they are really difficult to use from this point of view, in contrast to the simple moments of order 2 and 3 in the figure 2.16 to 2.19, which are easier to use. This example illustrates the need to consider simple moments in our calculations rather than the Feynman moment. The following case present an example where the Feynman moment is more useful.

2.4.2 A second case

The first test case was used to verify the calculation of the direct problem with different methods. A second test case is defined where the physical parameters are those that will be used, in the next chapter, to calculate the a posteriori distribution of the parameters.

We consider the following set of parameters

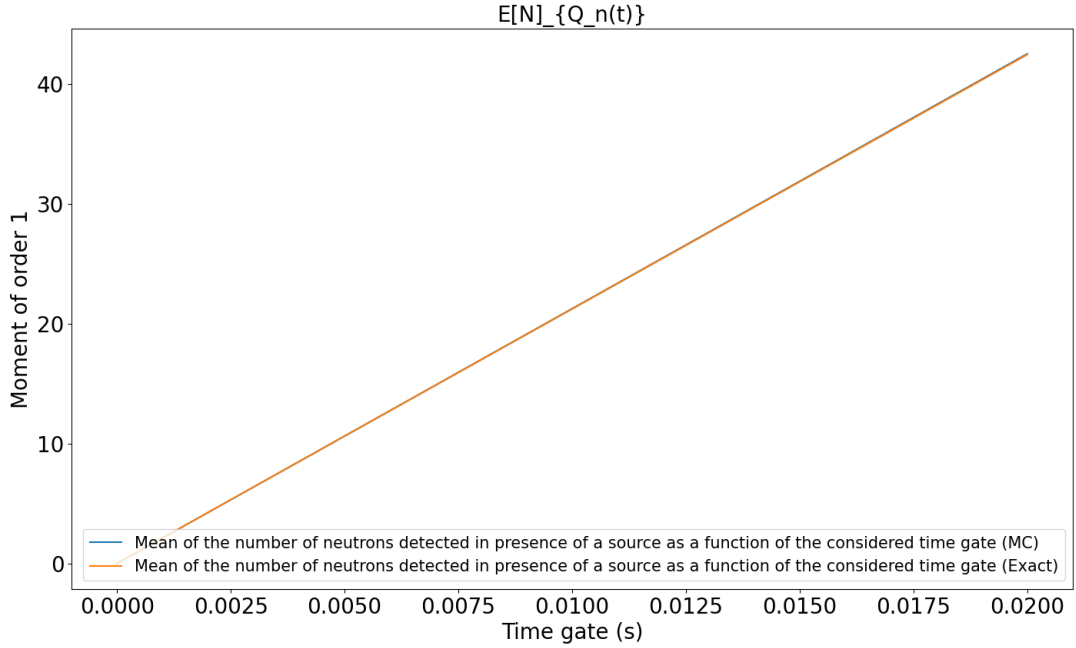
$$\mathbf{p} = \begin{pmatrix} S \\ k_{eff} \\ \varepsilon_C \\ \mathbf{x} \\ \alpha \end{pmatrix} = \begin{pmatrix} 70 \text{ m s}^{-1} \\ 0,95 \\ 0,25 \cdot 10^{-2} \\ 0 \\ 2 \text{ m s}^{-1} \end{pmatrix} \quad (2.56)$$

we recall that $k_{eff} = 0,95 \iff \rho = -0.05263157894$.

Nuclear mater $\left\{ \begin{array}{l} \text{The induced fission material is } {}^{235}\text{U}. \\ \text{The source is poissonian.} \end{array} \right.$

The nuclear constants are

$$\begin{pmatrix} \bar{\nu} \\ D_2 \\ D_3 \end{pmatrix} = \begin{pmatrix} 2,4130 \\ 0,7992 \\ 0,4819 \end{pmatrix} \quad \begin{pmatrix} \bar{\nu}_S \\ D_{2S} \\ D_{3S} \end{pmatrix} = \begin{pmatrix} 1 \\ 0 \\ 0 \end{pmatrix} \quad (2.57)$$

Figure 2.25: $E[N]_{Q_n(t)}$, t is in ms

The measurement time is equal to 36s.

For a time gate $T = \frac{6}{\alpha}$, there are 12000 time gates of duration T . We consider three observables, which are the average count and the Feynman moments of order 2 and 3. The calculation of these observables using the test case parameters is shown in the following figure 2.25, 2.26 and 2.27 respectively.

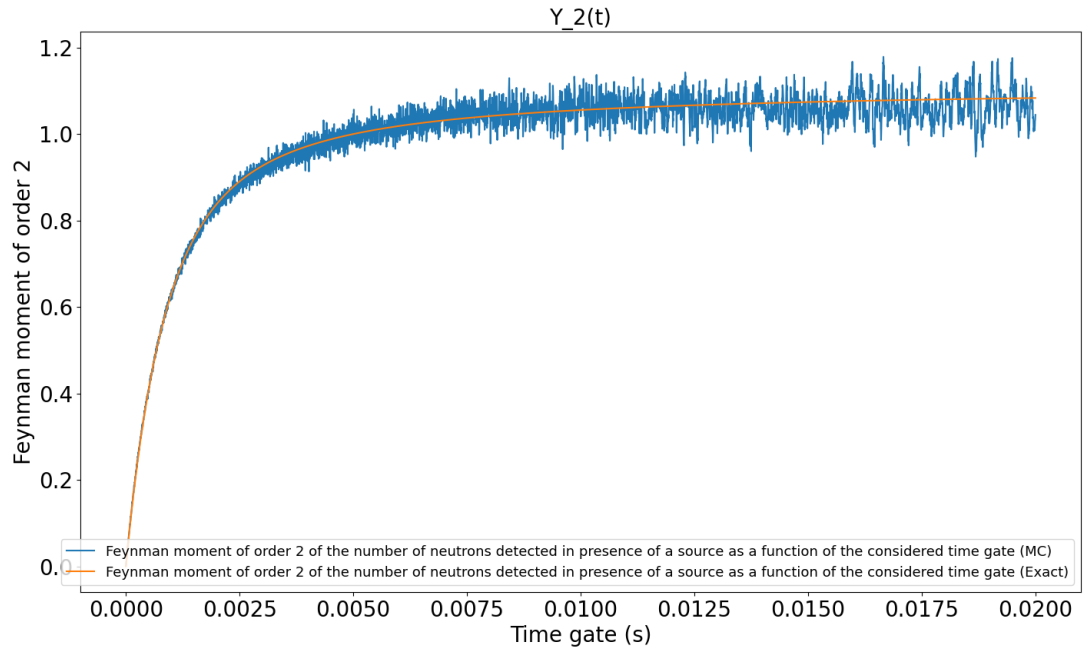
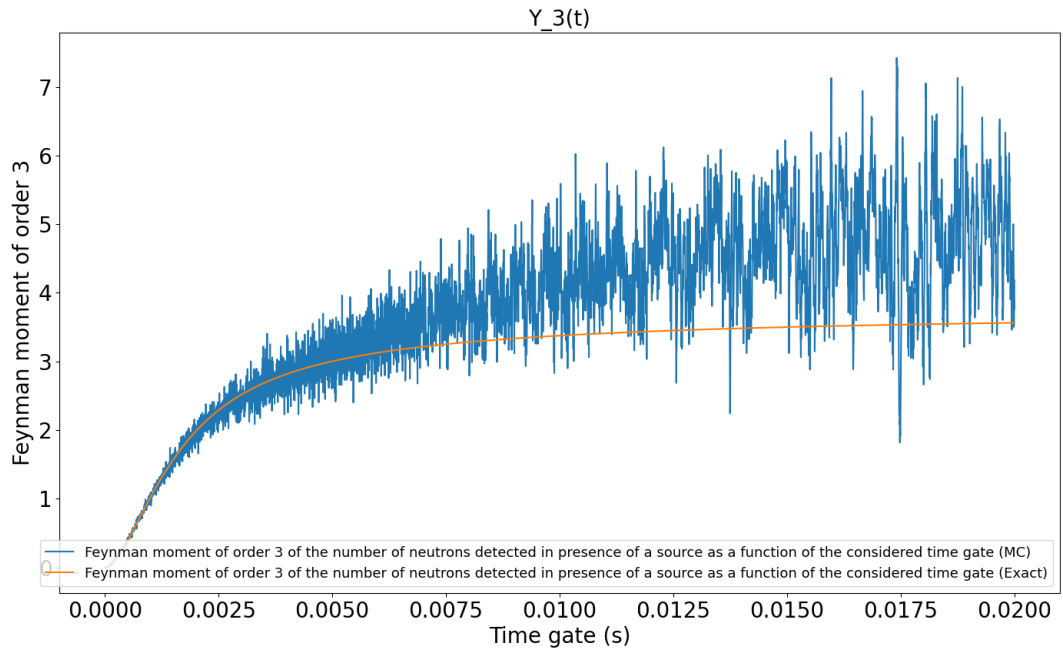
The mean $\mathbb{E}[N]_{Q_n(t)}$ is represented in figure 2.25. As the number of MC realisations is very high, the exact and MC curves are superimposed. The following figure shows further details.

The figure 2.26 is the plot of the Feynman moment of order 2 $Y_2(t)$ with exact formula and MC estimation. The MC estimation of Y_2 is noisy and tends to be 5% close to the exact formula (for $t \in [0, 0.013]$). Then the MC estimation are 20% close to the exact formula (for $t \in [0.013, 0.02]$). These fluctuations are centred but correlated in time. Since $k_{eff} = 0,95$ there are more correlations than in the previous case.

The figure 2.27 is the plot of the Feynman moment of order 3 $Y_3(t)$ with exact formula and MC estimation. The MC estimation of Y_3 is noisier than for Y_2 because it uses the moment of order 3 $E[N^3]_{Q_n(t)}$. For $t \in [0, 0.03]$ the MC estimation of Y_3 is around 20% of the exact value of Y_3 , then the MC estimation gets noisier and noisier, the fluctuations can go to 200% of the exact value for $t = 0.019$. As previously, the fluctuations are centred but correlated in time.

The calculated covariance matrix of the three measurements is:

$$\mathbf{Cov}(\mathbf{M}(\mathbf{p})) = \begin{pmatrix} 1,09887 \cdot 10^{-3} & 1,81672 \cdot 10^{-2} & 0,27707 \\ 1,81672 \cdot 10^{-2} & 0,33449 & 5,57235 \\ 0,27707 & 5,57235 & 100,24600 \end{pmatrix} \quad (2.58)$$

Figure 2.26: $Y_2(t)$, t is in sFigure 2.27: $Y_3(t)$, t is in s

with python, we obtain the following associated eigenvalues

$$\begin{pmatrix} \lambda_1 \\ \lambda_2 \\ \lambda_3 \end{pmatrix} = \begin{pmatrix} 1.00557 \cdot 10^2 \\ 2.35786 \cdot 10^{-5} \\ 2.49747 \cdot 10^{-2} \end{pmatrix} \quad (2.59)$$

Python provides also the conditioning of the covariance matrix $Cond(\mathbf{Cov}(\mathbf{M}(\mathbf{p}))) = 4956145.66857$.

As the ratio between the maximum and minimum eigenvalues is $\approx 10^7$ the associated quadratic formula is degenerate. Therefore, sampling the distribution a posteriori is rather difficult.

2.4.3 A third case

We present a last test case whose parameters are as follows

$$\mathbf{p} = \begin{pmatrix} S \\ k_{eff} \\ \varepsilon_C \\ x \\ \alpha \end{pmatrix} = \begin{pmatrix} 70 \text{ ms}^{-1} \\ 0,95 \\ 0,25 \cdot 10^{-2} \\ 0 \\ 2 \text{ ms}^{-1} \end{pmatrix} \quad (2.60)$$

we recall that $k_{eff} = 0,95 \iff \rho = -0,05263157894$.

Nuclear mater $\left\{ \begin{array}{l} \text{The induced fission material is } {}^{235}\text{U}. \\ \text{The source is poissonian.} \end{array} \right.$

The nuclear constants parameters

$$\begin{pmatrix} \bar{\nu} \\ D_2 \\ D_3 \end{pmatrix} = \begin{pmatrix} 2,5304 \\ 0,8119 \\ 0,5187 \end{pmatrix} \quad \begin{pmatrix} \bar{\nu}_S \\ D_{2S} \\ D_{3S} \end{pmatrix} = \begin{pmatrix} 1 \\ 0 \\ 0 \end{pmatrix} \quad (2.61)$$

The Diven factors correspond to a normalized fission distribution.

The measurement time is $3600 \cdot 10^3 \text{ ms}$ i.e. 1 hour. Considering two time gates $T = \frac{1}{\alpha}$ and $T = \frac{10}{\alpha}$, there are $72 \cdot 10^8$ time gates of length T_1 and $72 \cdot 10^7$ time gates of length T_2 .

The mean and Feynman moments of order 2 and 3 are presented in figure 2.28, 2.29 and 2.30 respectively. We draw almost the same conclusions as for the previous case, except the time of measurement is 100 times higher than for the previous case. On the figure 2.29 we can see that the Feynman moment of order 2 is still noisy. On the figure 2.30 we can see the fluctuations goes higher for the previous case.

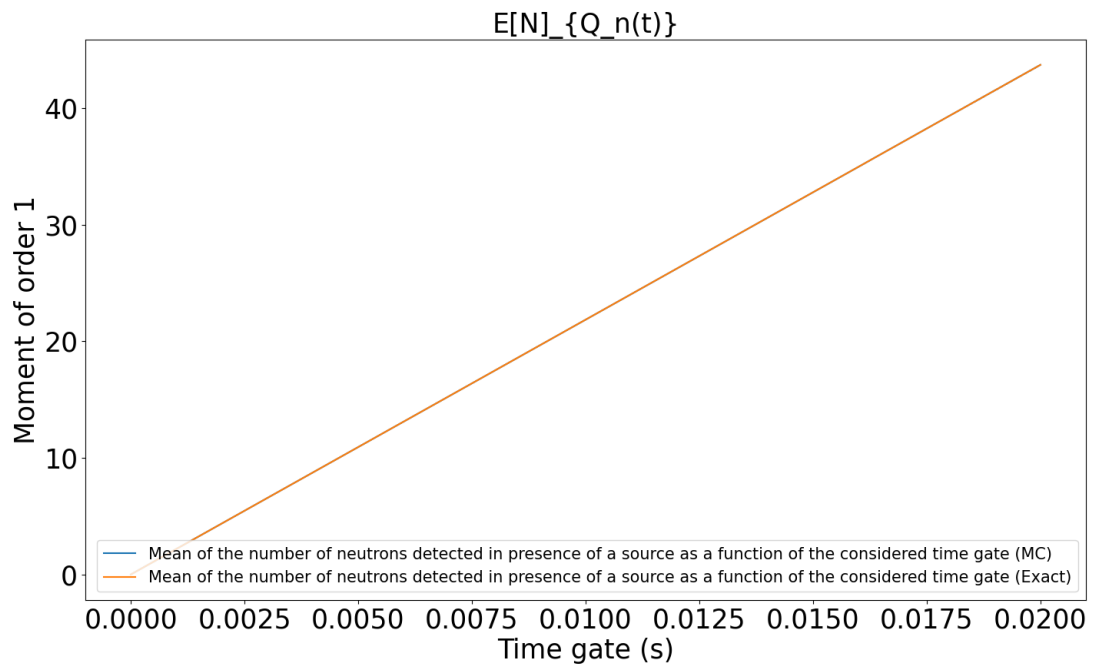


Figure 2.28: $E[N]_{Q_n(t)}$, t is in s

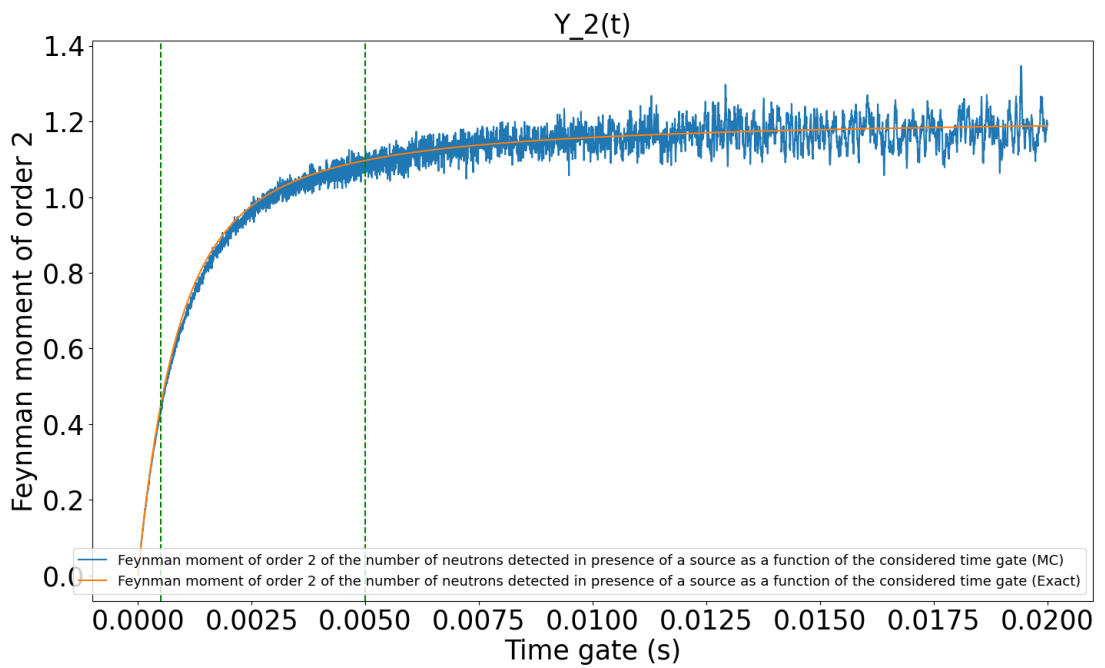


Figure 2.29: $Y_2(t)$ with two vertical indication on $T = \frac{1}{\alpha}$ and $T = \frac{10}{\alpha}$, t is in s

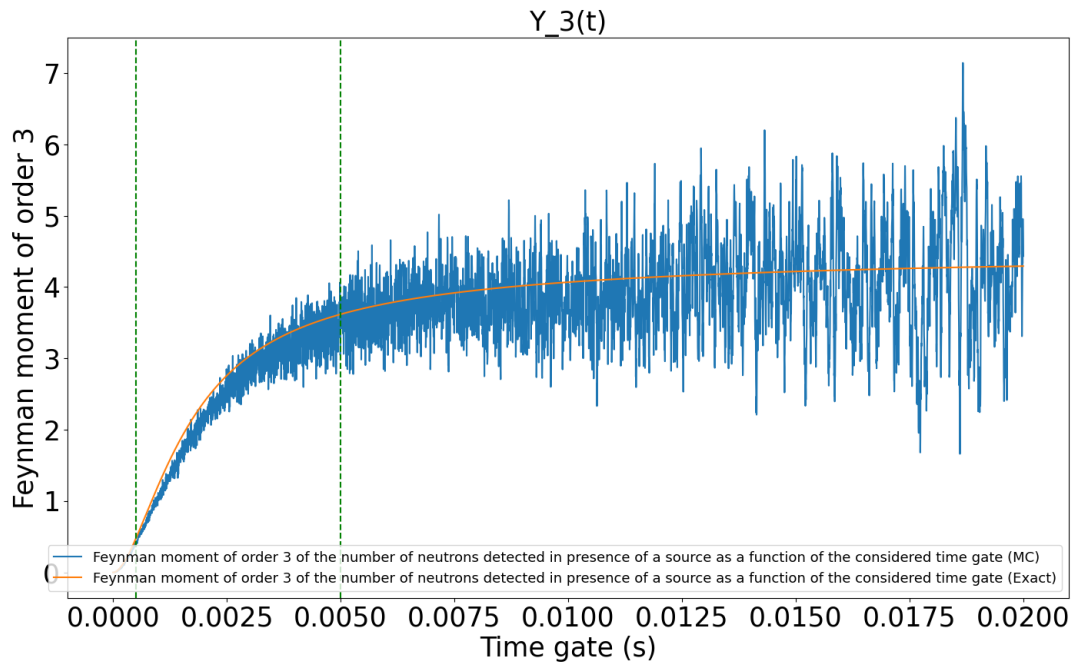


Figure 2.30: $Y_3(t)$ with two vertical indication on $T = \frac{1}{\alpha}$ and $T = \frac{10}{\alpha}$, t is in s

2.5 Neutronic code check

The main objective of this section is to compare the Feynman moments of order 1 to 3 on two cases with two neutron codes: MCNP6 and Tripoli-4. The comparison will allow verifying the observed asymptotic values.

MCNP6 (see [Goo+13]), which stands for Monte Carlo N-Particle transport, is a code developed by the Los Alamos laboratory since the Manhattan Project to simulate nuclear physics processes, 37 types of particles in particular the neutron transport equations and the evolution of gamma rays.

An MCNP file contains the following information

| Case |
|--|
| System geometry |
| Precise composition of the system (present element, density, etc...) |
| Type of data we want to compute (Tally) |

Then MCNP6 provides a ptrac file. This file is used to retrieve the timelist file using "ap2list" (see algorithm 5).

Algorithm 5: Pseudo-code of ap2list

```

Initialisation of the number of subdivisions of the file nb_batch, t_max the
time of the experiment;
Index of the previous mother index settled npsp = 0;
Reading of the ptrac file;
Computation of the length of the file: imax;
Building the TimeList file;
for  $i = 1, imax$  do
    Read the index of the mother nps and the detection time  $t_d$ ;
    if  $t_d \geq 0$  then
        if  $nps \neq npsp$  then
             $u \sim \mathcal{U}[0, 1]$ ;
             $t\_source = u * t\_max$ ;
        Conversion for MCNP
        (time in MCNP is in  $10^{-8}$ s to convert in ms  $t\_d * 10^{-5}$ ms):
         $t'_d = t\_source + t\_d * 10^{-5}$  ;
         $npsp = nps$  ;
        Updating additional variables for next loop;
        Sorting of the detection times in increasing order;
    Writing the detection times in nb_batch files;

```

Exhaustive details can be found in [Goo+13].

Tripoli-4 is a general purpose transport code, it calculates the transport of electrons, neutrons, positrons, photons by the Monte Carlo method in 3D geometries. The main fields of application are radiation protection, criticality safety and reactor physics. A variance reduction technique is implemented, but it will not be useful here. Exhaustive details can be found in [tea17]. All the work with Tripoli-4 was done with Davide Mancusi whom I thank again for his advice and help.

More precisely, we will use the analog mode here. This allows similar calculations to be made with respect to collisions and the transport between collisions. This calculation does not provide criticality calculations, and only the neutron or photon can be considered as a particle type in this context (the two cannot be considered together because photons produced by the reaction induced by neutron interactions are not yet available).

The results of the code are stored in the file track.roots which is a branch tree resulting from the Tripoli-4 calculation. In the generated branching tree, we call "mother" the primary neutron of an induced fission chain. In order to process the tracks.roots file, we used post-treatment.py which is summarised in the following algorithm 6.

2.5.1 Modelisation of the data of a first case

We study the data of the spherical case

Algorithm 6: Pseudo-code of post-traitement.py

```

Importation of ROOT, etc...;
Loading of the library "libtripoli4depletion.so";
Loading the tracks.roots file of the corresponding case;
Initialisation of simulation directory, the batch number and the number of
particles;
Open TimeList file to fill with the counts;
for batch_key in batch_keys do
    Initialisation of batch_dir, packet_keys, new_batch = True;
    for packet_key in packet_keys do
        Consider the current batch;
        if new_batch then
            n_particles += batch.size();
            new_batch = False;
        n_tracks = batch.getNbtracks();
        for i in n_tracks do
            Compute the properties of the mother of the points its position,
            time and energy of the point
            (x_mother,y_mother,z_mother,t_mother,e_mother);
            for j in x_range(n_points) do
                point = track.GetPoint(j);
                Affectation of the position, time and energy of the point
                (x,y,z,t,e);
                Computing the time of detection on the  ${}^3\text{He}$  of the current
                point in the TimeList file;

```

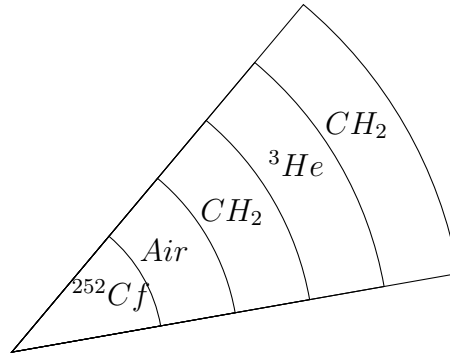
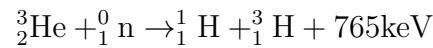


Figure 2.31: Scheme of the first case

The composition of the different layers are

- ^{252}Cf : Spontaneous fission source, compound Poisson type (thickness 0.01cm)
- *Air*: The neutron passes through it almost without any interaction (thickness 19.99cm, $0.0013\text{g}/\text{cm}^3$)
- CH_2 : The neutron collides with the polyethylene atoms to give rise to a random walk (thickness 2cm, $0.9\text{g}/\text{cm}^3$)
- ^3He : enables to capture the neutron by the reaction (thickness 2cm, $0.001\text{g}/\text{cm}^3$)



(thickness 2cm)

Details of the Tripoli-4 file are given in the annexes A.2.12.

The advantage of polyethylene is that it slows down the neutron on its path to facilitate its capture and detection in the ^3He .

In practice, we obtain the detection times through the presence of electrodes at the interface between the polyethylene and Helium-3. The outputs of the code can be processed as follows thanks to dedicated routines (see algorithm 5 and 6).

Physical data extraction of the test case

We have given the geometry of the simulation, we now exploit the results.

Tripoli-4 allows access to the energies after their emission or before their detection (via `post-traitement.py` allowing the processing of `tracks.root` files, i.e. the file containing the branching trees of the fission process). Thus, we search for the distribution of neutron energies after their emission or before their detection, we obtain the following histograms:

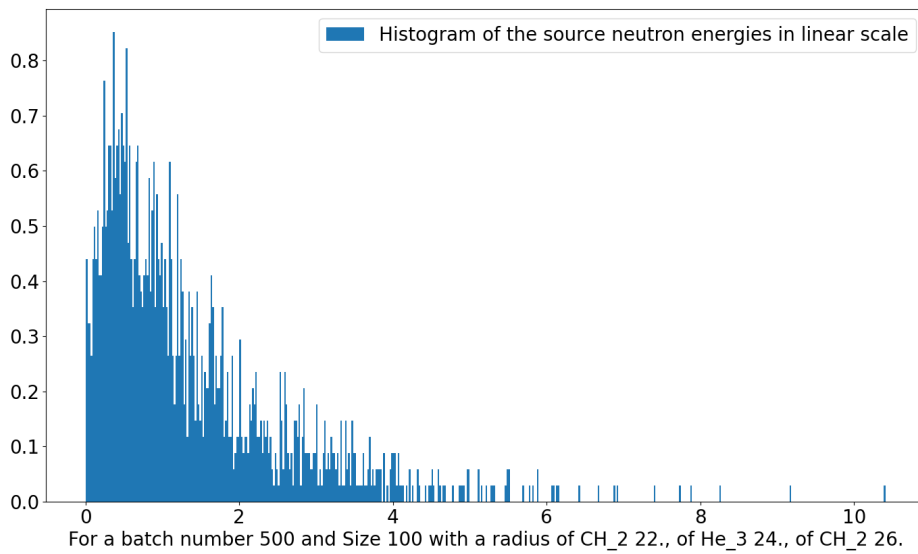


Figure 2.32: Histogram of neutron energies in MeV after emission in linear scale, for a batch number 500 and size 100

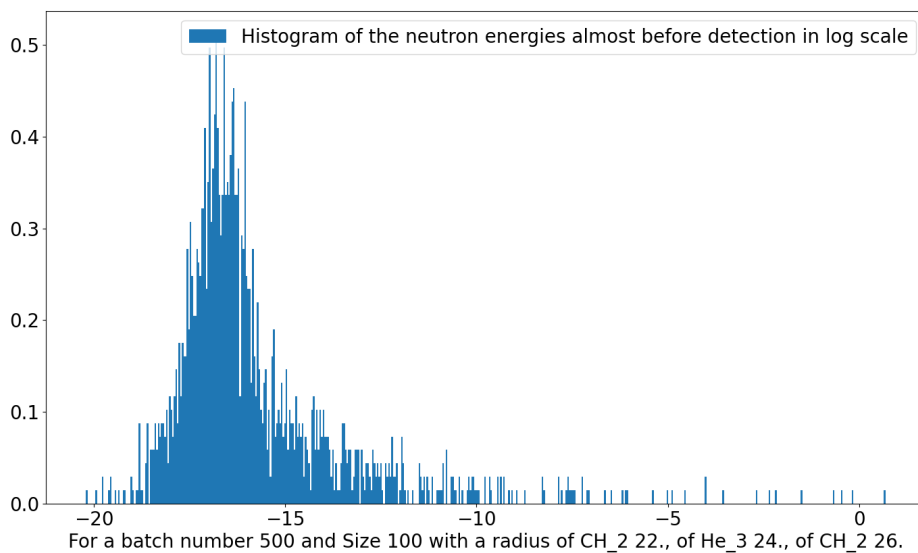


Figure 2.33: Histogram of neutron energies in MeV just before detection in log scale, for a batch number 500 and size 100

In order to better understand the correlation between the energies associated with a neutron before its detection and its detection time, we display the following diagram

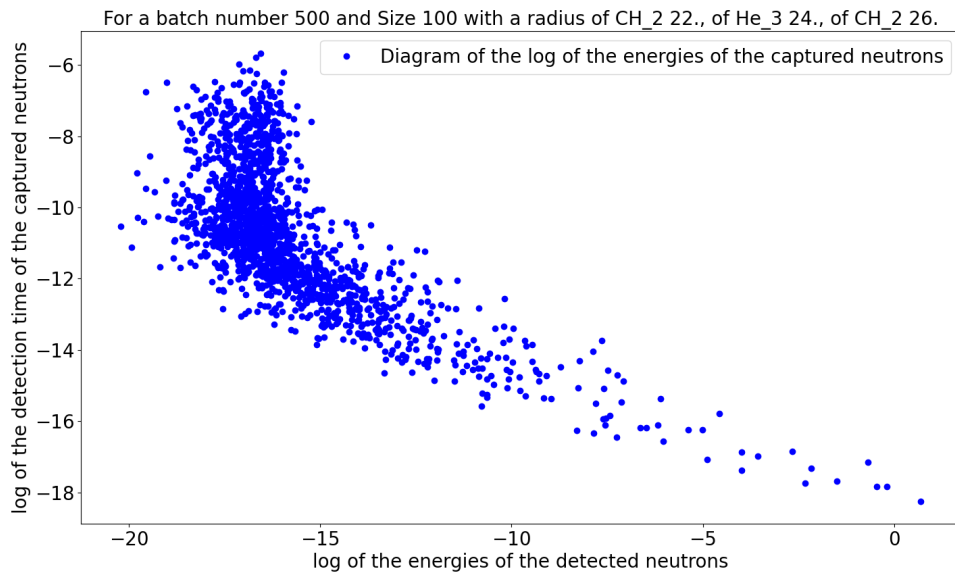


Figure 2.34: Diagram of the log of the detection times in function of the log of the energies in MeV of neutrons just before detection

Thus, we note that a large majority of the detected neutrons have low energy and low to high detection times.

Furthermore, in order to observe more precisely the average energies of the neutrons before their detection or just after their emission as a function of the number of neutrons emitted by the source, we draw the following diagrams

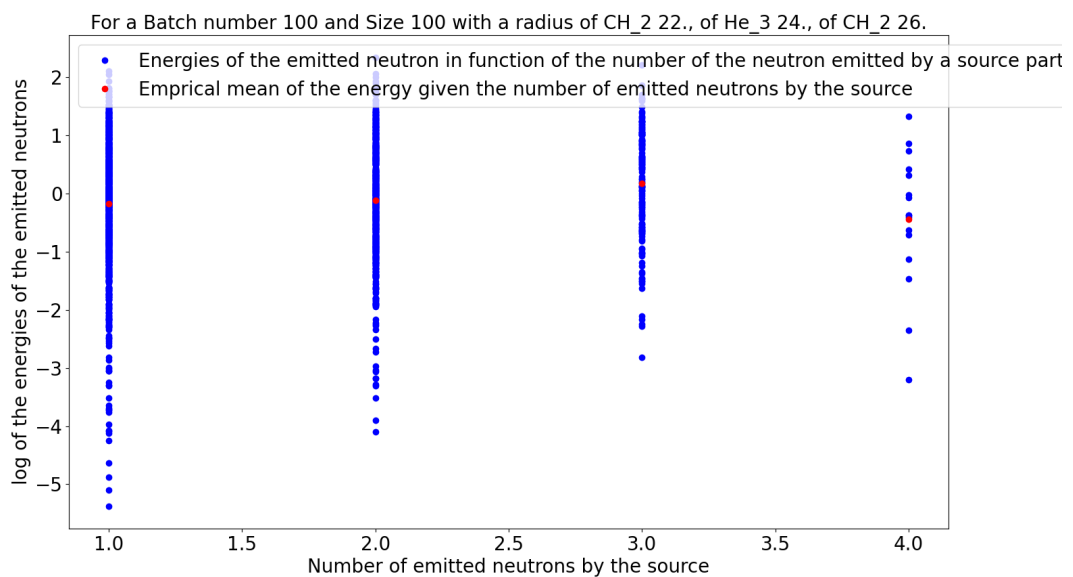


Figure 2.35: Diagram of the log of the neutron energies in MeV just after the emission as a function of the number of source particles emitted

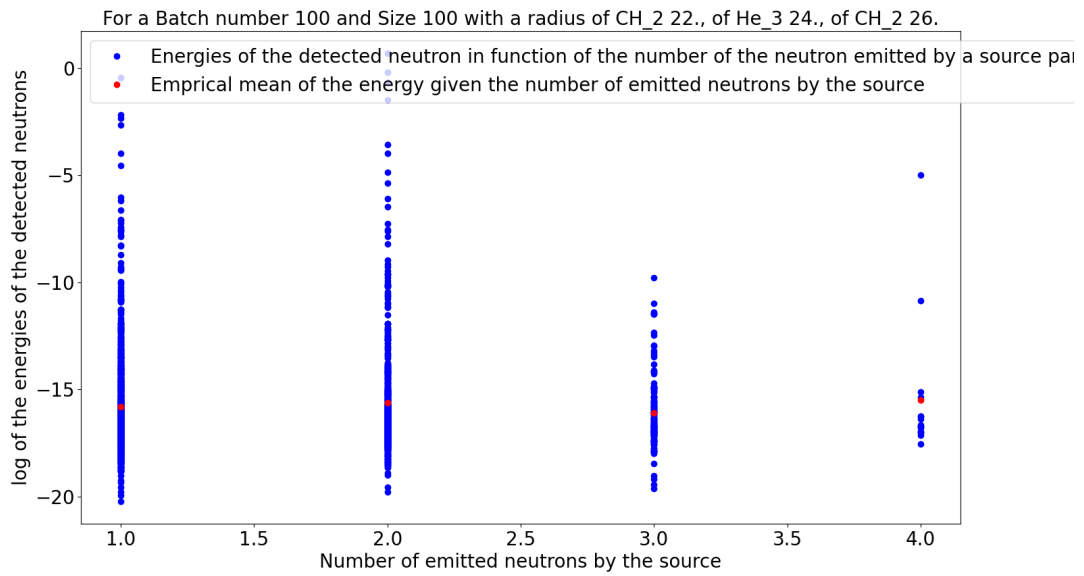


Figure 2.36: Diagram of the log of the energies in MeV before their detection as a function of the number of source particles emitted

It can be seen from the two previous figures that the average value of the neutron energies considered has approximately the same value (red dot), whatever the number of neutrons emitted by the source.

Thus, the average value of the neutron energies considered does not depend on the number of neutrons emitted by the source.

The histograms of the neutron energies just after emission and before detection suggest that they may be Gaussian distributions. To do this, we use the kernel density estimate (KDE) to confirm this hypothesis. We have the following graphical representations:

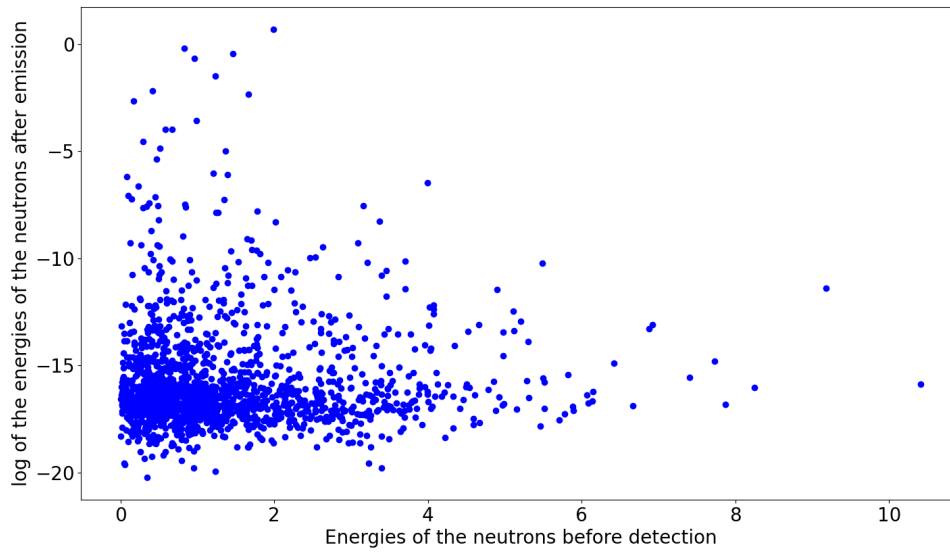


Figure 2.37: Scatter plot of the log of the energies in MeV before their detection as a function of the neutron energies just after the emission

We recall the formula of the kernel density estimation

$$p(\mathbf{x}) = \frac{1}{nh^d} \sum_{i=1}^n K\left(\frac{\mathbf{x} - \mathbf{x}_i}{h}\right) \quad (2.62)$$

where $\mathbf{x} \in \mathbb{R}^d$, $d \in \mathbb{N}^*$ the dimension of the considered mesh, the Gaussian peaks are positioned at the $\mathbf{x}_i \in \mathbb{R}^d$ and

$$K(\mathbf{y}) = \prod_{j=1}^d \frac{1}{\sqrt{2\pi}} e^{-\frac{y_j^2}{2}}. \quad (2.63)$$

We provide a representation of this kernel density estimation in the following

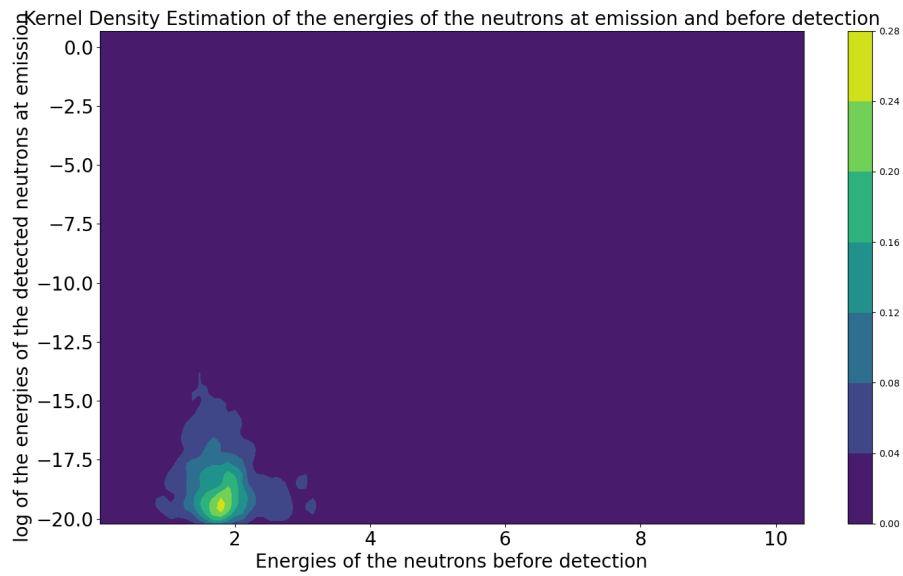


Figure 2.38: Kernel density estimation of the log of the energies of the neutrons detected as a function of the energies before detection

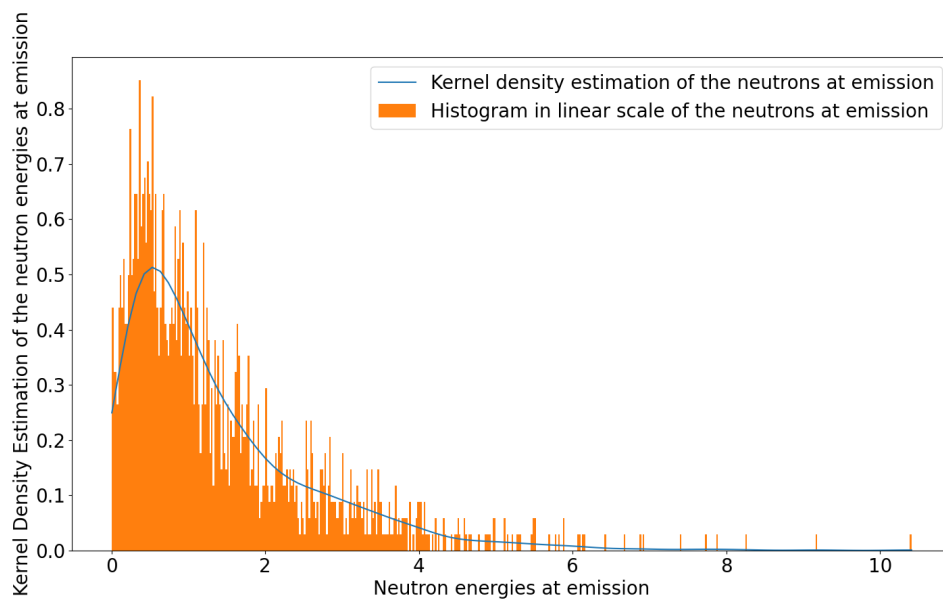


Figure 2.39: Kernel density estimation and histogram of the energies of the neutrons just after the emission

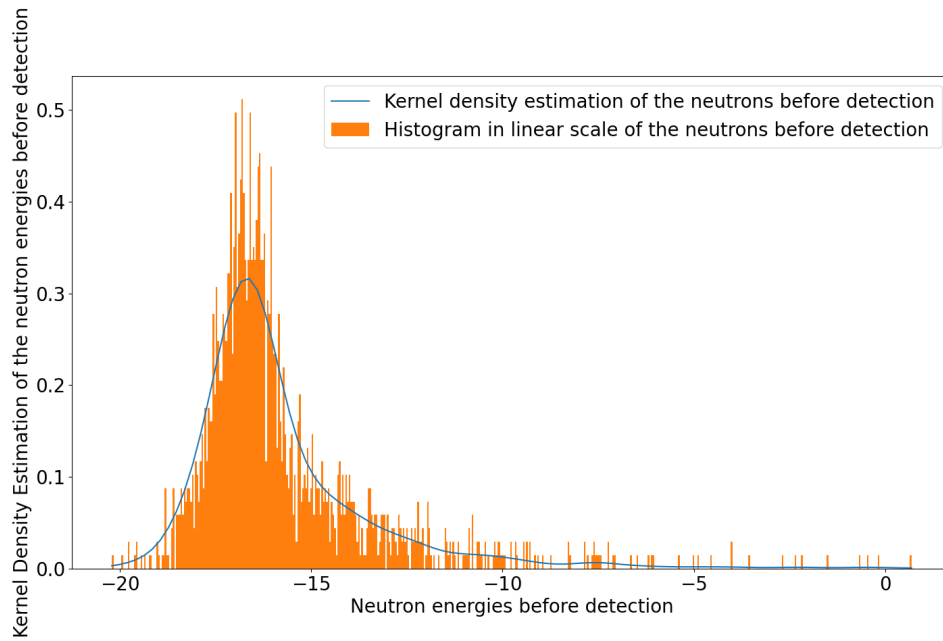


Figure 2.40: Kernel density estimation and histogram of the energies of the neutrons just before detection

Processing of the file of the detection times

Finally, we construct the detection time histogram from the timelist file produced by `post-traitement.py` (used to process the `tracks.root` files, i.e. the file containing the branching trees of fission)

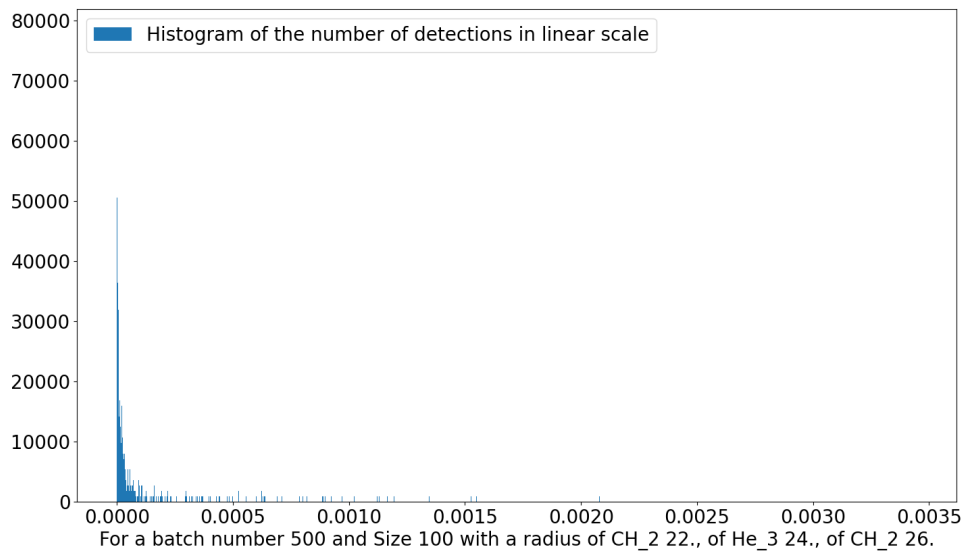


Figure 2.41: Detection time histogram in linear scale for 50000 sources particles

We assume that the corresponding distribution is exponential. In order to approximate the parameter of the exponential distribution.

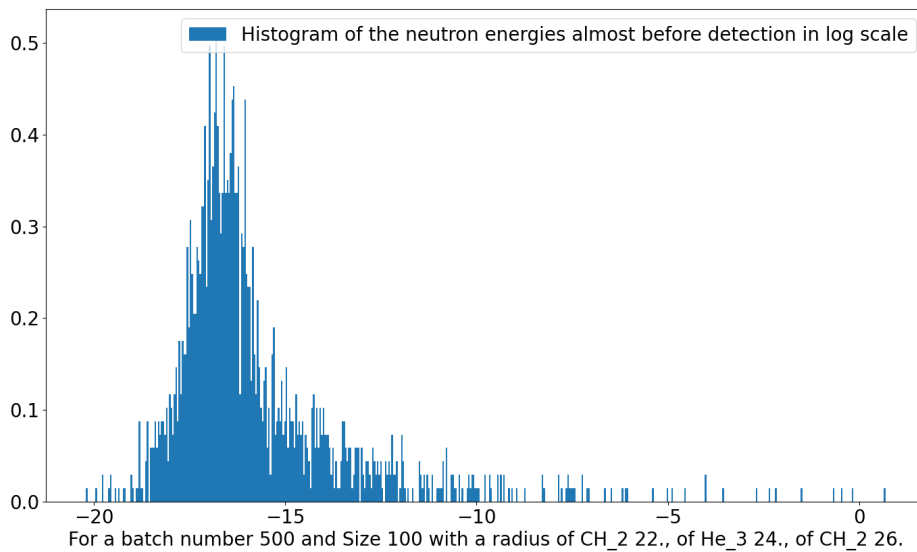


Figure 2.42: Histogram of the detection times in log scale and associated cumulative distribution function

In order to better understand the number of neutrons in the logarithmic scale representation, we plot the cumulative distribution function of the corresponding distribution. By drawing a vertical line at the end of the first part of detected neutrons, at the intersection of this line with the graph of the cumulative distribution function we notice that 70% of the neutrons correspond to this part of the exponential distribution. There is therefore a small proportion of neutrons that should be taken into account in the model with a second exponential.

The detection time file provided by the codes allows us to make a comparison between the different Feynman moments (MCNP, Tripoli and the asymptotic values given by the point model).

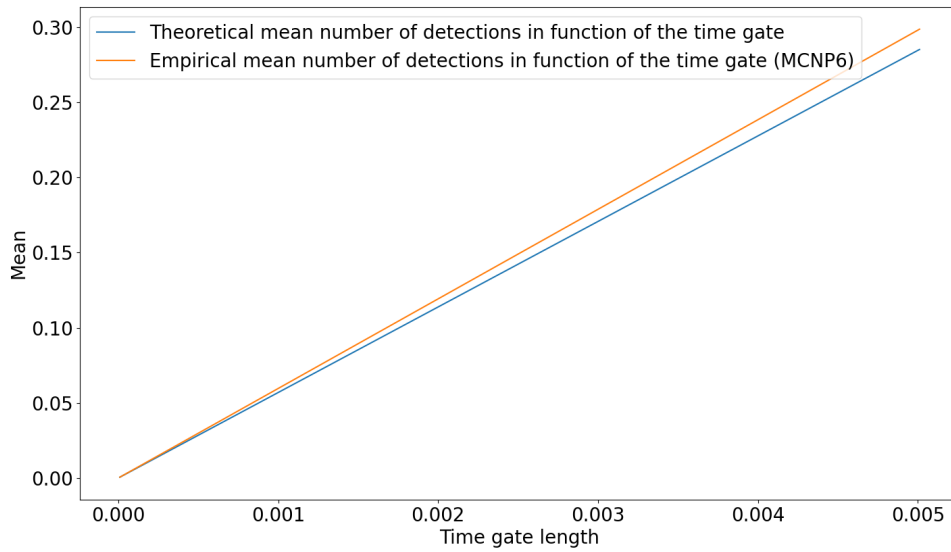


Figure 2.43: Mean number of detections as a function of the time gate, t is in s

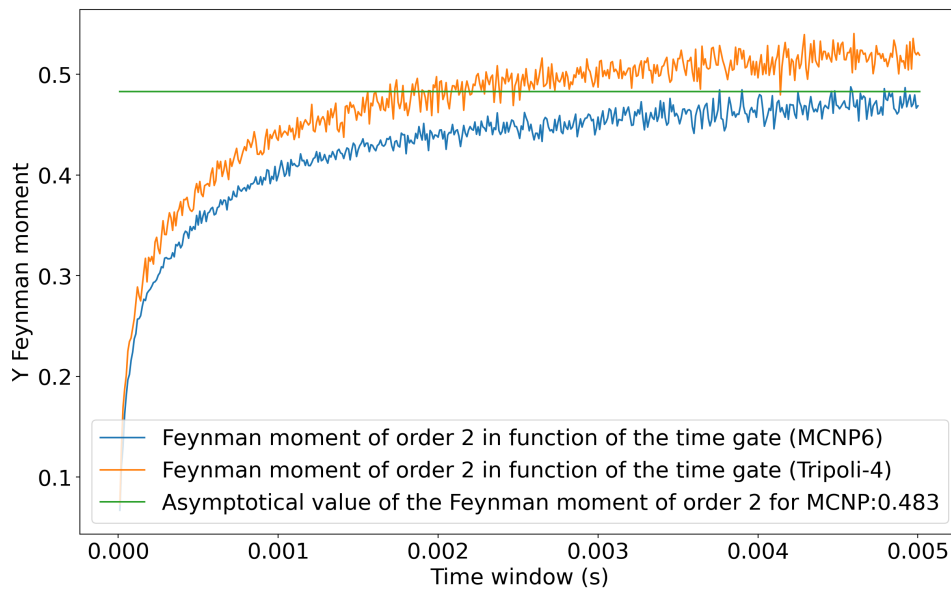


Figure 2.44: Comparison of the Feynman moment of order 2 calculated with MCNP, Tripoli as well as asymptotical value in the point model approximation (green), t is in s

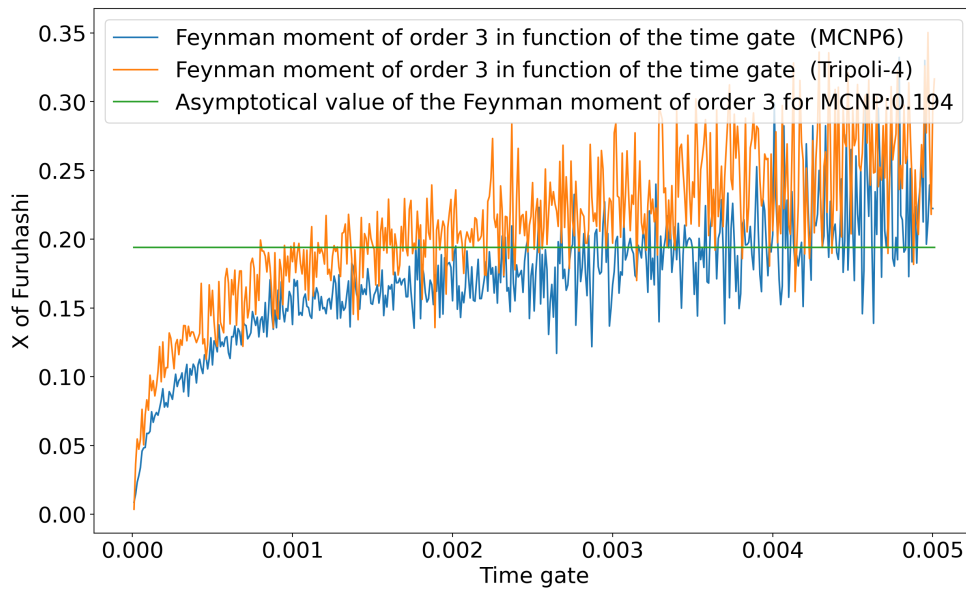


Figure 2.45: Comparison of the Feynman moment of order 3 calculated with MCNP, Tripoli as well as asymptotical value in the point model approximation (green), t is in s

Remark 2.5.1. *The same set of parameters \mathbf{p} is calculated with different nuclear data; the Terrel distribution for MCNP and Freya for Tripoli-4. The asymptotes for MCNP and Tripoli-4 in figure 2.44 and 2.45 are very close because only one element is considered: ^{252}Cf and the spontaneous fission distributions are similar.*

Details of the calculations of the asymptotic values of the Feynman moments can be found in the state-of-the-art, see section 1.6.3.

2.5.2 Modelling of the data of the second case

As before, the spherical case where a uranium solution is placed in the centre:

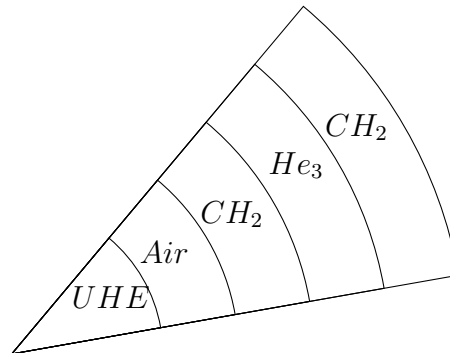
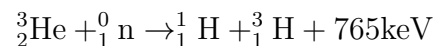


Figure 2.46: Scheme of the second case

The composition of the different layers are

- *UHE*: Mixture composed of 90% ^{235}U and ^{238}U , the 10% left being reserved to water (thickness 14cm)
- *Air*: The neutron passes through it almost without any interaction (thickness 19.99cm, $0.0013\text{g}/\text{cm}^3$)
- *CH₂*: The neutron collides with the polyethylene atoms to give rise to a random walk (thickness 2cm, $0.9\text{g}/\text{cm}^3$)
- ^3He : enables to capture the neutron by the reaction (thickness 2cm, $0.001\text{g}/\text{cm}^3$)



(thickness 2cm)

Tripoli-4 file details are given in annexes A.2.12.

The interest of polyethylene is to slow down the neutron in its trajectory to facilitate its capture and detection.

In practice, we obtain the detection times through the presence of electrodes at the interface between the polyethylene and Helium-3. The outputs of the code can be processed as follows thanks to dedicated routines (see algorithm 5 and 6).

Physical data extraction of the test case

We make progress by analysing the neutron energy distributions just after emission and just before detection.

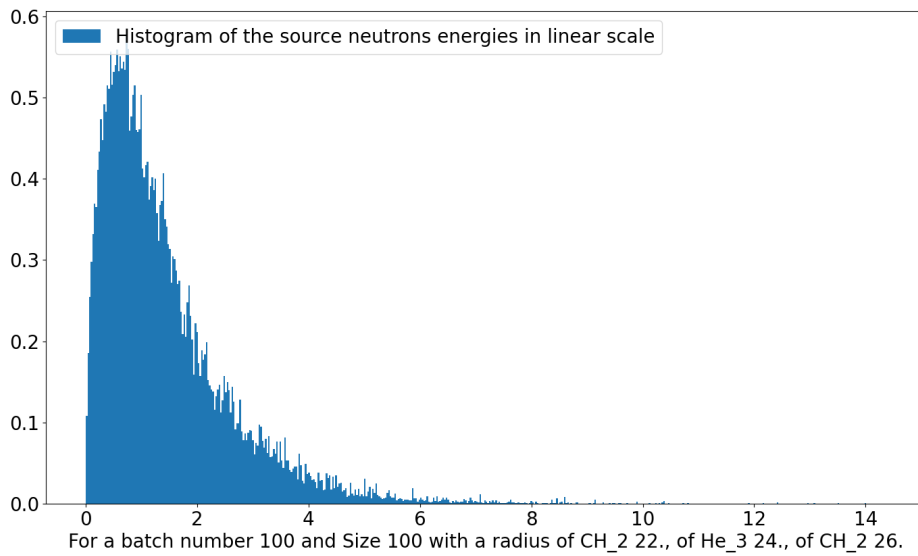


Figure 2.47: Histogram of the neutron energies just after the emission

As the previous graph does not allow a correct visualisation of the neutron energy distribution just before detection, we use the logarithmic scale.

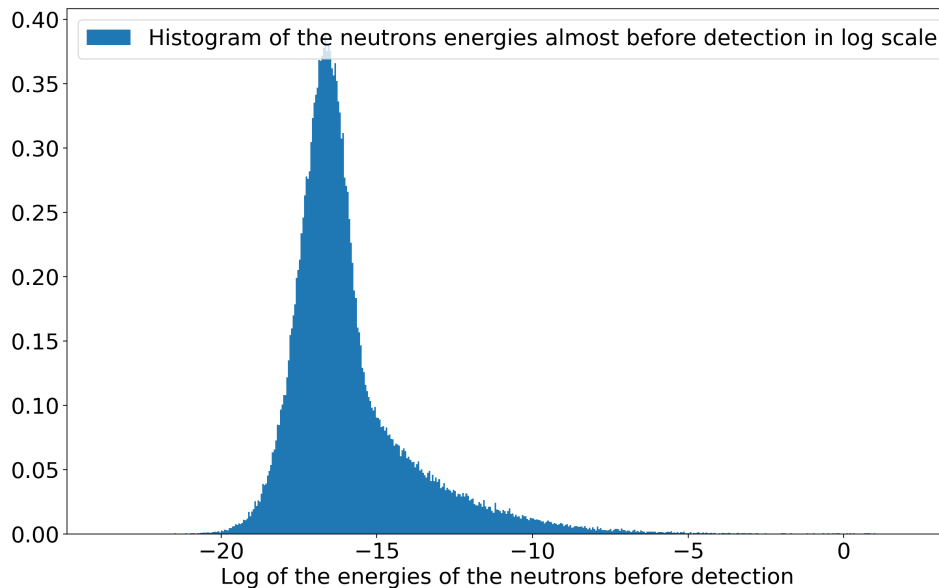


Figure 2.48: Histogram of the neutron energies just before detection in log scale

As in the first case, we study the diagram showing the detection times as a function of the neutron energy just before detection.

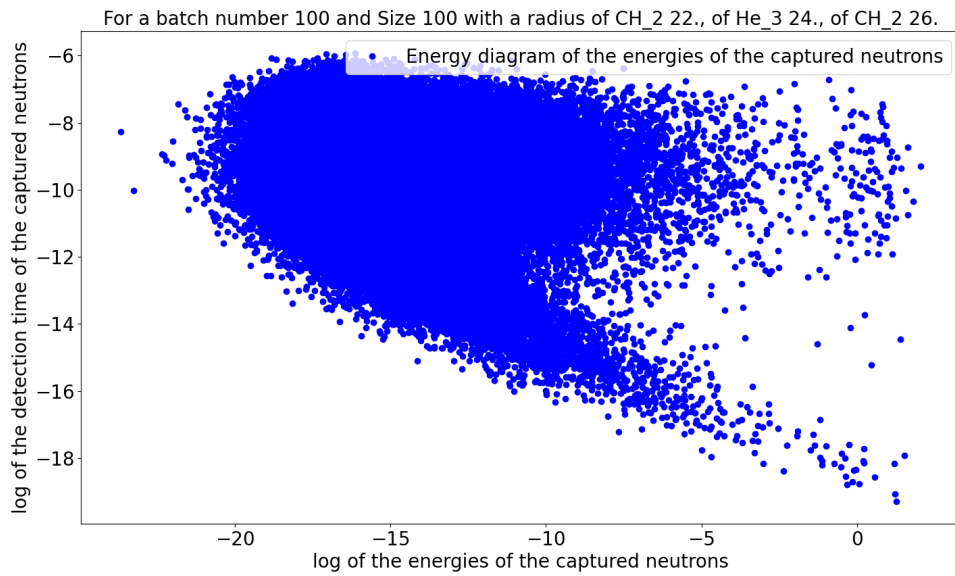


Figure 2.49: Diagram of the log of the detection times as a function of the log of the neutron energies just before detection

To further investigate the data on neutron transport through polyethylene, we plot the neutron energies against the number of neutrons emitted by the source.

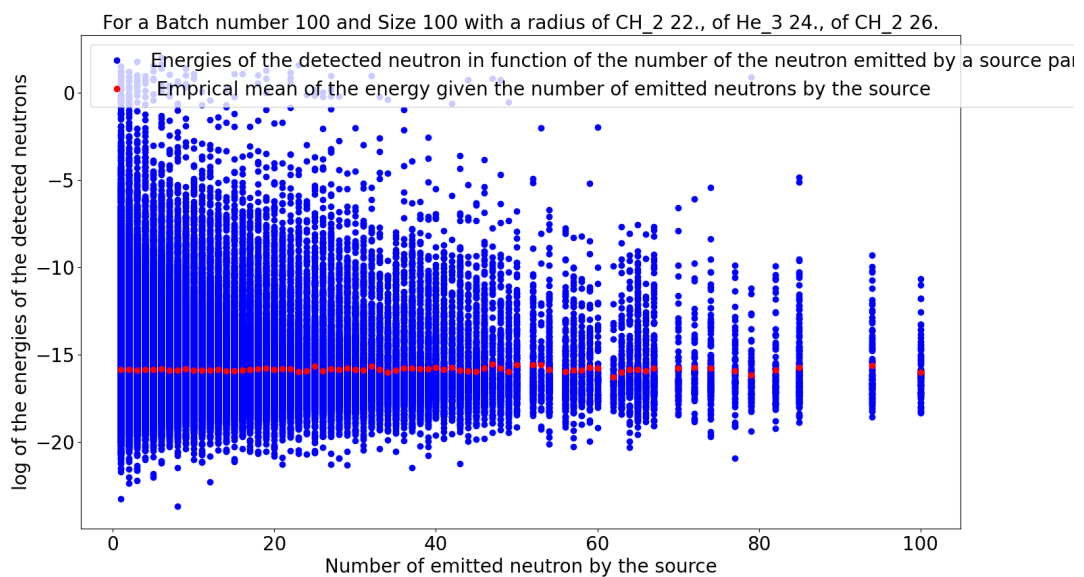


Figure 2.50: Diagram of the log of the neutron energies as a function of the number of neutrons after emission

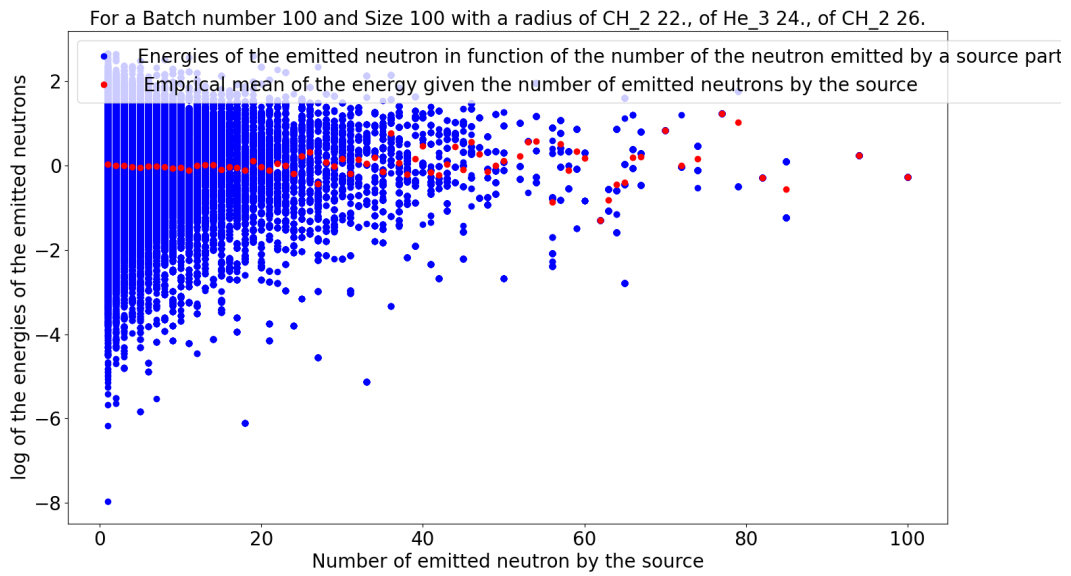


Figure 2.51: Diagram of the log of the neutron energies as a function of the number of neutrons before detection

As we have conjectured that the distribution of neutron energies just after emission and before detection are Gaussian, we try to approximate the distribution of the energy pair considered. To do so, we use a method of estimating the density of the nucleus, as in the first case.

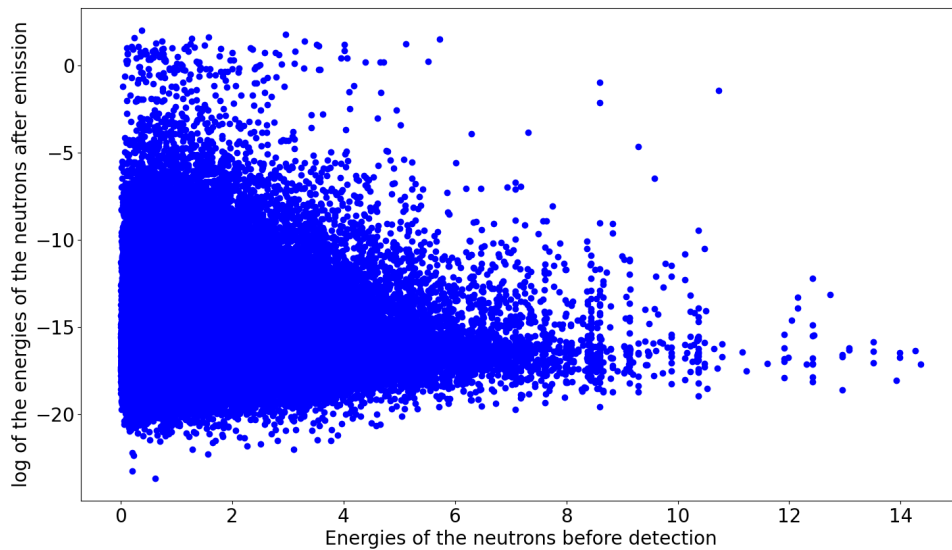


Figure 2.52: Scatter plot of the neutron energies before the detection in function of the energies of the neutrons just after the emission

Kernel Density Estimation of the energies of the neutrons at emission and before detection

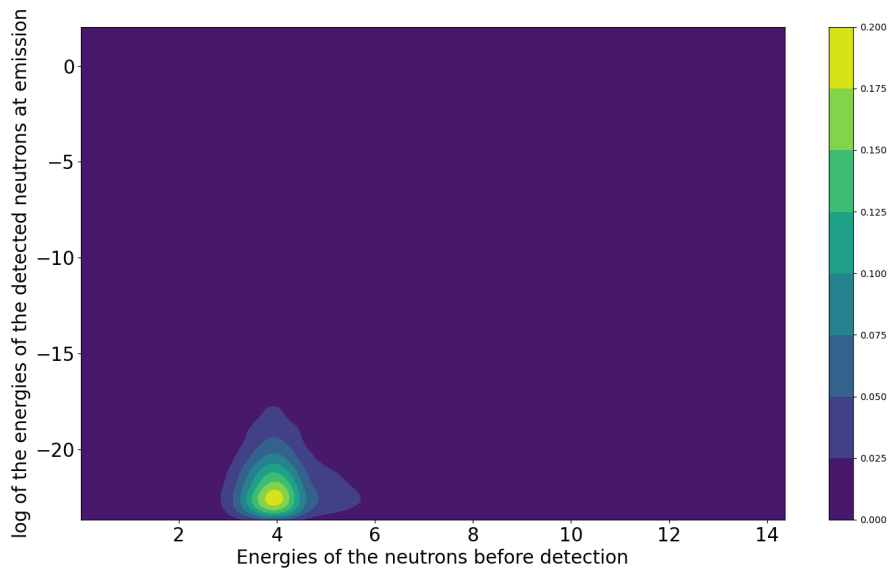


Figure 2.53: Kernel density estimation of the energies of the neutrons just before detection and of the energies of the neutrons just after the emission

Furthermore, for each type of energy considered, we plot the KDE method in dimension 1 and compare it to the marginal distribution of the couple distribution.

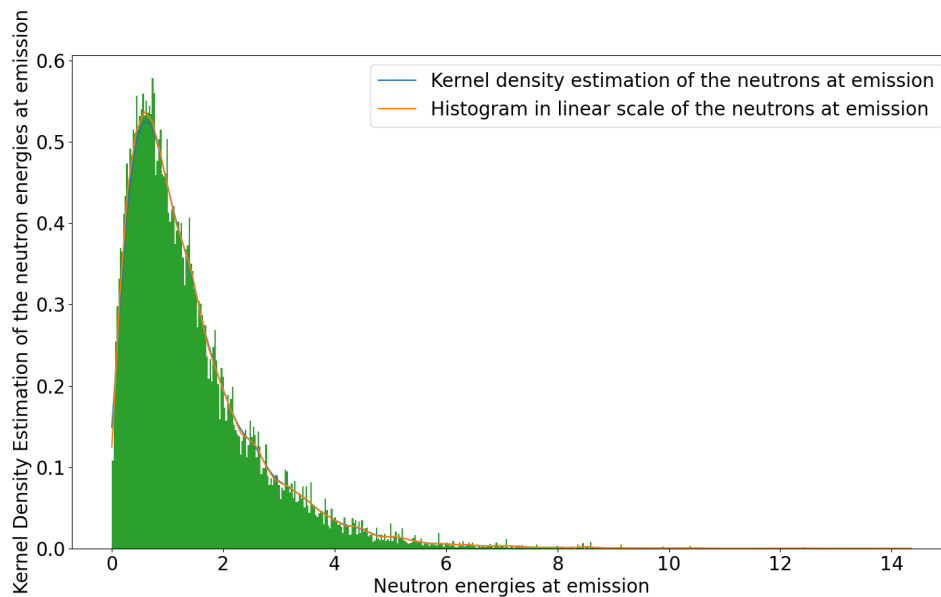


Figure 2.54: Comparison of the histogram of the neutron energy just after the emission, of the 1D KDE method and of the marginal distribution

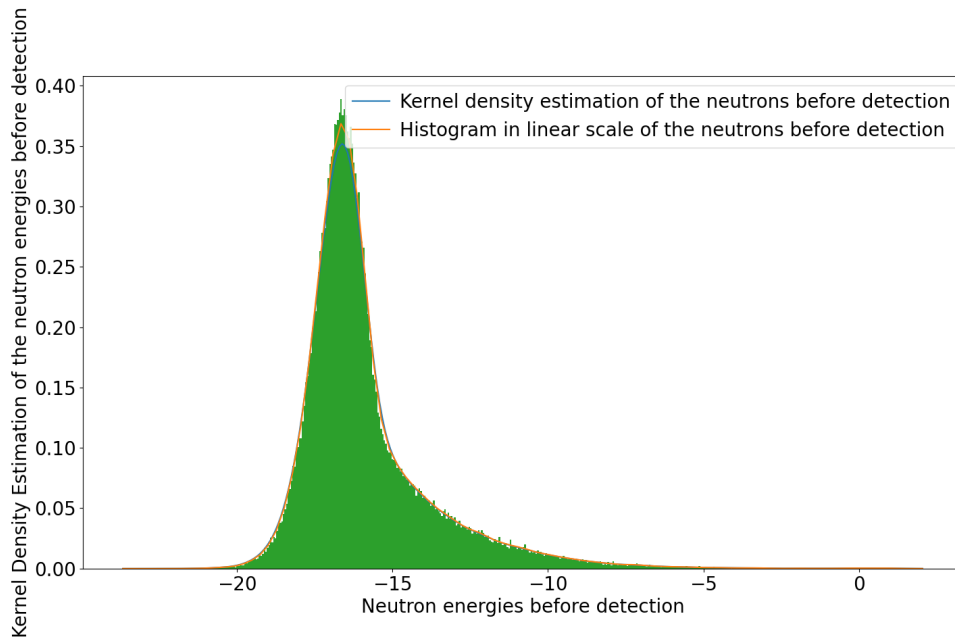


Figure 2.55: Comparison of the histogram of the energy of the neutrons just before detection of the 1D KDE method and of the associated marginal distribution (2D KDE)

TimeList file processing

Finally, we elaborate a histogram of the detection times from the TimeList file provided by `post-traitement.py` (allowing the processing of the `tracks.root` file, i.e. the file containing the branch trees of the fission)

As before, we plot the histogram of detection times aided by the python functions

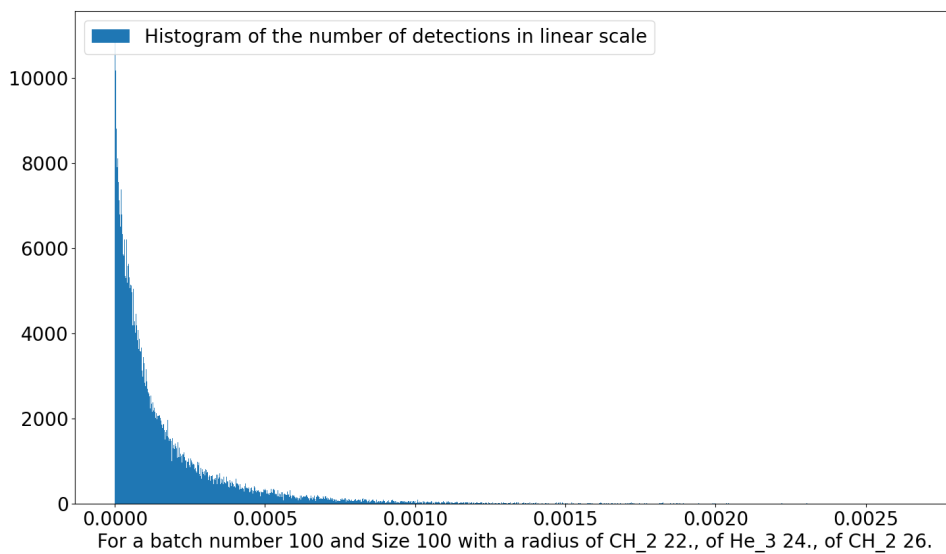


Figure 2.56: Histogram of the detection times in linear scale

The appearance of the histogram also suggests that the actual distribution is an exponential distribution.

Thus, the log scale histogram 2.57 shows two behaviours of the neutron detection times. There is an exponential asymptote for short detection times and another asymptote for longer detection times. Furthermore, we plot the associated cumulative distribution function, so the total proportion of neutrons detected can be read.

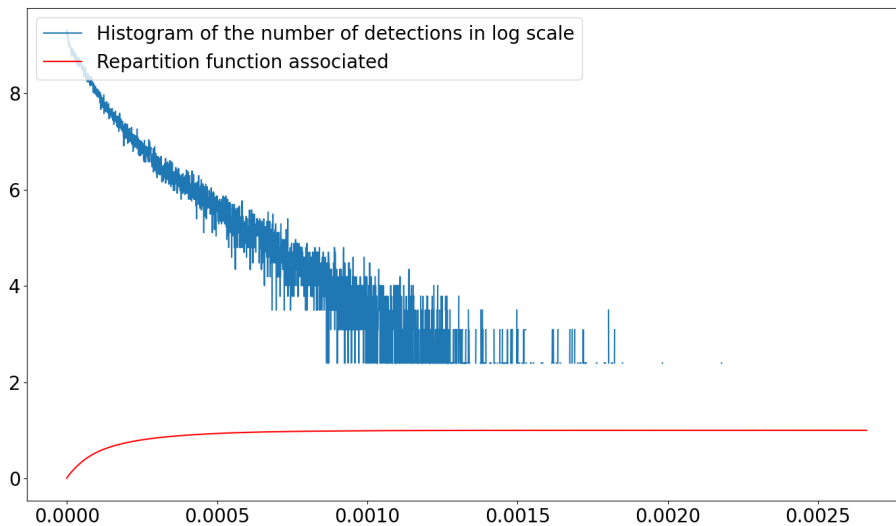


Figure 2.57: Histogram of the detection times in log scale and associated cumulative distribution function

We note that, contrary to the first case, the detected fast neutrons are in low proportion (24%, read on the graph of the cumulative distribution function). This is due to the fission and thickness of the UHE mixture.

The detection time file provided by Tripoli allows us to establish a comparison between the different Feynman moments given (MCNP, Tripoli) and the asymptotic values predicted by the point model approximation.

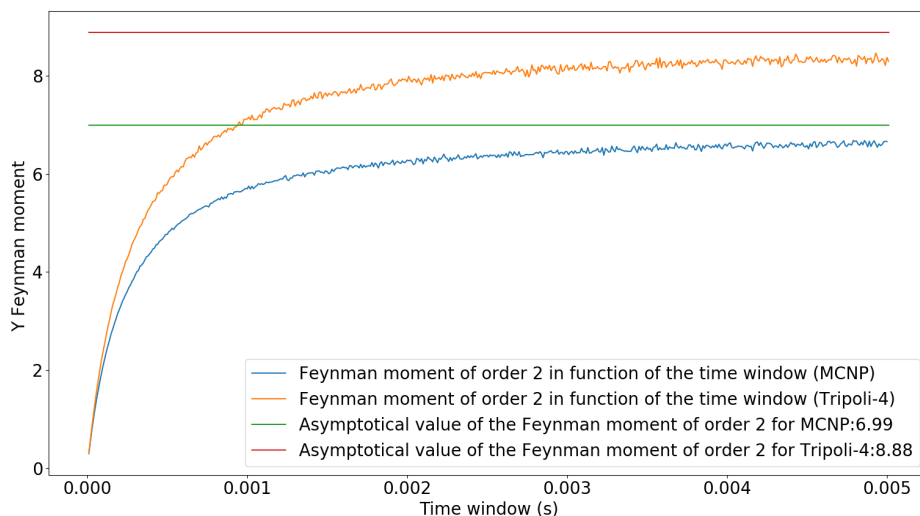


Figure 2.58: Comparison of the Feynman moment of order 2 with MCNP, Tripoli and with the values given by the point model approximation

Remark 2.5.2. *The same set of parameters \mathbf{p} is calculated with different nuclear data; the Terrel distribution (see [Ter57]) for MCNP and Freya for Tripoli-4 (see [VP15]). The asymptotes for MCNP and Tripoli-4 in Figure 2.58 are then different because of the two different elements present and their Diven factors.*

Finally, we can conclude after studying the results of this comparison that MCNP6 and Tripoli-4 provide similar Feynman moments.

To conclude this chapter, we have established the analytical expressions for the first three moments of the distribution of the neutrons counted between T and t during the stationary state and verified them by using a Monte-Carlo code in the neutron point model approximation.

Chapter 3

The neutron noise inverse problem

3.1 Inverse problem

The general form of the direct problem is as follows

$$\begin{aligned} \mathbf{M} : \mathbb{R}^5 &\rightarrow \mathbb{R}^3 \\ \mathbf{p} &\mapsto \mathbf{M}(\mathbf{p}) \end{aligned} \quad (3.1)$$

where

$$\mathbf{p} = \begin{pmatrix} \varepsilon_C \\ k_{eff} \\ \alpha \\ S \\ x \end{pmatrix} \quad (3.2)$$

is the parameter vector of the point model and

$$\mathbf{M}(\mathbf{p}) = \begin{pmatrix} \mathbb{E}[N_{[0,t]}] \\ \mathbb{E}[N_{[0,t]}^2] \\ \mathbb{E}[N_{[0,t]}^3] \end{pmatrix} \quad (3.3)$$

is the vector of observations of the simple moments of the distribution $N_{[0,t]}$ of the number of neutrons detected during a time gate t . Most often, the first three moments are taken into account. However, when the ε_C range is large enough, the fourth order moment can be considered.

We recall

- ε_C is the capture neutron detector efficiency
- k_{eff} is the effective multiplication factor eigenvalue of the system
- α is the prompt neutron decay constant
- S is the intensity of the source, i.e. the number of neutrons emitted per unit of time
- x is the proportion of spontaneous fission source neutrons, it is equal to 1 for a pure spontaneous fission source and 0 when there is only an (α, n) source

The first three parameters are related to fission and detection, the last two are related to source characteristics.

Remark 3.1.1. *Another parameter ρ can be expressed in terms of the multiplication factor $\rho = \frac{k_{eff}-1}{k_{eff}}$ and will be considered in the following.*

From the relation $\lambda_F \varepsilon_F = \lambda_C \varepsilon_C$, we can deduce ε_C (average number of detections per neutron capture) is related to the fission efficiency ε_F (average number of detections per fission) thanks to the relation

$$\left(1 - \frac{k_{eff}}{\bar{\nu}}\right) \varepsilon_C = \frac{k_{eff}}{\bar{\nu}} \varepsilon_F \quad (3.4)$$

In the context of this study, we will consider an inverse problem with only three parameters to recover

Definition 3.1.2. *Given the observations \mathbf{y} , we want to determine the input \mathbf{p}^* of the model \mathbf{M} such that*

$$\mathbf{y} = \mathbf{M}(\mathbf{p}^*) \quad (3.5)$$

where

$$\begin{aligned} \mathbf{M} : \mathbb{R}^3 &\rightarrow \mathbb{R}^3 \\ \mathbf{p} &\mapsto \mathbf{M}(\mathbf{p}) \end{aligned} \quad (3.6)$$

with

$$\mathbf{p} = \begin{pmatrix} \varepsilon_C \\ k_{eff} \\ S \end{pmatrix} \quad \mathbf{M}(\mathbf{p}) = \begin{pmatrix} \mathbb{E}[N_{[0,t]}] \\ \mathbb{E}[N_{[0,t]}^2] \\ \mathbb{E}[N_{[0,t]}^3] \end{pmatrix} \quad (3.7)$$

To this end, we first recall the work of [al.98] where the analytical resolution of the Böhnel equations [Bö85] was proposed in order to solve the inverse problem.

Remark 3.1.3. *The interested reader can consult [Shi+19] to have a complete nomenclature of the notation of neutronics.*

Another way is to consider minimising the square norm of the difference between the observations and the model, i.e. to find

$$\underset{\mathbf{p}}{\operatorname{argmin}} \|\mathbf{y} - \mathbf{M}(\mathbf{p})\|^2 \quad (3.8)$$

We focus on the behaviour of this norm with one parameter, two parameters and three parameters. Then, we will also take into account the covariance matrix of the measurements in quadratic form that determines the least-squares misfit function 3.8.

The least-square problem 3.8 is a non-convex optimization problem. We will consider the simulated annealing method in order to have an estimate of the position of the minimum of $\|\mathbf{y} - \mathbf{M}(\mathbf{p})\|^2$. In a second part, we will use Bayesian methods and MCMC sampling methods on the cost function $\|\mathbf{y} - \mathbf{M}(\mathbf{p})\|^2$, the Bayesian methods provide the a posteriori distribution of the parameters of the system given the observations $\mathbf{p}|\mathbf{y}$. The MCMC sampling methods are the Metropolis-Hastings (MH) algorithm, the version of [HST99; HST01] and the MH algorithm with covariance matrix adaptation (CMA) in order to sample the a posteriori distribution of $\mathbf{p}|\mathbf{y}$.

3.1.1 Analytical inversion method

In the Böhnel method, four unknowns are deduced from the measurements of the number of singles, doubles, and triples counts (see next definition). In [PEP09] Pázsit provided a rigorous derivation of the solution. A complete view of the notation dealing with this question can be found in [Shi+19]. We expose here how to proceed in our case.

We recall first the Böhnel method, which is dealing with an equivalent problem of the problem 3.6. This method is used to solve analytically the following inverse problem. Some details can be found in [Hum16].

Remark 3.1.4. *We recall the stationary regime is established when, for $k_{eff} < 1$, the ergodicity for X_t is achieved. This is the same thing as in the state-of-art, see 1.6.33.*

Here, we define the output that will be used in the current problem.

Definition 3.1.5. *Let a time gate of duration t . We consider here the stationary regime is established. We introduce the singles count detected during t given the stationary regime $N_{1,C}(t)$, the number doubles correlated counts $N_{2,C}(t)$ during t given the stationary regime, and the number triples correlated counts $N_{3,C}(t)$ during t given the stationary regime, where the singles counts rate is *Singles*, the doubles correlated counts rate is *Doubles* and the triples correlated counts rate is *Triples* (cf. Chapter 2)*

$$\begin{aligned}
 N_{1,C}(t) &:= \text{Singles} = \sum_{n \in \mathbb{N}^*} n Q_n(t) \\
 N_{2,C}(t) &:= \text{Doubles} = \sum_{n \in \mathbb{N}^*} \frac{n(n-1)}{2} Q_n(t) \\
 N_{3,C}(t) &:= \text{Triples} = \sum_{n \in \mathbb{N}^*} \frac{n(n-1)(n-2)}{6} Q_n(t)
 \end{aligned} \tag{3.9}$$

where $N_{1,C}(t) = \mathbb{E}[N_{[0,t]}]$. A neutron is considered to be a leak when it does not induce fission, in the point model approximation this refers to capture of a neutron. Leakage efficiency is

$$\boxed{\varepsilon_C := \text{Probability that a captured neutron is detected}} \tag{3.10}$$

According to [Ser45], the leakage multiplication of the system is

$$\boxed{M_L := \text{the number of neutrons that escape permanently from the active material when a single neutron is introduced as a primary source,}} \tag{3.11}$$

This term reflects the fact that not all the new neutrons produced by induced fissions escape from the sample. Instead, some will be captured in the sample. We also define the quantity

$$\boxed{\alpha_x := \frac{S_x}{\bar{\nu}_S S_F}} \tag{3.12}$$

Then the input parameters of the Böhnel equations are

$$\mathbf{p}^{Böhnel} = \begin{pmatrix} \varepsilon_C \\ M_L \\ \alpha_x \\ S_F \end{pmatrix} \quad (3.13)$$

The reader will notice that in this subsection the input parameters are noted $\mathbf{p}^{Böhnel}$ but are different from those of the problem 3.6.

From the definition, we can deduce

Proposition 3.1.6. *Multiplication leakage*

We have

$$M_L = \frac{1 - \frac{k_{eff}}{\nu}}{1 - k_{eff}} \quad (3.14)$$

Proof. We recall the equation of the mean (eq. 1.135 from the state-of-the-art)

$$\frac{d}{dt}n_t + \alpha n_t = \bar{S} \quad (3.15)$$

where $\bar{S} = S_\alpha + \bar{\nu}_S S_F$. During the stationary regime

$$\frac{d}{dt}n_t = 0 \quad (3.16)$$

then

$$\begin{aligned} n_t &= \frac{\bar{S}}{\alpha} \\ &= \frac{\bar{S}\theta}{1 - k_{eff}}, \text{ where } \theta = \frac{1}{\lambda_T} \text{ is the mean lifetime of the neutrons} \\ &= \frac{\bar{S}}{\lambda_T(1 - k_{eff})} \end{aligned} \quad (3.17)$$

The rate of capture (leak) is

$$\begin{aligned} \lambda_C n_t &= \frac{1 - \frac{\lambda_F}{\lambda_T}}{1 - k_{eff}} \bar{S} \\ &= \frac{1 - \frac{k_{eff}}{\bar{\nu}}}{1 - k_{eff}} \bar{S} = M_L \bar{S} \text{ by definition} \end{aligned} \quad (3.18)$$

Then by identification

$$M_L = \frac{1 - \frac{k_{eff}}{\nu}}{1 - k_{eff}} \quad (3.19)$$

□

For further computations, we define

Definition 3.1.7. *The asymptotic Feynman moment of order 3 $Y_{3,\infty}$ is the sum of the two quantities*

$$\begin{aligned} Y_{3,2,\infty} &:= \left(\frac{\varepsilon_F D_2}{\rho^2} \right)^2 \left(1 - \alpha \rho \frac{\bar{\nu}_S D_{2S}}{\bar{\nu} D_2} \right) \\ Y_{3,3,\infty} &:= \left(- \frac{\varepsilon_F^2 D_3}{\rho^3} \right) \end{aligned} \quad (3.20)$$

The link with the Feynman equations neutron multiplicity counting is

Proposition 3.1.8. *We can establish*

$$\begin{aligned} Y_2(t) &= \frac{2N_{2,C}(t)}{N_{1,C}(t)} \\ Y_3(t) &= \frac{6N_{3,C}(t)}{N_{1,C}(t)} \end{aligned} \quad (3.21)$$

Proof. This result is established thanks to

$$Y_p(T-t) = \frac{p! \Gamma_p(T-t)}{\Gamma_1(T-t)} \quad (3.22)$$

from the state-of-the-art, section Stochastic neutronics, stochastic neutronics equations, Feynman moments. \square

We can establish the results

Proposition 3.1.9. *Böhnel equations and direct problem
The direct problem of the Böhnel equations is*

$$\begin{aligned} \mathbf{M} : \mathbb{R}^4 &\rightarrow \mathbb{R}^3 \\ \mathbf{p}_{Böhnel} &\mapsto \mathbf{M}_{Böhnel}(\mathbf{p}_{Böhnel}) \end{aligned} \quad (3.23)$$

where

$$\mathbf{p}_{Böhnel} = \begin{pmatrix} \varepsilon_C \\ M_L \\ \alpha_x \\ S_F \end{pmatrix} \quad (3.24)$$

is the parameter vector of the point model and

$$\mathbf{M}_{Böhnel}(\mathbf{p}_{Böhnel}) = \begin{pmatrix} \text{Singles} \\ \text{Doubles} \\ \text{Triples} \end{pmatrix} \quad (3.25)$$

where the Böhnel equations are

$$\begin{aligned} \text{Singles} &= \varepsilon_C M_L \bar{\nu}_S S_F (1 + \alpha_x) \\ \text{Doubles} &= \frac{\varepsilon_C^2 M_L^2 S_F}{2} (\nu_{2S} + (1 + \alpha_x) \frac{M_L - 1}{\bar{\nu} - 1} \nu_2 \bar{\nu}_S) \\ \text{Triples} &= \frac{\varepsilon_C^3 M_L^3 S_F}{6} \left(\nu_{3S} + \frac{M_L - 1}{\bar{\nu} - 1} ((1 + \alpha_x) \nu_3 \bar{\nu}_S + 3\nu_{2S} \nu_2) + 3 \left(\frac{M_L - 1}{\bar{\nu} - 1} \right)^2 (1 + \alpha_x) \bar{\nu}_S \right) \end{aligned} \quad (3.26)$$

Proof. The number of single counts is

$$\begin{aligned} Singles &= \bar{S} \frac{\varepsilon_F}{-\rho\bar{\nu}} \\ &= \varepsilon_C M_L \bar{S} \end{aligned} \quad (3.27)$$

We use the following variable

$$\alpha_x = \frac{S_\alpha}{\bar{\nu}_S S_F} \quad (3.28)$$

then since $\bar{S} = S_\alpha + \bar{\nu}_S S_F$, $\bar{S} = \bar{\nu}_S S_F (1 + \alpha_x)$.

We deduce the first equation of Böhnel

$$\boxed{Singles = \varepsilon_C M_L \bar{\nu}_S S_F (1 + \alpha_x)} \quad (3.29)$$

The number of double correlated counts is

$$\begin{aligned} Doubles &= \frac{Singles Y_{2,\infty}}{2} \\ &= \frac{Singles \varepsilon_F D_2}{2 \rho^2} \left(1 - x \rho \frac{\bar{\nu}_S D_{2S}}{\bar{\nu} D_2} \right) \end{aligned} \quad (3.30)$$

To express this quantity in the variables ε_L, M_L we use

$$\frac{M_L - 1}{\bar{\nu} - 1} = \left(\frac{k_{eff}}{1 - k_{eff}} \right) \frac{1}{\bar{\nu}} \quad (3.31)$$

what enables to deduce

$$\frac{\varepsilon_F D_2}{\rho^2} = \varepsilon_C M_L \frac{M_L - 1}{\bar{\nu} - 1} \nu_2 \quad (3.32)$$

We can deduce the second equation of Böhnel

$$\boxed{Doubles = \frac{\varepsilon_C^2 M_L^2 S_F}{2} (\nu_{2S} + (1 + \alpha_x) \frac{M_L - 1}{\bar{\nu} - 1} \nu_2 \bar{\nu}_S)} \quad (3.33)$$

The number of triples correlated counts is

$$Triples = \frac{Singles Y_{3,\infty}}{6} \quad (3.34)$$

We use $Triples_2$

$$Triples_2 := \frac{Singles Y_{3,2,\infty}}{6} = \frac{Singles}{6} \left(\frac{\varepsilon_F D_2}{\rho^2} \right)^2 \left(1 - x \rho \frac{\bar{\nu}_S D_{2S}}{\bar{\nu} D_2} \right) \quad (3.35)$$

We also use $Triples_3$

$$Triples_3 := \frac{Singles Y_{3,3,\infty}}{6} = \frac{Singles}{6} \left(- \frac{\varepsilon_F^2 D_3}{\rho^3} \right) \quad (3.36)$$

Then we can decompose equation 3.34 into two different parts

$$Triples = \frac{Singles Y_{3,2,\infty}}{6} + \frac{Singles Y_{3,3,\infty}}{6} = Triples_2 + Triples_3 \quad (3.37)$$

But

$$-\frac{\varepsilon_F^2 D_3}{\rho^3} = \varepsilon_C^2 M_L^2 \frac{M_L - 1}{\bar{\nu} - 1} \nu_3 \quad (3.38)$$

Moreover

$$-x\rho \frac{\bar{\nu}_S^2 D_{3S}}{\bar{\nu}^2 D_3} = \frac{1}{1 + \alpha_x} \left(\frac{\bar{\nu} - 1}{M_L - 1} \right) \frac{\nu_{3S}}{\nu_3 \nu_S} \quad (3.39)$$

Then

$$Triples_3 = \frac{\varepsilon_C^3 M_L^3 S_F}{6} (\nu_{3S} + (1 + \alpha_x) \frac{M_L - 1}{\bar{\nu} - 1} \nu_{3S} \bar{\nu}_S) \quad (3.40)$$

Finally the third Böhnel equation is

$$Triples = \frac{\varepsilon_C^3 M_L^3 S_F}{6} \left(\nu_{3S} + \frac{M_L - 1}{\bar{\nu} - 1} ((1 + \alpha_x) \nu_3 \bar{\nu}_S + 3\nu_{2S} \nu_2) + 3 \left(\frac{M_L - 1}{\bar{\nu} - 1} \right)^2 (1 + \alpha_x) \bar{\nu}_S \right) \quad (3.41)$$

To sum up, the proposition is established. \square

Moreover, we know that

Proposition 3.1.10. *The asymptotic Feynman equations*
The asymptotic Feynman equations are

$$\begin{aligned} \frac{\mathbb{E}[N_{[0,t]}]}{t} &= \bar{S} \frac{\varepsilon_F}{-\rho \bar{\nu}} \\ Y_{2,\infty} &= \frac{\varepsilon_F D_2}{\rho^2} \left(1 - x\rho \frac{\bar{\nu}_S D_{2S}}{\bar{\nu} D_2} \right) \\ Y_{3,\infty} &= 3 \left(\frac{\varepsilon_F D_2}{-\rho^2} \right)^2 \left(1 - x\rho \frac{\bar{\nu}_S D_{2S}}{\bar{\nu} D_2} \right) - \frac{\varepsilon_F^2 D_3}{\rho^3} \left(1 - x\rho \frac{\bar{\nu}_S D_{3S}}{\bar{\nu} D_3} \right) \end{aligned} \quad (3.42)$$

These equations were established in the state-of-the-art, the first chapter.

Now we can solve analytically the inverse problem

Proposition 3.1.11. *Böhnel inversion equations, and another inverse problem*
Knowing the direct problem of Böhnel equations 3.23, the inverse problem of Böhnel equations knowing the observations

$$\mathbf{y}_{obs} = \mathbf{M}_{Böhnel}(\mathbf{p}_{Böhnel}) = \begin{pmatrix} N_{1,C}(t) \\ N_{2,C}(t) \\ N_{3,C}(t) \end{pmatrix} \quad (3.43)$$

we can deduce the parameters $\mathbf{p}_{Böhnel}$.

Now, we consider α_x known. The inverse problem is the following : knowing the

mean $\mathbb{E}[N_{[0,t]}]$ and the asymptotical Feynman moments of order 2 and 3 $Y_{2,\infty}$, $Y_{3,\infty}$ as observations

$$\mathbf{y}_{obs} = \mathbf{M}(\mathbf{p}) = \begin{pmatrix} \mathbb{E}[N_{[0,t]}] \\ Y_{2,\infty} \\ Y_{3,\infty} \end{pmatrix} \quad (3.44)$$

we want to recover the parameters \mathbf{p} . Then, considering $a_1 = \frac{\bar{v}_S D_{2S}}{\bar{v} D_2}$, $a_2 = \frac{\bar{v}_S^2 D_{3S}}{\bar{v}^2 D_3}$, $a_3 = \frac{D_3}{3D_2^2}$, $\rho \in [0, 1]$ is the solution of

$$x(xa_1^2 z - a_2 a_3) \rho^2 + (xa_1(1 - 2z) + a_3) \rho z - 1 = 0 \quad (3.45)$$

Then the inversion procedure provides

$$\mathbf{p} = \begin{pmatrix} \rho \\ \varepsilon_F \\ S_F \end{pmatrix} = \begin{pmatrix} \text{solution of equation 3.45} \\ \frac{\rho^2 Y_{2,\infty}}{D_2} \\ \frac{\mathbb{E}[N_{[0,t]}]}{\bar{v}_S \frac{\varepsilon_F}{-\rho \bar{v}} t} \end{pmatrix} \quad (3.46)$$

From this last results we can deduce k_{eff} and ε_C .

Proof. We can consider the analytical inversion using the quantities $\frac{\mathbb{E}[N_{[0,t]}]}{t}$, $Y_{2,\infty}$, $Y_{3,\infty}$.

In order to use the analytical inversion, we consider

$$\begin{aligned} z &= \frac{Y_{3,\infty}}{3Y_{2,\infty}^2} \\ &= \frac{\left(\frac{\varepsilon_F D_2}{-\rho^2}\right)^2 \left(1 - x\rho \frac{\bar{v}_S D_{2S}}{\bar{v} D_2}\right) - \frac{\varepsilon_F^2 D_3}{\rho^3} \left(1 - x\rho \frac{\bar{v}_S D_{3S}}{3\bar{v} D_3}\right)}{\left(\frac{\varepsilon_F D_2}{\rho^2}\right)^2 \left(1 - x\rho \frac{\bar{v}_S D_{2S}}{\bar{v} D_2}\right)^2} \\ &= \frac{\left(1 - x\rho \frac{\bar{v}_S D_{2S}}{\bar{v} D_2}\right) - \rho \frac{D_3}{3D_2^2} \left(1 - x\rho \frac{\bar{v}_S D_{3S}}{3\bar{v} D_3}\right)}{\left(1 - x\rho \frac{\bar{v}_S D_{2S}}{\bar{v} D_2}\right)^2} \end{aligned} \quad (3.47)$$

Considering $a_1 = \frac{\bar{v}_S D_{2S}}{\bar{v} D_2}$, $a_2 = \frac{\bar{v}_S^2 D_{3S}}{\bar{v}^2 D_3}$, $a_3 = \frac{D_3}{3D_2^2}$ we have

$$z = \frac{(1 - x\rho a_1) - \rho a_3 (1 - x\rho a_2)}{(1 - x\rho a_1)^2} \quad (3.48)$$

Then the reactivity ρ is the solution of the equation

$$x(xa_1^2 z - a_2 a_3) \rho^2 + (xa_1(1 - 2z) + a_3) \rho z - 1 = 0 \quad (3.49)$$

Knowing ρ we can deduce

$$\begin{aligned} k_{eff} &= \frac{1}{1 - \rho} \\ M &= 1 - \frac{1}{\rho} \\ M_L &= \frac{1 - \frac{k_{eff}}{\bar{v}}}{1 - k_{eff}} \end{aligned} \quad (3.50)$$

Then, depending on the application, we have to consider different subcases.

- When $x = 0$, the source is only Poisson type ($S_F = 0$). So $z > 1$, $\rho = \frac{1-z}{\frac{D_3}{3D_2^2}}$, then $k_{eff} = \frac{a_3}{a_3+z-1}$ and so $M_L = 1 + \frac{a_3}{z-1}$
- When $x = 1$, the source is compound Poisson ($S_\alpha = 0$). So $z < 1$.
- If $k_{eff} = 0$, there is no induced fission $z = \frac{1}{x} \frac{D_{3S}}{3D_{2S}^2}$
- If $k_{eff} \rightarrow 1$, $z \rightarrow 1$ for all x .
- Most of the time, there is only one solution $\rho \in [0, 1]$ for one (z, x) . But in some cases, there can be two admissible solutions.

a plot of z in function of k_{eff} can help to have a better understanding of these cases.

The Böhnel equations can be deduced from the equations of $\mathbb{E}[N_{[0,t]}]$, $Y_{2,\infty}$, $Y_{3,\infty}$ and conversely. In the case where α_x is known, we now have an analytical inversion method. \square

Application

Now we consider again the case with the point model parameters

$$\mathbf{p}^* = \begin{pmatrix} S_F^* = 70 \text{ n.ms}^{-1} \\ \rho^* = -1 \\ \varepsilon_C^* = 0,25 \cdot 10^{-2} \\ x^* = 0 \\ \alpha^* = 2 \text{ ms}^{-1} \end{pmatrix} \quad (3.51)$$

where $\rho^* = -1$ corresponds to $k_{eff}^* = 0.5$. All the computations will be done in ms^{-1} . The measurements are done for a time duration 3600 s. The spontaneous fission emits at most 1 neutron, the induced fission emits at most 7 neutrons (with Terrel distribution) and the nuclear constants are

$$\begin{pmatrix} \bar{\nu} \\ D_2 \\ D_3 \end{pmatrix} = \begin{pmatrix} 2,53108 \\ 0,81168 \\ 0,51843 \end{pmatrix} \quad \begin{pmatrix} \bar{\nu}_S \\ D_{2S} \\ D_{3S} \end{pmatrix} = \begin{pmatrix} 1 \\ 0 \\ 0 \end{pmatrix} \quad (3.52)$$

In the present case $x = 0$, the equation 3.47 becomes

$$z = 1 - \rho \frac{D_3}{3D_2^2} \quad (3.53)$$

which is equivalent to

$$\begin{aligned} \rho \frac{D_3}{3D_2^2} &= 1 - z \\ \rho &= \frac{1 - z}{\frac{D_3}{3D_2^2}} \end{aligned} \quad (3.54)$$

thanks to the fact that $\rho = 1 - \frac{1}{k_{eff}}$

$$\begin{aligned} 1 - \frac{1}{k_{eff}} &= \frac{1 - z}{\frac{D_3}{3D_2^2}} \\ 1 - \frac{1 - z}{\frac{D_3}{3D_2^2}} &= \frac{1}{k_{eff}} \end{aligned} \quad (3.55)$$

$$\boxed{k_{eff} = \frac{\frac{D_3}{3D_2^2}}{\frac{D_3}{3D_2^2} + z - 1}} \quad (3.56)$$

Moreover

$$\varepsilon_F = \frac{\rho^2 Y_{2,\infty}}{D_2} \quad (3.57)$$

and because of the equation 3.4 we dispose of

$$\boxed{\varepsilon_C = \frac{\frac{\rho^2 Y_{2,\infty}}{D_2}}{\frac{\nu}{k_{eff}} - 1}} \quad (3.58)$$

And finally, we can deduce the intensity of the source

$$\boxed{S_F = \frac{\mathbb{E}[N_{[0,t]}]}{\bar{\nu}_S \frac{\varepsilon_F}{-\rho \bar{\nu}} t}} \quad (3.59)$$

In the current case, we have the numerical values

$$\mathbf{y}_{obs} = \begin{pmatrix} \mathbb{E}[N_{[0,t]}] \\ Y_{2,\infty} \\ Y_{3,\infty} \end{pmatrix} = \begin{pmatrix} 0.28086 t \\ 8.24294 \cdot 10^{-3} \\ 2.57305 \cdot 10^{-4} \end{pmatrix} \quad (3.60)$$

Then

$$\begin{aligned} k_{eff} &= \frac{\frac{D_3}{3D_2^2}}{\frac{D_3}{3D_2^2} + \frac{Y_{3,\infty}}{3Y_{2,\infty}^2} - 1} \\ &= 0.50000 \end{aligned} \quad (3.61)$$

Also

$$\begin{aligned} \varepsilon_C &= \frac{\rho^2 Y_{2,\infty}}{D_2 \left(\frac{\nu}{k_{eff}} - 1 \right)} \\ &= 0.25 \cdot 10^{-2} \end{aligned} \quad (3.62)$$

And finally

$$\begin{aligned} S_F &= \frac{\mathbb{E}[N_{[0,t]}]}{\bar{\nu}_S \frac{\varepsilon_F}{-\rho \bar{\nu}} t} \\ &= 70.00000 \end{aligned} \quad (3.63)$$

To sum up

$$\mathbf{p} = \begin{pmatrix} k_{eff} \\ \varepsilon_C \\ S_F \end{pmatrix} = \begin{pmatrix} 0.5000 \\ 0.25 \cdot 10^{-2} \\ 70.00000 \end{pmatrix} \quad (3.64)$$

We conclude that the results of the analytical inversion are exact, but the observations are noisy in practice.

We can consider noisy observations, and try to recover $(k_{eff}, S_F, \varepsilon_C)$. For a time gate $t = \frac{10}{\alpha}$, we have the following MC realisation using "Counting" (see Chapter 2, algo 3)

$$\mathbf{y}_{obs,1,MC} = \begin{pmatrix} \mathbb{E}[N_{[0,t]}] \\ Y_2(t) \\ Y_3(t) \end{pmatrix} = \begin{pmatrix} 1.3871428966522217 \\ 0.10204351973567416 \\ 0.13522437794891484 \end{pmatrix} \quad (3.65)$$

With these values, we obtain the numerical result

$$\mathbf{p}_{1,MC} = \begin{pmatrix} k_{eff} \\ \varepsilon_C \\ S_F \end{pmatrix} = \begin{pmatrix} 7.30428 \cdot 10^{-2} \\ 4.86016 \cdot 10^{-2} \\ 27.242536 \end{pmatrix} \quad (3.66)$$

This set of values is inoperable in practice. Moreover, we compute the following L_2 norms $\|\mathbf{s}\|_2 = \sqrt{\sum_i |s_i|^2}$

$$\begin{aligned} \|\mathbf{M}(\mathbf{p}^*) - \mathbf{y}_{obs,1,MC}\|_2 &= 1.118423 \\ \|\mathbf{p}^* - \mathbf{p}_{1,MC}\|_2 &= 42.75962 \end{aligned} \quad (3.67)$$

Remark 3.1.12. *We can obtain negative values for $Y_3(t)$, which provides absurd results.*

We use again the code "Counting" 3, each new launch of the code the pseudo-random seed is changed, and it provides independent realisations of the first experiment. We obtain

$$\mathbf{y}_{obs,2,MC} = \begin{pmatrix} \mathbb{E}[N_{[0,t]}] \\ Y_2(t) \\ Y_3(t) \end{pmatrix} = \begin{pmatrix} 1.42714 \\ 5.83425 \cdot 10^{-2} \\ 0.34410 \end{pmatrix} \quad (3.68)$$

With these values, we obtain the numerical result

$$\mathbf{p}_{2,MC} = \begin{pmatrix} k_{eff} \\ \varepsilon_C \\ S_F \end{pmatrix} = \begin{pmatrix} 7.95818 \cdot 10^{-3} \\ 0.49774 \\ 2.85338 \end{pmatrix} \quad (3.69)$$

This value is also not useful in practice. Moreover, we compute the following L_2 norms

$$\begin{aligned} \|\mathbf{M}(\mathbf{p}^*) - \mathbf{y}_{obs,2,MC}\|_2 &= 1.19779 \\ \|\mathbf{p}^* - \mathbf{p}_{2,MC}\|_2 &= 67.1502467 \end{aligned} \quad (3.70)$$

Moreover, we can compute the L_2 norms

$$\begin{aligned} \|\mathbf{y}_{obs,1,MC} - \mathbf{y}_{obs,2,MC}\|_2 &= 0.21712 \\ \|\mathbf{p}_{1,MC} - \mathbf{p}_{2,MC}\|_2 &= 24.39338 \end{aligned} \quad (3.71)$$

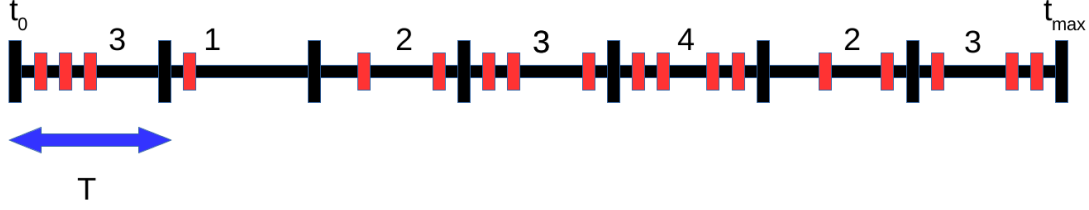


Figure 3.1: Measurements of the number of neutrons detected during a time gate T between t_0 and t_{max} : $N_{1,[0,T]} = 3$, $N_{2,[0,T]} = 1$, $N_{3,[0,T]} = 2, \dots$

The equations 3.67 and 3.70 provide the order of magnitude of the deviation at $\mathbf{M}(\mathbf{p}^*)$ of the observations generated by the "Counting" MC code 3. Both quantities $\|\mathbf{M}(\mathbf{p}^*) - \mathbf{y}_{obs,1,MC}\|_2$ and $\|\mathbf{M}(\mathbf{p}^*) - \mathbf{y}_{obs,2,MC}\|_2$ are quite the same order of magnitude, i.e. 1.1 or 1.2 respectively. This means that the noise in $\mathbf{y}_{obs,MC} = \mathbf{M}(\mathbf{p}^*) + \epsilon$ is small and almost the same here. Furthermore, we can consider the difference in norm L_2 of the corresponding parameters $\|\mathbf{p}^* - \mathbf{p}_{1,MC}\|_2$ and $\|\mathbf{p}^* - \mathbf{p}_{2,MC}\|_2$, these two quantities are not as close as the noise, they are more different and the equation 3.71 confirms it. This highlights the fact that analytical inversion using noisy observations is not robust enough to be used in practice.

3.1.2 The observations

In this chapter, the observations \mathbf{y}_{obs} are provided by the Monte Carlo "Counting" code 3 or taken as $\mathbf{M}(\mathbf{p}^*)$ where \mathbf{p}^* refers to the actual parameters of the current system. It can also be experimental data provided in a Time List file.

As indicated in Figure 3.1, the realisations of $N_{[0,T]}$ are calculated by storing the detection times (the red bars) over a measurement time between t_0 and t_{max} by subdividing them into time gates of duration T providing the number of neutrons detected during the l -th time gate of length T : $N_{l,[0,T]}$.

Then, we can define the observations $\mathbf{y}_{obs} = \hat{\mathbf{M}}$ to refer to the Monte Carlo estimates of the first three simple moments of $N_{[0,t]}$

$$\begin{aligned} \mathbf{y}_{obs} &= \hat{\mathbf{M}} \\ &= \begin{pmatrix} \widehat{\mathbb{E}[N_{[0,t]}]} \\ \widehat{\mathbb{E}[N_{[0,t]}^2]} \\ \widehat{\mathbb{E}[N_{[0,t]}^3]} \end{pmatrix} \\ &= \mathbf{M}(\mathbf{p}^*) + \epsilon \end{aligned} \quad (3.72)$$

where, for $N_{realisations} \in \mathbb{N}^*$,

$$\widehat{\mathbb{E}[N_{[0,t]}^j]} = \frac{1}{N_{realisations}} \sum_{l=1}^{N_{realisations}} N_{l,[0,t]}^j \quad (3.73)$$

and ϵ is the noise of observations.

These estimates will be taken into account when estimating the moments for the whole of this chapter. The notation $\hat{\mathbf{M}}$ will refer to these estimates when they are mentioned.

3.1.3 The mean square error, a first consideration for the inverse problem

In the first part, we will study the influence of ρ on several norms.

We consider here the parameters of the point model

$$\mathbf{p}^* = \begin{pmatrix} \varepsilon_C^* = 0, 25 \cdot 10^{-2} \\ \rho^* = -1 \\ \alpha^* = 2 \text{ m.s}^{-1} \\ S^* = 70 \text{ n.m.s}^{-1} \\ x^* = 0 \end{pmatrix} \quad (3.74)$$

where $\rho^* = -1$ corresponds to $k_{eff}^* = 0.5$. One spontaneous fission emits at most 1 neutron, one induced fission emits at most 7 neutrons and the nuclear constants are

$$\begin{pmatrix} \bar{\nu} \\ D_2 \\ D_3 \end{pmatrix} = \begin{pmatrix} 2, 53108 \\ 0, 81168 \\ 0, 51843 \end{pmatrix} \quad \begin{pmatrix} \bar{\nu}_S \\ D_{2S} \\ D_{3S} \end{pmatrix} = \begin{pmatrix} 1 \\ 0 \\ 0 \end{pmatrix} \quad (3.75)$$

An inverse problem with the reactivity ρ

In order to study the influence of ρ on the outputs of our model, we will focus on several cost functions. In this particular case, it will be clearer whether the inverse problem is well posed: this means that we can recover ρ^* using the observed cost function. We recall the value $\rho^* = -1$.

We first study the cost function $Cost_1$.

$$Cost_1(\rho) = \sum_{j=1}^3 \frac{\|\hat{\mathcal{M}}_j(t) - \mathcal{M}_j(\rho, t)\|^2}{\|\hat{\mathcal{M}}_j(t)\|^2}, \quad (3.76)$$

where $\hat{\mathcal{M}}_j(t)$ is the estimation of $\frac{\mathbb{E}[N_{[0,t]}(N_{[0,t]}-1)\dots(N_{[0,t]}-j+1)]}{j!}$, $j \in \llbracket 2, +\infty \llbracket$ using the Monte-Carlo code "Counting" 3 in the point model approximation and $\mathcal{M}_j(\rho, t) = \frac{1}{j!} \left[\frac{\partial^j}{\partial x^j} \mathcal{G} \right]_{x=1}$ where \mathcal{G} is defined in the state-of-the-art (see Chapter 1 or index of notations).

We have considered three different time gates which correspond to

$$\begin{aligned} t_1 &= \frac{1}{\alpha} \\ t_2 &= \frac{2}{\alpha} \\ t_3 &= \frac{10}{\alpha} \end{aligned} \quad (3.77)$$

The MC code "Counting" 3 provide the observations

$$\begin{aligned} y_{obs}(t_1) &= \begin{pmatrix} 0.13716 \\ 0.15689 \\ 0.19797 \end{pmatrix} \\ y_{obs}(t_2) &= \begin{pmatrix} 0.27432 \\ 0.35703 \\ 0.55324 \end{pmatrix} \\ y_{obs}(t_3) &= \begin{pmatrix} 1.37286 \\ 3.28714 \\ 9.70429 \end{pmatrix} \end{aligned} \quad (3.78)$$

the associated covariance matrices are

$$\begin{aligned} \widehat{\mathbf{Cov}}(t_1) &= \begin{pmatrix} 1.86592 \cdot 10^{-5} & 2.38450 \cdot 10^{-5} & 3.484340 \cdot 10^{-5} \\ 2.38450 \cdot 10^{-5} & 3.51872 \cdot 10^{-5} & 5.98092 \cdot 10^{-5} \\ 3.48440 \cdot 10^{-5} & 5.98092 \cdot 10^{-5} & 1.15613 \cdot 10^{-4} \end{pmatrix} \\ \widehat{\mathbf{Cov}}(t_2) &= \begin{pmatrix} 7.61549 \cdot 10^{-5} & 1.23055 \cdot 10^{-4} & 2.41304 \cdot 10^{-4} \\ 1.23055 \cdot 10^{-4} & 2.47872 \cdot 10^{-4} & 5.81751 \cdot 10^{-4} \\ 2.41304 \cdot 10^{-4} & 5.81751 \cdot 10^{-4} & 1.54774 \cdot 10^{-3} \end{pmatrix} \\ \widehat{\mathbf{Cov}}(t_3) &= \begin{pmatrix} 2.00344 \cdot 10^{-3} & 7.41644 \cdot 10^{-3} & 2.90106 \cdot 10^{-2} \\ 7.41644 \cdot 10^{-3} & 3.26067 \cdot 10^{-2} & 0.14227 \\ 2.90106 \cdot 10^{-2} & 0.14227 & 0.670244 \end{pmatrix} \end{aligned} \quad (3.79)$$

Figure 3.2 shows the evolution of the cost function $Cost_1(\rho)$ for $\rho \in [-2; -0.16]$ and three different time gates. We have chosen to draw the logarithm of the cost function because we can observe the minimum. We can observe that the three curves have a similar behaviour but that the minimum is more or less accentuated. This variation of level can be explained by the variation of the time gate. Indeed, the simple moments of order 2 and 3 are very noisy, the curve of the simple moments in function of the time gate t is erratic and thus the cost function $Cost_1(\rho)$ is minimal on the cost function $\rho + \varepsilon_t$ where ε_t is an estimation error induced by the noise ϵ (see eq. 3.72).

First consider the curve for $t_3 = \frac{10}{\alpha}$ in Figure 3.2. The minimum of this function is approximately $\rho^* \pm 0.05$, so the minimum of this function is relatively well-marked with a small bias of 0.05.

The minimum of this curve is at $\rho^* + \varepsilon_t$, which is consistent with the fact that the observations are noisy.

We note the convergence to the ρ solution by improving the precision of the mesh. By definition, there is a component $\frac{\mathcal{M}_1^j(t)}{j!}$ in $\mathcal{M}^j(t), \forall j \in \llbracket 2, +\infty \llbracket$ so we study the second cost function

$$Cost_2(\rho) = \frac{\|\hat{\mathcal{M}}_1(t) - \mathcal{M}_1(\rho, t)\|^2}{\|\hat{\mathcal{M}}_1(t)\|^2} + \sum_{j=2}^3 \frac{\|\hat{\mathcal{M}}_j(t) - \frac{\hat{\mathcal{M}}_1^j(t)}{j!} - (\mathcal{M}_j(\rho, t) - \frac{\mathcal{M}_1^j(\rho, t)}{j!})\|^2}{\|\hat{\mathcal{M}}_j(t) - \frac{\hat{\mathcal{M}}_1^j(t)}{j!}\|^2} \quad (3.80)$$

where $\hat{\mathcal{M}}_j(t)$ is the estimation of $\frac{\mathbb{E}[N_{[0,t]}(N_{[0,t]}-1)\cdots(N_{[0,t]}-j+1)]}{j!}$, $j \in \llbracket 2, +\infty \llbracket$ using the Monte-Carlo code "Counting" 3 in the point model approximation.

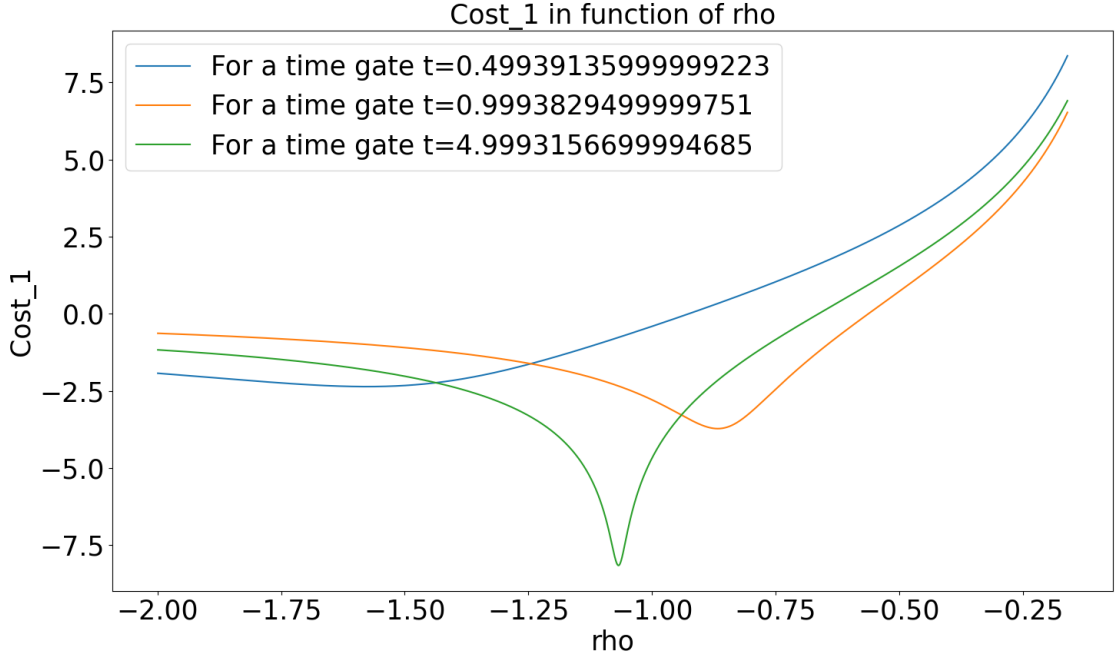


Figure 3.2: The log of $\sum_{j=1}^3 \frac{\|\hat{\mathcal{M}}_j(t) - \mathcal{M}(\rho, t)\|^2}{\|\hat{\mathcal{M}}_j(t)\|^2}$ for ρ in $[-2; -0.16]$

Figure 3.3 shows less information than the previous cost functions. Since the simple moment of order j has a $\frac{\mathcal{M}_1^j(t)}{j!}$ component, the rest of the cost function considered is not sufficient to estimate the real parameter ρ^* . This shows also the error depends on the time gate t but is not monotone in t .

To conclude for this part, we considered two cost functions with the moment of the distribution $N_{[0,t]}$, they have different minimums. The curve showing the most information to conclude is for $t_3 = \frac{10}{\alpha}$. We can choose the first cost function in our calculations because the second one does not provide enough information. This could be useful when minimising a square norm, such as in the simulated annealing use.

Influence of the type of moment

Still considering ρ and trying to obtain ρ^* , we want to study the influence of the time gate using the following cost function

$$Cost_3(\rho) = \sum_{j=1}^3 \frac{\|\hat{\mathcal{M}}_1(t_j) - \mathcal{M}_1(\rho, t_j)\|^2}{\|\hat{\mathcal{M}}_1(t_j)\|^2} \quad (3.81)$$

where $t_1 = \frac{1}{\alpha}$, $t_2 = \frac{2}{\alpha}$ and $t_3 = \frac{10}{\alpha}$ and $\hat{\mathcal{M}}_j(t)$ is the estimation of $\frac{\mathbb{E}[N_{[0,t]}(N_{[0,t]}-1)\cdots(N_{[0,t]}-j+1)]}{j!}$, $j \in \llbracket 2, +\infty \rrbracket$ using the Monte-Carlo code "Counting" 3 in the point model approximation.

Knowing the outputs of our model and the chosen time gates, we draw the Figure 3.4. The three configurations correspond to the consideration of the three

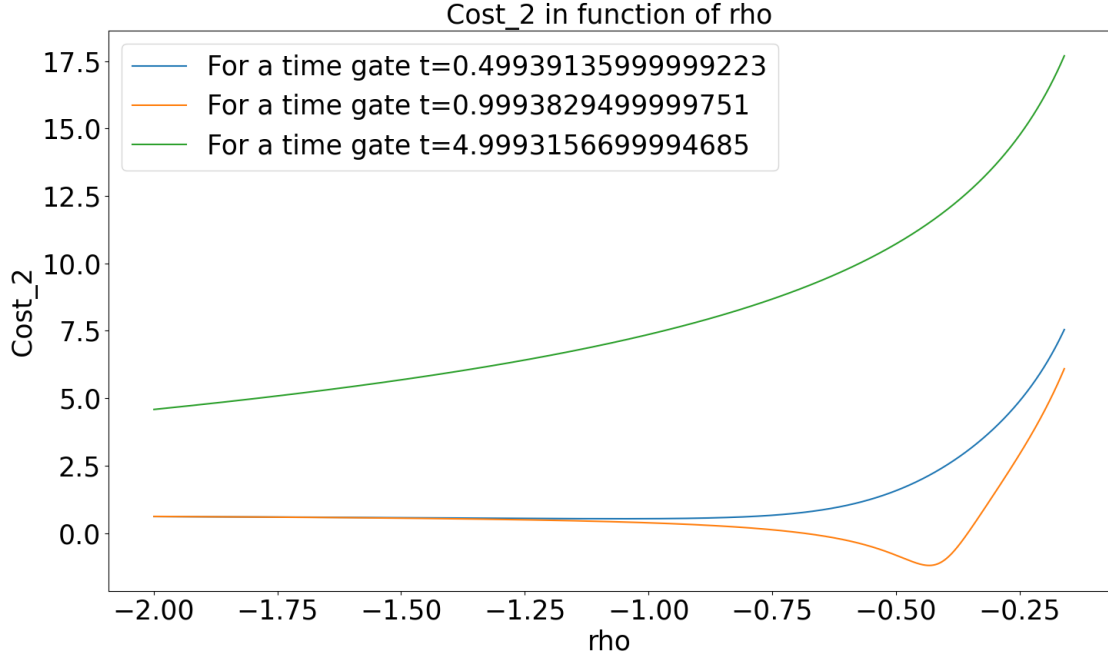


Figure 3.3: The log of $\frac{\|\hat{\mathcal{M}}_1(t) - \mathcal{M}_1(\rho, t)\|^2}{\|\hat{\mathcal{M}}_1(t)\|^2} + \sum_{j=2}^3 \frac{\|\hat{\mathcal{M}}_j(t) - \frac{\hat{\mathcal{M}}_1^j(t)}{j!} - (\mathcal{M}_j(\rho, t) - \frac{\mathcal{M}_1^j(\rho, t)}{j!})\|^2}{\|\hat{\mathcal{M}}_j(t) - \frac{\hat{\mathcal{M}}_1^j(t)}{j!}\|^2}$ for ρ in $[-2; -0.16]$

moments $\mathcal{M}_j(t)$, $j \in \llbracket 1, 3 \rrbracket$ and thus we observe that there is a curve which provides more information than the others; the green curve is flat and does not provide any information, the orange and blue curves are sharper, but the blue one is the sharpest. This means that we have to consider the moment of order one or two to get the best estimate of ρ^* . We still have the effect of the erratic behaviour of $\hat{\mathbf{M}}$.

We can see that the orange curve correctly estimates $\rho^* = -1$.

Using a covariance matrix

In order to take into account the covariance between the measurements, we compute the covariance matrix of the measurements, more precisely we will consider the empirical covariance matrix of the observations (which we obtain from the Monte Carlo realisations). This covariance matrix allows us to have a good approximation of the shape of the a posteriori distribution, in particular it controls the width of the a posteriori distribution which can be really degenerate when the number of realisations of $N_{[0,t]}$ is high.

We recall the shape of the covariance matrix, we will apply it to the neutron counts distribution $N_{[0,t]}$.

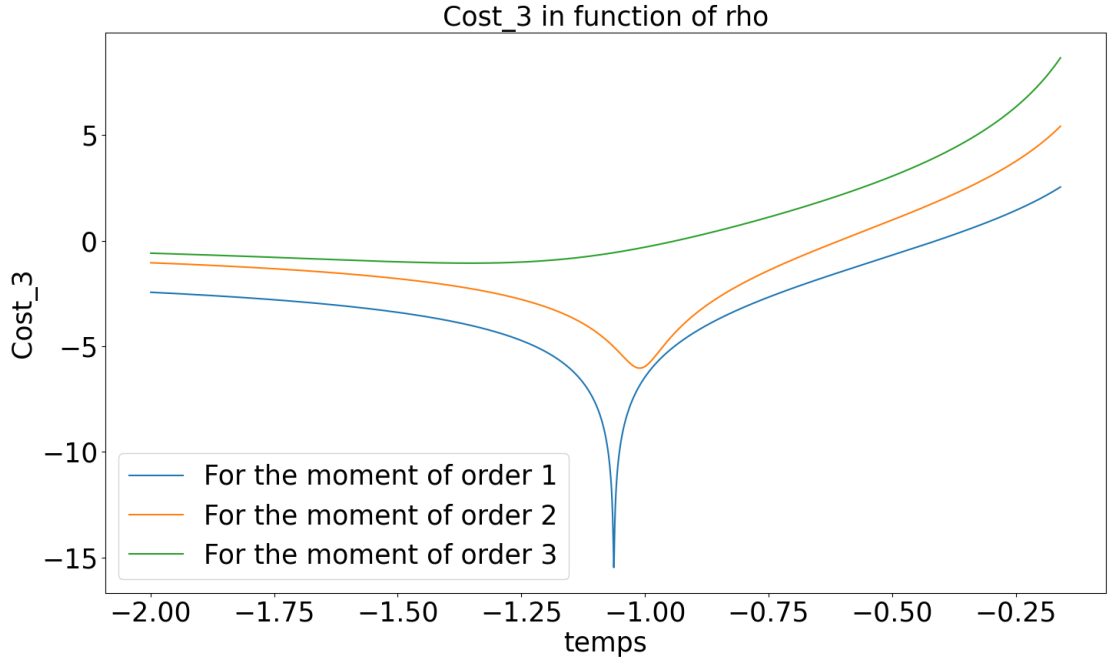


Figure 3.4: The log of $\sum_{j=1}^3 \frac{\|\hat{\mathcal{M}}_l(t_j) - \mathcal{M}_l(\rho, t_j)\|^2}{\|\hat{\mathcal{M}}_l(t_j)\|^2}$ for ρ in $[-2; -0.16]$ and $l = 1, 2$ or 3

Proposition 3.1.13. *The empirical covariance matrix of $\mathbf{X}_l = (N_l^k)_{k=1,3}$ is*

$$\widehat{\mathbf{K}} := \widehat{\mathbf{Cov}}(\mathbf{X}_l) = \begin{pmatrix} \widehat{\mathbb{E}}[N^2] - \widehat{\mathbb{E}}[N]^2 & \widehat{\mathbb{E}}[N^3] - \widehat{\mathbb{E}}[N]\widehat{\mathbb{E}}[N^2] & \widehat{\mathbb{E}}[N^4] - \widehat{\mathbb{E}}[N]\widehat{\mathbb{E}}[N^3] \\ \widehat{\mathbb{E}}[N^3] - \widehat{\mathbb{E}}[N]\widehat{\mathbb{E}}[N^2] & \widehat{\mathbb{E}}[N^4] - \widehat{\mathbb{E}}[N^2]^2 & \widehat{\mathbb{E}}[N^5] - \widehat{\mathbb{E}}[N^2]\widehat{\mathbb{E}}[N^3] \\ \widehat{\mathbb{E}}[N^4] - \widehat{\mathbb{E}}[N]\widehat{\mathbb{E}}[N^3] & \widehat{\mathbb{E}}[N^5] - \widehat{\mathbb{E}}[N^2]\widehat{\mathbb{E}}[N^3] & \widehat{\mathbb{E}}[N^6] - \widehat{\mathbb{E}}[N^3]^2 \end{pmatrix} \quad (3.82)$$

Definition 3.1.14. *Let $n \in \mathbb{N}^*$, the norm associated to a matrix $\mathbf{K} \in PD(\mathbb{R})$ is*

$$\|\mathbf{y}\|_{\mathbf{K}}^2 = \mathbf{y}^T \mathbf{K}^{-1} \mathbf{y}, \text{ for any vector } \mathbf{y} \in \mathbb{R}^n. \quad (3.83)$$

where $PD(\mathbb{R})$ refers to the set of positive-definite matrices on \mathbb{R} .

This norm defines a quadratic form.

Thanks to the chapter on the state-of-the-art (and 8.2.1 [Gar17]), when the likelihood is a Gaussian distribution $\mathcal{N}(\mathbf{M}(\mathbf{p}), \mathbf{Cov}(\mathbf{p}))$, it is known that the a posteriori distribution $\mu_{\text{posterior}}$ has the form

$$\mu_{\text{posterior}}(\mathbf{p}) \simeq e^{-\frac{\|\mathbf{y}_{\text{obs}} - \mathbf{M}(\mathbf{p})\|_{\widehat{\mathbf{Cov}}(\mathbf{p})}^2}{2} - \frac{1}{2} \log(\det(\mathbf{Cov}(\mathbf{p})))}. \quad (3.84)$$

The computation of the covariance matrix requires to compute the exact simple moments up to the order 6, and this is too much complicated. So we suggest use the empirical covariance matrix $\widehat{\mathbf{Cov}}$, and this is efficient because $\widehat{\mathbf{Cov}}^{-1} \rightarrow \mathbf{Cov}(\mathbf{p}^*)^{-1}$, when the number of realisations tends to infinity $n \rightarrow +\infty$ (see A.4.2).

And then when we focus on the mode of the a posteriori distribution, we find the maximum a posteriori (MAP):

$$\underset{\mathbf{p} \in \mathbb{R}^5}{\operatorname{argmin}} \|\mathbf{y}_{\text{obs}} - \mathbf{M}(\mathbf{p})\|_{\widehat{\mathbf{Cov}}}^2 \quad (3.85)$$

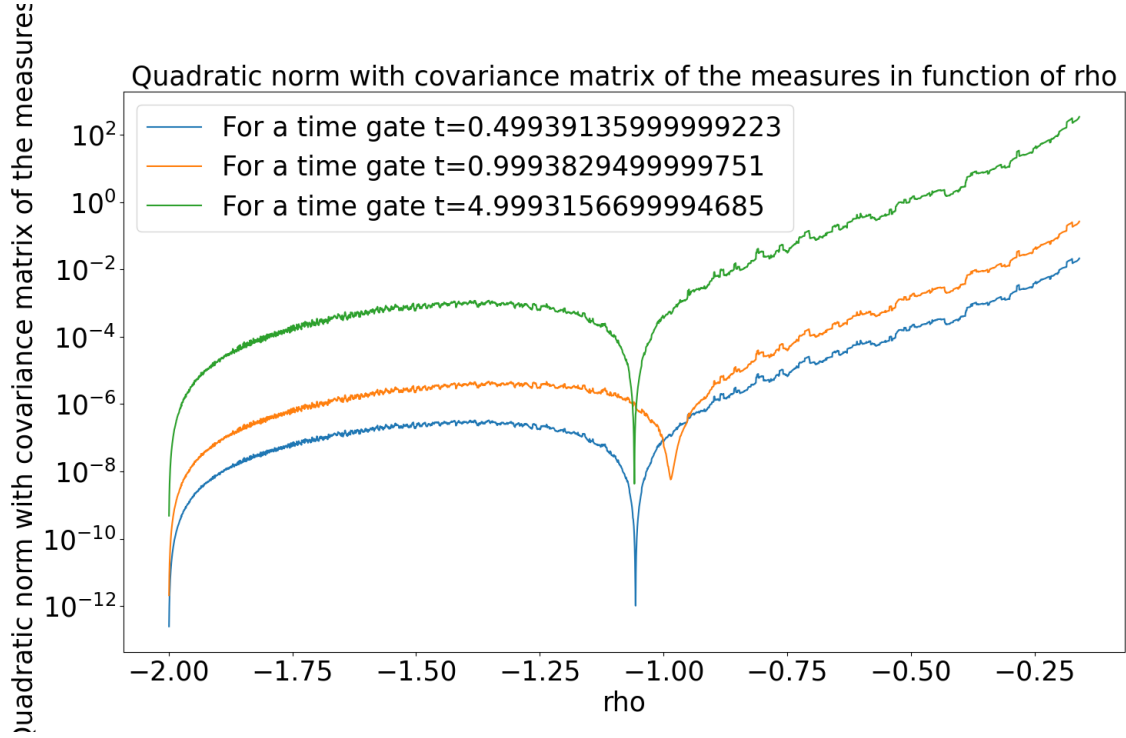


Figure 3.5: $\|\hat{\mathcal{M}}(t) - \mathcal{M}(\rho, t)\|_{\hat{K}}^2$ for ρ in $[-2; -0.16]$

The norm associated with the covariance of the measurements is considered in Figure 3.5. We observe three curves linked to three different time gates t_1, t_2, t_3 . As before, we observe a noise on the minimum of the curve, which can be explained by the noise in $\hat{\mathbf{M}}$. The curve corresponding to the time gate $t_2 = \frac{2}{\alpha}$ allows us to estimate ρ^* precisely.

Now we will consider a point estimation of \mathbf{p}^* with this norm because the minimum is the best emphasized.

3.1.4 Simulated annealing

We introduce here a classical optimization method: simulated annealing (more details are given in [KGV83; Kir84]). It was introduced by Metropolis et al. as an adaptation of the Metropolis-Hastings algorithm. This algorithm is designed to search for the global minimum of functions, but it does not give information about the uncertainty on the parameters (as do the Bayesian-MCMC methods). Here we study this algorithm and analyse the efficiency of the algorithm.

The simulated annealing algorithm is inspired by metallurgy, where the temperature of the medium is successively cooled and warmed in order to decrease the energy of the medium.

In this algorithm, the temperature pattern, the energy and the density must be specified. And must be adapted empirically to the considered problem.

Thus, the algorithm is initialized with a point with the initial energy, this energy is calculated with the energy scheme. And the initial temperature is chosen arbitrarily in the definition domain. The density allows taking into account or not

the new neighbour.

First, we choose the temperature pattern as

Definition 3.1.15. *Temperature choice*

At the iteration number i , the current temperature is T_i , we use T_{i-1} and a coefficient τ_T such that

$$T_i = \tau_T T_{i-1} \text{ where } \tau_T < 1$$

Then, the temperature decreases. We made the choice of $\tau_T = 0.9999$ and the algorithm converges in our case, in 3D the temperature needs to be slow, and this choice enables slow decreasing for the present case.

Secondly, with regard to the choice of the new neighbour

Definition 3.1.16. *Choice of the new neighbour*

We choose the new neighbour \mathbf{p}_{new} with a Gaussian distribution centred on the current point

$$p_{j,new} \sim \mathcal{N}(p_j, \text{frac}^2(p_{max,j} - p_{min,j})^2]$$

in each component, where $[p_{min,j}, p_{max,j}]$ will specify the research interval and frac is the scale adaptation factor.

Then we compute the energy scheme as

Definition 3.1.17. *Energy of for the simulated annealing*

For $\mathbf{p} = (\varepsilon_F, S, \rho)$ the energy is chosen as

$$E(\mathbf{p}) = \|\widehat{\mathbf{M}}(t) - \mathbf{M}(\mathbf{p}, t)\|_{\widehat{\mathbf{Cov}}}^2 \quad (3.86)$$

where t is the considered time gate.

We have implemented an energy version using the empirical covariance matrix in the definition of the norm.

Definition 3.1.18. *Density function of the temperature*

For two energies E' , E , the density in function of the temperature is the following

$$\mathbb{P}(E, E', T) = \begin{cases} 1 & \text{when } E' < E \\ e^{-\frac{E'-E}{T}} & \end{cases} \quad (3.87)$$

To sum up, at each new iteration the algorithm cools the temperature thanks to the temperature scheme T , propose a new neighbour \mathbf{p}_{new} , compute the acceptance rate thanks to the energy scheme E and the density with the Metropolis rule:

- we compute the variation of energy of the current point \mathbf{p} and \mathbf{p}_{new} : $\Delta_E = E(\mathbf{p}) - E(\mathbf{p}_{new})$
- When the variation of energy is negative, the new point \mathbf{p}_{new} is taken into account
- Else, the new point \mathbf{p}_{new} is accepted with probability $\mathbb{P}(E(\mathbf{p}), E(\mathbf{p}_{new}), T)$

Moreover, we will use an adapting factor $frac$ in order to have an acceptance rate between 0.25 and 0.5:

- If the acceptance rate is smaller than 0.25, then $frac = 0.99frac$,
- If the acceptance rate is larger than 0.5, then $frac = 1.01frac$.

Then we cool down the temperature, and the next iteration of the algorithm is executed.

Finally, we obtain a point estimate of the solution of our optimisation problem.

More precisely, we have

Algorithm 7: Pseudo-code of the simulated annealing for the inverse problem

```

Initialization of :
-the current point, its energy;
-the temperature;
for  $i = 0, iMax$  do
    Update the temperature  $T_i = \tau_T T_{i-1}$ ;
    Choice of a new neighbor  $\mathbf{p}_{new}$  in a ball centered in  $\mathbf{p}$ ;
    if  $\mathbb{P}(E(\mathbf{p}), E(\mathbf{p}_{new}), T) \geq u$  where  $u \sim \mathcal{U}[0; 1]$  then
        Store the evolution of the energy and the number of selections;
         $\mathbf{p} = \mathbf{p}_{new}$ ;
         $i_{acc,loc} = i_{acc,loc} + 1$ ;
    end
    if  $i \equiv 0(mod\ 1000)$  then
         $tx_{acc} = \frac{i_{acc,loc}}{1000}$ ;
        If  $0.25 > tx_{acc}$ , then  $frac = 0.99frac$ ;
        If  $tx_{acc} > 0.5$ , then  $frac = 1.01frac$ ;
         $i_{acc,loc} = 0$ ;
        If  $frac > 1$ , then  $frac = 1$ ;
        If  $frac < 10^{-4}$ , then  $frac = 10^{-4}$ ;
    end
end

```

Now, in the case where the parameter $x = 0$, we study the performance of simulated annealing with the following complexity levels:

- One parameter is unknown
- Two parameters are unknown
- Third parameters are unknown

For the whole study of the simulated annealing, we consider the following entries:

a time gate $t = \frac{10}{\alpha}$, and the set of parameters is

$$\mathbf{p}^* = \begin{pmatrix} \varepsilon_C^* = 0, 25.10^{-2} \\ \rho^* = -1 \\ \alpha^* = 2 \text{ ms}^{-1} \\ S^* = 70 \text{ n.ms}^{-1} \\ x^* = 0 \end{pmatrix} \quad (3.88)$$

and in this context

$$\hat{\mathbf{M}} = \begin{pmatrix} \widehat{\mathbb{E}[N_{[0,t]}]} \\ \widehat{\mathbb{E}[N_{[0,t]}^2]} \\ \widehat{\mathbb{E}[N_{[0,t]}^3]} \end{pmatrix} = \begin{pmatrix} 1.38714 \\ 3.45286 \\ 11.03000 \end{pmatrix} \quad (3.89)$$

estimated with MC code "Counting" 3 and the covariance matrix of measurements

$$\widehat{\mathbf{Cov}} = \begin{pmatrix} 2.18385 \cdot 10^{-3} & 8.91485 \cdot 10^{-3} & 4.14834 \cdot 10^{-2} \\ 8.91485 \cdot 10^{-3} & 4.63091 \cdot 10^{-2} & 0.25866 \\ 4.14834 \cdot 10^{-2} & 0.25866 & 1.65500 \end{pmatrix} \quad (3.90)$$

this matrix is positive definite, and the conditioning is 14320.71261 and its eigenvalues are 1.69663, $1.18474 \cdot 10^{-4}$, $6.74996 \cdot 10^{-3}$. We now analyse the result of the simulated annealing algorithm applied to the neutron multiplicity counting problem.

One unknown parameter

First, we look for one parameter and the other two are fixed.

To verify that the simulated annealing is well coded, we use it to solve the inverse problem in 1D as follows.

For this subsection we will consider 10^7 iterations of the simulated annealing, with an initial temperature $T_0 = 10^7$, and the initial value of the parameter $\frac{s_{max,j} + s_{min,j}}{2}$. At the end of the computations the algorithm provides the following results

| | |
|--------------------|-------------|
| Unknown parameter | S |
| Research interval | $[0, 1000]$ |
| Obtained parameter | 68.81691 |
| Expected parameter | 70 |

which is a deviation of 1.18309 to the real value of S .

The evolution of the energy as a function of the number of selections is shown in Figure 3.6. First, in the output file we can see there are 86 873 acceptations among 10 000 000 iterations, in fact the 86 873 first acceptations happen in the $8 \cdot 10^{-2}$ fraction of first iterations, the algorithm reject always after. In the Figure 3.6, the energy decreases before 58 000 iterations and then stabilises until the solution is well approximated. We can see many fluctuations in the evolution of the energy in function of the number of selection, this is due to the use of the adaptation factor *frac*, the convergence to the minimum of the quadratic form correspond to the diminution of the energy. The simulated annealing is designed to traverse the

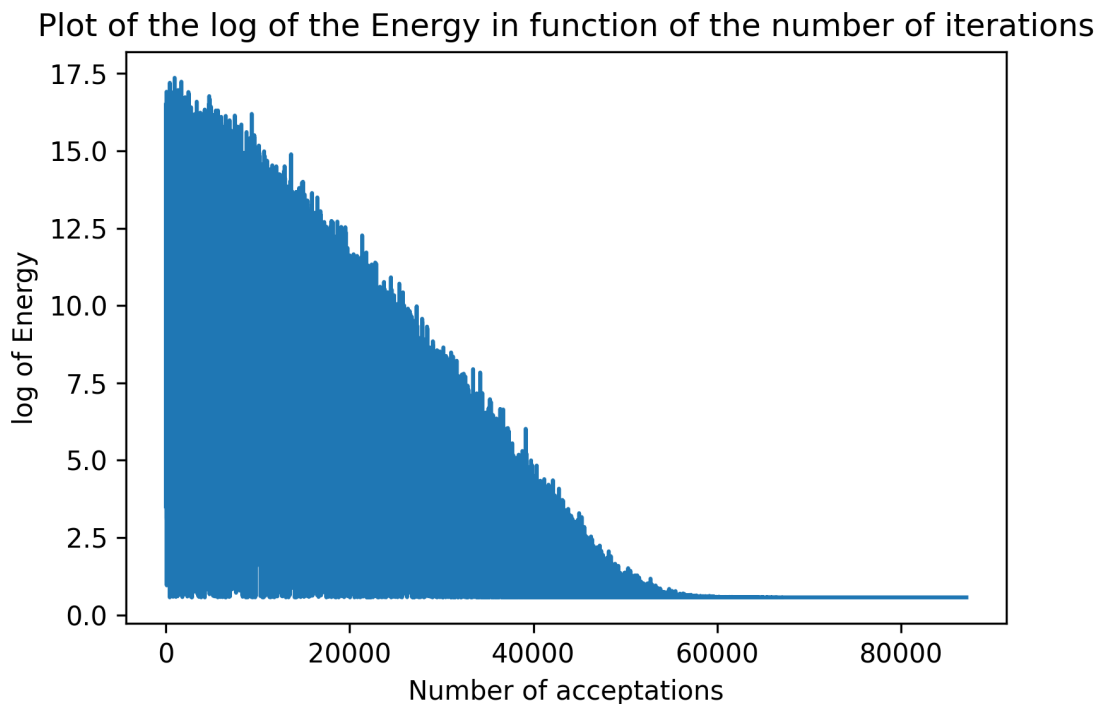


Figure 3.6: Log of the energy of S as a function of the number of selections using the simple moments of order 1 to 3

energy landscape in such a way that it does not get stuck in a local minimum or saddle point and finally finds the global minimum (when it exists). In figure 3.7, the simulated annealing finds the minimum, the function is convex in a neighbourhood of its minimum. This landscape is nice in 1D, but it will more complex to handle in 2D and 3D. On the Figure 3.7, the value that the simulated annealing finds is closed to 70 and is well-marked so the algorithm has not many difficulties to find the minimum of $E(S)$.

We provide here the same kind of results for k_{eff} and ε_C , to be exhaustive.

For k_{eff} , the Figure 3.9 shows the energy in function of the value of k_{eff} . The curve is well picked around $k_{eff} = k^*$, the curve is also less curved in this region than before. As before, there are many fluctuations of the value of $E(k_{eff})$ because the algorithm visits the whole energy landscape. As showed in algorithm 7, the factor $frac$ is used to adapt the proposition law in order to have a local acceptance rate between 0.25 and 0.5, which guarantees we explore as much as possible the energy landscape.

| | |
|--------------------|-----------|
| Unknown parameter | k_{eff} |
| Research interval | $[0, 1]$ |
| Obtained parameter | 0.48895 |
| Expected parameter | 0.5 |

Concerning the Figure 3.8, in the output file we can see there are 110 890 acceptations among 10 000 000 iterations, this is due to the fact that the 110 887 first

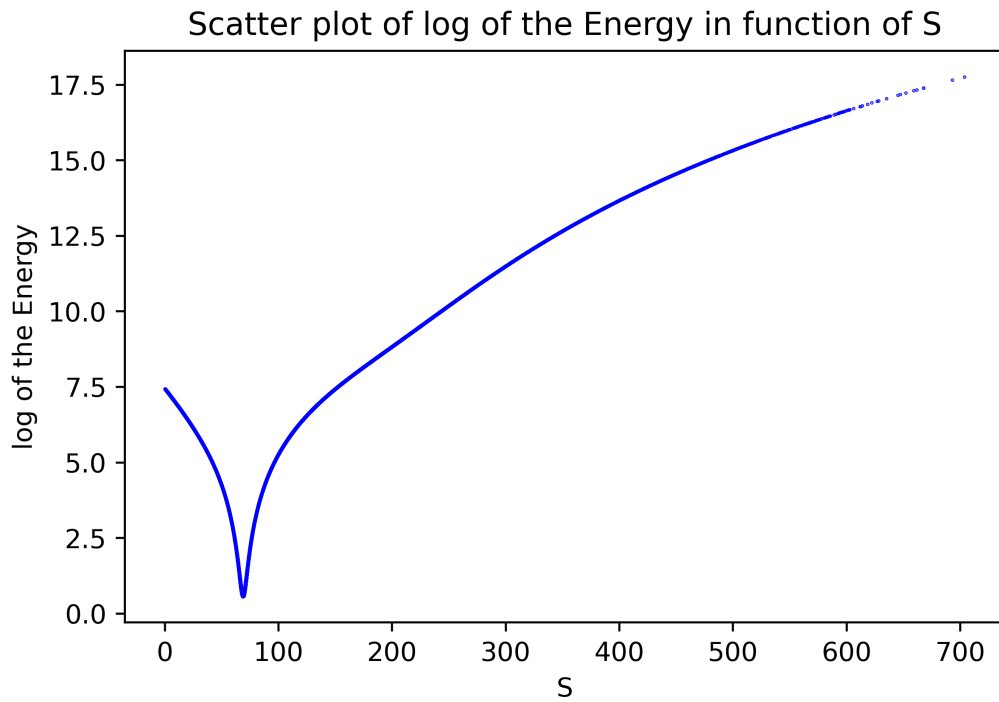


Figure 3.7: Log of the energy as a function of S using the simple moments of order 1 to 3

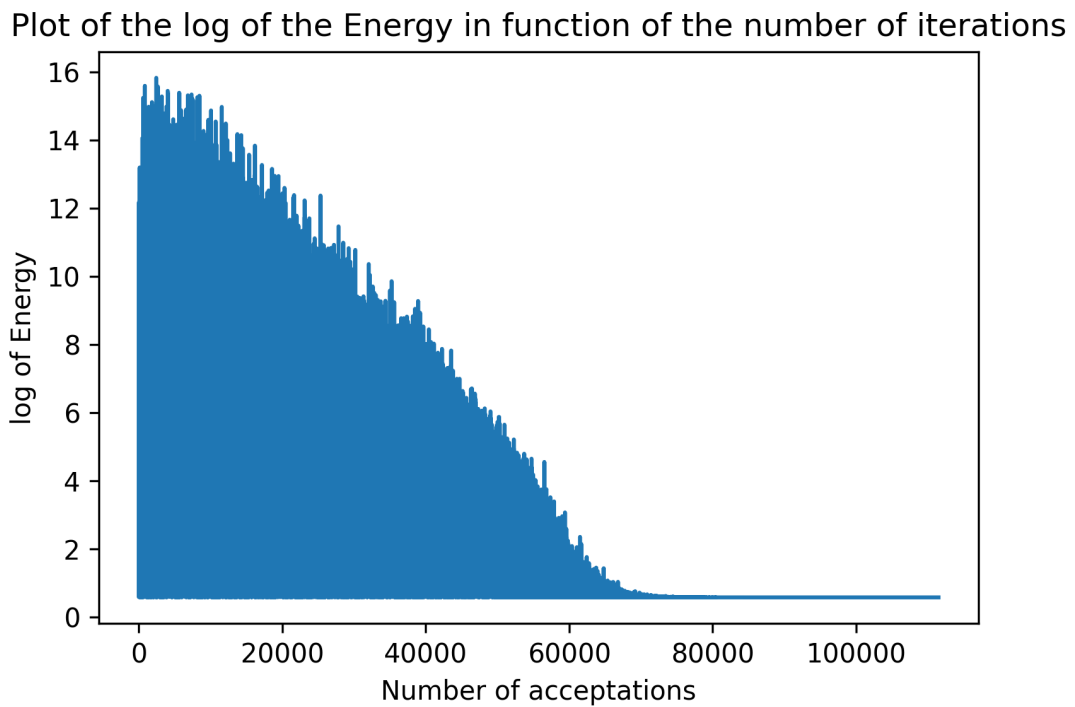


Figure 3.8: Log of the energy of k_{eff} as a function of the number of selections using the simple moments of order 1 to 3

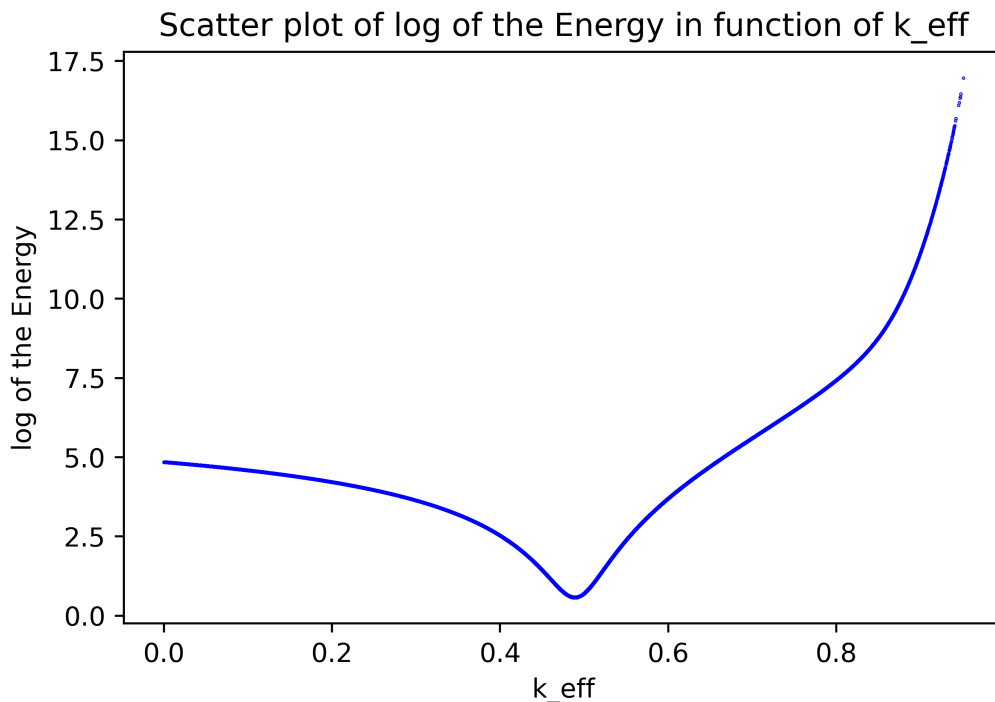


Figure 3.9: Log of the energy as a function of k_{eff} using the simple moments of order 1 to 3

acceptations happen in the $8 \cdot 10^{-2}$ fraction of first iterations, the last three acceptations happen in the remaining iterations which implies the algorithm is stuck fast. In the Figure 3.8, the energy decreases before 78 000 iterations and then stabilises until the solution is well approximated. The same kind of issue happen for ε_C .

Finally, we also obtain interesting results for ε_C . The energy landscape of ε_C (see Figure 3.11) is the most marked. The minimum of this landscape is easier to estimate with simulated annealing, which is why there are fewer fluctuations in the evolution of the energy as a function of the number of acceptances (see Figure 3.10).

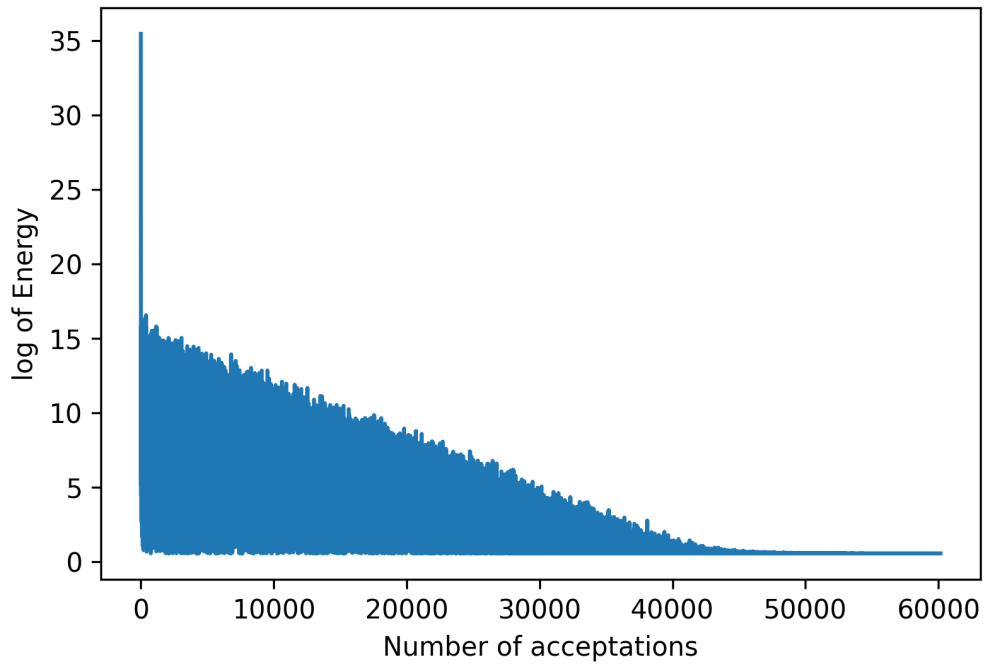
| | |
|--------------------|-------------------------|
| Unknown parameter | ε_C |
| Research interval | $[0, 1]$ |
| Obtained parameter | $2.45816 \cdot 10^{-3}$ |
| Expected parameter | $2.5 \cdot 10^{-3}$ |

Finally, we can conclude the estimation of one parameter with the simulated annealing is achievable easily because of the energies landscape in function of the parameter.

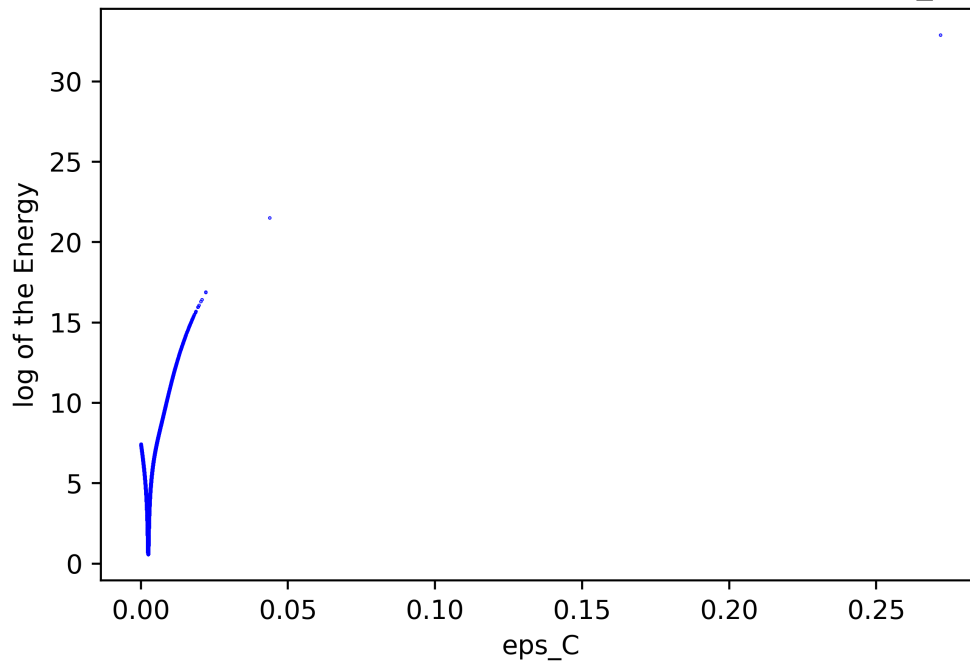
Two unknown parameters

Still considering the same case ($\widehat{\mathbf{M}}$ and $\widehat{\mathbf{Cov}}$ from MC estimation) as before, we use the three first simple moments with 10^7 iterations, initial temperature 10^7 and the initial parameters are $(\frac{s_{max,j} + s_{min,j}}{2}, j \in \llbracket 1; 3 \rrbracket)$ for a time gate $t = \frac{10}{\alpha}$. We still consider the parameter of the simulated annealing as before ($\tau_T = 0.9999$,

Plot of the log of the Energy in function of the number of iterations

Figure 3.10: Log of the energy of ε_C as a function of the number of selections using the simple moments of order 1 to 3

Scatter plot of log of the Energy in function of eps_C

Figure 3.11: Log of the energy as a function of ε_C using the simple moments of order 1 to 3

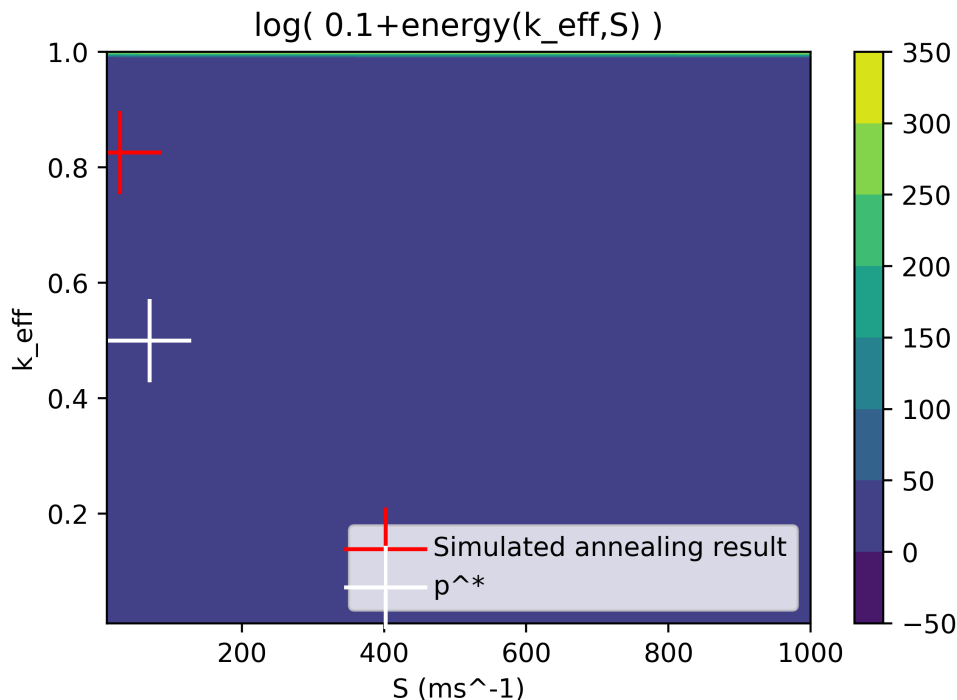


Figure 3.12: The log of energy as a function of (k_{eff}, S) using the three first simple moments, $\varepsilon_C = \varepsilon_C^*$

etc...). First, we will plot the energy landscape as a function of the two parameters considered (considering that the last one is known) and zoom in to see what is interesting in the neighbourhood of the real values. Then we analyse the behaviour of the energy as a function of the number of acceptances.

We specify that the energy landscape is drawn with an explicit mesh with 100 points in each direction, and the remaining parameter is set to the exact value of the parameter. Zooming in on the energy landscape is done by changing the domain boundaries still with 100 points in each direction.

Figure 3.12 shows that the minimal points are not well distinguished. We therefore need to zoom in, as shown in Figure 3.13. This Figure shows there is a whole range (k_{eff}, S) is minimal, and the minimum is not well-defined, thus the simulated annealing has difficulties to find the minimum. We add the figure 3.13 could be enhanced in order to show the simulated annealing result and the point \mathbf{p}^* are in the same valley, but the simulated annealing result is deeper in the valley. The difficulty to find the minimum can be overcome, but it will be done in the Bayesian method part.

Then the simulated annealing ends with the results in the following table.

| | |
|---------------------|---------------------------|
| Unknown parameters | k_{eff} and S |
| Research interval | $[0, 1] \times [0, 1000]$ |
| Obtained parameters | $(0.82588, 28.58705)$ |
| Expected parameters | $(0.5, 70)$ |

The evolution of the energy in function of the number of acceptations is presented

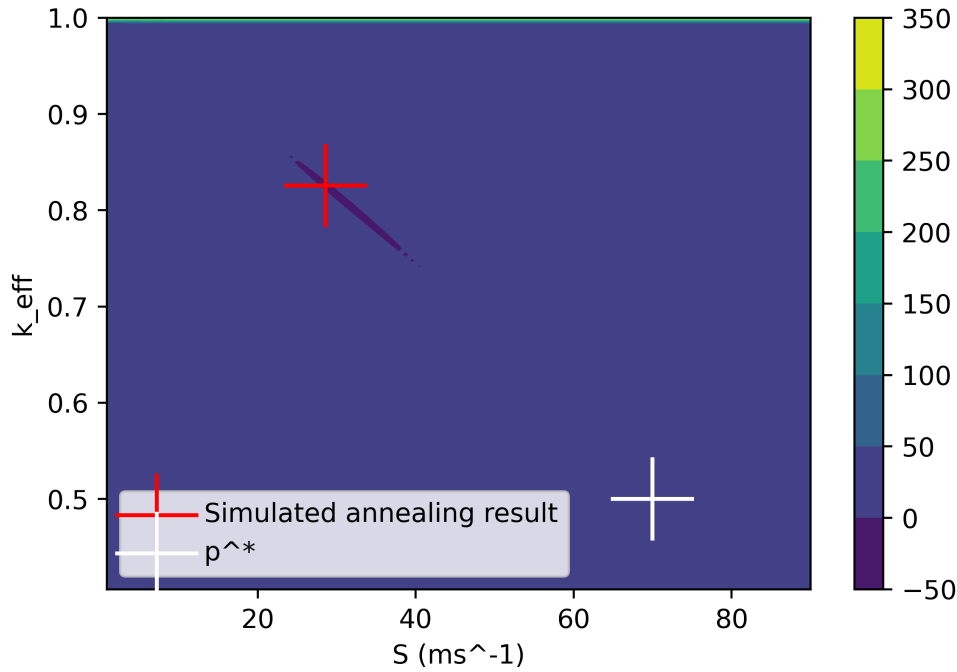


Figure 3.13: Zoom on the log of energy as a function of (k_{eff}, S) using the three first simple moments, $\varepsilon_C = \varepsilon_C^*$ showing the relative position of the result of the simulated annealing and \mathbf{p}^*

in the Figure 3.14. The output file shows 80947 acceptations among 10 000 000 iterations. As in 1D, this is due to the fact that the algorithm accept in the $8 \cdot 10^{-2}$ fraction of first iterations and then reject. We observe the energy fluctuates then stabilises, this means the simulated annealing is over. The same goes for the next computations.

As before, we draw the same conclusions about the energy landscape for (S, ε_C) .

| | |
|---------------------|------------------------------------|
| Unknown parameters | S and ε_C |
| Research interval | $[0, 1000] \times [0, 1]$ |
| Obtained parameters | $(5.88253, 2.92955 \cdot 10^{-2})$ |
| Expected parameters | $(70, 2.5 \cdot 10^{-3})$ |

We plot the evolution of the energy as a function of the number of selections (cf. Figure 3.17). We also observe the energy fluctuates around a constant value, then decreases to a constant value (a larger number of iterations confirms the algorithm stays a long time in this area).

The two previous numerical experiments show the simulated annealing has lots of difficulties finding the real value \mathbf{p}^* . It is due to the shape of energy landscape, where there is a portion of surface that is minimal. This issue is also present in 3D.

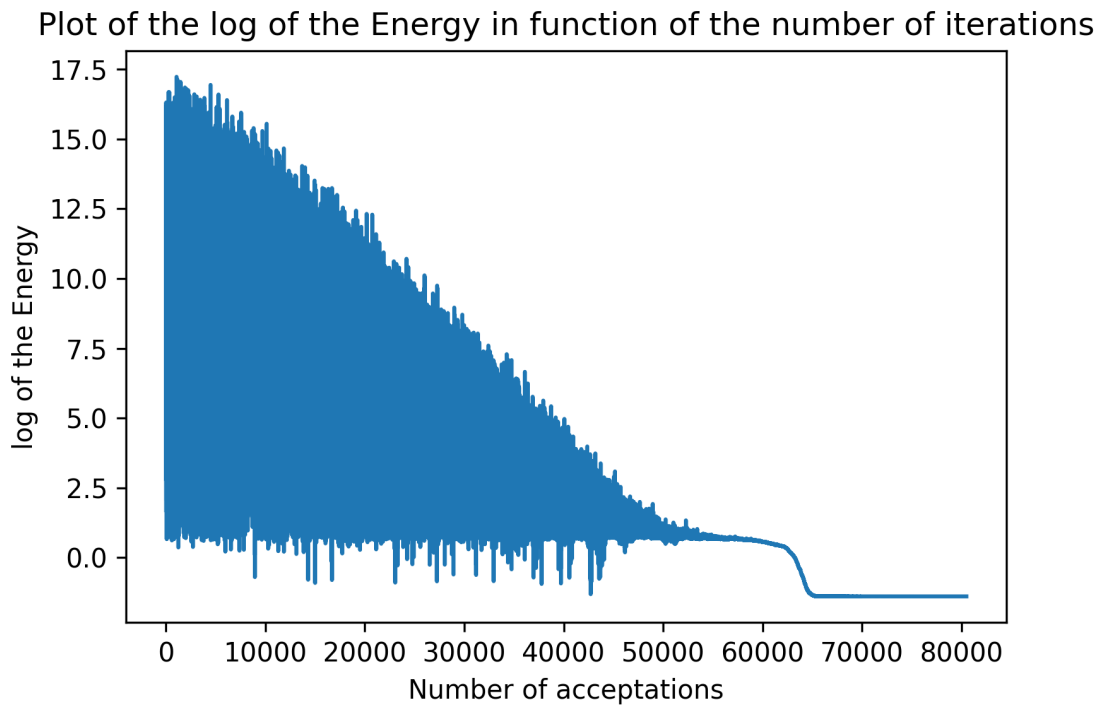


Figure 3.14: Log of energy in function of the number of acceptations using the three first simple moments, $\varepsilon_C = \varepsilon_C^*$

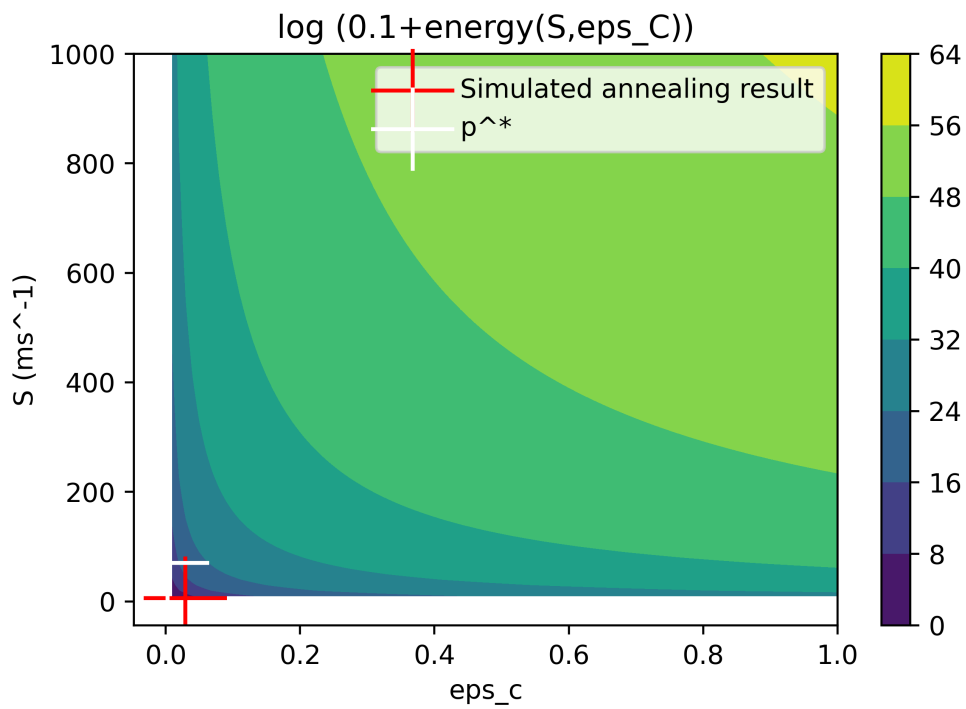


Figure 3.15: The log of energy as a function of (S, ε_C) using the three first simple moments, $k_{eff} = k_{eff}^*$

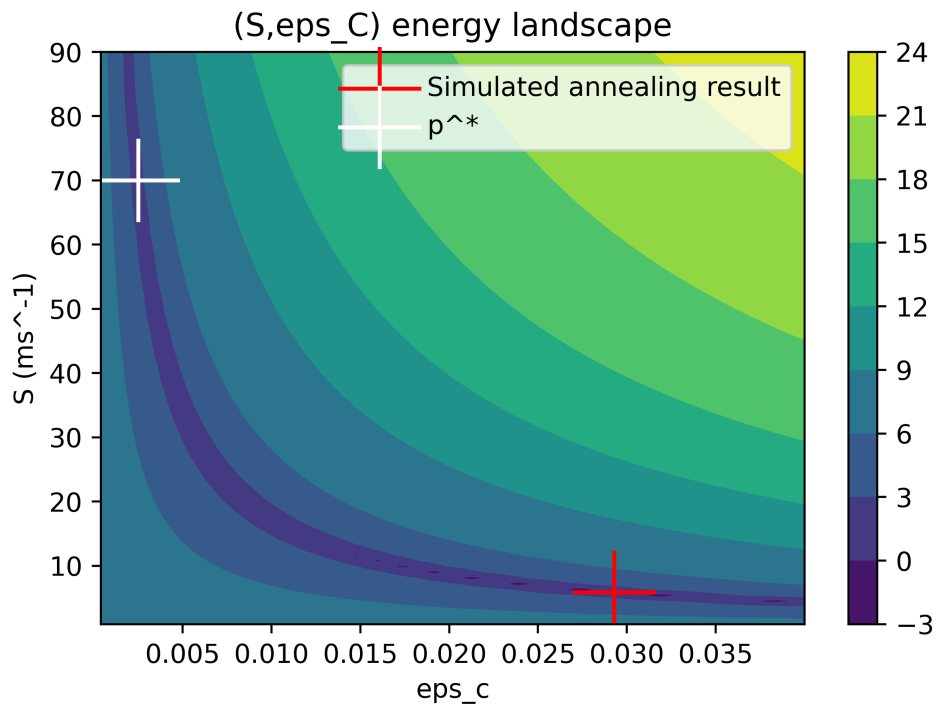


Figure 3.16: Zoom on the log of energy as a function of (S, ε_C) using the three first simple moments, $k_{eff} = k_{eff}^*$

Plot of the log of the Energy in function of the number of iterations

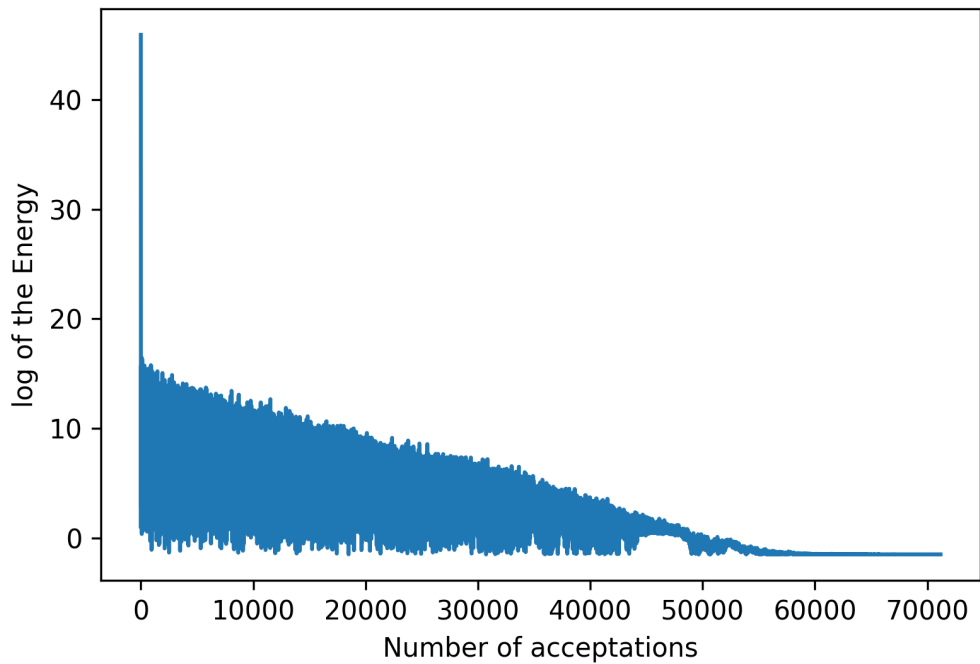


Figure 3.17: Log of energy in function of the number of acceptations using the three first simple moments, $k_{eff} = k_{eff}^*$

Three unknown parameters

We still consider the same case ($\widehat{\mathbf{M}}$ and $\widehat{\mathbf{Cov}}$ from MC estimation) as before, we use the three first simple moments with $5 \cdot 10^8$ iterations, initial temperature 10^7 and the initial parameters are $(\frac{s_{max,j} - s_{min,j}}{2}, j \in \llbracket 1; 3 \rrbracket)$ for a time gate $t = \frac{10}{\alpha}$. We still consider the parameter of the simulated annealing as before ($\tau_T = 0.9999$, etc...). First, we will plot the projection of the energy landscape as a function of the two parameters considered (the projection is made in the last direction) and zoom in to see what is interesting in the neighbourhood of the real values. Then we analyse the behaviour of the energy as a function of the number of acceptances.

Simulated annealing provides

| | |
|---------------------|--|
| Unknown parameters | k_{eff}, S and ε_C |
| Research interval | $[0, 1] \times [0, 1000] \times [0, 1]$ |
| Obtained parameters | $(0.94259, 99.33642, 2.54623 \cdot 10^{-4})$ |
| Expected parameters | $(0.5, 70, 2.5 \cdot 10^{-3})$ |

The curve in Figure 3.18 shows the evolution of the energy as a function of the number of selections by the algorithm. Here there is 198 882 acceptations among $5 \cdot 10^8$ iterations, the algorithm accept regularly during the 20% iterations of the first iterations and then reject almost every time. We observe the algorithm search and goes to a decreasing state.

Plot of the log of the Energy in function of the number of iterations

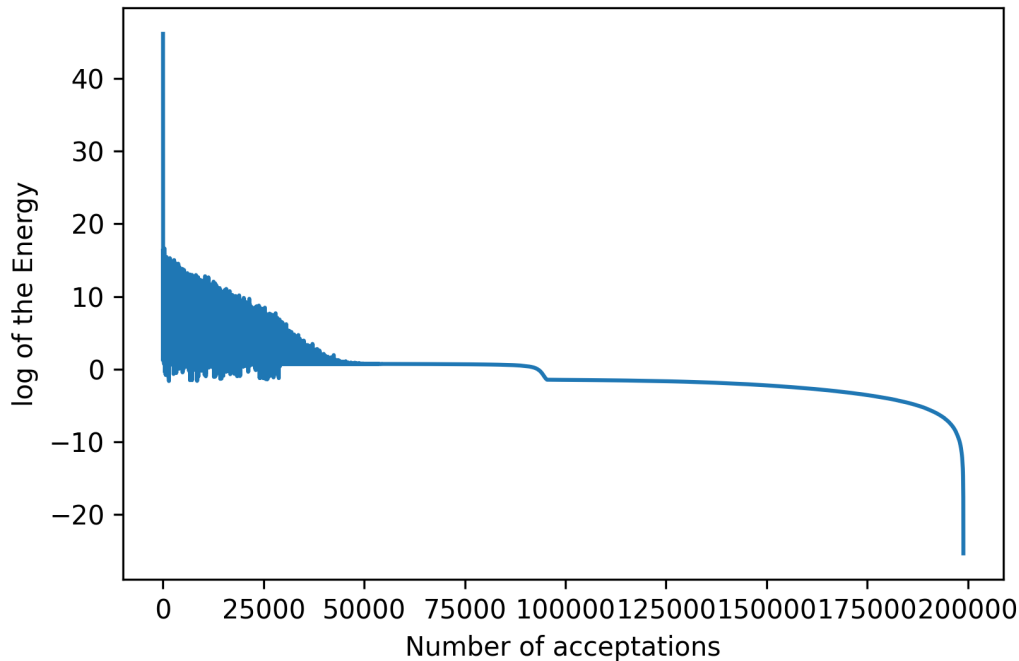


Figure 3.18: The log of the energy in function of the number of selections using the three first simple moments of $Q_n(t)$

We can observe the energy landscape $E(k_{eff}, S, \varepsilon_C)$ by fixing $k_{eff} = k_{eff}^*$ or $\varepsilon_C = \varepsilon_C^*$. The Figure 3.19 provides a global view of the energy landscape of (k_{eff}, S)

when $\varepsilon_C = \varepsilon_C^*$, on this Figure we can see the different position of the real set of parameter \mathbf{p}^* and the result of the simulated annealing $\mathbf{p}^{\text{Simulated annealing}}$. The result needs to be specified by Figure 3.20, when $\varepsilon_C = \varepsilon_C^*$, i.e. for the figure (a), we observe the real parameter is in a valley and not the simulated annealing result. If the algorithm search in the landscape $E(k_{eff}, S, \varepsilon_C)$, so it has difficulties to find \mathbf{p}^* in the landscape (a). We obtained the figure (b) for the results of the simulated annealing, we see the result is in a valley but not the real parameter (k_{eff}, S) . This underlines the difficulty for the algorithm to find \mathbf{p}^* . The Figure 3.21 provides a global view of the energy landscape projected on (S, ε_C) with $k_{eff} = k_{eff}^*$, we observe we need more precision to have a better understanding of the two positions of \mathbf{p}^* and $\mathbf{p}^{\text{Simulated annealing}}$. The details of figure 3.22 (a) show the real point \mathbf{p}^* and the result of the simulated annealing seems on the same valley, the figure (b) shows the same fact. The point \mathbf{p}^* and $\mathbf{p}^{\text{Simulated annealing}}$ are at the two extreme of the observed valley, to have a coherent result with the system observed \mathbf{p}^* , this technique will be done in the next sections.

To conclude on this use of the simulated annealing, the energy landscape we are dealing with is really difficult to tackle because of the previous statements.

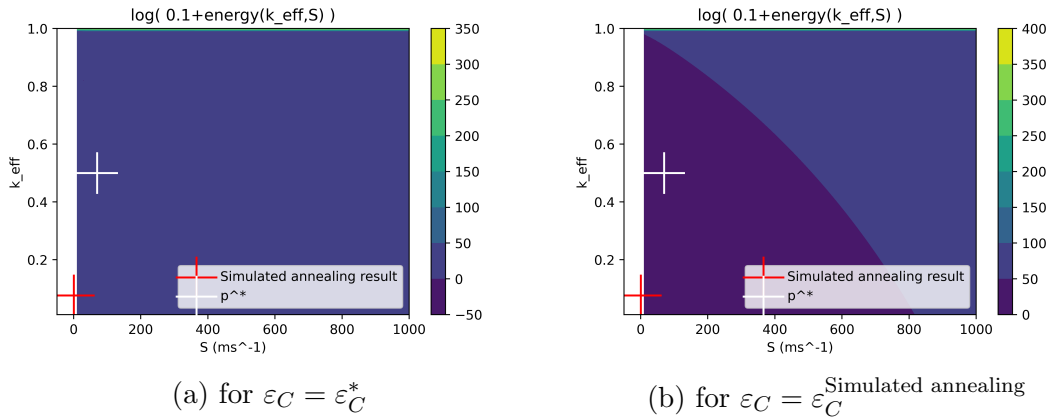


Figure 3.19: Log of the energy landscape of (k_{eff}, S)

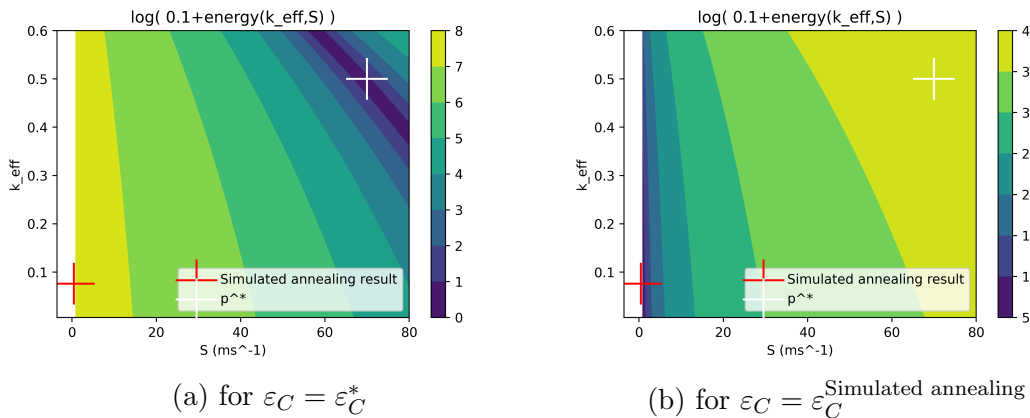


Figure 3.20: Zoom Log of the energy landscape of (k_{eff}, S)

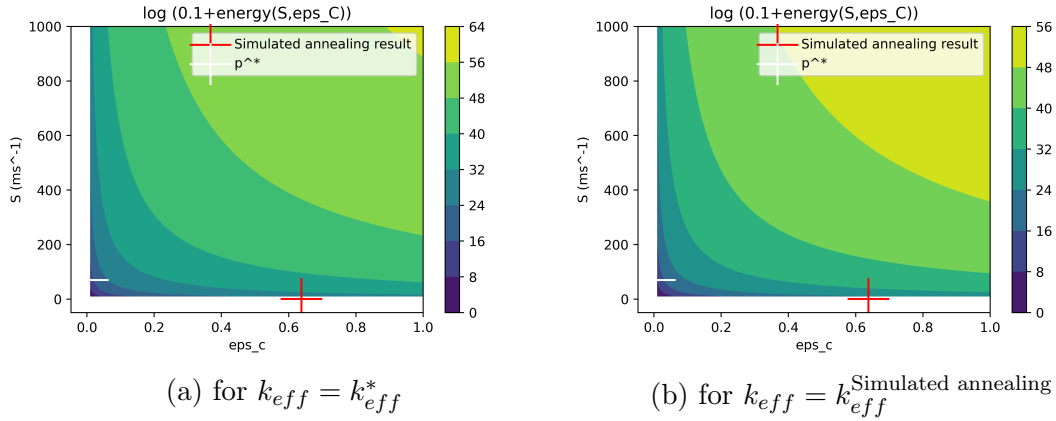


Figure 3.21: Log of the energy landscape of (S, ε_C)

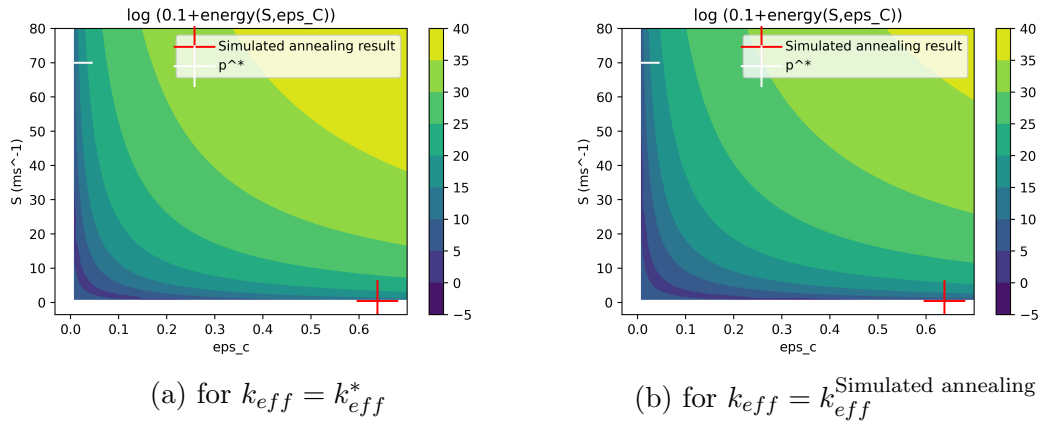


Figure 3.22: Zoom Log of the energy landscape of (S, ε_C)

Except in 1D, the simulated annealing hardly obtains a minimum consistent with the system we observe. The energy landscape shows a range of probable values of the \mathbf{p} parameters. In its minimality domain, the simulated annealing does not know which direction to choose. We could have used a strategy to lead the simulated annealing to the right minimum. In order to obtain an a posteriori distribution of the parameters knowing observations (the measurements) we will use Bayesian methods and sample the a posteriori distribution with MCMC methods. In this case, a good strategy to sample a degenerated distribution is the use of adaptation of the covariance matrix (CMA).

3.1.5 Use of Bayesian methods

We want to obtain an a posteriori distribution of the parameters \mathbf{p} knowing the observations \mathbf{y}_{obs} . To this end, we use Bayesian methods. Then we will use MCMC samplings such as the Metropolis algorithm with adaptive proposal and Metropolis Hastings with Covariance Matrix Adaptation.

In our context, the support of the a posteriori distribution can be very thin and the classical MH algorithm fails when sampling the a posteriori distribution of

three or more parameters. To overcome this difficulty, we will consider the MCMC method with adaptation to sample the proposed distribution.

Explicit sampling of the a posteriori distribution

A simple approach to obtain the explicit sampling of the a posteriori distribution is to use a compactly supported a priori distribution in the domain $[\varepsilon_{C,min}, \varepsilon_{C,max}] \times [k_{min}, k_{max}] \times [S_{min}, S_{max}]$ and to compute the a posteriori distribution over each point of a regular mesh. There are N_e points in each direction. The total number of evaluations of the direct model (defined by the equation 3.6) is therefore N_e^3 . We also calculate the moments of the distribution in order to have quantitative information: mean and variance to compare with the MCMC results.

In addition, this method is useful when checking the next MCMC method with another sample when the number of parameters is low (typically less than or equal to 3). However, it becomes too expensive in terms of computation time when the number of parameters increases.

Bayesian methods in neutron noise

Bayes inference for neutronics appears in Verbeke et al. [VP15; Ver16; VP16]. In particular, [Ver16] consider the point model approximation using [VP15] where the input parameters are

$$\mathbf{p} = \begin{pmatrix} M \\ \varepsilon_C \\ \bar{\nu}_S S_F \end{pmatrix} \quad (3.91)$$

where $M = \frac{1}{1-k_{eff}}$ is the multiplication of the system. The output of the case considered in [Ver16] is the distribution $Q_n(t)$. Then, using the code BigFit, the best set of parameters that fits the distribution $Q_n(t)$ of the measurements is determined. They also compute the Feynman moments of order 2 and 3 in order to confirm the results. The measurements are computed with Tripoli-4 using Freya. The code BigFit was developed in Livermore, further details about it are in the patents [PSR10; PSR12]. The authors present the results on several test cases, such as a PuO₂ ball and a BeRP ball. The computation of the posterior distribution is done on a uniform grid with explicit sampling.

This method enables to obtain the a posteriori distribution of 2 and 3 parameters knowing the observations. The use of BigFit when the a posteriori distribution is computed is costly, and the method is limited to three parameters. The next methods will be used in order to get the a posteriori distribution of three parameters knowing the observations $\mathbf{p}|\mathbf{y}_{obs}$, but can also be used for more parameters, thanks to the use of a more involved Markov-Chain Monte Carlo sampling method.

Haario et al. MCMC methods

Haario et al. have proposed two alternative versions of the MH algorithm for sampling distributions.

The first was proposed in the article [HST99].

The aim is to sample the a posteriori distribution of the parameters

$$\mathbf{p} = (p_1, p_2, p_3). \quad (3.92)$$

and we define $p_{1,min} = \varepsilon_{C,min}$, $p_{1,max} = \varepsilon_{C,max}$, $p_{2,min} = k_{min}$, $p_{2,max} = k_{max}$, $p_{3,min} = S_{min}$, $p_{3,max} = S_{max}$. The target distribution is denoted π .

The next algorithm is the Adaptive Proposal Metropolis algorithm. This algorithm is built with the basis algorithm 2 (see state-of-the-art) in order to sample the a posteriori distribution taking into account a sample of the last accepted points. More precisely, the algorithm generates a sample of a given number of last accepted points, concatenate these points, compute the associated empirical covariance matrix and use it in order to make the next proposition of the Metropolis-Hastings algorithm and adapt the width of the covariance matrix in order to propose in the support of the target distribution more often.

For $\mathbf{C}_i = [\mathbf{p}_{k-H}, \dots, \mathbf{p}_k]$, we recall that $\widehat{\mathbb{E}[\mathbf{C}_i]} = \frac{1}{H} \sum_{j=k-H}^k \mathbf{p}_j$.

Algorithm 8: Pseudo-code of the Adaptive Proposal Metropolis (AP) algorithm

The integer $H > 1$ is settled. We consider the sample \mathbf{S} of the concatenated H last accepted points.

Initialisation of

- The empirical acceptance x_{rate}
- The target acceptance rate x_{obj}
- The initial scale factor of the instrumental law $frac$
- The frequency of update of the scale factor $N_{MC,1}$
- The burn-in phase duration N_{bp}
- The number of iteration of the algorithm $N_{maxiter}$
- The initial parameter \mathbf{p}_0 is chosen with the uniform distribution over $\bigotimes_{k=1}^3 [p_{k,min}, p_{k,max}]$

for $i = 1, N_{bp}$ **do**

- We use as instrumental law

$$\mathbf{q}_{i+1} \sim \mathcal{N}(\mathbf{p}_i, frac^2 \mathbf{C}_{bi}) \quad (3.93)$$

where \mathbf{q}_{i+1} the proposal, \mathbf{p}_i the last accepted point,
 $\mathbf{C}_{bi} = diag(((p_{k,max} - p_{k,min})^2)_{k=1}^3)$ the diagonal matrix with diagonal elements $((p_{k,max} - p_{k,min})^2)_{k=1}^3$.

The burning phase generates a sample of length $k \geq H$ (H is fixed, and so k is) in $\mathbb{R}^d \{\mathbf{p}_1, \dots, \mathbf{p}_k\}$;

for $i = N_{bp} + 1, N_{maxiter}$ **do**

- We compute the covariance matrix of the last H selected points

$$\begin{aligned} \mathbf{C}_i &= [\mathbf{p}_{k-H}, \dots, \mathbf{p}_k] \\ \tilde{\mathbf{C}}_i &= \mathbf{C}_i - \widehat{\mathbb{E}[\mathbf{C}_i]} \\ \mathbf{R}_i &= \frac{1}{H} \tilde{\mathbf{C}}_i^T \tilde{\mathbf{C}}_i; \end{aligned} \quad (3.94)$$

- $\mathbf{q}_{i+1} \sim \mathcal{N}(\mathbf{p}_i, frac^2 \mathbf{R}_i)$;
- Computation of the local acceptance rate using the likelihood of the proposal and the previous accepted point

$$\alpha(\mathbf{q}_{i+1}, \mathbf{p}_i) = \min\left(1, \frac{\pi(\mathbf{q}_{i+1})}{\pi(\mathbf{p}_i)}\right)$$

Then $\mathbf{p}_{i+1} = \mathbf{q}_{i+1}$ with probability α ; $\mathbf{p}_{i+1} = \mathbf{p}_i$ with probability $1 - \alpha$.

- We update the scale factor when $i \equiv 0 \pmod{N_{MC,1}}$. The scale factor $frac$

$$frac \leftarrow frac \exp(x_{rate} - x_{obj})$$

$$x_{rate} = \frac{\text{Number of acceptations}}{\text{Number of iterations}}$$

MH-CMA algorithm

The principle of the covariance matrix adaptation (CMA) is to consider the last points accepted by the Metropolis-Hastings algorithm, and to propose a new neighbour with a Gaussian distribution centred on the last point accepted by the algorithm and with the covariance of the concatenated accepted points. The difference between the next algorithm and the algorithm 8 are : the covariance matrix update, and we consider all the accepted points.

We use this approach because the a priori distribution can be very degenerate so that the classical MH fails the sampling. We then choose to use the CMA to take into account the previous points of the distribution and to control the width of the proposal law. Thus, the points calculated are in the support of the a posteriori distribution π .

We have implemented the Metropolis-Algorithm with covariance matrix adaptation of [AT08] and [HST01]. As previously we consider the parameter \mathbf{p} and we consider the same parameter bounds $p_{1,min} = \varepsilon_{C,min}$, $p_{1,max} = \varepsilon_{C,max}$, $p_{2,min} = k_{min}$, $p_{2,max} = k_{max}$, $p_{3,min} = S_{min}$, $p_{3,max} = S_{max}$. The target distribution is still denoted π .

We first initiate

- The empirical acceptance x_{rate} .
- The initial scale factor of the instrumental law $frac$
- The target acceptance rate x_{obj}
- The frequency of update of the scale factor $N_{MC,1}$
- The burn-in phase duration N_{bp}
- The initial parameter \mathbf{p}_0 is chosen with the uniform distribution over $\bigotimes_{k=1}^3 [p_{k,min}, p_{k,max}]$

Iteration $i \rightarrow i + 1$

1. During $i \leq N_{bp}$, we use as instrumental law

$$\mathbf{q}_{i+1} \sim \mathcal{N}(\mathbf{p}_i, frac^2 \mathbf{C}_{bi}) \quad (3.95)$$

where \mathbf{q}_{i+1} the proposal, \mathbf{p}_i the last accepted point, $\mathbf{C}_{bi} = diag(((p_{k,max} - p_{k,min})^2)_{k=1}^3)$.

2. After the burnin we use the instrumental law as in algorithm 4 of [AT08]

$$\mathbf{q}_{i+1} \sim \mathcal{N}(\mathbf{p}_i, frac^2 \mathbf{C}_i) \quad (3.96)$$

where \mathbf{C}_i is defined by 3.99.

3. Finally, we compute the acceptance rate α using the likelihood ratio of the proposal and the previous accepted point

$$\alpha(\mathbf{q}_{i+1}, \mathbf{p}_i) = \min\left(1, \frac{\pi(\mathbf{q}_{i+1})}{\pi(\mathbf{p}_i)}\right) \quad (3.97)$$

4. The acceptance-rejection criterion

$$u \sim \mathcal{U}([0, 1])$$

$$\text{If } u \leq \alpha(\mathbf{q}_{i+1}, \mathbf{p}_i) \text{ then } \mathbf{q}_{i+1} \text{ is accepted: } \mathbf{p}_{i+1} = \mathbf{q}_{i+1} \text{ otherwise } \mathbf{p}_{i+1} = \mathbf{p}_i \quad (3.98)$$

is applied

5. We update the scale factor when $i \equiv 0 \pmod{N_{MC,1}}$. The scale factor $frac$

$$\begin{aligned} frac &= frac \exp(x_{rate} - x_{obj}) \\ x_{rate} &= \frac{\text{Number of acceptations}}{\text{Number of iterations}} \end{aligned}$$

This is an algorithm with global scaling and vanishing adaptation, so that the ergodicity of the algorithm is achieved. Here the vanishing factor is $\gamma_i = \frac{1}{i}$, it must be chosen such that $\sum_i \gamma_i = +\infty$ (explained in [AT08]), more explanation in the next paragraphs.

The covariance matrix is updated as in [Mü10]

$$\begin{aligned} \bar{\mathbf{p}}_{i+1} &= (1 - \gamma_{i+1})\bar{\mathbf{p}}_i + \gamma_{i+1}\mathbf{p}_i \\ \mathbf{C}_{i+1} &= (1 - \gamma_{i+1})\mathbf{C}_i + \gamma_{i+1}(\mathbf{p}_i - \bar{\mathbf{p}}_i)^T(\mathbf{p}_i - \bar{\mathbf{p}}_i) \end{aligned} \quad (3.99)$$

The work of [GRG96] provides an analysis of the Metropolis-Hastings algorithm regarding the acceptance rate. Then we choose $frac = \frac{2.4}{\sqrt{d}}$ where $d = \dim(\mathbf{p})$ as suggested in [GRG96].

The empirical covariance matrix and the mean of the proposal are updated as follows: The target $x_{obj} = 0.234$ is chosen thanks to [GRG96]. As the a posteriori distribution can be highly degenerate, the use of \mathbf{C} and the global adaptation of the factors allows the distribution to be well sampled, even if it is highly degenerate.

The target distribution is really degenerate, it is difficult to sample it with a classical Metropolis-Hastings algorithm. The best algorithm we can have is an algorithm whose exploration law is equal to our target distribution. To sample this target distribution, we use a vanishing factor γ_i (here $\gamma_i = \frac{1}{i}$) so that the exploration distribution coincides with the target distribution. The vanishing factor γ_i will tend to zero so that the exploration law fits the target distribution well.

We have seen that the algorithm works well in the cases studied, but the more parameters we take into account, the more difficult the algorithm becomes. The MCMC methods provide a sampling of the distribution of the parameters \mathbf{p} given the observations of our system $\hat{\mathbf{M}}$.

In the following, we present the results of the calculation of the posterior distribution obtained on test cases. Two numerical methods are used. The first one, the explicit method, is deterministic and based on the discretisation of the calculated distribution on a regular grid. In the second method, the distribution is sampled using an MCMC algorithm. The explicit method becomes very expensive when the parameter space is large. It is used for verification of the MCMC method when the number of parameters is less than or equal to three. The advantage of the MCMC method is that it can be used at a reasonable cost when the number of parameters is greater than three.

3.2 Inverse problem: posterior distributions

3.2.1 A posteriori distribution of $(k_{eff}, \varepsilon_C, S)$ given the three first moments of $N_{[0,T]}$ for $k_{eff} = 0.95$

These results were presented in [GHH21]. The input parameters and the global case specifications correspond to the second case studied in the direct problem. More precisely, the observations are calculated using the model with the exact parameters.

$$\mathbf{y}_{obs} = \mathbf{M}(\mathbf{p}^*) \quad (3.100)$$

where the expected parameters are

$$\mathbf{p}^* = \begin{pmatrix} \varepsilon_C^* \\ k_{eff}^* \\ S^* \end{pmatrix} = \begin{pmatrix} 0, 25 \cdot 10^{-2} \\ 0, 5 \text{ or } 0, 75 \text{ or } 0, 95 \\ 70 \text{ ms}^{-1} \end{pmatrix} \quad (3.101)$$

The a priori distribution is uniform over a bounded parameter domain. We use the following limits for the a priori distribution

$$\begin{aligned} \varepsilon_{C,min} &= 0, 1 \cdot 10^{-2} \\ \varepsilon_{C,max} &= 0, 4 \cdot 10^{-2} \\ k_{min} &= 0 \\ k_{max} &= 1 \\ S_{min} &= 20 \\ S_{max} &= 200 \end{aligned} \quad (3.102)$$

The measured function of interest is $N_{[0,T]}$ when the time gate is $T = 10 \text{ ms}$ and for three duration measurements $T_{meas} = 36, 360, 3600 \text{ s}$. We also considered a neutron decay constant $\alpha_Y = 2 \text{ ms}^{-1}$ and the following fission multiplicity data:

$$\begin{aligned} \bar{\nu} &= 2.4130 & \bar{\nu}_S &= 1 \\ D_2 &= 0.7992 & D_{2S} &= 0 \\ D_3 &= 0.4819 & D_{3S} &= 0 \end{aligned} \quad (3.103)$$

The initialization parameters of the AM algorithm are

$$\begin{aligned} x_{rate} &= 1 \\ x_{obj} &= 0.234 \\ frac &= 0.1 \\ N_{bp} &= 10^7 \\ N_{MC,1} &= \max\left(\frac{N_{MC}}{10000}, 1\right) \end{aligned} \quad (3.104)$$

Regarding the explicit sampling, there are N_e^3 points in the grid with $N_e = 400$.

In order to observe the effect of measurement duration and criticality levels on the shape of the posterior distribution of the parameters, calculations are performed for: $T_{meas} = 36, 360$ and 3600s . For each measurement time, the following multiplication factors are considered: $k_{eff} = 0.5, 0.75$ and 0.95 .

Remark 3.2.1. *In the following, the acronym 3P3M refers to the inverse problem*

$$\begin{aligned} \mathbf{M} : \mathbb{R}^3 &\rightarrow \mathbb{R}^3 \\ \mathbf{p} &\mapsto \mathbf{M}(\mathbf{p}) \end{aligned} \quad (3.105)$$

where $\mathbf{p} = (\varepsilon_C, k_{eff}, S)$ and $\mathbf{M}(\mathbf{p})$ refers to the three first simple moments of $Q_n(t)$.

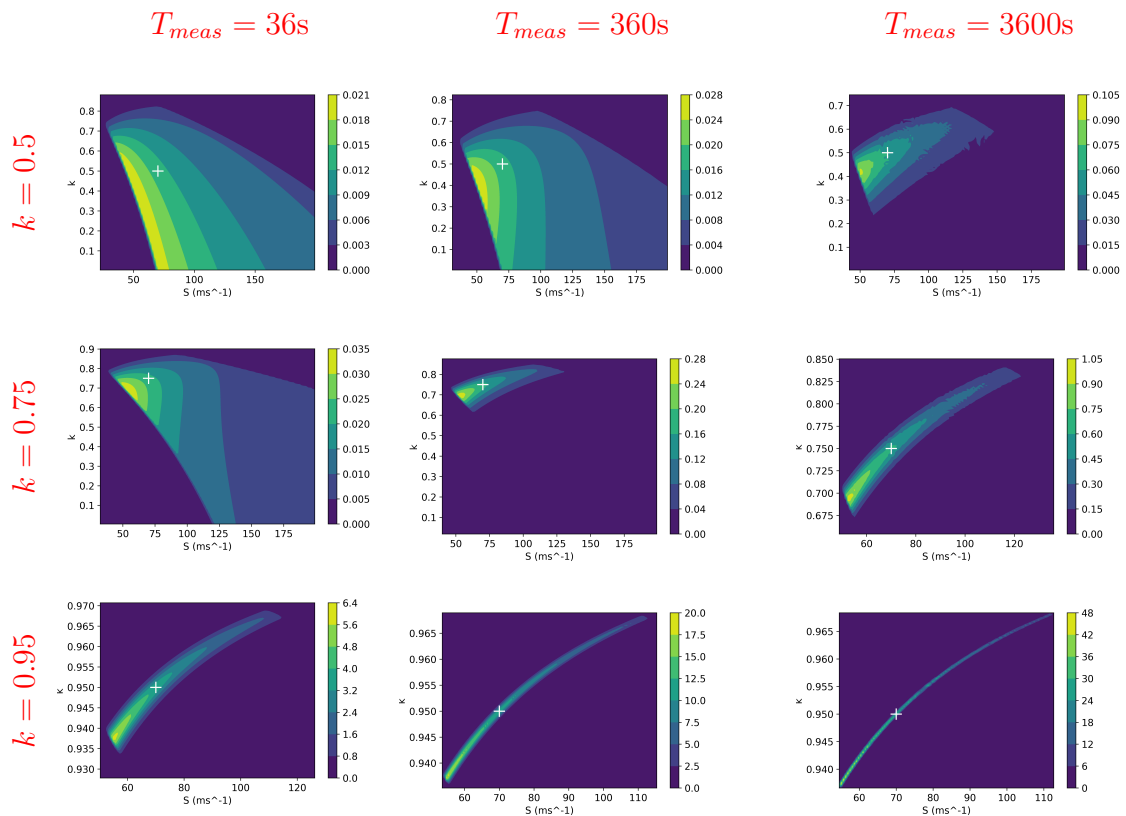


Figure 3.23: A posteriori distribution for (k_{eff}, S) using 3P3M with explicit sampling

We can compare it to the result using the MCMC method

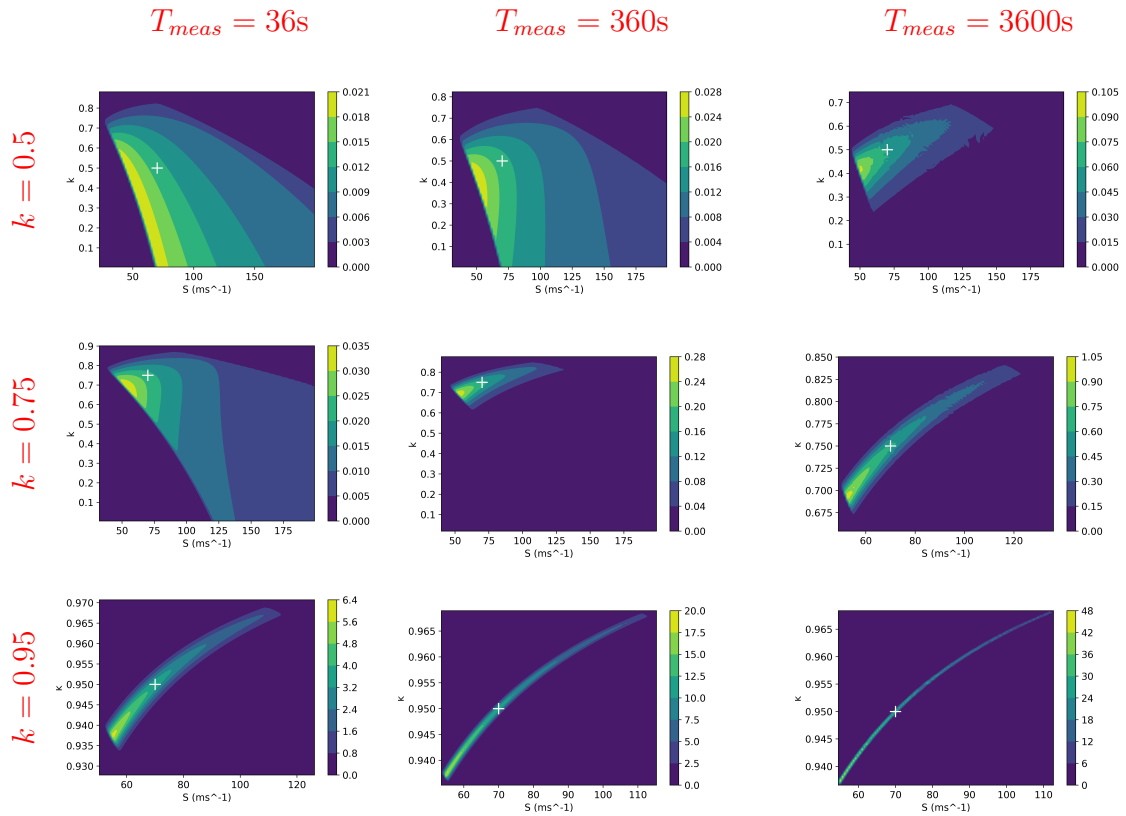


Figure 3.24: A posteriori distribution for (k_{eff}, S) using 3P3M with MCMC sampling

We can also observe the a posteriori distribution for (k, ε_C)

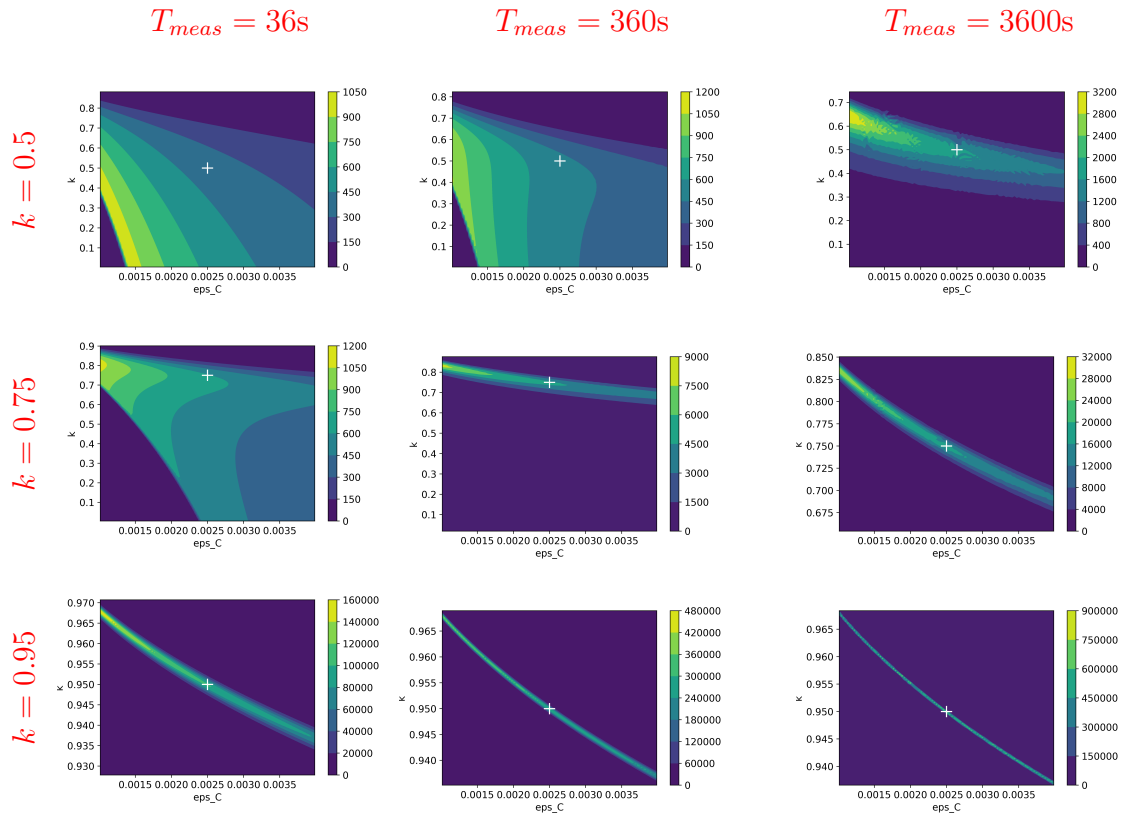
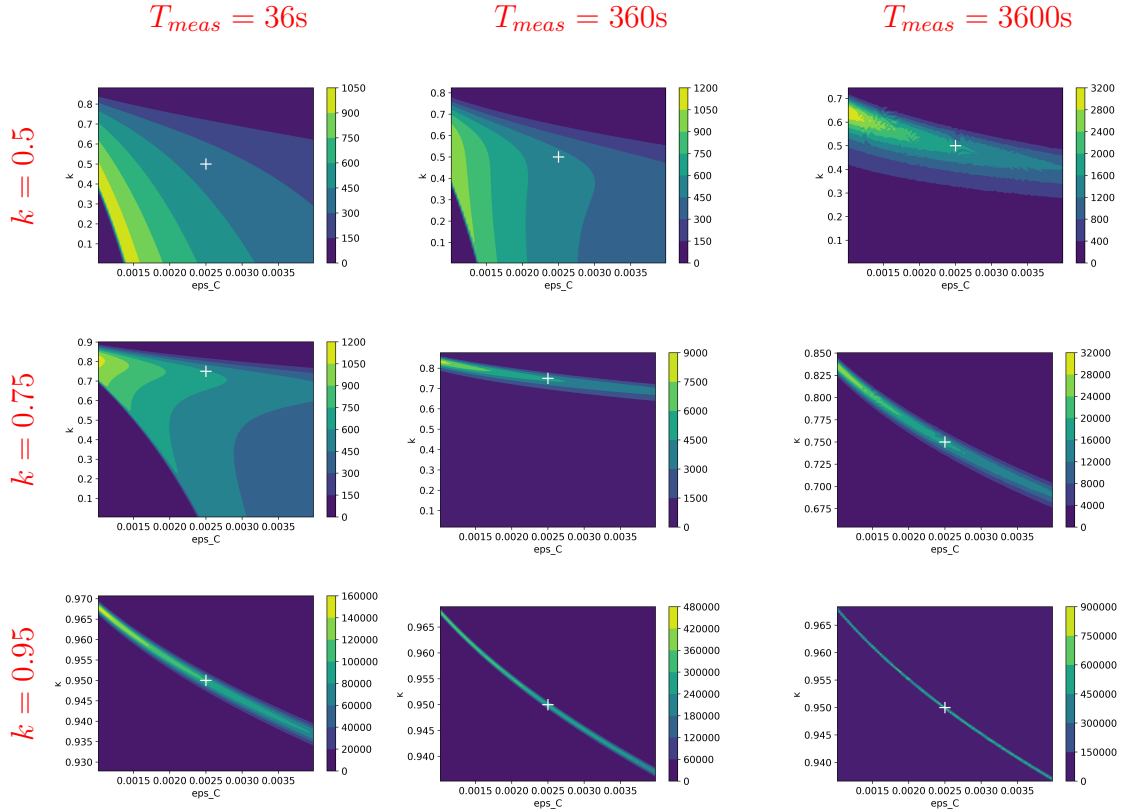


Figure 3.25: A posteriori distribution for (k_{eff}, ϵ_C) using 3P3M with explicit sampling

We can compare these results to the MCMC method results

Figure 3.26: A posteriori distribution for (k_{eff}, ε_C) using 3P3M with MCMC

When the width of the time gate is short $T_1 = \frac{1}{\alpha}$, there will be no correlated counts, and thus no information beyond the first moment (average number of counts). When the time gate is large $T_2 = \frac{10}{\alpha}$ the proportion of correlated detections saturates, but the number of gates is smaller for a given total measurement time. In the following, we will consider two time gate widths: $T_1 = \frac{1}{\alpha}$ and $T_2 = \frac{10}{\alpha}$. The use of several time gates could give access to a fourth parameter, the time constant of the prompt neutron α .

We present here the results of taking into account two different time gates $T_1 = \frac{1}{\alpha}$ and $T_2 = \frac{10}{\alpha}$. We recall that we consider the following set of parameters.

Since the simple moments have a different behaviour according to the considered regime ($T - t \rightarrow 0$ or $T - t \rightarrow +\infty$) cf. chapter 2, the direct problem, we make the hypothesis that the a posteriori distributions will have different profiles.

Moreover, we consider an improvement of the previous MCMC method in order to properly plot the a posteriori distribution of the \mathbf{p} parameters knowing the observations $\mathbf{M}(\mathbf{p}^*)$.

From now, we consider $\mathbf{Cov}(\mathbf{p}) = \mathbf{Cov}(\mathbf{p}^*)$ in the problem 3.85, computed using `ntc0b_cov2` (see annexes).

A posteriori distribution of $(k_{eff}, \varepsilon_C, S)$ given the three first moments of $N_{[0, T_1]}$ for $T_1 = \frac{1}{\alpha}$

For a time of measurements of 3600s, we consider the parameters

$$\mathbf{p}^* = \begin{pmatrix} S \\ k_{eff} \\ \varepsilon_C \\ x \\ \alpha \end{pmatrix} = \begin{pmatrix} 70 \text{ ms}^{-1} \\ 0,95 \\ 0,25 \cdot 10^{-2} \\ 0 \\ 2 \text{ ms}^{-1} \end{pmatrix} \quad (3.106)$$

we recall that $k_{eff} = 0,95 \iff \rho = -0.05263157894$.

Nuclear mater $\left\{ \begin{array}{l} \text{The fissile material is } {}^{235}\text{U}. \\ \text{The source is poissonian.} \end{array} \right.$

The nuclear constants for nuclear parameters

$$\begin{pmatrix} \bar{\nu} \\ D_2 \\ D_3 \end{pmatrix} = \begin{pmatrix} 2,4130 \\ 0,7992 \\ 0,4819 \end{pmatrix} \quad \begin{pmatrix} \bar{\nu}_S \\ D_{2S} \\ D_{3S} \end{pmatrix} = \begin{pmatrix} 1 \\ 0 \\ 0 \end{pmatrix} \quad (3.107)$$

The results of the numerical experiments here and for all subsequent numerical experiments, the first three moments and the covariance matrix, are calculated using the software `ntc0b_cov2` (see annexes). This computer program solves the moment equations in the point model using deterministic methods.

We consider the observations for a time gate $T_1 = \frac{1}{\alpha} = \frac{1}{2}$ ms, provided by `ntc0b_cov2`.

$$\mathbf{y}_{obs} = \mathbf{M}(\mathbf{p}^*) = \begin{pmatrix} 1,0930 \\ 2,7777 \\ 9,5764 \end{pmatrix} \quad (3.108)$$

The covariance matrix is

$$\mathbf{Cov}(\mathbf{p}^*) = \begin{pmatrix} 0,2198306 \cdot 10^{-6} & 0,90818 \cdot 10^{-6} & 0,51613 \cdot 10^{-5} \\ 0,90818 \cdot 10^{-6} & 0,47888 \cdot 10^{-5} & 0,32488 \cdot 10^{-4} \\ 0,51613 \cdot 10^{-5} & 0,32488 \cdot 10^{-4} & 0,25484 \cdot 10^{-3} \end{pmatrix} \quad (3.109)$$

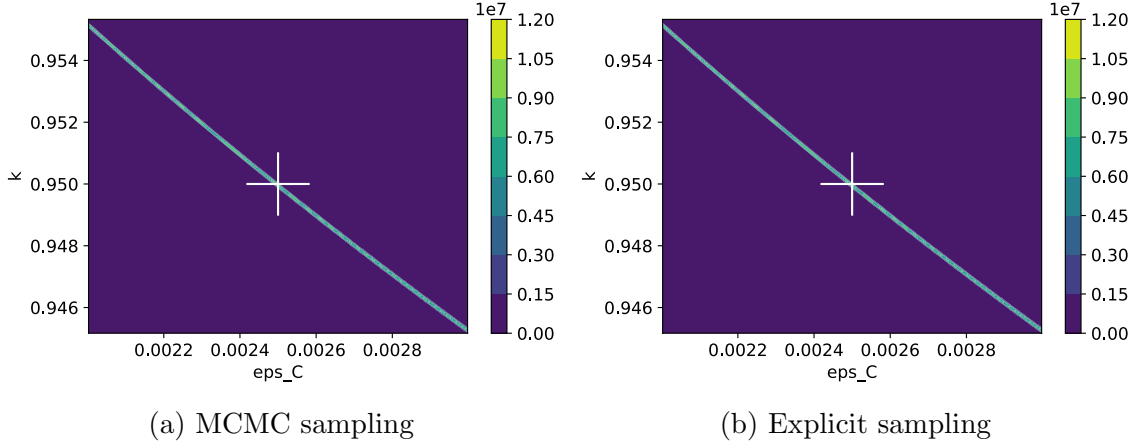
with python, we obtain the following associated eigenvalues

$$\begin{pmatrix} \lambda_1 \\ \lambda_2 \\ \lambda_3 \end{pmatrix} = \begin{pmatrix} 2,59098 \cdot 10^{-4} \\ 1,60808 \cdot 10^{-8} \\ 7,34625 \cdot 10^{-7} \end{pmatrix} \quad (3.110)$$

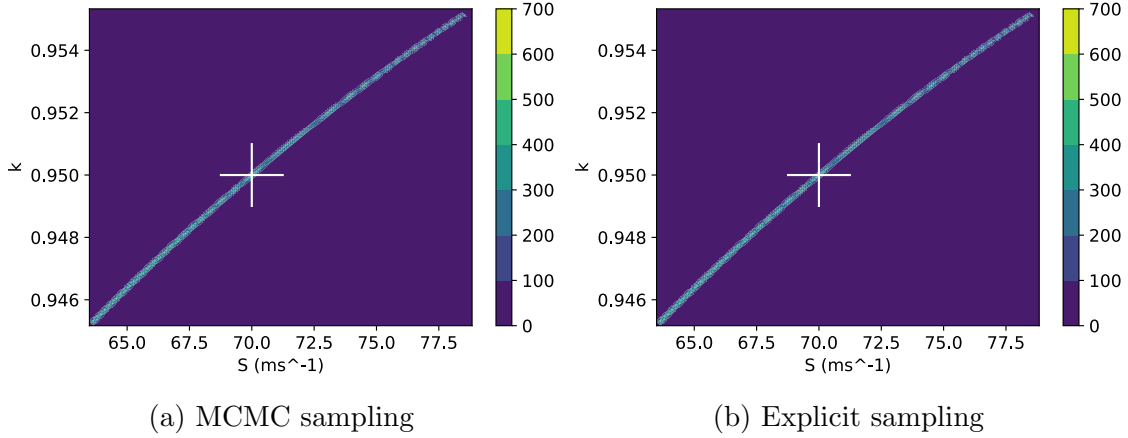
Python provides also the conditioning of the covariance matrix $Cond(\mathbf{Cov}(\mathbf{p})) = 22308,89421$.

The spectral deviation and the $\mathbf{Cov}(\mathbf{p})$ conditioning are high, which means that the a posteriori distribution is degenerate. It is therefore difficult to sample.

The MCMC method use $N_{bp} = 10^7$ and the explicit samplings use $N_e = 400$. We considered an a priori on the parameters as previously on $[\varepsilon_{C,min}, \varepsilon_{C,max}] \times [k_{eff,min}, k_{eff,max}] \times [S_{min}, S_{max}]$.


 Figure 3.28: Marginal distribution of k_{eff} and ε_C

We observe the a posteriori distributions


 Figure 3.27: Marginal distribution of k_{eff} and S

The results are the same with explicit sampling or MCMC methods. As before, we can observe that the a posteriori distribution is really thin due to a measurement time of 3600s and a high level of subcriticality, $k_{eff}=0.95$. We observe that the input parameter \mathbf{p}^* is in the support of the a posteriori distribution.

A posteriori distribution of $(k_{eff}, \varepsilon_C, S)$ given the three first moments of $N_{[0, T_2]}$ for $T_2 = \frac{10}{\alpha}$

The set of nuclear parameters is the same as before, and the parameters $N_{bp} = 10^7$ and $N_e = 400$ of the MCMC method and explicit sampling remain the same.

For a time of measurements of 3600s, we consider the observations for a time gate $T_2 = \frac{10}{\alpha} = 5ms$.

$$\mathbf{y}_{obs} = \mathbf{M}(\mathbf{p}^*) = \begin{pmatrix} 10, 930 \\ 142, 38 \\ 2143, 7 \end{pmatrix} \quad (3.111)$$

$$\mathbf{Cov}(\mathbf{p}^*) = \begin{pmatrix} 0,31832 \cdot 10^{-4} & 0,81587 \cdot 10^{-3} & 0,18297 \cdot 10^{-1} \\ 0,81587 \cdot 10^{-3} & 0,22680 \cdot 10^{-1} & 0,54756 \\ 0,18297 \cdot 10^{-1} & 0,54756 & 14,185 \end{pmatrix} \quad (3.112)$$

with python, we obtain the following associated eigenvalues

$$\begin{pmatrix} \lambda_1 \\ \lambda_2 \\ \lambda_3 \end{pmatrix} = \begin{pmatrix} 1,42061625 \cdot 10^1 \\ 4,48725675 \cdot 10^{-7} \\ 1,54892527 \cdot 10^{-3} \end{pmatrix} \quad (3.113)$$

Python provides also the conditioning of the covariance matrix $Cond(\mathbf{Cov}(\mathbf{p})) = 35077411,03653$.

As before, the spectral gap and the conditioning of $\mathbf{Cov}(\mathbf{p})$ are high, which means that the a posteriori distribution is degenerate. It is therefore difficult to sample.

We observe the a posteriori distributions

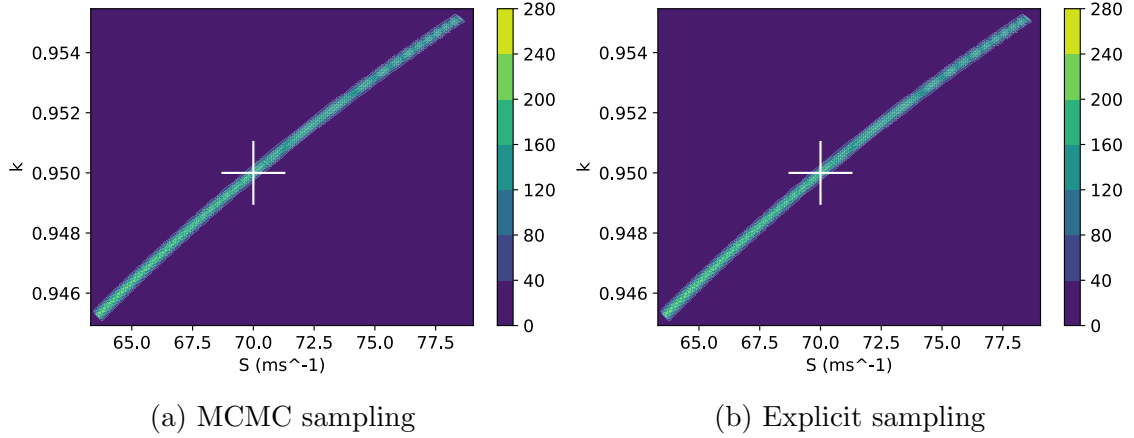


Figure 3.29: Marginal distribution of k_{eff} and S

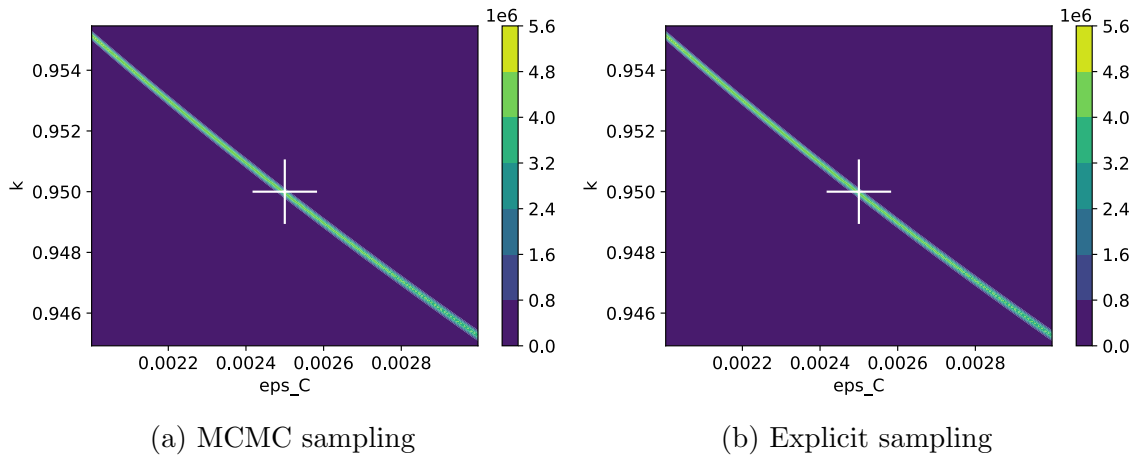


Figure 3.30: Marginal distribution of k_{eff} and ϵ_C

We draw the same conclusions as above.

where $\text{diag}(\mathbf{A}, \mathbf{B})$ is diagonal matrix formed of \mathbf{A} and \mathbf{B} in the diagonal of the block matrix.

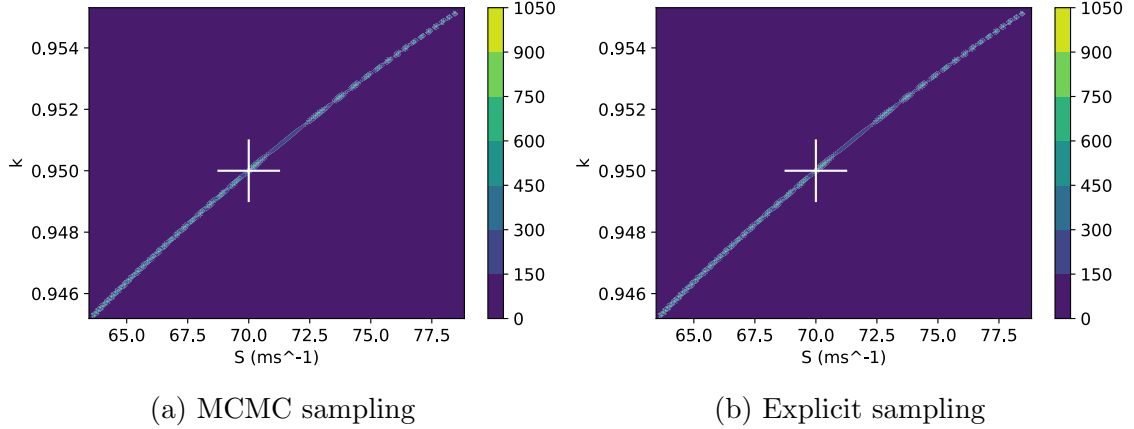


Figure 3.32: Marginal distribution of k_{eff} and S

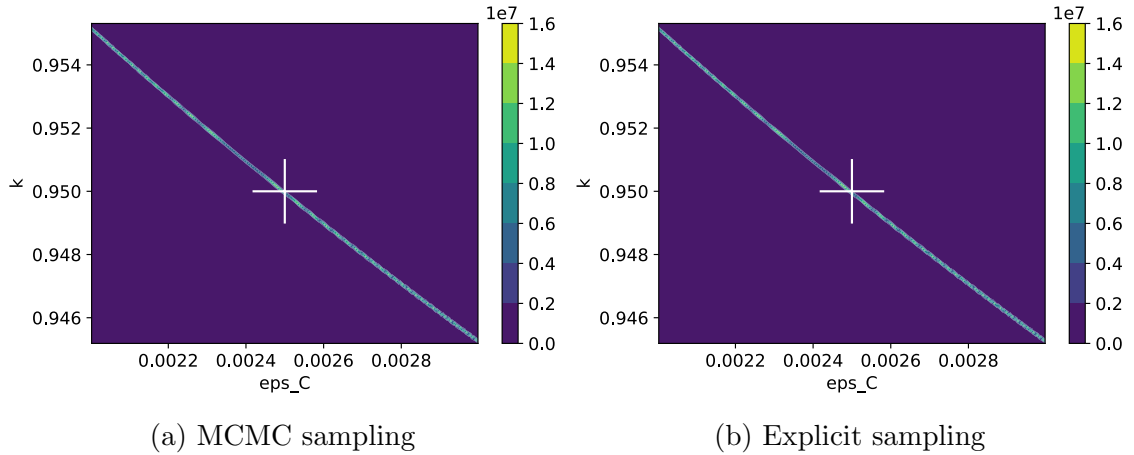


Figure 3.33: Marginal distribution of k_{eff} and ε_C

3.2.3 A posteriori distribution of $(k_{eff}, \varepsilon_C, S)$ given the three first moments of $N_{[0,T]}$ where $T = \frac{1}{\alpha}$ or $T = \frac{10}{\alpha}$ and $k_{eff} = 0.5$

We now consider the case where the criticality is lower, i.e. $k_{eff} = 0.5$. It is then expected that the a posteriori distributions are less degenerate and therefore easier to sample for $N_{bp} = 5 \cdot 10^7$. We considered 1000 points on each direction for explicit sampling.

We want to have a better view of the impact of considering two different time gates in a case where the a posteriori distribution is wide, so considering two time gates in different regimes (in the establishment of the regime or during the steady state) will give more information on the parameters to be estimated.

First, for a time of measurements of 3600s, we consider the following system for a time gate $T = \frac{1}{\alpha}$.

$$\mathbf{p}^* = \begin{pmatrix} S \\ k_{eff} \\ \varepsilon_C \\ x \\ \alpha \end{pmatrix} = \begin{pmatrix} 70 \text{ ms}^{-1} \\ 0,5 \\ 0,25 \cdot 10^{-2} \\ 0 \\ 2 \text{ ms}^{-1} \end{pmatrix} \quad (3.116)$$

we recall that $k_{eff} = 0,5 \iff \rho = -1$.

The nuclear mater is $\begin{cases} \text{The induced fission material is } {}^{235}\text{U}. \\ \text{The source is poissonian.} \end{cases}$

The nuclear constants for nuclear parameters

$$\begin{pmatrix} \bar{\nu} \\ D_2 \\ D_3 \end{pmatrix} = \begin{pmatrix} 2,53108 \\ 0,81168 \\ 0,51843 \end{pmatrix} \quad \begin{pmatrix} \bar{\nu}_S \\ D_{2S} \\ D_{3S} \end{pmatrix} = \begin{pmatrix} 1 \\ 0 \\ 0 \end{pmatrix} \quad (3.117)$$

The corresponding observations are

$$\mathbf{y}_{obs} = \mathbf{M}(\mathbf{p}^*) = \begin{pmatrix} 0,14043 \\ 0,16058 \\ 0,20382 \end{pmatrix} \quad (3.118)$$

The associated covariance matrix is

$$\mathbf{Cov}(\mathbf{p}^*) = \begin{pmatrix} 0,19563 \cdot 10^{-7} & 0,25177 \cdot 10^{-7} & 0,37637 \cdot 10^{-7} \\ 0,25177 \cdot 10^{-7} & 0,38033 \cdot 10^{-7} & 0,67808 \cdot 10^{-7} \\ 0,37637 \cdot 10^{-7} & 0,67808 \cdot 10^{-7} & 0,14152 \cdot 10^{-6} \end{pmatrix} \quad (3.119)$$

We considered a uniform a priori distribution on each parameter $[0; 1] \times [0; 400] \times [0; 0,01]$. Moreover, we specified with a Gaussian a priori on ε_C of mean $3 \cdot 10^{-3}$ and standard deviation 10^{-3} . This a priori choice was considered thanks to the first results without a Gaussian a priori, which were not conclusive because the marginal distribution on (k_{eff}, S) showed that $(k_{eff}, S) = (\epsilon, \epsilon)$, where ϵ is small, had a high probability. This was counterintuitive. Indeed, when $\epsilon \rightarrow 0$ the system detects no neutron, so the average number of neutrons detected should be 0 as well as the second and third order simple moments: no detection provides observations that are 0.

First, we observe the 1D marginal distribution of each parameter. We can see that each marginal distribution corresponds to explicit sampling and MCMC sampling. The statistical noise is smaller than the aliasing noise (here the fact that the mesh is not refined so that the likelihood plot is well done) and therefore the MCMC sampling is more accurate than the explicit sampling.

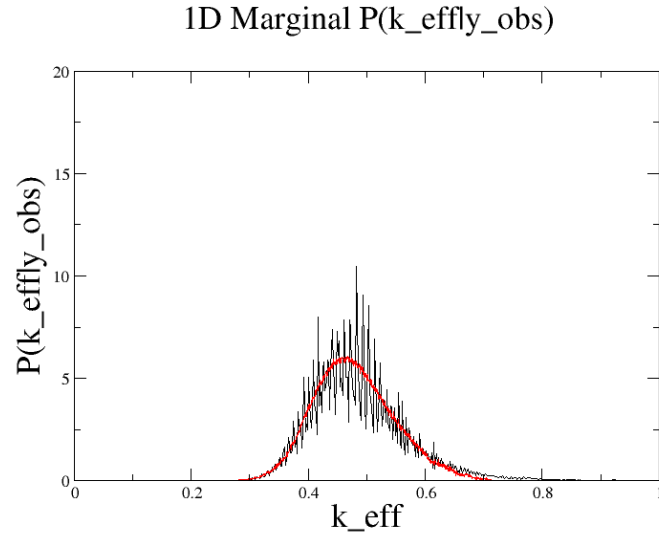


Figure 3.34: Marginal distribution of k_{eff} with explicit sampling (black) and MCMC sampling (red)

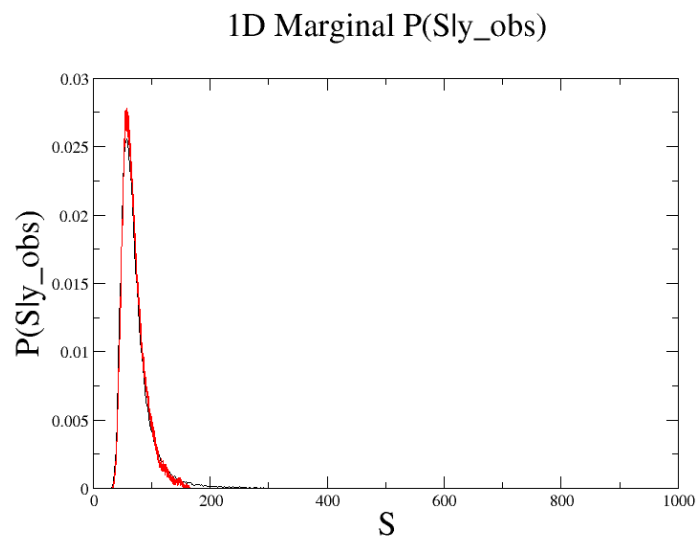


Figure 3.35: Marginal distribution of S with explicit sampling (black) and MCMC sampling (red)

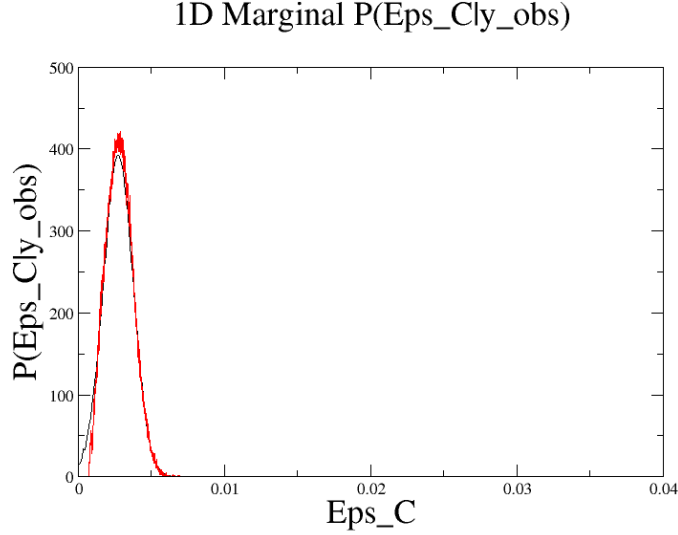


Figure 3.36: Marginal distribution of ε_C with explicit sampling (black) and MCMC sampling (red)

We have obtained the following mean and standard deviation for the MCMC sampling:

$$\begin{aligned}
 \mathbb{E}[k_{eff}|\hat{\mathbf{M}}] &= 0,47937 & \sqrt{\mathbb{E}[(k_{eff} - \mathbb{E}[k_{eff}|\hat{\mathbf{M}}])^2|\hat{\mathbf{M}}]} &= 0,84720 \cdot 10^{-1} \\
 \mathbb{E}[S|\hat{\mathbf{M}}] &= 74,412 & \sqrt{\mathbb{E}[(S - \mathbb{E}[S|\hat{\mathbf{M}}])^2|\hat{\mathbf{M}}]} &= 38,431 \\
 \mathbb{E}[\varepsilon_C|\hat{\mathbf{M}}] &= 0,27933 \cdot 10^{-2} & \sqrt{\mathbb{E}[(\varepsilon_C - \mathbb{E}[\varepsilon_C|\hat{\mathbf{M}}])^2|\hat{\mathbf{M}}]} &= 0,10082 \cdot 10^{-2}
 \end{aligned} \tag{3.120}$$

$$\tag{3.121}$$

We have obtained the following mean and standard deviation for the explicit sampling:

$$\begin{aligned}
 \mathbb{E}[k_{eff}|\hat{\mathbf{M}}] &= 0,48266 & \sqrt{\mathbb{E}[(k_{eff} - \mathbb{E}[k_{eff}|\hat{\mathbf{M}}])^2|\hat{\mathbf{M}}]} &= 0,85346 \cdot 10^{-1} \\
 \mathbb{E}[S|\hat{\mathbf{M}}] &= 74,651 & \sqrt{\mathbb{E}[(S - \mathbb{E}[S|\hat{\mathbf{M}}])^2|\hat{\mathbf{M}}]} &= 40,788 \\
 \mathbb{E}[\varepsilon_C|\hat{\mathbf{M}}] &= 0,27389 \cdot 10^{-2} & \sqrt{\mathbb{E}[(\varepsilon_C - \mathbb{E}[\varepsilon_C|\hat{\mathbf{M}}])^2|\hat{\mathbf{M}}]} &= 0,10094 \cdot 10^{-2}
 \end{aligned} \tag{3.122}$$

$$\tag{3.123}$$

These numerical values provide qualitative results, more accurate than those of the 1D or 2D marginal distributions.

The 2D marginal distribution on k_{eff} and S (in the next figure) shows that the a posteriori distributions on (k_{eff}, S) are concentrated around the real value of the point and decrease when k_{eff} and S increase, the Gaussian a priori on ε_C flattens out the a posteriori distribution when k_{eff} and S are too small or too large. The 2D marginals show that the shapes of the curves are the same with MCMC or explicit

sampling. We can observe that the MCMC distribution has some statistical noise, and that the explicit sampling has aliasing problems. These aliasing problems can be overcome by using regularisation techniques.

The actual parameters \mathbf{p}^* are indicated by a black cross, and show that the actual parameter is highly probable.

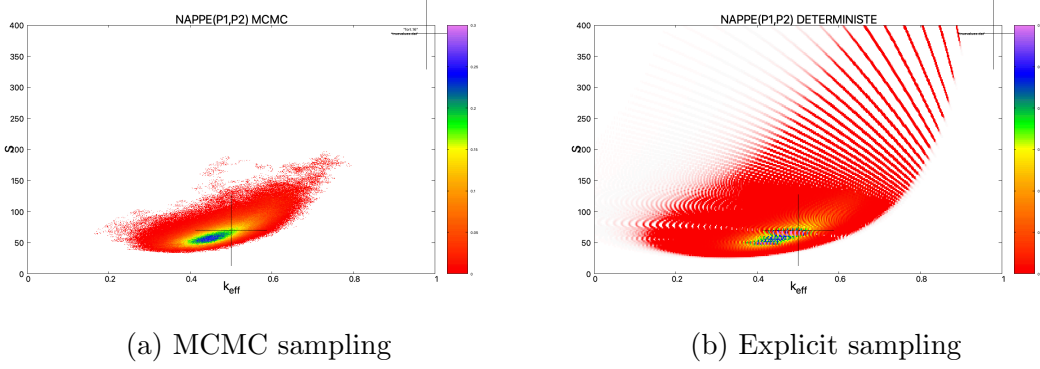


Figure 3.37: Marginal distribution of k_{eff} and S

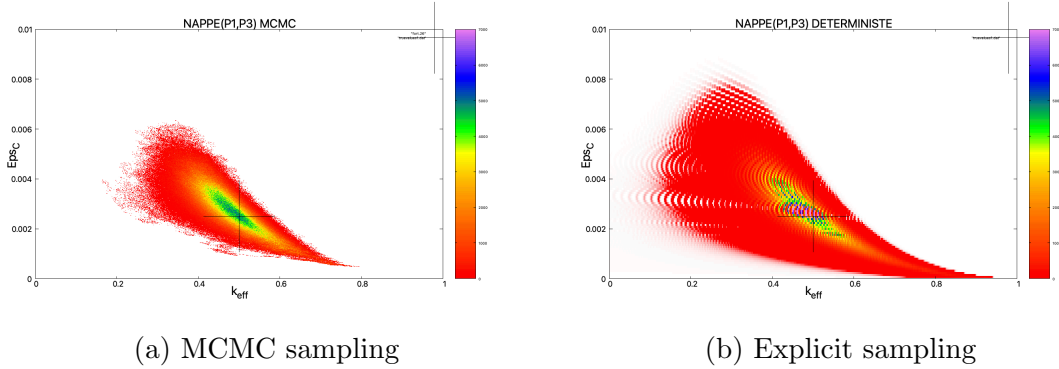


Figure 3.38: Marginal distribution of k_{eff} and ε_C

The marginal distribution on k_{eff} and ε_C also shows that the true parameter \mathbf{p}^* is in the support of the posterior distributions (which are the same but plotted by two different methods).

Then, for a measurement time of 3600s, we consider the same system as before for a time gate $T = \frac{10}{\alpha}$.

The corresponding observations are

$$\mathbf{M}(\mathbf{p}^*) = \begin{pmatrix} 1, 4043 \\ 3, 3868 \\ 10, 165 \end{pmatrix} \quad (3.124)$$

The associated covariance matrix is

$$\mathbf{Cov}(\mathbf{p}^*) = \begin{pmatrix} 0, 19649 \cdot 10^{-5} & 0, 75127 \cdot 10^{-5} & 0, 30420 \cdot 10^{-4} \\ 0, 75127 \cdot 10^{-5} & 0, 34313 \cdot 10^{-4} & 0, 15688 \cdot 10^{-3} \\ 0, 30420 \cdot 10^{-4} & 0, 15688 \cdot 10^{-3} & 0, 78938 \cdot 10^{-3} \end{pmatrix} \quad (3.125)$$

As previously, we consider a Gaussian a priori on ε_C with mean 3.10^{-3} and variance 10^{-3} .

First, we observe the 1D marginal distribution of each parameter. We can see that each marginal distribution corresponds to explicit sampling and MCMC sampling. The statistical noise is smaller than the aliasing noise.

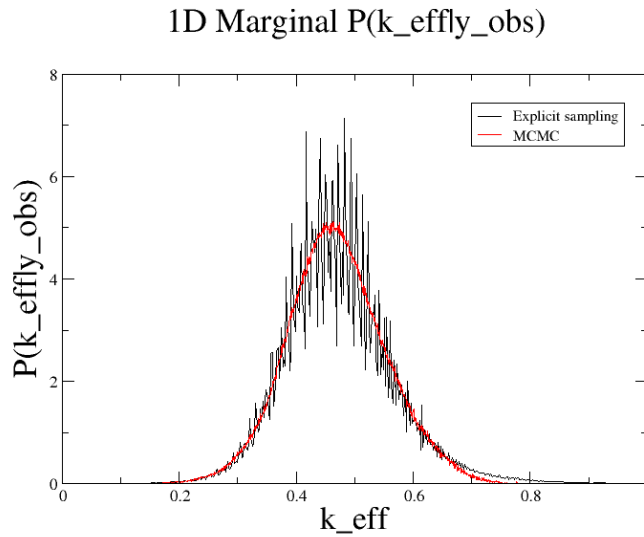


Figure 3.39: Marginal distribution of k_{eff} with explicit sampling (black) and MCMC sampling (red)

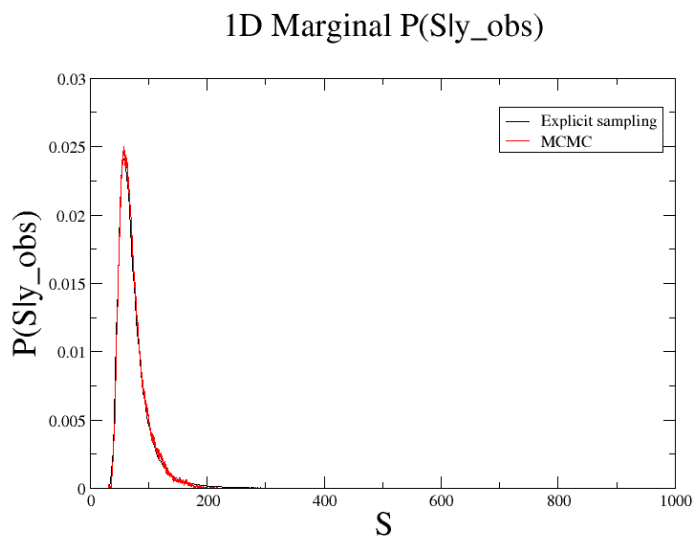


Figure 3.40: Marginal distribution of S with explicit sampling (black) and MCMC sampling (red)

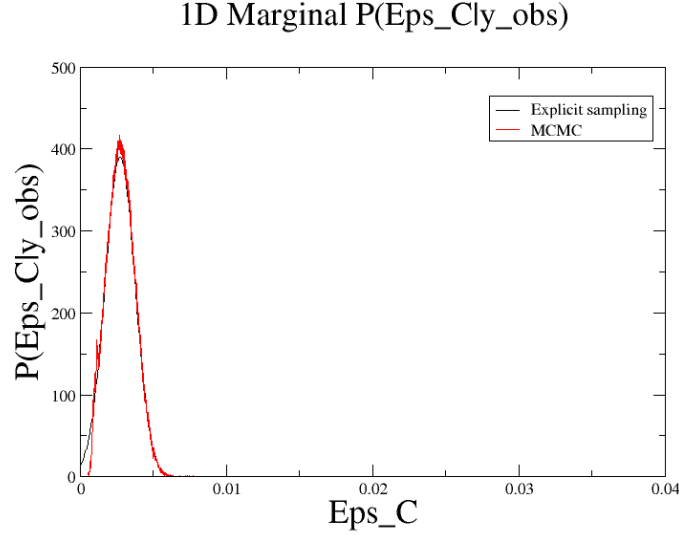


Figure 3.41: Marginal distribution of ε_C with explicit sampling (black) and MCMC sampling (red)

We have obtained the following mean and standard deviation for the MCMC sampling:

$$\begin{aligned}
 \mathbb{E}[k_{eff}|\hat{\mathbf{M}}] &= 0,46896 & \sqrt{\mathbb{E}[(k_{eff}|\hat{\mathbf{M}} - \mathbb{E}[k_{eff}|\hat{\mathbf{M}}])^2]} &= 0,84000 \cdot 10^{-1} \\
 \mathbb{E}[S|\hat{\mathbf{M}}] &= 72,762 & \sqrt{\mathbb{E}[(S|\hat{\mathbf{M}} - \mathbb{E}[S|\hat{\mathbf{M}}])^2]} &= 23,656 \\
 \mathbb{E}[\varepsilon_C|\hat{\mathbf{M}}] &= 0,27800 \cdot 10^{-2} & \sqrt{\mathbb{E}[(\varepsilon_C|\hat{\mathbf{M}} - \mathbb{E}[\varepsilon_C|\hat{\mathbf{M}}])^2]} &= 0,95656 \cdot 10^{-3}
 \end{aligned} \tag{3.126}$$

$$\tag{3.127}$$

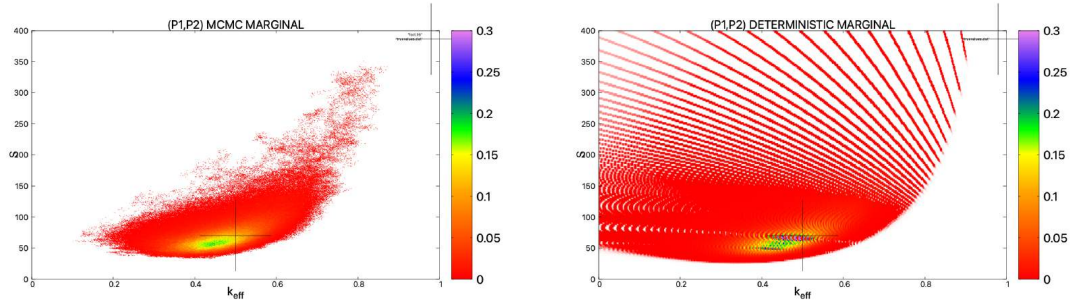
And for the explicit sampling:

$$\begin{aligned}
 \mathbb{E}[k_{eff}|\hat{\mathbf{M}}] &= 0,47358 & \sqrt{\mathbb{E}[(k_{eff} - \mathbb{E}[k_{eff}|\hat{\mathbf{M}}])^2|\hat{\mathbf{M}}]} &= 0,92548 \cdot 10^{-1} \\
 \mathbb{E}[S|\hat{\mathbf{M}}] &= 76,137 & \sqrt{\mathbb{E}[(S - \mathbb{E}[S|\hat{\mathbf{M}}])^2|\hat{\mathbf{M}}]} &= 42,643 \\
 \mathbb{E}[\varepsilon_C|\hat{\mathbf{M}}] &= 0,27300 \cdot 10^{-2} & \sqrt{\mathbb{E}[(\varepsilon_C - \mathbb{E}[\varepsilon_C|\hat{\mathbf{M}}])^2|\hat{\mathbf{M}}]} &= 0,10107 \cdot 10^{-2}
 \end{aligned} \tag{3.128}$$

$$\tag{3.129}$$

We draw the same quantitative conclusions (shape of the curve, influence of the Gaussian a posteriori, position of \mathbf{p}^*).

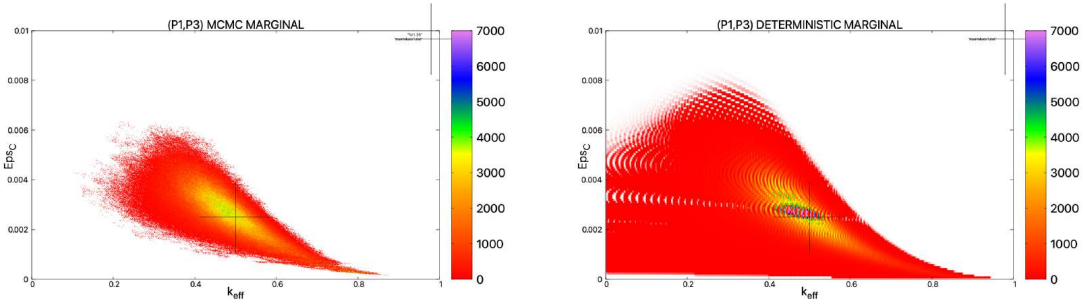
We observe the 2D a posteriori distributions



(a) MCMC sampling

(b) Explicit sampling

Figure 3.42: Marginal distribution of k_{eff} and S



(a) MCMC sampling

(b) Explicit sampling

Figure 3.43: Marginal distribution of k_{eff} and ε_C

We draw almost the same conclusions as for $T = \frac{1}{\alpha}$, except that the most probable points are less probable than for the previous time gate (the a posteriori distributions are normalised). The a posteriori distributions of the two time gates have common values in their support, and we hope to obtain more information by combining these two results. This is the objective of the next subsection.

3.2.4 A posteriori distribution of $(k_{eff}, \varepsilon_C, S)$ given the three first moments of $N_{[0,T_1]}$, $N_{[0,T_2]}$ where $T_1 = \frac{1}{\alpha}$, $T_2 = \frac{10}{\alpha}$ and $k_{eff} = 0.5$

Now that we have obtained the results for two distinct regimes, we will consider the product of the a posteriori distribution of the two previous experiments for $N_{bp} = 5.10^7$, always considering 1000 points in each direction for explicit sampling.

The observations are

$$\mathbf{y}_{obs} = \mathbf{M}(\mathbf{p}^*) = \begin{pmatrix} 0, 14043 \\ 0, 16058 \\ 0, 20382 \\ 1, 4043 \\ 3, 3868 \\ 10, 165 \end{pmatrix} \quad (3.130)$$

Since the measurements associated with the two time gates are not correlated, the covariance matrix is

$$\mathbf{Cov}(\mathbf{p}^*)_{T_1, T_2} = \begin{pmatrix} 0, 19563.10^{-7} & 0, 25177.10^{-7} & 0, 37637.10^{-7} & & & \\ 0, 25177.10^{-7} & 0, 38033.10^{-7} & 0, 67808.10^{-7} & & & \\ 0, 37637.10^{-7} & 0, 67808.10^{-7} & 0, 14152.10^{-6} & & & \\ & & & 0, 19649.10^{-5} & 0, 75127.10^{-5} & 0, 30420.10^{-4} \\ & & & 0, 75127.10^{-5} & 0, 34313.10^{-4} & 0, 15688.10^{-3} \\ & & & 0, 30420.10^{-4} & 0, 15688.10^{-3} & 0, 78938.10^{-3} \end{pmatrix} \quad (0) \quad (3.131)$$

First, we observe the 1D marginal distribution of each parameter. We can see that each marginal distribution corresponds to explicit sampling and MCMC sampling. The statistical noise is smaller than the aliasing noise.

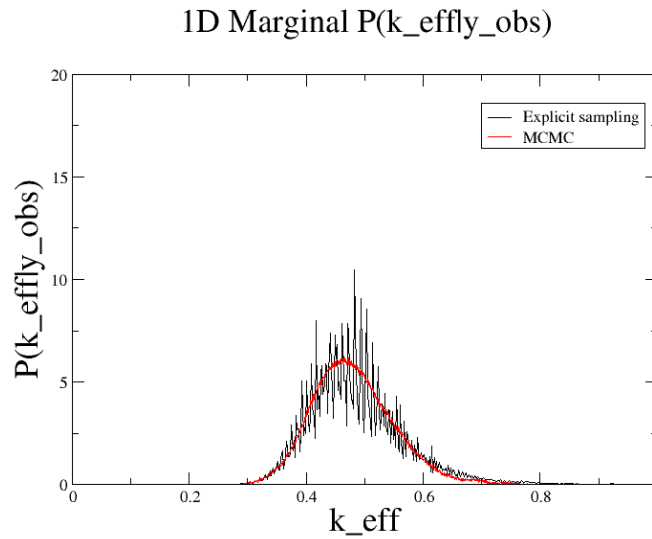


Figure 3.44: Marginal distribution of k_{eff} with explicit sampling (black) and MCMC sampling (red)

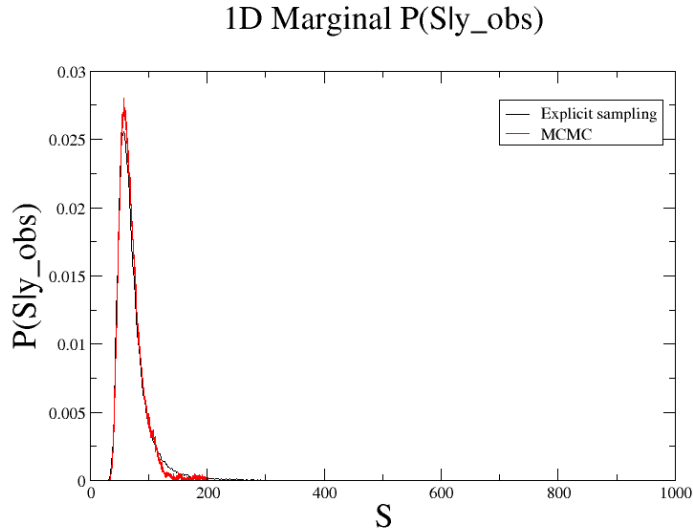


Figure 3.45: Marginal distribution of S with explicit sampling (black) and MCMC sampling (red)

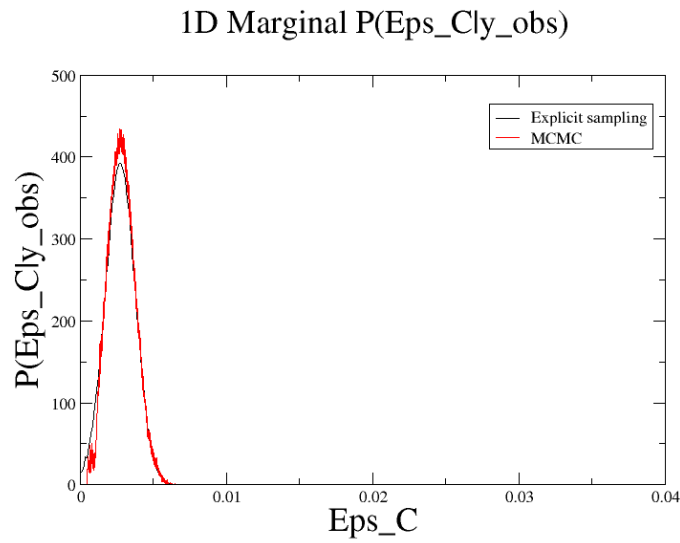


Figure 3.46: Marginal distribution of ε_C with explicit sampling (black) and MCMC sampling (red)

We have obtained the following mean and standard deviation for the MCMC sampling:

$$\begin{aligned}
 \mathbb{E}[k_{eff}|\hat{\mathbf{M}}] &= 0,48026 & \sqrt{\mathbb{E}[(k_{eff} - \mathbb{E}[k_{eff}|\hat{\mathbf{M}}])^2|\hat{\mathbf{M}}]} &= 0,69752 \cdot 10^{-1} \\
 \mathbb{E}[S|\hat{\mathbf{M}}] &= 69,441 & \sqrt{\mathbb{E}[(S - \mathbb{E}[S|\hat{\mathbf{M}}])^2|\hat{\mathbf{M}}]} &= 20,656 \\
 \mathbb{E}[\varepsilon_C|\hat{\mathbf{M}}] &= 0,28338 \cdot 10^{-2} & \sqrt{\mathbb{E}[(\varepsilon_C - \mathbb{E}[\varepsilon_C|\hat{\mathbf{M}}])^2|\hat{\mathbf{M}}]} &= 0,92588 \cdot 10^{-3}
 \end{aligned}
 \tag{3.132}$$

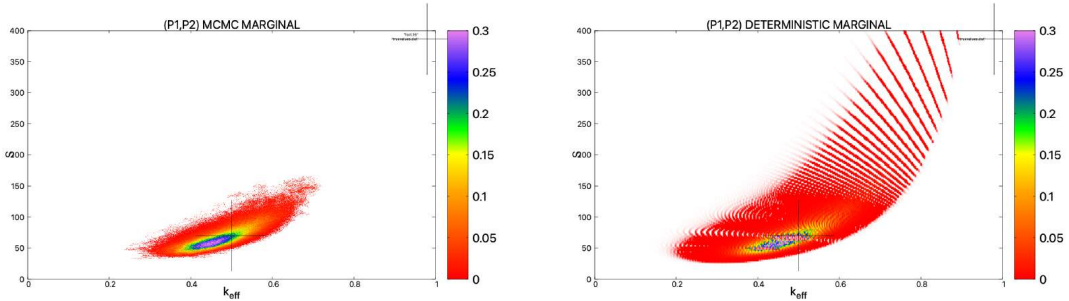
$$\tag{3.133}$$

And for the explicit sampling:

$$\begin{aligned}
 \mathbb{E}[k_{eff}|\hat{\mathbf{M}}] &= 0,48723 & \sqrt{\mathbb{E}[(k_{eff} - \mathbb{E}[k_{eff}|\hat{\mathbf{M}}])^2|\hat{\mathbf{M}}]} &= 0,82327 \cdot 10^{-1} \\
 \mathbb{E}[S|\hat{\mathbf{M}}] &= 74,019 & \sqrt{\mathbb{E}[(S - \mathbb{E}[S|\hat{\mathbf{M}}])^2|\hat{\mathbf{M}}]} &= 40,178 \\
 \mathbb{E}[\varepsilon_C|\hat{\mathbf{M}}] &= 0,27424 \cdot 10^{-2} & \sqrt{\mathbb{E}[(\varepsilon_C - \mathbb{E}[\varepsilon_C|\hat{\mathbf{M}}])^2|\hat{\mathbf{M}}]} &= 0,10101 \cdot 10^{-2}
 \end{aligned}
 \tag{3.134}$$

$$\tag{3.135}$$

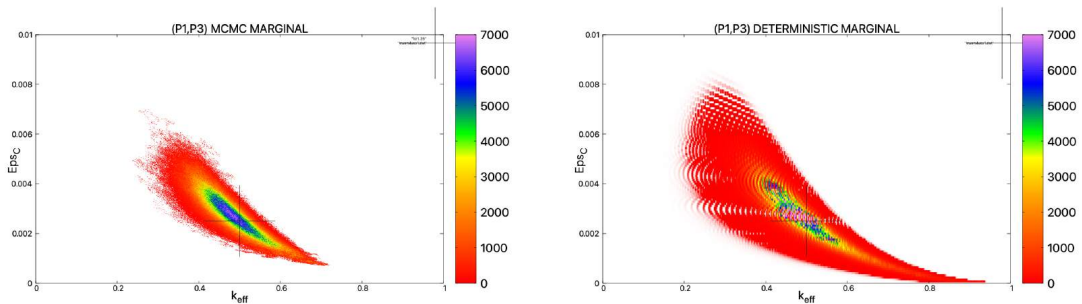
We draw the following conclusions: for $T_1 = \frac{1}{\alpha}$ and $T_2 = \frac{10}{\alpha}$, MCMC sampling is better than explicit sampling. But the standard deviation for each parameter is smaller than for T_1 and T_2 , so the approximation is better, an improvement of order 10^{-1} is made with this approach.



(a) MCMC sampling

(b) Explicit sampling

Figure 3.47: Marginal distribution of k_{eff} and S



(a) MCMC sampling

(b) Explicit sampling

Figure 3.48: Marginal distribution of k_{eff} and ε_C

We provide the Figure 3.49 and 3.50 in order to have a better comparison of the marginals for $T_1 = \frac{1}{\alpha}$, $T_2 = \frac{10}{\alpha}$ and (T_1, T_2) .

The results of the MCMC sampling using (T_1, T_2) in subfigure (c) of Figure 3.49 and 3.50 are as follows.

With three equations, such as the equations of the first three simple moments of $N_{[0,t]}$, we can expect to find at most three parameters. When there are more than three parameters to estimate, we have to find a way to calculate more. Taking into account the Feynman moment of order 4 could have been considered but only when ε_C is high. We recall that the equations of $\mathbb{E}[N_{[0,t]}]$, $Y_2(t)$, $Y_3(t)$ depend on t . So here we will consider two observation regimes: $t \ll \frac{1}{\alpha}$ and $t \gg \frac{1}{\alpha}$. Both regimes can be taken into account in order to cross-check the information, thus obtaining a better estimate of $\mathbf{p}|\mathbf{y}_{obs}$. We will explain this in the following paragraphs.

Considering the 1D marginal distribution for k_{eff} of the MCMC sampling with (T_1, T_2) , we know that the mean of this 1D marginal distribution have a mean of 0,48026 and a standard deviation of $0,69752 \cdot 10^{-1}$ (where the mean is 0.47937 and the standard deviation is $0,84720 \cdot 10^{-1}$ for T_1 , and 0,46896 and $0,84000 \cdot 10^{-1}$ for T_2). So regarding the MCMC sampling, the 1D marginal distribution of k_{eff} with (T_1, T_2) is a better estimation of $k_{eff}^* = 0.5$ than with T_1 or T_2 alone because the mean is closer to the real value and the standard deviation is smaller than for the two other time gates.

The same kind of result can be observed for S and ε_C . So, regarding the 1D marginal distribution, the use of (T_1, T_2) is more recommended than T_1 or T_2 alone.

For the 2D marginal distribution of k_{eff} and S , we notice that the mode of the a posteriori distribution has a higher probability in figure (c) than in figures (a) and (b). Thus, the marginal distribution over k_{eff} and S is more concentrated, and thus gives a better estimate of \mathbf{p}^* .

In the same way, we can analyse the marginal distribution of k_{eff} and ε_C , we also notice that the mode is more likely than the two previous figures.

We can conclude that considering two time gates (T_1, T_2) , in this case, enables to gain information through the marginal distributions. As the Figures 3.23, 3.24, 3.25 and 3.26 shows, the a posteriori distribution is wider when k_{eff} is low and the time of measurements T_{meas} is low, so considering the two regimes when $T \gg \frac{1}{\alpha}$ and $T \ll \frac{1}{\alpha}$ provide more information in these cases rather than when k_{eff} is high and the time of measurements T_{meas} is high. In these last cases, considering $T \gg \frac{1}{\alpha}$ and $T \ll \frac{1}{\alpha}$ provide no significant information gain.

As the behaviour of the simple moments depends on the regime considered (see Chapter 2), we conjectured that the corresponding posterior distributions are not the same, and that we can obtain more information by considering observations from the two previous posterior distributions.

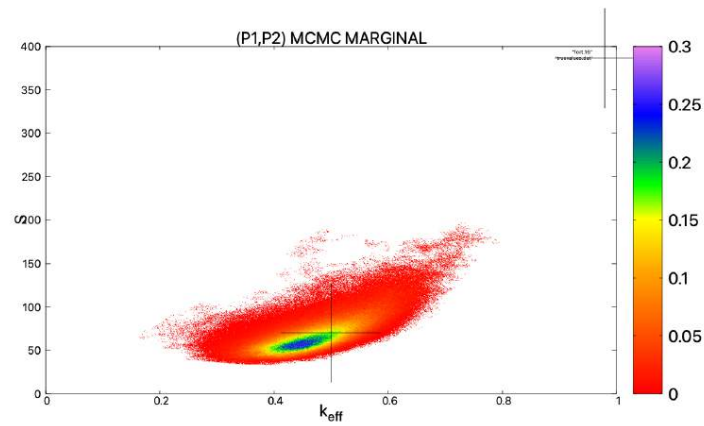
This is confirmed by the observations, as before the true parameter \mathbf{p}^* is in the support of the a posteriori distribution. This technique allows us to gain information.

What is interesting in the applications.

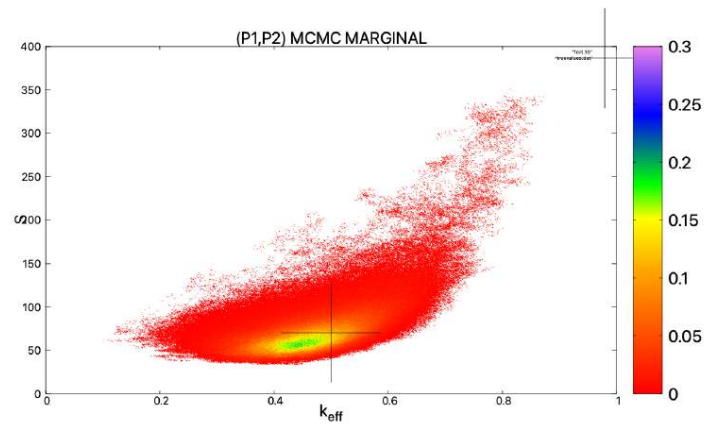
3.2.5 Influence of the prior distribution

Due to physical assumptions, we restrict the prior to a uniform distribution added to a Gaussian a priori on ε_C . In fact, our \mathbf{p}^* parameters are bounded:

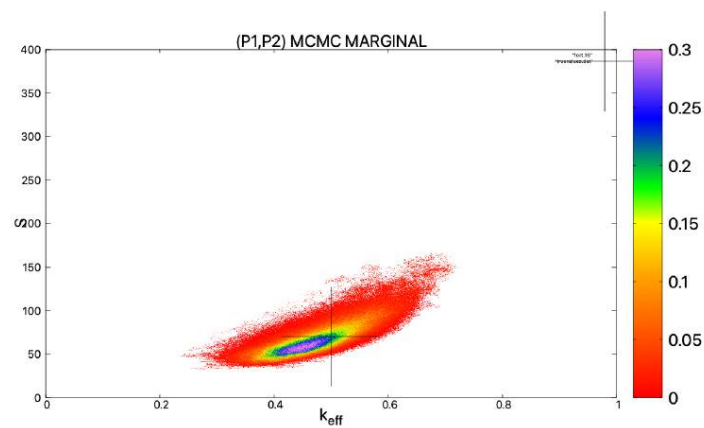
- The intensity S is non-negative since the spontaneous fission produces neutron.



(a) $T_1 = \frac{1}{\alpha}$

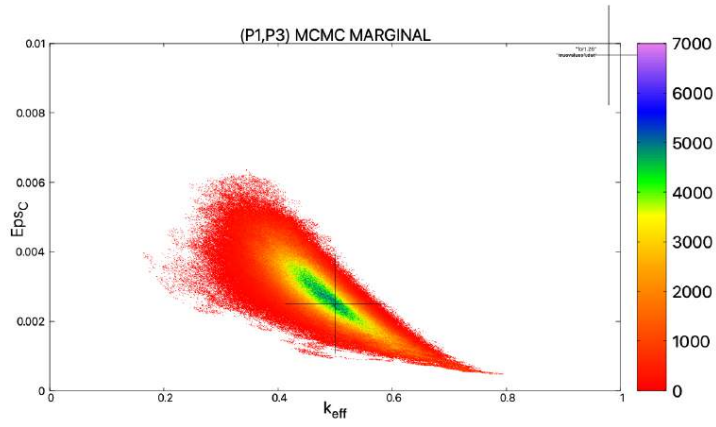


(b) $T_2 = \frac{10}{\alpha}$

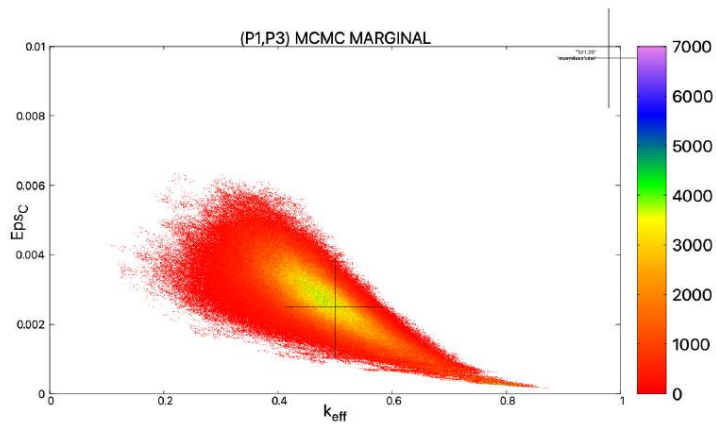


(c) (T_1, T_2)

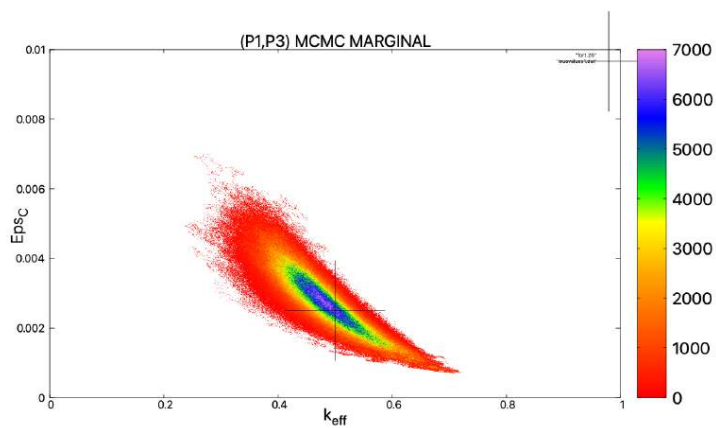
Figure 3.49: Marginal distribution of k_{eff} and S for T_1 , T_2 and (T_1, T_2) with MCMC sampling



(a) $T_1 = \frac{1}{\alpha}$



(b) $T_2 = \frac{10}{\alpha}$



(c) (T_1, T_2)

Figure 3.50: Marginal distribution of k_{eff} and ε_C for T_1 , T_2 and (T_1, T_2) with MCMC sampling

An upper bound can be found using the mean of the neutron detected $\mathcal{M}_1(1)$. Physicists empirically observe $\frac{\mathcal{M}_1(1)}{10\varepsilon_C} \leq S \leq 10\frac{\mathcal{M}_1(1)}{\varepsilon_C}$.

- The spontaneous fission rate x is by definition in $[0, 1]$
- Since the system is sub-critical (stationary), the multiplication factor k_{eff} of the system is between 0 and 1 (strictly lower than 1)
- The efficiency of the detector ε_C is a probability, so it is in $[0, 1]$. By the relation $\lambda_C\varepsilon_C = \lambda_F\varepsilon_F$ and $\varepsilon_C \leq 1$ we can deduce $\varepsilon_F \leq \frac{\lambda_C}{\lambda_F}$ where the last ratio is supposed to be known.
- The decreasing coefficient of the system α can be estimated using the fit of Y_2 with the formula of the point model

Thus, with these physical considerations, we have a uniform a priori distribution over the domain studied added to a Gaussian a priori on ε_C , the a posteriori distribution sampled is then more accentuated around the real value \mathbf{p}^* .

When we have other information provided by measurements (gamma spectroscopy, X-ray, expert opinion etc.) they can be taken into account in the a priori distribution. Therefore, they modify the a posteriori distribution.

The γ spectroscopy and the 3He neutron detection are independent because they are performed by different methods and by different people.

The γ spectroscopy gives information on the efficiency, which makes it possible to reduce the search area.

Chapter 4

Conclusion

4.1 Conclusions

The main objective of this work was to develop a methodology for inferring nuclear system parameters with uncertainty quantification from neutron multiplicity count (NMC) measurements. The chosen method is based on Bayesian inference and Monte Carlo Markov Chain Sampling (MCMC) of the a posteriori probability distribution in the parameter space. A second objective was to study the direct problem and derive the point model equations for the first three moments of the neutron count distribution.

This thesis has been structured as follows. In the first part, the state of the art chapter, we recalled some basics about random processes (like Markov chains), inverse problems and neutron physics.

Then, in the chapter on direct problems, we established all the analytical expressions of the first three moments of the distribution of the number of neutrons present or detected

- in the absence of a source,
- in transitional regime with an external source,
- in stationary regime with an external source.

Then, we verified and compared numerically these expressions with the analytical expression using the explicit Euler method and Monte Carlo estimation in three different cases. In addition, the accuracy of the point model approximation was checked against the MCNP6 and Tripoli-4 simulations.

In the chapter on the inverse problem, we examined several numerical methods for recovering the parameters of the \mathbf{p} system knowing the \mathbf{y}_{obs} observations. This methodology has been applied on several test cases in order to verify its efficiency. We also considered measurements using two time gates of different duration, allowing to obtain more accurate a posteriori distributions and to have a better characterization of the considered system.

In summary, in the direct problem, we have fully established the analytical point model expressions for the first three moments of the distribution of neutrons present

and detected in the system during the steady state. Some specific test cases have shown the difference between the point model neutron approximation and the more accurate calculations performed with MCNP6 or Tripoli-4.

On the other hand, the inverse problem on the considered cases has shown that the use of MCMC methods with adaptation of the covariance matrix allows to compute the conditional a posteriori distribution of $\mathbf{p}|\mathbf{y}_{obs}$. In addition, the use of the length of two time gates gives more accurate information.

4.2 Perspectives

The calculations of the a posteriori distributions were performed using three parameters, namely the multiplication coefficient, the source intensity and the detection efficiency. Using two uncorrelated time gates, future work could include inference of the five point model parameters, namely the previous three plus the fast neutron decay constant and the spontaneous fission source proportion. In this case, explicit sampling fails and the use of MCMC sampling is mandatory. In the cases presented, we used synthetic measurements obtained by Monte Carlo simulations. The application of the method to real measurements will be considered.

In order to have a direct model that is faster than MCNP-6 or Tripoli-4 and more accurate than the point model approximation, the use of Gaussian process metamodeling will be considered.

We can also consider a non-informative prior on the \mathbf{p} parameters, such as the Jeffreys prior.

The γ spectroscopy can be used in the Gaussian prioritisation of data as it is independent of other measurements (see [HM17] for use of γ spectroscopy to obtain a prior on ε_F and for further details see also [MM08; MM10; AF12; BFA11; Fav04]).



Un vieil adage latin t'aidera, je l'espère, comme il m'a aidé. Quid est hoc æternitate : qu'est-ce que ceci au regard de l'éternité ? Aussitôt cette question posée, tu pourras prendre du recul et faire la part des choses. Tu discerneras alors entre leurs parts d'ombre et de lumière. Certains de tes objectifs te paraîtront pour ce qu'ils sont, tout à fait vains. D'autres brilleront d'un éclat jusqu'alors caché parce que tu verras leur dimension d'amour.

Soeur Emmanuelle "Vivre à quoi ça sert ?" Flammarion, 2004

Appendix A

Appendix

A.1 Note on the state-of-the-art

In this section, we provide here the clues in order to prove 1.1.10. The reader is led to notice we can also express the variance in function of the partial derivatives of the generating function.

$$\text{Var}[X] = \mathbb{E}[X^2] - \mathbb{E}[X]^2 = \left[\frac{\partial^2}{\partial x^2} G_{\mathbb{P}} \right]_{x=1} + \left[\frac{\partial}{\partial x} G_{\mathbb{P}} \right]_{x=1} - \left[\frac{\partial}{\partial x} G_{\mathbb{P}} \right]_{x=1}^2 \quad (\text{A.1})$$

Since $\text{Var}[X] = \mathbb{E}[(X - \mathbb{E}[X])^2]$ a variance is always positive.

Proof. proof of Prop 3.4.3 of MAP 361 [GMT19] + We know that

$$\left[\frac{\partial}{\partial x} G_{\mathbb{P}} \right]_{x=1} = \sum_{n \geq 0} n \mathbb{P}(X = n) = \mathbb{E}[X] \quad (\text{A.2})$$

Moreover

$$\left[\frac{\partial^2}{\partial x^2} G_{\mathbb{P}} \right]_{x=1} = \sum_{n \geq 0} n(n-1) \mathbb{P}(X = n) = \mathbb{E}[X(X-1)] \quad (\text{A.3})$$

What provides

$$\mathbb{E}[X^2] = \left[\frac{\partial^2}{\partial x^2} G_{\mathbb{P}} + \frac{\partial}{\partial x} G_{\mathbb{P}} \right]_{x=1} \quad (\text{A.4})$$

In the same way

$$\left[\frac{\partial^3}{\partial x^3} G_{\mathbb{P}} \right]_{x=1} = \sum_{n \geq 0} n(n-1)(n-2) \mathbb{P}(X = n) = \mathbb{E}[X(X-1)(X-2)] = \mathbb{E}[X^3] - 3\mathbb{E}[X^2] + 2\mathbb{E}[X] \quad (\text{A.5})$$

What provides

$$\mathbb{E}[X^3] = \left[\frac{\partial^3}{\partial x^3} G_{\mathbb{P}} \right]_{x=1} + 3 \left[\frac{\partial^2}{\partial x^2} G_{\mathbb{P}} + \frac{\partial}{\partial x} G_{\mathbb{P}} \right]_{x=1} - 2 \left[\frac{\partial}{\partial x} G_{\mathbb{P}} \right]_{x=1} \quad (\text{A.6})$$

□

A.1.1 Markov chains on finite set of space

We present here some results necessary to the existence of the invariant measure for a Markov chain on a finite set of space, the reader is invited to read [Bod20]. This subsection is useful for the ergodicity of the discrete-time Markov chains 1.3.4.

Theorem 7. *For an irreducible Markov chain X on a finite set of space, the unique invariant probability distribution Π is given by*

$$\Pi(x) = \frac{1}{\mathbb{E}_x[T_1^{(x)}]}, \forall x \in FCS \quad (\text{A.7})$$

A.1.2 Linear algebra

We present here the Woodbury formula that is useful in Bayesian and inverse problem subsection of the state-of-the-art 1.7.2.

Lemma A.1.1. *Woodbury's formula*

Let $\mathbf{B} \in GL_r(\mathbb{R})$, $\mathbf{A} \in \mathcal{M}_{r,s}(\mathbb{R})$, and $\mathbf{C} \in GL_s(\mathbb{R})$ such that $\mathbf{A}^T \mathbf{B}^{-1} \mathbf{A} + \mathbf{C}^{-1}$. Then the matrix $\mathbf{B} + \mathbf{A} \mathbf{C} \mathbf{A}^T$ is invertible and we have:

$$\mathbf{B} + \mathbf{A} \mathbf{C} \mathbf{A}^T = \mathbf{B}^{-1} - \mathbf{B}^{-1} \mathbf{A} (\mathbf{A}^T \mathbf{B}^{-1} \mathbf{A} + \mathbf{C}^{-1})^{-1} \mathbf{A} \mathbf{B}^{-1} \quad (\text{A.8})$$

Now we define some clues for the Tikhonov regularisation, see 1.7.1.

We define the meaning of s -sparse

Definition A.1.2. *\mathbf{p} is said s -sparse when*

$$\|\mathbf{p}\|_0 \leq s \quad (\text{A.9})$$

And here are some clues about the RIP (Restricted Isometric Property), mentioned in the state-of-the-art dealing with Tykhonov's regularisation. The idea was introduced by E. Candès and T. Tao in [CT05] for proofs of theorems in the compressed sensing field, and we can find more considerations of this field in [SF13], on p. 22 we can find

Definition A.1.3. *RIP*

Let $\delta_s \in (0, 1)$ be what we call the restricted isometric constant of a matrix \mathbf{M} , by definition this is the smallest real such that

$$(1 - \delta_s) \|\mathbf{p}\|_2^2 \leq \|\mathbf{M} \mathbf{p}\|_2^2 \leq (1 + \delta_s) \|\mathbf{p}\|_2^2, \text{ for all } s\text{-sparse } \mathbf{p} \quad (\text{A.10})$$

In an informal way, \mathbf{M} is said to satisfy the RIP if the restricted isometric constant δ_s is small for s sufficiently large.

A.1.3 Classical methods of estimation in statistics

The following theorem is useful in the state-of-the-art 1.7.2.

Theorem A.1.4. *Gaussian conditioning theorem*

Let $\begin{pmatrix} \mathbf{Y}_1 \\ \mathbf{Y}_2 \end{pmatrix}$ be a random Gaussian vector (with \mathbf{Y}_1 of length r_1 and \mathbf{Y}_2 of length r_2):

$$\mathcal{L}\left(\begin{pmatrix} \mathbf{Y}_1 \\ \mathbf{Y}_2 \end{pmatrix}\right) = \mathcal{N}\left(\begin{pmatrix} \mu_1 \\ \mu_2 \end{pmatrix}, \begin{pmatrix} \mathbf{R}_{1,1} & \mathbf{R}_{1,2} \\ \mathbf{R}_{2,1} & \mathbf{R}_{2,2} \end{pmatrix}\right) \quad (\text{A.11})$$

with the mean vectors μ_1 and μ_2 of length r_1 and r_2 , and the covariance matrix $\mathbf{R}_{1,1}$ of size $r_1 \times r_1$, $\mathbf{R}_{1,2}$ of size $r_1 \times r_2$, $\mathbf{R}_{2,1} = \mathbf{R}_{1,2}^T$ of size $r_2 \times r_1$ and $\mathbf{R}_{2,2}$ of size $r_2 \times r_2$ invertible.

Then the law of \mathbf{Y}_1 conditionally to \mathbf{Y}_2 is Gaussian

$$\mathcal{L}(\mathbf{Y}_1 | \mathbf{Y}_2 = \mathbf{y}_2) = \mathcal{N}(\mu_1 + \mathbf{R}_{1,2}\mathbf{R}_{2,2}^{-1}(\mathbf{y}_2 - \mu_2), \mathbf{R}_{1,1} - \mathbf{R}_{1,2}\mathbf{R}_{2,2}^{-1}\mathbf{R}_{2,1}) \quad (\text{A.12})$$

This theorem show that the Bayesian analysis reduces to linear algebra.

A.2 Direct problem: proof of the propositions and lemma

The reader can find the computations of the different moments necessary to the study of the direct problem, the chapter 2.

Before these computations, we recall some tools.

A.2.1 Some key integrals

First, we recall some basic integral

$$\int_t^T e^{-k\alpha(T-s)} ds = e^{-k\alpha T} \left[\frac{e^{k\alpha s}}{k\alpha} \right]_t^T = \frac{1 - e^{-k\alpha(T-t)}}{k\alpha}, \quad \forall k \in \mathbb{N}^* \quad (\text{A.13})$$

Hence,

$$\begin{aligned} \int_t^T e^{-\alpha(T-s)} ds &= \frac{1 - e^{-\alpha(T-t)}}{\alpha} \\ \int_t^T e^{-2\alpha(T-s)} ds &= \frac{1 - e^{-2\alpha(T-t)}}{2\alpha} \\ \int_t^T e^{-3\alpha(T-s)} ds &= \frac{1 - e^{-3\alpha(T-t)}}{3\alpha} \end{aligned} \quad (\text{A.14})$$

Then we recall here some important integrals computations. The first is the following

$$\begin{aligned} \int_0^{T-t} -\alpha s e^{-\alpha s} ds &= \left[s e^{-\alpha s} \right]_0^{T-t} - \int_0^{T-t} e^{-\alpha s} ds \\ &= (T-t)e^{-\alpha(T-t)} - \frac{1 - e^{-\alpha(T-t)}}{\alpha} \end{aligned} \quad (\text{A.15})$$

The second is

$$\begin{aligned} \int_0^{T-t} -2\alpha s e^{-2\alpha s} ds &= \left[s e^{-2\alpha s} \right]_0^{T-t} - \int_0^{T-t} e^{-2\alpha s} ds \\ &= (T-t)e^{-2\alpha(T-t)} - \frac{1 - e^{-2\alpha(T-t)}}{2\alpha} \end{aligned} \quad (\text{A.16})$$

Finally, we have

$$\begin{aligned} \int_0^{T-t} -\alpha s^2 e^{-\alpha s} ds &= \left[s^2 e^{-\alpha s} \right]_0^{T-t} - 2 \int_0^{T-t} s e^{-\alpha s} ds \\ &= (T-t)^2 e^{-\alpha(T-t)} + 2 \frac{(T-t)}{\alpha} e^{-\alpha(T-t)} - 2 \frac{1 - e^{-\alpha(T-t)}}{\alpha^2} \end{aligned} \quad (\text{A.17})$$

A.2.2 Cumulants of the distribution of presence

In order to compute the asymptotic values $\bar{\nu}_{II,\infty}$ (eq. 2.1.4), $\nu_{2,II,\infty}$ (eq. 2.12), $\nu_{3,II,\infty}$ (eq. 2.14) we need in part 2.1.1 of chapter 2 we will use the following integrals. In the following $S = S_F$ will refer to the intensity of the source and $S_\alpha = 0$.

Starting from

$$\Gamma_{II,n}(t) = S \int_0^{T-t} \nu_{\pi,n}(T-s) ds \quad (\text{A.18})$$

So,

$$\begin{aligned} \Gamma_{II,1}(t) &= S I_1(t) = \bar{\nu}_S S I_1(t) \\ &= \bar{\nu}_S S \frac{1 - e^{-\alpha(T-t)}}{\alpha} \end{aligned} \quad (\text{A.19})$$

In accordance with line 1 of eq. 2.27, we deduce the asymptotical value

$$\boxed{\Gamma_{II,1,\infty} = \frac{\bar{\nu}_S S}{\alpha}} \quad (\text{A.20})$$

Moreover,

$$\begin{aligned} \Gamma_{II,2}(t) &= \bar{\nu}_S S I_2(t) + \nu_{2S} S I_1^{(2)}(t) \\ &= \bar{\nu}_S S \frac{\nu_2}{-\rho \bar{\nu}} \left(\frac{1 - e^{-\alpha(T-t)}}{\alpha} - \frac{1 - e^{-2\alpha(T-t)}}{2\alpha} \right) + \nu_{2S} S \frac{1 - e^{-2\alpha(T-t)}}{2\alpha} \\ &= \bar{\nu}_S S \frac{\nu_2}{-\rho \bar{\nu}} \frac{1 - e^{-\alpha(T-t)}}{\alpha} + (\nu_{2S} S - \bar{\nu}_S S \frac{\nu_2}{-\rho \bar{\nu}}) \frac{1 - e^{-2\alpha(T-t)}}{2\alpha} \end{aligned} \quad (\text{A.21})$$

In accordance with line 2 of eq. 2.27, we deduce the asymptotical value

$$\boxed{\Gamma_{II,2,\infty} = \frac{S}{2\alpha} \left(\bar{\nu}_S \frac{\nu_2}{-\rho \bar{\nu}} + \nu_{2S} \right)} \quad (\text{A.22})$$

Also

$$\begin{aligned}
\Gamma_{II,3}(t) &= \bar{\nu}_S S I_3(t) + \nu_{3S} S I_1^{(3)}(t) + 2\nu_{2S} S I_{1,2} \\
&= \bar{\nu}_S S \frac{1}{-\rho\bar{\nu}} \left(\frac{\nu_2^2}{-\rho\bar{\nu}} \left(\frac{1 - e^{-\alpha(T-t)}}{\alpha} - 2 \frac{1 - e^{-2\alpha(T-t)}}{2\alpha} + \frac{1 - e^{-3\alpha(T-t)}}{3\alpha} \right) \right. \\
&\quad \left. + \frac{\nu_3}{2} \left(\frac{1 - e^{-\alpha(T-t)}}{\alpha} - \frac{1 - e^{-3\alpha(T-t)}}{3\alpha} \right) \right) \\
&\quad + \nu_{3S} S \frac{1 - e^{-3\alpha(T-t)}}{3\alpha} + 2\nu_{2S} S \frac{\nu_2}{-\rho\bar{\nu}} \left(\frac{1 - e^{-2\alpha(T-t)}}{2\alpha} - \frac{1 - e^{-3\alpha(T-t)}}{3\alpha} \right)
\end{aligned} \tag{A.23}$$

Finally, in accordance with line 3 of eq. 2.27, we deduce the asymptotical value

$$\boxed{\Gamma_{II,3,\infty} = \frac{S}{3\alpha} \left(\frac{\bar{\nu}_S}{-\rho\bar{\nu}} \left(\frac{\nu_2^2}{-\rho\bar{\nu}} + \nu_3 \right) + \frac{\nu_2\nu_{2S}}{-\rho\bar{\nu}} + \nu_{3S} \right)} \tag{A.24}$$

These values are then used in order to compute $\bar{\nu}_{II,\infty}$, $\nu_{2,II,\infty}$, $\nu_{3,II,\infty}$.

A.2.3 Moments of the distribution of presence $\pi_n(t)$ and $II_n(t)$

This subsection refers to the computation of the moments of the distributions $\pi_n(t)$ and $II_n(t)$.

Moments of the distribution $\pi_n(t)$

We present here the details of computation of the three first simple moments of $\pi_n(t)$, as in subsection 2.1

For a presence distribution $\pi_n(t)$, we denote

$$\nu_{p,\pi}(t) = \frac{1}{p!} \left[\frac{\partial^p g_\pi}{\partial x^p} \right]_{x=1} \tag{A.25}$$

For the three first moments of the number of neutrons present in the system, we dispose of

$$\begin{cases} \mathbb{E}[N]_{(\pi_n(t))_n} = \bar{\nu}(t) \\ \mathbb{E}[N^2]_{(\pi_n(t))_n} = 2\nu_{2,\pi}(t) + \bar{\nu}(t) \\ \mathbb{E}[N^3]_{(\pi_n(t))_n} = 6(\nu_{3,\pi}(t) + \nu_{2,\pi}(t)) + \bar{\nu}(t) \end{cases} \tag{A.26}$$

Now, we provide a proof of the analytical expression and property 2.1.1 of $\bar{\nu}_\pi(t)$.

Proof. Differentiating the equation 1.162 with respect to x

$$-\frac{\partial}{\partial t} \frac{\partial g_\pi}{\partial x} = -(\lambda_F \sum_{i \neq 1} f_i + \lambda_C) \frac{\partial g_\pi}{\partial x} + \lambda_F \sum_i i f_i \frac{\partial g_\pi}{\partial x} g_\pi^{i-1}(t) \tag{A.27}$$

Then evaluating in $x = 1$, we obtain

$$\begin{aligned} -\frac{d\bar{\nu}_\pi}{dt} &= -(\lambda_F \sum_{i \neq 1} f_i + \lambda_C) \bar{\nu}_\pi + \lambda_F \sum_{i=2}^m i f_i \bar{\nu}_\pi \\ &= -\lambda_C \bar{\nu}_\pi + \lambda_F \sum_i (i-1) f_i \bar{\nu}_\pi \end{aligned} \quad (\text{A.28})$$

That can become

$$\frac{d\bar{\nu}_\pi}{dt} = \bar{\nu}_\pi \alpha \quad (\text{A.29})$$

As a result, we have

$$\bar{\nu}_\pi(t) = \text{Constant} e^{\alpha t} \quad (\text{A.30})$$

Using the final condition, we have the knowledge that

$$1 = \bar{\nu}_\pi(T) = \text{Constant} e^{\alpha T} \quad (\text{A.31})$$

Which enables us to deduce (eq. 2.3)

$$\boxed{\bar{\nu}_\pi(t) = e^{-\alpha(T-t)}} \quad (\text{A.32})$$

And thus

$$\boxed{\bar{\nu}_{\pi, \infty} = 0} \quad (\text{A.33})$$

□

Now we provide a proof of the analytical expression and properties of $\nu_{2,\pi}(t)$

Proof. Starting from 1.172, we are in the presence of a linear differentiate equation of the first order with associated homogeneous equation

$$\frac{\partial}{\partial t} \nu_{2,\pi} = (\lambda_C - \lambda_F \sum_{i \neq 1} (i-1) f_i) \nu_{2,\pi} = \alpha \nu_{2,\pi} \quad (\text{A.34})$$

A solution of this differentiate equation is

$$\nu_{2,\pi} = \text{Cste} e^{\alpha t} \quad (\text{A.35})$$

type.

Remark A.2.1. By definition $\nu_{2,\pi}(T) = 0$ and so $\text{Cste}(T) = 0$.

Using the constant variation method in order to obtain the general solution of the equation 1.172

$$\text{Cste}' e^{\alpha t} = -\nu_2 \lambda_F \bar{\nu}_\pi^2 \quad (\text{A.36})$$

This equation becomes

$$\text{Cste}' = -\nu_2 e^{-2\alpha(T-t)} e^{-\alpha t} = -\nu_2 \lambda_F e^{-2\alpha T} e^{\alpha t} \quad (\text{A.37})$$

By integrating

$$\text{Cste}(T) - \text{Cste}(t) = -\nu_2 e^{-2\alpha T} \frac{e^{\alpha T} - e^{\alpha t}}{\alpha} = -\nu_2 \lambda_F e^{-\alpha T} \frac{1 - e^{-\alpha(T-t)}}{\alpha} \quad (\text{A.38})$$

Using the initial condition, we can deduce

$$Cste(t) = \nu_2 \lambda_F e^{-\alpha T} \frac{1 - e^{-\alpha(T-t)}}{\alpha} \quad (\text{A.39})$$

Which finally leads us to the following result

$$\nu_{2,\pi} = \nu_2 \lambda_F e^{-\alpha(T-t)} \frac{1 - e^{-\alpha(T-t)}}{\alpha} \quad (\text{A.40})$$

But $\frac{\nu_2 \lambda_F}{\alpha} = \nu_2 \frac{\lambda_F}{\lambda_T - \bar{\nu} \lambda_F} = \nu_2 \frac{1}{\frac{\lambda_T}{\bar{\nu} \lambda_F} - 1} = \frac{\nu_2}{-\rho \bar{\nu}}$, and so we obtain eq. 2.5

$$\boxed{\nu_{2,\pi} = \frac{\nu_2}{-\rho \bar{\nu}} e^{-\alpha(T-t)} (1 - e^{-\alpha(T-t)})} \quad (\text{A.41})$$

From this fact,

$$\boxed{\nu_{2,\pi,\infty} = 0} \quad (\text{A.42})$$

□

Finally, we provide a proof of the analytical expression and property of $\nu_{3,\pi}(t)$

Proof. Starting from 1.175, we dispose of the same type of differential equation as the one checked by $\nu_{2,\pi}$, the same goes for the solution of the associated homogeneous differential equation

$$\nu_{3,\pi} = Cste e^{\alpha t} \quad (\text{A.43})$$

The variation constants method leads us to the following equation

$$\begin{aligned} Cste' e^{\alpha t} &= -\lambda_F (2\nu_2 \bar{\nu} \nu_{2,\pi} + \nu_3 \bar{\nu}^3) \\ &= -\lambda_F \left(2 \frac{\nu_2^2}{-\rho \bar{\nu}} e^{-2\alpha(T-t)} (1 - e^{-\alpha(T-t)}) + \nu_3 e^{-3\alpha(T-t)} \right) \end{aligned} \quad (\text{A.44})$$

What gives us so

$$Cste' = -\lambda_F \left(2 \frac{\nu_2^2}{-\rho \bar{\nu}} (e^{-2\alpha T} e^{\alpha t} - e^{-3\alpha T} e^{2\alpha t}) + \nu_3 e^{-3\alpha T} e^{2\alpha t} \right) \quad (\text{A.45})$$

By integrating, we obtain

$$Cste(T) - Cste(t) = -\lambda_F \left(2 \frac{\nu_2^2}{-\rho \bar{\nu}} \left(e^{-2\alpha T} \frac{e^{\alpha T} - e^{\alpha t}}{\alpha} - e^{-3\alpha T} \frac{e^{2\alpha T} - e^{2\alpha t}}{2\alpha} \right) + \nu_3 e^{-3\alpha T} \frac{e^{2\alpha T} - e^{2\alpha t}}{2\alpha} \right) \quad (\text{A.46})$$

Using the condition at time T , we obtain

$$Cste(t) = \lambda_F e^{-\alpha T} \left(2 \frac{\nu_2^2}{-\rho \bar{\nu}} \left(\frac{1 - e^{-\alpha(T-t)}}{\alpha} - \frac{1 - e^{-2\alpha(T-t)}}{2\alpha} \right) + \nu_3 \frac{1 - e^{-2\alpha(T-t)}}{2\alpha} \right) \quad (\text{A.47})$$

Finally, by multiplying the previous results by $e^{\alpha t}$, we can deduce eq. 2.7

$$\boxed{\nu_{3,\pi}(t) = \frac{e^{-\alpha(T-t)}}{-\rho \bar{\nu}} \left(\frac{\nu_2^2}{-\rho \bar{\nu}} (1 - e^{-\alpha(T-t)})^2 + \nu_3 \frac{1 - e^{-2\alpha(T-t)}}{2} \right)} \quad (\text{A.48})$$

and

$$\boxed{\nu_{3,\pi,\infty} = 0} \quad (\text{A.49})$$

□

The three first moment of $\pi_n(t)$ are now computed and can be used in the following.

Moments of the distribution $\Pi_n(t)$

In the following $S = S_F$ will refer to the intensity of the source and $S_\alpha = 0$. We now compute the moment of the distribution $\Pi_n(t)$. Then we provide the proof of the analytical expression of the first simple moment of $(\Pi_{n,\infty})_{n \in \mathbb{N}}$

Proof. From the equation 1.191, we know that

$$\bar{\nu}_{\Pi}(T) - \bar{\nu}_{\Pi}(t) = -\bar{\nu}_S S e^{-\alpha T} \frac{(e^{\alpha T} - e^{\alpha t})}{\alpha} \quad (\text{A.50})$$

Then we obtain the eq. 2.9

$$\boxed{\bar{\nu}_{\Pi}(t) = \bar{\nu}_S S \frac{1 - e^{-\alpha(T-t)}}{\alpha}} \quad (\text{A.51})$$

And so, we obtain the eq. 2.1.4

$$\boxed{\bar{\nu}_{\Pi,\infty} = \frac{\bar{\nu}_S S}{\alpha}} \quad (\text{A.52})$$

□

Now we dispose of the expression of $\bar{\nu}_{\Pi}(t)$ and $\bar{\nu}_{\Pi,\infty}$.

Then we provide the proof of the analytical expression and property of $\nu_{2,\Pi}(t)$.

Proof. Starting from 1.194

$$\begin{aligned} -\frac{\partial \nu_{2,\Pi}}{\partial t} &= \bar{\nu}_S S \left(\bar{\nu}_S S \frac{1 - e^{-\alpha(T-t)}}{\alpha} e^{-\alpha(T-t)} + \frac{\nu_2}{-\rho \bar{\nu}} e^{-\alpha(T-t)} (1 - e^{-\alpha(T-t)}) \right) + \nu_{2S} S e^{-2\alpha(T-t)} \\ &= \bar{\nu}_S S \left(\frac{\bar{\nu}_S S}{\alpha} + \frac{\nu_2}{-\rho \bar{\nu}} \right) (e^{-\alpha T} e^{\alpha t} - e^{-2\alpha T} e^{2\alpha t}) + \nu_{2S} S e^{-2\alpha T} e^{2\alpha t} \end{aligned} \quad (\text{A.53})$$

Integrating between T and t , we obtain

$$\begin{aligned} \nu_{2,\Pi}(T) - \nu_{2,\Pi}(t) &= -\bar{\nu}_S S \left(\frac{\bar{\nu}_S S}{\alpha} + \frac{\nu_2}{-\rho \bar{\nu}} \right) \left(e^{-\alpha T} \frac{e^{\alpha T} - e^{\alpha t}}{\alpha} - e^{-2\alpha T} \frac{e^{2\alpha T} - e^{2\alpha t}}{2\alpha} \right) \\ &\quad - \nu_{2S} S e^{-2\alpha T} \frac{e^{2\alpha T} - e^{2\alpha t}}{2\alpha} \end{aligned} \quad (\text{A.54})$$

What enables us to deduce the eq. 2.11, by the use of A.51

$$\boxed{\nu_{2,\Pi}(t) = \bar{\nu}_S S \left(\frac{\bar{\nu}_S S}{\alpha} + \frac{\nu_2}{-\rho \bar{\nu}} \right) \frac{1 - e^{-\alpha(T-t)}}{\alpha} + \left(-\bar{\nu}_S S \left(\frac{\bar{\nu}_S S}{\alpha} + \frac{\nu_2}{-\rho \bar{\nu}} \right) + \nu_{2S} S \right) \frac{1 - e^{-2\alpha(T-t)}}{2\alpha}} \quad (\text{A.55})$$

When $T - t \rightarrow +\infty$, we obtain the eq. 2.12

$$\boxed{\nu_{2,\Pi,\infty} = \frac{S}{2\alpha} \left(\bar{\nu}_S \frac{\nu_2}{-\rho \bar{\nu}} + \nu_{2S} \right) + \frac{\bar{\nu}_S^2 S^2}{2\alpha^2}} \quad (\text{A.56})$$

□

Now we dispose of the expression of $\nu_{2,\Pi}$ and $\nu_{2,\Pi,\infty}$.

Then we provide a proof of the analytical expression and property of $\nu_{3,\Pi}(t)$

Proof. Starting from 1.196, we obtain

$$-\frac{d}{dt}\nu_{3,\Pi} = S(\nu_{2,\Pi}\bar{\nu}_\pi\bar{\nu}_S + \nu_{\Pi}(\nu_{2\pi}\bar{\nu}_S + \bar{\nu}_\pi^2\nu_{2S}) + \nu_{3,\pi}\bar{\nu}_S + 2\bar{\nu}_\pi\nu_{2,\pi}\nu_{2S} + \bar{\nu}_\pi^3\nu_{3S}), \quad \nu_{3,\Pi}(T) = 0 \quad (\text{A.57})$$

This equation has 6 sub-members, we compute them here. The first sub-member is

$$\begin{aligned} & \bar{\nu}_S S \nu_{2,\Pi}(t) \bar{\nu}_\pi(t) \\ &= \bar{\nu}_S S \left(\bar{\nu}_S S \left(\frac{\bar{\nu}_S S}{\alpha} + \frac{\nu_2}{-\rho\bar{\nu}} \right) \frac{1 - e^{-\alpha(T-t)}}{\alpha} + \left(-\bar{\nu}_S S \left(\frac{\bar{\nu}_S S}{\alpha} + \frac{\nu_2}{-\rho\bar{\nu}} \right) + \nu_{2S} S \right) \frac{1 - e^{-2\alpha(T-t)}}{2\alpha} \right) e^{-\alpha(T-t)} \\ &= \bar{\nu}_S S \left(\bar{\nu}_S S \left(\frac{\bar{\nu}_S S}{\alpha} + \frac{\nu_2}{-\rho\bar{\nu}} \right) \frac{e^{-\alpha(T-t)} - e^{-2\alpha(T-t)}}{\alpha} \right. \\ &+ \left. \left(-\bar{\nu}_S S \left(\frac{\bar{\nu}_S S}{\alpha} + \frac{\nu_2}{-\rho\bar{\nu}} \right) + \bar{\nu}_S \nu_{2S} S^2 \right) \frac{e^{-\alpha(T-t)} - e^{-3\alpha(T-t)}}{2\alpha} \right) \\ &= \left(\frac{(\bar{\nu}_S S)^2}{\alpha} \left(\frac{\bar{\nu}_S S}{\alpha} + \frac{\nu_2}{-\rho\bar{\nu}} \right) - \left(\frac{(\bar{\nu}_S S)^2}{2\alpha} \left(\frac{\bar{\nu}_S S}{\alpha} + \frac{\nu_2}{-\rho\bar{\nu}} \right) - \frac{\bar{\nu}_S \nu_{2S} S^2}{2\alpha} \right) \right) e^{-\alpha(T-t)} \\ &- \left(\frac{(\bar{\nu}_S S)^2}{\alpha} \left(\frac{\bar{\nu}_S S}{\alpha} + \frac{\nu_2}{-\rho\bar{\nu}} \right) \right) e^{-2\alpha(T-t)} + \left(\frac{(\bar{\nu}_S S)^2}{2\alpha} \left(\frac{\bar{\nu}_S S}{\alpha} + \frac{\nu_2}{-\rho\bar{\nu}} \right) - \frac{\bar{\nu}_S \nu_{2S} S^2}{2\alpha} \right) e^{-3\alpha(T-t)} \\ &= \left(\frac{(\bar{\nu}_S S)^2}{2\alpha} \left(\frac{\bar{\nu}_S S}{\alpha} + \frac{\nu_2}{-\rho\bar{\nu}} \right) + \frac{\bar{\nu}_S \nu_{2S} S^2}{2\alpha} \right) e^{-\alpha(T-t)} \\ &- \left(\frac{(\bar{\nu}_S S)^2}{\alpha} \left(\frac{\bar{\nu}_S S}{\alpha} + \frac{\nu_2}{-\rho\bar{\nu}} \right) \right) e^{-2\alpha(T-t)} \\ &+ \left(\frac{(\bar{\nu}_S S)^2}{2\alpha} \left(\frac{\bar{\nu}_S S}{\alpha} + \frac{\nu_2}{-\rho\bar{\nu}} \right) - \frac{\bar{\nu}_S \nu_{2S} S^2}{2\alpha} \right) e^{-3\alpha(T-t)} \end{aligned} \quad (\text{A.58})$$

The second sub-member is

$$\begin{aligned} \bar{\nu}_S S \bar{\nu}_{\Pi}(t) \nu_{2,\pi}(t) &= (\bar{\nu}_S S)^2 \frac{1 - e^{-\alpha(T-t)}}{\alpha} \frac{\nu_2}{-\rho\bar{\nu}} e^{-\alpha(T-t)} (1 - e^{-\alpha(T-t)}) \\ &= \frac{(\bar{\nu}_S S)^2}{\alpha} \frac{\nu_2}{-\rho\bar{\nu}} e^{-\alpha(T-t)} (1 - e^{-\alpha(T-t)})^2 \\ &= \frac{(\bar{\nu}_S S)^2}{\alpha} \frac{\nu_2}{-\rho\bar{\nu}} e^{-\alpha(T-t)} (1 - 2e^{-\alpha(T-t)} + e^{-2\alpha(T-t)}) \\ &= \frac{(\bar{\nu}_S S)^2}{\alpha} \frac{\nu_2}{-\rho\bar{\nu}} (e^{-\alpha(T-t)} - 2e^{-2\alpha(T-t)} + e^{-3\alpha(T-t)}) \end{aligned} \quad (\text{A.59})$$

The third sub-member is

$$\begin{aligned} \nu_{2S} S \bar{\nu}_{\Pi}(t) \bar{\nu}_\pi^2(t) &= \nu_{2S} \bar{\nu}_S S^2 \frac{1 - e^{-\alpha(T-t)}}{\alpha} e^{-2\alpha(T-t)} \\ &= \nu_{2S} \frac{\bar{\nu}_S S^2}{\alpha} (e^{-2\alpha(T-t)} - e^{-3\alpha(T-t)}) \end{aligned} \quad (\text{A.60})$$

Using the computation done for the second sub-member, the fourth sub-member is

$$\begin{aligned}
\bar{\nu}_S S \nu_{3,\pi}(t) &= \bar{\nu}_S S \frac{e^{-\alpha(T-t)}}{-\rho\bar{\nu}} \left(\frac{\nu_2^2}{-\rho\bar{\nu}} (1 - e^{-\alpha(T-t)})^2 + \nu_3 \frac{1 - e^{-2\alpha(T-t)}}{2} \right) \\
&= \frac{\bar{\nu}_S S}{-\rho\bar{\nu}} \left(\frac{\nu_2^2}{-\rho\bar{\nu}} (e^{-\alpha(T-t)} - 2e^{-2\alpha(T-t)} + e^{-3\alpha(T-t)}) + \nu_3 \frac{e^{-\alpha(T-t)} - e^{-3\alpha(T-t)}}{2} \right) \\
&= \frac{\bar{\nu}_S S}{-\rho\bar{\nu}} \left(\frac{\nu_2^2}{-\rho\bar{\nu}} + \frac{\nu_3}{2} \right) e^{-\alpha(T-t)} \\
&\quad - 2\bar{\nu}_S S \frac{\nu_2^2}{(-\rho\bar{\nu})^2} e^{-2\alpha(T-t)} \\
&\quad + \frac{\bar{\nu}_S S}{-\rho\bar{\nu}} \left(\frac{\nu_2^2}{-\rho\bar{\nu}} - \frac{\nu_3}{2} \right) e^{-3\alpha(T-t)}
\end{aligned} \tag{A.61}$$

The fifth sub-member is

$$\begin{aligned}
2\nu_{2S} S \bar{\nu}_\pi(t) \nu_{2,\pi}(t) &= 2\nu_{2S} S e^{-\alpha(T-t)} \frac{\nu_2}{-\rho\bar{\nu}} e^{-\alpha(T-t)} (1 - e^{-\alpha(T-t)}) \\
&= 2\nu_{2S} S \frac{\nu_2}{-\rho\bar{\nu}} e^{-2\alpha(T-t)} (1 - e^{-\alpha(T-t)}) \\
&= 2\nu_{2S} S \frac{\nu_2}{-\rho\bar{\nu}} (e^{-2\alpha(T-t)} - e^{-3\alpha(T-t)})
\end{aligned} \tag{A.62}$$

The sixth sub-member is

$$\nu_{3S} S \bar{\nu}_\pi^3(t) = \nu_{3S} S e^{-3\alpha(T-t)} \tag{A.63}$$

Now, each sub-member can be integrated between t and T we use the key integral of equation A.13, then the first member integrated provides

$$\begin{aligned}
&\int_t^T \bar{\nu}_S S \nu_{2,\Pi}(s) \bar{\nu}_\pi(s) ds \\
&= \left(\frac{(\bar{\nu}_S S)^2}{2\alpha} \left(\frac{\bar{\nu}_S S}{\alpha} + \frac{\nu_2}{-\rho\bar{\nu}} \right) + \frac{\bar{\nu}_S \nu_{2S} S^2}{2\alpha} \right) \frac{1 - e^{-\alpha(T-t)}}{\alpha} \\
&\quad - \left(\frac{(\bar{\nu}_S S)^2}{\alpha} \left(\frac{\bar{\nu}_S S}{\alpha} + \frac{\nu_2}{-\rho\bar{\nu}} \right) \right) \frac{1 - e^{-2\alpha(T-t)}}{2\alpha} \\
&\quad + \left(\frac{(\bar{\nu}_S S)^2}{2\alpha} \left(\frac{\bar{\nu}_S S}{\alpha} + \frac{\nu_2}{-\rho\bar{\nu}} \right) - \frac{\bar{\nu}_S \nu_{2S} S^2}{2\alpha} \right) \frac{1 - e^{-3\alpha(T-t)}}{3\alpha}
\end{aligned} \tag{A.64}$$

Then the limit of this quantity when $T - t \rightarrow +\infty$

$$\lim_{T-t \rightarrow +\infty} \int_t^T \bar{\nu}_S S \nu_{2,\Pi}(s) \bar{\nu}_\pi(s) ds = \frac{(\bar{\nu}_S S)^2}{6\alpha^2} \left(\frac{\bar{\nu}_S S}{\alpha} + \frac{\nu_2}{-\rho\bar{\nu}} \right) + \frac{\bar{\nu}_S \nu_{2S} S^2}{3\alpha^2} \tag{A.65}$$

The second member integrated between t and T provides

$$\int_t^T \bar{\nu}_S S \bar{\nu}_\pi(s) \nu_{2,\pi}(s) ds = \frac{(\bar{\nu}_S S)^2}{\alpha} \frac{\nu_2}{-\rho\bar{\nu}} \left(\frac{1 - e^{-\alpha(T-t)}}{\alpha} - 2 \frac{1 - e^{-2\alpha(T-t)}}{2\alpha} + \frac{1 - e^{-3\alpha(T-t)}}{3\alpha} \right) \tag{A.66}$$

This quantity has a limit when $T - t \rightarrow +\infty$

$$\lim_{T-t \rightarrow +\infty} \int_t^T \bar{\nu}_S S \bar{\nu}_{II}(s) \nu_{2,\pi}(s) ds = \frac{(\bar{\nu}_S S)^2}{3\alpha^2} \frac{\nu_2}{-\rho \bar{\nu}} \quad (\text{A.67})$$

The third member provides

$$\int_t^T \nu_{2S} \bar{\nu}_{II}(s) \bar{\nu}_\pi^2(s) = \nu_{2S} \frac{\bar{\nu}_S S}{\alpha} \left(\frac{1 - e^{-2\alpha(T-t)}}{2\alpha} - \frac{1 - e^{-3\alpha(T-t)}}{3\alpha} \right) \quad (\text{A.68})$$

Then the previous quantity has a limit when $T - t \rightarrow +\infty$

$$\lim_{T-t \rightarrow +\infty} \int_t^T \nu_{2S} \bar{\nu}_{II}(s) \bar{\nu}_\pi^2(s) = \frac{\nu_{2S} \bar{\nu}_S S}{6\alpha^2} \quad (\text{A.69})$$

The fourth member integrated over time is

$$\begin{aligned} \int_t^T \bar{\nu}_S S \nu_{3,\pi}(s) ds &= \frac{\bar{\nu}_S S}{-\rho \bar{\nu}} \left(\frac{\nu_2^2}{-\rho \bar{\nu}} + \frac{\nu_3}{2} \right) \frac{1 - e^{-\alpha(T-t)}}{\alpha} \\ &\quad - 2\bar{\nu}_S S \frac{\nu_2^2}{(-\rho \bar{\nu})^2} \frac{1 - e^{-2\alpha(T-t)}}{2\alpha} \\ &\quad + \frac{\bar{\nu}_S S}{-\rho \bar{\nu}} \left(\frac{\nu_2^2}{-\rho \bar{\nu}} - \frac{\nu_3}{2} \right) \frac{1 - e^{-3\alpha(T-t)}}{3\alpha} \end{aligned} \quad (\text{A.70})$$

This quantity has a limit when $T - t \rightarrow +\infty$

$$\lim_{T-t \rightarrow +\infty} \int_t^T \bar{\nu}_S S \nu_{3,\pi}(s) ds = \frac{\bar{\nu}_S S}{-\rho \bar{\nu}} \left(\frac{1}{3} \frac{\nu_2^2}{-\rho \bar{\nu}} + \frac{\nu_3}{3} \right) \quad (\text{A.71})$$

The fifth member integrated between t and T is

$$\int_t^T 2\nu_{2S} S \bar{\nu}_\pi(s) \nu_{2,\pi}(s) ds = 2\nu_{2S} S \frac{\nu_2}{-\rho \bar{\nu}} \left(\frac{1 - e^{-2\alpha(T-t)}}{2\alpha} - \frac{1 - e^{-3\alpha(T-t)}}{3\alpha} \right) \quad (\text{A.72})$$

When $T - t \rightarrow +\infty$ this quantity tends to

$$\lim_{T-t \rightarrow +\infty} \int_t^T 2\nu_{2S} S \bar{\nu}_\pi(s) \nu_{2,\pi}(s) ds = \frac{\nu_{2S} S}{3\alpha} \frac{\nu_2}{-\rho \bar{\nu}} \quad (\text{A.73})$$

The sixth sub-member integrated is

$$\int_t^T \nu_{3S} S \bar{\nu}_\pi^3(s) ds = \nu_{3S} S \frac{1 - e^{-3\alpha(T-t)}}{3\alpha} \quad (\text{A.74})$$

The limit of the previous quantity when $T - t \rightarrow +\infty$ is

$$\lim_{T-t \rightarrow +\infty} \int_t^T \nu_{3S} S \bar{\nu}_\pi^3(s) ds = \frac{\nu_{3S} S}{3\alpha} \quad (\text{A.75})$$

Then the whole expression integrated between t and T is

$$\begin{aligned}
& \nu_{3,\Pi}(t) - \nu_{3,\Pi}(T) \\
&= \left[\left(\frac{(\bar{\nu}_S S)^2}{2\alpha} \left(\frac{\bar{\nu}_S S}{\alpha} + \frac{\nu_2}{-\rho\bar{\nu}} \right) + \frac{\bar{\nu}_S \nu_{2S} S^2}{2\alpha} \right) + \frac{(\bar{\nu}_S S)^2}{\alpha} \frac{\nu_2}{-\rho\bar{\nu}} + \frac{\bar{\nu}_S S}{-\rho\bar{\nu}} \left(\frac{\nu_2^2}{-\rho\bar{\nu}} + \frac{\nu_3}{2} \right) \right] \frac{1 - e^{-\alpha(T-t)}}{\alpha} \\
&+ \left[- \left(\frac{(\bar{\nu}_S S)^2}{\alpha} \left(\frac{\bar{\nu}_S S}{\alpha} + \frac{\nu_2}{-\rho\bar{\nu}} \right) \right) - 2 \frac{(\bar{\nu}_S S)^2}{\alpha} \frac{\nu_2}{-\rho\bar{\nu}} \right. \\
&+ \left. \frac{\bar{\nu}_S \nu_{2S} S^2}{\alpha} - 2 \bar{\nu}_S S \frac{\nu_2^2}{(-\rho\bar{\nu})^2} + 2 \nu_{2S} S \frac{\nu_2}{-\rho\bar{\nu}} \right] \frac{1 - e^{-2\alpha(T-t)}}{2\alpha} \\
&+ \left[\left(\frac{(\bar{\nu}_S S)^2}{2\alpha} \left(\frac{\bar{\nu}_S S}{\alpha} + \frac{\nu_2}{-\rho\bar{\nu}} \right) - \frac{\bar{\nu}_S \nu_{2S} S^2}{2\alpha} \right) + \frac{(\bar{\nu}_S S)^2}{\alpha} \frac{\nu_2}{-\rho\bar{\nu}} \right. \\
&- \left. \frac{\bar{\nu}_S \nu_{2S} S^2}{\alpha} + \frac{\bar{\nu}_S S}{-\rho\bar{\nu}} \left(\frac{\nu_2^2}{-\rho\bar{\nu}} - \frac{\nu_3}{2} \right) - 2 \nu_{2S} S \frac{\nu_2}{-\rho\bar{\nu}} + \nu_{3S} S \right] \frac{1 - e^{-3\alpha(T-t)}}{3\alpha}
\end{aligned} \tag{A.76}$$

Finally, by taking into account $\nu_{3,\Pi}(T) = 0$, the simplified expressions of the moment of order 3 of the neutron present in the system in presence of a source is, as in eq. 2.13,

$$\begin{aligned}
\nu_{3,\Pi}(t) &= \left[\left(\frac{(\bar{\nu}_S S)^2}{2\alpha} \left(\frac{\bar{\nu}_S S}{\alpha} + 3 \frac{\nu_2}{-\rho\bar{\nu}} \right) + \frac{\bar{\nu}_S \nu_{2S} S^2}{2\alpha} \right) + \frac{\bar{\nu}_S S}{-\rho\bar{\nu}} \left(\frac{\nu_2^2}{-\rho\bar{\nu}} + \frac{\nu_3}{2} \right) \right] \frac{1 - e^{-\alpha(T-t)}}{\alpha} \\
&+ \left[- \left(\frac{(\bar{\nu}_S S)^2}{\alpha} \left(\frac{\bar{\nu}_S S}{\alpha} + 3 \frac{\nu_2}{-\rho\bar{\nu}} \right) \right) + \frac{\bar{\nu}_S \nu_{2S} S^2}{\alpha} - 2 \bar{\nu}_S S \frac{\nu_2^2}{(-\rho\bar{\nu})^2} + 2 \nu_{2S} S \frac{\nu_2}{-\rho\bar{\nu}} \right] \frac{1 - e^{-2\alpha(T-t)}}{2\alpha} \\
&+ \left[\left(\frac{(\bar{\nu}_S S)^2}{2\alpha} \left(\frac{\bar{\nu}_S S}{\alpha} + 3 \frac{\nu_2}{-\rho\bar{\nu}} \right) - \frac{3 \bar{\nu}_S \nu_{2S} S^2}{2\alpha} \right) \right. \\
&+ \left. \frac{\bar{\nu}_S S}{-\rho\bar{\nu}} \left(\frac{\nu_2^2}{-\rho\bar{\nu}} - \frac{\nu_3}{2} \right) - 2 \nu_{2S} S \frac{\nu_2}{-\rho\bar{\nu}} + \nu_{3S} S \right] \frac{1 - e^{-3\alpha(T-t)}}{3\alpha}
\end{aligned} \tag{A.77}$$

Now we consider the asymptotic integrated sub-members in order to compute $\nu_{3,\Pi,\infty}$.

The first term in $\frac{(\bar{\nu}_S S)^2}{2\alpha} \left(\frac{\bar{\nu}_S S}{\alpha} + 3 \frac{\nu_2}{-\rho\bar{\nu}} \right) \frac{1}{\alpha}$ cancels with the corresponding term in the line below.

Then the next term $\frac{\bar{\nu}_S \nu_{2S} S^2}{\alpha}$ in $\frac{1}{\alpha}$ is added to the second term in $\frac{1}{2\alpha}$ and the second term in $\frac{1}{3\alpha}$

$$\frac{\bar{\nu}_S \nu_{2S} S^2}{2\alpha} \left(\frac{1}{\alpha} + \frac{1}{2\alpha} - \frac{1}{2\alpha} \right) = \frac{\bar{\nu}_S S}{\alpha} \frac{S}{2\alpha} \nu_{2S} \tag{A.78}$$

The next term $\frac{\bar{\nu}_S S}{-\rho\bar{\nu}} \frac{\nu_2^2}{-\rho\bar{\nu}}$ in $\frac{1}{\alpha}$ with the third term in $\frac{1}{2\alpha}$ and the third term in $\frac{1}{3\alpha}$

$$\frac{\bar{\nu}_S S}{-\rho\bar{\nu}} \frac{\nu_2^2}{-\rho\bar{\nu}} \left(\frac{1}{\alpha} - 2 \frac{1}{2\alpha} + \frac{1}{3\alpha} \right) = \frac{S}{3\alpha} \frac{\bar{\nu}_S}{-\rho\bar{\nu}} \frac{\nu_2^2}{-\rho\bar{\nu}} \tag{A.79}$$

Then, the last term $\frac{\bar{\nu}_S S}{-\rho\bar{\nu}} \frac{\nu_3}{2}$ in $\frac{1}{\alpha}$ can be added to the sixth term in $\frac{1}{3\alpha}$

$$\frac{\bar{\nu}_S S}{-\rho\bar{\nu}} \frac{\nu_3}{2} \left(\frac{1}{\alpha} - \frac{1}{3\alpha} \right) = \frac{S}{3\alpha} \frac{\bar{\nu}_S}{-\rho\bar{\nu}} \nu_3 \tag{A.80}$$

Now we consider the remaining term $2\nu_{2S}S\frac{\nu_2}{-\rho\bar{\nu}}$ in $\frac{1}{2\alpha}$ can be added to the seventh term in $\frac{1}{3\alpha}$

$$2\nu_{2S}S\frac{\nu_2}{-\rho\bar{\nu}}\left(\frac{1}{2\alpha} - \frac{1}{3\alpha}\right) = \frac{S}{3\alpha} \frac{\bar{\nu}_S}{-\rho\bar{\nu}} \frac{\nu_2\nu_{2S}}{-\rho\bar{\nu}} \quad (\text{A.81})$$

The second term $\frac{(\bar{\nu}_S S)^2}{2\alpha} 3\frac{\nu_2}{-\rho\bar{\nu}}$ in $\frac{1}{3\alpha}$ can be rewritten

$$\frac{(\bar{\nu}_S S)^2}{2\alpha} 3\frac{\nu_2}{-\rho\bar{\nu}} \frac{1}{3\alpha} = \frac{\bar{\nu}_S S}{\alpha} \frac{S}{2\alpha} \bar{\nu}_S \frac{\nu_2}{-\rho\bar{\nu}} \quad (\text{A.82})$$

The two remaining terms in $\frac{1}{3\alpha}$ are $\frac{\bar{\nu}_S^3 S^3}{6\alpha^3}$ and $\frac{S}{3\alpha}\nu_{3S}$. Then adding equations A.79, A.80, A.81 and $\frac{S}{3\alpha}\nu_{3S}$, adding equations A.78 and A.82, and adding also $\frac{\bar{\nu}_S^3 S^3}{6\alpha^3}$, we obtain the eq. 2.14

$$\nu_{3,II,\infty} = \frac{S}{3\alpha} \left(\frac{\bar{\nu}_S}{-\rho\bar{\nu}} \left(\frac{\nu_2^2}{-\rho\bar{\nu}} + \nu_3 \right) + \frac{\nu_2\nu_{2S}}{-\rho\bar{\nu}} + \nu_{3S} \right) + \frac{\bar{\nu}_S S}{\alpha} \frac{S}{2\alpha} \left(\bar{\nu}_S \frac{\nu_2}{-\rho\bar{\nu}} + \nu_{2S} \right) + \frac{\bar{\nu}_S^3 S^3}{6\alpha^3} \quad (\text{A.83})$$

□

We now dispose of all the expression of the moment for the presence of the neutron in the system

- at time t , $\bar{\nu}_\pi(t)$, $\nu_{2,\pi}(t)$, $\nu_{3,\pi}(t)$ and $\bar{\nu}_{II}(t)$, $\nu_{2,II}(t)$, $\nu_{3,II}(t)$,
- their asymptotic values 0 and $\bar{\nu}_{II,\infty}$, $\nu_{2,II,\infty}$, $\nu_{3,II,\infty}$.

A.2.4 Moments of the distribution of detection $p_n(t)$, $P_n(t)$, $Q_n(t)$

Here we provide the detail of all the computation needed for the moments of the distribution of the neutron detected $p_n(t)$, $P_n(t)$, $Q_n(t)$.

Moments of the distribution $p_n(t)$

First, we provide a proof of the analytical expression of the first moment of $(p_n(t))_{n \in \mathbb{N}}$.

Proof. For the moment of order 1, by differentiating the equation 1.214 with respect to x then evaluating in $x = 1$, we obtain

$$-\frac{dm_1}{dt}(t) + \lambda_T m_1(t) = \lambda_F \sum_{\nu=0}^{\infty} \nu f_\nu m_1(t) + \lambda_C \varepsilon_C, \quad m_1(T) = 0 \quad (\text{A.84})$$

which becomes

$$-\frac{dm_1}{dt}(t) + (\lambda_T - \lambda_F \bar{\nu}) m_1(t) = \lambda_C \varepsilon_C \quad (\text{A.85})$$

but, as $\alpha = \lambda_T - \lambda_F \bar{\nu}$, we can deduce that

$$-\frac{1}{\alpha} \frac{dm_1}{dt}(t) + m_1(t) = \frac{\lambda_F \varepsilon_F}{\alpha} \quad (\text{A.86})$$

Moreover, we know the fact that

$$\begin{aligned}\frac{\lambda_F}{\alpha} &= \frac{\lambda_F}{\lambda_T - \bar{\nu}\lambda_F} \\ &= \frac{1}{\bar{\nu}} \frac{1}{\frac{\lambda_T}{\bar{\nu}\lambda_F} - 1} \\ &= \frac{1}{-\rho\bar{\nu}}\end{aligned}\tag{A.87}$$

because $\rho = 1 - \frac{\lambda_T}{\bar{\nu}\lambda_F}$.

The knowledge of the differential equations allows obtaining the simple moments in the absence of a source, we need to compute them.

We suppose here that $s \in [t, T]$. Computing the simple moment of order 1 in the absence of a source, we search to solve the differential equation

$$-\frac{1}{\alpha} \frac{dm_1}{ds} + m_1 = \frac{\varepsilon_F}{-\rho\bar{\nu}}, \quad m_1(T) = 0\tag{A.88}$$

with homogeneous equation associated

$$-\frac{1}{\alpha} \frac{dm_1}{ds} + m_1 = 0\tag{A.89}$$

the corresponding solution is

$$m_{1H} = Ke^{\alpha s}\tag{A.90}$$

A particular solution of the equation A.88

$$m_{1particuliere} = \frac{\varepsilon_F}{-\rho\bar{\nu}}\tag{A.91}$$

So, we dispose of

$$m_1 = Ke^{\alpha s} + \frac{\varepsilon_F}{-\rho\bar{\nu}}\tag{A.92}$$

Moreover, we are in the presence of the initial condition

$$m_1(T) = 0\tag{A.93}$$

Which signifies that

$$K = -\frac{\varepsilon_F}{-\rho\bar{\nu}}e^{-\alpha T}\tag{A.94}$$

So, when $t < T$

$$\mathbb{E}[N_{[t,T]}]_{(p_n(t))_n} = m_1(t) = \frac{\varepsilon_F}{-\rho\bar{\nu}}(1 - e^{-\alpha(T-t)})\tag{A.95}$$

Thus, we can conclude eq. 2.32

$$\boxed{\mathbb{E}[N_{[t,T]}]_{(p_n(t))_n} = m_1(t) = \frac{\varepsilon_F}{-\rho\bar{\nu}}(1 - e^{-\alpha(T-t)})}\tag{A.96}$$

□

Then we dispose of the expression of $p_n(t)$.

Now we compute the moment of order 2 of $p_n(t)$, $m_2(t)$. So we provide the proof of the analytical expression of the second moment of $(p_n(t))_{n \in \mathbb{N}}$

Proof. Differentiating two times the equation 1.214 with respect to x then evaluating in $x = 1$, we obtain

$$-\frac{1}{\alpha} \frac{dm_2}{dt} + m_2 = \frac{\nu_2}{-\rho\bar{\nu}} m_1^2, \quad m_2(T) = 0 \quad (\text{A.97})$$

The associated homogeneous equation is the same as for m_1 , we refer the reader to the previous computations.

Using the previous expression by introducing the expression of m_1 , we obtain

$$-\frac{1}{\alpha} \frac{dm_2}{dt} + m_2 = \frac{\nu_2}{-\rho\bar{\nu}} \left(\frac{\varepsilon_F}{-\rho\bar{\nu}} \right)^2 (1 - e^{-\alpha(T-t)})^2, \quad m_2(T) = 0 \quad (\text{A.98})$$

the second member of the differential equation in question is an exponential polynomial, so we search a particular solution of the form of an exponential polynomial. More explicitly, this equation becomes for $\tau = T - t$

$$\frac{dm_2}{d\tau} + \alpha m_2 = \alpha \frac{\nu_2}{-\rho\bar{\nu}} \left(\frac{\varepsilon_F}{-\rho\bar{\nu}} \right)^2 (1 - e^{-\alpha\tau})^2, \quad m_2(0) = 0 \quad (\text{A.99})$$

multiplying by $e^{\alpha\tau}$, we obtain

$$\frac{dm_2 e^{\alpha\tau}}{d\tau} = \alpha e^{\alpha\tau} \frac{\nu_2}{-\rho\bar{\nu}} \left(\frac{\varepsilon_F}{-\rho\bar{\nu}} \right)^2 (1 - e^{-\alpha\tau})^2, \quad m_2(0) = 0 \quad (\text{A.100})$$

integrating between 0 and t , we obtain

$$\begin{aligned} m_2 &= \alpha e^{-\alpha\tau} \frac{\nu_2}{-\rho\bar{\nu}} \left(\frac{\varepsilon_F}{-\rho\bar{\nu}} \right)^2 \int_0^\tau e^{\alpha u} (1 - e^{-\alpha u})^2 du, \quad m_2(0) = 0 \\ &= \alpha e^{-\alpha\tau} \frac{\nu_2}{-\rho\bar{\nu}} \left(\frac{\varepsilon_F}{-\rho\bar{\nu}} \right)^2 \int_0^\tau (e^{\alpha u} - 2 + e^{-\alpha\tau}) du \\ &= \frac{\nu_2}{-\rho\bar{\nu}} \left(\frac{\varepsilon_F}{-\rho\bar{\nu}} \right)^2 \alpha e^{-\alpha\tau} \left(\frac{e^{\alpha\tau} - 1}{\alpha} - 2\tau + \frac{e^{-\alpha\tau} - 1}{-\alpha} \right) \end{aligned} \quad (\text{A.101})$$

We can deduce the eq. 2.35

$$\boxed{m_2(t) = \frac{\nu_2 \varepsilon_F^2}{(-\rho\bar{\nu})^3} (1 - 2\alpha(T-t)e^{-\alpha(T-t)} - e^{-2\alpha(T-t)})} \quad (\text{A.102})$$

But, we know that

$$\begin{aligned} \mathbb{E}[N_{[t,T]}^2]_{(p_n(t))_n} &= \left[\frac{\partial^2 g}{\partial x^2} \right]_{x=1} (t) + \left[\frac{\partial g}{\partial x} \right]_{x=1} (t) \\ &= 2m_2(t) + m_1(t) \end{aligned} \quad (\text{A.103})$$

To conclude, we dispose of eq. 2.34

$$\mathbb{E}[N_{[t,T]}^2]_{(p_n(t))_n} = 2 \frac{\nu_2 \varepsilon_F^2}{(-\rho \bar{\nu})^3} (1 - 2\alpha(T-t)e^{-\alpha(T-t)} - e^{-2\alpha(T-t)}) + \frac{\varepsilon_F}{-\rho \bar{\nu}} (1 - e^{-\alpha(T-t)}) \quad (\text{A.104})$$

□

Now we dispose of the expression of the moment of order 2 of $p_n(t)$, $m_2(t)$ and the associated simple moment $\mathbb{E}[N_{[t,T]}^2]_{(p_n(t))_n}$.

Then we compute the expression of the moments of order 3 of $p_n(t)$. Here is the proof of the analytical expression of the third simple moment of $(p_n(t))_{n \in \mathbb{N}}$

Proof. Deriving three time the equation 1.214 with respect to x then evaluating in $x = 1$, we are in presence of

$$-\frac{1}{\alpha} \frac{dm_3}{dt} + m_3 = \frac{1}{-\rho \bar{\nu}} (\nu_3 m_1^3 + 2\nu_2 m_1 m_2), \quad m_3(T) = 0 \quad (\text{A.105})$$

We retold the solution of the homogeneous associated equation is given by

$$m_3(t) = cste e^{\alpha t} \quad (\text{A.106})$$

Reinjecting the expression of m_1 and m_2 in A.105, we dispose of

$$\begin{aligned} -\frac{1}{\alpha} \frac{dm_3}{dt} + m_3 &= \frac{1}{-\rho \bar{\nu}} \nu_3 \frac{\varepsilon_F^3}{(-\rho \bar{\nu})^3} (1 - e^{-\alpha(T-t)})^3 \\ &+ 2\nu_2 \frac{\varepsilon_F}{-\rho \bar{\nu}} (1 - e^{-\alpha(T-t)}) \frac{\nu_2 \varepsilon_F^2}{(-\rho \bar{\nu})^3} (1 - 2\alpha(T-t)e^{-\alpha(T-t)} - e^{-2\alpha(T-t)}), \quad m_3(T) = 0 \end{aligned} \quad (\text{A.107})$$

By the use of the change of variable $\tau = T - t$, and multiplying by $e^{\alpha\tau}$,

$$\begin{aligned}
\frac{dm_3 e^{\alpha\tau}}{d\tau} &= \frac{\alpha e^{\alpha\tau}}{-\rho\bar{\nu}} \left(\nu_3 \left(\frac{\varepsilon_F}{-\rho\bar{\nu}} \right)^3 (1 - e^{-\alpha\tau})^3 + 2\nu_2 \left(\frac{\varepsilon_F}{-\rho\bar{\nu}} \right) (1 - e^{-\alpha\tau}) \frac{\nu_2 \varepsilon_F^2}{(-\rho\bar{\nu})^3} (1 - 2\alpha\tau e^{-\alpha\tau} - e^{-2\alpha\tau}) \right) \\
&= \frac{\alpha}{-\rho\bar{\nu}} \left(\nu_3 \left(\frac{\varepsilon_F}{-\rho\bar{\nu}} \right)^3 e^{\alpha\tau} (1 - e^{-\alpha\tau})^3 \right. \\
&\quad \left. + 2\nu_2 \left(\frac{\varepsilon_F}{-\rho\bar{\nu}} \right) \frac{\nu_2 \varepsilon_F^2}{(-\rho\bar{\nu})^3} e^{\alpha\tau} (1 - e^{-\alpha\tau}) (1 - 2\alpha\tau e^{-\alpha\tau} - e^{-2\alpha\tau}) \right) \\
&= \frac{\alpha}{-\rho\bar{\nu}} \left(\nu_3 \left(\frac{\varepsilon_F}{-\rho\bar{\nu}} \right)^3 (1 - 3e^{-\alpha\tau} + 3e^{-2\alpha\tau} - e^{-3\alpha\tau}) e^{\alpha\tau} \right. \\
&\quad \left. + 2\nu_2^2 \frac{\varepsilon_F^3}{(-\rho\bar{\nu})^4} e^{\alpha\tau} (1 - (2\alpha\tau + 1)e^{-\alpha\tau} + (2\alpha\tau - 1)e^{-2\alpha\tau} + e^{-3\alpha\tau}) \right) \\
&= \frac{\alpha}{-\rho\bar{\nu}} \left(\nu_3 \left(\frac{\varepsilon_F}{-\rho\bar{\nu}} \right)^3 (e^{\alpha\tau} - 3 + 3e^{-\alpha\tau} - e^{-2\alpha\tau}) \right. \\
&\quad \left. + 2\nu_2^2 \frac{\varepsilon_F^3}{(-\rho\bar{\nu})^4} (e^{\alpha\tau} - (2\alpha\tau + 1) + (2\alpha\tau - 1)e^{-\alpha\tau} + e^{-2\alpha\tau}) \right) \\
&= \frac{\alpha}{-\rho\bar{\nu}} \left(\frac{\varepsilon_F}{-\rho\bar{\nu}} \right)^3 \left(\left(\nu_3 + 2 \frac{\nu_2^2}{-\rho\bar{\nu}} \right) e^{\alpha\tau} - \nu_3 - 4\alpha\tau \frac{\nu_2^2}{-\rho\bar{\nu}} - 2 \frac{\nu_2^2}{-\rho\bar{\nu}} \right) \\
&\quad \left. + \left(3\nu_3 - 2 \frac{\nu_2^2}{-\rho\bar{\nu}} \right) e^{-\alpha\tau} - \left(\nu_3 - \frac{2\nu_2^2}{-\rho\bar{\nu}} \right) e^{-2\alpha\tau} + 4\alpha\tau \frac{\nu_2^2}{-\rho\bar{\nu}} e^{-\alpha\tau} \right)
\end{aligned} \tag{A.108}$$

Integrating between 0 and τ we obtain

$$\begin{aligned}
m_3 e^{\alpha\tau} &= \frac{1}{-\rho\bar{\nu}} \left(\frac{\varepsilon_F}{-\rho\bar{\nu}} \right)^3 \left(\left(\nu_3 + 2 \frac{\nu_2^2}{-\rho\bar{\nu}} \right) (e^{\alpha\tau} - 1) - (3\nu_3 + 2 \frac{\nu_2^2}{-\rho\bar{\nu}}) \alpha\tau - 2(\alpha\tau)^2 \frac{\nu_2^2}{-\rho\bar{\nu}} \right. \\
&\quad \left. + (3\nu_3 - 2 \frac{\nu_2^2}{-\rho\bar{\nu}}) (-e^{-\alpha\tau} + 1) - \left(\nu_3 - 2 \frac{\nu_2^2}{-\rho\bar{\nu}} \right) \frac{1 - e^{-2\alpha\tau}}{2} - 4 \frac{\nu_2^2}{-\rho\bar{\nu}} \left(\alpha\tau e^{-\alpha\tau} - 1 + e^{-\alpha\tau} \right) \right)
\end{aligned} \tag{A.109}$$

What enables us to come to

$$\begin{aligned}
m_3(\tau) &= \frac{1}{-\rho\bar{\nu}} \left(\frac{\varepsilon_F}{-\rho\bar{\nu}} \right)^3 \left(\left(\nu_3 + 2 \frac{\nu_2^2}{-\rho\bar{\nu}} \right) (1 - e^{-\alpha\tau}) - (3\nu_3 + 2 \frac{\nu_2^2}{-\rho\bar{\nu}}) \alpha\tau e^{-\alpha\tau} - 2(\alpha\tau)^2 \frac{\nu_2^2}{-\rho\bar{\nu}} e^{-\alpha\tau} \right. \\
&\quad \left. + (3\nu_3 - 2 \frac{\nu_2^2}{-\rho\bar{\nu}}) (e^{-\alpha\tau} - e^{-2\alpha\tau}) - \left(\nu_3 - 2 \frac{\nu_2^2}{-\rho\bar{\nu}} \right) \frac{e^{-\alpha\tau} - e^{-3\alpha\tau}}{2} \right. \\
&\quad \left. - 4 \frac{\nu_2^2}{-\rho\bar{\nu}} \left(e^{-\alpha\tau} - \alpha\tau e^{-2\alpha\tau} - e^{-2\alpha\tau} \right) \right)
\end{aligned} \tag{A.110}$$

which becomes de facto

$$\begin{aligned}
m_3(\tau) = \frac{1}{-\rho\bar{\nu}} \left(\frac{\varepsilon_F}{-\rho\bar{\nu}} \right)^3 & \left(\nu_3 + 2 \frac{\nu_2^2}{-\rho\bar{\nu}} \right. \\
& + e^{-\alpha\tau} \left(-(\nu_3 + 2 \frac{\nu_2^2}{-\rho\bar{\nu}}) + (3\nu_3 - 2 \frac{\nu_2^2}{-\rho\bar{\nu}}) - \frac{1}{2}(\nu_3 - 2 \frac{\nu_2^2}{-\rho\bar{\nu}}) + 4 \frac{\nu_2^2}{-\rho\bar{\nu}} \right) \\
& - \alpha\tau e^{-\alpha\tau} (3\nu_3 + 2 \frac{\nu_2^2}{-\rho\bar{\nu}}) - 2 \frac{\nu_2^2}{-\rho\bar{\nu}} (\alpha\tau)^2 e^{-\alpha\tau} + e^{-2\alpha\tau} (-3\nu_3 + 2 \frac{\nu_2^2}{-\rho\bar{\nu}} - 4 \frac{\nu_2^2}{-\rho\bar{\nu}}) \\
& \left. + 4 \frac{\nu_2^2}{-\rho\bar{\nu}} \alpha\tau e^{-2\alpha\tau} + \frac{1}{2}(\nu_3 - 2 \frac{\nu_2^2}{-\rho\bar{\nu}}) e^{-3\alpha\tau} \right)
\end{aligned} \tag{A.111}$$

which is in fact

$$\begin{aligned}
m_3(\tau) = \frac{1}{-\rho\bar{\nu}} \left(\frac{\varepsilon_F}{-\rho\bar{\nu}} \right)^3 & (\nu_3 + 2 \frac{\nu_2^2}{-\rho\bar{\nu}} + (3\nu_3(\frac{1}{2} - \alpha\tau) + 2 \frac{\nu_2^2}{-\rho\bar{\nu}}(\frac{1}{2} - \alpha\tau(1 + \alpha\tau)))e^{-\alpha\tau} \\
& - (3\nu_3 + 2 \frac{\nu_2^2}{-\rho\bar{\nu}}(1 + 2\alpha\tau))e^{-2\alpha\tau} + \frac{1}{2}(\nu_3 - 2 \frac{\nu_2^2}{-\rho\bar{\nu}})e^{-3\alpha\tau})
\end{aligned} \tag{A.112}$$

Introducing the constants

$$\boxed{\begin{cases} \text{A} = \nu_3 \frac{\varepsilon_F^3}{(-\rho\bar{\nu})^4} \\ \text{B} = 2\nu_2^2 \frac{\varepsilon_F^3}{(-\rho\bar{\nu})^5} \end{cases}} \tag{A.113}$$

Finally, the expression can be rearranged as eq. 2.38

$$\boxed{\begin{aligned}
m_3(t) = & -\frac{1}{2}(-2(\text{A} + \text{B})) \\
& + (-(3\text{A} + \text{B}) + 2\alpha(T - t)(3\text{A} + \text{B}) + 2\alpha^2\text{B}(T - t)^2)e^{-\alpha(T-t)} \\
& + (2(3\text{A} + \text{B}) + 4\alpha\text{B}(T - t))e^{-2\alpha(T-t)} \\
& + (-\text{A} + \text{B})e^{-3\alpha(T-t)}
\end{aligned}} \tag{A.114}$$

But we know that

$$\begin{aligned}
\mathbb{E}[N_{[t,T]}^3]_{(p_n(t))_n} & = \left[\frac{\partial^3 g}{\partial x^3} \right]_{x=1} (t) + 3 \left[\frac{\partial^2 g}{\partial x^2} \right]_{x=1} (t) + \left[\frac{\partial g}{\partial x} \right]_{x=1} (t) \\
& = 6(m_3(t) + m_2(t)) + m_1(t)
\end{aligned} \tag{A.115}$$

We can conclude by the eq. 2.37

$$\begin{aligned} \mathbb{E}[N_{[t,T]}^3]_{(p_n(t))_n} = & 6 \left[-\frac{1}{2}(-2(A+B) + (-(3A+B) + 2\alpha(T-t)(3A+B) + 2\alpha^2 B(T-t)^2)e^{-\alpha(T-t)} \right. \\ & + (2(3A+B) + 4\alpha B(T-t))e^{-2\alpha(T-t)} + (-A+B)e^{-3\alpha(T-t)} \\ & \left. + \frac{\nu_2 \varepsilon_F^2}{(-\rho \bar{\nu})^3} (1 - 2\alpha(T-t)e^{-\alpha(T-t)} - e^{-2\alpha(T-t)}) \right] \\ & + \frac{\varepsilon_F}{-\rho \bar{\nu}} (1 - e^{-\alpha(T-t)}) \end{aligned}$$

(A.116)

□

Finally, we dispose of all the expression the three first moment of $p_n(t)$

- $m_1(t)$, $m_2(t)$, $m_3(t)$
- $\mathbb{E}[N_{[t,T]}]_{(p_n(t))_n}$, $\mathbb{E}[N_{[t,T]}^2]_{(p_n(t))_n}$, $\mathbb{E}[N_{[t,T]}^3]_{(p_n(t))_n}$

Moments of the distribution $P_n(t)$

In the following $S = S_F$ will refers to the intensity of the source and $S_\alpha = 0$. Now we will compute the three first moment of $P_n(t)$. Then we begin with the proof of Prop 2.32

Proof. We differentiate 2.39

$$\begin{aligned} \frac{\partial G}{\partial x}(x, t) = & \left\{ \int_t^T S \sum_{\nu=0}^{+\infty} \nu \hat{f}_\nu \frac{\partial g}{\partial x}(x, s) g^{\nu-1}(x, s) ds \right\} G(x, t) \\ = & \left\{ \int_0^{T-t} S \sum_{\nu=0}^{+\infty} \nu \hat{f}_\nu \frac{\partial g}{\partial x}(x, T-s) g^{\nu-1}(x, T-s) ds \right\} G(x, t) \end{aligned} \quad (\text{A.117})$$

Evaluating in $x = 1$, we find that

$$\begin{aligned} \left[\frac{\partial G}{\partial x} \right]_{x=1}(t) = & \int_0^{T-t} S \sum_{\nu=0}^{+\infty} \nu \hat{f}_\nu m_1(T-s) ds \\ = & \int_0^{T-t} S \sum_{\nu=0}^{+\infty} \nu \hat{f}_\nu \frac{\varepsilon_F}{-\rho \bar{\nu}} (1 - e^{-\alpha(T-(T-s))}) ds \\ = & S \frac{\varepsilon_F}{-\rho \bar{\nu}} \sum_{\nu=0}^{+\infty} \nu \hat{f}_\nu \int_0^{T-t} (1 - e^{-\alpha s}) ds \end{aligned} \quad (\text{A.118})$$

After the computation of the integral, we obtain eq. 2.40

$$\mathbb{E}[N_{[t,T]}]_{(P_n(t))_n} = M_1(t) = \bar{\nu} S \frac{\varepsilon_F}{-\rho \bar{\nu}} \left[(T-t) - \frac{1 - e^{-\alpha(T-t)}}{\alpha} \right] \quad (\text{A.119})$$

□

Now we dispose of the expression of the first moment of $P_n(t)$. Then we compute the moment of order 2 of the distribution $P_n(t)$. Thus, the proof of Prop 2.2.1 is

Proof. We take back the equation for 1.222 where

$$\begin{cases} m_1(T-s) = \frac{\varepsilon_F}{-\rho\bar{\nu}}(1 - e^{-\alpha(T-(T-s))}) \\ m_2(T-s) = \frac{\nu_2\varepsilon_F^2}{(-\rho\bar{\nu})^3}(1 - 2\alpha(T - (T-s))e^{-\alpha(T-(T-s))} - e^{-2\alpha(T-(T-s))}) \end{cases} \quad (\text{A.120})$$

what enables to deduce

$$\left(\int_0^{T-t} S\bar{\nu}_S m_1(T-s) ds \right)^2 = \left(\bar{\nu}_S S \frac{\varepsilon_F}{-\rho\bar{\nu}} \left[T-t - \frac{1 - e^{-\alpha(T-t)}}{\alpha} \right] \right)^2 \quad (\text{A.121})$$

and

$$\begin{aligned} \int_0^{T-t} S\nu_{2S} m_1^2(T-s) &= \nu_{2S} S \frac{\varepsilon_F^2}{(-\rho\bar{\nu})^2} \int_0^{T-t} (1 - 2e^{-\alpha s} + e^{-2\alpha s}) ds \\ &= \nu_{2S} S \frac{\varepsilon_F^2}{(-\rho\bar{\nu})^2} \left[T-t - 2\frac{1 - e^{-\alpha(T-t)}}{\alpha} + \frac{1 - e^{-2\alpha(T-t)}}{2\alpha} \right] \\ \int_0^{T-t} \bar{\nu}_S S m_2(T-s) &= \bar{\nu}_S S \frac{\nu_2\varepsilon_F^2}{(-\rho\bar{\nu})^3} \int_0^{T-t} (1 - 2\alpha(T - (T-s))e^{-\alpha(T-(T-s))} - e^{-2\alpha(T-(T-s))}) ds \\ &= \bar{\nu}_S S \frac{\nu_2\varepsilon_F^2}{(-\rho\bar{\nu})^3} \left(T-t - 2 \left[\alpha s \frac{e^{-\alpha s}}{-\alpha} \right]_0^{T-t} - 2 \left[\frac{e^{-\alpha s}}{\alpha} \right]_0^{T-t} + \left[\frac{e^{-2\alpha s}}{2\alpha} \right]_0^{T-t} \right) \\ &= \bar{\nu}_S S \frac{\nu_2\varepsilon_F^2}{(-\rho\bar{\nu})^3} \left\{ T-t + 2(T-t)e^{-\alpha(T-t)} - 2\frac{1 - e^{-\alpha(T-t)}}{\alpha} - \frac{1 - e^{-2\alpha(T-t)}}{2\alpha} \right\} \end{aligned} \quad (\text{A.122})$$

So, we can conclude by eq. 2.42

$$\begin{aligned} M_2(t) &= \bar{\nu}_S S \frac{\nu_2\varepsilon_F^2}{(-\rho\bar{\nu})^3} \left[T-t + 2(T-t)e^{-\alpha(T-t)} - 2\frac{1 - e^{-\alpha(T-t)}}{\alpha} - \frac{1 - e^{-2\alpha(T-t)}}{2\alpha} \right] \\ &\quad + \nu_{2S} S \frac{\varepsilon_F^2}{(-\rho\bar{\nu})^2} \left[T-t - 2\frac{1 - e^{-\alpha(T-t)}}{\alpha} + \frac{1 - e^{-2\alpha(T-t)}}{2\alpha} \right] \\ &\quad + \frac{1}{2} \left[\bar{\nu}_S S \frac{\varepsilon_F}{-\rho\bar{\nu}} \left\{ T-t - \frac{1 - e^{-\alpha(T-t)}}{\alpha} \right\} \right]^2 \end{aligned} \quad (\text{A.123})$$

And, as $\mathbb{E}[N_{[t,T]}^2]_{(P_n(t))_n} = 2M_2(t) + M_1(t)$, we can deduce eq. 2.41

$$\begin{aligned}
\mathbb{E}[N_{[t,T]}^2]_{(P_n(t))_n} &= 2\bar{\nu}_S S \frac{\nu_2 \varepsilon_F^2}{(-\rho\bar{\nu})^3} \left[T - t + 2(T - t)e^{-\alpha(T-t)} - 2\frac{1 - e^{-\alpha(T-t)}}{\alpha} - \frac{1 - e^{-2\alpha(T-t)}}{2\alpha} \right] \\
&\quad + 2\nu_2 S S \frac{\varepsilon_F^2}{(-\rho\bar{\nu})^2} \left[T - t - 2\frac{1 - e^{-\alpha(T-t)}}{\alpha} + \frac{1 - e^{-2\alpha(T-t)}}{2\alpha} \right] \\
&\quad + \left[\bar{\nu}_S S \frac{\varepsilon_F}{-\rho\bar{\nu}} \left\{ T - t - \frac{1 - e^{-\alpha(T-t)}}{\alpha} \right\} \right]^2 + \bar{\nu}_S S \frac{\varepsilon_F}{-\rho\bar{\nu}} \left\{ T - t - \frac{1 - e^{-\alpha(T-t)}}{\alpha} \right\}
\end{aligned}
\tag{A.124}$$

□

Now we dispose of the expression of the moment of order 2 of $P_n(t)$. Then we provide the proof of the Prop

Proof. We have the knowledge that most of the terms in previous equation, we have to compute now the first term of the left part of 1.241.

Moreover, we know that

$$\begin{aligned}
\int_0^{T-t} m_1(T-s)ds &= \frac{\varepsilon_F}{-\rho\bar{\nu}} \int_0^{T-t} (1 - e^{-\alpha(T-(T-s))})ds = \frac{\varepsilon_F}{-\rho\bar{\nu}} \left(T-t - \frac{1 - e^{-\alpha(T-t)}}{\alpha} \right) \\
\int_0^{T-t} m_2(T-s)ds &= \int_0^{T-t} \nu_2 \frac{\varepsilon_F^2}{(-\rho\bar{\nu})^3} (1 - 2\alpha s e^{-\alpha s} - e^{-2\alpha s}) ds \\
&= \frac{\nu_2 \varepsilon_F^2}{(-\rho\bar{\nu})^3} \left(T-t + 2 \left((T-t)e^{-\alpha(T-t)} - \frac{1 - e^{-\alpha(T-t)}}{\alpha} \right) - \frac{1 - e^{-2\alpha(T-t)}}{2\alpha} \right) \\
\int_0^{T-t} m_3(T-s)ds &= \int_0^{T-t} -\frac{1}{2} \left(-2(A+B) + (-(3A+B) + 2\alpha s(3A+B) + 2\alpha^2 B s^2) e^{-\alpha s} \right. \\
&\quad \left. + (2(3A+B) + 4\alpha B s) e^{-2\alpha s} + (-A+B) e^{-3\alpha s} \right) ds \\
&= -\frac{1}{2} \left(-2(A+B)(T-t) - (3A+B) \frac{1 - e^{-\alpha(T-t)}}{\alpha} \right. \\
&\quad \left. - 2(3A+B) \left((T-t)e^{-\alpha(T-t)} - \frac{1 - e^{-\alpha(T-t)}}{\alpha} \right) \right. \\
&\quad \left. + 2B(-\alpha(T-t)^2 e^{-\alpha(T-t)} - 2(T-t)e^{-\alpha(T-t)} + 2 \frac{1 - e^{-\alpha(T-t)}}{\alpha}) \right. \\
&\quad \left. + 2(3A+B) \frac{1 - e^{-2\alpha(T-t)}}{2\alpha} - 2B \left((T-t)e^{-2\alpha(T-t)} - \frac{1 - e^{-2\alpha(T-t)}}{2\alpha} \right) + (-A+B) \frac{1 - e^{-3\alpha(T-t)}}{3\alpha} \right) \\
\int_0^{T-t} m_1^2(T-s)ds &= \int_0^{T-t} \frac{\varepsilon_F^2}{(-\rho\bar{\nu})^2} (1 - e^{-\alpha(T-(T-s))})^2 ds \\
&= \frac{\varepsilon_F^2}{(-\rho\bar{\nu})^2} \int_0^{T-t} (1 - 2e^{-\alpha s} + e^{-2\alpha s}) ds \\
&= \frac{\varepsilon_F^2}{(-\rho\bar{\nu})^2} \left(T-t - 2 \frac{1 - e^{-\alpha(T-t)}}{\alpha} + \frac{1 - e^{-2\alpha(T-t)}}{2\alpha} \right) \\
\int_0^{T-t} m_1^3(T-s)ds &= \int_0^{T-t} \frac{\varepsilon_F^3}{(-\rho\bar{\nu})^3} (1 - e^{-\alpha(T-(T-s))})^3 ds \\
&= \frac{\varepsilon_F^3}{(-\rho\bar{\nu})^3} \left(T-t - 3 \frac{1 - e^{-\alpha(T-t)}}{\alpha} + 3 \frac{1 - e^{-2\alpha(T-t)}}{2\alpha} - \frac{1 - e^{-3\alpha(T-t)}}{3\alpha} \right) \\
\int_0^{T-t} m_1 m_2(T-s)ds &= \int_0^{T-t} \frac{\nu_2 \varepsilon_F^3}{(-\rho\bar{\nu})^4} (1 - e^{-\alpha s})(1 - 2\alpha s e^{-\alpha s} - e^{-2\alpha s}) ds \\
&= \frac{\nu_2 \varepsilon_F^3}{(-\rho\bar{\nu})^4} \int_0^{T-t} (1 - (2\alpha s + 1)e^{-\alpha s} + (2\alpha s - 1)e^{-2\alpha s} + e^{-3\alpha s}) ds \\
&= \frac{\nu_2 \varepsilon_F^3}{(-\rho\bar{\nu})^4} \left((T-t) + 2(T-t)e^{-\alpha(T-t)} - 3 \frac{1 - e^{-\alpha(T-t)}}{\alpha} \right. \\
&\quad \left. - (T-t)e^{-2\alpha(T-t)} + \frac{1 - e^{-3\alpha(T-t)}}{3\alpha} \right)
\end{aligned} \tag{A.125}$$

Remark A.2.2. We retold the reader that

$$\begin{cases} A = \nu_3 \frac{\varepsilon_F^3}{(-\rho\bar{\nu})^4} \\ B = 2\nu_2^2 \frac{\varepsilon_F^3}{(-\rho\bar{\nu})^5} \end{cases} \quad (\text{A.126})$$

Hence, we can conclude by eq. 2.44

$$\begin{aligned} M_3(t) = & -\frac{S\bar{\nu}_S}{2} \left(-2(A+B)(T-t) - (3A+B) \frac{1-e^{-\alpha(T-t)}}{\alpha} \right. \\ & - 2(3A+B) \left((T-t)e^{-\alpha(T-t)} - \frac{1-e^{-\alpha(T-t)}}{\alpha} \right) \\ & + 2B(-\alpha(T-t)^2 e^{-\alpha(T-t)} - 2(T-t)e^{-\alpha(T-t)} + 2 \frac{1-e^{-\alpha(T-t)}}{\alpha}) \\ & + 2(3A+B) \frac{1-e^{-2\alpha(T-t)}}{2\alpha} - 2B \left((T-t)e^{-2\alpha(T-t)} - \frac{1-e^{-2\alpha(T-t)}}{2\alpha} \right) + (-A+B) \frac{1-e^{-3\alpha(T-t)}}{3\alpha} \Big) \\ & + 2\nu_{2S} S \frac{\nu_2 \varepsilon_F^3}{(-\rho\bar{\nu})^4} \left((T-t) + 2(T-t)e^{-\alpha(T-t)} - 3 \frac{1-e^{-\alpha(T-t)}}{\alpha} \right. \\ & \left. - (T-t)e^{-2\alpha(T-t)} + \frac{1-e^{-3\alpha(T-t)}}{3\alpha} \right) \\ & + \nu_{3S} S \frac{\varepsilon_F^3}{(-\rho\bar{\nu})^3} \left(T-t - 3 \frac{1-e^{-\alpha(T-t)}}{\alpha} + 3 \frac{1-e^{-2\alpha(T-t)}}{2\alpha} - \frac{1-e^{-3\alpha(T-t)}}{3\alpha} \right) \\ & + \left(\bar{\nu}_S S \frac{\nu_2 \varepsilon_F^2}{(-\rho\bar{\nu})^3} \left(T-t + 2 \left((T-t)e^{-\alpha(T-t)} - \frac{1-e^{-\alpha(T-t)}}{\alpha} \right) - \frac{1-e^{-2\alpha(T-t)}}{2\alpha} \right) \right. \\ & + \nu_{2S} \frac{\varepsilon_F^2}{(-\rho\bar{\nu})^2} \left(T-t - 2 \frac{1-e^{-\alpha(T-t)}}{\alpha} + \frac{1-e^{-2\alpha(T-t)}}{2\alpha} \right) \\ & \left. + \frac{\bar{\nu}_S^2 S^2}{6} \frac{\varepsilon_F^2}{(-\rho\bar{\nu})^2} \left(T-t - \frac{1-e^{-\alpha(T-t)}}{\alpha} \right)^2 \right) \bar{\nu}_S S \frac{\varepsilon_F}{(-\rho\bar{\nu})} \left[(T-t) - \frac{1-e^{-\alpha(T-t)}}{\alpha} \right] \end{aligned} \quad (\text{A.127})$$

The term produces

$$-\frac{1-e^{-\alpha(T-t)}}{\alpha} + 2 \frac{1-e^{-\alpha(T-t)}}{\alpha} = \frac{1-e^{-\alpha(T-t)}}{\alpha} \quad (\text{A.128})$$

$$+4B \frac{1-e^{-\alpha(T-t)}}{\alpha} = (3A+5B) \frac{1-e^{-\alpha(T-t)}}{\alpha} \quad (\text{A.129})$$

and also

What can be simplified as eq. 2.44

$$\begin{aligned}
M_3(t) = & -\frac{S\bar{\nu}_S}{2} \left(-2(A+B)(T-t) + (3A+5B)\frac{1-e^{-\alpha(T-t)}}{\alpha} \right. \\
& - 2(3A+B)(T-t)e^{-\alpha(T-t)} \\
& + 2B(-\alpha(T-t))^2 e^{-\alpha(T-t)} - 2(T-t)e^{-\alpha(T-t)} + 2\frac{1-e^{-\alpha(T-t)}}{\alpha} \\
& + (6A+4B)\frac{1-e^{-2\alpha(T-t)}}{2\alpha} - 2B(T-t)e^{-2\alpha(T-t)} + (-A+B)\frac{1-e^{-3\alpha(T-t)}}{3\alpha} \left. \right) \\
& + 2\nu_{2S}S\frac{\nu_2\varepsilon_F^3}{(-\rho\bar{\nu})^4} \left((T-t) + 2(T-t)e^{-\alpha(T-t)} - 3\frac{1-e^{-\alpha(T-t)}}{\alpha} \right. \\
& \left. - (T-t)e^{-2\alpha(T-t)} + \frac{1-e^{-3\alpha(T-t)}}{3\alpha} \right) \\
& + \nu_{3S}S\frac{\varepsilon_F^3}{(-\rho\bar{\nu})^3} \left(T-t - 3\frac{1-e^{-\alpha(T-t)}}{\alpha} + 3\frac{1-e^{-2\alpha(T-t)}}{2\alpha} - \frac{1-e^{-3\alpha(T-t)}}{3\alpha} \right) \\
& + \left(\bar{\nu}_S S\frac{\nu_2\varepsilon_F^2}{(-\rho\bar{\nu})^3} \left(T-t + 2((T-t)e^{-\alpha(T-t)} - \frac{1-e^{-\alpha(T-t)}}{\alpha}) - \frac{1-e^{-2\alpha(T-t)}}{2\alpha} \right) \right. \\
& + \nu_{2S}\frac{\varepsilon_F^2}{(-\rho\bar{\nu})^2} \left(T-t - 2\frac{1-e^{-\alpha(T-t)}}{\alpha} + \frac{1-e^{-2\alpha(T-t)}}{2\alpha} \right) \\
& \left. + \frac{\bar{\nu}_S^2 S^2}{6} \frac{\varepsilon_F^2}{(-\rho\bar{\nu})^2} \left(T-t - \frac{1-e^{-\alpha(T-t)}}{\alpha} \right)^2 \right) \bar{\nu}_S S\frac{\varepsilon_F}{(-\rho\bar{\nu})} \left[(T-t) - \frac{1-e^{-\alpha(T-t)}}{\alpha} \right]
\end{aligned} \tag{A.130}$$

What we can consider in a more ordinate manner as

$$\mathbb{E}[N_{[t,T]}^3]_{(P_n(t))_n} = 6(M_3(t) + M_2(t)) + M_1(t) \tag{A.131}$$

To conclude, we dispose of eq. 2.43

$$\begin{aligned}
& \mathbb{E}[N_{[t,T]}^3]_{(P_n(t))_n} \\
&= 6 \left(-\frac{S\bar{\nu}_S}{2} \left(-2(A+B)(T-t) - (3A+B) \frac{1-e^{-\alpha(T-t)}}{\alpha} \right. \right. \\
&\quad \left. \left. - 2(3A+B)((T-t)e^{-\alpha(T-t)} - \frac{1-e^{-\alpha(T-t)}}{\alpha}) \right) \right. \\
&\quad \left. + 2B(-\alpha(T-t)^2 e^{-\alpha(T-t)} - 2(T-t)e^{-\alpha(T-t)} + 2 \frac{1-e^{-\alpha(T-t)}}{\alpha}) \right. \\
&\quad \left. + 2(3A+B) \frac{1-e^{-2\alpha(T-t)}}{2\alpha} - 2B((T-t)e^{-2\alpha(T-t)} - \frac{1-e^{-2\alpha(T-t)}}{2\alpha}) + (-A+B) \frac{1-e^{-3\alpha(T-t)}}{3\alpha} \right) \\
&\quad + 2\nu_{2S} S \frac{\nu_2 \varepsilon_F^3}{(-\rho\bar{\nu})^4} \left((T-t) + 2(T-t)e^{-\alpha(T-t)} - 3 \frac{1-e^{-\alpha(T-t)}}{\alpha} \right. \\
&\quad \left. - (T-t)e^{-2\alpha(T-t)} + \frac{1-e^{-3\alpha(T-t)}}{3\alpha} \right) \\
&\quad + \nu_{3S} S \frac{\varepsilon_F^3}{(-\rho\bar{\nu})^3} \left(T-t - 3 \frac{1-e^{-\alpha(T-t)}}{\alpha} + 3 \frac{1-e^{-2\alpha(T-t)}}{2\alpha} - \frac{1-e^{-3\alpha(T-t)}}{3\alpha} \right) \\
&\quad + \left(\bar{\nu}_S S \frac{\nu_2 \varepsilon_F^2}{(-\rho\bar{\nu})^3} \left(T-t + 2((T-t)e^{-\alpha(T-t)} - \frac{1-e^{-\alpha(T-t)}}{\alpha}) - \frac{1-e^{-2\alpha(T-t)}}{2\alpha} \right) \right. \\
&\quad \left. + \nu_{2S} \frac{\varepsilon_F^2}{(-\rho\bar{\nu})^2} \left(T-t - 2 \frac{1-e^{-\alpha(T-t)}}{\alpha} + \frac{1-e^{-2\alpha(T-t)}}{2\alpha} \right) \right. \\
&\quad \left. + \frac{\bar{\nu}_S^2 S^2}{6} \frac{\varepsilon_F^2}{(-\rho\bar{\nu})^2} \left(T-t - \frac{1-e^{-\alpha(T-t)}}{\alpha} \right)^2 \right) \bar{\nu}_S S \frac{\varepsilon_F}{(-\rho\bar{\nu})} \left[(T-t) - \frac{1-e^{-\alpha(T-t)}}{\alpha} \right] \\
&\quad + 6 \left(\bar{\nu}_S S \frac{\nu_2 \varepsilon_F^2}{(-\rho\bar{\nu})^3} \left[T-t + 2(T-t)e^{-\alpha(T-t)} - 2 \frac{1-e^{-\alpha(T-t)}}{\alpha} - \frac{1-e^{-2\alpha(T-t)}}{2\alpha} \right] \right. \\
&\quad \left. + \nu_{2S} S \frac{\varepsilon_F^2}{(-\rho\bar{\nu})^2} \left[T-t - 2 \frac{1-e^{-\alpha(T-t)}}{\alpha} + \frac{1-e^{-2\alpha(T-t)}}{2\alpha} \right] \right. \\
&\quad \left. + \frac{1}{2} \left[\bar{\nu}_S S \frac{\varepsilon_F}{-\rho\bar{\nu}} \left\{ T-t - \frac{1-e^{-\alpha(T-t)}}{\alpha} \right\} \right]^2 \right) \\
&\quad + \bar{\nu}_S S \frac{\varepsilon_F}{-\rho\bar{\nu}} \left\{ T-t - \frac{1-e^{-\alpha(T-t)}}{\alpha} \right\}
\end{aligned}$$

(A.132)

□

Thus, we dispose of the expression of the three first moment of the distribution $P_n(t)$

- $M_1(t)$, $M_2(t)$, $M_3(t)$,
- $\mathbb{E}[N_{[t,T]}]_{(P_n(t))_n}$, $\mathbb{E}[N_{[t,T]}^2]_{(P_n(t))_n}$, $\mathbb{E}[N_{[t,T]}^3]_{(P_n(t))_n}$.

Moments of the distribution $Q_n(t)$

In the following $S = S_F$ will refer to the intensity of the source and $S_\alpha = 0$. Now we want to compute the expressions of the three first moments of $Q_n(t)$. First, we compute the expression of Prop 2.2.8

Proof. We can sum it in

$$\mathbb{E}[N_{[t,T]}]_{(Q_n(t))_n} = \varepsilon_F \frac{\bar{\nu}_S S}{-\rho \bar{\nu}} \left[(T-t) - \frac{1 - e^{-\alpha(T-t)}}{\alpha} \right] + \frac{\varepsilon_F}{-\rho \bar{\nu}} (1 - e^{-\alpha(T-t)}) \bar{\nu}_{II,\infty} \quad (\text{A.133})$$

By the use of A.51, we conclude by stating the simple moment of order 1 in presence of a source is (eq. 2.45)

$$\boxed{\mathbb{E}[N_{[t,T]}]_{(Q_n(t))_n} = \bar{\nu}_S S \frac{\varepsilon_F}{-\rho \bar{\nu}} (T-t)} \quad (\text{A.134})$$

□

Now we dispose of the expression of \mathcal{M}_1 . Then we want to compute the expression of \mathcal{M}_2 and thus the expression of $\mathbb{E}[N_{[t,T]}^2]_{(Q_n(t))_n}$. So we do the proof of Prop 2.2.9

Proof. We retold

$$\mathbb{E}[N_{[t,T]}^2]_{(Q_n(t))_n} = 2\mathcal{M}_2(t) + \mathcal{M}_1 \quad (\text{A.135})$$

Carefully repeating the previous formula, we can write

$$\begin{aligned} \mathcal{M}_2(t) &= \bar{\nu}_S S \frac{\nu_2 \varepsilon_F^2}{(-\rho \bar{\nu})^3} \left[T - t + 2(T-t)e^{-\alpha(T-t)} - 2 \frac{1 - e^{-\alpha(T-t)}}{\alpha} - \frac{1 - e^{-2\alpha(T-t)}}{2\alpha} \right] \\ &+ \nu_2 S S \frac{\varepsilon_F^2}{(-\rho \bar{\nu})^2} \left[T - t - 2 \frac{1 - e^{-\alpha(T-t)}}{\alpha} + \frac{1 - e^{-2\alpha(T-t)}}{2\alpha} \right] \\ &+ \frac{1}{2} \left[\bar{\nu}_S S \frac{\varepsilon_F}{-\rho \bar{\nu}} \left\{ T - t - \frac{1 - e^{-\alpha(T-t)}}{\alpha} \right\} \right]^2 \\ &+ \frac{\bar{\nu}_S S}{\alpha} \bar{\nu}_S S \frac{\varepsilon_F}{-\rho \bar{\nu}} \left[(T-t) - \frac{1 - e^{-\alpha(T-t)}}{\alpha} \right] \frac{\varepsilon_F}{-\rho \bar{\nu}} (1 - e^{-\alpha(T-t)}) \\ &+ \frac{\bar{\nu}_S S}{\alpha} \frac{\nu_2 \varepsilon_F^2}{(-\rho \bar{\nu})^3} (1 - 2\alpha(T-t)e^{-\alpha(T-t)} - e^{-2\alpha(T-t)}) \\ &+ \left[\frac{\bar{\nu}_S S}{2\alpha} \left(\frac{\bar{\nu}_S S}{\alpha} + \frac{\nu_2}{-\rho \bar{\nu}} \right) + \frac{\nu_2 S}{2\alpha} \right] \left(\frac{\varepsilon_F}{-\rho \bar{\nu}} \right)^2 (1 - e^{-\alpha(T-t)})^2 \end{aligned} \quad (\text{A.136})$$

In the subparts A.2.4 and 2.2 we have already computed the $(m_i)_{i \in \llbracket 1;2 \rrbracket}$, $(M_i)_{i \in \llbracket 1;2 \rrbracket}$ and the moments of the distribution of the number of neutrons present in the system

in presence of a source or in the absence of a source, we can now state

$$\begin{aligned}
\mathbb{E}[N_{[t;T]}^2]_{(Q_n(t))_n} &= 2 \left\{ \bar{\nu}_S S \frac{\nu_2 \varepsilon_F^2}{(-\rho \bar{\nu})^3} \left[T - t + 2(T - t)e^{-\alpha(T-t)} - 2 \frac{1 - e^{-\alpha(T-t)}}{\alpha} - \frac{1 - e^{-2\alpha(T-t)}}{2\alpha} \right] \right. \\
&\quad + \nu_{2S} S \frac{\varepsilon_F^2}{(-\rho \bar{\nu})^2} \left[T - t - 2 \frac{1 - e^{-\alpha(T-t)}}{\alpha} + \frac{1 - e^{-2\alpha(T-t)}}{2\alpha} \right] \\
&\quad + \frac{1}{2} \left[\bar{\nu}_S S \frac{\varepsilon_F}{-\rho \bar{\nu}} \left\{ T - t - \frac{1 - e^{-\alpha(T-t)}}{\alpha} \right\} \right]^2 \\
&\quad + \frac{\bar{\nu}_S S}{\alpha} \bar{\nu}_S S \frac{\varepsilon_F}{-\rho \bar{\nu}} \left[(T - t) - \frac{1 - e^{-\alpha(T-t)}}{\alpha} \right] \frac{\varepsilon_F}{-\rho \bar{\nu}} (1 - e^{-\alpha(T-t)}) \\
&\quad + \frac{\bar{\nu}_S S}{\alpha} \frac{\nu_2 \varepsilon_F^2}{(-\rho \bar{\nu})^3} (1 - 2\alpha(T - t)e^{-\alpha(T-t)} - e^{-2\alpha(T-t)}) \\
&\quad + \left[\frac{\bar{\nu}_S S}{2\alpha} \left(\frac{\bar{\nu}_S S}{\alpha} + \frac{\nu_2}{-\rho \bar{\nu}} \right) + \frac{\nu_{2S} S}{2\alpha} \right] \left(\frac{\varepsilon_F}{-\rho \bar{\nu}} \right)^2 (1 - e^{-\alpha(T-t)})^2 \left. \right\} \\
&\quad + \bar{\nu}_S S \frac{\varepsilon_F}{-\rho \bar{\nu}} (T - t)
\end{aligned} \tag{A.137}$$

We remark we can add the first and fifth line of A.137

$$\begin{aligned}
&\bar{\nu}_S S \frac{\nu_2 \varepsilon_F^2}{(-\rho \bar{\nu})^3} \left[T - t + 2(T - t)e^{-\alpha(T-t)} - 2 \frac{1 - e^{-\alpha(T-t)}}{\alpha} - \frac{1 - e^{-2\alpha(T-t)}}{2\alpha} \right] \\
&+ \frac{\bar{\nu}_S S}{\alpha} \frac{\nu_2 \varepsilon_F^2}{(-\rho \bar{\nu})^3} (1 - 2\alpha(T - t)e^{-\alpha(T-t)} - e^{-2\alpha(T-t)}) \\
&= \bar{\nu}_S S \frac{\nu_2 \varepsilon_F^2}{(-\rho \bar{\nu})^3} \left(T - t - 2 \frac{1 - e^{-\alpha(T-t)}}{\alpha} + \frac{1 - e^{-2\alpha(T-t)}}{2\alpha} \right)
\end{aligned} \tag{A.138}$$

Factorising the third and the fourth line of A.137 by $2\bar{\nu}_S^2 S^2 \left(\frac{\varepsilon_F}{-\rho \bar{\nu}} \right)^2 \left(T - t - \frac{1 - e^{-\alpha(T-t)}}{\alpha} \right)$ then added provides

$$\begin{aligned}
&2\bar{\nu}_S^2 S^2 \left(\frac{\varepsilon_F}{-\rho \bar{\nu}} \right)^2 \left(T - t - \frac{1 - e^{-\alpha(T-t)}}{\alpha} \right) \left(\frac{1}{2}(T - t) - \frac{1}{2} \frac{1 - e^{-\alpha(T-t)}}{\alpha} + \frac{1 - e^{-\alpha(T-t)}}{\alpha} \right) \\
&= \frac{2}{2} \bar{\nu}_S^2 S^2 \left(\frac{\varepsilon_F}{-\rho \bar{\nu}} \right)^2 \left((T - t)^2 - \left(\frac{1 - e^{-\alpha(T-t)}}{\alpha} \right)^2 \right)
\end{aligned} \tag{A.139}$$

The right side of this equation simplifies with the first term of $2\nu_2 \Pi m_1^2$.

In the same manner, we can add A.138 and the second member of the fifth line

of A.137.

$$\begin{aligned}
& 2\bar{\nu}_S S \frac{\nu_2 \varepsilon_F^2}{(-\rho\bar{\nu})^3} \left(T - t - 2 \frac{1 - e^{-\alpha(T-t)}}{\alpha} + \frac{1 - e^{-2\alpha(T-t)}}{2\alpha} \right) \\
& + 2 \frac{\bar{\nu}_S S}{2\alpha} \frac{\nu_2 \varepsilon_F^2}{(-\rho\bar{\nu})^3} (1 + 2e^{-2\alpha(T-t)} - e^{-\alpha(T-t)}) \\
& = 2\nu_S S \nu_2 \frac{\varepsilon_F^2}{(-\rho\bar{\nu})^3} \left(T - t - \frac{1 - e^{-\alpha(T-t)}}{\alpha} \right)
\end{aligned} \tag{A.140}$$

Moreover, the second line added to the third term of the fifth line of A.137

$$\begin{aligned}
& 2\nu_2 S S \frac{\varepsilon_F^2}{(-\rho\bar{\nu})^2} \left[T - t - 2 \frac{1 - e^{-\alpha(T-t)}}{\alpha} + \frac{1 - e^{-2\alpha(T-t)}}{2\alpha} \right] \\
& + 2 \frac{\nu_2 S S}{2\alpha} \frac{\varepsilon_F^2}{(-\rho\bar{\nu})^2} (1 + e^{-2\alpha(T-t)} - 2e^{-\alpha(T-t)}) \\
& = 2\nu_2 S S \frac{\varepsilon_F^2}{(-\rho\bar{\nu})^2} \left(T - t - \frac{1 - e^{-\alpha(T-t)}}{\alpha} \right)
\end{aligned} \tag{A.141}$$

Finally, the whole expression is simplified as eq. 2.46

$$\begin{aligned}
\mathbb{E}[N_{[t;T]}^2]_{(Q_n(t))_n} &= \nu_S^2 S^2 \frac{\varepsilon_F^2}{(-\rho\bar{\nu})^2} (T-t)^2 \\
&+ 2 \frac{\varepsilon_F^2}{(-\rho\bar{\nu})^2} \left(\nu_S S \frac{\nu_2}{(-\rho\nu)} + \nu_2 S S \right) \left(T - t - \frac{1 - e^{-\alpha(T-t)}}{\alpha} \right) \\
&+ \bar{\nu}_S S \frac{\varepsilon_F}{-\rho\bar{\nu}} (T-t)
\end{aligned} \tag{A.142}$$

we can notice this expression contains $\mathbb{E}[N_{[t;T]}]_{(Q_n(t))_n}^2$ and $\mathbb{E}[N_{[t;T]}]_{(Q_n(t))_n}$.

We can use the same tricks for $\mathcal{M}_2(t)$ and we obtain eq. 2.47

$$\begin{aligned}
\mathcal{M}_2(t) &= \frac{1}{2} \nu_S^2 S^2 \frac{\varepsilon_F^2}{(-\rho\nu_2)^2} (T-t)^2 \\
&+ \frac{\varepsilon_F^2}{(-\rho\nu_2)^2} \left(\nu_S S \frac{\nu_2}{(-\rho\nu)} + \nu_2 S S \right) \left(T - t - \frac{1 - e^{-\alpha(T-t)}}{\alpha} \right)
\end{aligned} \tag{A.143}$$

□

Then the expression of \mathcal{M}_2 and the expression of $\mathbb{E}[N_{[t;T]}^2]_{(Q_n(t))_n}$ are computed.

And so, we find the analytical expression of $Y_2(T-t)$.

Then the expression of \mathcal{M}_3 and $\mathbb{E}[N_{[t;T]}^3]_{(Q_n(t))_n}$ can be computed. So we do the proof of Prop 2.2.10

Proof. We dispose of the equation

$$\mathbb{E}[N_{[t;T]}^3] = 6\mathcal{M}_3(t) + 6\mathcal{M}_2(t) + \mathcal{M}_1(t) \tag{A.144}$$

In order to get a more simplified version of the computations, we recall the form of $M_3(t)$

$$\begin{aligned}
M_3(t) = & \int_0^{T-t} S(\bar{\nu}_S m_3(T-s) + 2\nu_{2S} m_1(T-s)m_2(T-s) + \nu_{3S} m_1^3(T-s)) ds \\
& + \left(\int_0^{T-t} S(\bar{\nu}_S m_2(T-s) + \nu_{2S} m_1^2(T-s)) ds + \frac{1}{6} \left(\int_0^{T-t} S \bar{\nu}_S m_1(T-s) ds \right)^2 \right) M_1(t)
\end{aligned}
\tag{A.145}$$

We assign a term of $M_3(t)$ with respect to another term in function of the nuclear parameter of the source.

$$\begin{aligned}
& \int_0^{T-t} S \bar{\nu}_S m_3(T-s) ds + \bar{\nu}_{II, \infty} m_3(t) \\
&= -\frac{\bar{\nu}_S S}{2} \left(-2(A+B)(T-t) - (3A+B) \frac{1-e^{-\alpha(T-t)}}{\alpha} \right. \\
&\quad \left. - 2(3A+B) \left((T-t)e^{-\alpha(T-t)} - \frac{1-e^{-\alpha(T-t)}}{\alpha} \right) \right. \\
&\quad \left. + 2B(-\alpha(T-t)^2 e^{-\alpha(T-t)} - 2(T-t)e^{-\alpha(T-t)} + 2 \frac{1-e^{-\alpha(T-t)}}{\alpha}) \right. \\
&\quad \left. + 2(3A+B) \frac{1-e^{-2\alpha(T-t)}}{2\alpha} - 2B \left((T-t)e^{-2\alpha(T-t)} - \frac{1-e^{-2\alpha(T-t)}}{2\alpha} \right) + (-A+B) \frac{1-e^{-3\alpha(T-t)}}{3\alpha} \right) \\
&\quad - \frac{\bar{\nu}_S S}{2\alpha} (-2(A+B) \\
&\quad + (-(3A+B) + 2\alpha(T-t)(3A+B) + 2\alpha^2 B(T-t)^2) e^{-\alpha(T-t)} \\
&\quad + (2(3A+B) + 4\alpha B(T-t)) e^{-2\alpha(T-t)} \\
&\quad + (-A+B) e^{-3\alpha(T-t)}) \\
&= -\frac{\bar{\nu}_S S}{2} \left\{ -2 \frac{(A+B)}{\alpha} - \frac{(3A+B)}{\alpha} - 2(3A+B) \frac{-1}{\alpha} + 2B \frac{2}{\alpha} + 2(3A+B) \frac{1}{2\alpha} \right. \\
&\quad \left. - 2B \frac{-1}{2\alpha} + (-A+B) \frac{1}{3\alpha} \right. \\
&\quad \left. - 2(A+B)(T-t) \right. \\
&\quad \left. + \left(\frac{(3A+B)}{\alpha} - 2 \frac{(3A+B)}{\alpha} - 4 \frac{B}{\alpha} - \frac{(3A+B)}{\alpha} \right) e^{-\alpha(T-t)} \right. \\
&\quad \left. + \left(-2(3A+B) - 4B + 2 \frac{\alpha}{\alpha} (3A+B) \right) (T-t) e^{-\alpha(T-t)} \right. \\
&\quad \left. + \left(-2\alpha B + 2\alpha B \right) (T-t)^2 e^{-\alpha(T-t)} \right. \\
&\quad \left. + \left(-2 \frac{(3A+B)}{2\alpha} - 2 \frac{B}{2\alpha} + 2 \frac{(3A+B)}{\alpha} \right) e^{-2\alpha(T-t)} \right. \\
&\quad \left. + \left(-2B + 4B \frac{\alpha}{\alpha} \right) (T-t) e^{-2\alpha(T-t)} \right. \\
&\quad \left. + \left(\frac{-A+B}{3\alpha} + \frac{-A+B}{\alpha} \right) e^{-3\alpha(T-t)} \right\} \\
&= -\frac{\bar{\nu}_S S}{2} \left\{ \frac{11A+16B}{3\alpha} - 2(A+B)(T-t) - 6 \frac{A+B}{\alpha} e^{-\alpha(T-t)} - 4B(T-t) e^{-\alpha(T-t)} \right. \\
&\quad \left. + 3 \frac{A}{\alpha} e^{-2\alpha(T-t)} + 2B(T-t) e^{-2\alpha(T-t)} + 2 \frac{-A+B}{3\alpha} e^{-3\alpha(T-t)} \right\}
\end{aligned} \tag{A.146}$$

$$\begin{aligned}
& \int_0^{T-t} S\nu_2 S m_1(T-s)m_2(T-s)ds + \frac{\nu_2 S}{2\alpha} 2m_1(t)m_2(t) \\
&= S\nu_2 S \frac{\nu_2 \varepsilon_F^3}{(-\rho\bar{\nu})^4} \left((T-t) + 2(T-t)e^{-\alpha(T-t)} - 3\frac{1-e^{-\alpha(T-t)}}{\alpha} - (T-t)e^{-2\alpha(T-t)} + \frac{1-e^{-3\alpha(T-t)}}{3\alpha} \right) \\
&+ \frac{\nu_2 S}{\alpha} \frac{\nu_2 \varepsilon_F^3}{(-\rho\bar{\nu})^4} (1-e^{-\alpha(T-t)})(1-2\alpha(T-t)e^{-\alpha(T-t)} - e^{-2\alpha(T-t)}) \\
&= \nu_2 S \frac{\nu_2 \varepsilon_F^3}{(-\rho\bar{\nu})^4} \left((T-t) + 2(T-t)e^{-\alpha(T-t)} - 3\frac{1-e^{-\alpha(T-t)}}{\alpha} - (T-t)e^{-2\alpha(T-t)} + \frac{1-e^{-3\alpha(T-t)}}{3\alpha} \right. \\
&\left. + \frac{1-e^{-\alpha(T-t)}}{\alpha} (1-2\alpha(T-t)e^{-\alpha(T-t)} - e^{-2\alpha(T-t)}) \right) \\
&= \nu_2 S \frac{\nu_2 \varepsilon_F^3}{(-\rho\bar{\nu})^4} \left(T-t - 2\frac{1-e^{-\alpha(T-t)}}{\alpha} + (T-t - \frac{1}{\alpha})e^{-2\alpha(T-t)} + \frac{1}{3\alpha} - 2\frac{e^{-3\alpha(T-t)}}{3\alpha} \right)
\end{aligned} \tag{A.147}$$

$$\begin{aligned}
& \int_0^{T-t} S\nu_3 S m_1^3(T-s)ds + \frac{\nu_3 S}{3\alpha} m_1^3(t) \\
&= \nu_3 S \frac{\varepsilon_F^3}{(-\rho\bar{\nu})^3} \left((T-t - 3\frac{1-e^{-\alpha(T-t)}}{\alpha} + 3\frac{1-e^{-2\alpha(T-t)}}{2\alpha} - \frac{1-e^{-3\alpha(T-t)}}{3\alpha}) \right. \\
&\left. + \frac{1-3e^{-\alpha(T-t)} + 3e^{-2\alpha(T-t)} - e^{-3\alpha(T-t)}}{3\alpha} \right) \\
&= \nu_3 S \frac{\varepsilon_F^3}{(-\rho\bar{\nu})^3} \left(T-t - 2\frac{1-e^{-\alpha(T-t)}}{\alpha} - \frac{1+e^{-2\alpha(T-t)}}{2\alpha} \right)
\end{aligned} \tag{A.148}$$

$$\begin{aligned}
& \int_0^{T-t} S\bar{\nu}_S m_2(T-s)ds M_1(t) + \frac{\bar{\nu}_S S}{\alpha} M_1(t)m_2(t) \\
&= \bar{\nu}_S S M_1(t) \left(\int_0^{T-t} m_2(T-s)ds + m_2(t) \right) \\
&= \bar{\nu}_S S M_1(t) \left(\frac{\nu_2 \varepsilon_F^2}{(-\rho\bar{\nu})^3} (T-t + 2((T-t)e^{-\alpha(T-t)} - \frac{1-e^{-\alpha(T-t)}}{\alpha}) - \frac{1-e^{-2\alpha(T-t)}}{2\alpha}) \right. \\
&\left. + \frac{\nu_2 \varepsilon_F^2}{(-\rho\bar{\nu})^3} \frac{(1-2\alpha(T-t)e^{-\alpha(T-t)} - e^{-2\alpha(T-t)})}{\alpha} \right) \\
&= \bar{\nu}_S S \frac{\nu_2 \varepsilon_F^2}{(-\rho\bar{\nu})^3} M_1(t) \left(T-t - 2\frac{1-e^{-\alpha(T-t)}}{\alpha} \right)
\end{aligned} \tag{A.149}$$

$$\begin{aligned}
& \int_0^{T-t} S \nu_{2S} m_1^2(T-s) ds M_1(t) + \frac{\nu_{2S} S}{2\alpha} M_1(t) m_1^2(t) \\
&= \nu_{2S} S M_1(t) \left(\int_0^{T-t} m_1^2(T-s) ds + m_1^2(t) \right) \\
&= \nu_{2S} S \frac{\varepsilon_F^2}{(-\rho\bar{\nu})^2} M_1(t) \left((T-t) - 2 \frac{1-e^{-\alpha(T-t)}}{\alpha} + \frac{1-e^{-2\alpha(T-t)}}{2\alpha} \right) + \frac{1-2e^{-\alpha(T-t)}+e^{-2\alpha(T-t)}}{2\alpha} \\
&= \nu_{2S} S \frac{\varepsilon_F^2}{(-\rho\bar{\nu})^2} M_1(t) \left(T-t - \frac{1-e^{-\alpha(T-t)}}{\alpha} \right) \\
&= \frac{\nu_{2S}}{\bar{\nu}_S} \frac{\varepsilon_F}{-\rho\bar{\nu}} M_1^2(t)
\end{aligned} \tag{A.150}$$

$$\begin{aligned}
& \frac{1}{6} \left(\int_0^{T-t} S \bar{\nu}_S m_1(T-s) ds \right)^2 M_1(t) + \frac{\bar{\nu}_S^3 S^3}{6\alpha^3} m_1^3(t) \\
&= \frac{M_1^3(t)}{6} + \frac{\bar{\nu}_S^3 S^3}{6\alpha^3} m_1^3(t) \\
&= \frac{\bar{\nu}_S^3 S^3}{6} \frac{\varepsilon_F^3}{(-\rho\bar{\nu})^3} \left((T-t)^3 - 3(T-t)^2 \frac{1-e^{-\alpha(T-t)}}{\alpha} + 3(T-t) \frac{(1-e^{-\alpha(T-t)})^2}{\alpha^2} \right. \\
&\quad \left. - \frac{(1-e^{-\alpha(T-t)})^3}{\alpha^3} + \frac{(1-e^{-\alpha(T-t)})^3}{\alpha^3} \right) \\
&= \frac{\bar{\nu}_S^3 S^3}{6} \frac{\varepsilon_F^3}{(-\rho\bar{\nu})^3} (T-t) \left((T-t)^2 - 3(T-t) \frac{1-e^{-\alpha(T-t)}}{\alpha} + 3 \frac{(1-e^{-\alpha(T-t)})^2}{\alpha^2} \right)
\end{aligned} \tag{A.151}$$

It remains $(\nu_{3,II,\infty} - \frac{\nu_{3S} S}{3\alpha} - \frac{\bar{\nu}_S^3 S^3}{6\alpha^3}) m_1^3(t)$ and $\bar{\nu}_{II,\infty} M_2(t) m_1(t)$

$$\begin{aligned}
& (\nu_{3,II,\infty} - \frac{\nu_{3S} S}{3\alpha} - \frac{\bar{\nu}_S^3 S^3}{6\alpha^3}) m_1^3(t) \\
&= \left(\frac{S}{3\alpha} \left(\frac{\bar{\nu}_S}{-\rho\bar{\nu}} \left(\frac{\nu_2^2}{-\rho\bar{\nu}} + \nu_3 \right) + \frac{\nu_2 \nu_{2S}}{-\rho\bar{\nu}} + \nu_{3S} \right) \right. \\
&\quad \left. + \frac{\bar{\nu}_S S}{\alpha} \frac{S}{2\alpha} \left(\bar{\nu}_S \frac{\nu_2}{-\rho\bar{\nu}} + \nu_{2S} \right) + \frac{\bar{\nu}_S^3 S^3}{6\alpha^3} \right) m_1^3(t) - \frac{\nu_{3S} S}{3\alpha} m_1^3(t) - \frac{\bar{\nu}_S^3 S^3}{6\alpha^3} m_1^3(t) \\
&= \left(\frac{S}{3\alpha} \left(\frac{\bar{\nu}_S}{-\rho\bar{\nu}} \left(\frac{\nu_2^2}{-\rho\bar{\nu}} + \nu_3 \right) + \frac{\nu_2 \nu_{2S}}{-\rho\bar{\nu}} \right) + \frac{\bar{\nu}_S S}{\alpha} \frac{S}{2\alpha} \left(\bar{\nu}_S \frac{\nu_2}{-\rho\bar{\nu}} + \nu_{2S} \right) \right) m_1^3(t)
\end{aligned} \tag{A.152}$$

We have to take care of 5 terms in order to simplify the $e^{-3\alpha(T-t)}$

$$\begin{aligned}
& \bar{\nu}_{II,\infty} M_2(t) m_1(t) \\
&= \frac{\bar{\nu}_S S}{\alpha} \left(\frac{\varepsilon_F}{(-\rho\bar{\nu})} \left(1 - e^{-\alpha(T-t)} \right) \right) \left(\bar{\nu}_S S \frac{\nu_2 \varepsilon_F^2}{(-\rho\bar{\nu})^3} \left[T - t + 2(T-t)e^{-\alpha(T-t)} - 2 \frac{1 - e^{-\alpha(T-t)}}{\alpha} \right. \right. \\
&\quad \left. \left. - \frac{1 - e^{-2\alpha(T-t)}}{2\alpha} \right] \right. \\
&\quad \left. + \nu_2 S \frac{\varepsilon_F^2}{(-\rho\bar{\nu})^2} \left[T - t - 2 \frac{1 - e^{-\alpha(T-t)}}{\alpha} + \frac{1 - e^{-2\alpha(T-t)}}{2\alpha} \right] \right. \\
&\quad \left. + \frac{1}{2} \left[\bar{\nu}_S S \frac{\varepsilon_F}{-\rho\bar{\nu}} \left\{ T - t - \frac{1 - e^{-\alpha(T-t)}}{\alpha} \right\} \right]^2 \right)
\end{aligned} \tag{A.153}$$

Then summing each previous sub results, we obtain the simplified version.

More explicitly we have

$$\begin{aligned}
\mathcal{M}_3(t) = & -\frac{S\bar{\nu}_S}{2} \left(-2(A+B)(T-t) - (3A+B) \frac{1-e^{-\alpha(T-t)}}{\alpha} \right. \\
& - 2(3A+B) \left((T-t)e^{-\alpha(T-t)} - \frac{1-e^{-\alpha(T-t)}}{\alpha} \right) \\
& + 2B(-\alpha(T-t)^2 e^{-\alpha(T-t)} - 2(T-t)e^{-\alpha(T-t)} + 2 \frac{1-e^{-\alpha(T-t)}}{\alpha}) \\
& + 2(3A+B) \frac{1-e^{-2\alpha(T-t)}}{2\alpha} - 2B \left((T-t)e^{-2\alpha(T-t)} - \frac{1-e^{-2\alpha(T-t)}}{2\alpha} \right) + (-A+B) \frac{1-e^{-3\alpha(T-t)}}{3\alpha} \left. \right) \\
& + 2\nu_{2S} S \frac{\nu_2 \varepsilon_F^3}{(-\rho\bar{\nu})^4} \left((T-t)(1+2e^{-\alpha(T-t)} - e^{-2\alpha(T-t)}) - 3 \frac{1-e^{-\alpha(T-t)}}{\alpha} + \frac{1-e^{-3\alpha(T-t)}}{3\alpha} \right) \\
& + \nu_{3S} S \frac{\varepsilon_F^3}{(-\rho\bar{\nu})^3} \left(T-t - 3 \frac{1-e^{-\alpha(T-t)}}{\alpha} + 3 \frac{1-e^{-2\alpha(T-t)}}{2\alpha} - \frac{1-e^{-3\alpha(T-t)}}{3\alpha} \right) \\
& + \left(\bar{\nu}_S S \frac{\nu_2 \varepsilon_F^2}{(-\rho\bar{\nu})^3} \left(T-t + 2 \left((T-t)e^{-\alpha(T-t)} - \frac{1-e^{-\alpha(T-t)}}{\alpha} \right) - \frac{1-e^{-2\alpha(T-t)}}{2\alpha} \right) \right. \\
& + \nu_{2S} \frac{\varepsilon_F^2}{(-\rho\bar{\nu})^2} \left(T-t - 2 \frac{1-e^{-\alpha(T-t)}}{\alpha} + \frac{1-e^{-2\alpha(T-t)}}{2\alpha} \right) \\
& + \frac{\bar{\nu}_S^2 S^2}{6} \frac{\varepsilon_F^2}{(-\rho\bar{\nu})^2} \left(T-t - \frac{1-e^{-\alpha(T-t)}}{\alpha} \right)^2 \bar{\nu}_S S \frac{\varepsilon_F}{(-\rho\bar{\nu})} \left[(T-t) - \frac{1-e^{-\alpha(T-t)}}{\alpha} \right] \\
& + \frac{\bar{\nu}_S S}{\alpha} \left(\frac{\varepsilon_F}{(-\rho\bar{\nu})} \left(1 - e^{-\alpha(T-t)} \right) \right) \left(\bar{\nu}_S S \frac{\nu_2 \varepsilon_F^2}{(-\rho\bar{\nu})^3} \left[T-t + 2(T-t)e^{-\alpha(T-t)} - 2 \frac{1-e^{-\alpha(T-t)}}{\alpha} \right. \right. \\
& \left. \left. - \frac{1-e^{-2\alpha(T-t)}}{2\alpha} \right] \right) \\
& + \nu_{2S} S \frac{\varepsilon_F^2}{(-\rho\bar{\nu})^2} \left[T-t - 2 \frac{1-e^{-\alpha(T-t)}}{\alpha} + \frac{1-e^{-2\alpha(T-t)}}{2\alpha} \right] \\
& + \frac{1}{2} \left[\bar{\nu}_S S \frac{\varepsilon_F}{-\rho\bar{\nu}} \left\{ T-t - \frac{1-e^{-\alpha(T-t)}}{\alpha} \right\} \right]^2 \left. \right) \\
& + \bar{\nu}_S S \frac{\varepsilon_F}{(-\rho\bar{\nu})} \left[(T-t) - \frac{1-e^{-\alpha(T-t)}}{\alpha} \right] \frac{\nu_2 \varepsilon_F^2}{(-\rho\bar{\nu})^3} (1 - 2\alpha(T-t)e^{-\alpha(T-t)} - e^{-2\alpha(T-t)}) \\
& - \frac{\bar{\nu}_S S}{2\alpha} \left(-2(A+B) \right. \\
& + (-(3A+B) + 2\alpha(T-t)(3A+B) + 2\alpha^2 B(T-t)^2) e^{-\alpha(T-t)} \\
& + (2(3A+B) + 4\alpha B(T-t)) e^{-2\alpha(T-t)} \\
& \left. + (-A+B) e^{-3\alpha(T-t)} \right) \\
& + \frac{S}{\alpha^2} \left(\bar{\nu}_S (1 + \bar{\nu}_S S) + \frac{\nu_{2S}}{2} \right) \left(\frac{\varepsilon_F}{(-\rho\bar{\nu})} \left[(T-t) - \frac{1-e^{-\alpha(T-t)}}{\alpha} \right] \right) \left(\frac{\varepsilon_F}{(-\rho\bar{\nu})} (1 - e^{-\alpha(T-t)}) \right)^2 \\
& + 2 \frac{\varepsilon_F}{(-\rho\bar{\nu})} (1 - e^{-\alpha(T-t)}) \frac{\nu_2 \varepsilon_F^2}{(-\rho\bar{\nu})^3} (1 - 2\alpha(T-t)e^{-\alpha(T-t)} - e^{-2\alpha(T-t)}) \left. \right) \\
& + \left(\frac{S}{3\alpha} \left(\frac{\bar{\nu}_S}{-\rho\bar{\nu}} \left(\frac{\nu_2^2}{-\rho\bar{\nu}} + \nu_3 \right) + \frac{\nu_2 \nu_{2S}}{-\rho\bar{\nu}} + \nu_{3S} \right) \right. \\
& \left. + \frac{\bar{\nu}_S S}{\alpha} \frac{S}{2\alpha} \left(\bar{\nu}_S \frac{\nu_2}{-\rho\bar{\nu}} + \nu_{2S} \right) + \frac{\bar{\nu}_S^3 S^3}{6\alpha^3} \right) \left(\frac{\varepsilon_F}{(-\rho\bar{\nu})} (1 - e^{-\alpha(T-t)}) \right)^3
\end{aligned}$$

This expression can be simplified. We point at the reader that

$$\mathbb{E}[N_{[t;T]}^3]_{(Q_n(t))_n} = 6(\mathcal{M}_3 + \mathcal{M}_2) + \mathcal{M}_1 \quad (\text{A.155})$$

that can be shortened as eq. 2.48

$$\begin{aligned} \mathbb{E}[N_{[t;T]}^3]_{(Q_n(t))_n} &= \bar{\nu}_S S \frac{\varepsilon_F}{(-\rho\bar{\nu})} (T-t) 3 \left(\frac{\varepsilon_F D_2}{-\rho^2} \right)^2 \left(1 - \rho \frac{\bar{\nu}_S D_{2S}}{\bar{\nu} D_2} \right) \left(1 + e^{-\alpha(T-t)} - 2 \frac{1 - e^{-\alpha(T-t)}}{\alpha(T-t)} \right) \\ &\quad - \frac{\varepsilon_F D_3}{\rho^3} \left(1 - \rho \frac{\bar{\nu}_S^2 D_{3S}}{\bar{\nu}^2 D_3} \right) \left(1 - \frac{3 - 4e^{-\alpha(T-t)} + 2e^{-2\alpha(T-t)}}{2\alpha(T-t)} \right) \\ &\quad + 6 \frac{\varepsilon_F^2}{(-\rho\bar{\nu})^2} \left(\nu_S S \frac{\nu_2}{(-\rho\nu)} + \nu_{2S} S \right) \left(T-t - \frac{1 - e^{-\alpha(T-t)}}{\alpha} \right) \left(\bar{\nu}_S S \frac{\varepsilon_F}{(-\rho\bar{\nu})} (T-t) + 1 \right) \\ &\quad + \bar{\nu}_S^3 S^3 \frac{\varepsilon_F^3}{(-\rho\bar{\nu})^3} (T-t)^3 + 6\bar{\nu}_S^2 S^2 \frac{\varepsilon_F^2}{(-\rho\bar{\nu})^2} (T-t)^2 + 2\bar{\nu}_S S \frac{\varepsilon_F}{(-\rho\bar{\nu})} (T-t) \end{aligned} \quad (\text{A.156})$$

Then the asymptotical behaviour of the moments can be settled. \square

Proof of the computation of the Feynman moments of order 2 and 3.

Finally, we have computed the three first moment of $Q_n(t)$

- $\mathcal{M}_1, \mathcal{M}_2, \mathcal{M}_3,$
- $\mathbb{E}[N_{[t;T]}^3]_{(Q_n(t))_n}, \mathbb{E}[N_{[t;T]}^2]_{(Q_n(t))_n}, \mathbb{E}[N_{[t;T]}]_{(Q_n(t))_n}.$

A.2.5 Generating functions

We recall here the principal use of a generating function, and we give the details of the previous computations of the annexes.

We denote $g(x, t)$ a generating function associated to the distribution $p_n(t)$: $g(x, t) := \sum_{n=0}^{+\infty} x^n p_n(t)$. What enables us to get

$$p_n(t) = \frac{1}{n!} \left[\frac{\partial^n g}{\partial x^n} \right]_{x=0} (t) \quad (\text{A.157})$$

We denote $g_\nu(x, t)$ the generated function associated to $p_{n,\nu}(t)$: $g_\nu(x, t) := \sum_{n=0}^{+\infty} x^n p_{n,\nu}(t)$

$$g_\nu = g^\nu \quad (\text{A.158})$$

because $p_{n,\nu}$ is a conditional probability, which can be broken down as follows $p_{n,\nu} = \sum_{n_1+\dots+n_\nu=n} \prod_{j=1}^\nu p_{n_j}$.

In order to get the moment of g_ν , we can differentiate with respect to the space variable x :

$$\left(\frac{\partial g^\nu}{\partial x}\right) = \nu g^{\nu-1} \frac{\partial g}{\partial x} \quad (\text{A.159})$$

$$\left(\frac{\partial^2 g^\nu}{\partial x^2}\right) = \nu(\nu-1)g^{\nu-2} \left(\frac{\partial g}{\partial x}\right)^2 + \nu g^{\nu-1} \left(\frac{\partial^2 g}{\partial x^2}\right) \quad (\text{A.160})$$

$$\begin{aligned} \left(\frac{\partial^3 g^\nu}{\partial x^3}\right) &= \nu(\nu-1)(\nu-2)g^{\nu-3} \left(\frac{\partial g}{\partial x}\right)^3 + \nu(\nu-1)g^{\nu-2} 2 \left(\frac{\partial g}{\partial x}\right) \left(\frac{\partial^2 g}{\partial x^2}\right) \\ &+ \nu(\nu-1)g^{\nu-2} \left(\frac{\partial g}{\partial x}\right) \left(\frac{\partial^2 g}{\partial x^2}\right) + \nu g^{\nu-1} \left(\frac{\partial^3 g}{\partial x^3}\right) \\ &= \nu(\nu-1)(\nu-2)g^{\nu-3} \left(\frac{\partial g}{\partial x}\right)^3 + 3\nu(\nu-1)g^{\nu-2} \left(\frac{\partial g}{\partial x}\right) \left(\frac{\partial^2 g}{\partial x^2}\right) + \nu g^{\nu-1} \left(\frac{\partial^3 g}{\partial x^3}\right) \end{aligned} \quad (\text{A.161})$$

$$\begin{aligned} \left(\frac{\partial^4 g^\nu}{\partial x^4}\right) &= \nu(\nu-1)(\nu-2)(\nu-3)g^{\nu-4} \left(\frac{\partial g}{\partial x}\right)^3 + 3\nu(\nu-1)(\nu-2)g^{\nu-3} \frac{\partial g}{\partial x} \\ &+ 3\nu(\nu-1)g^{\nu-2} \left(\frac{\partial^2 g}{\partial x^2}\right)^2 + 3\nu(\nu-1)g^{\nu-2} \left(\left(\frac{\partial^2 g}{\partial x^2}\right)^2 + \frac{\partial g}{\partial x} \frac{\partial^3 g}{\partial x^3}\right) \\ &+ \nu(\nu-1)g^{\nu-2} \frac{\partial^3 g}{\partial x^3} \frac{\partial g}{\partial x} + \nu g^{\nu-1} \frac{\partial^4 g}{\partial x^4} \quad (\text{A.162}) \\ &= \nu(\nu-1)(\nu-2)(\nu-3)g^{\nu-4} \left(\frac{\partial g}{\partial x}\right)^3 + 3\nu(\nu-1)(\nu-2)g^{\nu-3} \frac{\partial g}{\partial x} \\ &+ 4\nu(\nu-1)g^{\nu-2} \frac{\partial g}{\partial x} \frac{\partial^3 g}{\partial x^3} + 3\nu(\nu-1)g^{\nu-2} \left(\frac{\partial^2 g}{\partial x^2}\right)^2 + \nu g^{\nu-1} \frac{\partial^4 g}{\partial x^4} \end{aligned}$$

In order to get the differential equations for the considered moments (simple, factorial, etc...), we write properly the Fokker-Planck equations, which reads

$$-\frac{dg}{dt} + \lambda_T g = \lambda_F \sum_{\nu=0}^{\infty} f_\nu g^\nu + \lambda_C(\varepsilon_C x + (1 - \varepsilon_C)), \quad g(T) = 1 \quad (\text{A.163})$$

A first differentiation with respect to x provides

$$-\frac{d}{dt} \frac{\partial g}{\partial x} + \lambda_T \frac{\partial g}{\partial x} = \lambda_F \sum_{\nu=0}^{\infty} \nu f_\nu \frac{\partial g}{\partial x} g^{\nu-1} + \lambda_C \varepsilon_C, \quad \frac{\partial g}{\partial x}(T) = 0 \quad (\text{A.164})$$

A second one

$$-\frac{d}{dt} \frac{\partial^2 g}{\partial x^2} + \lambda_T \frac{\partial^2 g}{\partial x^2} = \lambda_F \sum_{\nu=0}^{\infty} \nu f_\nu \left\{ \frac{\partial^2 g}{\partial x^2} g^{\nu-1} + (\nu-1) \left(\frac{\partial g}{\partial x}\right)^2 g^{\nu-2} \right\}, \quad \frac{\partial^2 g}{\partial x^2}(T) = 0 \quad (\text{A.165})$$

A third one provides

$$-\frac{d}{dt} \frac{\partial^3 g}{\partial x^3} + \lambda_T \frac{\partial^3 g}{\partial x^3} = \lambda_F \sum_{\nu=0}^{\infty} \nu f_{\nu} \left\{ \frac{\partial^3 g}{\partial x^3} g^{\nu-1} + 3(\nu-1) \frac{\partial g}{\partial x} \frac{\partial^2 g}{\partial x^2} g^{\nu-2} + (\nu-1)(\nu-2) \left(\frac{\partial g}{\partial x} \right)^3 \right\}, \quad \frac{\partial^3 g}{\partial x^3}(T) = 0 \quad (\text{A.166})$$

A fourth one gives

$$\begin{aligned} -\frac{d}{dt} \frac{\partial^4 g}{\partial x^4} + \lambda_T \frac{\partial^4 g}{\partial x^4} &= \lambda_F \sum_{\nu=0}^{\infty} \nu f_{\nu} \left\{ \frac{\partial^4 g}{\partial x^4} g^{\nu-1} + 3(\nu-1) \left(\left(\frac{\partial^2 g}{\partial x^2} \right)^2 g^{\nu-2} + \frac{\partial g}{\partial x} \frac{\partial^3 g}{\partial x^3} g^{\nu-2} \right) \right. \\ &\quad \left. + 6(\nu-1)(\nu-2) \left(\frac{\partial g}{\partial x} \right) \frac{\partial^2 g}{\partial x^2} g^{\nu-3} + (\nu-1)(\nu-2)(\nu-3) \left(\frac{\partial g}{\partial x} \right)^4 g^{\nu-4} \right\}, \\ \frac{\partial^4 g}{\partial x^4}(T) &= 0 \end{aligned} \quad (\text{A.167})$$

A fifth one provides

$$\begin{aligned} -\frac{d}{dt} \frac{\partial^5 g}{\partial x^5} + \lambda_T \frac{\partial^5 g}{\partial x^5} &= \lambda_F \sum_{\nu=0}^{\infty} \nu f_{\nu} \left\{ \frac{\partial^5 g}{\partial x^5} g^{\nu-1} \right. \\ &\quad \left. + (\nu-1) \left(\frac{\partial g}{\partial x} \frac{\partial^4 g}{\partial x^4} g^{\nu-2} + 6 \frac{\partial^3 g}{\partial x^3} \frac{\partial^2 g}{\partial x^2} g^{\nu-2} + 3 \left(\frac{\partial^3 g}{\partial x^3} \frac{\partial^2 g}{\partial x^2} g^{\nu-2} + \frac{\partial g}{\partial x} \frac{\partial^4 g}{\partial x^4} \right) \right) \right. \\ &\quad \left. + 3(\nu-1)(\nu-2) \left(\frac{\partial g}{\partial x} \right) \frac{\partial^2 g}{\partial x^2} g^{\nu-3} \right. \\ &\quad \left. + 2(\nu-1)(\nu-2)(\nu-3) \frac{\partial^2 g}{\partial x^2} \left(\frac{\partial g}{\partial x} \right)^2 \left(3 + 2 \frac{\partial g}{\partial x} \right) g^{\nu-4} \right. \\ &\quad \left. + (\nu-1)(\nu-2)(\nu-3)(\nu-4) \left(\frac{\partial g}{\partial x} \right)^5 g^{\nu-5} \right\}, \\ \frac{\partial^5 g}{\partial x^5}(T) &= 0 \end{aligned} \quad (\text{A.168})$$

Generating function moments

We define the moments of the generating function g as

$$m_n(t) = \frac{1}{n!} \left[\frac{\partial^n g}{\partial x^n} \right]_{x=1} \quad (\text{A.169})$$

Using the Fokker-Planck equation for the moments, we obtain

$$\begin{aligned}
-\frac{1}{\alpha} \frac{dm_1}{dt} + m_1 &= \frac{1}{-\rho\bar{\nu}} \varepsilon_F(T-t), \quad m_1(T) = 0 \\
-\frac{1}{\alpha} \frac{dm_2}{dt} + m_2 &= \frac{\nu_2}{-\rho\bar{\nu}} m_1^2, \quad m_2(T) = 0 \\
-\frac{1}{\alpha} \frac{dm_3}{dt} + m_3 &= \frac{1}{-\rho\bar{\nu}} (\nu_3 m_1^3 + 2\nu_2 m_1 m_2), \quad m_3(T) = 0 \\
-\frac{1}{\alpha} \frac{dm_4}{dt} + m_4 &= \frac{1}{-\rho\bar{\nu}} (\nu_2(m_2^2 + \frac{3}{2} m_2 m_3) + \nu_3 m_1^2 m_2 + \nu_4 m_1^4), \quad m_4(T) = 0
\end{aligned} \tag{A.170}$$

From these equations we can get

$$m_{2,\nu} = \frac{1}{2} \left[\frac{\partial^2 g^\nu}{\partial x^2} \right]_{x=1} = \frac{\nu(\nu-1)}{2} m_1^2 + \nu m_2 \tag{A.171}$$

We can notice the fact that

$$\mathbb{E}[N(N-1)\cdots(N-n)] = n! m_n \tag{A.172}$$

More explicitly, we dispose of

$$\begin{cases} \mathbb{E}[N]_{(p_n(t))_n} = m_1(t) \\ \mathbb{E}[N^2]_{(p_n(t))_n} = 2m_2(t) + m_1(t) \\ \mathbb{E}[N^3]_{(p_n(t))_n} = 6(m_3(t) + m_2(t)) + m_1(t) \end{cases} \tag{A.173}$$

Generating function g_F

In this part we consider a specific generating function

Definition A.2.3. *We take into account the generating function associated to the induced fission*

$$g_F(x, t) = \sum_{\nu=0}^{+\infty} f_\nu g^\nu(x, t) \tag{A.174}$$

Proposition A.2.4. *The differentiate of g_F of order 1 to 3 with respect to x of the generating function g_F are*

$$\begin{aligned}
\frac{\partial g_F}{\partial x} &= \sum_{\nu=0}^{+\infty} \nu f_\nu \frac{\partial g}{\partial x} g^{\nu-1} \\
\frac{\partial^2 g_F}{\partial x^2} &= \sum_{\nu=0}^{+\infty} \nu f_\nu \frac{\partial^2 g}{\partial x^2} g^{\nu-1} + \sum_{\nu=0}^{+\infty} \nu(\nu-1) f_\nu \left(\frac{\partial g}{\partial x} \right)^2 g^{\nu-2} \\
\frac{\partial^3 g_F}{\partial x^3} &= \sum_{\nu=0}^{+\infty} \nu f_\nu \frac{\partial^3 g}{\partial x^3} g^{\nu-1} + \sum_{\nu=0}^{+\infty} \nu(\nu-1) f_\nu \frac{\partial g}{\partial x} \frac{\partial^2 g}{\partial x^2} g^{\nu-2} \\
&\quad + \sum_{\nu=0}^{+\infty} \nu(\nu-1) f_\nu 2 \frac{\partial g}{\partial x} \frac{\partial^2 g}{\partial x^2} g^{\nu-2} + \sum_{\nu=0}^{+\infty} \nu(\nu-1)(\nu-2) f_\nu \left(\frac{\partial g}{\partial x} \right)^3 g^{\nu-3}
\end{aligned} \tag{A.175}$$

By this fact we dispose of

$$\begin{aligned} \left[\frac{\partial g_F}{\partial x} \right]_{x=1} &= \bar{\nu}_S m_1(t) \\ \left[\frac{\partial^2 g_F}{\partial x^2} \right]_{x=1} &= 2\bar{\nu}_S m_2(t) + 2\nu_{2S} m_1^2(t) \\ \left[\frac{\partial^3 g_F}{\partial x^3} \right]_{x=1} &= 6\bar{\nu}_S m_3(t) + 12\nu_{2S} m_1(t) m_2(t) + 6\nu_{3S} m_1^3(t) \end{aligned} \quad (\text{A.176})$$

Proof. The two first equations are easy to obtain, the last one requires computing that

$$3 \times 2 \times 2 = 12 \quad (\text{A.177})$$

□

A.2.6 Feynman moments tools

This part is useful in 1.6.3.

In the following $S = S_F$ will refer to the intensity of the source and $S_\alpha = 0$. The Feynman moments can be computed thanks to the $\Gamma_{n,\infty}$.

The computation of $\Gamma_{1,\infty}(t)$ is

Proof. We retold that $\Gamma_{1,\infty}(t) = \left[\frac{\partial \mathcal{K}}{\partial x} \right]_{x=1}$ where $\mathcal{K} := \log \mathcal{G}$ and so

$$\mathcal{K} = \log G + \log G_{II,\infty}(g(x,t),t) \quad (\text{A.178})$$

Moreover

$$\log G = S \int_0^{T-t} \left(\sum_{\nu=0}^{+\infty} \hat{f}_\nu g^\nu(x, T-s) - 1 \right) ds \quad (\text{A.179})$$

Then when we differentiate \mathcal{K} one time with respect to x

$$\frac{\partial \mathcal{K}}{\partial x} = \frac{\partial \mathcal{K}}{\partial x} + \frac{\partial G_{II,\infty}(g(x,t),t)}{G_{II,\infty}(g(x,t),t)} \quad (\text{A.180})$$

where

$$\begin{aligned} \left[\frac{\partial G_{II,\infty}(g(x,t),t)}{\partial x} \right]_{x=1} &= \left[\frac{\partial g}{\partial x} \right]_{x=1} \left[\frac{\partial G_{II,\infty}(g(x,t),t)}{\partial x} \right]_{x=1} \\ &= m_1(t) \bar{\nu}_{II,\infty} \end{aligned} \quad (\text{A.181})$$

and so

$$\Gamma_{1,\infty}(t) = M_1(t) + m_1(t) \bar{\nu}_{II,\infty} \quad (\text{A.182})$$

what provides

$$\Gamma_{1,\infty}(t) = \bar{\nu}_S S \frac{\varepsilon_F}{-\rho \bar{\nu}} (T-t) \quad (\text{A.183})$$

□

The computation of $\Gamma_{2,\infty}(t)$ is

Proof. By definition, we know that

$$\Gamma_{2,\infty}(t) = \frac{1}{2} \left[\frac{\partial^2 \mathcal{K}}{\partial x^2} \right]_{x=1} \quad (\text{A.184})$$

and so we deduce

$$\Gamma_{2,\infty}(t) = \frac{1}{2} \left[\frac{\partial^2 K}{\partial x^2} \right]_{x=1} + \frac{1}{2} \left[\frac{\frac{\partial^2 G_{\Pi,\infty}(g(x,t),t)}{\partial x^2} G_{\Pi,\infty}(g(x,t),t) + \left(\frac{\partial G_{\Pi,\infty}(g(x,t),t)}{\partial x} \right)^2}{G_{\Pi,\infty}(g(x,t),t)^2} \right]_{x=1} \quad (\text{A.185})$$

But, we know that

$$G_{\Pi,\infty}(g(x,t),t) = 1 \quad (\text{A.186})$$

Moreover, we know

$$\begin{aligned} \frac{\partial^2 G_{\Pi,\infty}(g(x,t),t)}{\partial x^2} &= \frac{\partial}{\partial x} \frac{\partial G_{\Pi,\infty}(g(x,t),t)}{\partial x} \\ &= \frac{\partial}{\partial x} \left(\frac{\partial g}{\partial x} \frac{\partial G_{\Pi,\infty}}{\partial x}(g(x,t),t) \right) \\ &= \frac{\partial^2 g}{\partial x^2} \frac{\partial G_{\Pi,\infty}}{\partial x}(g(x,t),t) + \frac{\partial g}{\partial x} \frac{\partial^2 G_{\Pi,\infty}}{\partial x^2}(g(x,t),t) \end{aligned} \quad (\text{A.187})$$

what enables to understand that

$$\Gamma_{2,\infty}(t) = \Gamma_2(t) + m_2(t) \bar{\nu}_{\Pi,\infty} + m_1(t) \nu_{2,\Pi,\infty} + m_1^2(t) \bar{\nu}_{\Pi,\infty}^2 \quad (\text{A.188})$$

However

$$\begin{aligned} \Gamma_2(t) &= S \int_0^{T-t} \sum_{\nu=1}^{+\infty} \hat{f}_\nu m_{2,\nu}(T-s) ds \\ &= \nu_{2S} S I_1^{(2)}(t) + \bar{\nu}_S S I_2(t) \end{aligned} \quad (\text{A.189})$$

where

$$\begin{aligned} I_1^{(2)}(t) &= \int_0^{T-t} m_1^2(T-s) ds \\ &= \int_0^{T-t} \frac{\varepsilon_F^2}{\rho^2 \bar{\nu}^2} (1 - 2e^{-\alpha s} + e^{-2\alpha s}) ds \\ &= \frac{\varepsilon_F^2}{\rho^2 \bar{\nu}^2} \left(T-t - 2 \frac{1 - e^{-\alpha(T-t)}}{\alpha} + \frac{1 - e^{-2\alpha(T-t)}}{2\alpha} \right) \end{aligned} \quad (\text{A.190})$$

and also

$$\begin{aligned} I_2(t) &= \int_0^{T-t} m_2(T-s) ds \\ &= \frac{\varepsilon_F^2}{(-\rho \bar{\nu})^3} \int_0^{T-t} (1 - 2\alpha s e^{-\alpha s} - e^{-2\alpha s}) ds \\ &= \frac{\varepsilon_F^2}{(-\rho \bar{\nu})^3} \left(T-t + 2(T-t)e^{-\alpha(T-t)} - 2 \frac{1 - e^{-\alpha(T-t)}}{\alpha} - \frac{1 - e^{-2\alpha(T-t)}}{2\alpha} \right) \end{aligned} \quad (\text{A.191})$$

what provides

$$\begin{aligned} \Gamma_2(t) &= \nu_{2S} S \frac{\varepsilon_F^2}{\rho^2 \bar{\nu}^2} \left(T - t + 2 \frac{1 - e^{-\alpha(T-t)}}{\alpha} + \frac{1 - e^{-2\alpha(T-t)}}{2\alpha} \right) \\ &\quad + \bar{\nu}_S S \frac{\varepsilon_F^2}{(-\rho \bar{\nu})^3} \left(T - t + 2(T-t)e^{-\alpha(T-t)} - \frac{1 - e^{-\alpha(T-t)}}{\alpha} - \frac{1 - e^{-2\alpha(T-t)}}{2\alpha} \right) \end{aligned} \quad (\text{A.192})$$

Moreover, we know that

$$\begin{aligned} 2 \frac{m_2(t) \bar{\nu} \Pi_{1,\infty}}{\Gamma_{1,\infty}(t)} &= \frac{2 \frac{\varepsilon_F^2}{(-\rho \bar{\nu})^3} (1 - 2\alpha(T-t)e^{-\alpha(T-t)} - e^{-2\alpha(T-t)}) \frac{\bar{\nu}_S S}{\alpha}}{\bar{\nu}_S S \frac{\varepsilon_F}{-\rho \bar{\nu}} (T-t)} \\ &= 2 \frac{\varepsilon_F}{(-\rho \bar{\nu})^2} \left(-2e^{-\alpha(T-t)} + \frac{1 - e^{-2\alpha(T-t)}}{\alpha(T-t)} \right) \end{aligned} \quad (\text{A.193})$$

also

$$\begin{aligned} 2 \frac{m_1(t) \nu_{2,\infty}}{\Gamma_{1,\infty}(t)} &= \frac{2 \frac{\varepsilon_F}{-\rho \bar{\nu}} (1 - e^{-\alpha(T-t)}) \left(\frac{\bar{\nu}_S S}{2\alpha} \left(\frac{\bar{\nu}_S S}{\alpha} + \frac{\nu_2}{-\rho \bar{\nu}} \right) + \frac{\nu_{2S} S}{2\alpha} \right)}{\bar{\nu}_S S \frac{\varepsilon_F}{-\rho \bar{\nu}} (T-t)} \\ &= \left(\left(\frac{\bar{\nu}_S S}{\alpha} + \frac{\nu_2}{-\rho \bar{\nu}} \right) + \frac{\nu_{2S}}{\bar{\nu}_S} \right) \frac{1 - e^{-\alpha(T-t)}}{\alpha(T-t)} \end{aligned} \quad (\text{A.194})$$

in addition

$$\begin{aligned} 2 \frac{m_1^2(t) \bar{\nu}^2 \Pi_{1,\infty}}{\Gamma_{1,\infty}(t)} &= \frac{\left(\frac{\varepsilon_F}{-\rho \bar{\nu}} \right)^2 (1 - e^{-\alpha(T-t)})^2 \left(\frac{\bar{\nu}_S S}{\alpha} \right)^2}{\bar{\nu}_S S \frac{\varepsilon_F}{-\rho \bar{\nu}} (T-t)} \\ &= 2 \frac{\bar{\nu}_S S}{\alpha} \frac{\varepsilon_F}{-\rho \bar{\nu}} \frac{(1 - e^{-\alpha(T-t)})^2}{\alpha(T-t)} \end{aligned} \quad (\text{A.195})$$

And finally, we dispose of

$$\begin{aligned} \Gamma_{2,\infty}(t) &= \nu_{2S} S \frac{\varepsilon_F^2}{\rho^2 \bar{\nu}^2} \left(T - t + 2 \frac{1 - e^{-\alpha(T-t)}}{\alpha} + 2 \frac{1 - e^{-2\alpha(T-t)}}{2\alpha} \right) \\ &\quad + \bar{\nu}_S S \frac{\varepsilon_F^2}{(-\rho \bar{\nu})^3} \left(T - t + 2(T-t)e^{-\alpha(T-t)} - 2 \frac{1 - e^{-\alpha(T-t)}}{\alpha} - \frac{1 - e^{-2\alpha(T-t)}}{2\alpha} \right) \end{aligned} \quad (\text{A.196})$$

□

We can conclude the explicit expression of $Y_2(T)$

$$Y_2 = \frac{2\Gamma_{2,\infty}(t)}{\Gamma_{1,\infty}(t)} \quad (\text{A.197})$$

A.2.7 Feynman and simple moments: passage formula

We establish the equations between the Feynman and the simple moments in order to have less cost in computations in the inverse problem 3.1. We recall

$$Y_2 = \frac{\mathbb{E}[(N - \mathbb{E}[N])^2]}{\mathbb{E}[N]} - 1 \quad (\text{A.198})$$

Then

$$\boxed{Y_2 = \frac{\mathbb{E}[N^2]}{\mathbb{E}[N]} - \mathbb{E}[N] - 1} \quad (\text{A.199})$$

And reciprocally

$$\boxed{\mathbb{E}[N^2] = \mathbb{E}[N](Y_2 + \mathbb{E}[N] + 1)} \quad (\text{A.200})$$

On the other hand,

$$Y_3 = \frac{\mathbb{E}[(N - \mathbb{E}[N])^3]}{\mathbb{E}[N]} - 1 - 3\left(\frac{\mathbb{E}[(N - \mathbb{E}[N])^2]}{\mathbb{E}[N]} - 1\right) \quad (\text{A.201})$$

Then

$$\begin{aligned} Y_3 &= \frac{\mathbb{E}[N^3 - 3N^2\mathbb{E}[N] + 3N\mathbb{E}[N]^2 - \mathbb{E}[N]^3]}{\mathbb{E}[N]} - 3\left(\frac{\mathbb{E}[N^2]}{\mathbb{E}[N]} - \mathbb{E}[N] - 1\right) \\ &= \frac{\mathbb{E}[N^3] - 3\mathbb{E}[N^2]\mathbb{E}[N] + 2\mathbb{E}[N]^3}{\mathbb{E}[N]} - 3\left(\frac{\mathbb{E}[N^2]}{\mathbb{E}[N]} - \mathbb{E}[N] - 1\right) \end{aligned} \quad (\text{A.202})$$

Finally,

$$\boxed{Y_3 = \frac{\mathbb{E}[N^3]}{\mathbb{E}[N]} - 3\mathbb{E}[N^2] + 2\mathbb{E}[N]^2 - 3\left(\frac{\mathbb{E}[N^2]}{\mathbb{E}[N]} - \mathbb{E}[N]\right) + 2} \quad (\text{A.203})$$

Conversely,

$$\boxed{\mathbb{E}[N^3] = \mathbb{E}[N](Y_3 + 3\mathbb{E}[N^2] - 2\mathbb{E}[N]^2) + 3(\mathbb{E}[N^2] - \mathbb{E}[N]^2) - 2\mathbb{E}[N]} \quad (\text{A.204})$$

A.2.8 Euler's method for the moments of the neutrons detected

This subsection is useful in 2.4.

In the following $S = S_F$ will refer to the intensity of the source and $S_\alpha = 0$.

Starting again from the differential equation on G

$$-\frac{\partial G}{\partial t} = SG(g_F - 1) \quad (\text{A.205})$$

We differentiate a first time

$$-\frac{\partial}{\partial t} \frac{\partial G}{\partial x} = S\left(\frac{\partial G}{\partial x}(g_F - 1) + G\frac{\partial g_F}{\partial x}\right) \quad (\text{A.206})$$

Evaluated in $x = 1$, we obtain

$$\boxed{-\frac{d}{dt}M_1 = \bar{\nu}_S S m_1} \quad (\text{A.207})$$

Then we differentiate a second time the differential equation on G

$$-\frac{\partial}{\partial t} \frac{\partial^2 G}{\partial x^2} = S\left(\frac{\partial^2 G}{\partial x^2}(g_F - 1) + 2\frac{\partial G}{\partial x} \frac{\partial g_F}{\partial x} + G\frac{\partial^2 g_F}{\partial x^2}\right) \quad (\text{A.208})$$

Remark A.2.5. *Evaluated in $x = 1$ and divided by 2, we obtain*

$$\boxed{-\frac{d}{dt}M_2 = S(\bar{\nu}_S(M_1m_1 + m_2) + \nu_{2S}m_1^2)} \quad (\text{A.209})$$

In order to finally derive a last time

$$-\frac{\partial}{\partial t} \frac{\partial^3 G}{\partial x^3} = S\left(\frac{\partial^3 G}{\partial x^3}(g_F - 1) + 3\frac{\partial^2 G}{\partial x^2} \frac{\partial g_F}{\partial x} + 3\frac{\partial G}{\partial x} \frac{\partial^2 g_F}{\partial x^2} + G \frac{\partial^3 g_F}{\partial x^3}\right) \quad (\text{A.210})$$

By evaluating in $x = 1$ and dividing by 6, we obtain

$$\boxed{-\frac{d}{dt}M_3 = S(\bar{\nu}_S(M_2m_1 + M_1m_2 + m_3) + \nu_{2S}(M_1m_1^2 + 2m_1m_2) + \nu_{3S}m_1^3)} \quad (\text{A.211})$$

$(\mathcal{M}_j)_{j=1,3}$

Starting from the equation

$$\mathcal{G}(x, t) = G(x, t)G_{II,\infty}(g(x, t))$$

To obtain the explicit Euler scheme for $\mathcal{M}_1(t)$, we differentiate this equation with respect to x and evaluate in $x = 1$,

$$\mathcal{M}_1(t) = M_1(t) + \bar{\nu}_{II,\infty}m_1(t)$$

then we differentiate the obtained equation with respect to t ,

$$\boxed{\frac{d\mathcal{M}_1(t)}{dt} = \frac{dM_1(t)}{dt} + \bar{\nu}_{II,\infty} \frac{dm_1(t)}{dt}.} \quad (\text{A.212})$$

To obtain the explicit Euler scheme for $\mathcal{M}_2(t)$, we differentiate the equation 1.249 (state-of-the-art) with respect to x two times and divide by 2 and evaluate in $x = 1$,

$$\mathcal{M}_2(t) = M_2(t) + \bar{\nu}_{II,\infty}(M_1(t)m_1(t) + m_2(t)) + \nu_{2,II,\infty}m_1^2(t)$$

then we differentiate the obtained equation with respect to t ,

$$\boxed{\frac{d\mathcal{M}_2(t)}{dt} = \frac{dM_2(t)}{dt} + \bar{\nu}_{II,\infty} \frac{d(M_1(t)m_1(t) + m_2(t))}{dt} + \nu_{2,II,\infty} \frac{dm_1^2(t)}{dt}} \quad (\text{A.213})$$

To obtain the explicit Euler scheme for $\mathcal{M}_3(t)$, we differentiate the equation 1.249 (state-of-the-art) with respect to x three times and divide by 6 and evaluate in $x = 1$, then we differentiate the obtained equation with respect to t ,

$$\boxed{\begin{aligned} \frac{d\mathcal{M}_3}{dt} &= \frac{dM_3}{dt} + \bar{\nu}_{II,\infty} \frac{(dm_1M_2 + m_1dM_2 + dM_1m_2 + M_1dm_2)}{dt} \\ &+ \nu_{2,II,\infty} \frac{(2m_1dm_1M_1 + m_1^2dM_1 + 2(dm_1m_2 + m_1dm_2))}{dt} \\ &+ \bar{\nu}_{II,\infty} \frac{dm_3}{dt} + 3\nu_{3,II,\infty} \frac{m_1^2dm_1}{dt} \end{aligned}} \quad (\text{A.214})$$

A.2.9 Panjer formula

We retold here the Panjer formula the $\Gamma_p(T)$, useful in 1.6.3.

We still retold the expression so that the reader could bring closer to the equation for the $\Gamma_p(T)$.

Let start again from

$$\frac{\partial G}{\partial x}(x, t) = \left\{ \int_t^T S \frac{\partial g_F}{\partial x} ds \right\} G(x, t) \quad (\text{A.215})$$

Using the formula for the limited expansion in $x = 1$ of the generating function G in order to obtain the moments, we dispose of

$$\begin{aligned} \frac{\partial}{\partial x} \left(\sum_{n=0}^{\infty} (x-1)^n M_n \right) &= \int_t^T S \left(\frac{\partial}{\partial x} (x-1)^i m_i^F \right) dt \sum_{j=0}^{\infty} (x-1)^j M_j \\ \sum_{n=1}^{\infty} n(x-1)^{n-1} M_n &= \left(\sum_{i=1}^{\infty} i(x-1)^{i-1} \Gamma_i \right) \sum_{j=0}^{\infty} (x-1)^j M_j = \sum_{i=1}^{\infty} i(x-1)^{i-1} \Gamma_i \sum_{j=0}^{\infty} (x-1)^j M_j \\ &= \sum_{n=1}^{\infty} \left(n M_n \right) (x-1)^{n-1} = \sum_{n=1}^{\infty} \left(\sum_{i=1}^n i \Gamma_i M_{n-i} \right) (x-1)^{n-1} \end{aligned} \quad (\text{A.216})$$

What enables to get by identification of the general term of the present power series, and to conclude that

$$\boxed{n M_n = \sum_{i=1}^n \Gamma_i M_{n-i}} \quad (\text{A.217})$$

Thus, we expose what enables us to conclude the expression of the Feynman moments in function of the M_n .

$$\begin{aligned} M_0 &= 1 \\ M_1 &= \Gamma_1 \\ 2M_2 &= \Gamma_1 M_1 + 2\Gamma_2 \\ 3M_3 &= \Gamma_2 M_1 + 2\Gamma_2 M_1 + 3\Gamma_3 \end{aligned} \quad (\text{A.218})$$

What enables us to conclude that

$$\boxed{\begin{aligned} Y &= 2 \frac{\Gamma_2}{\Gamma_1} = 2 \frac{M_2}{M_1} - M_1 \\ X &= 6 \frac{\Gamma_3}{\Gamma_1} = 6 \frac{M_3}{M_1} - 6M_2 + 2M_1^2 \end{aligned}} \quad (\text{A.219})$$

A.2.10 Link between $Q_n(t)$ and $P_n(t)$

The aim of this subpart is to make a connection between $Q_n(t)$ and $P_n(t)$. To do so, we retold the definition of $P_n(t)$.

Definition A.2.6. *The probability of detecting n neutrons between t and T in the system knowing the fact there were 0 neutrons at time t is*

$$P_n(t) = \mathbb{P}(n, T|0, t) \quad (\text{A.220})$$

When the measure has begun at infinitesimal far time, we have

$$P_n(-\infty) = \mathbb{P}(n, T|0, -\infty) \quad (\text{A.221})$$

For $t < 0$, we can decompose $P_n(t)$ of the following manner

$$P_n(t) = \mathbb{P}(n, T|0, t) = \sum_{i=0}^{\infty} \mathbb{P}(n, T|i, 0) \Pi(i, 0|0, t) \quad (\text{A.222})$$

By moving t toward $-\infty$, we obtain

$$P_n(-\infty) = \sum_{i=0}^{\infty} \mathbb{P}(n, T|i, 0) \Pi(i, 0|0, -\infty) \quad (\text{A.223})$$

But $\Pi(i, 0|0, -\infty)$ is the stationary distribution of the number of neutrons present in the system.

So we can deduce

$$P_n(-\infty) = Q_n(t) \quad (\text{A.224})$$

We have an expression which depends on t and another that does not depend.

A.2.11 About ε_F , ε_C

This subsection is useful in the state-of-the-art 1.132 and in the inverse problem 3.1.

Now, we establish the relation

$$\varepsilon_F \lambda_F = \varepsilon_C \lambda_C \quad (\text{A.225})$$

Consider the following mean rate

$$\begin{aligned} \lambda_D &:= \text{mean rate of detections} \\ \lambda_F &:= \text{mean rate of fissions} \\ \lambda_C &:= \text{mean rate of capture} \end{aligned} \quad (\text{A.226})$$

and then we have the efficiencies of detection

$$\begin{aligned} \varepsilon_F &= \frac{\lambda_D}{\lambda_F} \\ \varepsilon_C &= \frac{\lambda_D}{\lambda_C} \end{aligned} \quad (\text{A.227})$$

then

$$\begin{aligned} \lambda_D &= \frac{\lambda_D}{\lambda_F} \lambda_F = \varepsilon_F \lambda_F \\ \lambda_D &= \frac{\lambda_D}{\lambda_C} \lambda_C = \varepsilon_C \lambda_C \end{aligned} \quad (\text{A.228})$$

and so

$$\boxed{\varepsilon_F \lambda_F = \varepsilon_C \lambda_C} \quad (\text{A.229})$$

Moreover, by definition of k_{eff} , we know that

$$\boxed{k_{eff} = \frac{\bar{\nu} \lambda_F}{\lambda_T}} \quad (\text{A.230})$$

We can deduce from the former equation

$$\begin{aligned} \lambda_T k_{eff} &= \bar{\nu} \lambda_F \\ \lambda_T &= \frac{\bar{\nu}}{k_{eff}} \lambda_F \\ \lambda_C + \lambda_F &= \frac{\bar{\nu}}{k_{eff}} \lambda_F \\ \lambda_C &= \lambda_F \left(\frac{\bar{\nu}}{k_{eff}} - 1 \right) \end{aligned} \quad (\text{A.231})$$

and so that

$$\boxed{\varepsilon_F = \varepsilon_C \left(\frac{\bar{\nu}}{k_{eff}} - 1 \right)} \quad (\text{A.232})$$

The different parameters are linked by the relations

$$\begin{aligned} \alpha &= \lambda_T - \bar{\nu} \lambda_F = \frac{1 - k_{eff}}{\theta_T} \\ \rho &= 1 - \frac{\lambda_T}{\bar{\nu} \lambda_F} = \frac{k_{eff} - 1}{k_{eff}} \end{aligned} \quad (\text{A.233})$$

k_{eff} is the multiplication factor (sub-critical system when $k_{eff} < 1$)
 α is the coefficient of the neutron decrease (sub-critical)

We notice that they are all linked by the cross-section notion. This notion is then crucial for the description of our system.

Remark A.2.7. *Here are some computations*

$$\frac{k_{eff}}{\theta_T \bar{\nu}} = \frac{1 - k_{eff}}{\theta_T} \frac{k_{eff}}{(1 - k_{eff}) \bar{\nu}} = \frac{\alpha \nu_2}{-\rho \bar{\nu}} \quad (\text{A.234})$$

$$\frac{\lambda_F}{\alpha} = \frac{\lambda_F}{\bar{\nu} \lambda_F} \frac{1}{\frac{\lambda_T}{\bar{\nu} \lambda_F} - 1} \quad (\text{A.235})$$

A.2.12 MCNP-6 and Tripoli-4 parameters

Here are the details of the numerical cases used in chapter 2, 2.5.

In the first case

We present here the Tripoli-4 data file for the case with Californium-252

| First test case | | |
|-------------------|-------|-------------------------------------|
| Layer composition | Width | Density |
| 252Cf | 0.01 | unknown |
| POLY, C, H_CH2 | 19.99 | 300 POLY 0.9 2 C 0.856 H_CH2 0.1438 |
| AIR, O16, N14 | 4 | 300 AIR 0.0013 2 O16 0.22 N14 0.78 |
| HELIUM3 | 2 | 300 HELIUM3 0.001 1 HE3 1 |

Here are some handling about the moments in the case of spontaneous fission source only.

$$\mathbb{E}[N_{[0,T]}] = \frac{\varepsilon_F S}{-\rho \bar{\nu}} = \varepsilon_S S \quad (\text{A.236})$$

What enables to deduce the following equation

$$\varepsilon_F = -\rho \bar{\nu} \varepsilon_S \quad (\text{A.237})$$

Remark A.2.8. *In the case of a pure spontaneous fission source, the reactivity ρ and the induced fission data (e.g. $\bar{\nu}$) are not defined.*

In the same way, we can establish that

$$Y_{2,\infty} = \varepsilon_S \bar{\nu}_S D_{2S} \quad (\text{A.238})$$

and

$$Y_{3,\infty} = \varepsilon_S^2 \bar{\nu}_S^2 D_{3S} \quad (\text{A.239})$$

For the second case

We present here the Tripoli-4 data file is

| Second test case | | |
|-------------------|-------|-------------------------------------|
| Layer composition | Width | Density |
| Water comp | 14 | PUNCTUAL 300 |
| POLY, C, H_CH2 | 6 | 300 POLY 0.9 2 C 0.856 H_CH2 0.1438 |
| AIR, O16, N14 | 4 | 300 AIR 0.0013 2 O16 0.22 N14 0.78 |
| HELIUM3 | 2 | 300 HELIUM3 0.001 1 HE3 1 |

We obtain the following moments:

$$\begin{aligned} \mathbb{E}[N_{[0,T]}] &= \frac{\varepsilon_F S}{-\rho \bar{\nu}} \\ Y_{2,\infty} &= \frac{\varepsilon_F D_2}{\rho^2} \left(1 - \rho \frac{\bar{\nu}_S D_{2S}}{\bar{\nu} D_2} \right) \\ Y_{3,\infty} &= 3 \left(\frac{\varepsilon_F D_2}{-\rho^2} \right)^2 \left(1 - \rho \frac{\bar{\nu}_S D_{2S}}{\bar{\nu} D_2} \right) - \frac{\varepsilon_F^2 D_3}{\rho^3} \left(1 - \rho \frac{\bar{\nu}_S^2 D_{3S}}{\bar{\nu}^2 D_3} \right) \end{aligned} \quad (\text{A.240})$$

A.3 Inverse problem

A.3.1 The program ntc0b_cov2

The following statements help to provide the data in 3.2.

In order to calculate an approximate version of the simple moments of order 1 to 6 of $Q_n(t)$ used in the covariance matrix of the measurements in the Inverse Problem chapter, we programmed the algorithm ntc0b_cov2. A general approach can be found in [Hum19].

In a first part, the algorithm ntc0b_cov2 uses an implicit Euler resolution of the backward EDO for $p_n(t)$

$$-\frac{dp_n}{dt}(t) + \lambda_T p_n(t) = \lambda_F \sum_{\nu=0}^{\nu_{max}} f_\nu p_{n,\nu}(t) + \lambda_C (\varepsilon_C \delta_{n,1} + (1 - \varepsilon_C) \delta_{n,0}), \quad p_n(T) = \delta_{n,0} \quad (\text{A.241})$$

By the use of the generating function

$$g(x, t) = \sum_n x^n p_n(t) \quad (\text{A.242})$$

and uses the Leibniz formula, in coupled equations.

In a second part, the algorithm ntc0b_cov2 uses an implicit Euler resolution of the backward EDO for $P_n(t)$

$$-\frac{dP_n}{dt}(t) = -S P_n(t) + S \sum_{\nu=0}^M f_{\nu,S} P_{n,\nu}(t), \quad P_n(T) = \delta_{n,0} \quad (\text{A.243})$$

for the binomial cumulants

$$\Gamma_p(T - t) := \frac{1}{p!} \left[\frac{\partial^p}{\partial x^p} \mathcal{K}_{Q_n(t)} \right]_{x=1}, \quad \forall p \in \mathbb{N}^* \quad (\text{A.244})$$

of order 1 to 6, where

$$\mathcal{K} = \log \mathcal{G} = \log G + \log G_{\Pi, \infty}(g(x, t)) \quad (\text{A.245})$$

and uses the Panjer formula (see State of art).

A.3.2 Vectorial version of CLT

This subsection is useful for the computation of the empirical covariance matrix of the observations 1.354.

The following results come from Central Limit Theorem. In a first part, we will examine the Cramér-Wold lemma.

Lemma A.3.1. *Cramér-Wold*

The sequence of random vectors $(\mathbf{X}_l)_{l \in \mathbb{N}}$ in the vectorial space E converges in law in E to \mathbf{X} if and only if for all linear form u on E , $u(\mathbf{X}_l)$ converges in law to $u(\mathbf{X})$.

This is a key point in order to prove the vectorial version of the CLT. Then we can establish the vectorial version of the central limit theorem.

Theorem A.3.2. *Let $(\mathbf{X}_l)_{l \in \mathbb{N}}$ be a sequence of independent and identically distributed random vectors in \mathbb{R}^d , and square-integrable (i.e. $\mathbf{E}[\mathbf{X}_1^2] < +\infty$) and $S_n := \sum_{i=1}^n \mathbf{X}_i$. Then*

$$\frac{S_n - n\mathbf{E}[\mathbf{X}_1]}{\sqrt{n}} \xrightarrow[n \rightarrow +\infty]{\text{law}} N(0, K) \quad (\text{A.246})$$

where K is the covariance matrix of \mathbf{X}_1 .

Proof. Let u be a linear form on \mathbb{R}^d . We will obtain the result thanks to the Cramér-Wold lemma by proving $u(n^{-\frac{1}{2}}(S_n - \mathbf{E}[S_n]))$ converges to $u(Z)$ where Z is a Gaussian random vector of law $N(0, K)$.

Note that $\mathbf{E}[u(Z)] = u(\mathbf{E}[Z]) = u(0) = 0$ and also $\text{Var}(u(Z)) = u(Ku) = \text{Var}(\mathbf{X}_1)$. Moreover,

$$u\left(\frac{S_n - n\mathbf{E}[\mathbf{X}_1]}{\sqrt{n}}\right) = \frac{1}{\sqrt{n}} \sum_{i=1}^n (u(\mathbf{X}_i) - \mathbf{E}[u(\mathbf{X}_i)]) \quad (\text{A.247})$$

$u(\mathbf{X}_i)$ are real independent random variables, with same law and square-integrable ($|\mathbf{E}u(\mathbf{X}_1)|^2 \leq |u| |\mathbf{E}(\mathbf{X}_1)|^2$). We can now apply the CLT for scalar. \square

Application

Let's settle $\mathbf{X}_l = (N_l^k)_{k \in \llbracket 1,3 \rrbracket}$ the vector of the power 1, 2, and 3 of the neutron detection distribution.

Proposition A.3.3. *The covariance matrix of \mathbf{X}_l is*

$$K := \text{Cov}(\mathbf{X}_l) = \begin{pmatrix} \mathbf{E}[N^2] - \mathbf{E}[N]^2 & \mathbf{E}[N^3] - \mathbf{E}[N]\mathbf{E}[N^2] & \mathbf{E}[N^4] - \mathbf{E}[N]\mathbf{E}[N^3] \\ \mathbf{E}[N^3] - \mathbf{E}[N]\mathbf{E}[N^2] & \mathbf{E}[N^4] - \mathbf{E}[N^2]^2 & \mathbf{E}[N^5] - \mathbf{E}[N^2]\mathbf{E}[N^3] \\ \mathbf{E}[N^4] - \mathbf{E}[N]\mathbf{E}[N^3] & \mathbf{E}[N^5] - \mathbf{E}[N^2]\mathbf{E}[N^3] & \mathbf{E}[N^6] - \mathbf{E}[N^3]^2 \end{pmatrix} \quad (\text{A.248})$$

Proof. By definition, we know

$$\begin{aligned} \text{Cov}(\mathbf{X}_l) = & \\ & \begin{pmatrix} \mathbf{E}[(X_1 - \mathbf{E}[X_1])(X_1 - \mathbf{E}[X_1])] & \mathbf{E}[(X_1 - \mathbf{E}[X_1])(X_2 - \mathbf{E}[X_2])] & \mathbf{E}[(X_1 - \mathbf{E}[X_1])(X_3 - \mathbf{E}[X_3])] \\ \mathbf{E}[(X_2 - \mathbf{E}[X_2])(X_1 - \mathbf{E}[X_1])] & \mathbf{E}[(X_2 - \mathbf{E}[X_2])(X_2 - \mathbf{E}[X_2])] & \mathbf{E}[(X_2 - \mathbf{E}[X_2])(X_3 - \mathbf{E}[X_3])] \\ \mathbf{E}[(X_3 - \mathbf{E}[X_3])(X_1 - \mathbf{E}[X_1])] & \mathbf{E}[(X_3 - \mathbf{E}[X_3])(X_2 - \mathbf{E}[X_2])] & \mathbf{E}[(X_3 - \mathbf{E}[X_3])(X_3 - \mathbf{E}[X_3])] \end{pmatrix} \end{aligned} \quad (\text{A.249})$$

This matrix is symmetrical by definition.

Then

$$\begin{aligned} \mathbf{E}[(X_1 - \mathbf{E}[X_1])(X_1 - \mathbf{E}[X_1])] &= \mathbf{E}[X_1^2 - 2\mathbf{E}[X_1]^2 + \mathbf{E}[X_1]^2] \\ &= \mathbf{E}[X_1^2] - \mathbf{E}[X_1]^2 \\ &= \mathbf{E}[N^2] - \mathbf{E}[N]^2 \end{aligned} \quad (\text{A.250})$$

and also

$$\begin{aligned}
\mathbb{E}[(X_2 - \mathbb{E}[X_2])(X_1 - \mathbb{E}[X_1])] &= \mathbb{E}[X_1X_2 - X_1\mathbb{E}[X_2] - X_2\mathbb{E}[X_1] + \mathbb{E}[X_2]\mathbb{E}[X_1]] \\
&= \mathbb{E}[X_1X_2] - \mathbb{E}[X_1]\mathbb{E}[X_2] \\
&= \mathbb{E}[N^3] - \mathbb{E}[N]\mathbb{E}[N^2]
\end{aligned} \tag{A.251}$$

Using the previous principle, we will do the same computation for the other matrix coefficient.

And so, we obtain the result. \square

Remark A.3.4. Let $e_j, j \in \llbracket 1; 3 \rrbracket$ be the j basis element of \mathbb{R}^3 . We can obtain the variance of each component of \mathbf{X}_t .

So

$$\begin{aligned}
\text{Var}[N] &= e_1^T K e_1 = \mathbb{E}[N^2] - \mathbb{E}[N]^2 \\
\text{Var}[N^2] &= e_2^T K e_2 = \mathbb{E}[N^4] - \mathbb{E}[N^2]^2 \\
\text{Var}[N^3] &= e_3^T K e_3 = \mathbb{E}[N^6] - \mathbb{E}[N^3]^2
\end{aligned} \tag{A.252}$$

A.3.3 Confidence interval

This subsection is useful for the first case of the case study 2.4.

We are about to settle the following result

$$\frac{\sqrt{n}(\hat{M}_j - M_j)}{\hat{\sigma}_j} \xrightarrow[n \rightarrow +\infty]{\text{law}} N(0, 1), \forall j \in \llbracket 1; 3 \rrbracket \tag{A.253}$$

in order to plot rightly the confidence interval of the M_j .

Firstly, the CLT claims

$$\frac{\sqrt{n}(\hat{M}_j - M_j)}{\sigma_j} \xrightarrow[n \rightarrow +\infty]{\text{law}} N(0, 1), \forall j \in \llbracket 1; 3 \rrbracket \tag{A.254}$$

Secondly, the Law of large number states

$$\hat{\sigma}_j = \sqrt{\hat{M}_{2j} - \hat{M}_j^2} \xrightarrow[n \rightarrow +\infty]{\text{probability}} \sigma \tag{A.255}$$

where $\sigma = \sqrt{M_{2j} - M_j^2}$.

Finally, we use the Slutsky theorem in order to settle

$$\boxed{\frac{\sqrt{n}(\hat{M}_j - M_j)}{\hat{\sigma}_j} = \frac{\sqrt{n}(\hat{M}_j - M_j)}{\sigma_j} \frac{\sigma_j}{\hat{\sigma}_j} \xrightarrow[n \rightarrow +\infty]{\text{law}} N(0, 1)} \tag{A.256}$$

It enables to draw confidence intervals of the $M_j, \forall j \in \llbracket 1; 3 \rrbracket$.

A.3.4 Approximation of the likelihood

This subsection is useful regarding the mode of 1.354.

We retold here some general aspects of the inverse problem's theory from [Sul15]. We introduce \mathcal{U} , \mathcal{Y} are Banach spaces.

Firstly, we talk about a direct problem.

Definition A.3.5. *Given an input $\mathbf{u} \in \mathcal{U}$ of a model $\mathbf{f} : \mathcal{U} \mapsto \mathcal{Y}$, we obtain \mathbf{y} the observations such that*

$$\mathbf{y} = \mathbf{f}(\mathbf{u}) \quad (\text{A.257})$$

Then, the inverse problem is

Definition A.3.6. *Given the observations \mathbf{y} , we want to determine the input \mathbf{u}^* of the model \mathbf{f} such that*

$$\mathbf{y} = \mathbf{f}(\mathbf{u}^*) \quad (\text{A.258})$$

About the direct problem

Here the observations are,

$$\hat{\mathbf{M}} \sim \mathcal{N}(\mathbf{M}(\mathbf{p}^*), \frac{1}{n} \mathbf{Cov}(\mathbf{p}^*)) \quad (\text{A.259})$$

where \mathbf{M} refers to the expression of the exact simple moments of the distribution of $N_{[t,T]}$ the number of neutrons detected between t and T .

Then

$$\hat{\mathbf{M}} = \mathbf{M}(\mathbf{p}^*) + \frac{1}{\sqrt{n}} \tilde{\mathbf{M}} \quad (\text{A.260})$$

where $\tilde{\mathbf{M}} \sim \mathcal{N}(\mathbf{0}, \mathbf{Cov}(\mathbf{p}^*))$.

We know \mathbf{p} the vector of the parameter, the law of $\hat{\mathbf{M}}$ has the following distribution

$$\mathbb{P}(\hat{\mathbf{M}}|\mathbf{p}) \approx \frac{1}{\sqrt{\det(\frac{1}{n} \mathbf{Cov}(\mathbf{p}))}} e^{-\frac{1}{2} {}^t(\hat{\mathbf{M}}-\mathbf{M}(\mathbf{p}))\mathbf{Cov}(\mathbf{p})^{-1}(\hat{\mathbf{M}}-\mathbf{M}(\mathbf{p}))n} \quad (\text{A.261})$$

which is the exact expression of the likelihood.

About the inverse problem

We dispose of $\hat{\mathbf{M}}$ the results of $\mathcal{N}(\mathbf{M}(\mathbf{p}^*), \frac{1}{n} \mathbf{Cov}(\mathbf{p}^*))$, we want to estimate \mathbf{p}^* that best fits the data.

So we use the Bayes theorem

$$\mathbb{P}(\mathbf{p}|\hat{\mathbf{M}}) \approx \mathbb{P}(\hat{\mathbf{M}}|\mathbf{p})\mathbb{P}(\mathbf{p}) \quad (\text{A.262})$$

We look for the mode of $\mathbb{P}(\mathbf{p}|\hat{\mathbf{M}})$ and $\mathbb{E}[\mathbf{p}|\hat{\mathbf{M}}]$.

Here are some notations

$$\begin{aligned}\mathbf{p}_{mode} &= \operatorname{argmax}_{\mathbf{p}} \mathbb{P}(\mathbf{p}|\hat{\mathbf{M}}) \\ \tilde{\mathbf{p}}_{mode} &= \operatorname{argmax}_{\mathbf{p}} \tilde{\mathbb{P}}(\mathbf{p}|\hat{\mathbf{M}})\end{aligned}\tag{A.263}$$

where

$$\tilde{\mathbb{P}}(\mathbf{p}|\hat{\mathbf{M}}) \approx \frac{1}{\sqrt{\det(\frac{1}{n}\widehat{\mathbf{Cov}})}} e^{-\frac{1}{2} {}^t(\hat{\mathbf{M}}-\mathbf{M}(\mathbf{p}))\widehat{\mathbf{Cov}}^{-1}(\hat{\mathbf{M}}-\mathbf{M}(\mathbf{p}))n}\tag{A.264}$$

Proposition A.3.7. *There exist $\varepsilon > 0$ such as $\|\mathbf{p}_{mode} - \tilde{\mathbf{p}}_{mode}\| < \varepsilon$ when $n \rightarrow +\infty$. Also, $\hat{\mathbf{M}} = \mathbf{M}(\mathbf{p}^*) + \frac{1}{\sqrt{n}}\mathbf{q}^* + o(\frac{1}{\sqrt{n}})$. And where*

$$\begin{aligned}\mathbf{p}_{mode} &= \mathbf{p}^* + \frac{1}{\sqrt{n}}\mathbf{q} + o(\frac{1}{\sqrt{n}}) \\ \tilde{\mathbf{p}}_{mode} &= \mathbf{p}^* + \frac{1}{\sqrt{n}}\mathbf{q} + o(\frac{1}{\sqrt{n}})\end{aligned}\tag{A.265}$$

Proof. Warning \mathbf{p}^* refers to real values of the parameters. By definition of the likelihood

$$\mathbb{P}(\hat{\mathbf{M}}|\mathbf{p}) \approx \frac{1}{\sqrt{\det(\frac{1}{n}\mathbf{Cov}(\mathbf{p}))}} e^{-\frac{1}{2} {}^t(\hat{\mathbf{M}}-\mathbf{M}(\mathbf{p}))\mathbf{Cov}(\mathbf{p})^{-1}(\hat{\mathbf{M}}-\mathbf{M}(\mathbf{p}))n}\tag{A.266}$$

which is maximal when

$$\|\hat{\mathbf{M}} - \mathbf{M}(\mathbf{p})\|_{\frac{\mathbf{Cov}(\mathbf{p})}{n}}^2 = 0\tag{A.267}$$

Thanks to A.259, we obtain,

$$\|\mathbf{M}(\mathbf{p}^*) - \mathbf{M}(\mathbf{p}) + \frac{1}{\sqrt{n}}\tilde{\mathbf{M}} + o(\frac{1}{\sqrt{n}})\|_{\frac{\mathbf{Cov}(\mathbf{p})}{n}}^2 = 0\tag{A.268}$$

which is equivalent to

$$\mathbf{M}(\mathbf{p}^*) - \mathbf{M}(\mathbf{p}) + \frac{1}{\sqrt{n}}\tilde{\mathbf{M}} + o(\frac{1}{\sqrt{n}}) = 0\tag{A.269}$$

We obtain

$$\mathbf{M}(\mathbf{p}^*) = \mathbf{M}(\mathbf{p}_{mode}) - \frac{1}{\sqrt{n}}\tilde{\mathbf{M}} + o(\frac{1}{\sqrt{n}})\tag{A.270}$$

Since the differential of \mathbf{M} in \mathbf{p}^* is invertible then we can apply the theorem of local inversion: there exist a neighbourhood \mathcal{V} of \mathbf{p}^* and \mathcal{W} of \mathbf{p}_{mode} such as $\mathbf{M}|_{\mathcal{V},\mathbf{p}^*}$ is a local diffeomorphism. So we deduce

$$\mathbf{p}^* = \mathbf{M}^{-1}|_{\mathcal{V},\mathbf{p}^*}(\mathbf{M}(\mathbf{p}_{mode}) - \frac{1}{\sqrt{n}}\tilde{\mathbf{M}} + o(\frac{1}{\sqrt{n}}))\tag{A.271}$$

Using a limited expansion at order one of the previous function, we can obtain

$$\mathbf{p}^* = \mathbf{p}_{mode} - d\mathbf{M}_{\mathcal{V},\mathbf{p}^*}^{-1}(\frac{1}{\sqrt{n}}\tilde{\mathbf{M}}) + o(\frac{1}{\sqrt{n}})\tag{A.272}$$

in the neighbourhood \mathcal{V} of \mathbf{p}^* . Then we can do the same reasoning for $\tilde{\mathbf{p}}_{mode}$, which leads to the announced result. \square

A.3.5 Delta method

We recall the result of the delta method from [GMT19] p 154., it is important for the confidence interval in the cases study 2.4

Theorem A.3.8. *Let X_1, \dots, X_n be a sequence of random vectors in \mathbb{R}^d , $g : \mathbb{R}^d \rightarrow \mathbb{R}^s$ a differentiable function in θ . If $\sqrt{n}(X_n - \theta) \xrightarrow[n \rightarrow +\infty]{law} N_d(0, \Sigma)$ where $N_d(0, \Sigma)$ refers to the normal law in dimension d with variance-covariance matrix Σ . Then the delta method is*

$$\sqrt{n}(g(X_n) - g(\theta)) \xrightarrow[n \rightarrow +\infty]{law} N_s(0, Dg(\theta)\Sigma Dg(\theta)^T) \quad (\text{A.273})$$

where $Dg(\theta)$ refers to the differentiate of g in θ .

A.3.6 Numerical results

This subsection is useful to illustrate the delta method applied to the first moment \mathcal{M}_1 .

We can observe that using the empirical or theoretical values of the standard deviation of \mathcal{M}_1 is similar, here is a result coming from the direct computation of the likelihood.

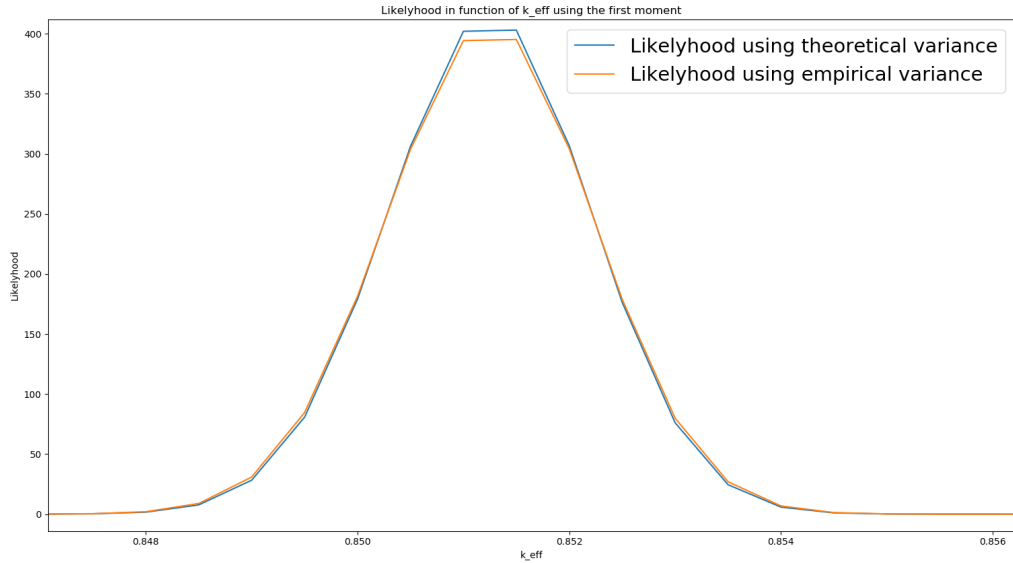


Figure A.1: Comparison of the use of the empirical or the theoretical standard deviation of \mathcal{M}_1 in the computation of the likelihood of k_{eff} for a time gate $T = 1.49018327$

A.4 Tools

A.4.1 Computation of confidence interval

Here are the explicit computations of the confidence interval of the cases study 2.4.

For the simple moments

We compute the expression of the confidence interval for $\mathbb{E}[N^2] - \mathbb{E}[N]^2$ and $\mathbb{E}[N^3] - \mathbb{E}[N]^3$.

We begin by computing the confidence interval for $\mathbb{E}[N^2] - \mathbb{E}[N]^2$.

Let $(Y_i)_{i=1}^n$ be an i.i.d. sample of a real-valued random variable with finite moments. Firstly, the asymptotic confidence interval for the expectation $I = \mathbb{E}[Y]$ is

$$[\hat{I}_n - 2\frac{\hat{\sigma}_n}{\sqrt{n}}, \hat{I}_n + 2\frac{\hat{\sigma}_n}{\sqrt{n}}] \quad (\text{A.274})$$

with $\hat{I}_n = \sum_{i=1}^n Y_i$ and $\hat{\sigma}_n^2 = \sum_{i=1}^n Y_i^2 - \hat{I}_n^2$.

We want to estimate $J = \mathbb{E}[Y^2] - \mathbb{E}[Y]^2$, so we will be using

$$\hat{J}_n = \frac{1}{n} \sum_{i=1}^n Y_i^2 - \left(\frac{1}{n} \sum_{i=1}^n Y_i \right)^2 = g_1(\hat{I}_n, \hat{K}_n), \quad g_1(I, K) = K - I^2 \quad (\text{A.275})$$

where $\hat{K}_n = \frac{1}{n} \sum_{i=1}^n Y_i^2$.

Thanks to the CLT, we dispose of

$$\left(\frac{\sqrt{n}(\frac{1}{n} \sum Y_i - \mathbb{E}[Y])}{\sqrt{n}(\frac{1}{n} \sum Y_i^2 - \mathbb{E}[Y^2])} \right) \xrightarrow{n \rightarrow +\infty} \mathcal{N} \left(0_{\mathbb{R}^2}, \begin{pmatrix} \text{Var}[Y] & \mathbb{E}[Y^3] - \mathbb{E}[Y]\mathbb{E}[Y^2] \\ \mathbb{E}[Y^3] - \mathbb{E}[Y]\mathbb{E}[Y^2] & \text{Var}[Y^2] \end{pmatrix} \right) \quad (\text{A.276})$$

We will note $C_1 = \begin{pmatrix} \text{Var}[Y] & \mathbb{E}[Y^3] - \mathbb{E}[Y]\mathbb{E}[Y^2] \\ \mathbb{E}[Y^3] - \mathbb{E}[Y]\mathbb{E}[Y^2] & \text{Var}[Y^2] \end{pmatrix}$

Using the delta method and the Slutsky theorem, we can obtain

$$\sqrt{n}(\hat{J}_n - J) \xrightarrow{n \rightarrow +\infty} \mathcal{N} \left(0, \nabla g_1(I, K) C_1 \nabla g_1(I, K)^T \right) \quad (\text{A.277})$$

where $\nabla g_1(I, K) C_1 \nabla g_1(I, K)^T = G_1(\mathbb{E}[Y], \dots, \mathbb{E}[Y^4])$.

More explicitly, we have

$$\nabla g_1(I, K) = (-2I, 1) \quad (\text{A.278})$$

and

$$\begin{aligned} \nabla g_1(I, K) C_1 \nabla g_1(I, K)^T &= (-2\mathbb{E}[Y], 1) \begin{pmatrix} \text{Var}[Y] & \mathbb{E}[Y^3] - \mathbb{E}[Y]\mathbb{E}[Y^2] \\ \mathbb{E}[Y^3] - \mathbb{E}[Y]\mathbb{E}[Y^2] & \text{Var}[Y^2] \end{pmatrix} \begin{pmatrix} -2\mathbb{E}[Y] \\ 1 \end{pmatrix} \\ &= (-2\mathbb{E}[Y], 1) \begin{pmatrix} -2\mathbb{E}[Y]\text{Var}[Y] + \mathbb{E}[Y^3] - \mathbb{E}[Y]\mathbb{E}[Y^2] \\ -2\mathbb{E}[Y]\mathbb{E}[Y^3] + 2\mathbb{E}[Y]^2\mathbb{E}[Y^2] + \text{Var}[Y^2] \end{pmatrix} \\ &= 4\mathbb{E}[Y]^2\text{Var}[Y] - 2\mathbb{E}[Y]\mathbb{E}[Y^3] + 2\mathbb{E}[Y]^2\mathbb{E}[Y^2] \\ &\quad - 2\mathbb{E}[Y]\mathbb{E}[Y^3] + 2\mathbb{E}[Y]^2\mathbb{E}[Y^2] + \text{Var}[Y^2] \\ &= 4\mathbb{E}[Y]^2\text{Var}[Y] - 4\mathbb{E}[Y]\mathbb{E}[Y^3] + 4\mathbb{E}[Y]^2\mathbb{E}[Y^2] + \text{Var}[Y^2] \end{aligned} \quad (\text{A.279})$$

So we can conclude that the bounds of the confidence interval for J is given by

$$\hat{J}_n \pm \frac{2}{\sqrt{n}} \sqrt{G_1\left(\frac{1}{n} \sum Y_i, \dots, \frac{1}{n} \sum Y_i^4\right)} \quad (\text{A.280})$$

where

$$\begin{aligned} G_1\left(\frac{1}{n} \sum Y_i, \dots, \frac{1}{n} \sum Y_i^4\right) &= 4 \left(\frac{1}{n} \sum Y_i\right)^2 \left(\frac{1}{n} \sum Y_i^2 - \left(\frac{1}{n} \sum Y_i\right)^2\right) \\ &\quad - 4 \left(\frac{1}{n} \sum Y_i\right) \left(\frac{1}{n} \sum Y_i^3\right) \\ &\quad + 4 \left(\frac{1}{n} \sum Y_i\right)^2 \left(\frac{1}{n} \sum Y_i^2\right) \\ &\quad + \frac{1}{n} \sum Y_i^4 - \left(\frac{1}{n} \sum Y_i^2\right)^2 \end{aligned} \quad (\text{A.281})$$

With the same principle, let's compute the confidence interval for $L = \mathbb{E}[Y^3] - \mathbb{E}[N]^3$. So we have

$$\hat{L}_n = \frac{1}{n} \sum_{i=1}^n Y_i^3 - \left(\frac{1}{n} \sum_{i=1}^n Y_i\right)^3 = g_2(\hat{I}_n, \hat{M}_n), \quad g_2(I, M) = M - I^3 \quad (\text{A.282})$$

Using the CLT, we dispose of

$$\left(\frac{\sqrt{n}(\frac{1}{n} \sum Y_i - \mathbb{E}[Y])}{\sqrt{n}(\frac{1}{n} \sum Y_i^3 - \mathbb{E}[Y^3])} \right) \xrightarrow{n \rightarrow +\infty} \mathcal{N}\left(0_{\mathbb{R}^2}, \begin{pmatrix} \text{Var}[Y] & \mathbb{E}[Y^4] - \mathbb{E}[Y]\mathbb{E}[Y^3] \\ \mathbb{E}[Y^4] - \mathbb{E}[Y]\mathbb{E}[Y^3] & \text{Var}[Y^3] \end{pmatrix}\right) \quad (\text{A.283})$$

We denote $C_2 = \begin{pmatrix} \text{Var}[Y] & \mathbb{E}[Y^4] - \mathbb{E}[Y]\mathbb{E}[Y^3] \\ \mathbb{E}[Y^4] - \mathbb{E}[Y]\mathbb{E}[Y^3] & \text{Var}[Y^3] \end{pmatrix}$, we have

$$\nabla g_2(I, M) = (-3I^2, 1) \quad (\text{A.284})$$

and

$$\begin{aligned} \nabla g_2(I, K) C_2 \nabla g_2(I, K)^T &= (-3\mathbb{E}[Y]^2, 1) \begin{pmatrix} \text{Var}[Y] & \mathbb{E}[Y^4] - \mathbb{E}[Y]\mathbb{E}[Y^3] \\ \mathbb{E}[Y^4] - \mathbb{E}[Y]\mathbb{E}[Y^3] & \text{Var}[Y^3] \end{pmatrix} \begin{pmatrix} -3\mathbb{E}[Y]^2 \\ 1 \end{pmatrix} \\ &= (-3\mathbb{E}[Y]^2, 1) \begin{pmatrix} -3\mathbb{E}[Y]^2 \text{Var}[Y] + \mathbb{E}[Y^4] - \mathbb{E}[Y]\mathbb{E}[Y^3] \\ -3\mathbb{E}[Y]^2(\mathbb{E}[Y^4] - \mathbb{E}[Y]\mathbb{E}[Y^3]) + \text{Var}[Y^3] \end{pmatrix} \\ &= (-3\mathbb{E}[Y]^2, 1) \begin{pmatrix} -3\mathbb{E}[Y]^2 \text{Var}[Y] + \mathbb{E}[Y^4] - \mathbb{E}[Y]\mathbb{E}[Y^3] \\ -3\mathbb{E}[Y]^2 \mathbb{E}[Y^4] + 3\mathbb{E}[Y]^2 \mathbb{E}[Y]\mathbb{E}[Y^3] + \text{Var}[Y^3] \end{pmatrix} \\ &= 9\mathbb{E}[Y]^4 \text{Var}[Y] - 3\mathbb{E}[Y]^2 \mathbb{E}[Y^4] + 3\mathbb{E}[Y]^3 \mathbb{E}[Y^3] \\ &\quad - 3\mathbb{E}[Y]^2 \mathbb{E}[Y^4] + 3\mathbb{E}[Y]^2 \mathbb{E}[Y]\mathbb{E}[Y^3] + \text{Var}[Y^3] \\ &= 9\mathbb{E}[Y]^4 \text{Var}[Y] - 6\mathbb{E}[Y]^2 \mathbb{E}[Y^4] + 6\mathbb{E}[Y]^3 \mathbb{E}[Y^3] + \text{Var}[Y^3] \end{aligned} \quad (\text{A.285})$$

Thanks to the delta method and the Slutsky theorem, we have

$$\sqrt{n}(\hat{L}_n - L) \xrightarrow{n \rightarrow +\infty} \mathcal{N}\left(0, \nabla g_2(I, K) C_2 \nabla g_2(I, K)^T\right) \quad (\text{A.286})$$

where $\nabla g_2(I, M) C_2 \nabla g_2(I, M)^T = G_2(\mathbb{E}[Y], \dots, \mathbb{E}[Y^6])$.

As conclusion, the bounds of the confidence interval for L is given by

$$\hat{L}_n \pm \frac{2}{\sqrt{n}} \sqrt{G_2\left(\frac{1}{n} \sum Y_i, \dots, \frac{1}{n} \sum Y_i^6\right)} \quad (\text{A.287})$$

For the Feynman moments

We suggest here to compute the covariance matrix for the Feynman moments. The delta method settles

$$\sqrt{n} \left(\begin{pmatrix} \hat{F}_1 \\ \hat{F}_2 \\ \hat{F}_3 \end{pmatrix} - \phi \left(\begin{pmatrix} \mathbb{E}[N] \\ \mathbb{E}[N^2] \\ \mathbb{E}[N^3] \end{pmatrix} \right) \right) \xrightarrow{n \rightarrow +\infty} \mathcal{N}\left(0, \nabla \phi K \nabla \phi^T\right) \quad (\text{A.288})$$

where $(\hat{F}_j)_{j=1,3} = \phi(\hat{N}^j)_{j=1,3}$.

We have previously established

$$\phi \left(\begin{pmatrix} \mathbb{E}[N] \\ \mathbb{E}[N^2] \\ \mathbb{E}[N^3] \end{pmatrix} \right) = \begin{pmatrix} \mathbb{E}[N] \\ \frac{\mathbb{E}[N^2] - \mathbb{E}[N]^2 - \mathbb{E}[N]}{\mathbb{E}[N]} \\ \frac{\mathbb{E}[N^3] - 3\mathbb{E}[N^2](\mathbb{E}[N] + 1) + 2\mathbb{E}[N]^3 + 3\mathbb{E}[N]^2 + 3\mathbb{E}[N]}{\mathbb{E}[N]} \end{pmatrix} \quad (\text{A.289})$$

So

$$\nabla \phi = \begin{pmatrix} 1 & -1 - \frac{\mathbb{E}[N^2]}{\mathbb{E}[N]^2} & -\frac{\mathbb{E}[N^3]}{\mathbb{E}[N]} + 3\frac{\mathbb{E}[N^2]}{\mathbb{E}[N]^2} + 4\mathbb{E}[N] + 3 \\ 0 & \frac{1}{\mathbb{E}[N]} & -3\frac{\mathbb{E}[N] + 1}{\mathbb{E}[N]} \\ 0 & 0 & \frac{1}{\mathbb{E}[N]} \end{pmatrix} \quad (\text{A.290})$$

We recall

$$K = \begin{pmatrix} \text{Var}(N) & \mathbb{E}[N^3] - \mathbb{E}[N]\mathbb{E}[N^2] & \mathbb{E}[N^4] - \mathbb{E}[N]\mathbb{E}[N^3] \\ \mathbb{E}[N^3] - \mathbb{E}[N]\mathbb{E}[N^2] & \text{Var}(N^2) & \mathbb{E}[N^5] - \mathbb{E}[N^2]\mathbb{E}[N^3] \\ \mathbb{E}[N^4] - \mathbb{E}[N]\mathbb{E}[N^3] & \mathbb{E}[N^5] - \mathbb{E}[N^2]\mathbb{E}[N^3] & \text{Var}(N^3) \end{pmatrix} \quad (\text{A.291})$$

And so, we will be able to compute the covariance of the Feynman moments $\nabla \phi K \nabla \phi^T$.

A.4.2 Differentiate for the computation of the empirical likelihood $\tilde{\mathbb{P}}(\mathbf{p}|\mathbf{y}_{obs})$

Here we compute the differentiate of the function used in A.3.4, and to justify the use of $\tilde{\mathbb{P}}(\mathbf{p}|\mathbf{y}_{obs})$ properly (see 1.7.2).

Firstly, thanks to the CLT

$$\begin{aligned} \det(\widehat{\mathbf{Cov}}) &= \det(\mathbf{Cov}(\mathbf{p}^*) + \frac{1}{\sqrt{n}}\widetilde{\mathbf{Cov}}), \\ &\text{where } \widetilde{\mathbf{Cov}} \sim \mathcal{N}(\mathbf{0}, \mathbf{Cov}(\mathbf{Cov}(\mathbf{p}^*))) \text{ and } \mathbf{Cov}(\mathbf{Cov}(\mathbf{p}^*)) = O(\mathbf{1}) \\ &= \det(\mathbf{Cov}(\mathbf{p}^*)) + \frac{1}{\sqrt{n}}\text{Tr}({}^t\text{Com}(\mathbf{Cov}(\mathbf{p}^*))\widetilde{\mathbf{Cov}}) + o\left(\frac{1}{\sqrt{n}}\right) \end{aligned} \quad (\text{A.292})$$

Then, applying the square root

$$\sqrt{\det(\widehat{\mathbf{Cov}})} = \sqrt{\det(\mathbf{Cov}(\mathbf{p}^*))} \sqrt{\left(1 + \mathbf{Cov}(\mathbf{p}^*)^{-1} \frac{1}{\sqrt{n}}\text{Tr}({}^t\text{Com}(\mathbf{Cov}(\mathbf{p}^*))\widetilde{\mathbf{Cov}}) + o\left(\frac{1}{\sqrt{n}}\right)\right)} \quad (\text{A.293})$$

Using the limited expansion of the square root, we can establish at order 1

$$\sqrt{\det(\widehat{\mathbf{Cov}})} \xrightarrow{n \rightarrow +\infty} \sqrt{\det(\mathbf{Cov}(\mathbf{p}^*))} \quad (\text{A.294})$$

Secondly, the CLT allows us to establish

$$\begin{aligned} \widehat{\mathbf{Cov}}^{-1} &= \left(\mathbf{Cov}(\mathbf{p}^*) + \frac{1}{\sqrt{n}}\widetilde{\mathbf{Cov}} \right)^{-1}, \text{ where } \widetilde{\mathbf{Cov}} \sim \mathcal{N}(\mathbf{0}, \mathbf{Cov}(\mathbf{Cov}(\mathbf{p}^*))) \\ &= \mathbf{Cov}(\mathbf{p}^*)^{-1} + \mathbf{Cov}(\mathbf{p}^*)^{-1} \frac{\widetilde{\mathbf{Cov}}}{\sqrt{n}} \mathbf{Cov}(\mathbf{p}^*)^{-1} + o\left(\frac{1}{\sqrt{n}}\right) \end{aligned} \quad (\text{A.295})$$

Then, at order 1

$$\widehat{\mathbf{Cov}}^{-1} \xrightarrow{n \rightarrow +\infty} \mathbf{Cov}(\mathbf{p}^*)^{-1} \quad (\text{A.296})$$

A.4.3 Distributions for induced fission

We provide here the numerical distributions used in the MC code in order to compute the induced fission

For the first case of the direct problem A.2.12, we used the Terrel distribution

$$\begin{aligned} f_0 &= 0,02800 \\ f_1 &= 0,15590 \\ f_2 &= 0,31490 \\ f_3 &= 0,30880 \\ f_4 &= 0,14810 \\ f_5 &= 0,03870 \\ f_6 &= 0,00496 \\ f_7 &= 0,00038 \end{aligned} \quad (\text{A.297})$$

Do not forget to normalise.

For the second case of the direct problem A.2.12, we have considered

$$\begin{aligned}f_0 &= 0,39658.10^{-1} \\f_1 &= 0,16205 \\f_2 &= 0,33160 \\f_3 &= 0,30869 \\f_4 &= 0,13069 \\f_5 &= 0,25066.10^{-1} \\f_6 &= 0,21643.10^{-2} \\f_7 &= 0,83505.10^{-4} \\f_8 &= 0,14403.10^{-5}\end{aligned}\tag{A.298}$$

For the third and the fourth case of the direct problem, we have considered

$$\begin{aligned}f_0 &= 0,02800 \\f_1 &= 0,15590 \\f_2 &= 0,31490 \\f_3 &= 0,30880 \\f_4 &= 0,14810 \\f_5 &= 0,03870 \\f_6 &= 0,00496 \\f_7 &= 0,00038\end{aligned}\tag{A.299}$$

Bibliography

- [AF12] J. Armstrong and J. Favorite. “Identification of Unknown Interface Locations in a Source/Shield System Using the Mesh Adaptive Direct Search Method”. In: *Transactions of the American Nuclear Society* 106 (Jan. 2012).
- [al.98] N. Ensslin et al. “Application Guide to Neutron Multiplicity Counting”. In: *Los Alamos National Laboratory LA-13422-M* (1998).
- [AT08] C. Andrieu and J. Thoms. “A tutorial on adaptive MCMC”. In: *Stat Comput* 18 (2008), 343–373.
- [Bas19] E. Bas. *Basics of Probability and Stochastic Processes*. Springer, 2019.
- [Bel65] G. I. Bell. “On the Stochastic Theory of Neutron Transport”. In: *Nuclear Science And Engineering* 21 (1965), pp. 390–401.
- [BFA11] K. C. Bledsoe, J. A. Favorite, and T. Aldemir. “Using the Levenberg-Marquardt Method for Solutions of Inverse Transport Problems in One- and Two-Dimensional Geometries”. In: *Nuclear Technology* 176.1 (2011), pp. 106–126.
- [BFG11] D. Bertolloto, P. Frajtag, and G. Girardin. *Flux Neutronique - Théorie et Mesures*. EPFL, 2011.
- [Bod20] T. Bodineau. *Modélisation de phénomènes aléatoires : introduction aux chaînes de Markov et aux martingales*. Cours de l’École polytechnique, 2020.
- [Bre16] M. Brener. “The effect of delayed neutrons and detector dead-time in Feynman distribution analysis”. PhD Thesis. The Pennsylvania State University The Graduate School The College of Engineering, 2016.
- [Bre69] L. Breiman. *Probability and Stochastic Processes: With a View Toward Applications*. Houston Mifflin Company - Boston, 1969.
- [Bre92] L. Breiman. *Probability*. SIAM Classics In Applied Mathematics, 1992.
- [Bö85] K. Böhnel. “The Effect of Multiplication on the Quantitative Determination of Spontaneously Fissioning Isotopes by Neutron Correlation Analysis”. In: *Nuclear Science And Engineering* 90 (1985), pp. 75–82.
- [CT05] E. J. Candès and T. Tao. “Decoding by linear programming”. In: *IEEE Transactions on Information Theory* 51.12 (2005), pp. 4203–4215.
- [Div+56] B. C. Diven et al. “Multiplicities of fission neutrons”. In: *Phys. Rev.* 101 (1956), pp. 1012–1015.

- [Ens+98] N. Ensslin et al. “Application Guide to Neutron Multiplicity Counting”. In: *Los Alamos National Laboratory LA-13422-M* (1998).
- [Fav04] J. A. Favorite. “Using the Schwinger Variational Functional for the Solution of Inverse Transport Problems”. In: *Nuclear Science and Engineering* 146.1 (2004), pp. 51–70.
- [Fel71] W. Feller. *An Introduction to Probability Theory and its Applications, Vol. II, second edition*. Wiley, New York, 1971.
- [FHS44] R. P. Feynman, F. de Hoffmann, and R. Serber. “Statistical fluctuations in the water boiler and the dispersion of neutrons emitted per fission”. In: *Los Alamos National Laboratory LA-101* (1944).
- [FHS56] R. P. Feynman, F. de Hoffmann, and R. Serber. “Dispersion of the neutron emission in U-235 fission”. In: *J. Nucl. Energy* 3.1-2 (1956), pp. 64–69.
- [FI67] A. Furuhashi and A. Izumi. “Third Moment of the Number of Neutrons Detected in Short Time Intervals”. In: *Journal of NUCLEAR SCIENCE and TECHNOLOGY* 5.2 (1967), pp. 48–59.
- [For09] G. Fort. “Méthode Monte-Carlo et Chaînes de Markov pour la simulation”. Habilitation à Diriger des Recherches (HDR). TELECOM ParisTech, 2009.
- [Gar17] J. Garnier. *Gestion des incertitudes et analyse de risque*. les Éditions de l’École polytechnique, 2017.
- [GHH21] J. Garnier, C. Houpert, and P. Humbert. “Inverse Problems for Stochastic Neutronics”. In: *Eccomas Proceedia UNCECOMP* (2021), pp. 63–74.
- [GMT19] J. Garnier, S. Méléard, and N. Touzi. *Aléatoire*. les Éditions de l’École polytechnique, 2019.
- [Goo+13] J. Goorley et al. *MCNP6 USER’S MANUAL Version 1.0*. Denise B. Pelowitz, 2013.
- [GRG96] A. Gelman, G.O. Roberts, and W. R. Gilks. “Efficient Metropolis Jumping Rules”. In: *Bayesian Statistics* 5 (1996), pp. 599–607.
- [Hag10] W. Hage. “Fissile mass determination by the active neutron correlation technique with the generalised Poisson parameters or its factorial moments”. In: *Nuclear Instruments and Methods in Physics Research Section A: Accelerators, Spectrometers, Detectors and Associated Equipment* 614.1 (2010), pp. 72–86.
- [Har02] T.E. Harris. *The Theory of Branching Processes*. Dover Phoenix Editions. Dover Publications, 2002.
- [HC85] W. Hage and D. M. Cifarelli. “Correlation Analysis with Neutron Count Distributions in Randomly or Signal Triggerred Time Intervals for Assay of Special Fissile Materials”. In: *Nuclear Science and Engineering* 89.2 (1985), pp. 159–176.
- [HM17] P. Humbert and Boukhmès Méchitoua. “Gamma ray transport simulations using SGarD code”. In: 3 (Mar. 2017), p. 9.

- [HST01] H. Haario, E. Saksman, and J. Tamminen. “An adaptive Metropolis algorithm”. In: *Bernoulli* 7.2 (2001), pp. 223–242.
- [HST99] H. Haario, E. Saksman, and J. Tamminen. “Adaptive proposal distribution for random walk Metropolis algorithm”. In: *Computational Statistics* 14.1 (1999), pp. 375–395.
- [Hum16] P. Humbert. “Application of Neutron Detection Third Order Time Correlation”. In: (June 2016), pp. 675–677.
- [Hum18] P. Humbert. “Simulation and Analysis of List Mode Measurements on SILENE Reactor”. In: *Journal of Computational and Theoretical Transport* (2018), pp. 1–14.
- [Hum19] P. Humbert. “Deterministic transport solution of multiplicity counting equations”. In: (Dec. 2019).
- [JEMSE18] Anil K. Prinja J. E. M. Saxby and M. D. Eaton. “Energy dependent Transport Model of the neutron number probability distribution in a subcritical multiplying assembly”. In: *Nuclear Science and Engineering* 189.1 (2018), pp. 1–25.
- [KGV83] S. Kirkpatrick, C. D. Gelatt, and M. P. Vecchi. “Optimization by Simulated Annealing”. In: *Science* 220 (1983), pp. 671–680.
- [Kir84] S. Kirkpatrick. “Optimization by Simulated Annealing: Quantitative Studies”. In: *Journal of Statistical Physics* 34 (1984), pp. 975–986.
- [MM08] D.J. Mitchell and J. Mattingly. “Rapid computation of gamma-ray spectra for one-dimensional source model”. In: *Trans. Am. Nucl. Soc.* 98 (2008), pp. 565–566.
- [MM10] J. Mattingly and D. J. Mitchell. “A Framework for the Solution of Inverse Radiation Transport Problems”. In: *IEEE Transactions on Nuclear Science* 57.6 (2010), pp. 3734–3743.
- [MP22] Jawad R. Moussa and Anil K. Prinja. “Reconstruction of neutron multiplicity distributions from low-order statistical information”. In: *Nuclear Instruments and Methods in Physics Research Section A: Accelerators, Spectrometers, Detectors and Associated Equipment* 1044 (2022), p. 167429.
- [Mé03] S. Méléard. *Modèles aléatoires en écologie et évolution*. École polytechnique, 2003.
- [Mü10] C. Müller. “Exploring the common concepts of adaptive MCMC and Covariance Matrix Adaptation schemes”. In: *Theory of Evolutionary Algorithms, 05.09. - 10.09.2010*. Ed. by Anne Auger et al. Vol. 10361. Dagstuhl Seminar Proceedings. Schloss Dagstuhl - Leibniz-Zentrum für Informatik, Germany, 2010.
- [Nag21] L. Nagy. “Neutron Multiplicity Counting with the Analysis of Continuous Detector Signals”. PhD Thesis. Chalmers University of Technology, Gothenburg, Sweden, Budapest University of Technology, and Economics, Budapest, Hungary, 2021.
- [Nic13] R. Nickl. *Statistical theory*. 2013. URL: http://www.statslab.cam.ac.uk/~nickl/Site/__files/stat2013.pdf.

- [OYS00] S. Okajima, Y. Yamane, and Y. Takemoto & T. Sakurai. “A Note on the Diven Factor in Fast Systems”. In: *Journal of Nuclear Science and Technology* 37.8 (2000), pp. 720–723.
- [Pan81] H. Panjer. “Recursive Evaluation Of a Family Of Compound Distributions”. In: *Astin Bulletin* 12 (1981), pp. 22–26.
- [PE08] Imre Pázsit and Andreas Enqvist. “Neutron Noise in Zero Power Systems”. In: 10 (2008), p. 171.
- [PEP09] Imre Pázsit, Andreas Enqvist, and Lénárd Pál. “A note on the multiplicity expressions in nuclear safeguards”. In: *Nuclear Instruments and Methods in Physics Research, Section A: Accelerators, Spectrometers, Detectors and Associated Equipment* 603.3 (2009), pp. 541–544.
- [PM07] P. Peerani and M. Marin Ferrer. “Sensitivity analysis of physical/operational parameters in neutron multiplicity counting”. In: *Nuclear Instruments and Methods in Physics Research Section A: Accelerators, Spectrometers, Detectors and Associated Equipment* 577.3 (2007), pp. 682–689.
- [PP08] I. Pázsit and L. Pal. *Neutron Fluctuations. A Treatise on the Physics of Branching Processes*. Elsevier Ltd, 2008.
- [PS12] M. K. Prasad and N. J. Snyderman. “Statistical Theory of Fission Chains and Generalized Poisson Neutron Counting Distribution”. In: *Nuclear Science and Engineering* 172.3 (2012), pp. 300–326.
- [PSR10] M. K. Prasad, N. J. Snyderman, and M. S. Rowland. “Absolute Nuclear Material Assay”. In: *U.S. Patent 7756237* (2010).
- [PSR12] M. K. Prasad, N. J. Snyderman, and M. S. Rowland. “Absolute Nuclear Material Assay Using Count Distribution (Lambda) Space”. In: *U.S. Patent 8194813* (2012).
- [Pà58] L. Pál. “On The Theory of Stochastic Processes in Nuclear Reactors”. In: *Nuovo Cimento* 10 7, Suppl. No. 1 (1958).
- [Pà62] L. Pál. “Statistical Theory of the Chain Reaction in Nuclear Reactors: Parts I, II, III”. In: *Acta Physica Hungaria, English Translation by V. Shibayev, Atomic Energy Authority Report, NP-TR-951 (HaP 31981), Harwell* (1962).
- [Reu03] P. Reuss. *Précis de neutronique*. EDP Sciences, 2003.
- [RS94] Robert and Smith. “Simple conditions for the convergence of the Gibbs sampler and Metropolis-Hastings algorithms”. In: *Stochastic Processes and their Applications* 49 (1994), pp. 207–216.
- [Sax17] J. Saxby. “Numerical Solution of the Phase-Space Dependent Backward Master Equation for the Probability Distribution of Neutron Number in a Subcritical Multiplying Sample”. PhD Thesis. Imperial College London Department of Mechanical Engineering, 2017.
- [Sch93] O. Scherzer. “The use of Morozov’s discrepancy principle for Tikhonov regularization for solving nonlinear ill-posed problems”. In: *SIAM J. Numer. Anal.* 6.30 (1993), pp. 1796–1838.
- [Ser45] R. Serber. “Distribution of Fission Neutron Numbers”. In: *Los Alamos National Laboratory LA-335* (1945).

- [SF13] Holger Rauhut Simon Foucart. *A Mathematical Introduction to Compressive Sensing*. Birkhäuser New York, NY, 2013.
- [Shi+19] T. Shin et al. “A Note on the Nomenclature in Neutron Multiplicity Mathematics”. In: *Nuclear Science and Engineering* 193.6 (2019), pp. 663–679.
- [SJ81] B. Sundt and W. S. Jewell. “Further Results on Recursive Evaluation of Compound Distributions”. In: *Astin Bulletin* 12 (1981).
- [Sul15] T.J. Sullivan. *Introduction to Uncertainty Quantification*. Springer International Publishing, 2015.
- [SWE16] J. Saxby, M.M.R. Williams, and M.D. Eaton. “The energy dependent Pál–Bell equation and the influence of the neutron energy on the survival probability in a supercritical medium”. In: *Annals of Nuclear Energy* 92 (2016), pp. 413–418.
- [Tar05] A. Tarantola. *Inverse Problem Theory and Methods for Model Parameter Estimation*. SIAM, 2005.
- [tea17] Tripoli-4 project team. *TRIPOLI-4 @VERSION 10 USER GUIDE*. CEA/DEN, 2017.
- [Ter57] J. Terrell. “Distribution of Fission Neutron Numbers”. In: *Physical Review* 108.3 (1957), pp. 783–789.
- [Tib96] R. Tibshirani. “Regression shrinkage and selection via the lasso”. In: *Journal of the Royal Statistical Society. Series B* 1 (1996), pp. 267–288.
- [TL15] N. Tsoufanidis and S. Landberger. *Measurements & Detection of radiation 4th edition*. CRC Press, 2015.
- [Ver16] J. M. Verbeke. “Neutron Multiplicity Counting: Credible Regions for Reconstruction Parameters”. In: *Nuclear Science and Engineering* 182.4 (2016), pp. 481–501.
- [Vot07] Arthur F. Voter. *INTRODUCTION TO THE KINETIC MONTE CARLO METHOD*. Ed. by Kurt E. Sickafus, Eugene A. Kotomin, and Blas P. Uberuaga. Dordrec: Springer Netherlands, 2007, pp. 1–23.
- [VP15] J.-M. Verbeke and O. Petit. “TRIPOLI-4 and FREYA for Stochastic Analog Neutron Transport. Application to Neutron Multiplicity Counting.” In: *37th ESARDA Annual Meeting (ESARDA Symposium 2015)*. Manchester, United Kingdom, 2015.
- [VP16] J. M. Verbeke and O. Petit. “Stochastic Analog Neutron Transport with Tripoli-4 and Freya: Bayesian Uncertainty Quantification for Neutron Multiplicity Counting”. In: *Nuclear Science and Engineering* 183.2 (2016), pp. 214–228.

Titre : Problèmes inverses pour la neutronique aléatoire

Mots clés : Neutronique, Processus de Markov, Méthodes bayésiennes, MCMC

Résumé : La détection et la caractérisation de la matière fissile sont des questions cruciales, notamment en matière de sûreté nucléaire, de garanties, de comptabilité de la matière et de mesures de réactivité. Dans ce contexte, nous voulons identifier une source de matière fissile en connaissant des mesures externes telles que les instants de détection pendant un intervalle de mesure donné. Ainsi, on observe les instants de détection des neutrons émis par la matière fissile et traversant le détecteur, puis on calcule les moments de la distribution empirique du nombre de neutrons détectés durant une porte temporelle T . Afin d'identifier la source, on doit obtenir les paramètres suivants : le facteur de multiplication k_{eff} du système, l'intensité de la source S , l'efficacité de détection ε_C . Compte tenu des paramètres de la source, il existe des modèles qui permettent de prédire les moments du nombre compté de neutrons pendant un temps T . Nous considérons un modèle ponctuel dans lequel les

neutrons monocinétiques se déplacent dans un milieu infini, isotrope et homogène. La méthode permet de calculer les moments de la distribution du nombre compté : les physiciens prennent généralement en compte les trois premiers moments (car les moments d'ordre supérieur à quatre sont trop bruités). Ensuite, étant donné les moments du nombre de neutrons comptés pendant un temps T , nous voulons obtenir les paramètres de la source fissile. Pour atteindre ce but, nous allons utiliser une approche bayésienne afin d'obtenir la distribution des paramètres. Cette distribution n'est pas triviale, les échantillons peuvent être obtenus avec des méthodes de Monte-Carlo par chaîne de Markov avec matrice d'adaptation de covariance (MCMC avec CMA). Après une étude de cas, et une analyse des formules des moments dans différents régimes de fonctionnement du système, nous utiliserons les mesures pour deux tailles de fenêtre différentes T_1 et T_2 .

Title : Inverse problems for stochastic neutronics

Keywords : Neutronics, Markov processes, Bayesian methods, MCMC

Abstract : Detection and characterisation of fissile material are crucial issues, especially in the area of nuclear safety, of guarantees, material accounting and reactivity measures. In this context, we want to identify a source of fissile material by knowing external measurements such as detection times during a given measurement interval. So, the detection times of the neutrons emitted by the fissile material and passing through the detector are observed, then the moments of the empirical distribution of the number of neutrons detected during a time gate T . In order to identify the source, the following parameters should be obtained : the multiplication factor of the system k_{eff} , the intensity of the source S , the detection efficiency ε_C . Given the parameters of the source, there are models that predict the moments of the counted number of neutrons during a time T . We consider a

point model in which monokinetic neutrons move in an infinite, isotropic and homogeneous medium. The method calculates the moments of the distribution of the number counted : physicists generally take into account the first three moments (because moments of order greater than four are too noisy). Then, given the moments of the number of neutrons counted during a time T , we want to obtain the parameters of the fissile source. To achieve this goal, we will use a Bayesian approach to obtain the distribution of the parameters. This distribution is not trivial, samples can be obtained with Markov Chain Monte Carlo methods with covariance adaptation matrix (MCMC with CMA). After a case study, and an analysis of the moment formulae in different operating regimes of the system, we will use the measurements for two different time gates T_1 and T_2 .